Title
Efforts Toward the Arcutines and Related Diterpenoid Natural Products

Author
Owens, Kyle Robert

Publication Date
2018

Peer reviewed|Thesis/dissertation

Efforts Toward the Arcutines and Related Diterpenoid Natural Products

by

Kyle Robert Owens

A dissertation submitted in partial satisfaction of the

requirements for the degree of

Doctor of Philosophy

in

Chemistry

in the

Graduate Division

of the

University of California, Berkeley

Committee in charge:

Professor Richmond Sarpong, Chair
Professor Thomas Maimone
Professor Wenjun Zhang

Spring 2018

Efforts Toward the Arcutines and Related Diterpenoid Natural Products

Abstract

Efforts Toward the Arcutines and Related Diterpenoid Natural Products

by

Kyle Robert Owens

Doctor of Philosophy in Chemistry

University of California, Berkeley

Professor Richmond Sarpong, Chair

This dissertation describes our approaches toward a variety of natural products, including the arcutine family and the related diterpenoid atropurpuran. A methodology developed to access several interesting terpenoids is also discussed. Chapter 1 is an introduction to the diterpenoid alkaloids, a large class biologically active natural products possessing highly caged scaffolds. Arcutine is the prototypical member of a small family of these molecules consisting of arcutine, arcutinine, aconicarmicharcutinium and the diterpenoid atropurpuran. This section includes a discussion of the biosynthesis of these molecules as well as our biosynthetic proposal. Previous work toward these molecules, including two total syntheses of atropupuran, is also discussed.

Chapter 2 describes our initial approaches toward arcutine and demonstrates many of the limitations of these approaches. In particular, much of the discussion focuses on synthetic disconnections that build on our groups previous approaches toward the diterpenoid alkaloids.

Chapter 3 describes our current approach toward the arcutines. While this approach has not led to a total synthesis to date, it has led to the first synthesis of the hexacyclic arcutine scaffold. Many of the transformations needed to access the arcutines from this scaffold have been completed and a total synthesis of all of the natural products in this family is well within reach. This approach hinges on an oxopyrrolium Diels–Alder cycloaddition that was developed to improve upon many of the shortcomings of previous approaches. This in turn led to a scalable synthesis of the hexacyclic arcutine framework.

Finally, Chapter 4 describes some previously published work that utilizes carvone derived cyclobutanols as precursors toward a variety of natural product and natural product like scaffolds. This work builds on our groups initial report based on these cyclobutanols, and extends it to allow further C–C bond formation. We use these new C–C bonds to forge a variety of interesting targets as well as a 4 step synthesis of the taxoid core. This work has spawned projects toward various diterpenoid natural products.

Dedicated in loving memory
of Aimi Owens

Contents

Acknowledgments . . . . . **iv**

Chapter 1: The C_{20} Diterpenoid Alkaloids **1**
1.1 Introduction & Biosynthesis 1
1.1.1 Biological Activity 2
1.1.2 Biosynthesis 2
1.2 The Arcutines & Atropurpuran 3
1.3 Biosynthetic Link Between the Arcutines and Hetidines 5
1.4 Previous Synthetic Approaches 8
1.4.1 Work by Yong Qin 8
1.4.2 Work by Susumu Kobayashi and Keiji Tanino 10
1.4.3 Work by other groups 11
1.5 References 13

Chapter 2: Initial Approaches Toward the Arcutines **15**
2.1 Topological Analysis & Retrosynthesis 15
2.2 Dipolar Cycloaddition Approach 16
2.3 Initial Diels–Alder Approach 18
2.3.1 Anhydride Based Dienophile 19
2.3.2 Imide Based Dienophile 21
2.3.3 Vinyl Group Installation 23
2.3.4 Arene Dearomatization 25
2.4 Experimental Contributors 26
2.5 Experimental Details 27
2.6 References 40
Appendix 2.A NMR Spectral Data for Chapter 2 41
Appendix 2.B X-ray Crystallography Data for Chapter 2 76

Chapter 3: Synthesis of Arcutine **97**
3.1 Introduction 97
3.2 Optimized Imide Synthesis 97
3.3 Oxopyrrolium Diels Alder 98
3.4 Tetracycle Functionalization 101
3.5 Oxidative Dearomatization & Diels-Alder Investigations 101
3.6 Pentacyclic Amide Functionalization 103

3.7 Synthesis of the Arcutine Core . . . 106
3.8 Synthetic Studies Toward Arcutinidine . . . 110
3.9 Experimental Contributors . . . 113
3.10 Experimental Details . . . 113
3.11 References . . . 128
Appendix 3.A NMR Spectral Data for Chapter 3 . . . 129
Appendix 3.B X-ray Crystallography Data for Chapter 3 . . . 174

Chapter 4: Synthesis of Natural Product Like Molecules Using C–C Activation . . . 201
4.1 Introduction . . . 201
4.2 Taxagifine: An Unusual Taxoid Natural Product . . . 203
4.3 Palladium Mediated C–C Bond Activation / Cross-Coupling . . . 204
4.4 Synthesis of Natural Product Like Scaffolds . . . 206
4.5 Experimental Contributors . . . 207
4.6 Experimental Details . . . 208
4.7 References . . . 221
Appendix 4.A NMR Spectral Data for Chapter 4 . . . 223
Appendix 4.B X-ray Crystallography Data for Chapter 4 . . . 276

Acknowledgments

First and foremost I would like to thank my family. Without their constant support I never would have made it this far. Thank you to my mother, for being an unceasing cheerleader, and for always lending a willing ear when I needed someone to vent to. Thank you to my dad, for his constant support and words of wisdom, and most of all, for keeping mom sane when I'm not around. Thanks to the rest of my family, especially the Tuckers, the Dauterives, and the Strykers. Thank you to Mimi for meatballs, cake balls, and casseroles when I needed them the most. Thank you to all the family that didn't get to see me finally finish school, I know you'd be proud.

Thank you to my advisor, Prof. Richmond Sarpong for taking a chance on a kid from Texas with no business getting into Berkeley. Thank you for providing me with the opportunities and support that I needed, and for being a constant source of new ideas and motivation. Thank you my Dissertation and Quailifying Exam committees, Professors Tom Maimone, John Hartwig, Dean Toste, Wenjun Zhang, and Mary Wildermuth.

Thank you too all of the support staff that make doing chemistry possible. Dr. Hasan Celic, and Nanette Jarenwattananon and Chris Canlas for keeping the NMR facility running even when everything was constantly falling apart. Thanks to Nick Settineri and Dr. Antonio DiPasquale for helping me figure out what the heck I was making.

Thank you to all of my previous mentors, especially Prof. Uttam Tambar, without whom I never would have gotten into Berkeley. Thanks to Manu, Amy, and David for teaching me so much and letting me tag along on their projects. Thanks to Ben Qi for being such a great mentor and teaching me so much about synthesis when I was a clueless undergrad. Thank you to all my old science teachers, especially Mr. Pfluegel and Dr. Thompson, without your enthusiastic teaching I never would have pursued a career in science.

And finally, thank you to all of the friends I've made over the course of these five years. Thanks Becca for constantly reminding me that it's ok to be going a little crazy at any given time. You've been a wonderful friend and this whole process would have been miserable without you around. Thanks to Shelby, for putting up with me, and for all that sweet, sweet, pinacol product. Thanks to all the other members of the group past and present. Especially, Jason, Paul, Lana, and Carol for being great friends and making me actually go outside occasionally. Thanks to all the past members of 907 and 832, especially Ben and Marco for helping balance out things in 832. Thanks to Adrian Gandara for being a good sport and having an unhealthy obsession with cleaning my glassware for me. Special thanks to Maddie, Jake, Harvest, and Mona for cheering me up every time I see them.

Lastly, thanks to whoever happens to be reading this. If you found my dissertation online then I hope it's helpful. I'm sure it's full of typos but I promise all the chemistry works great.

Chapter 1

The C_{20} Diterpenoid Alkaloids

1.1 Introduction & Biosynthesis

The diterpenoid alkaloids are a family of natural products with a long history in both traditional medicine and modern chemistry. From the initial isolation of aconitine (Figure 1.1) nearly 200 years ago,[1] to today, chemists have been enamored by their complex structures and potent biological activities. With over 1200 members isolated to date, the diterpenoid alkaloids are one of the largest classes of natural products. While primarily isolated from the *Aconitum* and *Delphenium* genera, small numbers of these alkaloids have been isolated from the plant genera *Consolida, Spiraea, Tricalysia, Anopterus, and Daphniphyllum.* Given the size of this family, as well as their diverse structures, the diterpenoid alkaloids have given rise to a complex system of classification. This has largely been codified in the works of Feng-Peng Wang in an effort to bring some consistency to this otherwise chaotic landscape.[2–5] The diterpenoid alkaloids are broadly classified by the number of carbons in their core skeleton. While many possess the full 20-carbon skeleton of a diterpenoid, C_{19} and C_{18} diterpenoid alkaloids arise from oxidative degradation of the C_{20} framework. In a 2002 review,[5] the C_{20} diterpenoid alkaloids alone were subdivided into 4 classes, with 19 types, 34 subtypes, and 42 groups, and this number has certainly grown in the intervening 16 years.

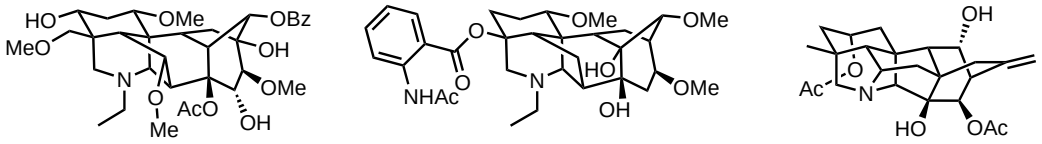

aconitine (**1.1**) lappaconitine (**1.2**) Guan-fu Base A (**1.3**)

Figure 1.1: Biologically active C_{20}, C_{19}, and C_{18} diterpenoid alkaloids.

While their complex structures have captured the interest of synthetic chemists for decades, the potent biological activities of the diterpenoid alkaloids have been known since antiquity. Often known by the more common names, wolfsbane and monkshood, plants from the genus *Aconitum* have been used as poisons and herbal remedies for at least 2000 years, appearing in ancient Greek literature and *Shennong bencao jin*, one of the earliest, and most important texts in traditional Chinese medicine.

1.1.1 Biological Activity

As modern chemistry has developed, many of the remedies used in traditional medicine have come under scientific scrutiny. This has led to efforts to determine the mechanisms of action of diterpenoid alkaloids. While many of the details are still unknown, it has been found that that many of the biological effects of the diterpenoid alkaloids can be attributed to their ability to modulate voltage-gated sodium (Na_v) channels, and to a lesser extent, potassium and calcium channels. These sodium channels exist as at least 9 isoforms in humans, $Na_v1.1$–9, and modulate a variety of physiological effects related to action potentials in muscles and neurons.[6] Development of small molecules that can selectively modulate these channels would be invaluable for treating a wide variety of conditions including hypertension and chronic pain.

Our limited understanding of the biological effects of the diterpenoid alkaloids is no better exemplified than by the comparison between aconitine (**1.1**) and lappaconitine (**1.2**). Despite their similar structures they have very different effects. Aconitine is a highly potent Na_v channel activator with a lethal dose in humans of approximately 2 mg. Conversely, lappaconitine is a Na_v channel blocker and is currently marketed in Russia and China as a treatment for arrhythmia.[7,8] Recent studies have shown that the physiological effects of the diterpenoid alkaloids are more complex than being simple blockers or activators, indicating that further study is necessary.

While the most potent members of the diterpenoid alkaloids are generally C_{19} alkaloids related to aconitine, the high toxicity of these compounds is problematic when considering pharmaceutical applications. In comparison, C_{20} diterpenoid alkaloids generally exhibit lower toxicity while still maintaining biological activity. Like lappaconitine **1.2**, guan-fu base A (**1.3**) has also been studied as a treatment for arrhythmias and is approved for human use in China.[9] Despite these clinical successes, there is still a great deal to learn about these molecules as there is little known about their protein binding and how changes in structure affect their bioactivity. Many of these natural products have only been isolated as complex mixtures with trace amounts of any particular natural product of interest. In contrast, total synthesis can provide access to individual members in a targeted fashion, and in quantities sufficient for biological studies.

1.1.2 Biosynthesis

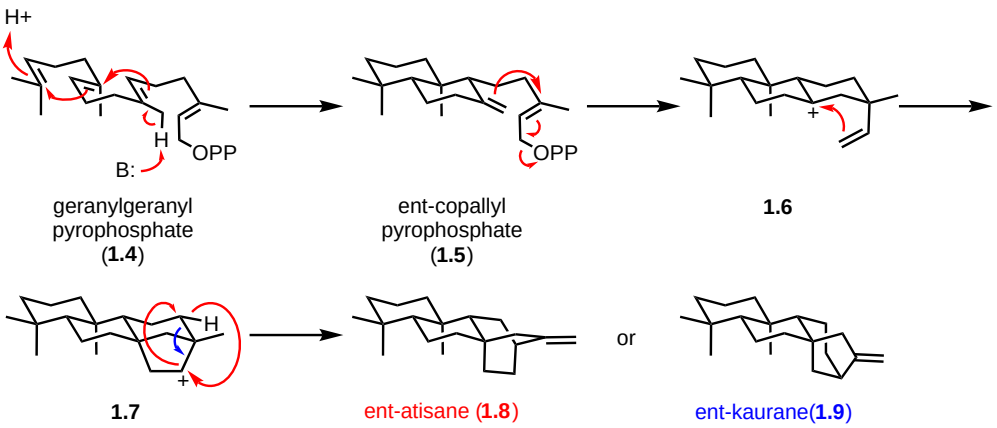

Figure 1.2: Proposed biosynthesis of the atisane core from geranylgeranylpyrophosphate (**1.4**).

All diterpenoid alkaloids arise biosynthetically[4] from geranylgeranyl pyrophosphate (GGPP, **1.4**), which undergoes a series of cationic cyclizations giving rise to carbocation **1.7**. With this tetracycle in place, a 1,2 hydride shift followed by 1,2 migration and loss of a proton gives the *ent*-atisane core (**1.8**), which serves as a precursor for most of the C_{20} diterpenoid alkaloids. Alternatively, a 1,2 migration and loss of a proton gives rise to the *ent*-kaurane skeleton (**1.9**). This process is facilitated by at least two enzymes, *ent*-copallyldiphosphate synthase and *ent*-kaurane synthase. Other enzymes related to the biosynthesis of the diterpenoid alkaloids have yet to be identified, but it is believed that cytochrome P450s play an important role. Following oxygenation, condensation with ethanolamine introduces a nitrogen. These adducts can then undergo reductive amination to form saturated nitrogen heterocycles. Oxidative loss of the ethanol fragment or reduction to the ethyl group is commonly observed, leading to secondary or tertiary N-ethyl amines. In a few instances the ethanolamine remains intact, resulting in an azaacetal.

At this stage in the biosynthesis, a wide variety of rearrangements and C–C or C–N bond forming events give rise to many of the more common diterpenoid alkaloid families. C–C bond formation, presumably via a Mannich reaction, gives rise to the hetidine (**1.11**) or denudatine (**1.13**) cores. The hetidine core can undergo an amination reaction to give the heptacyclic hetisine (**1.12**) core. The denudatine core can undergo a Wagner-Meerwein shift and oxidative loss of the C17 and C18 carbons to give the aconitine (**1.14**) and lappaconitine (**1.15**) scaffolds. Depending on which pathways are operative, plants are able to produce a wide array of these natural products. At the time of the last review in 2010, more than 80 C_{18}, 700 C_{19}, and 350 C_{20} diterpenoid alkaloids had been characterized.[2–5]

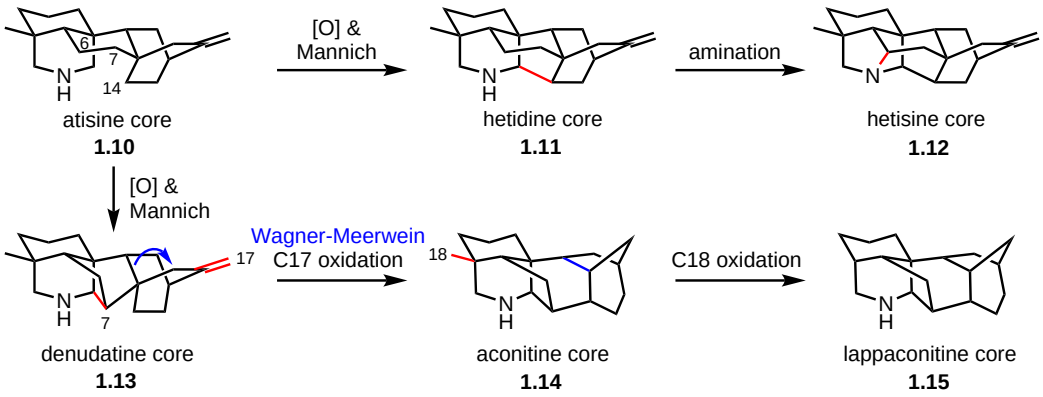

Figure 1.3: Biosynthesis of several major classes of atisane derived diterpenoid alkaloids.

;

1.2 The Arcutines & Atropurpuran

Among the numerous diterpenoid alkaloids isolated to date, the arcutines and the related diterpenoid atropurpuran stand out as some of the most unusual. This small family of natural products possesses structural elements unique to this class, most notably the presence of a [5.3.3.$0^{4,9}$.$0^{4,12}$] ring system. The arcutines are hexacyclic, highly caged natural products whereas the related diterpenoid atropurpuran possess a pentacyclic scaffold lacking the pyrrolidine ring found in the related alkaloids.

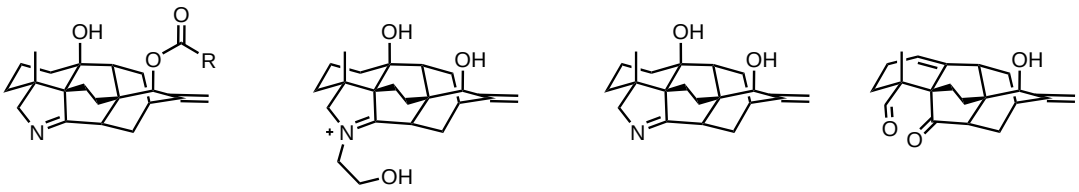

arcutine (**1.16**) R = *s*-Bu
arcutinine (**1.17**) R = *i*-Pr

aconicarmicharcutinium (**1.18**)

arcutinidine (**1.19**)

atropurpuran (**1.20**)

Figure 1.4: The arcutine family of natural products.

Arcutine (**1.16**), originally named arcutin, was isolated in 2000 by Saidkhodzhaeva and Bessonova from *Aconitum arcuatum* Maxim. in southeastern Russia.[10] Approximately 2 kilograms of dried aerial plant material was extracted to give 6.5 grams of crude alkaloids. These were further partitioned into hexane-insoluble (6.4 g) and hexane-soluble (140 mg) fractions. From the hexane soluble material, chromatography and recrystallization yielded 8 mg of a mixture of crystals. Manual separation of the crystals yielded arcutine (**1.16**), the structure of which was elucidated by X-ray crystallography. One year later, the same group published a follow up wherein they reported arcutinine (**1.17**) as the other crystalline component isolated alongside arcutine. ^{1}H NMR spectroscopy showed that these molecules were isolated as a roughly 2:1 mixture, with arcutine being the major component.[11] The structure of arcutinidine was determined by high resolution mass spectroscopy, which gave a fragmentation pattern indicating the presence of an isopropyl group rather than the *sec*-butyl moiety in arcutine. This was verified by saponification of the mixture of **1.16** and **1.17**, which gave arcutinidine (**1.19**) as the sole product. Since arcutine and arcutinine proved inseparable by chromatography, no ^{1}H NMR data was reported. However the ^{13}C chemical shifts of the mixture were provided. Arcutinidine was published with full ^{13}C and partial ^{1}H data.

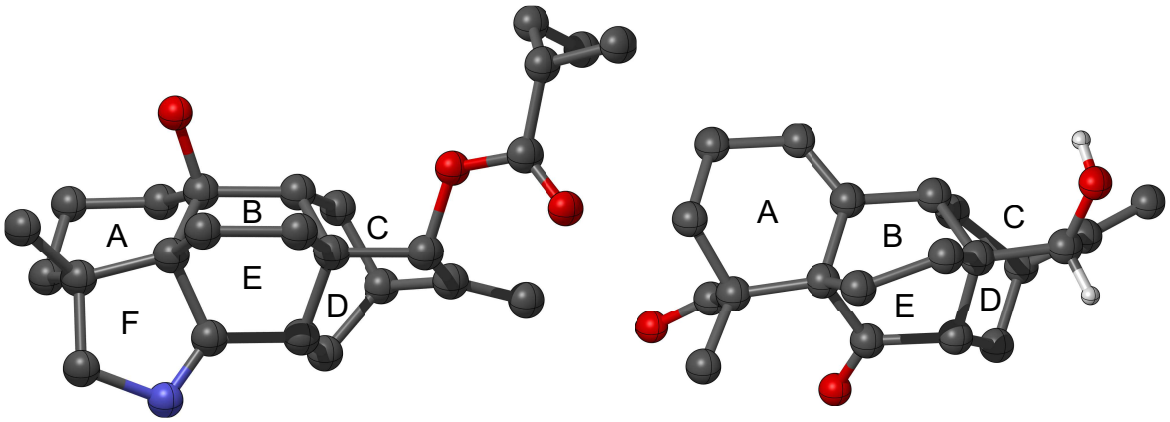

Figure 1.5: X-ray structure of arcutine (**1.16**, left) and atropurpuran (**1.20**, right) Rings are labeled clockwise from the top left ring. Ring F is absent in atropurpuran.

In 2016, the latest member of the arcutine family was isolated from *Aconitum carmichaelii*, one of the most common and thoroughly studied *Aconitum* varieties. Aconicarmicharcutinium (**1.18**) was isolated as part of the Shi group's efforts to characterize the water soluble constituents of aconitum roots, forgoing organic extractions and acid/base chemistry often used to preferentially isolate the alkaloidal constituents. When these plants are used in traditional medical practices it is often

as an aqueous solution. Therefore they hoped to identify new biologically active constituents that have eluded characterization by utilizing unadulterated aqueous extracts. They have been quite successful to date, isolating dozens of new alkaloids including the first new arcutine type alkaloid since the original isolation reports.[12] Starting from 50 kg of dried lateral roots they performed an exhaustive series of chromatographic separations, ultimately yielding 2.5 mg of aconicarmicharcutinium (**1.18**) as a mixture of the hydroxide and the trifluoroacetate salts. They did not report the azaacetal form of **1.18**, but previous reports show that this equilibrium is highly dependent on the structure of the molecule as well as the solvent.[13] Unlike arcutine and arcutinine, detailed spectroscopic information was provided for **1.18**.

The most unusual member of the arcutine family was isolated in 2009 by Feng-Peng Wang and coworkers. While the aconitum genus is a treasure trove of diterpenoid alkaloids, diterpenoids are relatively rare, despite being the presumed biosynthetic precursors to the alkaloids. Atropurpuran (**1.20**) was isolated from 2.4 kg of the dried roots of *Aconitum hemsleyanum* var. atropurpureum from Mount Emei in the Sichuan province of China. After typical alkaloid extraction procedures, 12 mg of **1.20** was isolated as a crystalline solid. The structure was determined by NMR studies and verified by X-ray crystallography. Surprisingly, the Wang group appears to have been unaware of arcutine and arcutinine at the time, as they report atropurpuran as the first known instance of a [5.3.3.$0^{4,9}$.$0^{4,12}$] tetracyclic system. This oversight was corrected by the time they published their review of the diterpenoid alkaloids in 2010.[5]

1.3 Biosynthetic Link Between the Arcutines and Hetidines

Given the unusual structure of the arcutine-type diterpenoid alkaloids, it is unsurprising that their biosynthesis has also garnered interest among the synthetic community. The initial biosynthetic proposal posited by Wang in the isolation paper for atropurpuran (**1.20**) clearly demonstrates the difficulty in identifying the connection between conventional diterpenoid alkaloids and the arcutines.[14] In this proposal, a hetidine type precursor **1.21** was thought to undergo a ring opening to form tricarbonyl compound **1.22**. They proposed an unusual step wherein oxidative loss of ethylene forms cyclohexadienone (**1.23**). Rather than tautomerize to the phenol, they proposed an addition of water to form diene **1.24**. Readdition of ethylene from the opposite face, in a Diels–Alder cycloaddition, then presumably provides **1.25**, which possesses all the carbon atoms in the natural product. This enolate could undergo an aldol reaction with the aldehyde generated in the first step of the biosynthesis to form the full atropurpuran skeleton **1.26**. At that stage, atropurpuran could arise from several redox manipulations.

When we approached this project, we too were very interested in the biosynthesis of these molecules. Given our group's previous difficulties in preparing diterpenoid alkaloids, we hoped that a greater understanding of the biosynthesis would provide insight and facilitate a bio-inspired approach. In studying the relative connectivity of the arcutines and the hetidine type diterpenoid alkaloids, we found that despite how dissimilar they appeared, they are actually only separated by a single difference in connectivity and stereochemistry. Our key insight was the recognition that the C5-C10-C20 connectivity common in most diterpenoid alkaloids was rearranged to a C10-C5-C20 triad in the arcutines and atropurpuran. Given that the structural diversity within the diterpenoid alkaloids is often derived from Wagner-Meerwein rearrangement of cationic intermediates, we posited that this could indeed be the source of the arcutines' unusual skeleton. Such a rearrange-

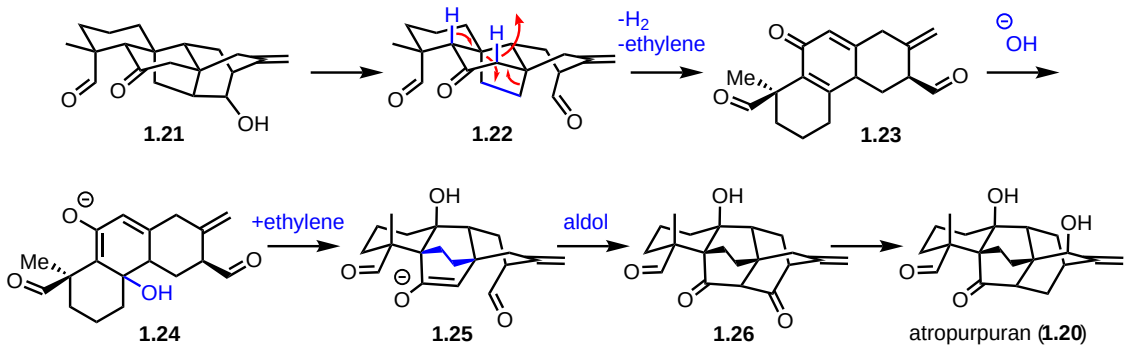

Figure 1.6: Wang's biosynthetic proposal to access atropurpuran (**1.20**) from a hetidine-type precursor.

ment also explains the stereochemical differences between these two families.

To this end, my colleague, Dr. Manuel Weber, and I began to explore this relationship computationally. While it is impossible to determine a biosynthesis without biochemical studies, we planned to model the conversion of known biosynthetic intermediates in the synthesis of C_{20} diterpenoid alkaloids to the arcutine framework. Utilizing DFT calculations, we hoped to show that the conversion between these scaffolds was feasible under biologically relevant conditions. We published the details of this study, which are summarized here.[15] Calculations were performed with mPW1K or B3LYP hybrid functionals in combination with the 6-31+G(d,p) basis set.

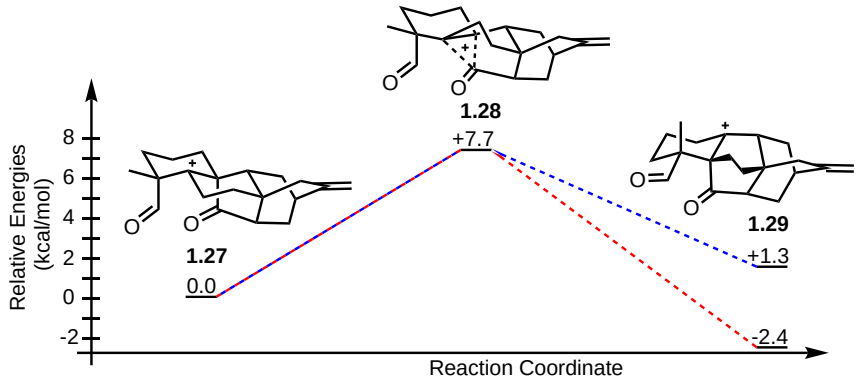

Figure 1.7: Relatives energies in the rearrangement of an atropurpuran type cation via a 1,2 acyl shift. blue (gas phase), red (water).

Since we were unsure whether the rearrangement would occur before or after addition of a nitrogen atom, we chose to explore the rearrangement on two relevant cationic substrates. The first was **1.27**, which could feasibly be an intermediate en route to a member of the hetidine class. In this case, the migration of a relatively high energy acyl cation would give the atropurpuryl cation, which could either eliminate a proton to from the alkene group found in **1.20** or be trapped by water. Calculations showed that the transition state for the cationic rearrangement of **1.28** had the same relative energy in both the gas phase as well as when modeling water as the solvent. Rearrangement to the atropurpuryl cation is thermodynamically favored in the aqueous case and slightly disfavored in the gas phase.

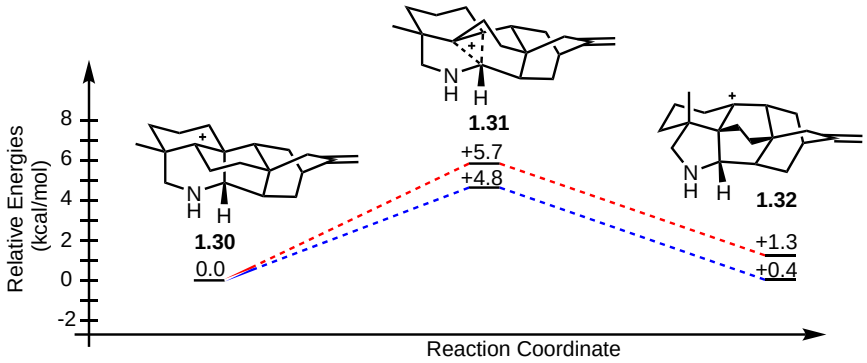

Figure 1.8: Relatives energies in the rearrangement of an hetidine type cation to an arcutine type cation via a 1,2 alkyl shift. blue (gas phase), red (water).

We also modeled this rearrangement on a cation containing a secondary amine as a possible biosynthetic precursor. Carbocation **1.30** possesses the full hetidine skeleton, albeit with unnatural stereochemistry α to the nitrogen. This stereochemistry is required for the rearrangement to give the desired product. Several hetidine type natural products possessing C5 hydroxylation have been isolated, and this hydroxyl group could serve as a viable precursor to the necessary carbocation. The alkyl migration showed a slightly lower barrier to migration as compared to the acyl cation, likely due to an interaction between the positive charge and the nitrogen lone pair that was readily apparent in the minimized structures. The gas phase and water solvated systems share similar energetics in this rearrangement, and were both slightly endothermic.

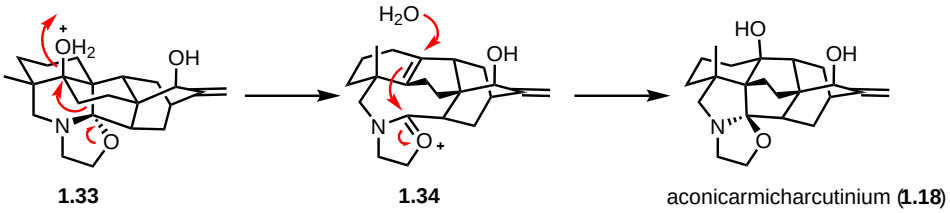

Figure 1.9: Possible biosynthetic pathway to aconicarmicharcutinium (**1.18**)

While these calculations cannot be used to determine which pathway is operative, they provide evidence for the feasibility of this transformation. Given the difficulty of synthesizing hetidine type skeletons to date, accessing the arcutines via a rearrangement of a hetidine type precursor is unlikely to prove effective. However, efficient access to the arcutine framework might provide a simpler pathway to the hetidine and hetisine type diterpenoid alkaloids.

Given the rarity of diterpenoid natural products isolated from *Aconitum* species, it seems likely that the introduction of a nitrogen would occur before rearrangement to the arcutine skeleton. Whether that rearrangement occurs from an amine that is later oxidized, or via an imine, is still unknown. However, the recent isolation of aconicarmicharcutinium (**1.18**) helps shed some light on the subject. Since ethanolamine is generally believed to be the nitrogen source in these natural products, it is reasonable to conclude that aconicarmicharcutinium (**1.18**) may be the precursor to the arcutines. If this is the case, then rearrangement of a hetidine-like scaffold (**1.33**) could be facilitated by an azaacetal as in **1.34**. This could then cyclize to give aconicarmicharcutinium (**1.18**).

DFT calculations show that this transformation is thermodynamically favored by 3 kcal/mol. Oxidative loss of the ethanolamine fragment could give the arcutines and hydrolysis of the azaacetal, and subsequent oxidation would lead to atropurpuran.

1.4 Previous Synthetic Approaches

In the nearly two decades since arcutine (**1.16**) was isolated, there has been significant synthetic interest in accessing it's unique skeleton, as well as related compounds. This has been especially true for atropurpuran (**1.20**), which has led to two total syntheses to date. No syntheses of the related alkaloids have been reported.

Following the isolation of atropurpuran (**1.20**) by Feng-Peng Wang in 2009, a great deal of synthetic work has been developed by his colleague Yong Qin, culminating in the first total synthesis of a member of this family of natural products.

1.4.1 Work by Yong Qin

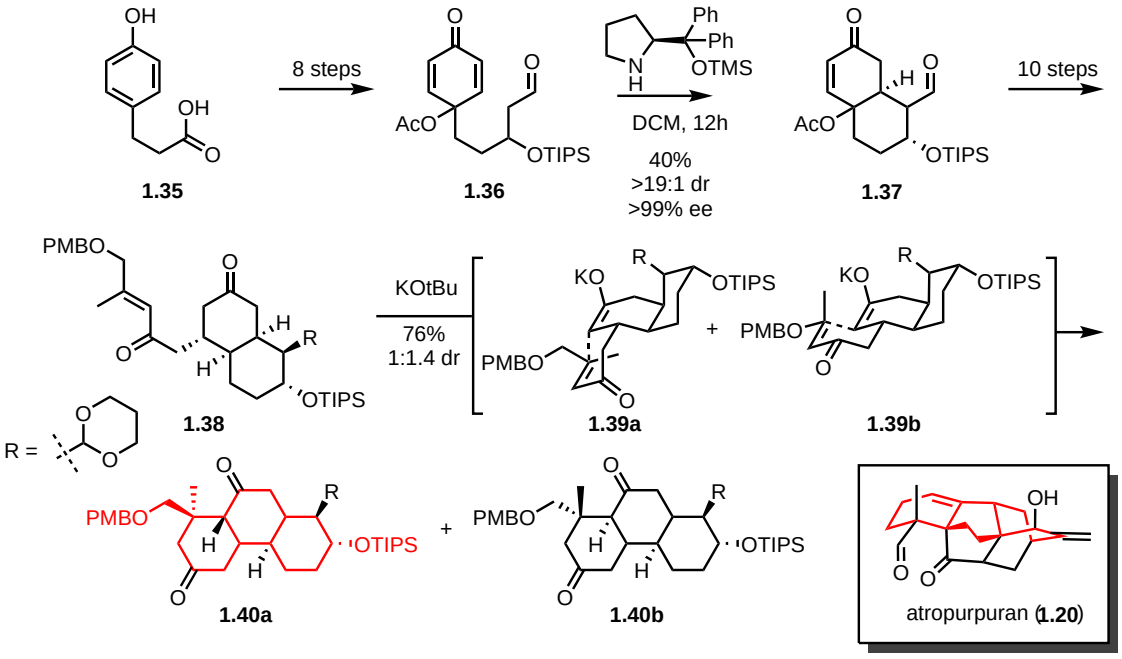

Scheme 1.1: Qin's enantioselective approach to the ABC ring system of atropurpuran (**1.20**).

The Qin group's initial work was the development of an enantioselective organocatalytic method for synthesizing an A-ring building block toward atropurpuran.[16] In 2016, they published a followup where they synthesized a highly functionalized tricycle that was used to form the A/B/C ring system.[17] Starting from the commercially available phenol **1.35**, they elaborated the side chain and performed an oxidative dearomatization to afford dienone **1.36**. This possessed an aldehyde poised for a Michael addition that furnished the B and C rings of atropurpuran. Building on their previous work, they developed a prolinol-catalyzed Michael addition, which gave the desired bicycle (**1.37**)

with excellent enantio- and diastereoselectivity. At this stage, 10 steps were needed to introduce a 6 carbon fragment at the β position of the enone. A second Michael addition using KO*t*-Bu furnished tricycle **1.40** as a mixture of diastereomers, slightly favoring the undesired **1.40b**. While this was the most advanced attempt toward atropurpuran (**1.20**) published at the time, at 20 steps, the length of the synthesis and relatively low overall yield would make it difficult to advance to the natural product.

Just a year later, the Qin group published a new approach to atropurpuran (Scheme 1.2). This approach relied on a new, racemic strategy, and ultimately led to the first total synthesis of atropurpuran.[18] Starting from substituted ethoxybenzene **1.41**, accessible in 5 steps from commercial materials, they were able to install an acrylate moiety as well as unmask the phenol to give **1.42**. From there, oxidative dearomatization afforded a dienone, which underwent a Diels–Alder cycloaddition with the pendant acrylate upon heating in xylene. This gave **1.43** as a single diastereomer and established the C and D rings of the natural product. The dimethylketal was reduced and the ketone protected as a cyclic ketal after which the lactone was opened with ethanethiol to give a thioester. The resulting primary alcohol group was oxidized to the aldehyde and then condensed with 1,3 cyclohexanedione, which would go on to form the A ring. The dione was then converted to the silyl enol ether to give **1.44**. The thioester was converted to an aldehyde, which then underwent a Mukaiyama type aldol reaction to forge the E ring. The resulting hydroxyl was protected as the silyl ether to give **1.45**. In what could be considered the key step, Qin et al. formed the B ring via a reductive cyclization yielding **1.46** as a single diastereomer. This product was converted to **1.47** via chlorination and elimination of the tertiary alcohol and hydrolysis of the ketal, followed by Wittig methylenation of the resulting ketone. Finally, Corey–Chaykovsky epoxidation of the A ring ketone followed by rearrangement with $BF_3 \cdot Et_2O$ installed a pendant aldehyde. The E ring hydroxyl was deprotected and oxidized to the ketone and the A ring aldehyde was alkylated with MeI to install the quaternary center to give **1.48**. Finally, allylic oxidation with selenium dioxide provided the epimeric natural product with only small amounts of atropurpuran. Oxidation to the enone followed by extensive screening of reductive conditions ultimately showed that $NaBH(OMe)_3$ reduction at low temperatures provided atropurpuran (**1.20**) with excellent diastereoselectivity.

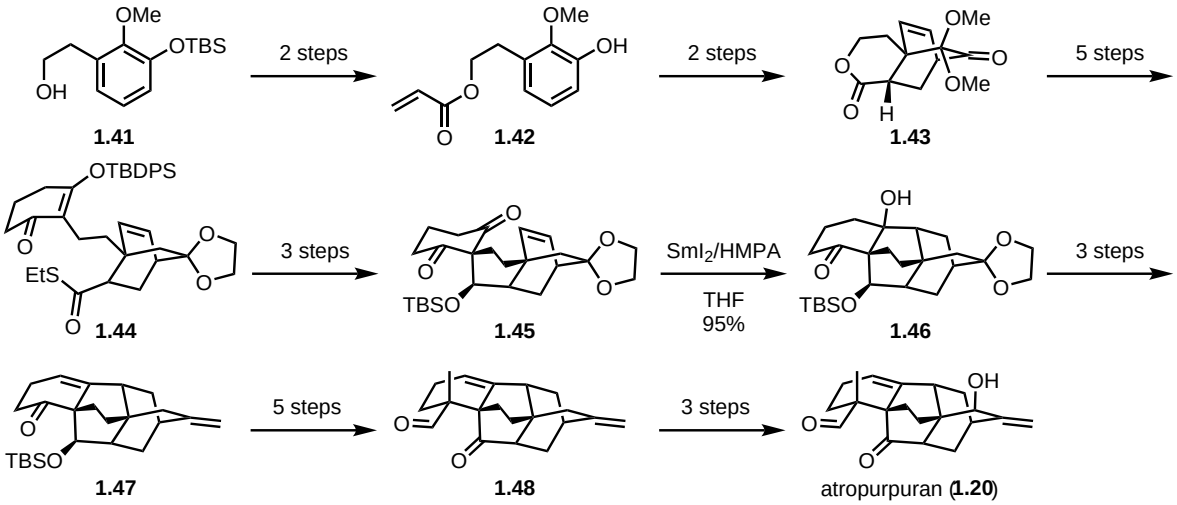

Scheme 1.2: Qin's total synthesis of atropurpuran (**1.20**).

1.4.2 Work by Susumu Kobayashi and Keiji Tanino

Some of the earliest work toward these natural products was reported[19] by Kobayashi and coworkers in 2011, just two years after atropurpuran was isolated. Given the uniqueness of the [5.3.3.$0^{4,9}$.$0^{4,12}$] ring system found in these natural products, it is no surprise that many of the synthetic efforts toward these molecules have focused on methods to install this unusual ring system. The Kobayashi group also opted to utilize an oxidative dearomatization/Diels–Alder sequence to enable the synthesis of this system, a feature that would be shared by many later approaches to these molecules.

The Kobayashi group's work starts with doubly protected tetralone **1.49**, which can be converted to the triply-allylated guiacol **1.50** in three steps. From this compound, oxidative dearomatization with PIDA afforded dienone **1.51**, which upon heating provided the desired cycloadduct (**1.52**) containing the [5.3.3.$0^{4,9}$.$0^{4,12}$] ring system. From there, ring closing metathesis with Grubb's second generation catalyst afforded **1.53** containing the full skeleton of atropurpuran (**1.20**). Further functionalization to complete the total synthesis, however, proved elusive.

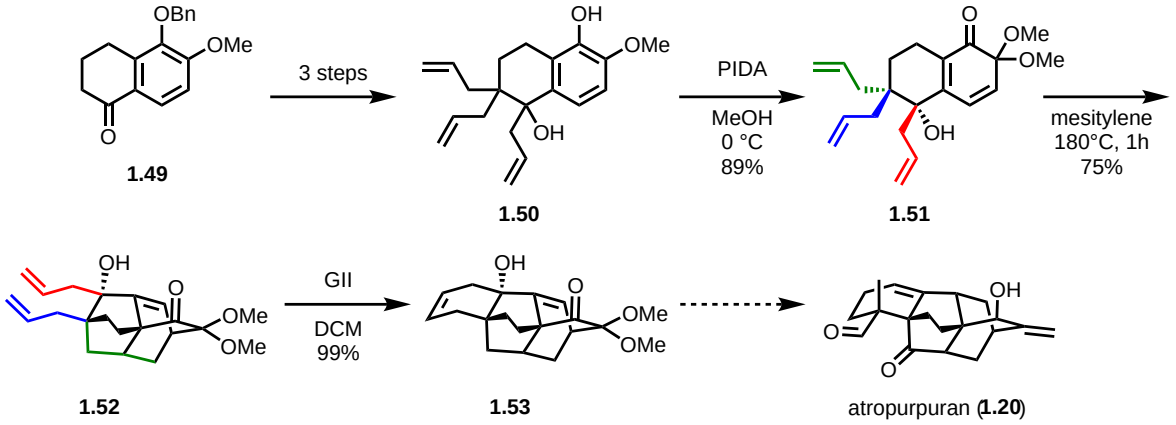

Scheme 1.3: Kobayashi's 2011 approach to the total synthesis of atropurpuran (**1.20**).

In 2014, the Kobayashi group published another[20] a synthetic study towards the [5.3.3.$0^{4,9}$.$0^{4,12}$] tetracyclic scaffold. This time, however, they were focused on achieving the synthesis of the underlying hydrocarbon skeleton, which they named dibarrelane (**1.59**) in reference to the well known barrelenes.[21] Unusual hydrocarbons have long interested synthetic chemists due to the challenge inherent in synthesizing complex molecules without any functional handles. This requires a great deal of strategy to forge the necessary bonds while also leaving room to remove any undesired functional groups at a later stage. In addition to their unusual structures, many of these hydrocarbons also possess interesting material properties.

Their work toward dibarrelane (**1.59**) begins similarly to their previous synthesis of the BCDE ring system of atropurpuran (**1.20**). Allylation and installation of a methyl ester on tetralone **1.49**, followed by reduction, protection of the resulting alcohol, and debenzylation afforded **1.54** in 5 steps. An oxidative dearomatization/Diels–Alder sequence once again afforded the [5.3.3.$0^{4,9}$.$0^{4,12}$] tetracycle containing **1.55** in good yield. Hydrogenation followed by treatment with acid afforded the diketone as well as unmasked the secondary alcohol in the B ring. An unusual Clemmensen reduction afforded not only reduction of the diketone, but deoxygenation of the secondary alcohol

group to afford dibarrelane carboxylic acid **1.58**. Finally, Barton decarboxylation afforded dibarrelane (**1.59**) in 11 steps from known tetralone **1.49**. Surprisingly, **1.58** crystallized as a dimer where each monomer was enantiomeric in the X-ray crystallographic structure. This is due to a small torsion in the 2 carbon bridges. Unfortunately, **1.59** failed to provide X-ray quality crystals, which, in addition to the relatively small calculated energy barrier between isomers, meant it was difficult to state whether dibarrelane is in fact chiral.

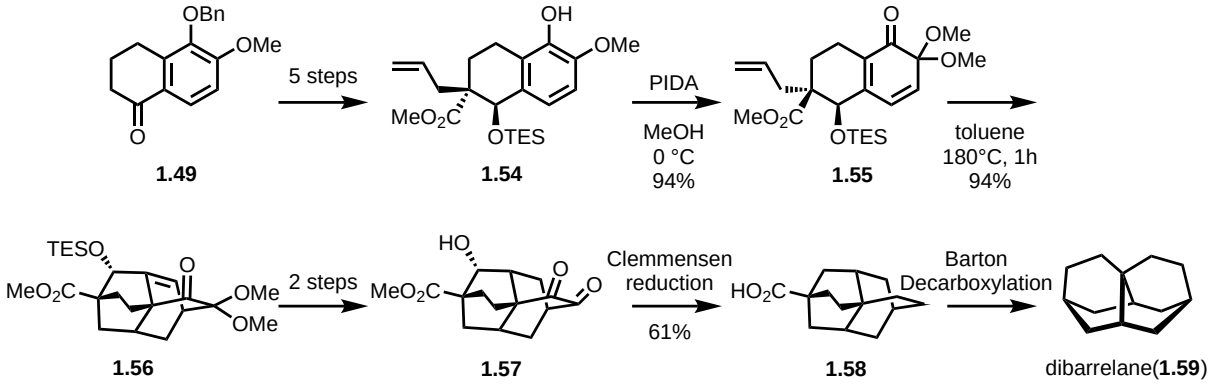

Scheme 1.4: Kobayashi's 2014 synthesis of the novel hydrocarbon dibarrelane (**1.59**).

In 2017, the Tanino and Kobayashi groups published[22] a followup to their work from 2011. By incorporating more densely functionalized building blocks early in the synthesis, they were able to complete the second total synthesis of atropurpuran to date. Utilizing the same tetralone (**1.49**) as in previous syntheses, they were able to elaborate it in 11 steps to their Diels–Alder precursor (**1.63**). Upon heating, an inverse demand Diels–Alder reaction occurred to afford an intermediate tetracycle (**1.64**). This adduct was then cyclized with the Hoveyda-Grubbs 2nd generation catalyst in the same flask to furnish **1.65**, which possesses the full pentacyclic core of atropurpuran. From there an additional 10 steps, the last of which is an allylic hydroxylation, furnished 15-epi-atropurpuran. Utilizing precedent from the Qin group, they oxidized and reduced the resulting enone selectively, which afforded atropurpuran (**1.20**) in good diastereoselectivity.

1.4.3 Work by other groups

The Sorensen group has also shown interest in these molecules, and although no papers were ever published, their efforts were reported in a Ph.D. dissertation. Their work began shortly after the isolation of atropurpuran in 2009, and while their initial approach unwittingly mirrored Kobayashi's,[19] it suffered from an unlucky choice of substrates to pursue the key step. They chose to approach the synthesis by targeting a less highly oxidized intermediate that utilized a normal demand Diels–Alder cycloaddition of an electron rich diene. They arrived at diene **1.67** in a short sequence of steps from the Wieland-Miescher ketone. The use of this starting material incorporates an undesirable ring fusion methyl group, which would have to be removed or replaced at some stage. This was necessary to prevent the aromatization of their diene, which was observed in some very early attempts with substrates bearing a ring fusion hydrogen. Upon heating **1.67** to 150 °C, they did observe some of the desired tetracycle (**1.68**) but also a substantial amount of undesired isomerization to give **1.69**. Kobayashi's related, but more highly oxidized, substrate (**1.51**)

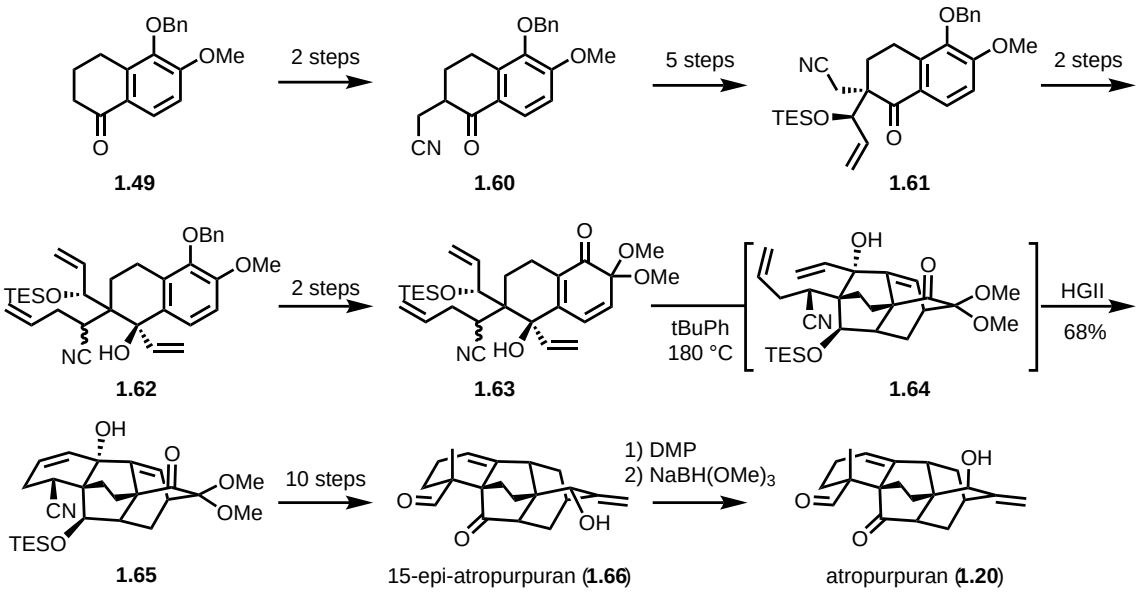

Scheme 1.5: Tanino's total synthesis of atropurpuran (**1.20**).

underwent the Diels–Alder reaction in good yields to give **1.52**. These observations illustrate the importance of choosing the appropriate redox level when developing a synthesis. While Sorensen's approach would give products much closer in redox level to the natural product, their chosen substrates suffered from diminished reactivity. This juxtaposes nicely with Kobayashi's high oxidation state approach, which ultimately costs steps but allows for much better control of which bonds can be made and broken. This choice is often difficult due to the desire to achieve shorter syntheses, especially in natural products with relatively low oxidation states. Walking the fine line between step economy and bond forming robustness is key to an efficient synthesis. Sorensen and coworkers also pursued a radical cyclization based approach but ultimately decided against pursuing the project further.

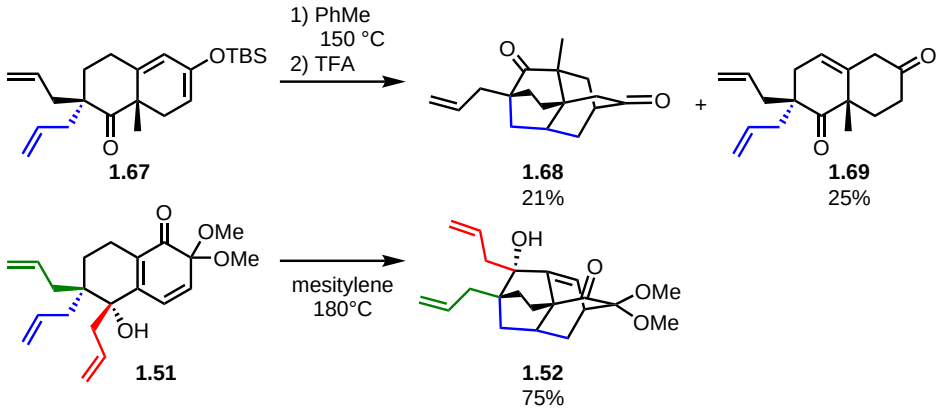

Scheme 1.6: Sorensen's first approach to the core of atropurpuran(**1.20**) (top), and Kobayashi's tetracycle synthesis (bottom).

In 2016, Singh and coworkers reported their synthesis of the atropurpuran BCDE ring system.[23]

Like Kobayashi, they planned to install the rightmost [2.2.2] bicycle with an oxidative dearomatization Diels–Alder sequence. Starting from a phenol (**1.70**) with an ortho benzylic hydroxyl, they were able to perform an oxidative dearomatization to give a dienone that rapidly dimerized to give **1.71**. Upon heating in the presence of the dienophile, a retro Diels–Alder followed by intermolecular Diels–Alder gave **1.72**. Following removal of the epoxide, the ethyl ester was twice homologated. In total, a 9 step sequence, including protection and deprotection of the ketone, was needed to access **1.73**. This ester was converted to an acyl radical, which cyclized onto the alkene to form **1.74**. Ether cleavage, and subsequent oxidation of the resulting hydroxyl to an aldehyde, led to a spontaneous aldol reaction and further oxidation to form the final bridge of the [5.3.3.$0^{4,9}$.$0^{4,12}$] tetracycle. In total, it took 15 steps to access this tetracyclic system from the starting phenol. The total step count is unknown given that no details on the synthesis of **1.70** are provided and no syntheses of their starting material have been reported to date.

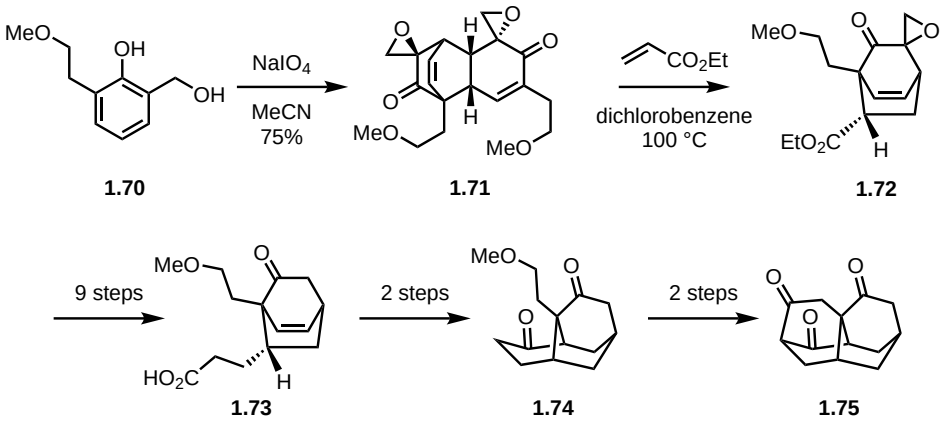

Scheme 1.7: Singh's approach to the [5.3.3.$0^{4,9}$.$0^{4,12}$] system.

1.5 References

1. Geiger, P. L. *Ann. der Pharm.* **1833**, *7*, 269–280.
2. Wang, F. P.; Chen, Q.-H.; Liang, X. T. *The Alkaloids* **2009**, *67*, 1–78.
3. Wang, F. P.; Chen, Q.-H. *The Alkaloids* **2010**, *69*, 1–577.
4. Wang, F. P.; Liang, X. T. *The Alkaloids* **2002**, *59*, 1–280.
5. Wang, F.-P.; Chen, Q.-H.; Liu, X.-Y. *Nat. Prod. Rep.* **2010**, *27*, 529–570.
6. (a) de Lera Ruiz, M.; Kraus, R. L. *J Med Chem* **2015**, *58*, 7093–7118; (b) Ahern, C. A.; Payandeh, J.; Bosmans, F.; Chanda, B. *J Gen Physiol* **2016**, *147*, 1–24.
7. Ameri, A. *Progress in Neurobiology* **1998**, *56*, 211–235.
8. Fujita, Y.; Terui, K.; Fujita, M.; Kakizaki, A.; Sato, N.; Oikawa, K.; Aoki, H.; Takahashi, K.; Endo, S. *Journal of Analytical Toxicology* **2007**, *31*, 132–137.
9. Sun, J. *et al. Drug Metab. Dispos.* **2015**, *43*, 713–724.
10. Tashkhodzhaev, B.; Saidkhodzhaeva, S. A.; Bessonova, I. A.; Antipin, M. Y. *Chem. Nat. Compd.* **2000**, *36*, 79–83.
11. Saidkhodzhaeva, S. A.; Bessonova, I. A.; Abdullaev, N. D. *Chem. Nat. Compd.* **2001**, *37*, 466–469.

12. Jiang, B.; Lin, S.; Zhu, C.; Wang, S.; Wang, Y.; Chen, M.; Zhang, J.; Hu, J.; Chen, N.; Yang, Y.; Shi, J. *J. Nat. Prod.* **2012**, *75*, 1145–1159.
13. Meng, X.-H.; Jiang, Z.-B.; Zhu, C.-G.; Guo, Q.-L.; Xu, C.-B.; Shi, J.-G. *Chin. Chem. Lett.* **2016**, *27*, 993–1003.
14. Tang, P.; Chen, Q.-H.; Wang, F.-P. *Tetrahedron Lett.* **2009**, *50*, 460–462.
15. Weber, M.; Owens, K.; Sarpong, R. *Tetrahedron Lett.* **2015**, *56*, 3600–3603.
16. Chen, H.; Zhang, D.; Xue, F.; Qin, Y. *Tetrahedron* **2013**, *69*, 3141 – 3148.
17. Chen, H.; Li, X.-H.; Gong, J.; Song, H.; Liu, X.-Y.; Qin, Y. *Tetrahedron* **2016**, *72*, 347–353.
18. Gong, J.; Chen, H.; Liu, X. Y.; Wang, Z. X.; Nie, W.; Qin, Y. *Nat. Commun.* **2016**, *7*, 12183.
19. Suzuki, T.; Sasaki, A.; Egashira, N.; Kobayashi, S. *Angew. Chem. Int. Ed.* **2011**, *50*, 9177–9179.
20. Suzuki, T.; Okuyama, H.; Takano, A.; Suzuki, S.; Shimizu, I.; Kobayashi, S. *J. Org. Chem.* **2014**, *79*, 2803–2808.
21. Zimmerman, H. E.; Paufler, R. M. *J. Am. Chem. Soc.* **1960**, *82*, 1514–1515.
22. Suzuki, T.; Nakanishi, K.; Kobayashi, S.; Tanino, K. *Symposium on the Chemistry of Natural Products, symposium papers* **2017**, *59*.
23. Jarhad, D. B.; Singh, V. *J. Org. Chem.* **2016**, *81*, 4304–4309.

Chapter 2

Initial Approaches Toward the Arcutines

2.1 Topological Analysis & Retrosynthesis

Our initial retrosynthesis of the arcutines was guided by topological analysis, a tool developed by Corey[1] and later Heathcock[2] in their respective longifolene and daphyniphyllum alkaloid syntheses, and codified by Corey[3] and Hoffmann[4] in their books on retrosynthesis analysis. This method was developed for highly caged molecules such as those in Figure 2.1, making it ideal for the diterpenoid alkaloids. Unlike many retrosynthetic approaches, it focuses on connectivity while being functional group agnostic. Due to their complex connectivity, these molecules can be difficult to understand intuitively. This method provides useful disconnections that might be missed by other approaches. The key premise of this strategy is the idea that bridging ring systems are inherently more complicated than fused systems. By identifying the maximally bridged ring and seeking retrosynthetic transforms that reduce the number of bridgehead atoms in highly complex caged structures, they can be rapidly reduced to simpler fused systems. Our group has previously applied this approach to the syntheses of other diterpenoid alkaloids.[5]

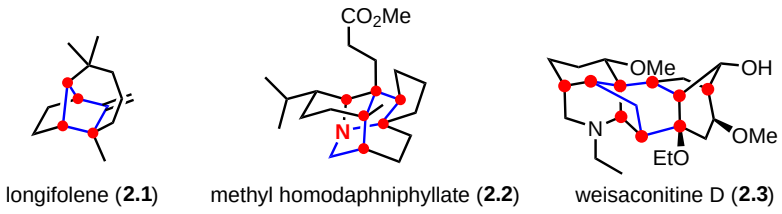

longifolene (**2.1**) methyl homodaphniphyllate (**2.2**) weisaconitine D (**2.3**)

Figure 2.1: Natural products synthesized utilizing topological analysis. Bridgehead atoms and maximally bridging ring.

My work on this project began several months after my colleague Dr. Manuel Weber initiated it. Our initial approach sought to utilize some chemistry we originally developed for several other total syntheses. The most notable step was a gallium (III)-catalyzed cycloisomerization reaction[6] to form 6-7-6 fused ring systems. I joined the project while these efforts were winding down in favor of developing an entirely new approach. At that time, we were aware of Kobayashi's approach[7] to the core of atropurpuran as well as the early work from the Qin group.[8] Given that much of the progress toward these molecules relied on building the rightmost [2.2.2] bicycle first, we instead opted to explore the early installation of the heterocyclic left hand portion, as this

challenge was still unaddressed in the literature. The early introduction of a nitrogen causes many of its own challenges, therefore developing a sufficiently robust synthesis that could tolerate this functionality was also a key consideration.

We identified arcutinidine (**1.19**, Figure 2.2) as our target since it would allow us to access the full suite of arcutines and atropurpuran. Utilizing topological analysis, we identified our first key disconnection as shown in Figure 2.2. After labeling all of the bridgehead carbons (red) it was immediately obvious that the central 6 membered ring with 6 bridgehead carbons was the maximally bridged <8-membered ring, and therefore an ideal place to start. We recognized that the Diels–Alder transform on the right hand [2.2.2] bicycle reduced this hexacyclic ring system with 8 bridgehead atoms to a tetracyclic all fused ring systems. In the forward sense, this transformation could be achieved by addition of a vinyl group into the ketone group of **2.4** followed by Birch reduction and Diels–Alder cycloaddition. This strategy (Figure 2.3) relied heavily on precedent from Gin and Peese's total synthesis of the hetisine type diterpenoid alkaloid nominine.[9] At the time, we were unaware of Sorensen's approach using a diene at a similar redox level, and their difficulties in achieving this transformation.

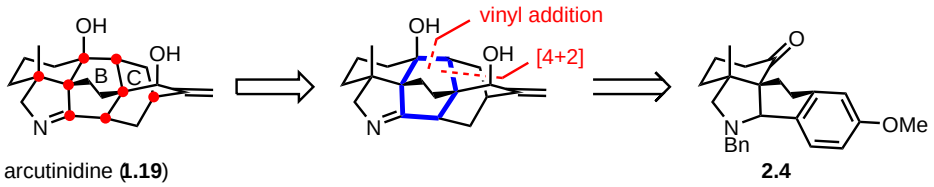

Figure 2.2: The first disconnection in our retrosynthesis was the removal of a 2 carbon fragment that would form the B and C rings. Bridgehead atoms are labeled in red, and the maximally bridged ring is shown in blue.

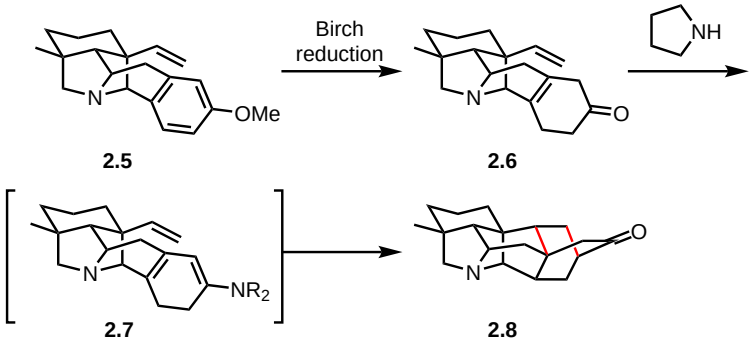

Figure 2.3: Gin's endgame makes use of a Diels–Alder cycloaddition with a transient aminodiene.

2.2 Dipolar Cycloaddition Approach

While we were confident in this analysis, the next disconnection of **2.4** was less obvious, as there were several possible candidates to take tetracycle **2.4** back to simpler materials. The first approach we decided to investigate was a 1,3 dipolar cycloaddition to form the F ring, as there

was some precedent from the synthesis of nominine. In Gin's approach to nominine they used an N-alkyl isoquinolinone 1,3 to generate a dipole (see **2.10**), which engaged a tethered electron deficient cyclohexene in a cycloaddition to form the F and G rings simultaneously as shown in **2.9**. Our proposal would utilize an azomethine ylide (**2.11**) to generate the E and F rings of arcutine simultaneously. One key challenge was the need for a tetrasubstituted dipolarophile, which generally impedes this type of cycloaddition reaction.

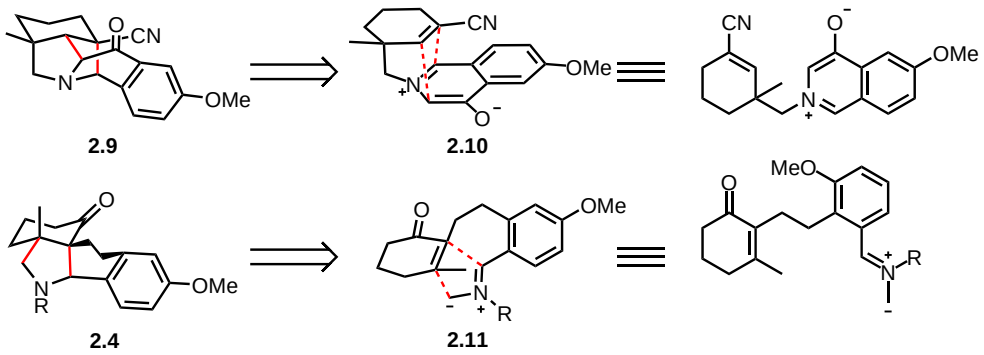

Figure 2.4: Gin's approach to the nominine core (top) and our proposed F ring synthesis.

We envisioned accessing this azomethine ylide from the corresponding aldehyde (**2.15**). Our synthesis started with known triflate **2.12**, which was be prepared in two steps from 3-methoxyphenol.[10] Sonogashira cross coupling with TMS acetylene followed by a strongly basic workup to cleave the silyl group gave **2.13**. A second Sonogashira cross coupling with 2-iodo-3-methyl cyclohexanone[11] gave **2.14**. Hydrogenation with Pd on $BaSO_4$ at 1 bar of H_2 gave the alkyne reduction product without overreduction, to afford our dipolar cycloaddition precursor **2.15**.

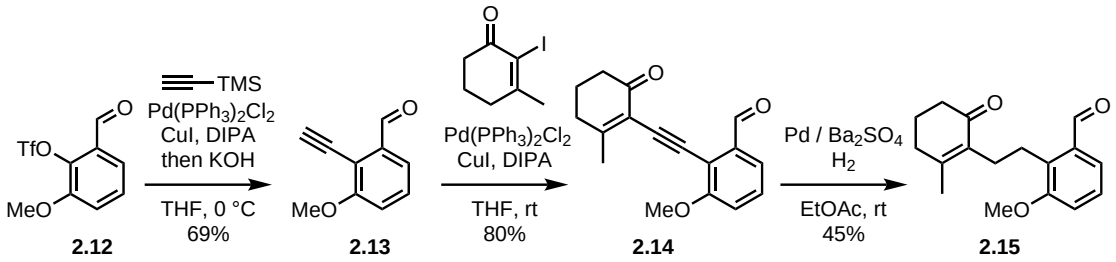

Scheme 2.1: Synthesis of dipolar cycloaddition precursor **2.57**.

We condensed aldehyde **2.58** with various glycine derivatives in an effort to form an azomethine ylide both thermally, as well as with various copper catalysts,.[12] All attempts gave back unreacted starting material or hydrolysis product **2.15**. Upon heating to higher temperatures, only nonspecific decomposition was observed. The problems with this approach appeared to lie in both the difficulty accessing an appropriate dipole as well as the addition of that dipole to the tetrasubstituted dipolarophile. Next, we tried an approach that would simplify generating the necessary carbanion. N-methyl imines with an appropriate heteroatom on the methyl group can be converted to α imino anions (aza-allyl anions) by metallation or desilylation. We chose the desilylative method (see Scheme 2.2) due to the ease of synthesizing the necessary silylated amine precursor.[13]

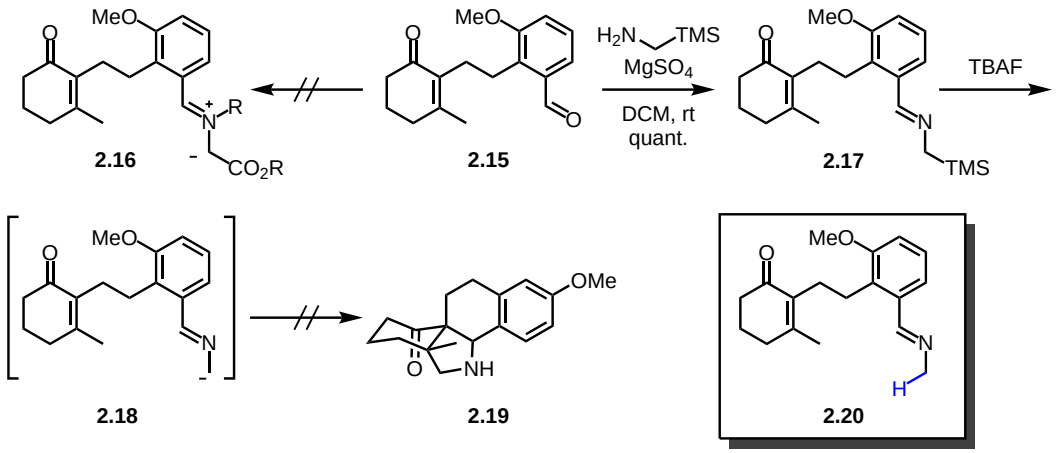

Scheme 2.2: Our attempts to perform a dipolar cycloaddition led to protodesilylation.

Condensation of **2.15** with trimethylsilylmethylamine gave our silylated nucleophile precursor **2.17**, in practically quantitative yields. When treated with a variety of fluoride sources such as tetrabutylammonium fluoride (TBAF), loss of the silicate gave carbanion **2.18**. Unfortunately no cyclization to give **2.19** was ever observed, and only the protodesilylated starting material (**2.20**) or the starting aldehyde (**2.15**) were recovered. Due to the difficulties in forming vicinal quaternary centers as well as the seven acidic α and γ protons in **2.18**, this approach became increasingly unappealing. In one final effort, we synthesized the desmethyl cyclohexanone in hopes that addition to a trisubstituted enone would be more favorable. However, the same protodesilylation issues were observed in that case as well.

2.3 Initial Diels–Alder Approach

It became clear that this dipolar cycloaddition approach was unlikely to progress further so we revised our plans. We still believed that our topological disconnection to the tetracycle was valid, but formation of the F ring wasn't the only approach to build the tetracycle. Synthesis of the A ring via a Diels–Alder cycloaddition with a heterocyclic dienophile would form a fragment with the A and F rings in place. We could also choose to introduce a nitrogen at various stages depending on our choice of dienophile. If a pendant aryl group was also present, it could be dearomatized to serve as a diene in a Diels–Alder cycloaddition as in Gin's synthesis of nominine. With these disconnections in mind we developed a new retrosynthesis (Figure 2.5). From tetracycle **2.21** we could build the E ring utilizing a Friedel-Crafts type alkylation, which would bring us back to fused bicycle **2.22**. Fused bicycle **2.22** could in turn be synthesized using a Diels–Alder cycloaddition between an oxygen containing diene (**2.23**) and a heterocyclic dienophile (**2.24**). The main challenge associated with the approach is the formation of vicinal quaternary centers in the Diels–Alder step, which is relatively uncommon and often requires very harsh conditions.

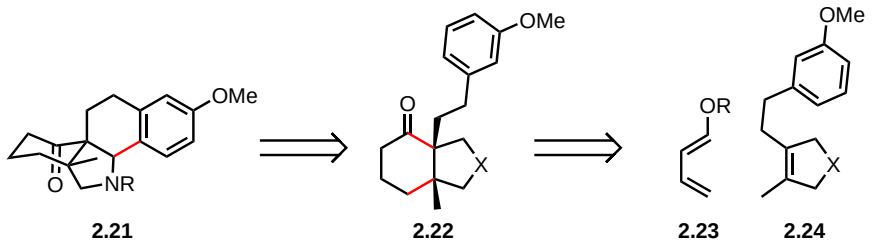

Figure 2.5: Retrosynthetic approach utilizing a Diels–Alder to build the A/F ring system.

2.3.1 Anhydride Based Dienophile

For the diene (**2.23**) we chose a TBS enol ether (i.e. R=TBS) as it was readily available in high isomeric purity in one step from crotonaldehyde.[14] For the dienophile coupling partner, we chose to target the anhydride as it was very electron deficient, which would help facilitate the Diels–Alder and could be converted to the imide in order to introduce the requisite nitrogen atom. Our group has utilized a comparable system en route to other diterpenoid alkaloids,[15] and we hoped to develop a similar approach. The first challenge was to synthesize the requisite anhydride. While there are many approaches to form trisubstituted anhydrides, there is relatively little precedent for forming tetrasubstituted anhydrides from simple precursors.

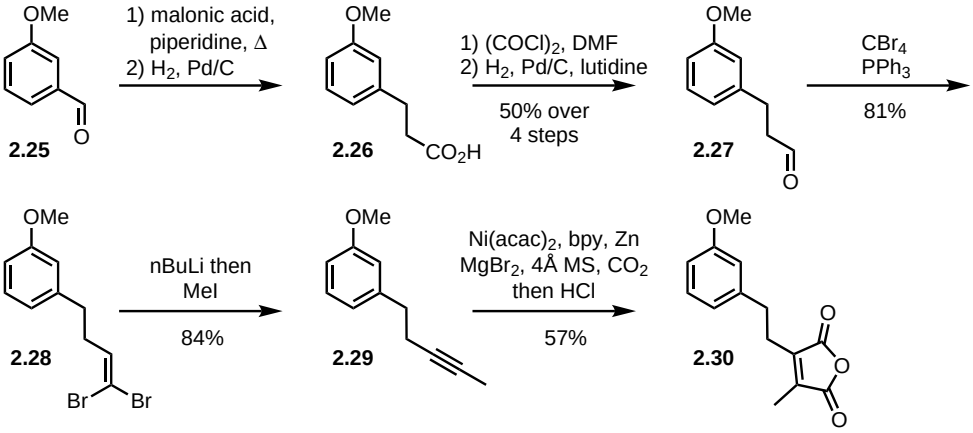

Scheme 2.3: Synthesis of target anhydride **2.30**.

Starting from 3-anisaldehyde (**2.25**, Scheme 2.3), Knoevenagel condensation with malonic acid gave an unsaturated carboxylic acid that was hydrogenated to give **2.26**. Treatment with oxalyl chloride and catalytic DMF led to the acid chloride, which was simply concentrated and subjected immediately to a Rosenmund reduction to give the corresponding aldehyde (**2.27**). Upon treatment with the Ohira-Bestmann reagent,[16] this aldehyde gave the desired terminal alkyne, but subsequent attempts to methylate it proved unsuccessful. Instead, Corey-Fuchs alkynylation followed by trapping of the intermediate lithium acetylide with iodomethane led to the desired alkyne (**2.29**). Access to **2.29** set the stage for our anhydride forming step. Initial attempts at forming the trisubstituted anhydride[15,17] by dicarboxylation of a terminal alkyne were moderately successful, but gave roughly equal amounts of the E and Z double bond isomers, of which only the Z isomer could be used to form an anhydride. Attempts to form a tetrasubstituted anhydride (**2.30**)

using the same conditions provided none of the desired product. Fortunately, a recent report by Tsuji demonstrated the synthesis of tetrasubstituted anhydrides directly from internal alkynes via a nickel catalyzed dicarboxylation reaction.[18] Our initial attempts failed to give any of the desired product, which we speculated was due to the presence of the methyl ether since the original report only demonstrated this reaction on hydrocarbon substrates. Attempts to replicate the work using the same substrates in the original report, however, also failed to give the expected products. After careful purification of all reagents, we found that our source of DMF was the culprit. Transferring all the reagents, including our anhydrous solvent, to a glovebox led to reproducible results, allowing us to access gram quantities of our desired dienophile (**2.30**). We also found that we could generate the active catalyst $Ni(acac)_2bpy$ in situ instead of synthesizing and isolating it separately as described in the initial report.

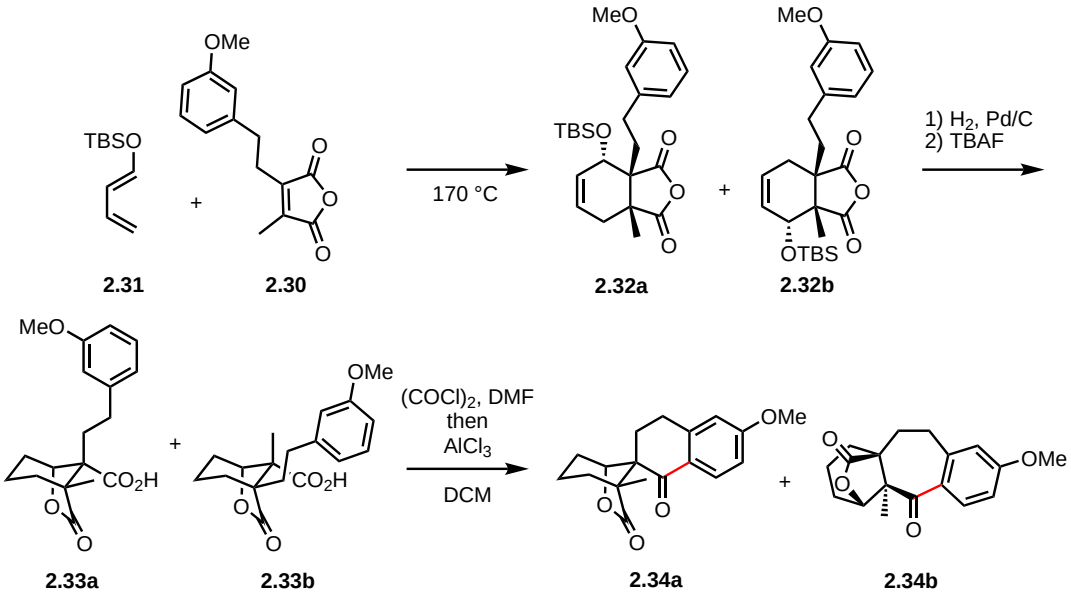

Scheme 2.4: Synthesis of tetracyclic lactones via a Friedel-Crafts acylation of **2.33a** and **2.59**.

With compound **2.30** in hand we investigated the Diels–Alder cycloaddition. After screening a variety of Lewis acid catalysts to help facilitate this reaction with unsatisfactory results, we found that judicious application of heat to a mixture of neat **2.30** and **2.31** led to the expected Diels–Alder adduct, albeit as an inseparable mixture of constitutional isomers, the desired **2.32a** and **2.32b**. Hydrogenation once again gave an inseparable mixture of the expected products. When this mixture was treated with TBAF, we found that none of the expected alcohol was present in our organic extracts despite formation of a product with the correct mass by LCMS. Upon closer inspection, we found **2.33a** and **2.33b** in our aqueous extracts. This was the result of desilylation followed by attack of the axial alkoxide onto the anhydride to form an inseparable mixture of two bicyclic lactones. While we had initially planned to perform a Friedel-Crafts cyclization with the anhydride, we found that formation of the acid chlorides under standard conditions followed by the addition of $AlCl_3$ led to a mixture of two Friedel–Crafts products **2.34a** and **2.34b**, which were separable by chromatography. 2D NMR studies of these lactones, namely their HMBC spectra, showed that the more polar of these isomeric products was consistent with the desired spiro-fused tetracycle. X-ray crystallography confirmed that it was **2.34a**.

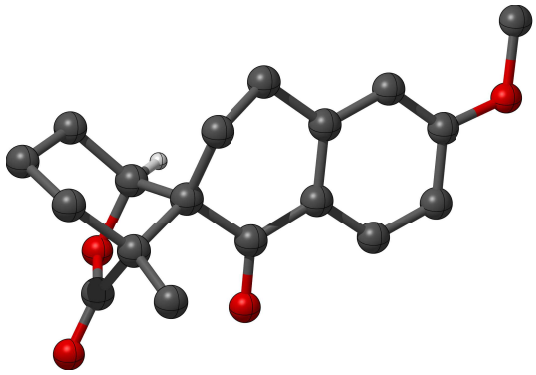

Figure 2.6: X-ray structure of **2.34a** visualized with CYLview.

With the modest amounts of material that this route afforded, we next investigated the installation of a nitrogen atom. This could be achieved either by reductive amination of the tetralone or via amidation of the lactone. Our attempts to condense ammonia onto the ketone group of the tetralone resulted in only recovered starting material. Electron rich tetralones are quite unreactive at the carbonyl. When coupled with the challenge of the adjacent quaternary center, this low reactivity was too much to overcome. Introduction of nitrogen at the lactone would allow us to achieve the same goal, however attempts to amidate the lactone with a variety amines led to no nitrogen incorporation.

2.3.2 Imide Based Dienophile

After coming to the realization that we would need to incorporate a nitrogen earlier in the sequence, we decided to do so before the Diels–Alder cycloaddition step. Treatment of anhydride **2.30** with benzylamine gave N-benzyl imide **2.35**. High temperatures were still required in order for the Diels–Alder to proceed and the products (**2.36a** and **2.36b**) were formed as an inseparable mixture of isomers. Fortunately, upon hydrogenation, **2.36a** and **2.36b** were separable. Deprotection of the 2°alcohol gave **2.38** and oxidation with Dess-Martin periodinane (DMP) gave ketone **2.39**. Treatment of **2.39** with vinyl magnesium bromide gave the allylic alcohol (**2.40**), as a single diastereomer with unknown stereochemistry at the tertiary center. At this stage we now needed to cyclize the aryl portion onto the imide carbonyl to form the E ring. Attempts at a Friedel-Crafts type cyclization showed that the imide was too unreactive for Friedel-Crafts cyclization, and that the allylic alcohol was prone to undesired side reactions.

Taking the unproductive cyclization and side reactions of the allylic alcohol into account, we sought more mild conditions to achieve this transformation we decided to use an anionic cyclization as shown in Scheme 2.6. We also considered that the quaternary center β to the imide might be too sterically encumbering, which could hinder this cyclization. We elected to take the TBS ether (**2.37**) forward as both the alcohol (**2.38**), and ketone (**2.39**) would be incompatible with the alkyllithium bases needed to generate our carbanion. Treatment of **2.37** with N-iodosuccinimide (NIS) gave para iodinated compound **2.41** exclusively. Upon treatment with Mg^0, no Grignard formation was detected. Treatment with *n*-BuLi gave the desired tetracycle (**2.42**), albeit in modest yields. *s*-BuLi and *t*BuLi gave inferior results. Ionic reduction conditions using $BF_3 \cdot Et_2O$ as a Lewis acid and Et_3SiH as a hydride source afforded **2.43** in good yields. Desilylation to unveil

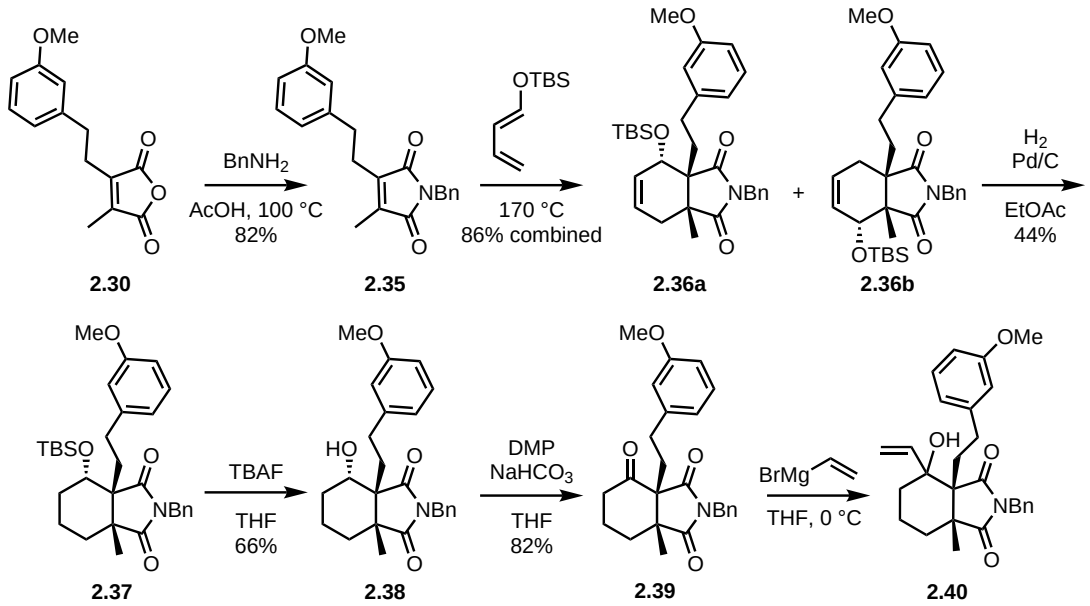

Scheme 2.5: Synthesis of a vinyl containing A/F ring system of arcutine.

the secondary alcohol proved unexpectedly difficult, but use of a large excess of TBAF at very high temperatures did give the desired alcohol (**2.44**). We found that sterically hindered alcohol **2.44** was unreactive to most common oxidants with the exception of DMP, which gave the expected product (**2.45**) in good yields. With **2.45** in hand, we had finally achieved the key intermediate from our retrosynthesis. We next set out to explore installation of the vinyl group and the subsequent dearomatization/Diels–Alder sequence.

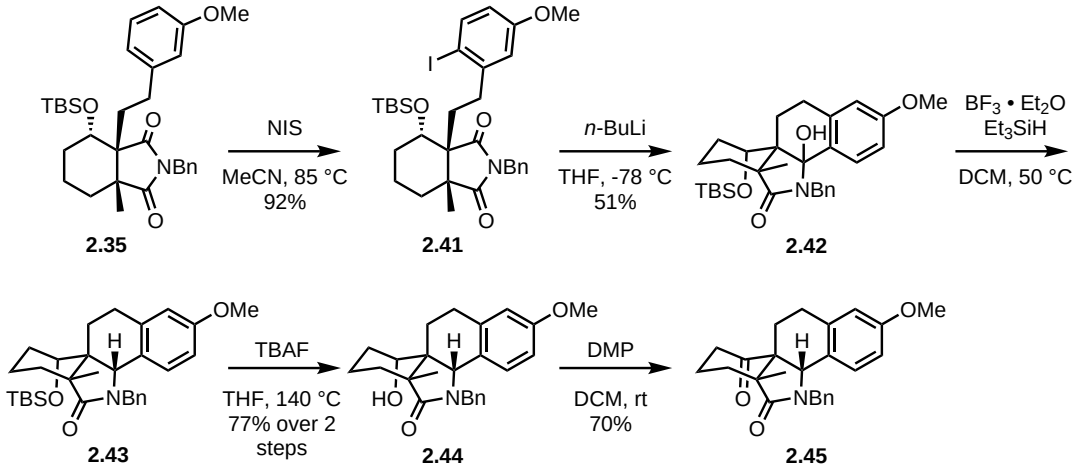

Scheme 2.6: Synthesis of the key tetracycle (**2.45**) from our initial retrosynthesis.

At this stage we wanted to confirm the structure of **2.45**, and to ensure that the silane reduction product, which was initially assigned via 1D NOE correlation, was the desired diastereomer. Additionally, since we were anticipating some difficulty adding nucleophiles to a neopentyl-like carbonyl, we hoped to gain some information about how accessible the ketone carbonyl was, as

well as what face nucleophiles might add from. X-ray structure determination of **2.45** showed that we did have the desired tetracycle, but that both Bürgi-Dunitz approaches were relatively similarly hindered.

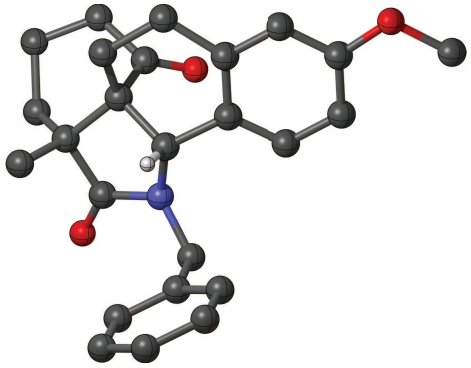

Figure 2.7: X-ray structure of **2.45**, visualized in CYLview.

2.3.3 Vinyl Group Installation

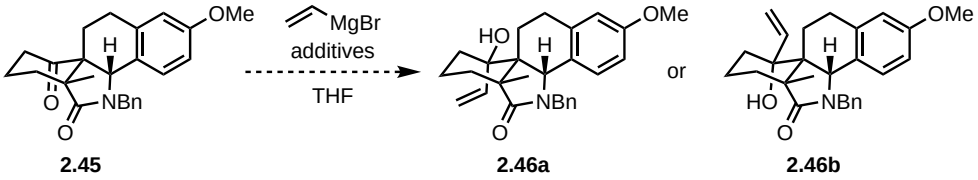

2.45 **2.46a** **2.46b**

Scheme 2.7: Addition of a vinyl group to ketone **2.45**. **2.46a** possesses the desired stereochemistry that matches that of the natural product.

Since we were unable to determine what the facial selectivity of a nucleophilic addition to the carbonyl in **2.60**, would be, we set out to install a vinyl group and rely on variation in experimental conditions to achieve selectivity. After our initial attempts utilizing vinylmagnesium bromide failed, it became readily apparent that this step would be even more challenging than expected. In addition to being surprisingly unreactive, ketone (**2.45**) was also extremely insoluble in all but chlorinated solvents, which were unsuitable for the reaction given the strongly basic conditions. It was difficult to say if this lack of reactivity was due to the steric environment of the ketone group or deprotonation and formation of an unreactive enolate. On the basis of the latter assumption, a variety of additives known to mitigate α deprotonation, namely $CeCl_3$ and $LaCl_3 \cdot 2\,LiCl$ were examined. Since it has been demonstrated that ketone preactivation as well as transmetalation of the organometallic reagent can be used, both possibilities were explored.[19] Given our difficulties installing the vinyl group, installation of an alkyne using the less sterically demanding ethynylmagnesium bromide was also attempted. The results of these efforts are summarized in Table 2.1.

Attempts to use the ketone "as is" or precomplexing the starting carbonyl with the vinyl Grignard alone failed to give any conversion. After screening the various combinations we found that activating the starting ketone with a commercial THF solution of $LaCl_3 \cdot 2\,LiCl$ and transmetalating the vinyl Grignard with anhydrous $CeCl_3$ provided the best conversion. High temperatures were

Table 2.1: Conditions for nucelophilic addition to ketone **2.45**. Reactions were performed in sealed microwave vials on 25 μmol scale in THF. When used, the starting ketone and organometallic reagents were precomplexed at room temperature for approximately two hours before use. a) reaction conducted on larger scale.

Entry	equiv	Nuc.	equiv	Ketone Act.	equiv	Nuc. Act.	Temp	Time	Conv.
1	1	vinyl	1.05	$LaCl_3$			23 °C	18 h	0%
2	1	vinyl	1.05	$CeCl_3$			23 °C	3 h	0%
3	3	vinyl					23 °C	18 h	0%
4	5	vinyl					50 °C	12 h	0%
5	5	vinyl				$CeCl_3$	70 °C	12 h	0%
6	5	vinyl				$LaCl_3$	70 °C	12 h	0%
7	3	vinyl	1.5	$CeCl_3$	3.5	$CeCl_3$	70 °C	12 h	0%
8	3	vinyl	2.5	$CeCl_3$	3.5	$CeCl_3$	100 °C	1 h	15%
9	3	vinyl	2.5	$CeCl_3$	3.5	$CeCl_3$	70 °C	12 h	15%
10	3	vinyl	2.5	$LaCl_3$	3.5	$LaCl_3$	100 °C	1 h	0%
11	3	vinyl	2.5	$LaCl_3$	3.5	$LaCl_3$	70 °C	12 h	trace
12	3	vinyl	2.5	$LaCl_3$	3.5	$CeCl_3$	100 °C	1 h	50%
13	3	vinyl	2.5	$CeCl_3$	3.5	$LaCl_3$	100 °C	1 h	0%
14	6	vinyl	2.5	$LaCl_3$	7	$CeCl_3$	100 °C	1 h	15%
15[a]	3	vinyl	2.5	$LaCl_3$	3.5	$CeCl_3$	100 °C	1 h	40%
16	5	ethynyl			5	$CeCl_3$	70 °C	12 h	80%
17[a]	5	ethynyl			5	$CeCl_3$	70 °C	12 h	30%

needed as the starting ketone was insoluble below 70 °C, even under relatively dilute conditions (approximately 0.02M). While addition of ethynylmagnesium bromide initially looked promising (Table 2.1, entry 16), the resulting proparygylic alcohol decomposed upon purification, even when deactivated silica was used. The best conditions for the vinyl addition (Table 2.1, entry 15) resulted from complexing the ketone with $LaCl_3 \cdot 2\,LiCl$, and using an excess of $CeCl_3$ to preform the organocerium reagent from vinyl magnesium bromide. Even with this optimization, we were only able to isolate a few milligrams of the resulting allylic alcohol. No NOE correlations were observed with the vinyl or hydroxyl protons, so once again the structure was determined by X-ray analysis, which showed that addition of the vinyl group occurred from the undesired face of the carbonyl to give **2.46b**.

In order to circumvent this troublesome Grignard addition step, we developed a second approach to introduce the vinyl group using a cross coupling. Since we believed that α deprotonation was an issue in the Grignard addition, we decided to use this to our advantage by converting ketone **2.45** to the corresponding vinyl triflate (**2.47**). Stille coupling provided the desired diene (**2.48**) in good yields but with poor reproducibility. This diene could also be selectively epoxidized, albeit in poor yields using mCPBA to give the vinyl epoxide (**2.49**). Given the low yields of this epoxidation, we opted to advance the synthesis using **2.48** instead.

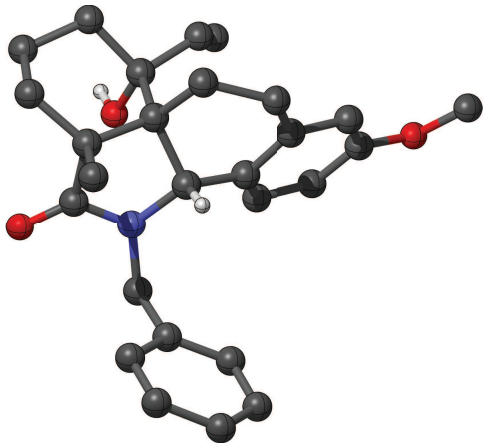

Figure 2.8: X-ray structure of **2.46b**, visualized in CYLview.

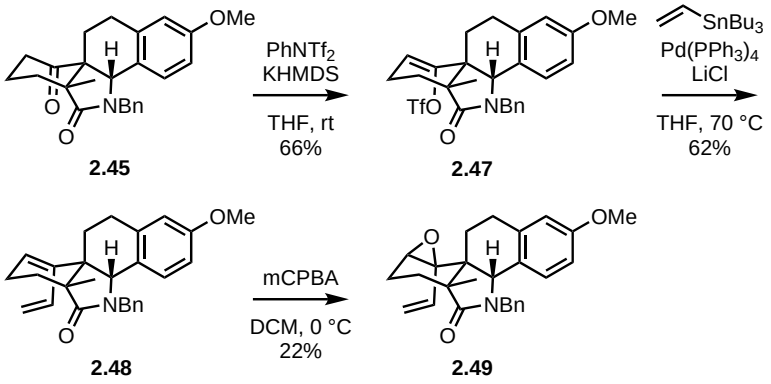

Scheme 2.8: Vinylation of ketone **2.45** via vinyl triflate formation then Stille coupling.

2.3.4 Arene Dearomatization

Our initial attempts at a Birch reduction focused on diene **2.48**. Using standard Birch conditions we were able to effect a Birch reduction, which gave a mixture of products including the debenzylated starting material, diene reduction, as well as the expected Birch reduced product **2.50**, albeit as a mixture of the conjugated and unconjugated methyl enol ether. The use of lithium as a reductant gave similar results and Na_2K impregnated silica gel[20] gave only diene reduction. Purification of these product mixtures proved difficult, and upon subjecting **2.50** to acidic conditions to unmask the ketone, decomposition occured. We next looked at the Birch reduction of the alcohol containing tetracycle **2.44**. Dissolving metal conditions using sodium metal gave the desired Birch reduced product **2.52** relatively cleanly, although purification was still a challenge. Once again, however, treating this enol ether with a variety of Brønsted and Lewis acids resulted only in decomposition.

Given our difficulties in effecting a useful reductive dearomatization, we decided to attempt an oxidative dearomatization. We were also motivated by Qin's recently reported synthesis of atropurpuran[21] that utilized an oxidative dearomatization. Since we were reluctant to develop a new route with more oxidized starting materials, we first opted to explore ways of utilizing the material we already had. Cleavage of the aryl methyl ether proved difficult on our tetracycle with

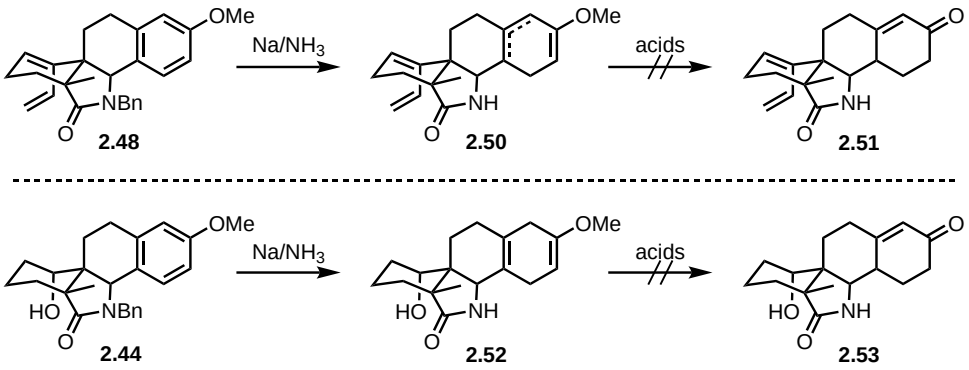

Scheme 2.9: Birch reduction of methoxy arenes.

both the free alcohol (**2.44**) and ketone (**2.45**) in place (Scheme 2.10). These substrates proved unreactive to EtSNa and related thiolates. Attempts to demethylate with a variety of common Lewis acids including BBr_3, AlI_3, and TMSI, showed that only BBr_3 gave any of the desired product. This transformation was low yielding, but enough of the resulting phenol (**2.54**) was accessed to attempt an oxidative dearomatization. Treatment with phenyliododiacetate (PIDA) in methanol did give the oxidative dearomatization product, but not the desired 1,3–diene needed for a Diels–Alder. Instead, addition of water gave the dienone (**2.55**), which proved too unstable to use in subsequent steps.

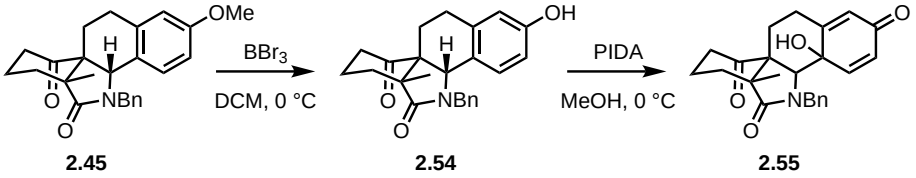

Scheme 2.10: Oxidative dearomatization of **2.45**.

With our inability to access any form of the dearomatized diene, we next attempted to oxidize the aromatic portion to install either another oxygen atom or some sort of halide that might allow for a more productive oxidative dearomatization. Ideally, we would be able to oxidize ortho to the alkyl and methoxy substituents in **2.56** to best set the stage for an oxidative dearomatization. Alcohol and ketone **2.44** and **2.45**, respectively, were explored as substrates for these oxidations. A variety of bromination and iodination reagents were screened as well as the phthaloyl peroxide developed by the Siegel group.[22] Common solvents for this type of halogenation were explored as well as both mild and forcing temperatures. Unfortunately, none of these attempts provided any detectable amount of the desired product (**2.56**).

2.4 Experimental Contributors

All of the work in Sections **2.1** and **2.2** were conducted jointly by Dr. Manuel Weber (M.W.) and Kyle Owens (K.O.), both authors contributed equally. All work in Section **2.3** and beyond was conducted solely by K.O..

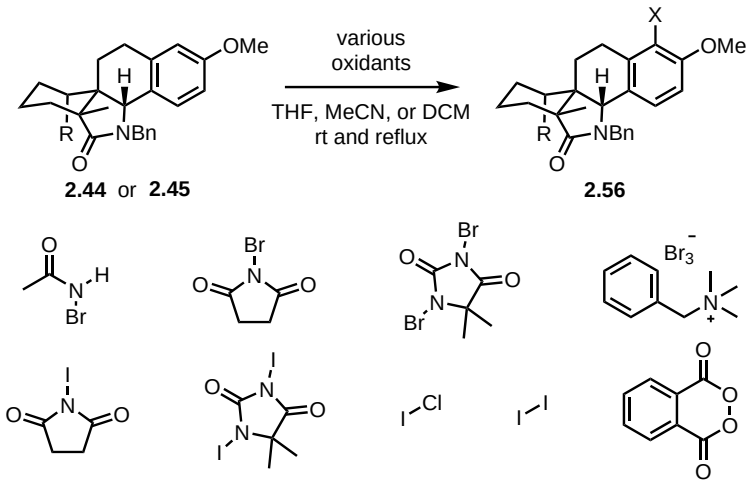

Scheme 2.11: Attempted oxidation of **2.44** and **2.45**.

2.5 Experimental Details

Materials and Methods for the Experiments in Chapter 2 Unless stated otherwise, reactions were performed in flame or oven dried glassware sealed with rubber septa under a nitrogen atmosphere and were stirred with Teflon-coated magnetic stir bars. Liquid reagents and solvents were transferred by syringe using standard Schlenk techniques. Reaction temperatures above room temperature (rt), 23 °C, were controlled by a temperature modulated stir plate. Reaction temperatures below room temperature were performed in appropriate cold baths maintained with dry ice, liquid N_2, or a portable cryostat. THF, Et_2O, PhH, PhMe, MeCN, Et_3N and MeOH were dried by passage over a column of activated alumina; DCM was distilled over calcium hydride; other solvents were obtained in a sure-seal bottles; all other reagents and solvents were used as received from commercial sources unless stated otherwise. Thin layer chromatography was performed using precoated (0.25 mm) silica gel 60 F-254 plates, which were visualized by UV irradiation and CAM or anisaldehyde stain when necessary. Silica gel (particle size 40-63 μm) was used for flash chromatography, or the reaction products were isolated and purified using an automated Yamazen flash system. $CDCl_3$ and C_6D_6 were obtained from commercial suppliers and were used as purchased. NMR experiments were performed on Bruker spectrometers operating at 300, 400, 500, or 600 MHz for 1H nuclei, 75, 100, 126, or 151 MHz for 13C experiments, and 376 MHz when 19F was observed. Chemical shifts (δ) are reported relative to TMS using the residual solvent signal as internal reference ($CDCl_3$: 7.26 ppm for 1H, 77.16 ppm for 13C; C_6D_6: 7.16 ppm for 1H, 128.06 ppm for 13C). NMR data are reported as follows: chemical shift (multiplicity, coupling constants J [Hz] where applicable, number of hydrogens). Abbreviations are as follows: s (singlet), d (doublet), t (triplet), q (quartet), sep (septet), m (multiplet), b (broad). High-resolution mass spectral data were obtained from the UCB Mass Spectral Facility using a Finnigan/Thermo LTQ/FT instrument for ESI, and a Waters Autospec Premiere instrument for EI. X-Ray data were collected on a Bruker APEX-II CCD diffractometer with Mo-Kα radiation (λ = 0.71073 Å) or a MicroStar-H X8 APEX-II diffractometer with Cu-Kα radiation (λ = 1.54178 Å) and analyzed by Dr. Antonio DiPasquale (University of California, Berkeley), structures were visualized with CYLview.

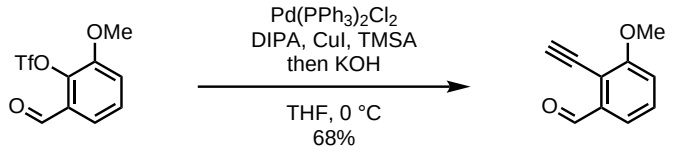

2.12 **2.13**

Alkyne 2.13: Triflate **2.12** (5 g, 17.6 mmol, 1 equiv) was dissolved in THF (120 mL, 0.15M) and $Pd(PPh_3)_2Cl_2$ (618 mg, 0.88 mmol, 0.05 equiv) and CuI (335 mg, 1.76 mmol, 0.10 equiv) were added and the flask was flushed with N_2. The reaction mixture was cooled to 0 °C and trimethylsilylacetylene (TMSA, 5.01 mL, 35.2 mmol, 2 equiv) then diisopropylamine (DIPA, 7.4 mL, 52.8 mmol, 3 equiv) was added. After 90 minutes TLC showed consumption of starting material so the reaction mixture was moved to room temperature and 1M KOH (150 mL, 150 mmol, 8.5 equiv) was added. The reaction mixture was stirred vigorously for 45 min until desilylation was complete by TLC. The reaction mixture was diluted with H_2O, extracted with EtOAc (3x150 mL), washed with brine, dried over $MgSO_4$ and filtered through celite to afford a dark brown solution that was concentrated and purified by flash chromatography (9:1 Hx:EtOAc) to give **2.13** (1.95 g, 69%) as a pale yellow powder. Spectral data was in good agreement with the literature reports.[23]

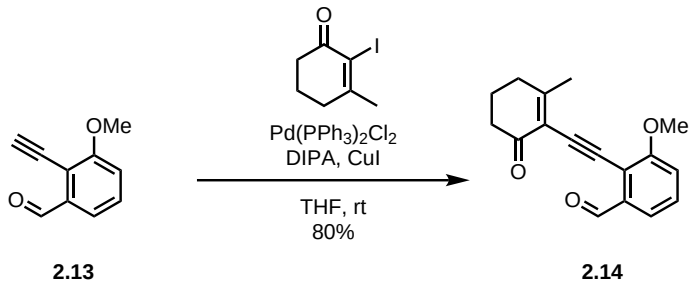

2.13 **2.14**

Alkyne **2.13** (1.36 g, 8.47 mmol, 2 equiv) and 2-iodo-3-methylcylohexanone (1.0 g, 4.24 mmol, 1 equiv) were dissolved in THF (30 mL, 0.15M) and $Pd(PPh_3)_2Cl_2$ (149 mg, 0.21 mmol, 0.05 equiv) and CuI (80 mg, 0.42 mmol, 0.10 equiv) were added and the flask was flushed with N_2. The reaction mixture was cooled to 0 °C and DIPA was added and the flask was moved to room temperature. After 6 hours no starting material was visible by TLC so the reaction mixture was diluted with 1N HCl (30 mL) and extracted with Et_2O (2x30 mL), washed with brine, dried over $MgSO_4$, filtered and concentrated. The resulting crude solid was purified by flash chromatography (0%–75% EtOAc in Hx) to give **2.14** (908 mg, 80%) as a colorless solid. **^{1}H NMR:** (300 MHz, $CDCl_3$) δ 10.48 (s, 1H), 7.89 (d, J = 8.8 Hz, 1H), 7.08 (d, J = 2.6 Hz, 1H), 6.95 (dd, J = 8.8, 2.6 Hz, 1H), 3.89 (s, 3H), 2.52 (q, J = 7.2, 6.8 Hz, 4H), 2.29 (s, 3H), 2.04 (t, J = 6.4 Hz, 2H).

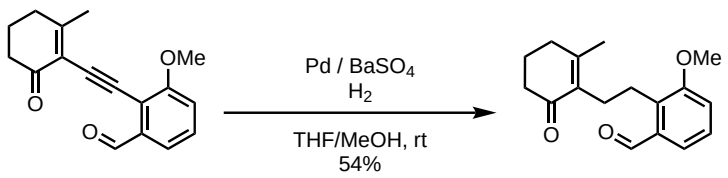

2.14 **2.15**

2.14 (539 mg, 2.01 mmol, 1 equiv) was dissolved in a 1:1 mixture of THF and MeOH (200 mL, 0.01M) and put under N_2. Pd on $BaSO_4$ (1070 mg, 0.5 mmol, 0.25 equiv) was added and the reaction mixture was sparged with H_2 for 5 minutes and then stirred under a balloon of H_2. After 80 minutes the reaction was complete by TLC. The reaction mixture was filtered through a celite plug, which was washed with EtOAc and then MeOH and concentrated. The crude product was purified by flash chromatography (25%–66% EtoAc in Hx) to give the **2.15** (306 mg, 56%) as a waxy white solid. **^{1}H NMR:** (300 MHz, $CDCl_3$) δ 10.09 (s, 1H), 7.78 (d, J = 8.6 Hz, 1H), 6.85 (dd, J = 8.6, 2.5 Hz, 1H), 6.78 (d, J = 2.6 Hz, 1H), 3.87 (s, 3H), 3.03 (dd, J = 8.8, 6.6 Hz, 2H), 2.59 (dd, J = 8.6, 6.8 Hz, 2H), 2.39 (dd, J = 7.5, 6.0 Hz, 2H), 2.29 (t, J = 6.1 Hz, 2H), 1.92 (p, J = 6.4 Hz, 2H), 1.76 (s, 3H).

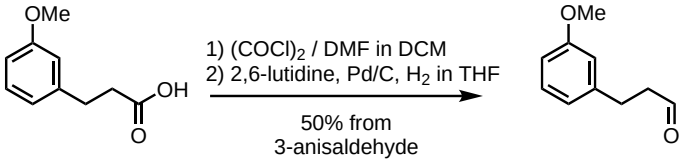

2.26 **2.27**

2.26 (20.16 g, 112 mmol, 1 equiv) was dissolved in DCM (375 mL, 0.3M) and a small amount of DMF (0.5 mL) was added. Oxalyl chloride (9.93 mL, 117 mmol, 1.05 equiv) was added and the flask was fitted with a bubbler full of 2N KOH. Warning: Extremely vigorous gas evolution occured upon addition of oxalyl chloride. After 90 minutes gas evolution and the reaction was concentrated and filtered through a celite plug under N_2. The plug was rinsed with 3x 10 mL DCM and the solution was concentrated to give the crude acid chloride as a viscous yellow oil (51.78g, 78% crude weight).

Two 1 L flasks were charged with THF (500 mL, 0.25M) and placed under N_2, Pd/C (10% Pd basis, 2.6 g, 10 wt. %) was added followed by 2,6 lutidine (15.1 mL, 130 mmol, 1 equiv). The flask was purged with H_2 3 times and then the crude acid chloride was added. After 150 min a small aliquot was quenched with iPrOH. ^{1}H showed no isopropyl ester so the reaction mixtures were filtered through celite and concentrated. The resulting yellow oil was filtered through a 3 cm silica plug with 10%–20% EtOAc in Hx to give a pale yellow oil. This was further purified by vacuum distillation (105 °C, 2 mtorr) to give **2.27** (32.76 g, 50% over 4 steps from 3-anisaldehyde) as a colorless oil. **^{1}H NMR:** (500 MHz, $CDCl_3$) δ 9.82 (t, J = 1.4 Hz, 1H), 7.21 (td, J = 7.7, 0.7 Hz, 1H), 6.80–6.73 (m, 3H), 3.80 (s, 3H), 2.94 (t, J = 7.6 Hz, 2H), 2.81–2.76 (m, 2H).

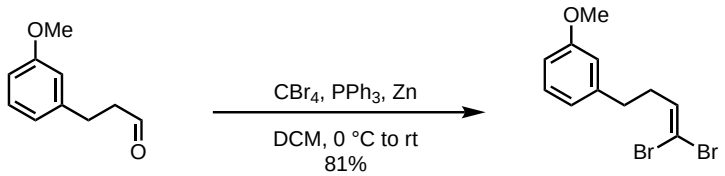

2.27 **2.28**

A dry 1 L round bottom flask was charged with CBr_4 (29.5 g, 89 mmol, 2 equiv) and DCM (300 mL, 0.15M) and cooled to 0 °C. PPh_3 was added (23.3 g, 89 mmol, 2 equiv). After stirring for 10 minutes, Zn powder (5.82 g, 89 mmol, 2 equiv) was added in 3 portions. After 10 minutes the reaction mixture was moved to room temperature. After 3 hours **2.27** was added and the resulting suspension was stirred overnight. After 18 hours no more aldehyde was visible by TLC so the reaction was concentrated to give a chunky brown/gray foam. 100 mL of Et_2O was added and the mixture was sonicated until no large chunks of solids remained. The Et_2O layer was filtered off and the process was repeated 4 more times. The resulting Et_2O fractions were partially concentrated to give a yellow solution that was washed with $Na_2S_2O_3$, brine, dried over $MgSO_4$, filtered and concentrated to give an orange oil that was dry loaded onto silica and flushed through a 5 cm silica plug with 800 mL 5% EtoAc in Hx to give the dibromoolefin **2.61** (22.81 g, 81%) as a pale yellow oil that was used without further purification. **^{1}H NMR:** (600 MHz, $CDCl_3$) δ 7.22 (t, J = 7.9 Hz, 1H), 6.77 (t, J = 9.3 Hz, 2H), 6.74 (s, 1H), 6.41 (t, J = 7.3 Hz, 1H), 3.81 (d, J = 1.3 Hz, 3H), 2.71 (t, J = 7.8 Hz, 2H), 2.41 (q, J = 7.5 Hz, 2H).

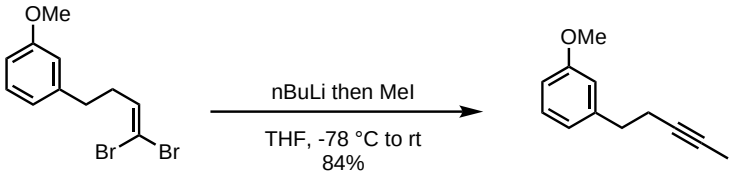

2.28 **2.29**

A dry 1 L 3 necked flask was charged with **2.61** (22.81 g, 71.3 mmol, 1 equiv) and then azeotroped 3 times with PhH. THF (360 mL, 0.2M) was added and the reaction was fitted with on oven dried dropping funnel and placed under N_2 atmosphere. The reaction mixture was cooled to -78 °C and nBuLi (2.2M in Hx, 68 mL, 149.7 mmol, 2.1 equiv) was added over 10 minutes. After 45 minutes, MeI (22 mL, 213.8 mmol, 5 equiv) was added and the reaction was allowed to slowly warm up to room temperature overnight. The reaction was quenched by the addition of sat. NH_4Cl and diluted with H_2O. The reaction mixture was concentrated to remove most of the THF and then extracted with pentane (3x150 mL), washed with brine, dried over $MgSO_4$, filtered and concentrated. The resulting orange oil was purified by vacuum distillation (95 °C, 2 mtorr) to give **2.29** (10.46 g, 84%) as a colorless oil. **^{1}H NMR:** (400 MHz, $CDCl_3$) δ 7.23 (t, J = 7.7 Hz, 0H), 6.88–6.68 (m, 1H), 3.81 (s, 1H), 2.80 (t, J = 7.7 Hz, 1H), 2.43 (ddt, J = 7.6, 5.0, 2.5 Hz, 1H), 1.80 (t, J = 2.6 Hz, 1H). **^{13}C NMR:** (101 MHz, $CDCl_3$) δ 159.7, 142.7, 129.4, 120.9, 114.3, 111.6, 78.7, 76.3, 55.2, 35.7, 21.0, 3.6.

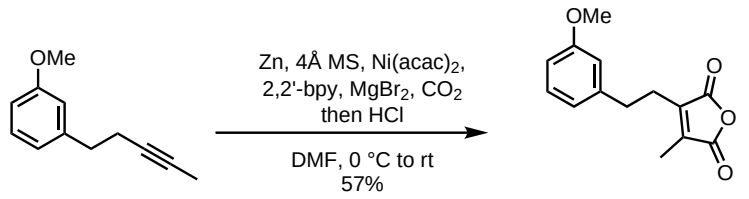

2.29 **2.30**

A flame dried 200 mL round bottom flask was transferred to a glovebox and charged with activated zinc powder (2.25 g, 34.44 mmol, 3 equiv), activated 4Å mol sieves (4.60 g, 400 mg/mmol), $Ni(acac)_2$ (295 mg, 1.15 mmol, 0.1 equiv), 2,2'-bipyridine (296 mg, 1.72 mmol, 0.15) followed by anhydrous DMF (77 mL, 0.15M). $MgBr_2$ (6.34 g, 34.44 mmol, 3 equiv) prepared by heating $MgBr_2 \cdot Et_2O$ under vacuum was added, which caused a strong exotherm. The reaction was quickly transferred to a fume hood and cooled to 0 ° before being purged 3x with CO_2 and fitted with a balloon of CO_2. **2.30** (2.0 g, 11.48 mmol, 1 equiv) was added and the reaction mixture was stirred at room temperature. After 18 hours HCl (6N, 100 mL, 50 equiv) was added (H_2 evolution, exotherm) and the reaction mixture was stirred for 2 hours then diluted with H_2O and extracted with Et_2O (3x100 mL). The combined organic layers were washed with saturated $NaHCO_3$, brine, dried over $MgSO_4$, filtered and concentrated. The resulting crude solid was dry loaded onto celite and purified by flash chromatography (10%–20% EtOAc in Hx) to give **2.30** (1620 mg, 57%) as a white powder. **^{1}H NMR:** (500 MHz, $CDCl_3$) δ 7.21 (t, J = 7.9 Hz, 1H), 6.77 (dd, J = 8.4, 2.5 Hz, 1H), 6.72 (dd, J = 7.6, 1.4 Hz, 1H), 6.68 (d, J = 2.1 Hz, 1H), 3.79 (s, 3H), 2.88 (t, J = 7.3 Hz, 2H), 2.76 (t, J = 7.3 Hz, 2H), 1.75 (d, J = 1.0 Hz, 3H).

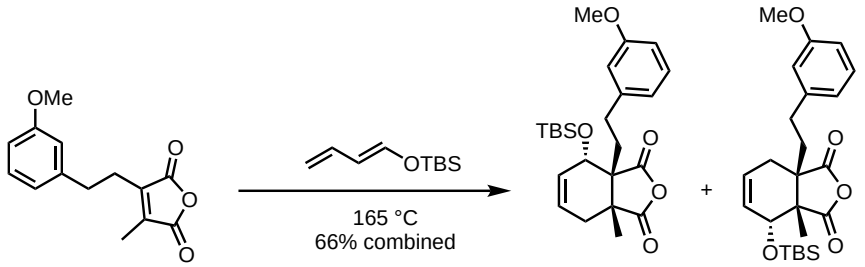

2.30 **2.32** TMP3

An oven dried 4 mL vial was charged with **2.30** (881 mg, 3.57 mmol, 1 equiv) and diene[14] (1.98g, 10.73 mmol, 3 equiv) and placed under high vacuum for 30 minutes. The vial was flushed with N_2 and fitted with a Teflon cap then heated to 165 °Cfor 23 hours. Upon cooling the reaction mixture solidified. The resulting solid was purified by flash chromatography (10%–20% EtOAc in Hx) to give **2.32a** and **2.62a** (995 mg, 65%) as a waxy colorless solid and a 1:1 mixture. **^{1}H NMR:** (500 MHz, $CDCl_3$) δ 7.21 (td, J = 8.0, 4.6 Hz, 2H), 6.78–6.65 (m, 6H), 6.07–5.92 (m, 4H), 4.45 (dd, J = 4.2, 1.7 Hz, 1H), 4.15 (d, J = 5.7 Hz, 1H), 3.80 (s, 3H), 3.79 (s, 3H), 3.12–3.03 (m, 1H), 2.94 (td, J = 13.1, 4.4 Hz, 1H), 2.73–2.44 (m, 1H), 2.18–2.01 (m, 3H), 1.92–1.71 (m, 3H), 1.38 (s, 3H), 1.20 (s, 3H). **^{13}C NMR:** (101 MHz, $CDCl_3$) δ 176.4, 175.6, 174.7, 159.9, 159.9, 142.9, 142.0, 130.2, 129.9, 129.8, 129.7, 126.8, 126.6, 120.7, 120.6, 114.2, 111.8, 111.6, 70.4, 67.7, 56.2, 55.3, 54.4, 47.8, 45.0, 41.2, 31.9, 31.2, 30.8, 30.4, 28.4, 25.5, 25.5, 17.9, 14.4, -4.1, -4.1, -5.3, -5.3.

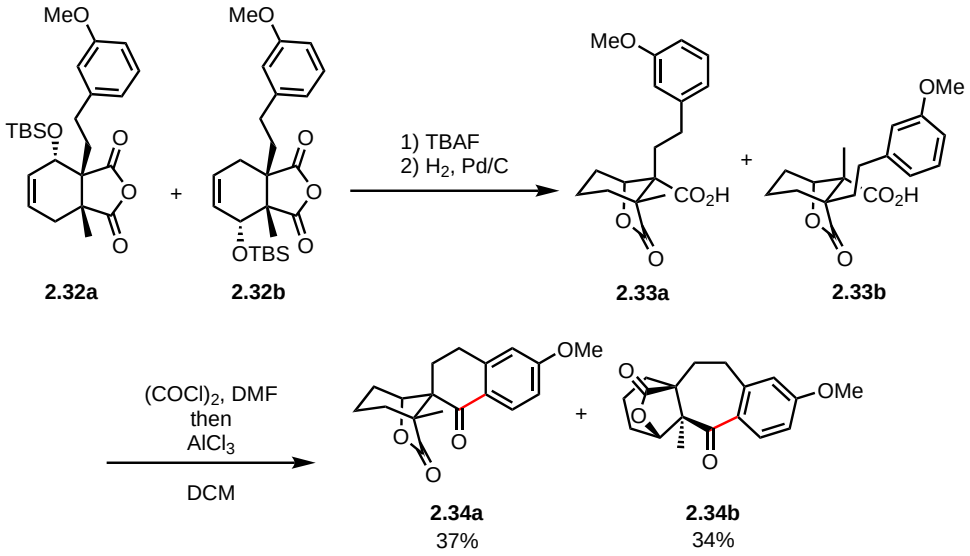

2.32a and **2.32b** (607 mg, 1.41 mmol, 1 equiv) were dissolved in THF (7 mL, 0.2M) and cooled to 0 °C. TBAF (1M in THF, 2.8 mL, 2.8 mmol, 2 equiv) was added. After 5 minutes TLC showed full conversion. The reaction was quenched with 2N HCl (4 mL) and extracted with EtOAc (3x10 mL) and washed with brine, dried over $MgSO_4$, filtered and concentrated to a pale yellow foam that was used without further purification. **^{1}H NMR:** (600 MHz, C_6D_6) δ 7.10 (td, J = 7.9, 2.1 Hz, 2H), 6.72 (d, J = 7.5 Hz, 1H), 6.69–6.62 (m, 4H), 6.59 (t, J = 2.1 Hz, 1H), 6.11–6.04 (m, 2H), 5.97 (d, J = 9.3 Hz, 1H), 5.90 (d, J = 9.4 Hz, 1H), 4.82 (dd, J = 5.7, 1.1 Hz, 1H), 4.64 (dd, J = 5.8, 1.2 Hz, 1H), 3.70 (d, J = 1.1 Hz, 6H), 2.98 (td, J = 13.0, 4.3 Hz, 1H), 2.64 (td, J = 12.6, 4.7 Hz, 1H), 2.58 (td, J = 13.0, 5.3 Hz, 1H), 2.47–2.11 (m, 6H), 2.05 (td, J = 12.8, 12.2, 4.7 Hz, 1H), 1.94–1.88 (m, 1H), 1.85–1.79 (m, 1H), 1.27 (d, J = 3.6 Hz, 5H).

The crude lactones were dissolved in EtOAc (7 mL, 0.2M) and Pd on charcoal (10% Pd basis, 45 mg, 10 wt. %) was added. The flask was evacuated and backfilled with H_2 5 times and then stirred under a balloon of H_2. After 3 hours the reaction mixture was filtered through celite and concentrated to give **2.33a** and **2.33b** (414 mg, 92% mass balance) as a white foam. **^{1}H NMR:** (500 MHz, $CDCl_3$) δ 11.17 (bs, 2H), 7.23 (t, J = 7.9 Hz, 1H), 7.17 (t, J = 7.8 Hz, 1H), 6.84–6.68 (m, 6H), 4.92 (d, J = 4.5 Hz, 1H), 4.69 (d, J = 4.4 Hz, 1H), 3.81 (s, 3H), 3.77 (s, 3H), 2.90 (td, J = 13.0, 4.5 Hz, 1H), 2.64 (qd, J = 12.4, 5.0 Hz, 2H), 2.50 (td, J = 12.8, 4.4 Hz, 1H), 2.17 (td, J = 13.2, 4.9 Hz, 1H), 2.11–1.99 (m, 2H), 1.92 (td, J = 13.1, 5.1 Hz, 4H), 1.83–1.67 (m, 8H), 1.56 (dd, J = 13.6, 6.1 Hz, 1H).

A dry flask was charged with **2.33a** and **2.33b** (20 mg, 63μmol, 1 equiv) and DCM (320 μL, 0.2M) and cooled to 0 °C. A bubbler was attached and DMF (5 μL) and oxalyl chloride (12 μL, 138 μmol, 2.2 equiv) were added. The and the reaction was stirred at room temperature for 1 hour then $AlCl_3$ (25 mg, 190 μmol, 3 equiv) was added and the reaction was sealed and heated to reflux for 2 hours. After the reaction was complete the reaction mixture was quenched with 2N HCl (1 mL) and extracted with Et_2O (3x1 mL). The combined organic layers were washed with saturated $NaHCO_3$, brine, dried over $MgSO_4$, filtered and concentrated. The crude products were purified by

flash chromatography (35%–55% EtOAc in Hx) to give **2.33a** (7.0 mg, 37%) and **2.33b** (6.4 mg, 34%) as white solids. **2.33a ^{1}H NMR:** (500 MHz, $CDCl_3$) δ 8.04 (d, J = 8.8 Hz, 1H), 6.85 (dd, J = 8.8, 2.5 Hz, 1H), 6.69 (d, J = 2.6 Hz, 1H), 4.64 (d, J = 4.7 Hz, 1H), 3.86 (s, 3H), 3.08–2.88 (m, 2H), 2.43 (dt, J = 13.9, 3.7 Hz, 1H), 2.12 (td, J = 13.2, 5.5 Hz, 1H), 2.06–1.95 (m, 1H), 1.84–1.67 (m, 4H), 1.61–1.51 (m, 1H), 1.16 (s, 3H). **^{13}C NMR:** (126 MHz, $CDCl_3$) δ 195.0, 179.9, 164.1, 144.9, 131.4, 124.6, 113.9, 112.4, 77.6, 56.3, 55.7, 45.6, 29.2, 24.9, 24.4, 23.7, 17.0, 16.3. **2.33b ^{1}H NMR:** (500 MHz, $CDCl_3$) δ 7.39 (d, J = 8.5 Hz, 1H), 6.77 (dd, J = 8.5, 2.5 Hz, 1H), 6.61 (d, J = 2.5 Hz, 1H), 4.99 (d, J = 4.6 Hz, 1H), 3.82 (s, 3H), 2.80–2.74 (m, 2H), 2.40 (ddd, J = 14.9, 8.8, 6.3 Hz, 1H), 1.97–1.79 (m, 3H), 1.77–1.57 (m, 3H), 1.53 (dd, J = 13.7, 6.8 Hz, 1H), 1.31 (s, 3H).

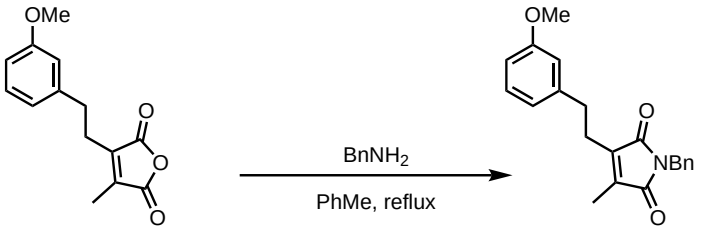

2.30 **2.35**

Anhydride **2.30** (1.33 g, 5.4 mmol, 1 equiv) was added to a dried flask and benzylamine (1.14 mL, 10.8 mmol, 2 equiv) was added. The mixture was dissolved in AcOH (10.8 mL, 1M) and the flask was fitted with a reflux condenser and put under a N_2 atmosphere and heated to 120 °C overnight. After 14 hours the flask was cooled to room temperature and the solution concentrated. The crude mixture was purified by flash chromatography (5%–10% EtOAc in Hx) and concentrated to a pale yellow oil. The oil was suspended in pentane and sonicated to precipitate the product (1.49 g, 82%) as a fine white powder. **^{1}H NMR:** (600 MHz, $CDCl_3$) δ 7.36–7.23 (m, 5H), 7.17 (t, J = 7.9 Hz, 1H), 6.76–6.69 (m, 3H), 6.67 (d, J = 2.1 Hz, 1H), 4.65 (s, 2H), 3.74 (s, 3H), 2.83 (t, J = 7.5 Hz, 2H), 2.69 (t, J = 7.5 Hz, 2H), 1.71 (s, 3H).

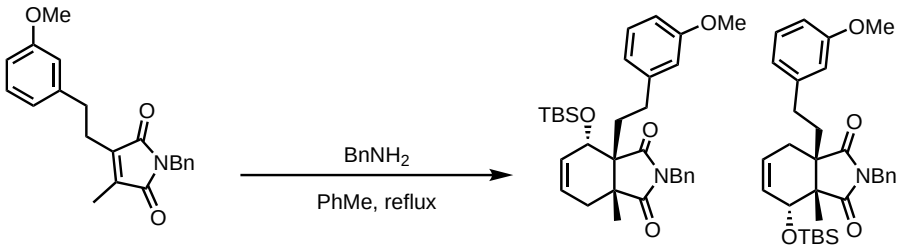

2.35 **2.36a** **2.36b**

TBS diene[14] (2.86 g, 15.53 mmol, 3 equiv) and imide **2.35** (1.74 g, 5.18 mmol, 1 equiv) were added to a dry 20 mL vial, flushed with N_2 and sealed with a Teflon cap. The vial was heated to 170 °Cfor 21 hours and then cooled to room temperature. The resulting waxy solid was purified by flash chromatography to give the the mixed Diels–Alder products (2.33g, 86% combined, 1.2:1 desired:undesired isomers) as a colorless oil.

^{1}H NMR: (500 MHz, $CDCl_3$) δ 7.39–7.33 (m, 2H), 7.33–7.17 (m, 8H), 7.09 (dt, J = 43.2, 7.8 Hz, 2H), 6.71–6.61 (m, 4H), 6.38–6.32 (m, 2H), 5.96–5.87 (m, 4H), 4.68–4.52 (m, 4H), 4.37 (d, J = 3.8 Hz, 1H), 4.07 (d, J = 5.1 Hz, 1H), 3.73 (s, 3H), 3.68 (s, 3H), 2.96–2.85 (m, 2H), 2.78 (td, J = 13.1, 4.5 Hz, 1H), 2.48 (td, J = 13.3, 4.9 Hz, 1H), 2.26 (td, J = 13.2, 4.8 Hz, 1H), 2.16 (td, J = 13.2, 4.6 Hz, 1H), 2.07–1.92 (m, 1H), 1.77 (ddd, J = 14.5, 12.8, 5.0 Hz, 2H), 1.71–1.61 (m, 1H), 1.49 (td, J = 13.1, 4.5 Hz, 0H), l1.17 (s, 3H), 1.13 (s, 3H), 0.83 (d, J = 1.4 Hz, 3H), 0.78 (s, 18H), -0.02 (dd, J = 7.6, 4.5 Hz, 12H). z

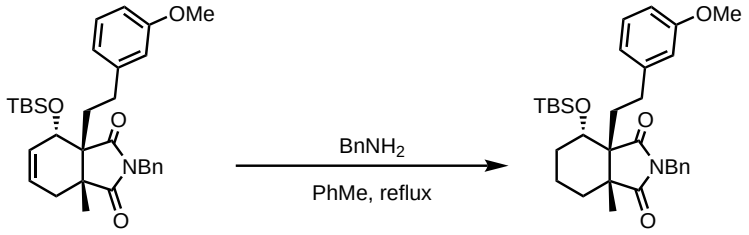

2.36a **2.37**

Diels–Alder adducts vinylimide-2.one,vinylimide-2.two (2,33gm 4.48 mmol, 1 equiv) were dissolved in EtOAc (23 mL, 0.2M) and Pd/C (10% Pd Basis, 230 mg, 10 wt%) was added. The flask was purged 5 times with H_2 and then fitted with a H_2 balloon and stirred at room temperature. After 21 hours the solution was filtered through a 2 cm celite plug and concentrated. The crude products were purified by Yamazen flash chromatography to give the desired product (1022 mg, 44%) contaminated with approximately 10% of an undesired isomeric product as a colorless oil. (desired isomer rf 0.42, undesired isomer rf 0.35 in 10% EtOAc in Hx)

^{1}H NMR: (500 MHz, $CDCl_3$) δ 7.35–7.14 (m, 5H), 6.80–6.72 (m, 3H), 4.64–4.55 (m, 2H), 4.29–4.19 (m, 1H), 3.80 (s, 3H), 3.03 (td, J = 13.0, 4.4 Hz, 1H), 2.67 (td, J = 12.9, 5.1 Hz, 1H), 2.28 (dt, J = 14.2, 4.9 Hz, 1H), 1.96 (ddd, J = 14.4, 12.8, 4.4 Hz, 1H), 1.86–1.65 (m, 4H), 1.56–1.38 (m, 2H), 1.34–1.24 (m, 1H), 1.02 (s, 3H), 0.87 (s, 9H), 0.06 (d, J = 11.8 Hz, 6H).

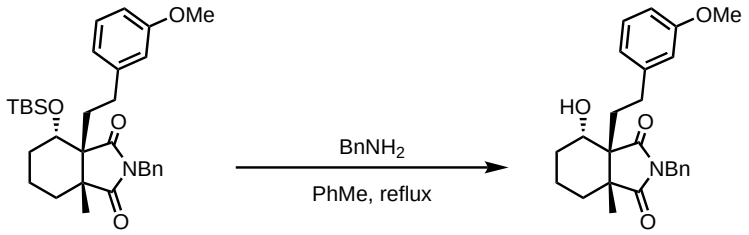

2.37 **2.38**

Silyl ether (**2.37** (51 mg, 0.1 mmol, 1 equiv) was dissolved in THF and cooled to 0°C. TBAF (1M in THF, 200 uL, 0.2 mmol, 2 equiv) was added and the reaction mixture was stirred for 1 hour at then moved to room temperature and stirred for an additional 4 hours until no starting material remained by TLC. The reaction was quenched by the addition of 1N HCl (1 mL) and extracted with EtOAc (3x5 mL), washed with brine, dried over $MgSO_4$, filtered and concentrated. The crude

product was purified by Yamazen flash chromatography to give the product (26 mg, 66%) as a colorless oil.

^{1}H NMR: (500 MHz, $CDCl_3$) δ 7.39 (dd, J = 7.8, 1.7 Hz, 1H), 7.35–7.28 (m, 30H), 7.14 (t, J = 8.0 Hz, 1H), 6.71 (dt, J = 8.4, 1.5 Hz, 1H), 6.60–6.49 (m, 2H), 4.74–4.56 (m, 2H), 4.35 (d, J = 3.6 Hz, 1H), 3.76 (s, 3H), 2.54 (td, J = 12.8, 5.0 Hz, 1H), 2.37 (td, J = 12.8, 4.3 Hz, 1H), 2.24 (td, J = 13.1, 5.0 Hz, 1H), 1.84–1.69 (m, 3H), 1.58–1.51 (m, 1H), 1.48–1.39 (m, 3H), 1.37–1.31 (m, 1H), 1.30 (s, 3H).

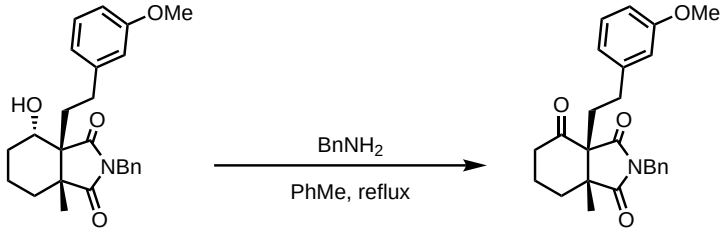

2.38 **2.39**

Alcohol **2.38** (7 mg, 17 μmol, 1 equiv) was dissolved in DCM (170 μL, 0.1M) and $NaHCO_3$ (3.5 mg, 42 μmol, 2.4 equiv) then DMP (9 mg, 21 μmol, 1.2 equiv) was added. After 1 hour the reaction mixture was filtered through celite and concentrated. The crude product was purified by pipette flash chromatography to give the product (5.7 mg, 82% as a colorless oil). **^{1}H NMR:** (600 MHz, $CDCl_3$) δ 7.38 (d, J = 5.1 Hz, 2H), 7.35–7.28 (m, 3H), 7.18 (t, J = 7.9 Hz, 1H), 6.73 (dd, J = 8.1, 2.5 Hz, 1H), 6.69 (d, J = 7.5 Hz, 1H), 6.65 (t, J = 2.1 Hz, 1H), 4.68 (q, J = 14.1 Hz, 2H), 3.78 (s, 3H), 2.66 (td, J = 13.2, 4.6 Hz, 1H), 2.51 (ddd, J = 16.0, 5.1, 3.5 Hz, 1H), 2.45–2.32 (m, 2H), 2.23 (dd, J = 11.5, 4.8 Hz, 1H), 2.13 (ddd, J = 14.1, 12.9, 4.7 Hz, 1H), 1.97 (ddd, J = 14.1, 12.9, 4.7 Hz, 1H), 1.93–1.85 (m, 21), 1.67–1.60 (m, 2H), 1.23 (s, 3H). **^{13}C NMR:** (151 MHz, $CDCl_3$) δ 206.0, 180.3, 175.2, 159.9, 142.8, 135.6, 129.7, 128.9, 128.9, 128.3, 120.7, 114.2, 111.8, 64.2, 55.3, 52.3, 43.0, 39.3, 32.8, 32.4, 31.5, 20.9, 20.8.

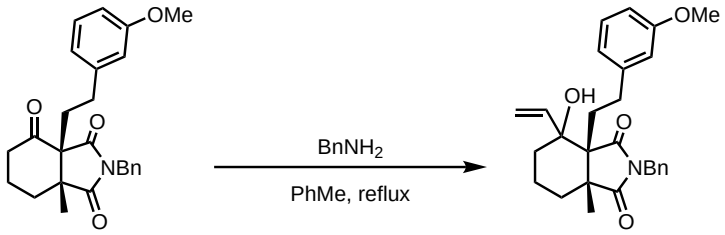

2.39 **2.40**

Ketone **2.40** (5.7 mg, 14 μL, 1 equiv) was dissolved in THF (140 μL) and cooled to 0 °C. Vinylmagnesium bromide (1M in THF, 42 μL, 3 equiv) was added and the reaction mixture was stirred for 2 hoursn and then quenched by the addition of NH_4Cl (100 μL). The reaction mixture was extracted with Et_2O (3x1 mL), washed with brine, dried over $MgSO_4$, filtered, and concentrated. The resulting crude residue was purified by pipette flash chromatography to give the product (<2

mg, yield not determined) as a colorless residue. **^{1}H NMR:** (600 MHz, $CDCl_3$) δ 7.42 (dd, J = 7.4, 2.2 Hz, 2H), 7.36–7.28 (m, 3H), 7.11 (t, J = 7.8 Hz, 1H), 6.72–6.64 (m, 1H), 6.46–6.39 (m, 2H), 6.03 (ddd, J = 17.1, 10.9, 1.5 Hz, 1H), 5.57 (dd, J = 16.9, 1.9 Hz, 1H), 5.24 (dd, J = 10.9, 1.9 Hz, 1H), 4.82–4.53 (m, 3H), 3.75 (s, 3H), 2.54 (td, J = 13.2, 4.5 Hz, 1H), 2.21 (td, J = 13.7, 4.5 Hz, 1H), 2.11 (td, J = 13.3, 4.0 Hz, 1H), 1.91–1.84 (m, 1H), 1.72 (d, J = 13.6 Hz, 1H), 1.66–1.57 (m, 3H), 1.46 (td, J = 13.7, 5.0 Hz, 1H), 1.30 (s, 3H).

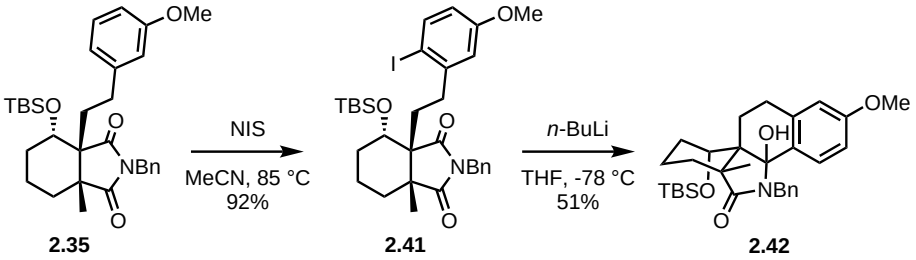

2.35 **2.41** **2.42**

Bicycle **2.35** (1522 mg, 2.91 mmol, 1 equiv) was dissolved in MeCN (15 mL, 0.2M) and transferred in a dry flask. N-iodosuccinimide (983 mg, 4.37 mmol, 1.5 equiv) was added and the flask was fitted with a reflux condenser and heated to 85 °C overnight. After 14 hours the vial was cooled to room temperature and the contents transferred to a flask and concentrated (prone to bumping in small containers). The crude residue was dissolved in Et_2O, washed with $Na_2S_2O_3$ and extracted with Et_2O (3x10 mL). The combined organic layers were washed with brine, dried over $MgSO_4$, filtered, and concentrated. The crude residue was purified by flash chromatography (0%–15%) to give the product (1604 mg, 85%) as an off white solid.

Crude aryl iodide (1604 mg, 2.48, 1 equiv) was dissolved in Et_2O (25 mL, 0.1M) and cooled to -78 °C. *n*-Bu Li (2.5M in hexane, 1.05 mL, 1.05 equiv) was added and stirred. After 4 hours ceNH4Cl (100 uL) was added and the reaction was allowed to slowly come to room temperature. The reaction mixture was diluted with H_2O and extracted with Et_2O (3x50 mL) , washed with brine, dried over $MgSO_4$, filtered and concentrated. The crude residue was purified by Yamazen flash chromatography to give the product (662 mg, 51%) as a white foam.

^{1}H NMR: (600 MHz, $CDCl_3$) δ 7.60 (d, J = 8.5 Hz, 1H), 7.17–6.97 (m, 5H), 6.76 (dd, J = 8.5, 2.7 Hz, 1H), 6.42 (d, J = 2.7 Hz, 1H), 4.15 (d, J = 15.0 Hz, 1H), 3.80 (s, 1H), 3.76 (s, 4H), 3.62 (dd, J = 11.5, 6.5 Hz, 1H), 2.30 (dt, J = 14.9, 3.4 Hz, 1H), 2.18 (td, J = 14.1, 2.9 Hz, 1H), 2.05 (td, J = 13.4, 3.0 Hz, 1H), 2.00–1.67 (m, 5H), 1.63 (td, J = 13.9, 3.3 Hz, 1H), 1.44 (dtd, J = 13.9, 10.8, 3.1 Hz, 1H), 1.29 (s, 3H), 0.56 (s, 9H), -0.02 (s, 3H), -0.33 (s, 3H). **^{13}C NMR:** (151 MHz, $CDCl_3$) δ 180.7, 159.5, 141.3, 138.6, 132.4, 128.3, 127.8, 126.8, 126.6, 112.8, 111.1, 91.7, 77.8, 55.5, 51.2, 45.6, 43.2, 37.4, 35.1, 33.4, 26.8, 25.5, 20.2, 20.0, 17.7, -4.0, -5.3.

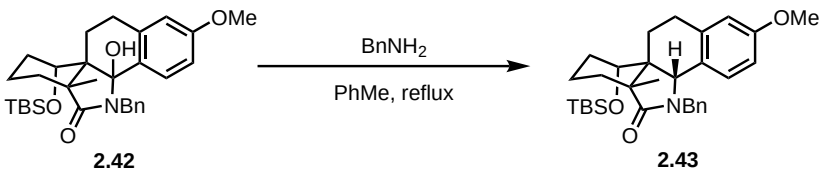

2.42 **2.43**

Hemiaminal **2.42** (662 mg, 1.27 mmol, 1 equiv) was dissolved in DCM (12.7 mL, 0.1M) and triethylsilane (2.03 mL, 12.7 mmol, 10 equiv) and $BF_3 \cdot OEt_2$ (1.57 equiv, 12.7 mmol, 10 equiv) were added. The flask was fitted with a reflux condenser and heated to 45 °Covernight. After 13 hours the reaction mixture was cooled to room temperature and sat. NH_4Cl was added carefully until no more gas evolution was observed. The reaction mixture was extracted with EtOAc (3x50 mL), washed with sat. $NaHCO_3$, water, brine, dried over $MgSO_4$ and concentrated to a white solid that was used without purification. **^{1}H NMR:** (600 MHz, $CDCl_3$) δ 7.57 (d, J = 8.4 Hz, 1H), 7.21 (s, 5H), 6.78 (dd, J = 8.4, 2.7 Hz, 1H), 6.68 (d, J = 2.7 Hz, 1H), 5.51 (d, J = 14.5 Hz, 1H), 4.39 (d, J = 14.5 Hz, 1H), 4.05 (s, 1H), 3.79 (s, 3H), 3.33 (d, J = 2.7 Hz, 1H), 2.80–2.65 (m, 2H), 2.27–2.19 (m, 1H), 1.79 (ddd, J = 13.8, 10.5, 5.1 Hz, 1H), 1.71 (ddd, J = 12.5, 8.4, 4.7 Hz, 1H), 1.61–1.55 (m, 1H), 1.51–1.37 (m, 2H), 1.29–1.11 (m, 3H), 0.85 (s, 9H), 0.74 (s, 3H), -0.19 (s, 3H), -0.55 (s, 3H).

The crude lactone **2.43** was dissolved in a solution of TBAF (1M in THF, 12.7 mL, 10 equiv) and heated under microwave irradiation to 100 °C for 1 hour. Upon cooling the reaction was quenched with 0.5 HCl (5 mL), and extracted with EtOAc (3x30 mL). The combined organic layers were washed with brine, dried over $MgSO_4$ and concentrated to an off white solid that was purified by Yamazen flash chromatography to give the product (461 mg, 93% over 2 steps) as a white solid. **^{1}H NMR:** (600 MHz, $CDCl_3$) δ (7.34 (d, J = 8.8 Hz, 1H), 7.29–7.18 (m, 5H), 6.80–6.70 (m, 2H), 5.22 (d, J = 14.8 Hz, 1H), 4.55 (d, J = 14.7 Hz, 1H), 4.16 (s, 1H), 3.80 (sp, 3H), 2.91 (s, 1H), 2.84–2.65 (m, 2H), 2.28–2.19 (m, 1H), 1.88 (ddd, J = 13.6, 10.8, 2.7 Hz, 1H), 1.72 (dddd, J = 17.2, 13.5, 8.7, 3.8 Hz, 1H), 1.56 (d, J = 25.2 Hz, 2H), 1.51 (d, J = 13.8 Hz, 1H), 1.39–1.32 (m, 2H), 1.31–1.23 (m, 2H), 1.13 (td, J = 13.7, 4.9 Hz, 1H), 0.85 (s, 3H).

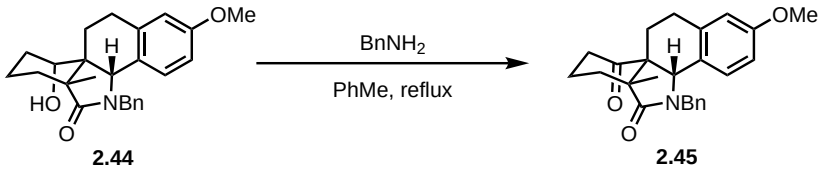

2.44 **2.45**

Alcohol **2.44** (405 mg, 1.03 mmol, 1 equiv) was dissolved in DCM (10.3 mL, 0.1M) and $NaHCO_3$ (433 mg, 5.17 mmol, 5 equiv) was added. The reaction mixture was cooled to 0 °C and DMP (526 mg, 1.24 mmol, 1.2 equiv) was added. After 45 minutes, LCMS showed no more starting material. After 1 hour the reaction mixture was diluted with H_2O and sat. $NaHCO_3$ and extracted with DCM (3x30 mL), washed with brine, dried over $MgSO_4$, filtered, and concentrated. The resulting crude orange solid was purified by Yamazen flash chromatography to give the product(269 mg, 67%) as a white solid. **^{1}H NMR:** (600 MHz, $CDCl_3$) δ 7.32–7.19 (m, 6H), 6.69 (dd, J = 8.5, 2.7 Hz, 1H), 6.64 (d, J = 2.7 Hz, 1H), 5.31 (d, J = 15.3 Hz, 1H), 4.65 (d, J = 15.3 Hz, 1H), 4.33 (s, 1H), 3.75 (s, 3H), 2.86–2.68 (m, 2H), 2.29 (t, J = 7.2 Hz, 2H), 2.24–2.18 (m, 1H), 2.08–1.93 (m, 2H), 1.86 (ddd, J = 10.3, 8.1, 4.6 Hz, 2H), 1.54 (ddd, J = 14.1, 11.1, 7.3 Hz, 1H), 1.12 (s, 3H). **^{13}C NMR:** (151 MHz, $CDCl_3$) δ 211.0, 180.6, 157.9, 137.0, 136.5, 128.8, 128.4, 128.1, 127.7, 123.6, 114.6, 111.0, 59.6, 59.2, 55.2, 51.3, 47.4, 38.3, 30.3, 27.6, 23.1, 22.6, 19.3.

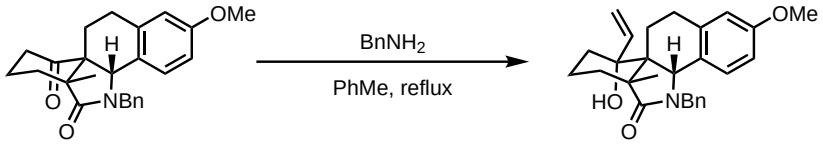

2.45 **2.46b**

A dry microwave vial was charged with **2.45** (40 mg, 103 μmol, 1 equiv) and THF (1 mL, 0.025M) was added. $LaCl_3 \cdot 2\,LiCl$ (0.57M in THF, 451 μL, 2.5 equiv) was added and the resulting suspension was stirred for 2 hours at room temperature. Concurrently, a dry vial was charged with anhydrous $CeCl_3$ (89 mg, 360 μmol, 3.5 equiv) and THF (1 mL, 0.025M) was added followed by vinylmagnesium bromide (1.1M in THF, 308 μL, 339 μmol, 3.3 equiv and the resulting suspension was stirred at room temperature for 2 hours. After complexing, the vinylcerium solution was added to the ketone solution and the reaction mixture was heated to 100 °C for 1 hour. After the reaction had cooled to room temperature it was quenched with sat. NH_4Cl solution, extracted with DCM (4x2 mL), washed with brine, dried over $MgSO_4$, filtered and concentrated. The product was combined with several batches of material and purified by Yamazen flash chromatography to give the product (12 mg, 27%) as a crystalline yellow solid.

add carbon

^{1}H NMR: (400 MHz, $CDCl_3$) δ 7.31–7.17 (m, 5H), 7.10 (d, J = 8.3 Hz, 1H), 6.72 (dd, J = 8.2, 2.6 Hz, 1H), 6.63 (d, J = 2.5 Hz, 1H), 5.13 (d, J = 14.5 Hz, 1H), 5.01 (dd, J = 16.8, 10.7 Hz, 1H), 4.49 (d, J = 14.5 Hz, 1H), 4.24 (d, J = 16.9 Hz, 1H), 4.15 (s, 1H), 4.02 (d, J = 10.4 Hz, 1H), 3.77 (s, 3H), 2.79–2.62 (m, 2H), 2.23 (d, J = 13.9 Hz, 1H), 1.95 (t, J = 12.4 Hz, 1H), 1.89–1.82 (m, 1H), 1.72–1.61 (m, 2H), 1.42 (t, J = 13.5 Hz, 1H), 1.21–1.03 (m, 3H), 0.86 (s, 3H).

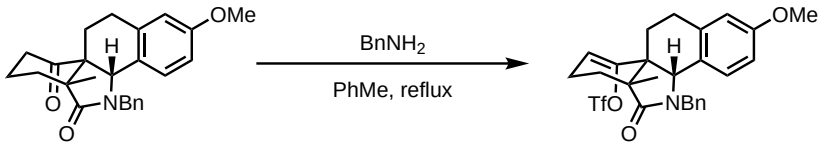

2.45 **2.47**

Ketone **2.47** (266 mg, 0.68 mmol, 1 equiv) was suspended in THF (7 mL, 0.1M) under N_2. The flask was cooled to 0 °C and KHMDS (1M in THF, 1.4 mL, 1.36 mmol, 2 equiv) was added. After 5 minutes the flask was moved to room temperature and stirred. After 90 minutes the flask was cooled to 0 °C and a solution of $PhNTf_2$ (1M in THF, 1.5 mL, 1.5 mmol, 2.2 equiv) was added dropwise. The flask was moved to room temperature and the reaction mixture was stirred overnight. After 18 hours the reaction was quenched with sat. NH_4Cl, diluted with H_2O, extracted with EtOAc (4x10 mL), washed with brine, dried over $MgSO_4$, filtered, and concentrated. The crude product was purified by Yamazen flash chromatography to give the triflate (236 mg, 66

^{1}H NMR: (500 MHz, $CDCl_3$) δ 7.33–7.13 (m, 6H), 6.82–6.69 (m, 1H), 5.77 (d, J = 6.8 Hz, 1H), 5.18 (d, J = 14.9 Hz, 1H), 4.57 (d, J = 15.0 Hz, 1H), 4.27 (s, 1H), 3.79 (s, 3H), 2.89 (dd, J = 15.6, 7.9 Hz, 1H), 2.77–2.61 (m, 1H), 2.37 (dq, J = 12.5, 7.0, 6.0 Hz, 1H), 2.19 (dd, J = 14.8, 9.8 Hz, 1H), 2.13–2.00 (m, 2H), 1.74 (dt, J = 15.6, 8.7 Hz, 1H), 1.42 (dt, J = 12.7, 6.4 Hz, 1H), 1.13 (s, 3H). **^{13}C NMR:** (126 MHz, $CDCl_3$) δ 181.4, 158.8, 150.7, 139.2, 136.4, 128.8, 128.3, 127.8, 126.9, 122.7, 122.1, 115.1, 111.2, 55.5, 50.4, 50.0, 47.2, 28.0, 28.0, 23.7, 21.3, 19.1.

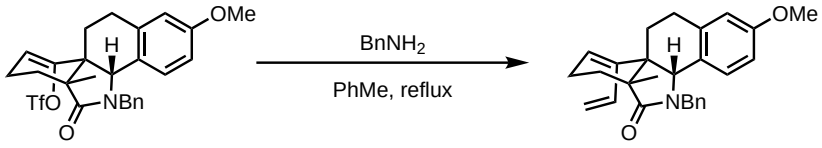

2.47 **2.48**

Diene **2.63**vinylcc-2. A 5 mL microwave vial was dried and transferred to a glovebox where $Pd(PPh_3)_3$ (25 mg, 20 μmol, 0.1 equiv) and LiCl (25 mg, 0.58 mmol, 3 equiv) were added. The vial was transferred to a Schlenk line and a solution of triflate **2.47** (100 mg, 0.19 mmol, 1 equiv) in THF (2 mL, 0.1M) was added. Tributyl(vinyl)tin (79 μL, 0.27 mmol, 1.4 equiv) was added and the vial was heated to 70 °C overnight. After 24 hours the reaction mixture was poured into a 10% aqueous solution of KF and extracted with DCM (3x10 mL), washed with brine, dried over $MgSO_4$, filtered and concentrated. The crude residue was purified by Yamazen flash chromatography to give the diene (47 mg, 62%) as a light yellow foam.

^{1}H NMR: (400 MHz, $CDCl_3$) δ 7.31–7.18 (m, 5H), 7.01 (d, J = 8.2 Hz, 1H), 6.72 (d, J = 2.6 Hz, 1H), 6.66 (dd, J = 8.4, 2.6 Hz, 1H), 5.81 (d, J = 5.5 Hz, 1H), 5.01 (d, J = 15.2 Hz, 1H), 4.89 (dd, J = 16.5, 10.5 Hz, 1H), 4.61 (d, J = 15.2 Hz, 1H), 4.55 (dd, J = 16.6, 2.4 Hz, 1H), 4.36 (s, 1H), 4.06 (dd, J = 10.5, 2.4 Hz, 1H), 3.79 (s, 3H), 2.90 pâĂŞ 2.58 (m, 2H), 2.32–2.19 (m, 1H), 2.12 (dd, J = 14.2, 9.4 Hz, 1H), 2.06–1.93 (m, 2H), 1.65 (ddd, J = 15.0, 10.4, 8.0 Hz, 1H), 1.46–1.25 (m, 2H), 1.11 (s, 3H), 0.93 (t, J = 7.3 Hz, 1H).

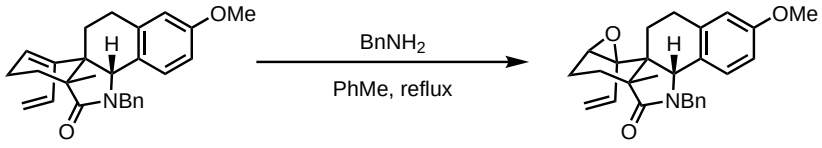

2.48 **2.49**

Diene **2.48** (20 mg, 0.05 mmol, 1 equiv) was dissolved in DCM (0.5 mL, 0.1M) in a 4 mL vial and cooled to 0 °C. mCPBA (70%, 15.4 mg, 60 μmol, 1.25 equiv) was added and the reaction was stirred at 0 °C. After 3 hours the reaction was quenched with sat. NH_4Cl, extracted with EtOAc (3x2 mL), washed with brine, dried over $MgSO_4$, filtered and concentrated. The product was purified via pipette column flash chromatography to give the epoxide (4.5 mg, 22%) as a colorless oil.

^{1}H NMR: (500 MHz, $CDCl_3$) δ 7.43–7.14 (m, 6H), 6.61 (dd, J = 8.7, 2.8 Hz, 1H), 6.54 (d, J = 2.7 Hz, 1H), 5.39 (dd, J = 16.7, 10.6 Hz, 1H), 5.23 (d, J = 15.7 Hz, 1H), 4.83–4.72 (m, 3H), 4.13 (dd, J = 10.5, 2.0 Hz, 1H), 3.74 (s, 3H), 2.94 (dt, J = 16.4, 8.0 Hz, 1H), 2.79 (s, 1H), 2.72 (ddd, J = 16.9, 8.0, 5.0 Hz, 1H), 2.16–2.03 (m, 2H), 1.95 (dd, J = 15.4, 5.3 Hz, 1H), 1.87 (dt, J = 13.5, 8.2 Hz, 1H), 1.77 (dd, J = 14.1, 5.7 Hz, 1H), 1.60 (s, 2H), 1.03 (s, 3H). **^{13}C NMR:** (126 MHz, $CDCl_3$) δ 182.0, 158.4, 139.0, 138.2, 137.0, 128.9, 128.5, 127.6, 127.5, 125.1, 114.3, 111.2, 108.9, 66.7, 63.6, 60.4, 55.3, 47.9, 47.2, 46.9, 27.9, 24.5, 23.9, 21.5, 18.7.

2.6 References

1. Corey, E. J.; Ohno, M.; Mitra, R. B.; Vatakencherry, P. A. *J. Am. Chem. Soc.* **1964**, *86*, 478–485.
2. (a) Heathcock, C. H.; Davidsen, S. K.; Mills, S.; Sanner, M. A. *J. Am. Chem. Soc.* **1986**, *108*, 5650–5651; (b) Heathcock, C. H. *Angew. Chem. Int. Ed.* **1992**, *31*, 665–681.
3. Corey, E. J.; Chelg, X.-M. *The Logic of Chemical Synthesis*; Wiley, 1995; pp 43–44.
4. Hoffmann, R. W. *Elements of Synthesis Planning*; Springer, 2009; pp 97–112.
5. (a) Marth, C. J.; Gallego, G. M.; Lee, J. C.; Lebold, T. P.; Kulyk, S.; Kou, K. G.; Qin, J.; Lilien, R.; Sarpong, R. *Nature* **2015**, *528*, 493–498; (b) Kou, K. G. M.; Kulyk, S.; Marth, C. J.; Lee, J. C.; Doering, N. A.; Li, B. X.; Gallego, G. M.; Lebold, T. P.; Sarpong, R. *J. Am. Chem. Soc.* **2017**, *139*, 13882–13896; (c) Kou, K. G.; Li, B. X.; Lee, J. C.; Gallego, G. M.; Lebold, T. P.; DiPasquale, A. G.; Sarpong, R. *J. Am. Chem. Soc.* **2016**, *138*, 10830–10833.
6. (a) Cortez, F. d. J.; Sarpong, R. *Org. Lett.* **2010**, *12*, 1428–1431; (b) Hamlin, A. M.; Cortez Fde, J.; Lapointe, D.; Sarpong, R. *Angew. Chem. Int. Ed.* **2013**, *52*, 4854–4857; (c) Hamlin, A. M.; Lapointe, D.; Owens, K.; Sarpong, R. *J. Org. Chem.* **2014**, *79*, 6783–6800.
7. Suzuki, T.; Sasaki, A.; Egashira, N.; Kobayashi, S. *Angew. Chem. Int. Ed.* **2011**, *50*, 9177–9179.
8. Chen, H.; Zhang, D.; Xue, F.; Qin, Y. *Tetrahedron* **2013**, *69*, 3141 – 3148.
9. Peese, K. M.; Gin, D. Y. *J. Am. Chem. Soc.* **2006**, *128*, 8734–8735.
10. Phan, D. H.; Kim, B.; Dong, V. M. *J. Am. Chem. Soc.* **2009**, *131*, 15608–15609.
11. Benhida, R.; Blanchard, P.; Fourrey, J.-L. *Tetrahedron Lett.* **1998**, *39*, 6849–6852.
12. Wang, C. J.; Liang, G.; Xue, Z. Y.; Gao, F. *J. Am. Chem. Soc.* **2008**, *130*, 17250–17251.
13. Letellier, M.; McPhee, D. J.; Griller, D. *Synth. Commun.* **1988**, *18*, 1975–1978.
14. Defoin, A.; Pires, J.; Streith, J. *Helv. Chim. Acta* **1991**, *74*, 1653–1670.
15. Pflueger, J. J.; Morrill, L. C.; deGruyter, J. N.; Perea, M. A.; Sarpong, R. *Org. Lett.* **2017**, *19*, 4632–4635.
16. (a) Ohira, S. *Synth. Commun.* **2006**, *19*, 561–564; (b) Roth, G.; Liepold, B.; Müller, S.; Bestmann, H. *Synthesis* **2003**, *2004*, 59–62.
17. Spiegel, D. A.; Njardarson, J. T.; Wood, J. L. *Tetrahedron* **2002**, *58*, 6545–6554.
18. Fujihara, T.; Horimoto, Y.; Mizoe, T.; Sayyed, F. B.; Tani, Y.; Terao, J.; Sakaki, S.; Tsuji, Y. *Org. Lett.* **2014**, *16*, 4960–4963.
19. Molander, G. A. *Chem. Rev.* **1992**, *92*, 29–68.
20. (a) Dye, J. L.; Cram, K. D.; Urbin, S. A.; Redko, M. Y.; Jackson, J. E.; Lefenfeld, M. *J. Am. Chem. Soc.* **2005**, *127*, 9338–9339; (b) Nandi, P.; Dye, J. L.; Jackson, J. E. *J. Org. Chem.* **2009**, *74*, 5790–5792.
21. Gong, J.; Chen, H.; Liu, X. Y.; Wang, Z. X.; Nie, W.; Qin, Y. *Nat. Commun.* **2016**, *7*, 12183.
22. Yuan, C.; Eliasen, A. M.; Camelio, A. M.; Siegel, D. *Nat. Protoc.* **2014**, *9*, 2624–2629.
23. Debrouwer, W.; Seigneur, R. A.; Heugebaert, T. S.; Stevens, C. V. *ChemComm* **2015**, *51*, 729–732.

2.A NMR Spectral Data for Chapter 2

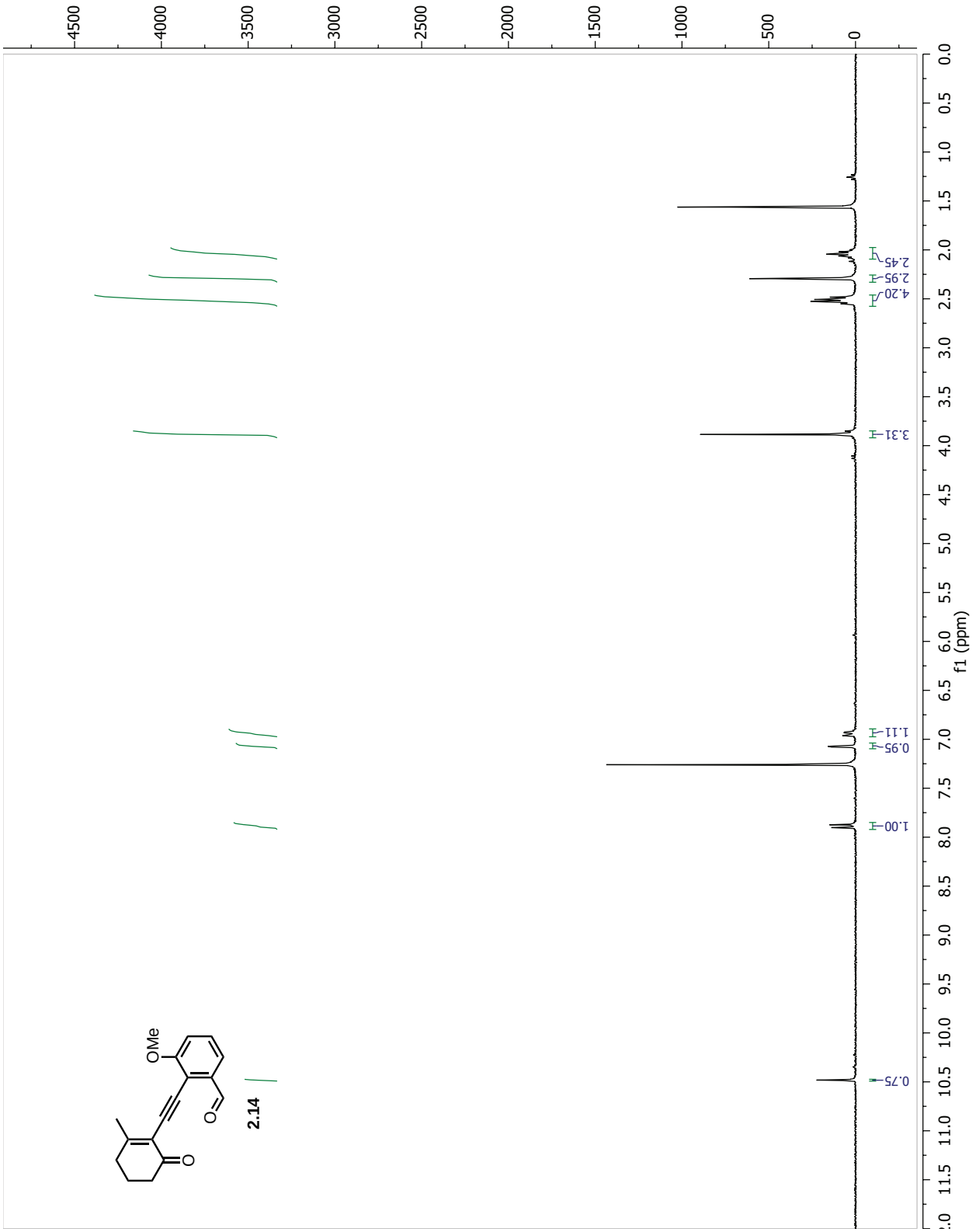

Figure 2.9: ^{1}H NMR of **2.14**

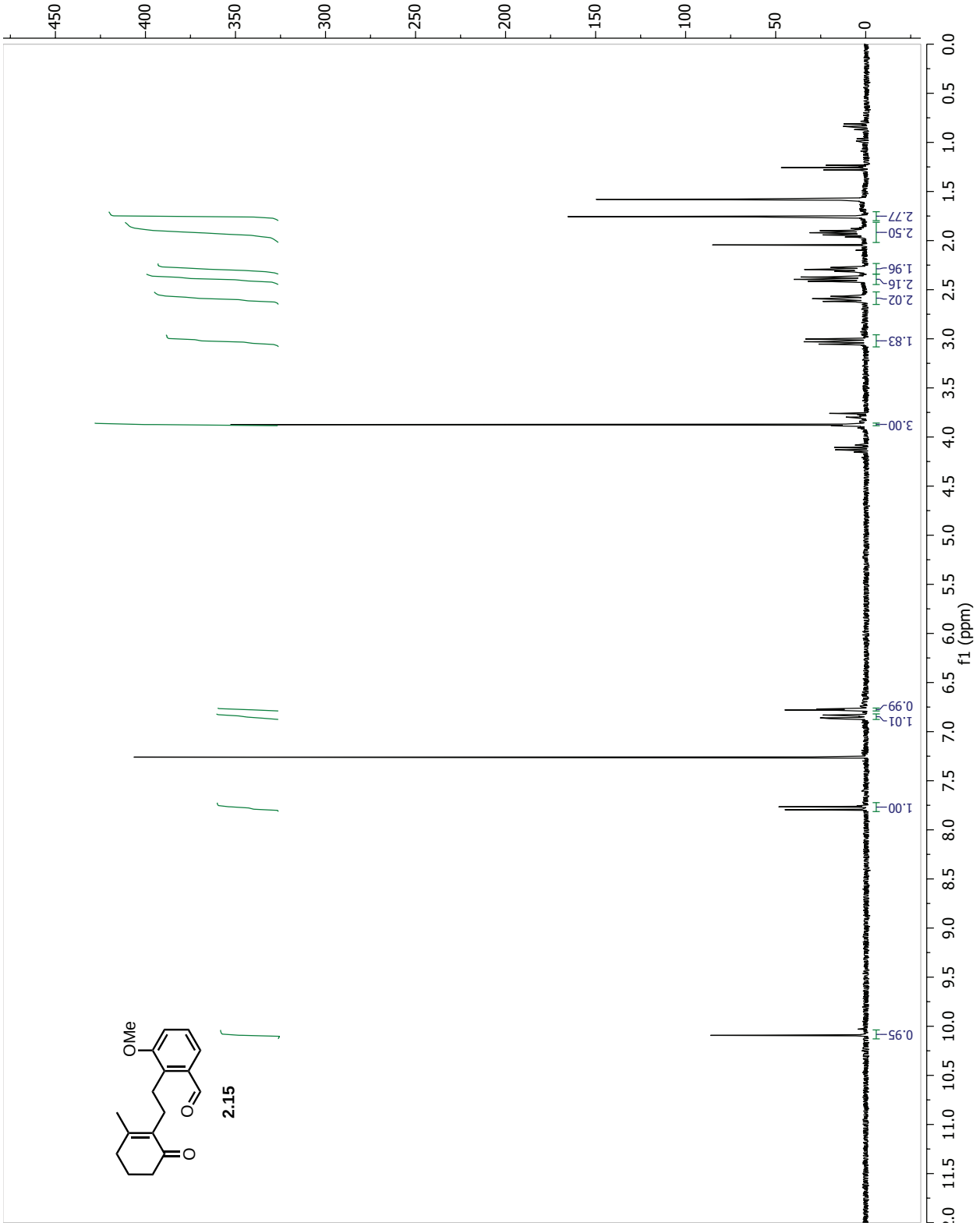

Figure 2.10: ^{1}H NMR of **2.15**

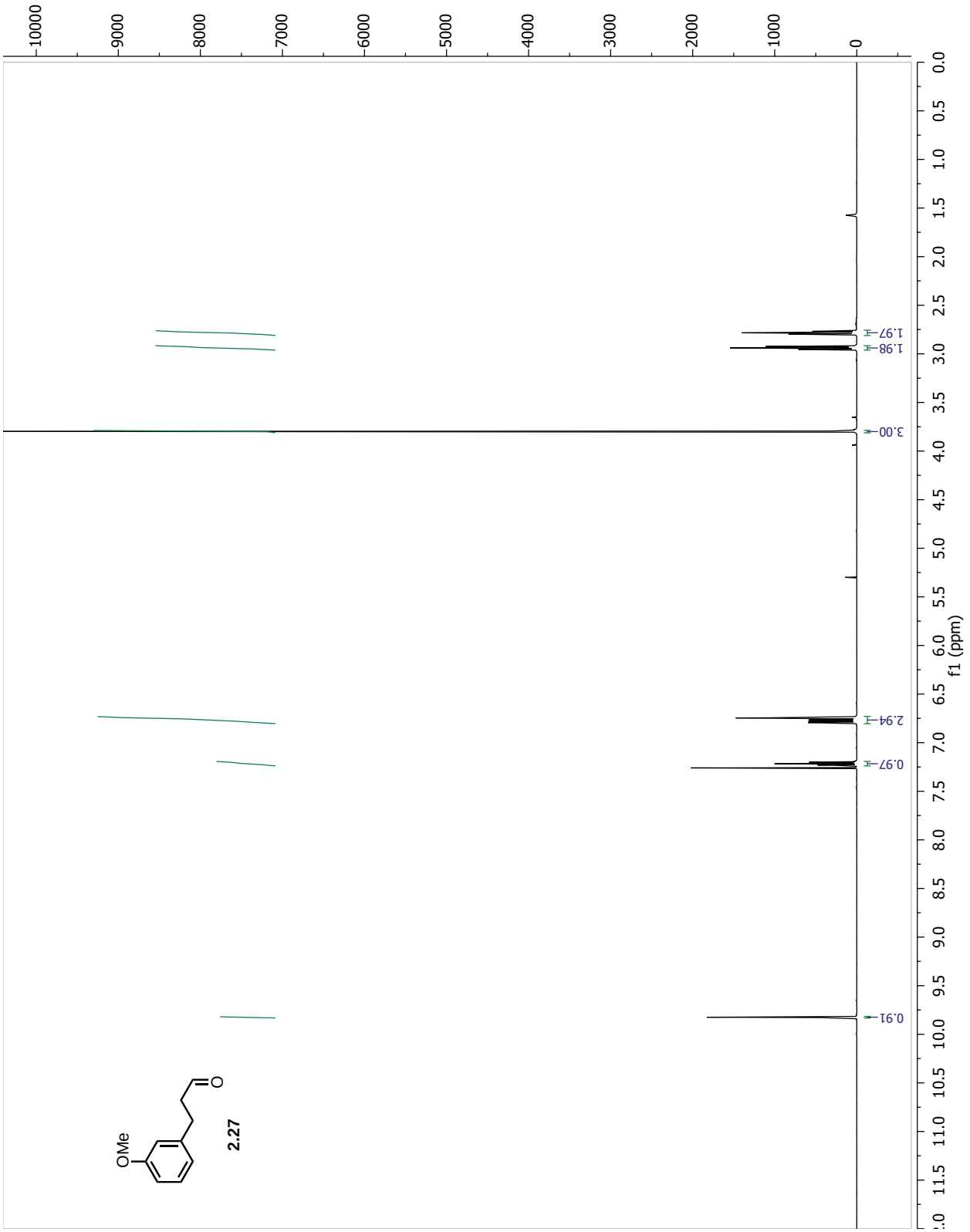

Figure 2.11: ^{1}H NMR of **2.27**

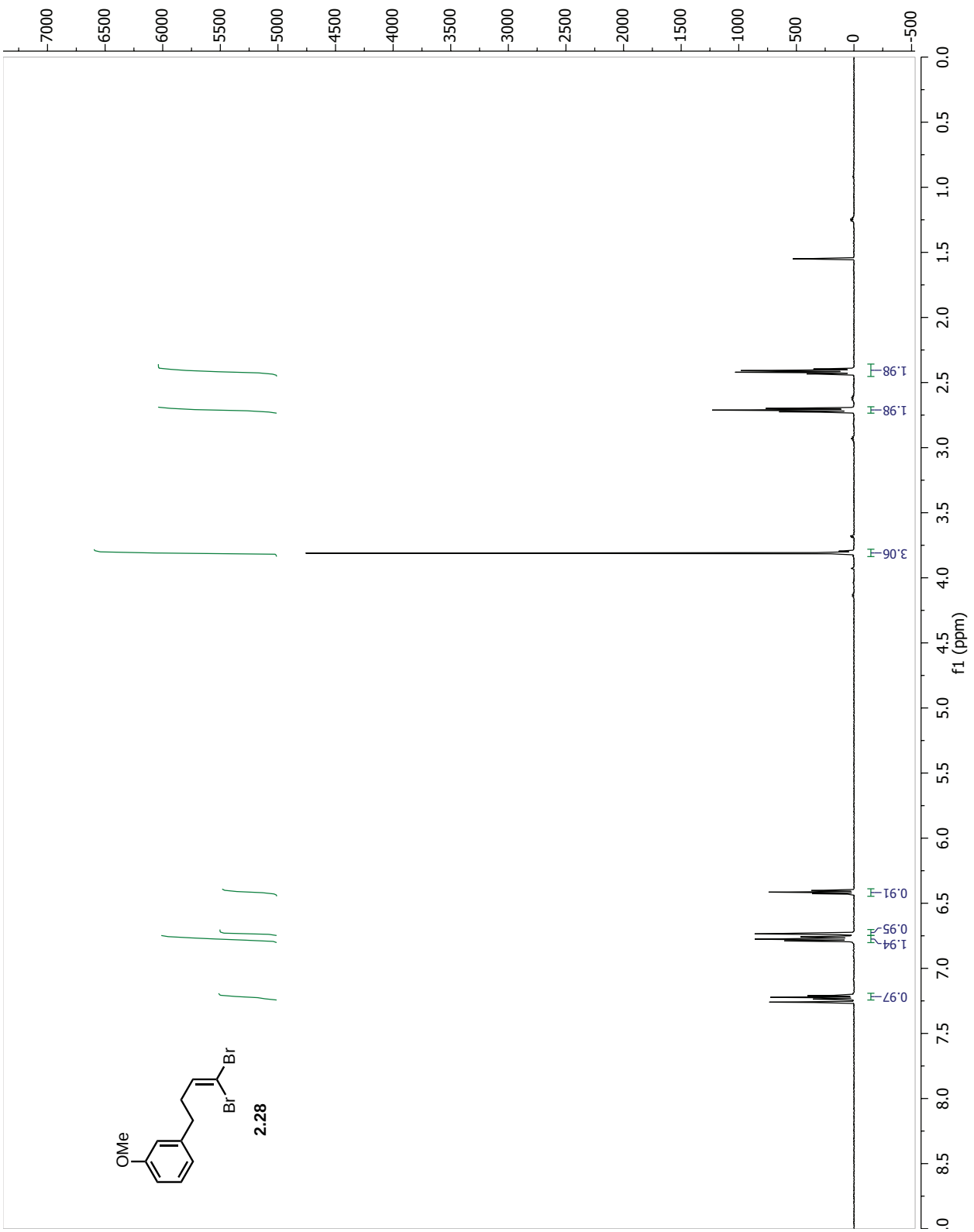

Figure 2.12: ^{1}H NMR of **2.28**

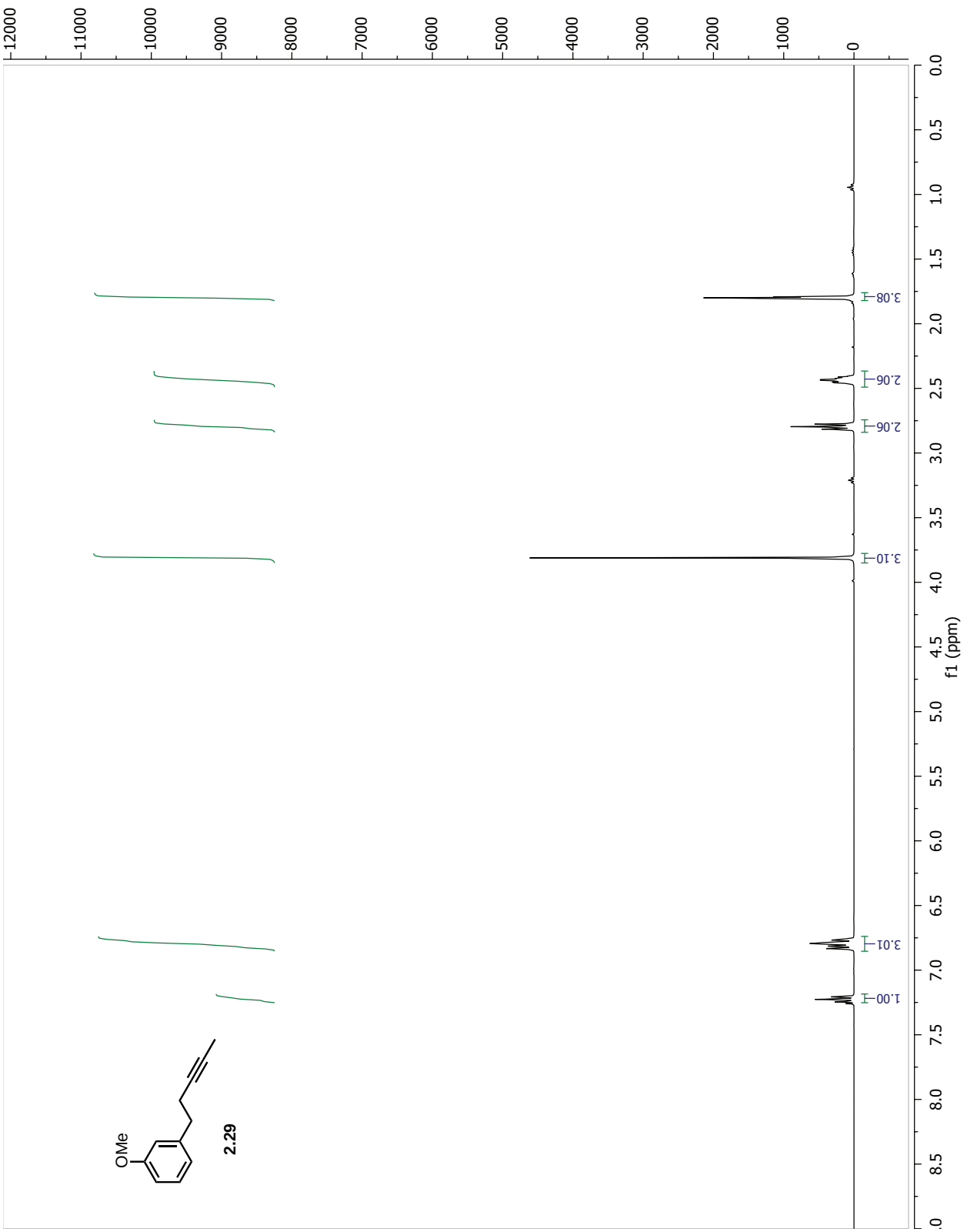

Figure 2.13: ^{1}H NMR of **2.29**

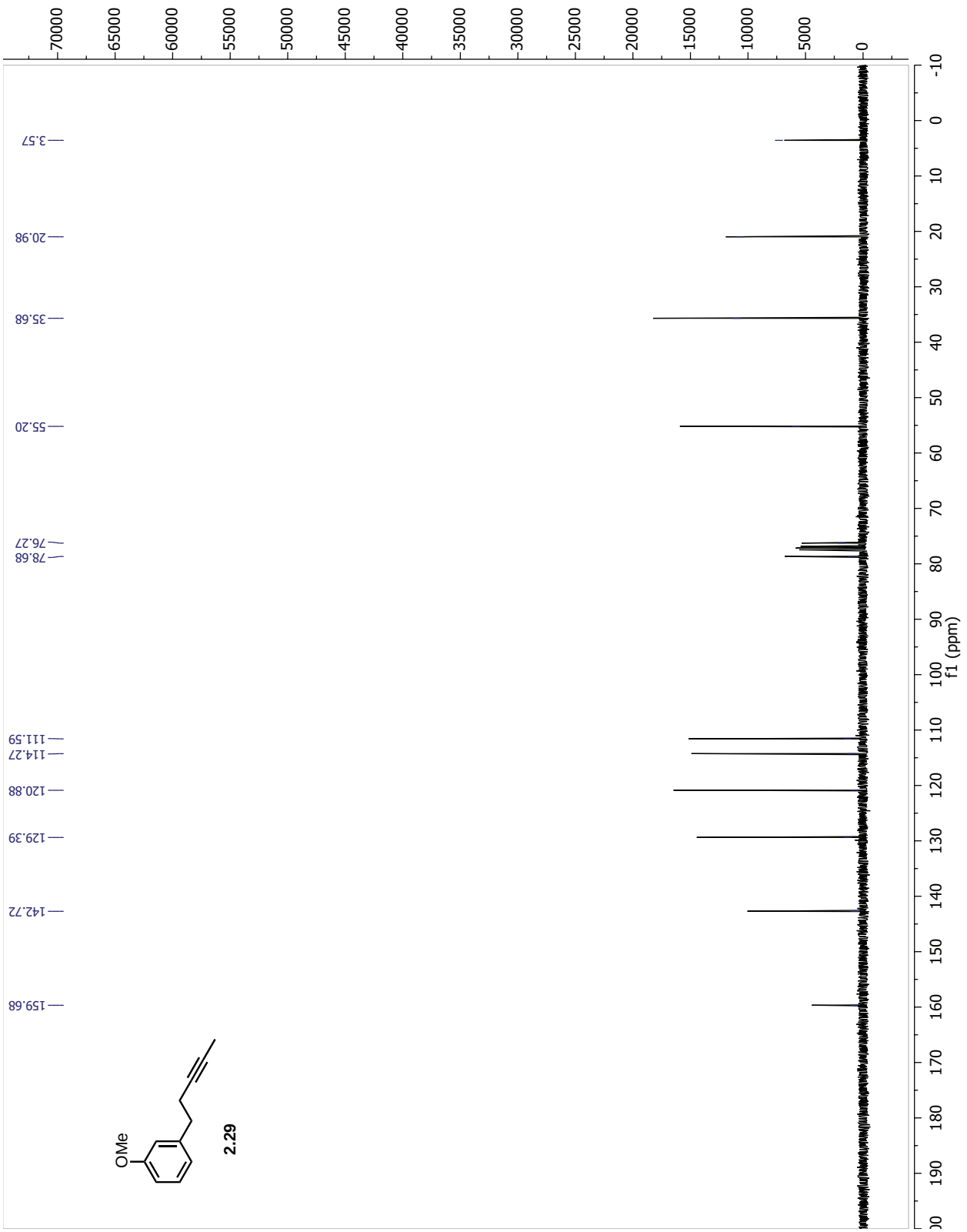

Figure 2.14: ^{13}C NMR of **2.29**

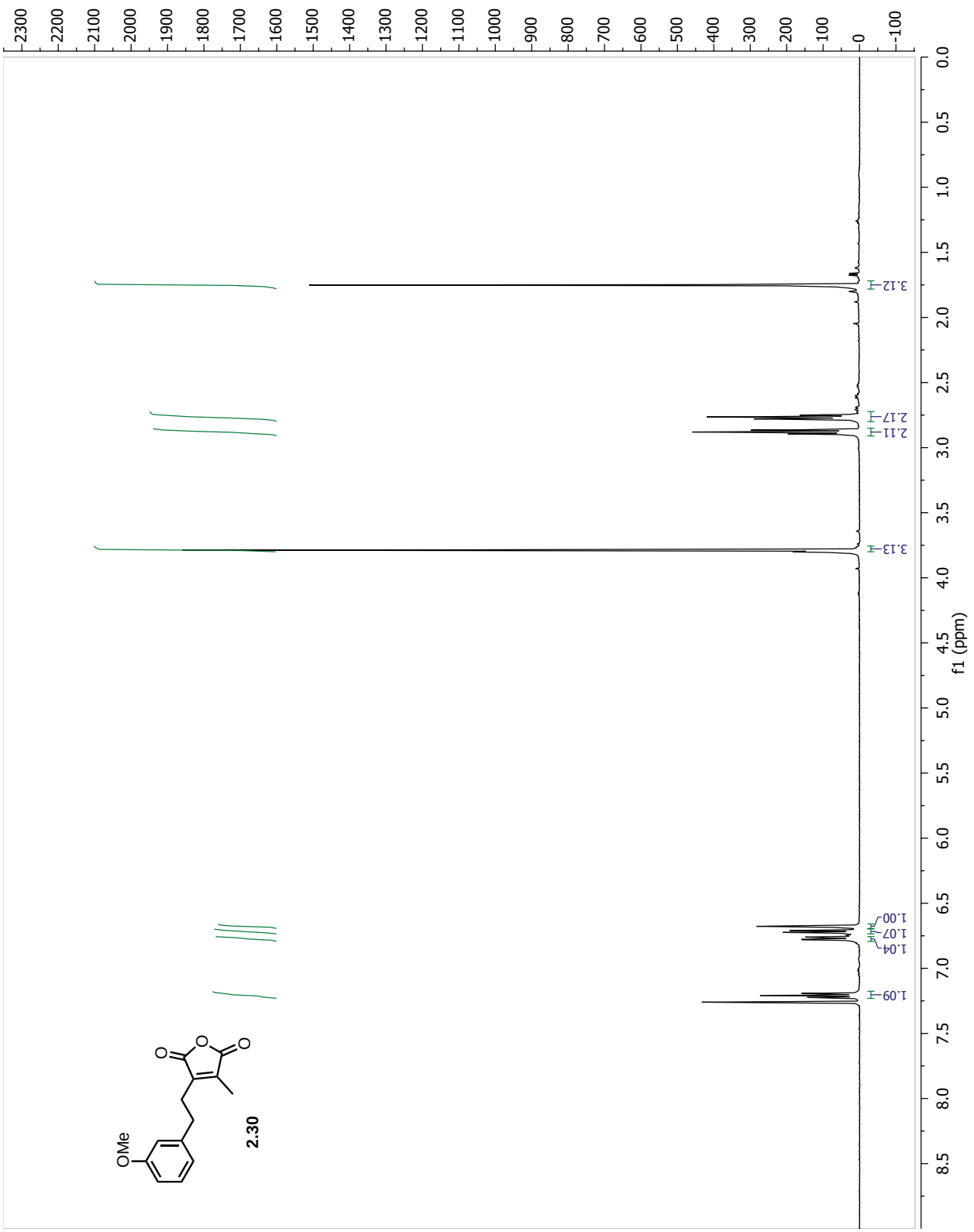

Figure 2.15: ^{1}H NMR of **2.30**

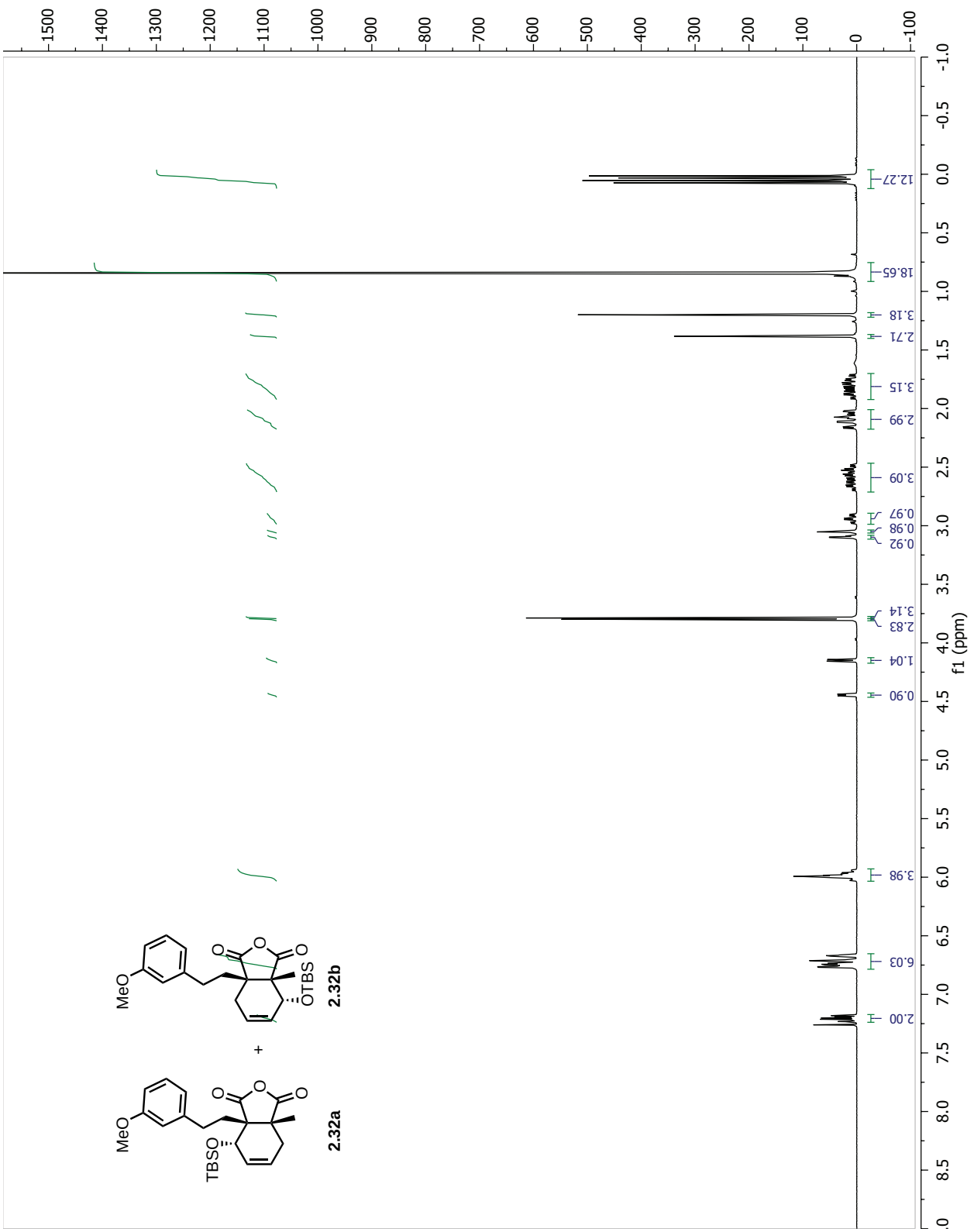

Figure 2.16: ^{1}H NMR of **2.32a** and **2.32b**

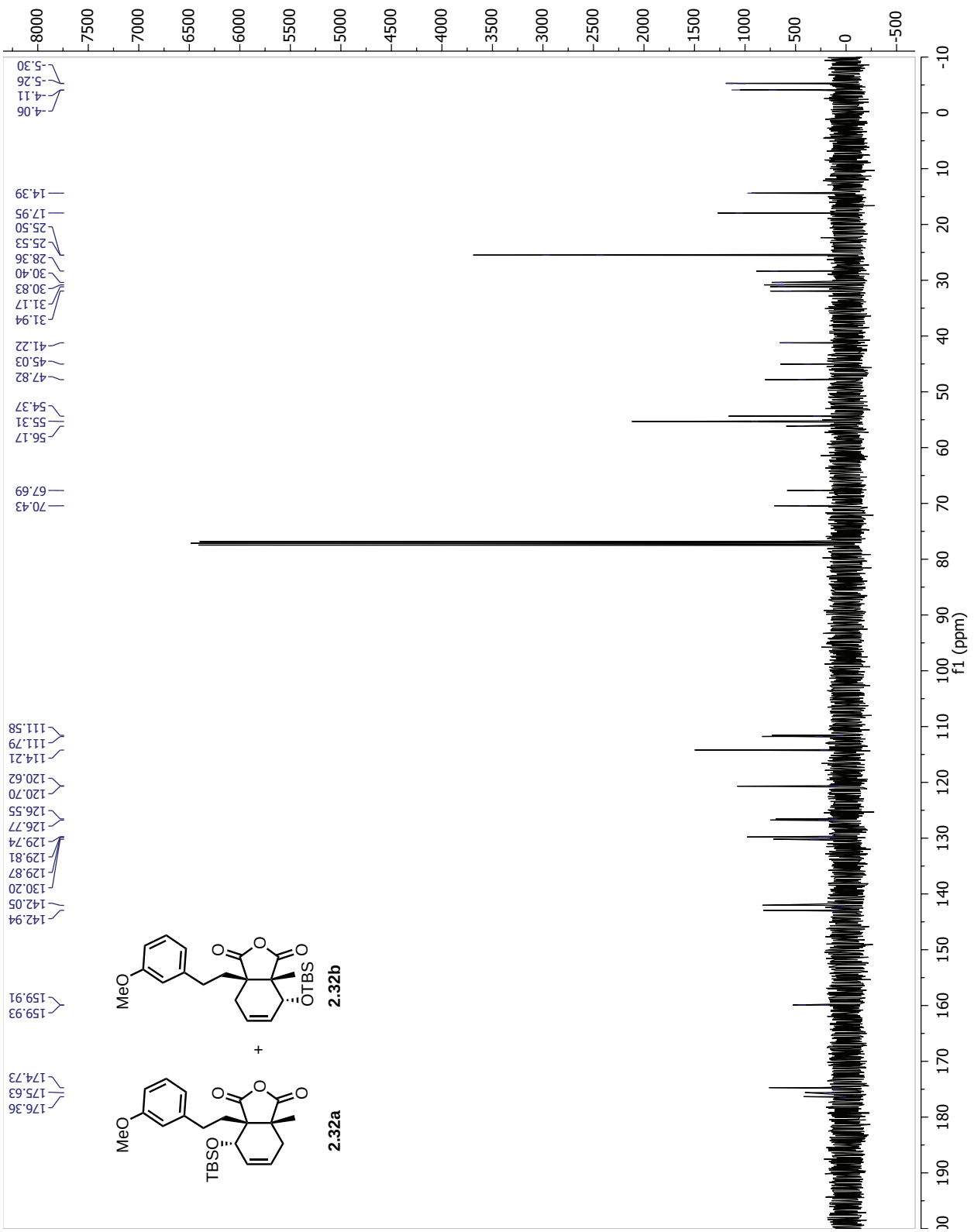

Figure 2.17: ^{13}C NMR of **2.32a** and **2.32b**

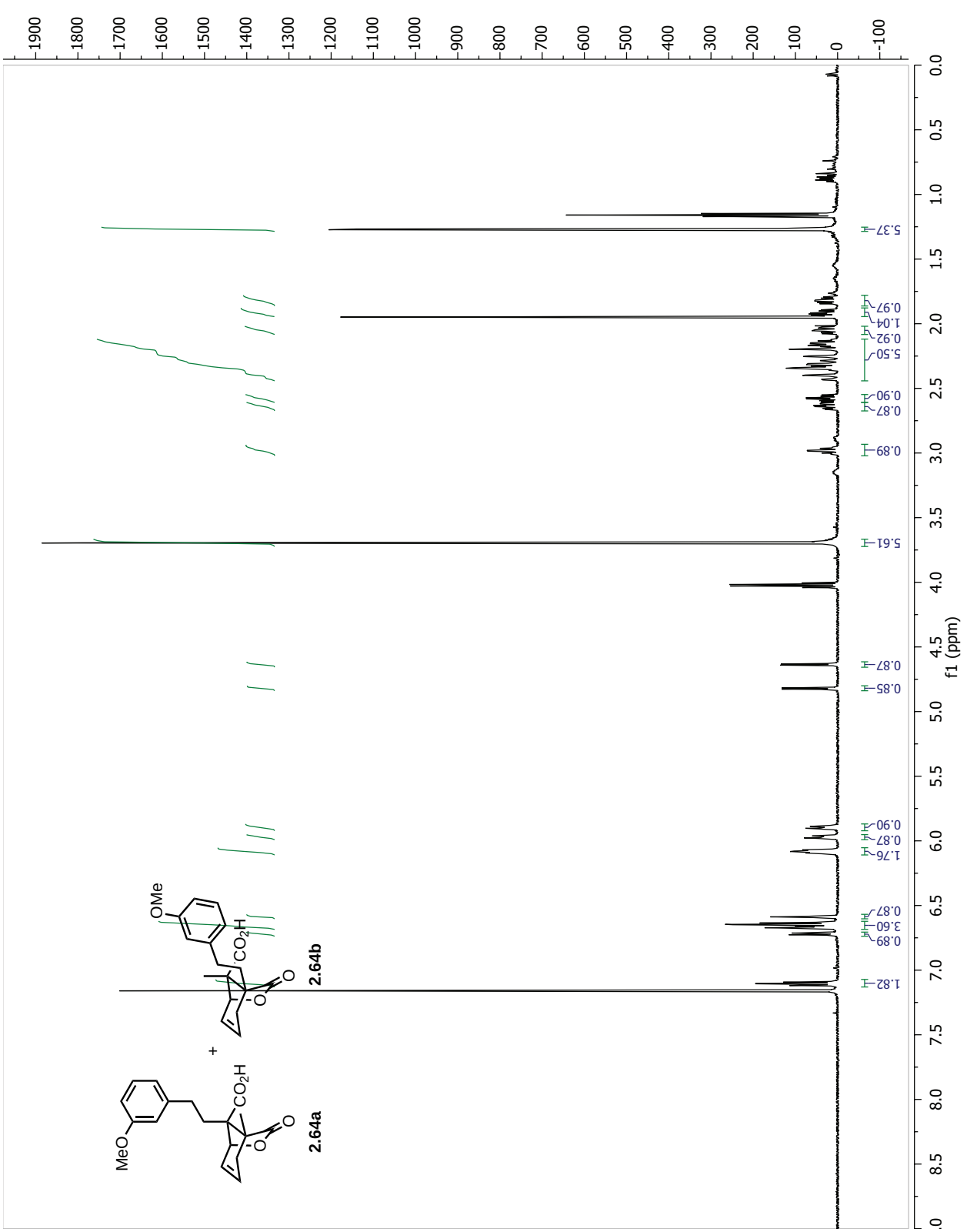

Figure 2.18: ^{1}H NMR of **2.64a** and **2.64b**

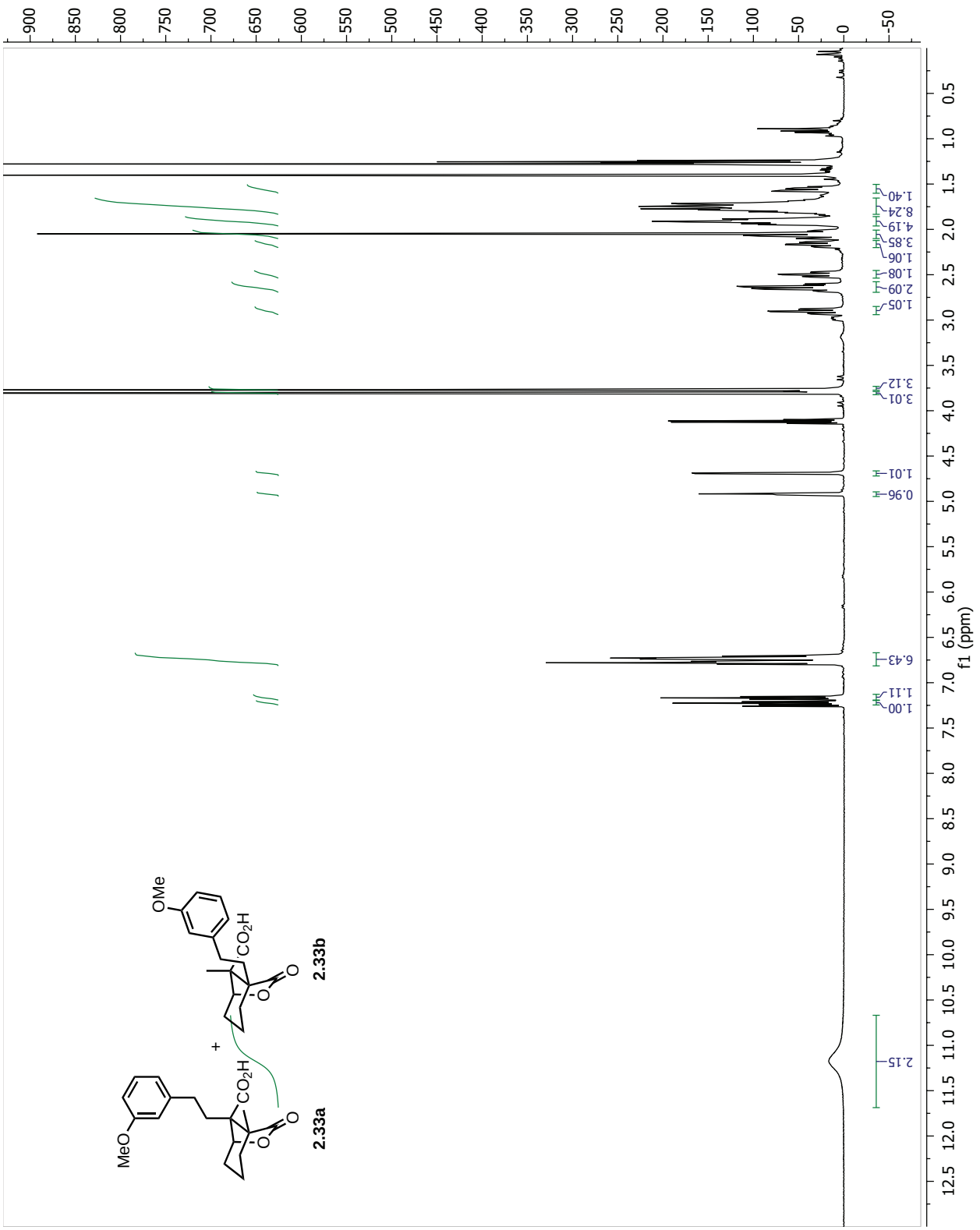

Figure 2.19: ^{1}H NMR of **2.33a** and **2.33b**

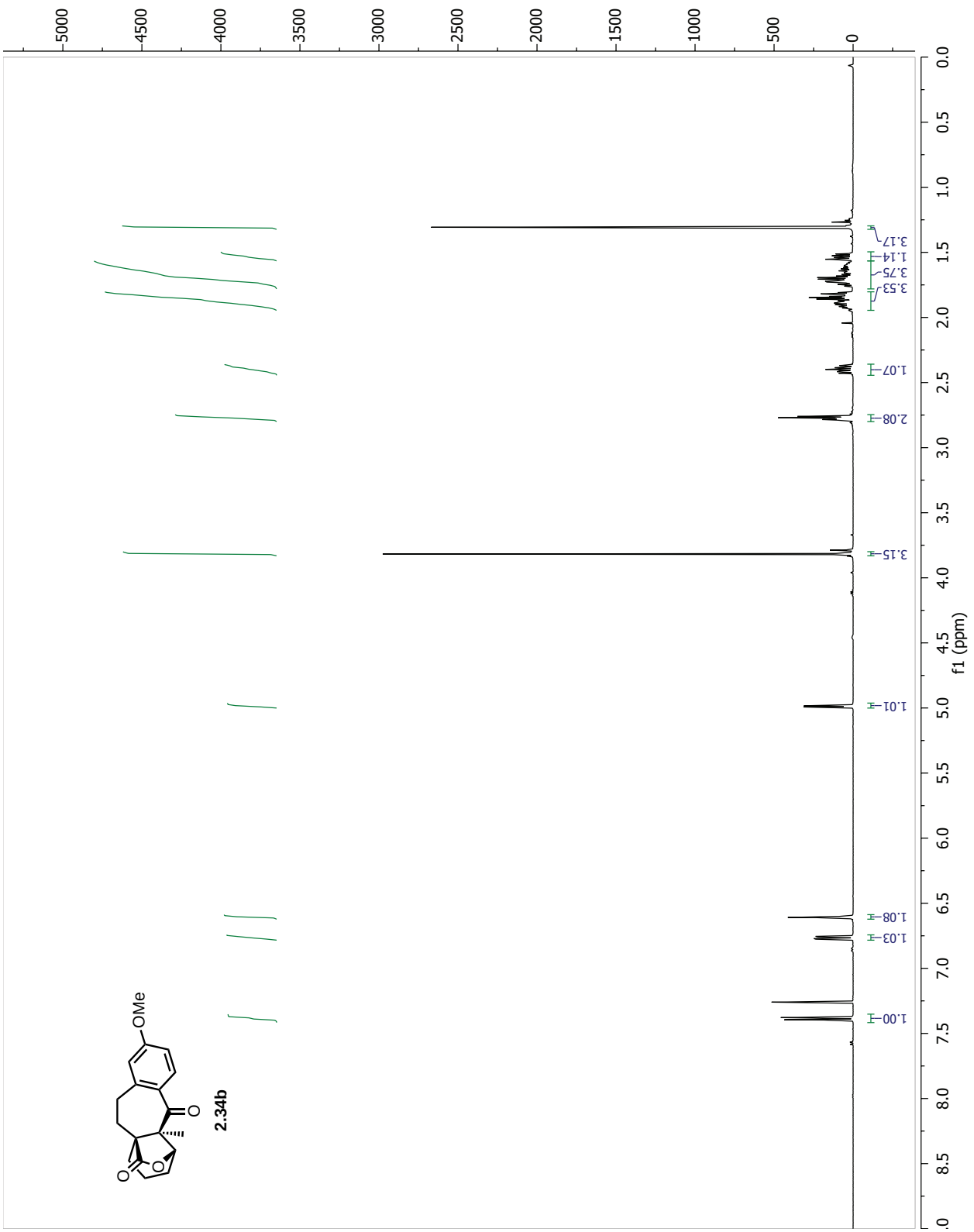

Figure 2.20: ^{1}H NMR of **2.34b**

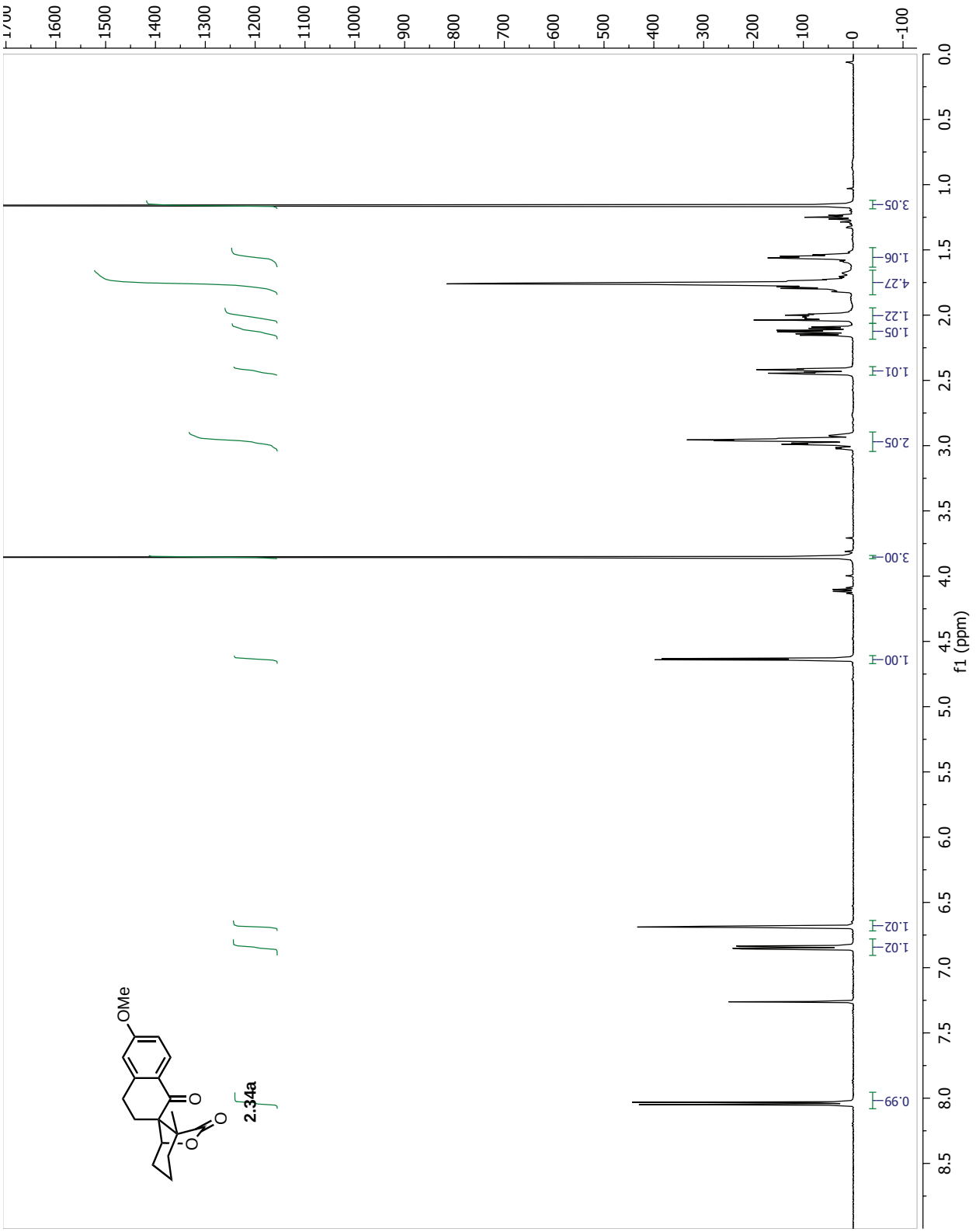

Figure 2.21: ^{1}H NMR of **2.34a**

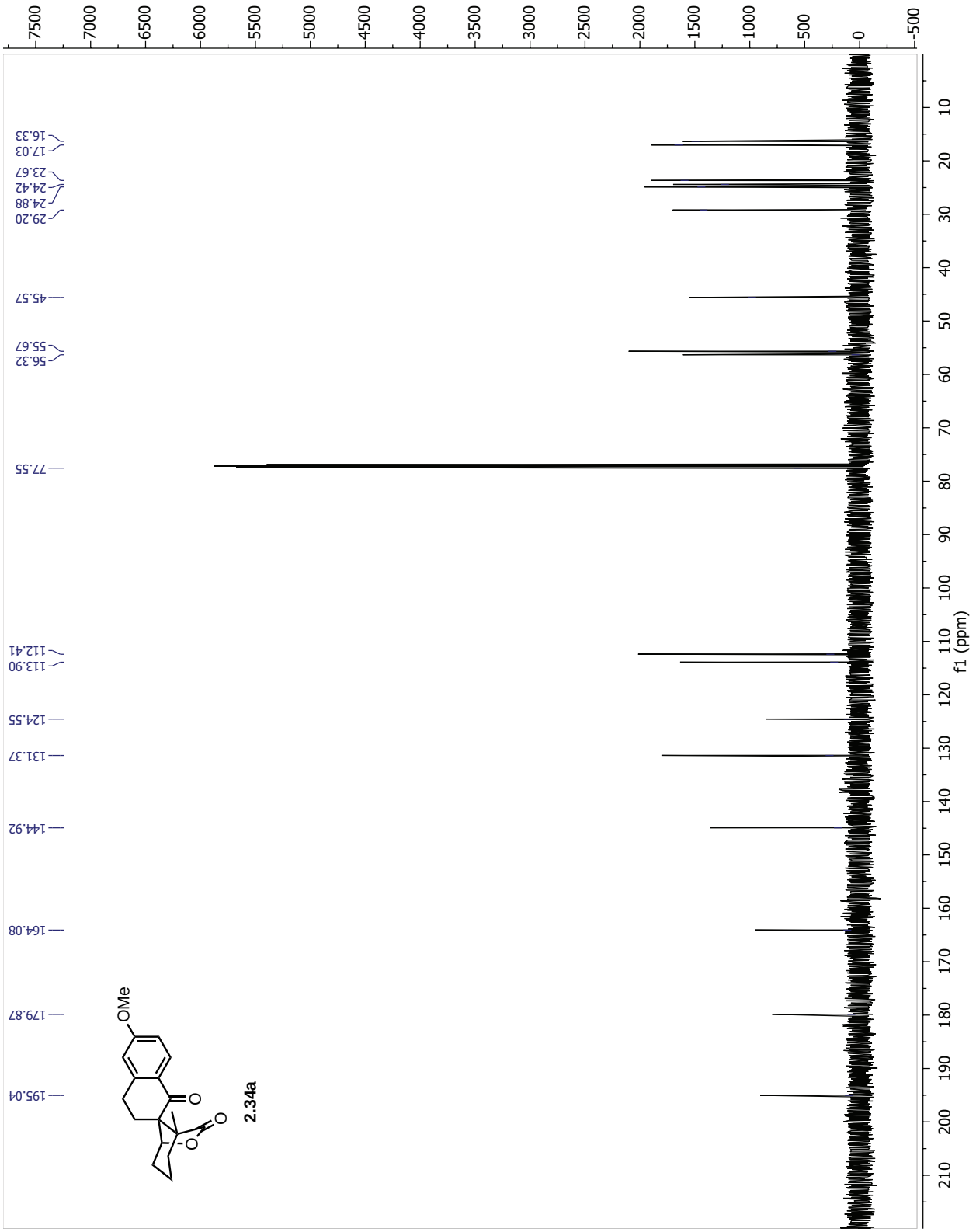

Figure 2.22: ^{1}H NMR of **2.34a**

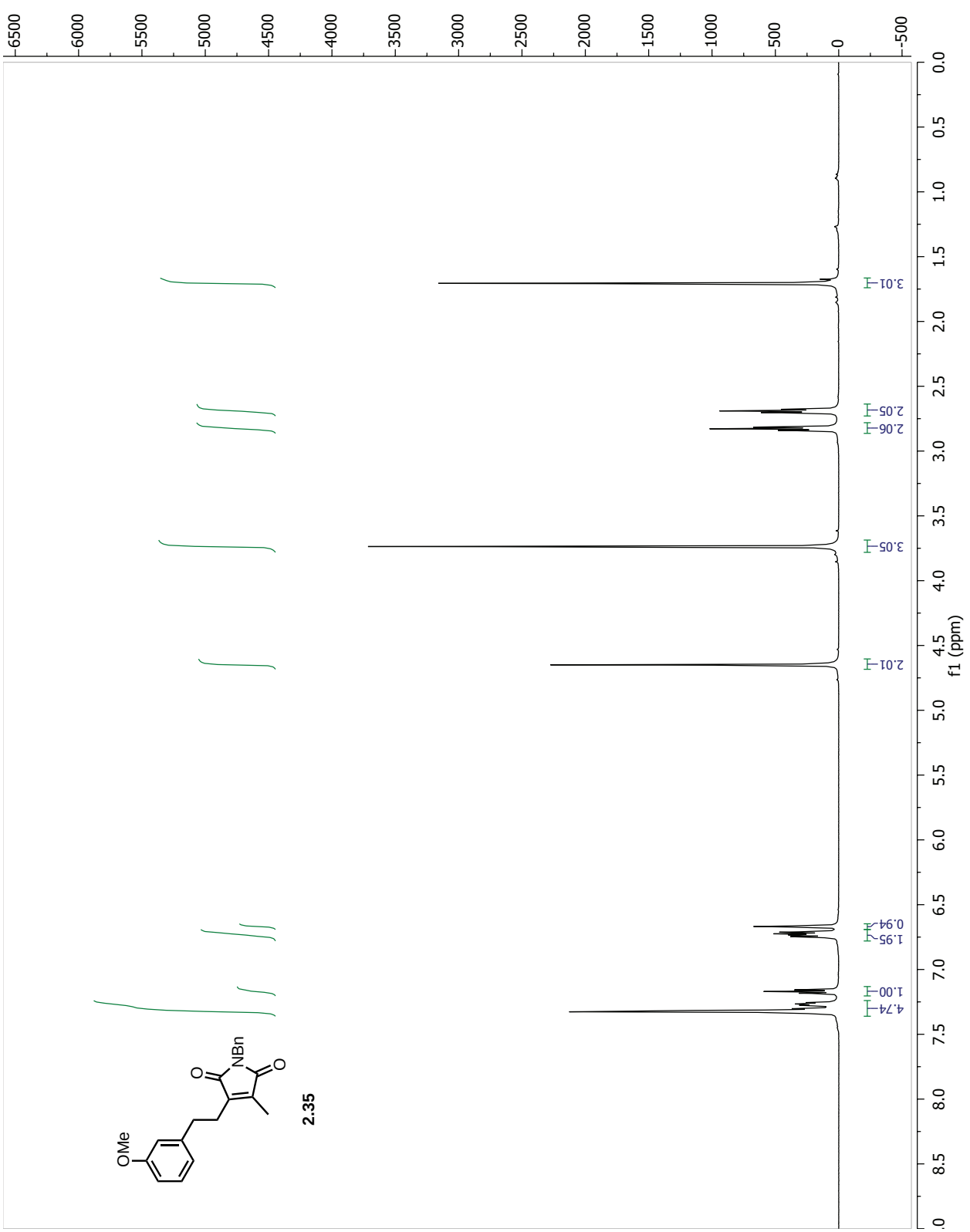

Figure 2.23: ^{1}H NMR of **2.35**

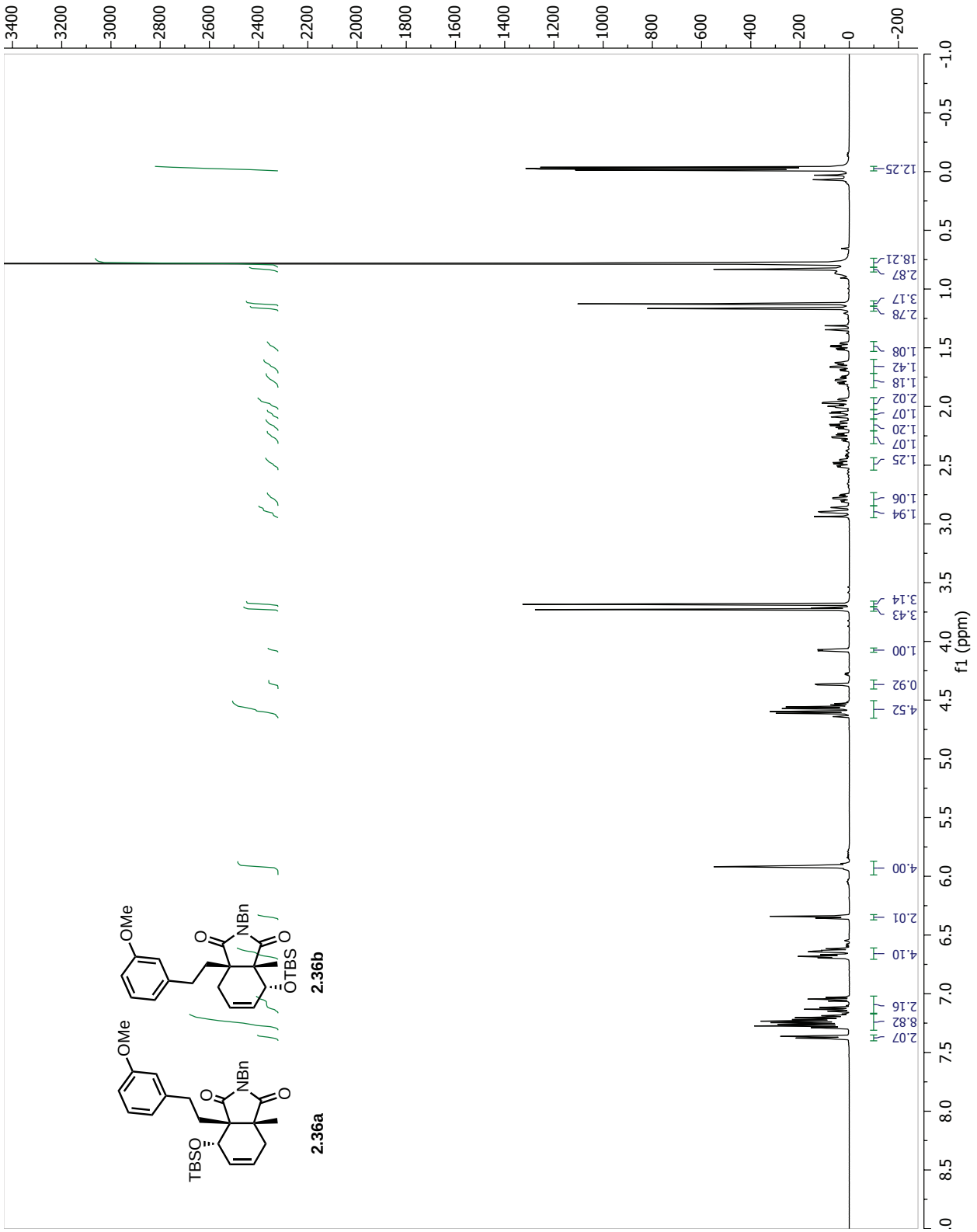

Figure 2.24: ^{1}H NMR of **2.36a** and **2.36b**

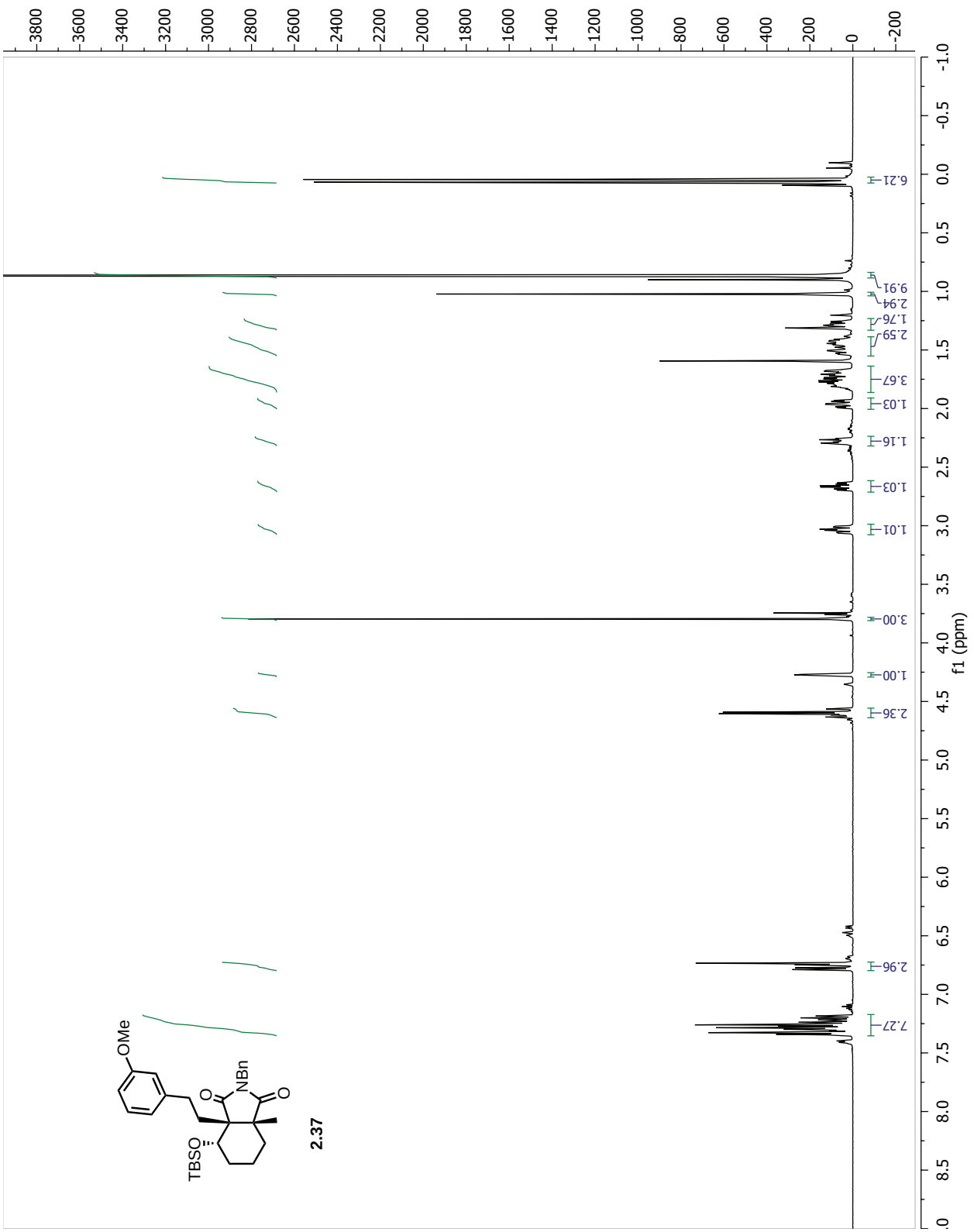

Figure 2.25: ^{1}H NMR of **2.37**

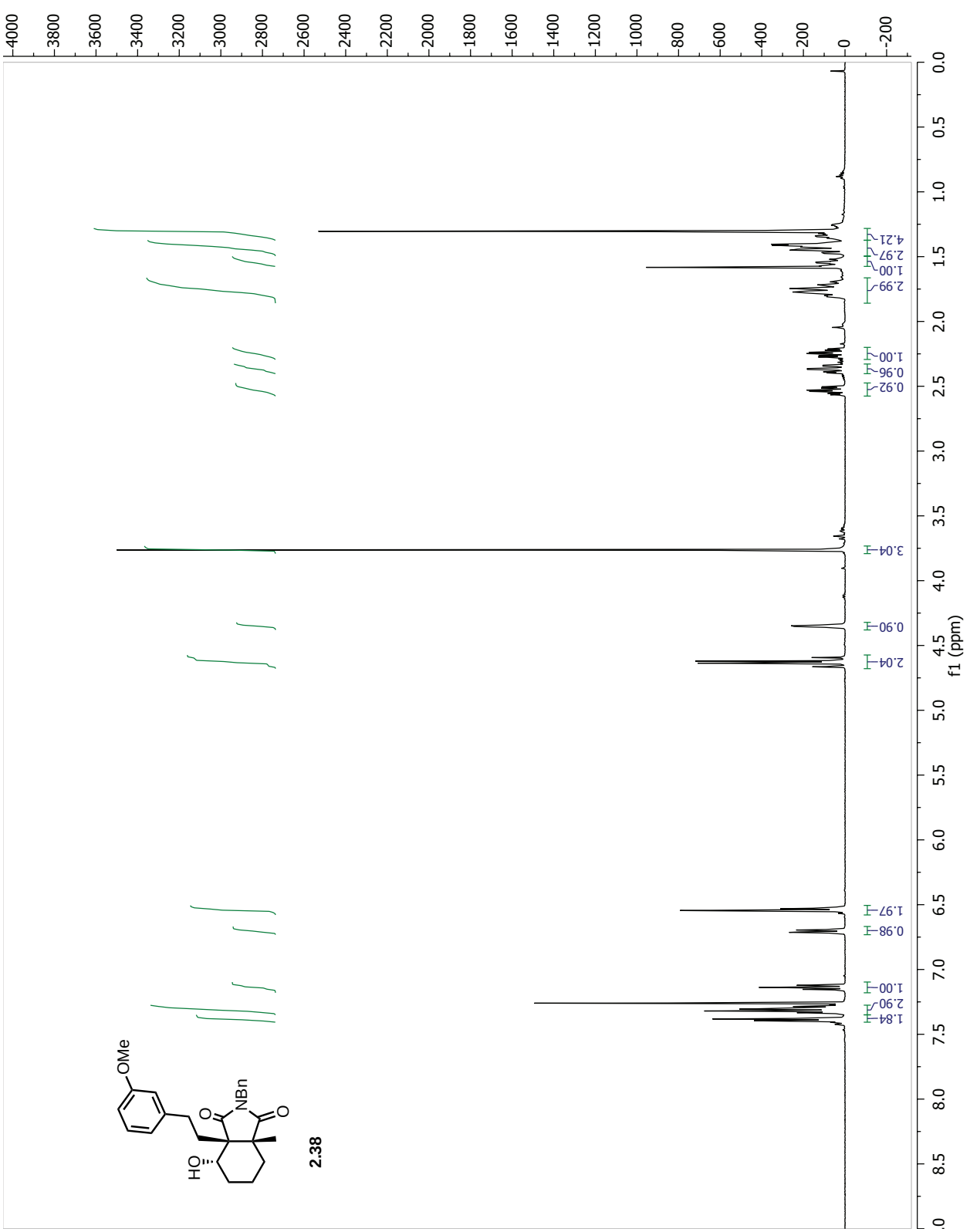

Figure 2.26: ^{1}H NMR of **2.38**

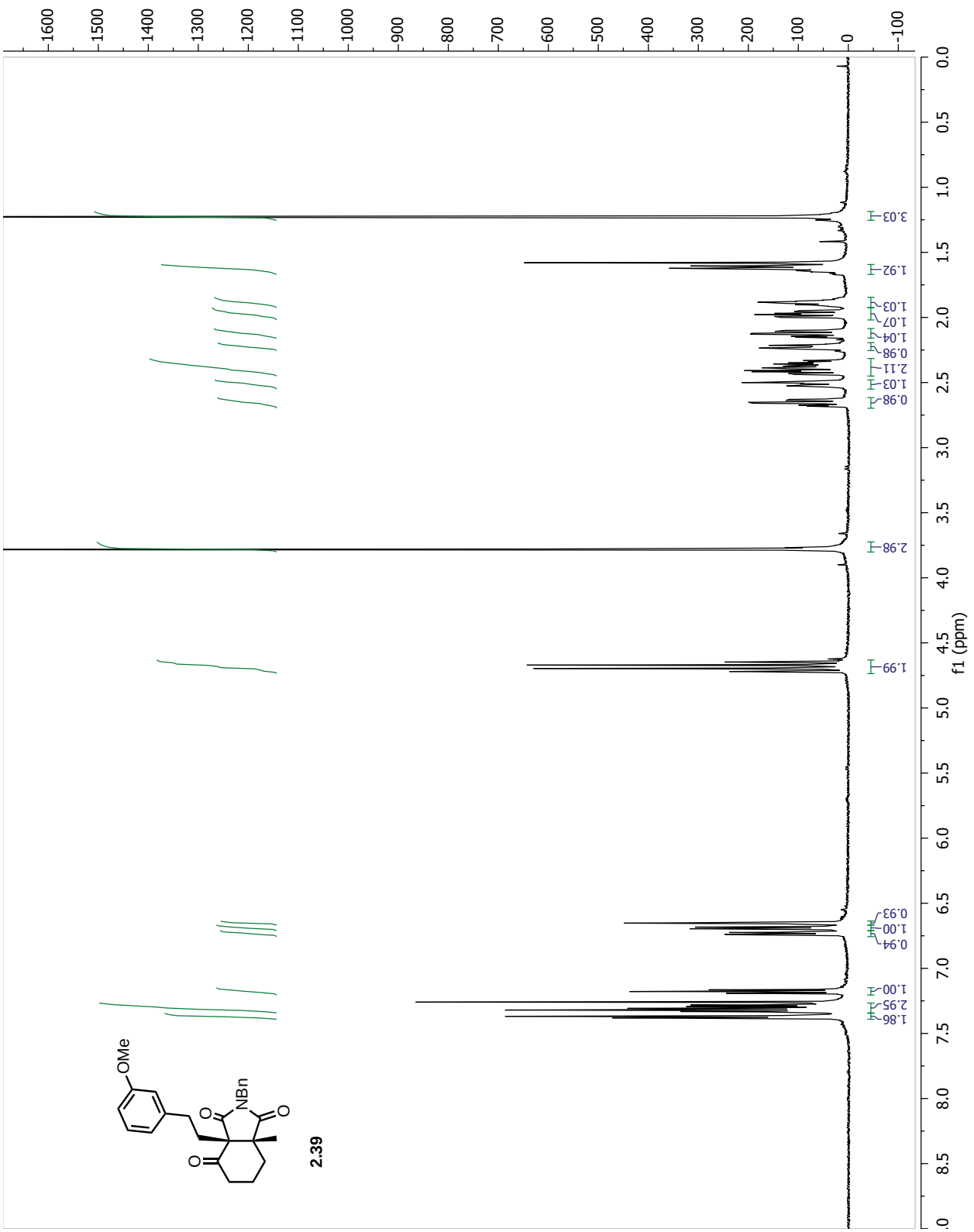

Figure 2.27: ^{1}H NMR of **2.39**

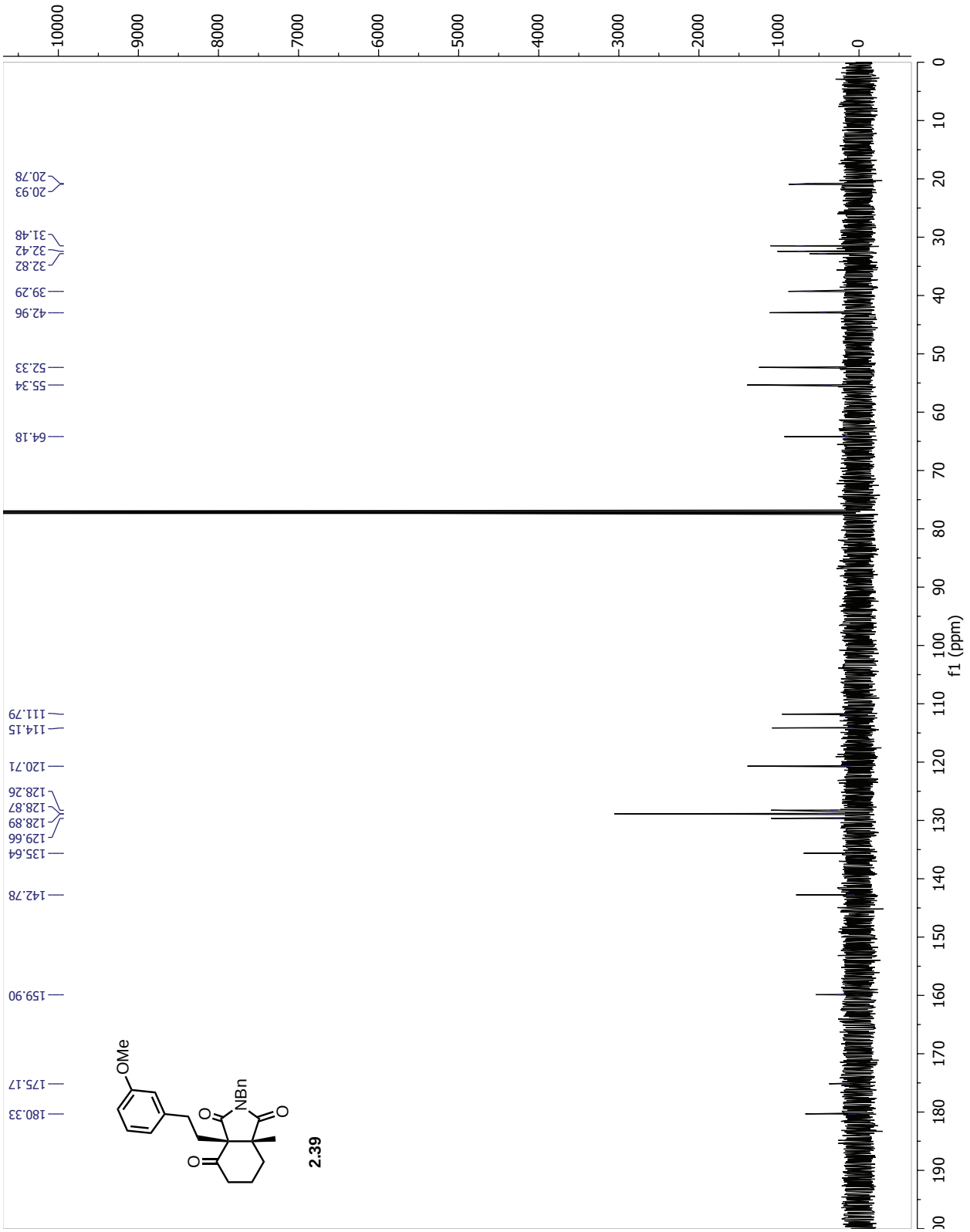

Figure 2.28: ^{13}C NMR of **2.39**

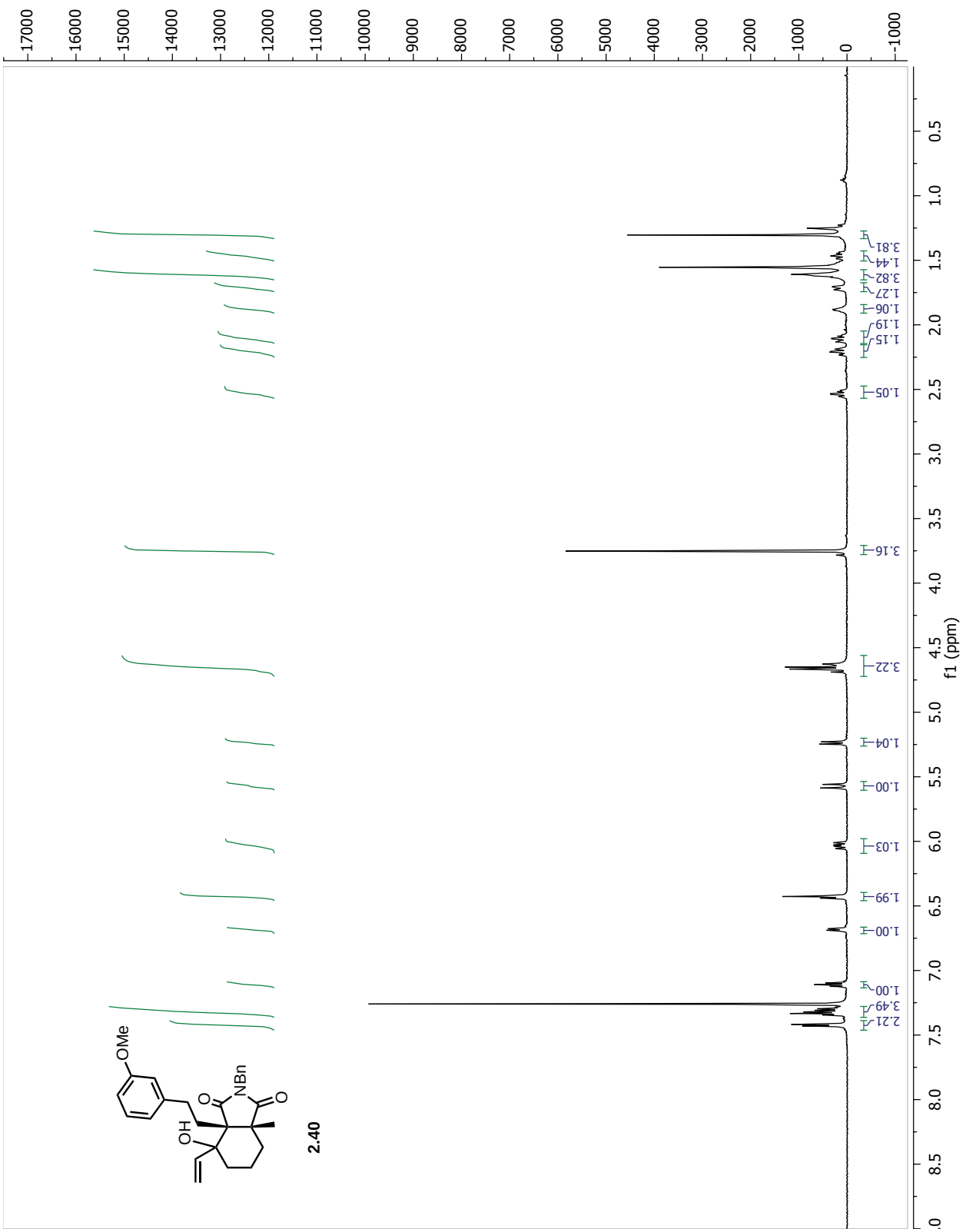

Figure 2.29: ^{1}H NMR of **2.40**

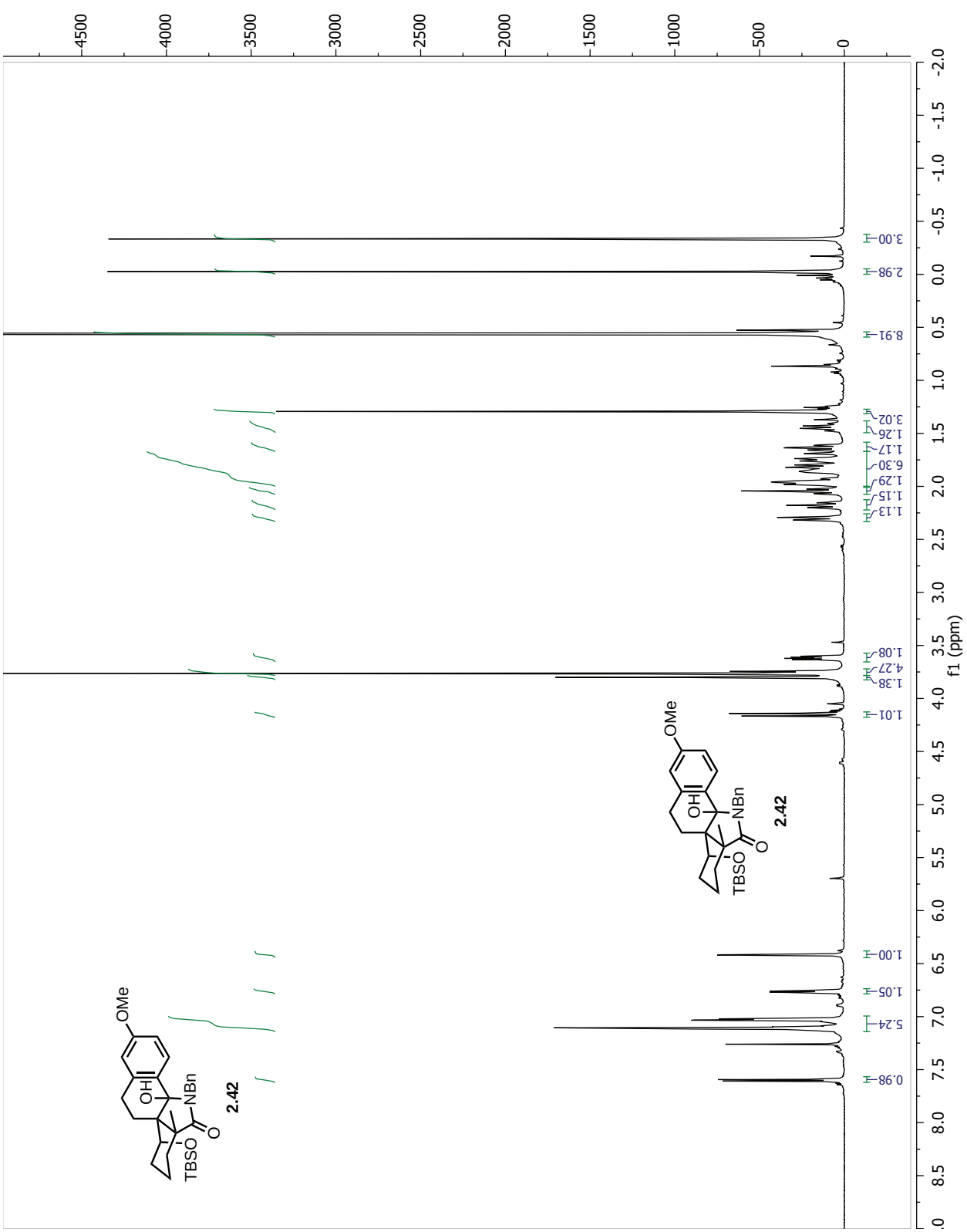

Figure 2.30: ^{1}H NMR of **2.42**

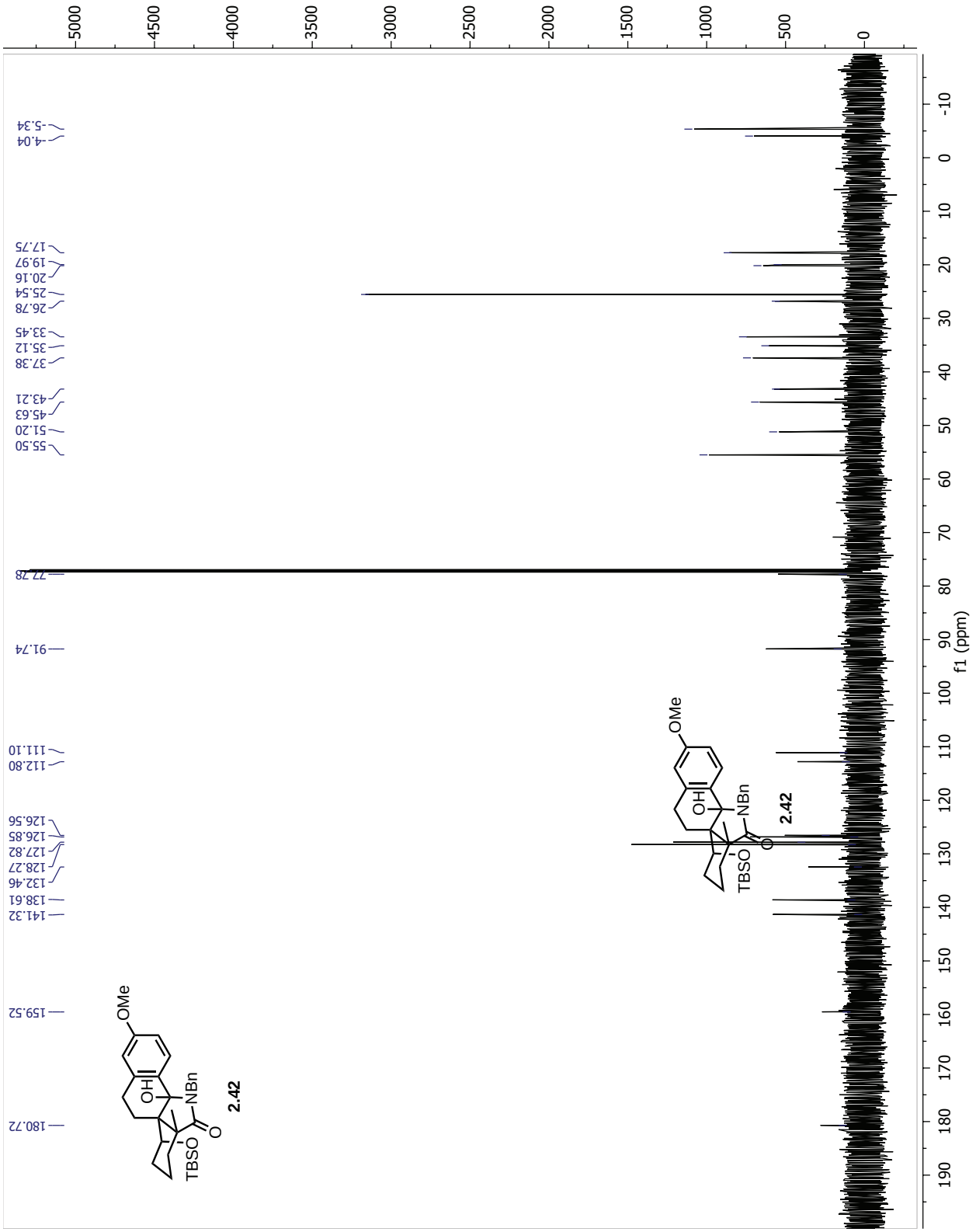

Figure 2.31: ^{13}C NMR of **2.42**

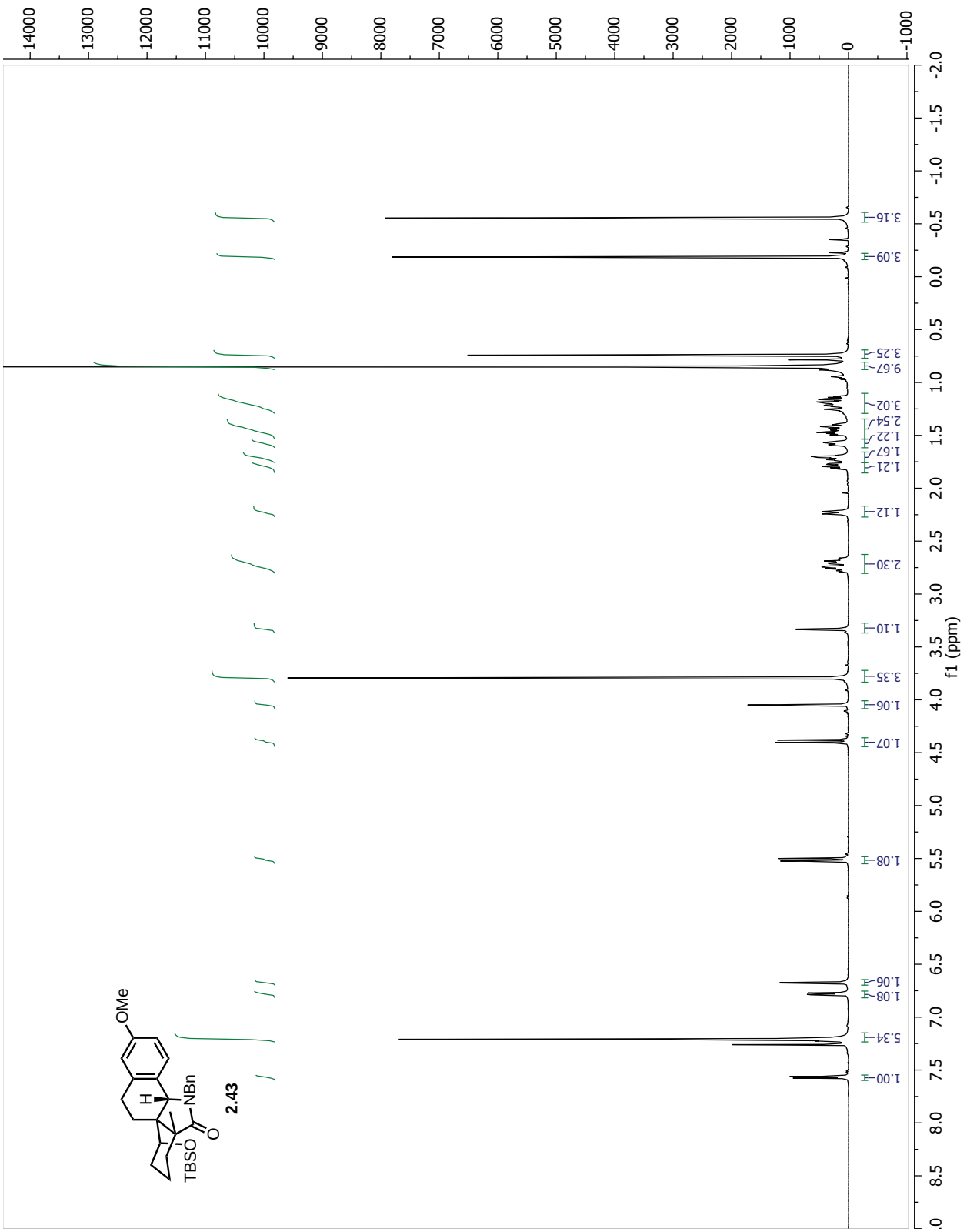

Figure 2.32: ^{1}H NMR of **2.43**

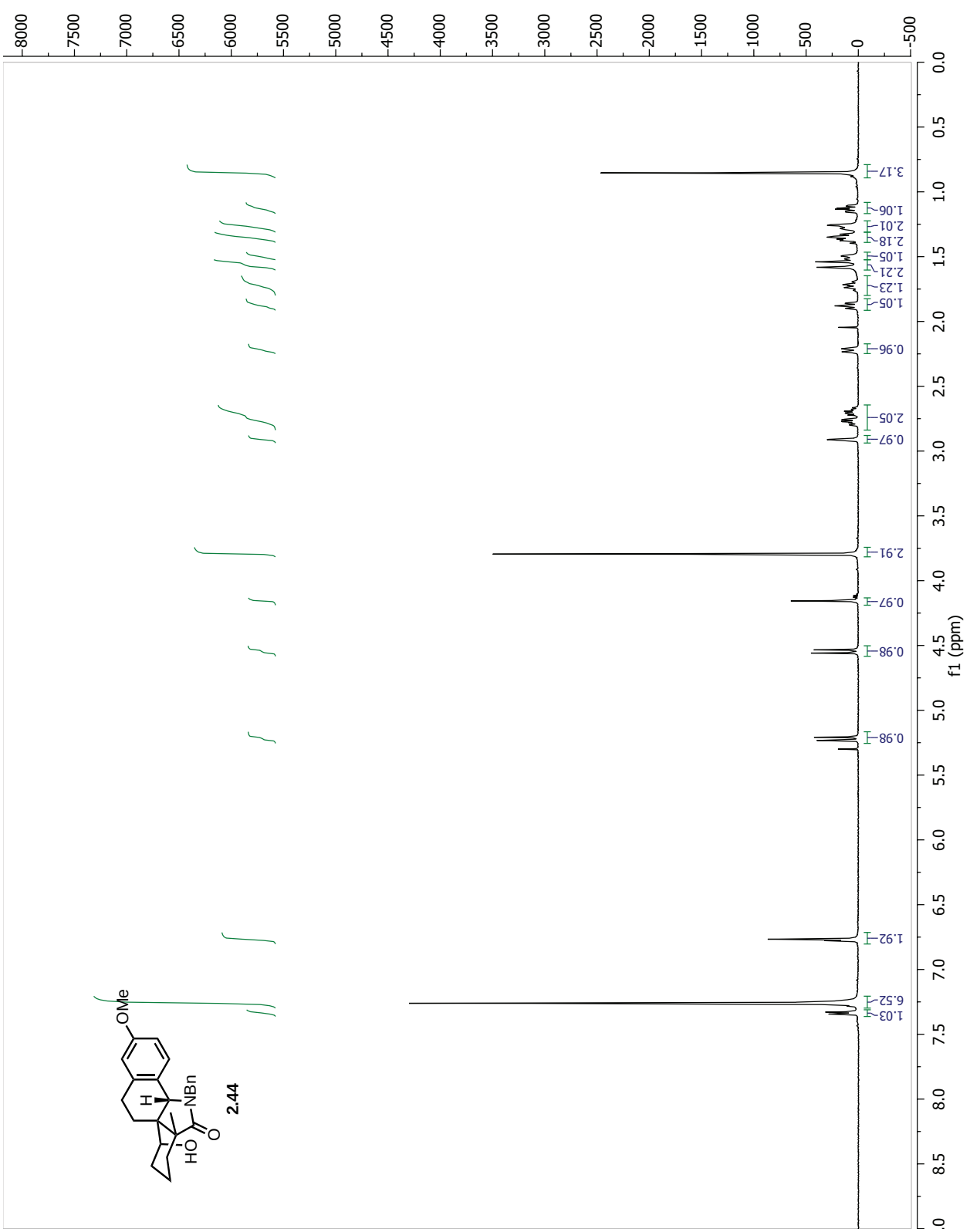

Figure 2.33: ^{1}H NMR of **2.44**

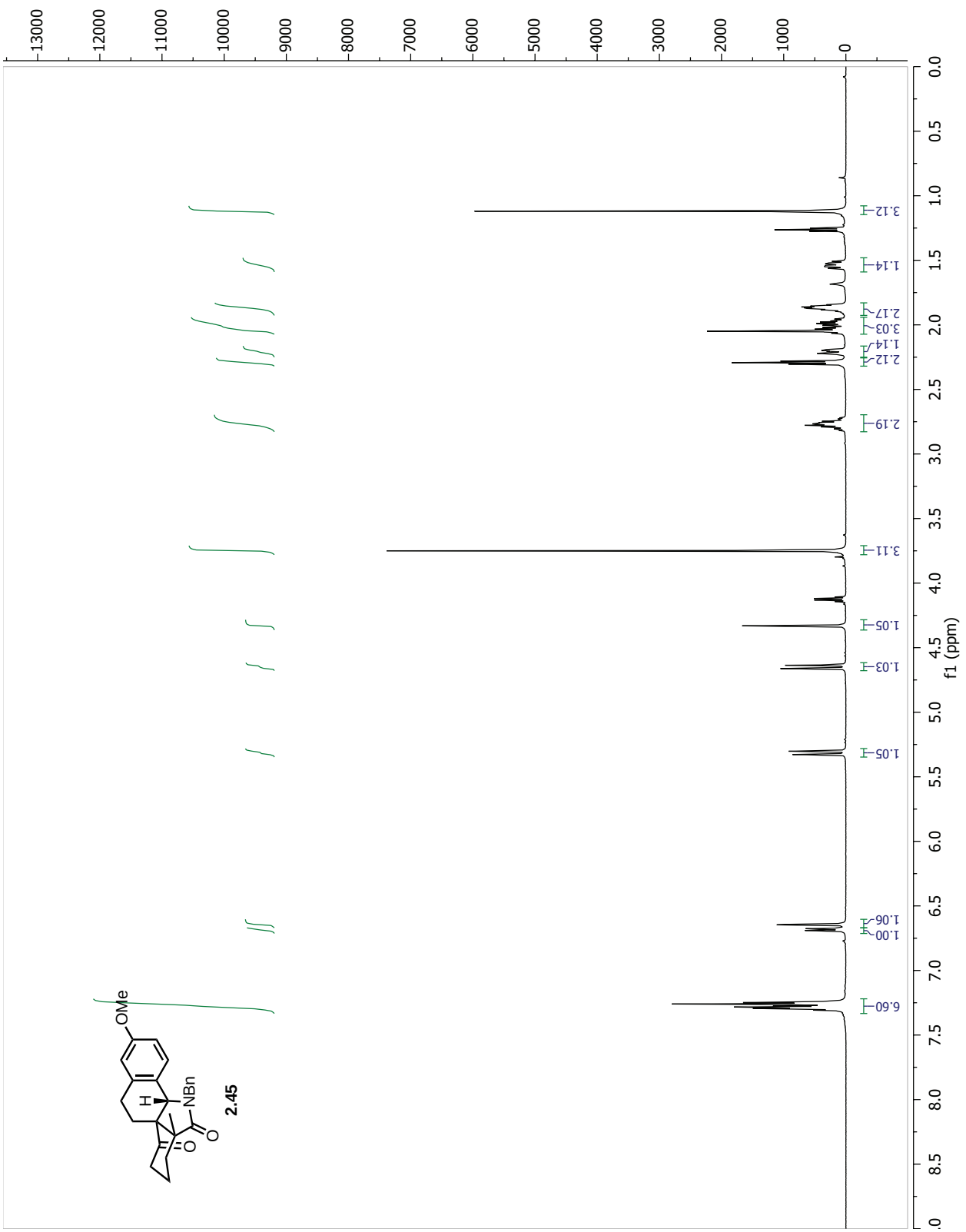

Figure 2.34: ^{1}H NMR of **2.45**

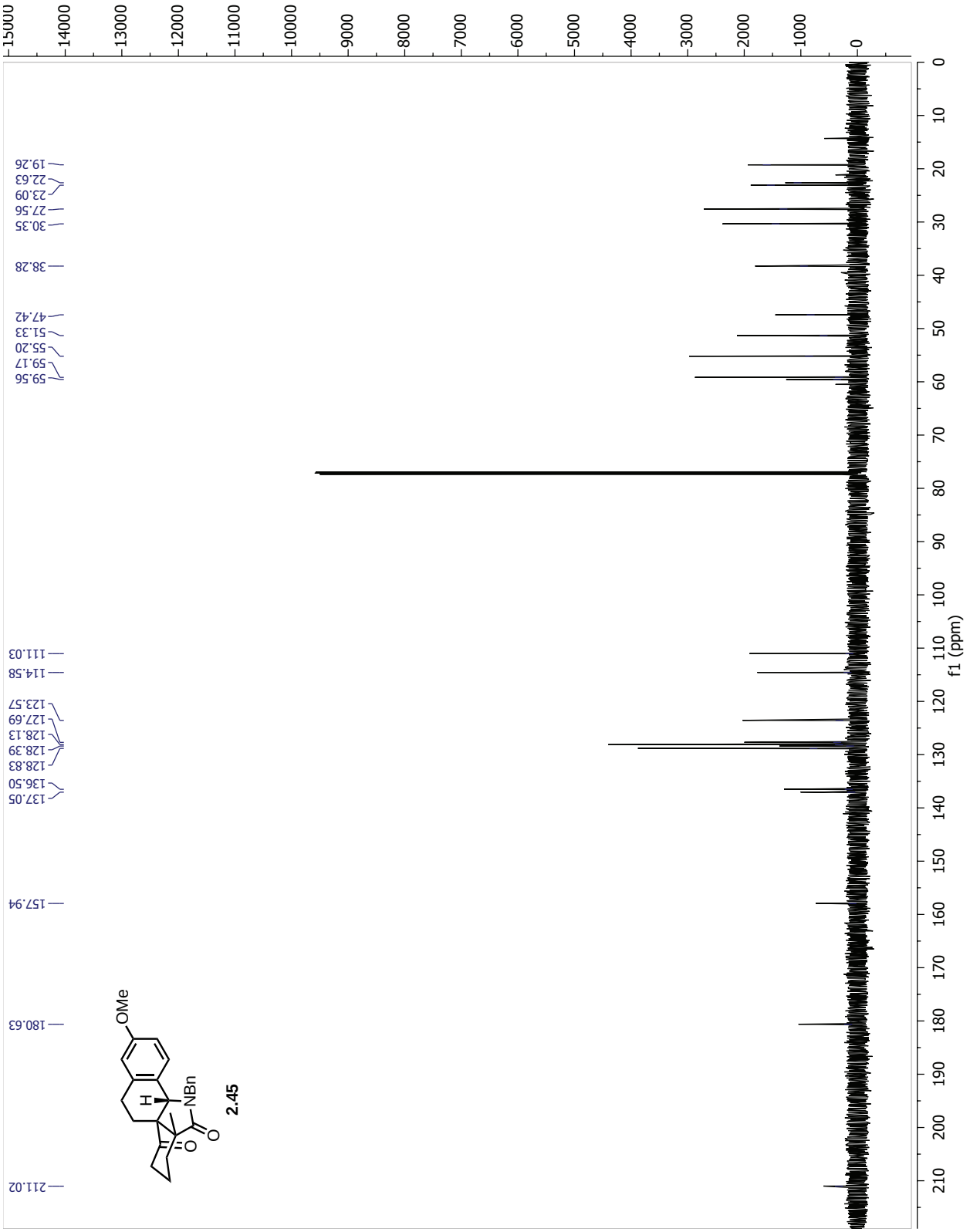

Figure 2.35: ^{1}H NMR of **2.45**

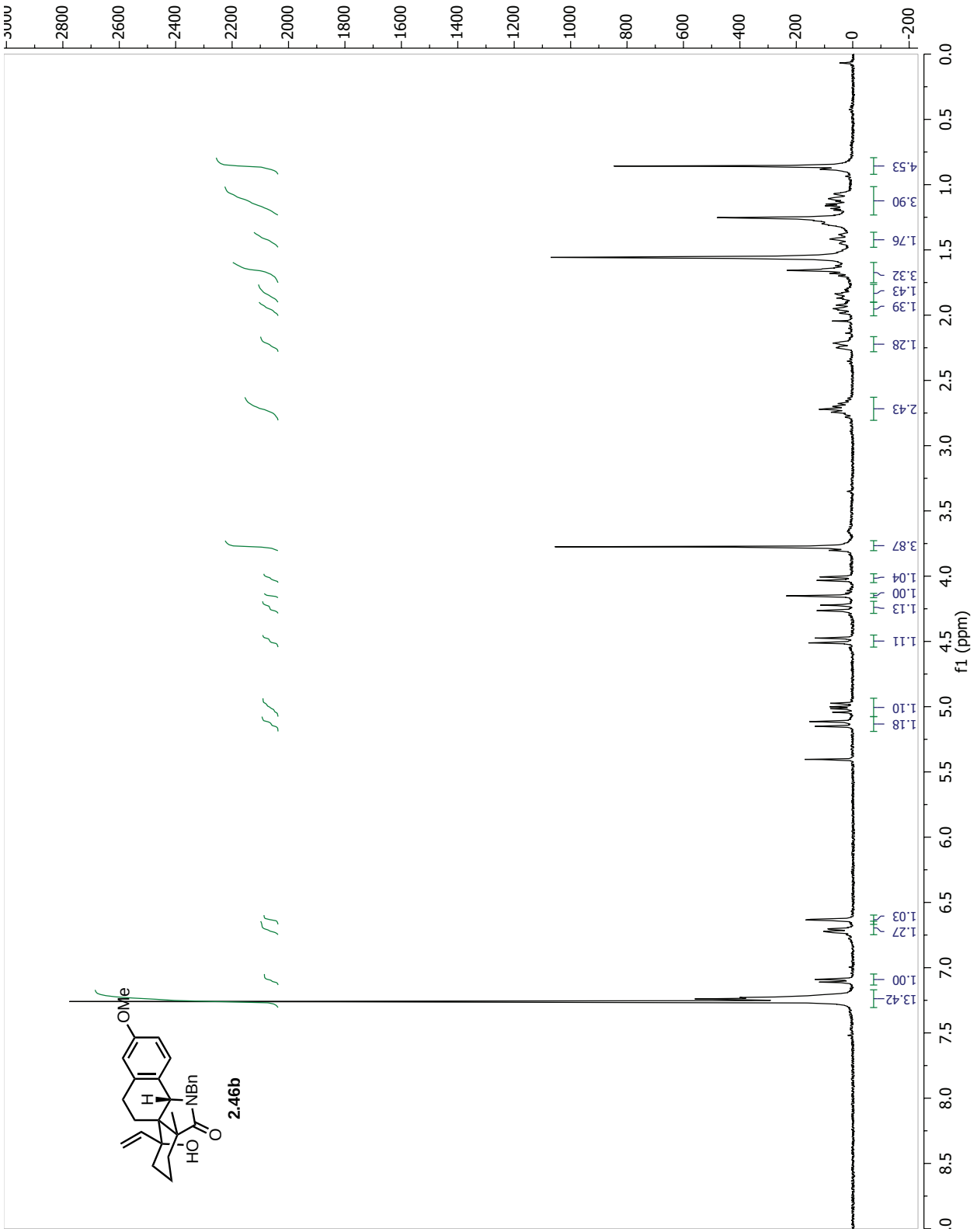

Figure 2.36: ^{1}H NMR of **2.46b**

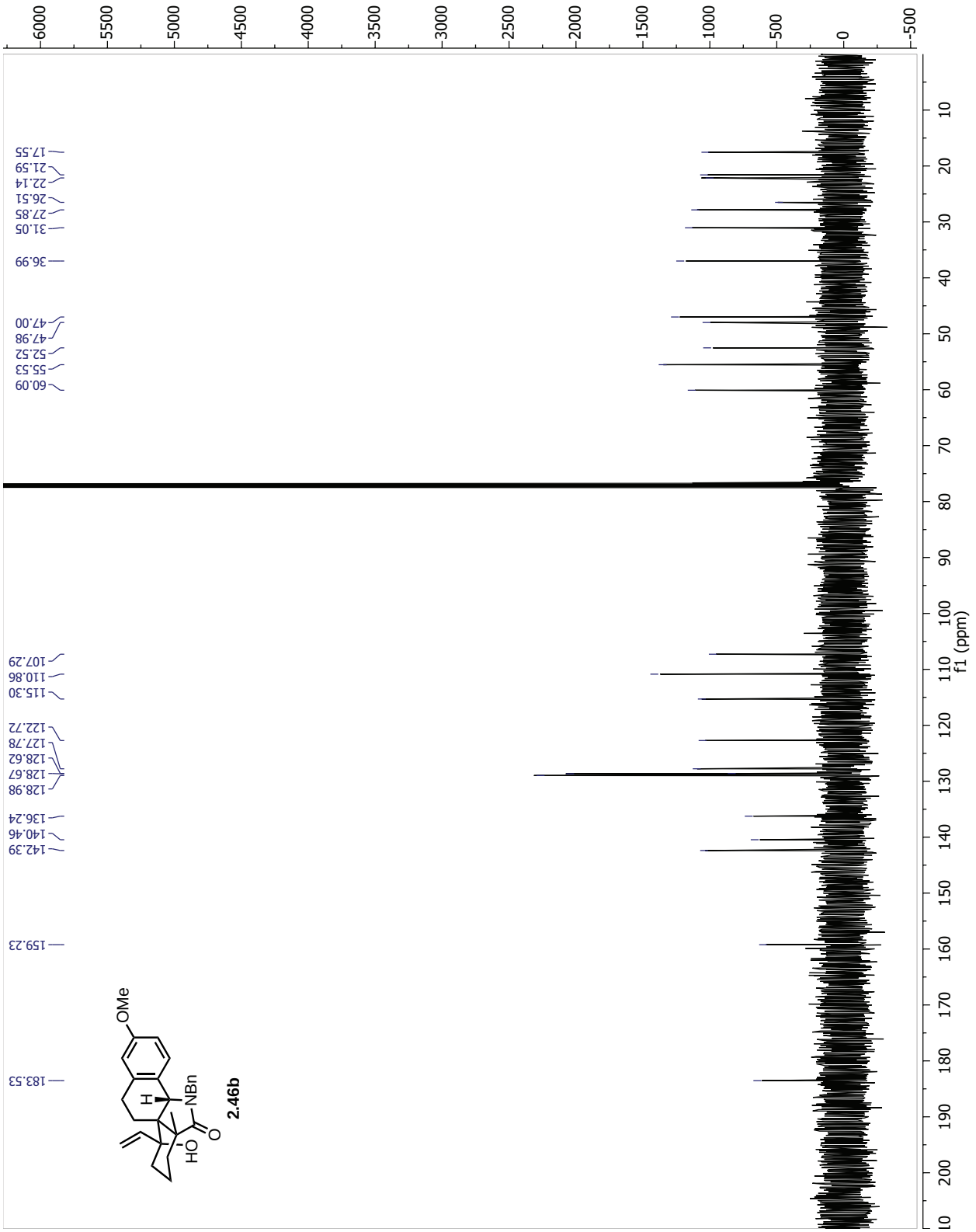

Figure 2.37: ^{13}C NMR of **2.46b**

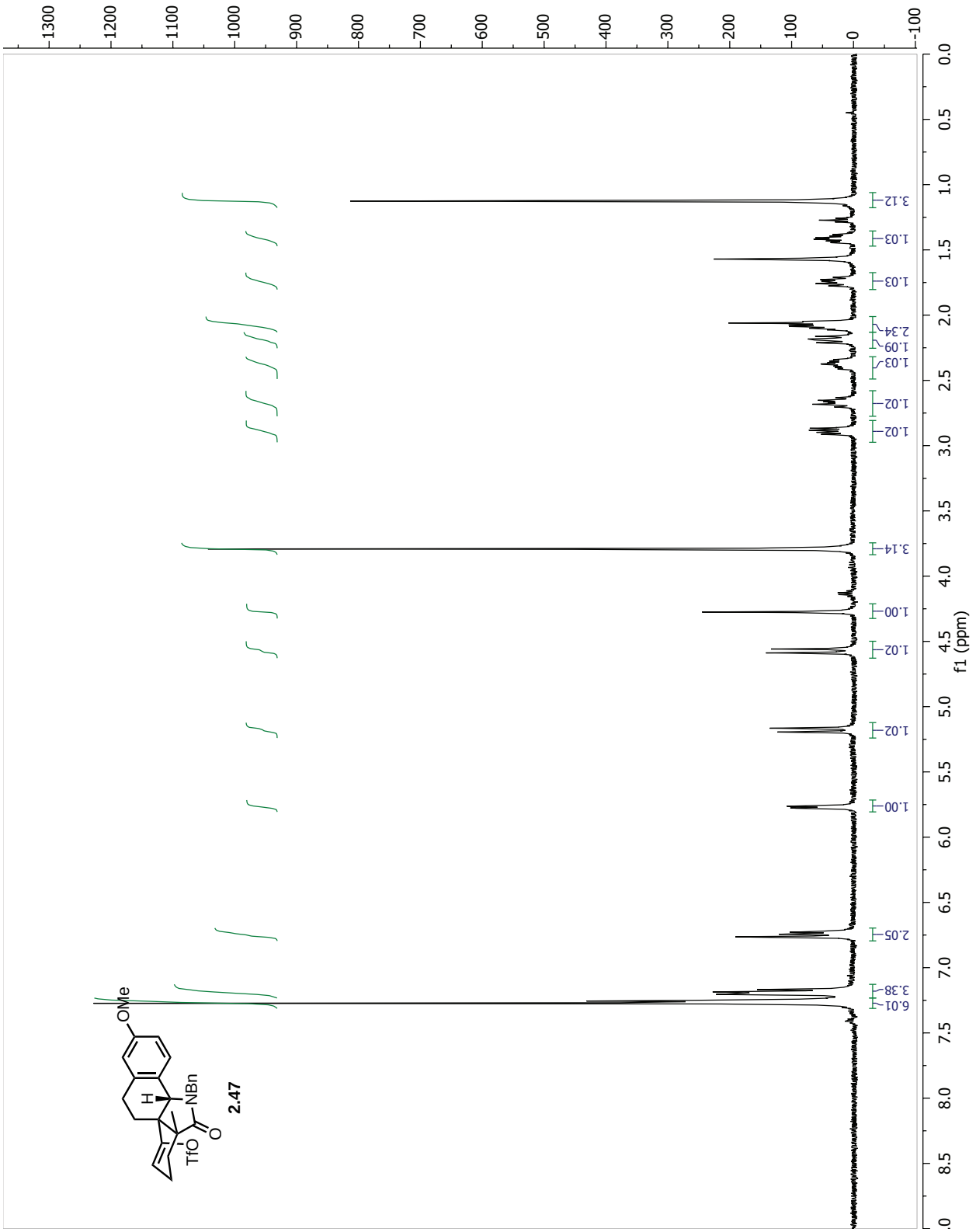

Figure 2.38: ^{1}H NMR of **2.47**

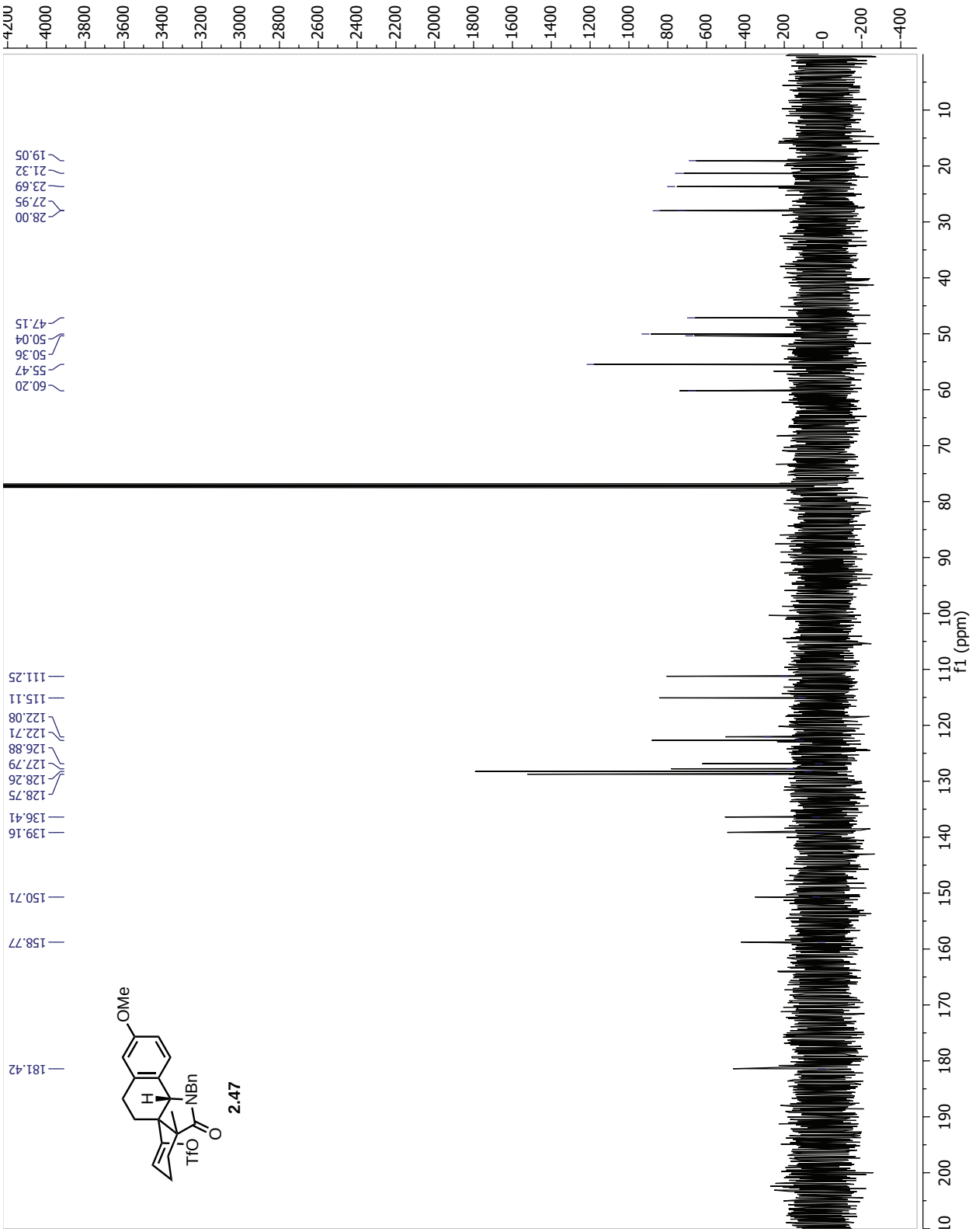

Figure 2.39: ^{13}C NMR of **2.47**

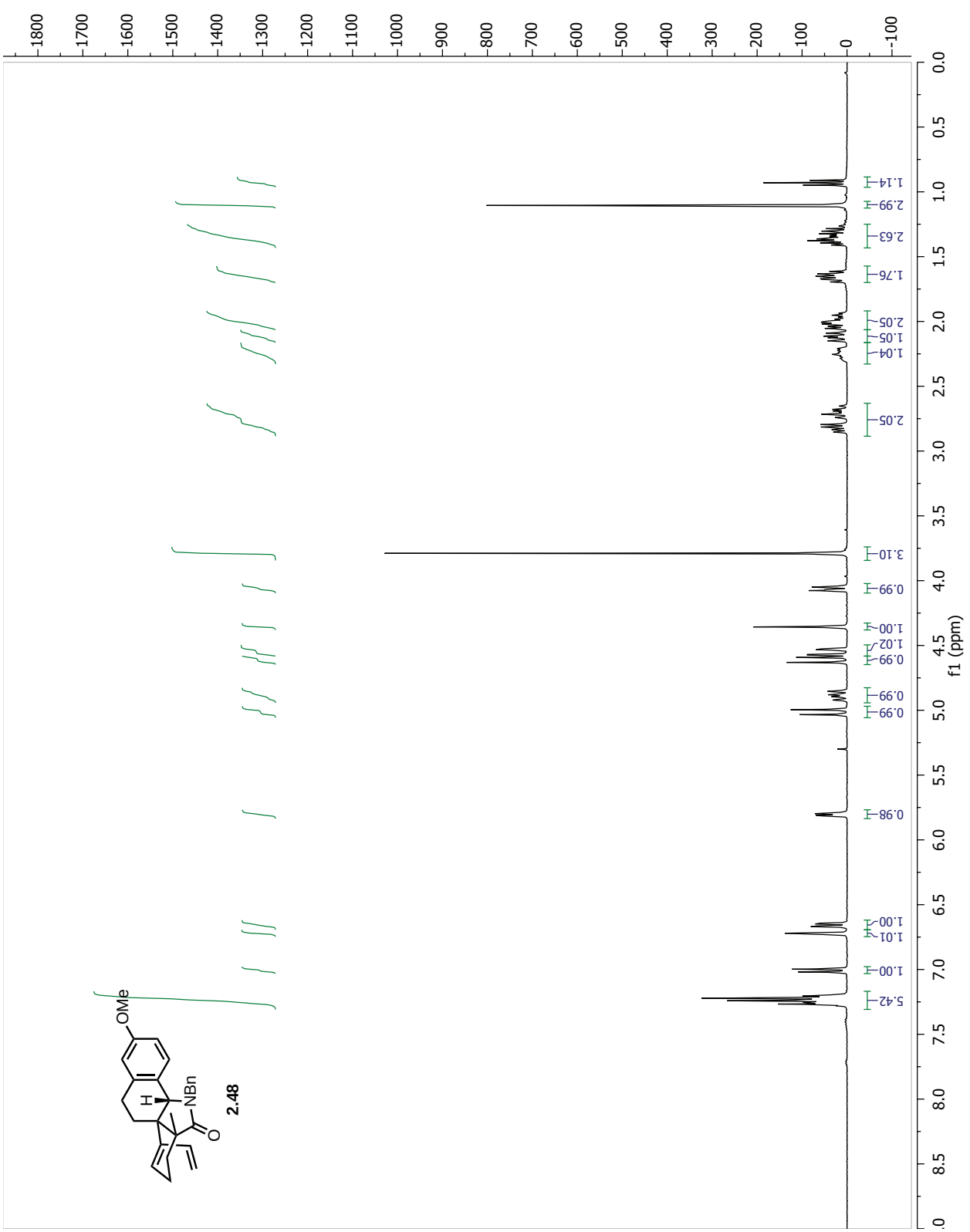

Figure 2.40: ^{1}H NMR of **2.48**

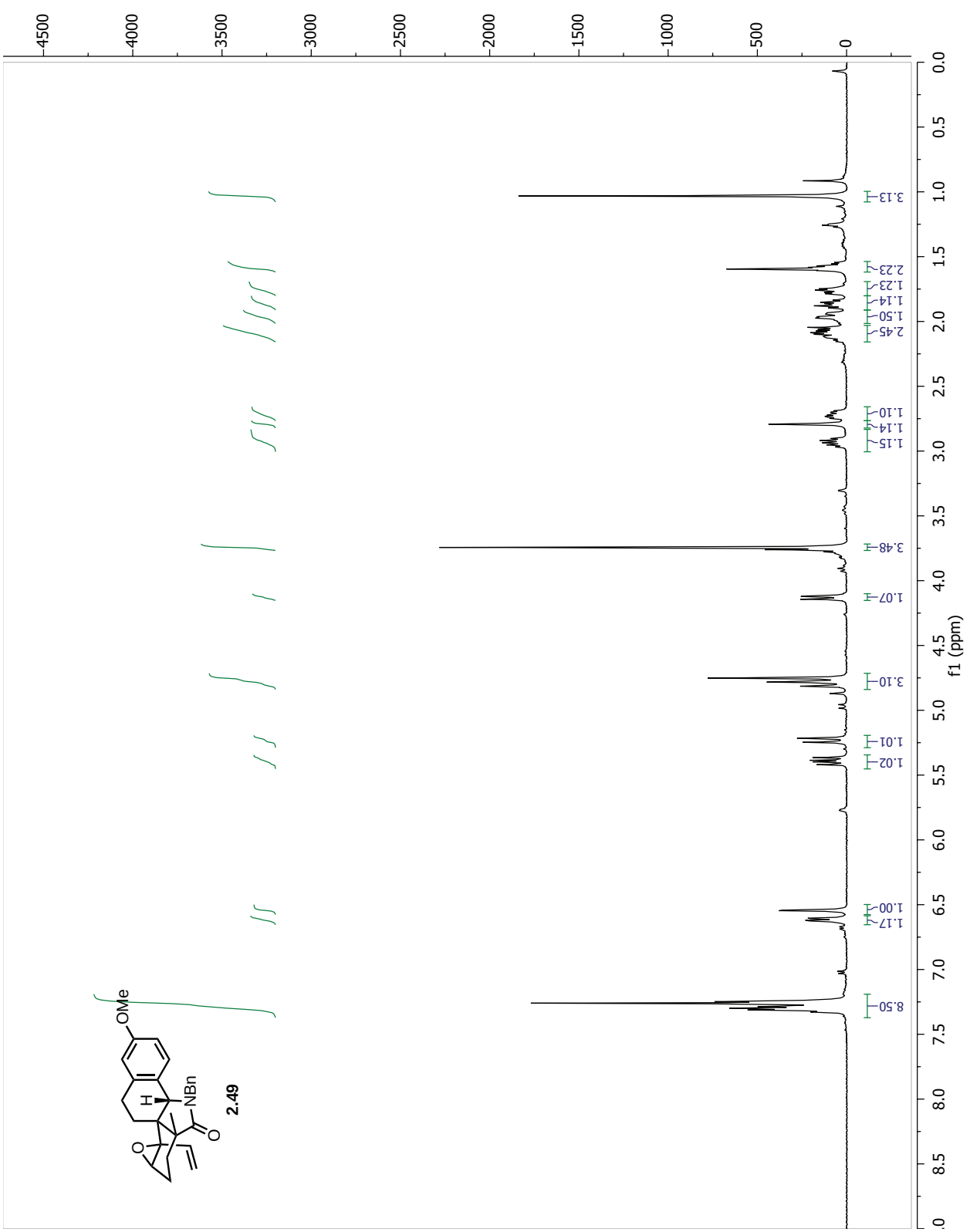

Figure 2.41: ^{1}H NMR of **2.49**

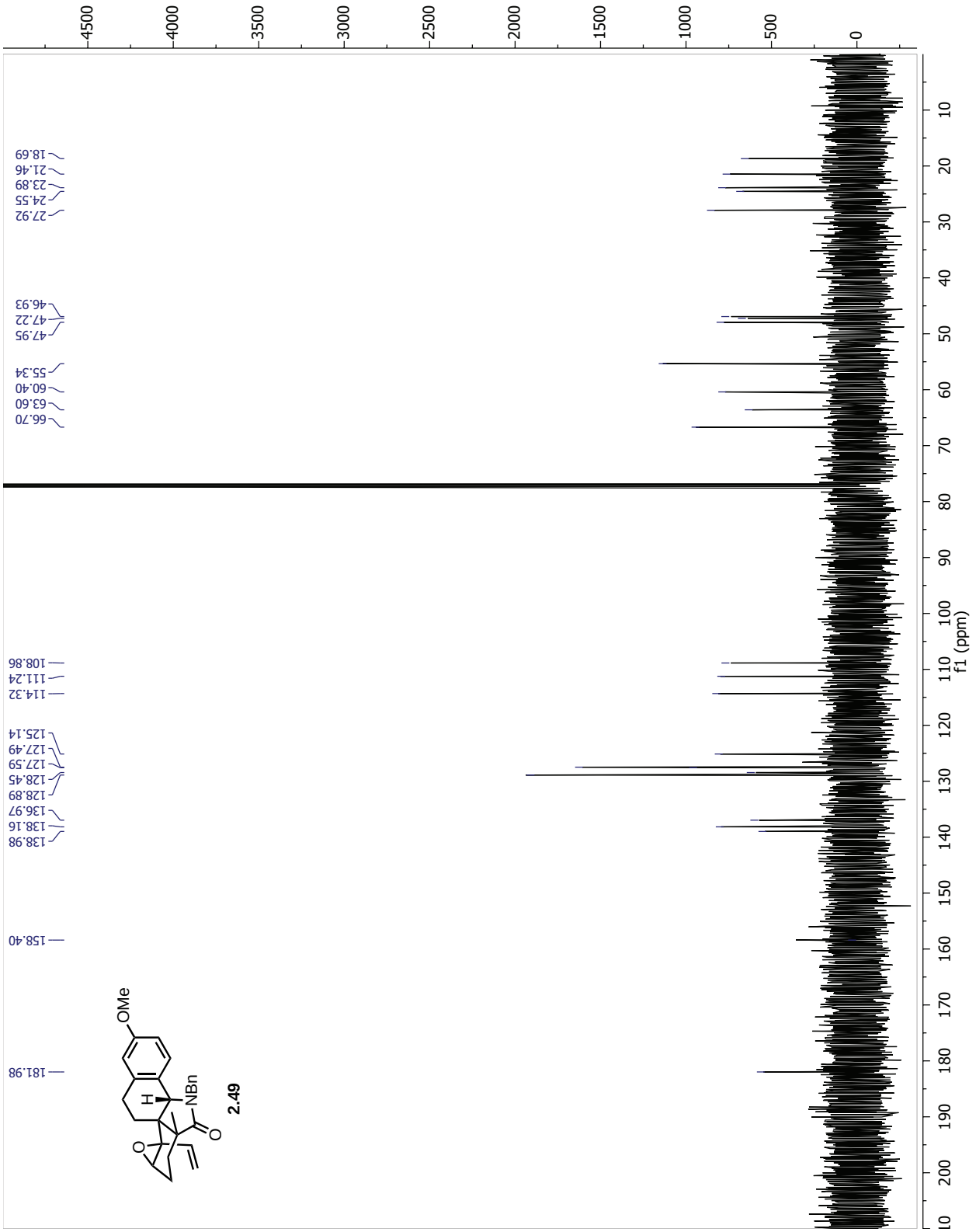

Figure 2.42: ^{13}C NMR of **2.49**

2.B X-ray Crystallography Data for Chapter 2

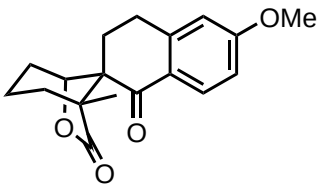

2.34a

A colorless plate 0.090 x 0.060 x 0.030 mm in size was mounted on a Cryoloop with Paratone oil. Data were collected in a nitrogen gas stream at 100(2) K using phi and omega scans. Crystal-to-detector distance was 50 mm and exposure time was 10 seconds per frame using a scan width of 1.0°. Data collection was 99.9% complete to 25.000° in θ. A total of 15628 reflections were collected covering the indices, -8<=h<=8, -11<=k<=11, -25<=l<=25. 2739 reflections were found to be symmetry independent, with an Rint of 0.0531. Indexing and unit cell refinement indicated a primitive, monoclinic lattice. The space group was found to be P 21/c (No. 14). The data were integrated using the Bruker SAINT software program and scaled using the SADABS software program. Solution by iterative methods (SHELXT) produced a complete heavy-atom phasing model consistent with the proposed structure. All non-hydrogen atoms were refined anisotropically by full-matrix least-squares (SHELXL-2014). All hydrogen atoms were placed using a riding model. Their positions were constrained relative to their parent atom using the appropriate HFIX command in SHELXL-2014.

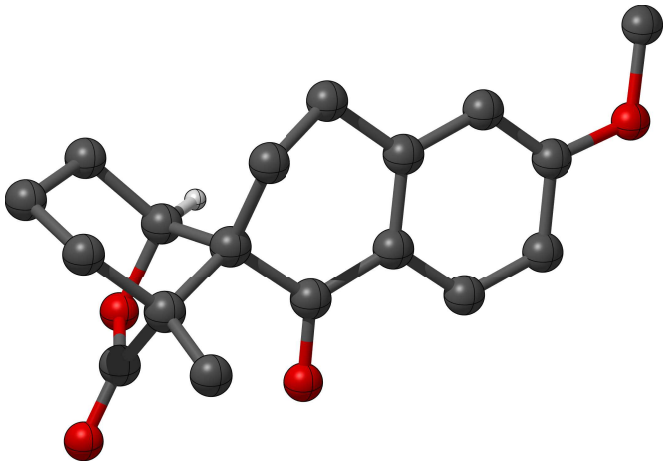

Table 2.2: Crystal data and structure refinement for **2.34a**.

X-ray ID	sarpong108	
Sample/notebook ID	kro3-160	
Empirical formula	C18 H20 O4	
Formula weight	300.34	
Temperature	100(2) K	
Wavelength	0.71073 Å	
Crystal system	Monoclinic	
Space group	P 21/c	
Unit cell dimensions	a = 7.2426(7) Å	a= 90°.
	b = 9.7698(10) Å	b= 92.020(2)°.
	c = 21.177(2) Å	g = 90°.
Volume	1497.5(3) Å3	
Z	4	
Density (calculated)	1.332 Mg/m^3	
Absorption coefficient	0.093 mm^{-1}	
F(000)	640	
Crystal size	0.090 x 0.060 x 0.030 mm^3	
Theta range for data collection	1.925 to 25.386°.	
Index ranges	-8<=h<=8, -11<=k<=11, -25<=l<=25	
Reflections collected	15628	
Independent reflections	2739 [R(int) = 0.0531]	
Completeness to theta = 25.000°	99.90%	
Absorption correction	Semi-empirical from equivalents	
Max. and min. transmission	0.928 and 0.711	
Refinement method	Full-matrix least-squares on F2	
Data / restraints / parameters	2739 / 0 / 201	
Goodness-of-fit on F2	1.083	
Final R indices [I>2sigma(I)]	R1 = 0.0495, wR2 = 0.1187	
R indices (all data)	R1 = 0.0627, wR2 = 0.1316	
Extinction coefficient	n/a	
Largest diff. peak and hole	0.352 and -0.238 e.$Å^{-3}$	

Table 2.3: Atomic coordinates (x 10^4) and equivalent isotropic displacement parameters (Å^{2}x 10^3) for sarpong108. U(eq) is defined as one third of the trace of the orthogonalized U^{ij} tensor.

	x	y	z	U(eq)
C(1)	6927(2)	1333(2)	3526(1)	22(1)
C(2)	5130(2)	1392(2)	3887(1)	23(1)
C(3)	4395(2)	2741(2)	4060(1)	21(1)
C(4)	2729(2)	2808(2)	4376(1)	24(1)
C(5)	1997(2)	4037(2)	4553(1)	25(1)
C(6)	2924(2)	5250(2)	4413(1)	22(1)
C(7)	4579(2)	5210(2)	4101(1)	22(1)
C(8)	5320(2)	3961(2)	3925(1)	22(1)
C(9)	7118(2)	3914(2)	3591(1)	26(1)
C(10)	8128(2)	2564(2)	3709(1)	25(1)
C(11)	2990(3)	7692(2)	4457(1)	26(1)
C(12)	6348(3)	1219(2)	2815(1)	30(1)
C(13)	7994(3)	1372(2)	2396(1)	36(1)
C(14)	9419(3)	250(2)	2531(1)	40(1)
C(15)	9697(3)	-88(2)	3237(1)	31(1)
C(16)	7872(3)	-88(2)	3601(1)	25(1)
C(17)	6542(3)	-972(2)	3213(1)	29(1)
C(18)	8227(3)	-616(2)	4270(1)	29(1)
O(1)	4295(2)	333(1)	4008(1)	33(1)
O(2)	2094(2)	6425(1)	4602(1)	28(1)
O(3)	5666(2)	-192(1)	2760(1)	34(1)
O(4)	6301(2)	-2189(1)	3244(1)	35(1)

Table 2.4: Bond lengths [Å] for sarpong108.

C(1)-C(10)	1.527(3)	C(11)-H(11A)	0.98
C(1)-C(2)	1.533(2)	C(11)-H(11B)	0.98
C(1)-C(16)	1.553(2)	C(11)-H(11C)	0.98
C(1)-C(12)	1.554(2)	C(12)-O(3)	1.467(2)
C(2)-O(1)	1.230(2)	C(12)-C(13)	1.519(3)
C(2)-C(3)	1.473(2)	C(12)-H(12)	1
C(3)-C(4)	1.401(2)	C(13)-C(14)	1.526(3)
C(3)-C(8)	1.402(2)	C(13)-H(13A)	0.99
C(4)-C(5)	1.371(3)	C(13)-H(13B)	0.99
C(4)-H(4)	0.95	C(14)-C(15)	1.538(3)
C(5)-C(6)	1.398(3)	C(14)-H(14A)	0.99
C(5)-H(5)	0.95	C(14)-H(14B)	0.99
C(6)-O(2)	1.363(2)	C(15)-C(16)	1.553(3)

C(6)-C(7)	1.390(2)	C(15)-H(15A)	0.99
C(7)-C(8)	1.390(2)	C(15)-H(15B)	0.99
C(7)-H(7)	0.95	C(16)-C(17)	1.514(3)
C(8)-C(9)	1.504(2)	C(16)-C(18)	1.520(2)
C(9)-C(10)	1.524(3)	C(17)-O(4)	1.204(2)
C(9)-H(9A)	0.99	C(17)-O(3)	1.364(2)
C(9)-H(9B)	0.99	C(18)-H(18A)	0.98
C(10)-H(10A)	0.99	C(18)-H(18B)	0.98
C(10)-H(10B)	0.99	C(18)-H(18C)	0.98
C(11)-O(2)	1.436(2)		

Table 2.5: Bond angles [°] for sarpong108.

C(10)-C(1)-C(2)	109.32(14)	H(11A)-C(11)-H(11C)	109.5
C(10)-C(1)-C(16)	115.68(15)	H(11B)-C(11)-H(11C)	109.5
C(2)-C(1)-C(16)	111.22(14)	O(3)-C(12)-C(13)	108.41(16)
C(10)-C(1)-C(12)	115.69(15)	O(3)-C(12)-C(1)	102.84(14)
C(2)-C(1)-C(12)	106.32(14)	C(13)-C(12)-C(1)	111.67(16)
C(16)-C(1)-C(12)	97.90(14)	O(3)-C(12)-H(12)	111.2
O(1)-C(2)-C(3)	121.07(16)	C(13)-C(12)-H(12)	111.2
O(1)-C(2)-C(1)	120.32(16)	C(1)-C(12)-H(12)	111.2
C(3)-C(2)-C(1)	118.57(15)	C(12)-C(13)-C(14)	111.04(16)
C(4)-C(3)-C(8)	118.92(16)	C(12)-C(13)-H(13A)	109.4
C(4)-C(3)-C(2)	119.02(16)	C(14)-C(13)-H(13A)	109.4
C(8)-C(3)-C(2)	122.05(15)	C(12)-C(13)-H(13B)	109.4
C(5)-C(4)-C(3)	121.29(16)	C(14)-C(13)-H(13B)	109.4
C(5)-C(4)-H(4)	119.4	H(13A)-C(13)-H(13B)	108
C(3)-C(4)-H(4)	119.4	C(13)-C(14)-C(15)	113.69(16)
C(4)-C(5)-C(6)	119.42(16)	C(13)-C(14)-H(14A)	108.8
C(4)-C(5)-H(5)	120.3	C(15)-C(14)-H(14A)	108.8
C(6)-C(5)-H(5)	120.3	C(13)-C(14)-H(14B)	108.8
O(2)-C(6)-C(7)	124.04(16)	C(15)-C(14)-H(14B)	108.8
O(2)-C(6)-C(5)	115.59(15)	H(14A)-C(14)-H(14B)	107.7
C(7)-C(6)-C(5)	120.37(16)	C(14)-C(15)-C(16)	113.43(17)
C(8)-C(7)-C(6)	119.99(16)	C(14)-C(15)-H(15A)	108.9
C(8)-C(7)-H(7)	120	C(16)-C(15)-H(15A)	108.9
C(6)-C(7)-H(7)	120	C(14)-C(15)-H(15B)	108.9
C(7)-C(8)-C(3)	120.00(15)	C(16)-C(15)-H(15B)	108.9
C(7)-C(8)-C(9)	120.13(16)	H(15A)-C(15)-H(15B)	107.7
C(3)-C(8)-C(9)	119.87(16)	C(17)-C(16)-C(18)	113.25(16)
C(8)-C(9)-C(10)	111.60(15)	C(17)-C(16)-C(15)	105.52(15)
C(8)-C(9)-H(9A)	109.3	C(18)-C(16)-C(15)	110.08(15)
C(10)-C(9)-H(9A)	109.3	C(17)-C(16)-C(1)	100.65(14)

C(8)-C(9)-H(9B)	109.3	C(18)-C(16)-C(1)	117.20(15)
C(10)-C(9)-H(9B)	109.3	C(15)-C(16)-C(1)	109.24(15)
H(9A)-C(9)-H(9B)	108	O(4)-C(17)-O(3)	121.67(17)
C(9)-C(10)-C(1)	112.00(15)	O(4)-C(17)-C(16)	128.68(18)
C(9)-C(10)-H(10A)	109.2	O(3)-C(17)-C(16)	109.50(16)
C(1)-C(10)-H(10A)	109.2	C(16)-C(18)-H(18A)	109.5
C(9)-C(10)-H(10B)	109.2	C(16)-C(18)-H(18B)	109.5
C(1)-C(10)-H(10B)	109.2	H(18A)-C(18)-H(18B)	109.5
H(10A)-C(10)-H(10B)	107.9	C(16)-C(18)-H(18C)	109.5
O(2)-C(11)-H(11A)	109.5	H(18A)-C(18)-H(18C)	109.5
O(2)-C(11)-H(11B)	109.5	H(18B)-C(18)-H(18C)	109.5
H(11A)-C(11)-H(11B)	109.5	C(6)-O(2)-C(11)	117.11(13)
O(2)-C(11)-H(11C)	109.5	C(17)-O(3)-C(12)	108.82(14)

Table 2.6: Anisotropic displacement parameters ($Å^2$x 10^3)for sarpong108. The anisotropic displacement factor exponent takes the form: -2$\sqrt{}$2[$h^2a^{*2}U^{11}$ + ... + 2 h k a* b* U^{12}]

	U^{11}	U^{22}	U^{33}	U^{23}	U^{13}	U^{12}
C(1)	24(1)	21(1)	21(1)	1(1)	0(1)	1(1)
C(2)	24(1)	21(1)	25(1)	3(1)	-4(1)	-1(1)
C(3)	21(1)	20(1)	22(1)	2(1)	-1(1)	1(1)
C(4)	25(1)	21(1)	26(1)	3(1)	1(1)	-4(1)
C(5)	22(1)	26(1)	28(1)	1(1)	5(1)	0(1)
C(6)	23(1)	20(1)	23(1)	-1(1)	-2(1)	2(1)
C(7)	24(1)	18(1)	23(1)	2(1)	-1(1)	-2(1)
C(8)	22(1)	23(1)	20(1)	2(1)	-1(1)	-1(1)
C(9)	26(1)	23(1)	29(1)	0(1)	5(1)	-3(1)
C(10)	25(1)	24(1)	26(1)	-1(1)	3(1)	0(1)
C(11)	29(1)	19(1)	31(1)	-2(1)	2(1)	0(1)
C(12)	39(1)	24(1)	26(1)	4(1)	-6(1)	-2(1)
C(13)	54(1)	34(1)	21(1)	1(1)	2(1)	-5(1)
C(14)	55(1)	37(1)	29(1)	-4(1)	15(1)	2(1)
C(15)	33(1)	27(1)	33(1)	-5(1)	5(1)	5(1)
C(16)	29(1)	22(1)	24(1)	-1(1)	1(1)	3(1)
C(17)	36(1)	27(1)	23(1)	-2(1)	0(1)	1(1)
C(18)	34(1)	27(1)	26(1)	0(1)	-5(1)	6(1)
O(1)	31(1)	21(1)	47(1)	5(1)	7(1)	-2(1)
O(2)	29(1)	20(1)	36(1)	-2(1)	8(1)	1(1)
O(3)	46(1)	27(1)	27(1)	2(1)	-10(1)	-6(1)
O(4)	51(1)	22(1)	31(1)	-3(1)	0(1)	-5(1)

Table 2.7: Hydrogen coordinates (x 10^4) and isotropic displacement parameters ($Å^2$x 10^3) for sarpong108.

	x	y	z	U(eq)
H(4)	2095	1985	4468	29
H(5)	871	4065	4769	30
H(7)	5203	6037	4008	26
H(9A)	7914	4680	3741	31
H(9B)	6873	4034	3132	31
H(10A)	8506	2498	4161	30
H(10B)	9261	2548	3460	30
H(11A)	4241	7697	4649	39
H(11B)	2282	8457	4624	39
H(11C)	3058	7786	3997	39
H(12)	5355	1893	2697	35
H(13A)	8572	2279	2469	43
H(13B)	7568	1325	1947	43
H(14A)	10617	541	2364	48
H(14B)	9026	-590	2303	48
H(15A)	10555	591	3434	37
H(15B)	10283	-1000	3280	37
H(18A)	7092	-540	4506	43
H(18B)	9205	-71	4479	43
H(18C)	8611	-1577	4254	43

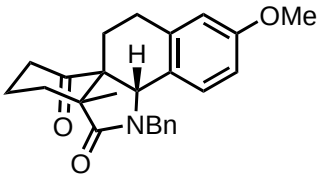

2.45

A colorless blade 0.060 x 0.040 x 0.030 mm in size was mounted on a Cryoloop with Paratone oil. Data were collected in a nitrogen gas stream at 100(2) K using and scans. Crystal-to-detector distance was 60 mm and exposure time was 10 seconds per frame using a scan width of 2.0°. Data collection was 97.9% complete to 67.000°in θ. A total of 16629 reflections were collected covering the indices, -9<=h<=11, -12<=k<=12, -14<=l<=14. 3427 reflections were found to be symmetry independent, with an Rint of 0.0234. Indexing and unit cell refinement indicated a primitive, triclinic lattice. The space group was found to be P -1 (No. 2). The data were integrated using the Bruker SAINT software program and scaled using the SADABS software program. Solution by iterative methods (SHELXT-2014) produced a complete heavy-atom phasing model consistent with the proposed structure. All non-hydrogen atoms were refined anisotropically by full-matrix least-squares (SHELXL-2014). All hydrogen atoms were placed using a riding model. Their positions were constrained relative to their parent atom using the appropriate HFIX command in SHELXL-2014.

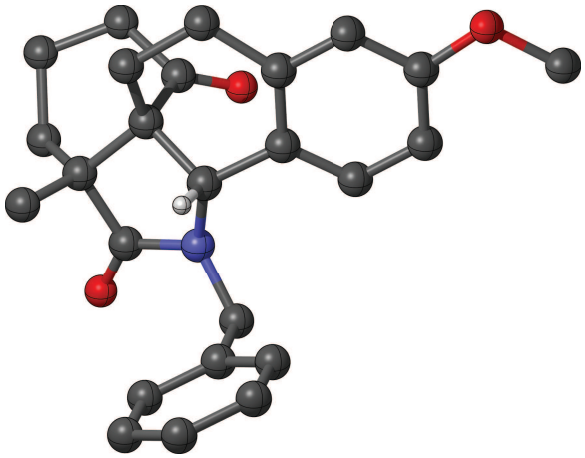

Table 2.8: Crystal data and structure refinement for **2.45**.

X-ray ID	sarpong122	
Sample/notebook ID	kro4.185	
Empirical formula	C25 H27 N O3	
Formula weight	389.47	
Temperature	100(2) K	
Wavelength	1.54178 Å	
Crystal system	Triclinic	
Space group	P -1	
Unit cell dimensions	a = 9.1549(6) Å	a= 98.346(2)°.
	b = 10.0413(6) Å	b= 91.324(2)°.
	c = 11.6705(7) Å	g = 114.6290(10)°.
Volume	960.73(10) Å3	
Z	2	
Density (calculated)	1.346 Mg/m3	
Absorption coefficient	0.697 mm^{-1}	
F(000)	416	
Crystal size	0.060 x 0.040 x 0.030 mm^3	
Theta range for data collection	3.845 to 68.319°.	
Index ranges	-9<=h<=11, -12<=k<=12, -14<=l<=14	
Reflections collected	16629	
Independent reflections	3427 [R(int) = 0.0234]	
Completeness to theta = 67.000°	97.90%	
Absorption correction	Semi-empirical from equivalents	
Max. and min. transmission	0.929 and 0.878	
Refinement method	Full-matrix least-squares on F2	
Data / restraints / parameters	3427 / 0 / 271	
Goodness-of-fit on F2	1.054	
Final R indices [I>2sigma(I)]	R1 = 0.0382, wR2 = 0.0972	
R indices (all data)	R1 = 0.0387, wR2 = 0.0975	
Extinction coefficient	n/a	
Largest diff. peak and hole	0.341 and -0.332 e.$Å^{-3}$	

Table 2.9: Atomic coordinates (x 10^4) and equivalent isotropic displacement parameters (Å^{2}x 10^3) for sarpong122. U(eq) is defined as one third of the trace of the orthogonalized U^{ij} tensor.

	x	y	z	U(eq)
C(1)	2482(2)	6363(1)	3038(1)	20(1)
C(2)	2084(2)	7712(1)	3200(1)	22(1)
C(3)	2279(2)	8360(1)	4499(1)	23(1)
C(4)	3589(1)	8232(1)	5242(1)	19(1)
C(5)	3820(1)	8849(1)	6413(1)	20(1)
C(6)	4906(2)	8701(1)	7179(1)	20(1)
C(7)	5770(2)	7903(1)	6768(1)	20(1)
C(8)	5542(2)	7283(1)	5596(1)	20(1)
C(9)	4479(1)	7440(1)	4814(1)	18(1)
C(10)	4253(1)	6918(1)	3509(1)	18(1)
C(11)	3719(2)	5001(1)	1941(1)	24(1)
C(12)	2453(2)	5589(1)	1778(1)	23(1)
C(13)	846(6)	4122(5)	1352(4)	25(1)
C(14)	-569(3)	4339(3)	1843(2)	28(1)
C(13A)	778(6)	4575(5)	1188(4)	25(1)
C(14A)	-315(3)	3532(3)	1950(2)	28(1)
C(15)	-405(2)	4450(2)	3136(1)	28(1)
C(16)	1319(2)	5132(1)	3654(1)	22(1)
C(17)	6229(2)	9331(2)	9099(1)	26(1)
C(18)	3099(2)	6691(2)	929(1)	31(1)
C(19)	6312(2)	5805(2)	3052(1)	24(1)
C(20)	7509(2)	7210(2)	2688(1)	23(1)
C(21)	8505(2)	8434(2)	3501(1)	28(1)
C(22)	9564(2)	9736(2)	3149(1)	33(1)
C(23)	9639(2)	9820(2)	1980(1)	34(1)
C(24)	8658(2)	8605(2)	1162(1)	35(1)
C(25)	7592(2)	7312(2)	1509(1)	29(1)
N(1)	4664(1)	5714(1)	2967(1)	21(1)
O(1)	5028(1)	9370(1)	8313(1)	24(1)
O(2)	3903(1)	4074(1)	1230(1)	37(1)
O(3)	1758(1)	4636(1)	4414(1)	30(1)

Table 2.10: Bond lengths [Å] for sarpong122.

C(1)-C(2)	1.5313(17)	C(14)-H(14B)	0.99
C(1)-C(10)	1.5352(17)	C(13A)-C(14A)	1.525(5)
C(1)-C(16)	1.5409(17)	C(13A)-H(13C)	0.99
C(1)-C(12)	1.5543(16)	C(13A)-H(13D)	0.99

C(2)-C(3)	1.5363(17)	C(14A)-C(15)	1.572(3)
C(2)-H(2A)	0.99	C(14A)-H(14C)	0.99
C(2)-H(2B)	0.99	C(14A)-H(14D)	0.99
C(3)-C(4)	1.5229(17)	C(15)-C(16)	1.5033(18)
C(3)-H(3A)	0.99	C(15)-H(15A)	0.99
C(3)-H(3B)	0.99	C(15)-H(15B)	0.99
C(4)-C(5)	1.3889(17)	C(16)-O(3)	1.2147(16)
C(4)-C(9)	1.4096(17)	C(17)-O(1)	1.4318(15)
C(5)-C(6)	1.3892(18)	C(17)-H(17A)	0.98
C(5)-H(5)	0.95	C(17)-H(17B)	0.98
C(6)-O(1)	1.3736(14)	C(17)-H(17C)	0.98
C(6)-C(7)	1.3899(18)	C(18)-H(18A)	0.98
C(7)-C(8)	1.3908(17)	C(18)-H(18B)	0.98
C(7)-H(7)	0.95	C(18)-H(18C)	0.98
C(8)-C(9)	1.3903(17)	C(19)-N(1)	1.4727(16)
C(8)-H(8)	0.95	C(19)-C(20)	1.5098(19)
C(9)-C(10)	1.5174(16)	C(19)-H(19A)	0.99
C(10)-N(1)	1.4734(15)	C(19)-H(19B)	0.99
C(10)-H(10)	1	C(20)-C(21)	1.3890(19)
C(11)-O(2)	1.2238(16)	C(20)-C(25)	1.3961(18)
C(11)-N(1)	1.3718(16)	C(21)-C(22)	1.392(2)
C(11)-C(12)	1.5243(18)	C(21)-H(21)	0.95
C(12)-C(13A)	1.519(5)	C(22)-C(23)	1.381(2)
C(12)-C(18)	1.5348(18)	C(22)-H(22)	0.95
C(12)-C(13)	1.590(5)	C(23)-C(24)	1.384(2)
C(13)-C(14)	1.512(6)	C(23)-H(23)	0.95
C(13)-H(13A)	0.99	C(24)-C(25)	1.384(2)
C(13)-H(13B)	0.99	C(24)-H(24)	0.95
C(14)-C(15)	1.497(3)	C(25)-H(25)	0.95
C(14)-H(14A)	0.99		

Table 2.11: Bond lengths [°] for sarpong122.

C(2)-C(1)-C(10)	107.04(10)	C(13)-C(14)-H(14B)	109.9
C(2)-C(1)-C(16)	110.69(10)	H(14A)-C(14)-H(14B)	108.3
C(10)-C(1)-C(16)	112.65(10)	C(12)-C(13A)-C(14A)	113.9(3)
C(2)-C(1)-C(12)	118.18(10)	C(12)-C(13A)-H(13C)	108.8
C(10)-C(1)-C(12)	102.54(10)	C(14A)-C(13A)-H(13C)	108.8
C(16)-C(1)-C(12)	105.64(10)	C(12)-C(13A)-H(13D)	108.8
C(1)-C(2)-C(3)	109.79(10)	C(14A)-C(13A)-H(13D)	108.8
C(1)-C(2)-H(2A)	109.7	H(13C)-C(13A)-H(13D)	107.7
C(3)-C(2)-H(2A)	109.7	C(13A)-C(14A)-C(15)	110.0(3)
C(1)-C(2)-H(2B)	109.7	C(13A)-C(14A)-H(14C)	109.7

C(3)-C(2)-H(2B)	109.7	C(15)-C(14A)-H(14C)	109.7
H(2A)-C(2)-H(2B)	108.2	C(13A)-C(14A)-H(14D)	109.7
C(4)-C(3)-C(2)	116.13(10)	C(15)-C(14A)-H(14D)	109.7
C(4)-C(3)-H(3A)	108.3	H(14C)-C(14A)-H(14D)	108.2
C(2)-C(3)-H(3A)	108.3	C(14)-C(15)-C(16)	113.37(14)
C(4)-C(3)-H(3B)	108.3	C(16)-C(15)-C(14A)	101.87(14)
C(2)-C(3)-H(3B)	108.3	C(14)-C(15)-H(15A)	108.9
H(3A)-C(3)-H(3B)	107.4	C(16)-C(15)-H(15A)	108.9
C(5)-C(4)-C(9)	119.51(11)	C(14)-C(15)-H(15B)	108.9
C(5)-C(4)-C(3)	117.13(11)	C(16)-C(15)-H(15B)	108.9
C(9)-C(4)-C(3)	123.22(11)	H(15A)-C(15)-H(15B)	107.7
C(4)-C(5)-C(6)	121.50(11)	O(3)-C(16)-C(15)	121.72(12)
C(4)-C(5)-H(5)	119.3	O(3)-C(16)-C(1)	123.64(12)
C(6)-C(5)-H(5)	119.3	C(15)-C(16)-C(1)	114.23(10)
O(1)-C(6)-C(5)	115.80(11)	O(1)-C(17)-H(17A)	109.5
O(1)-C(6)-C(7)	124.82(11)	O(1)-C(17)-H(17B)	109.5
C(5)-C(6)-C(7)	119.37(11)	H(17A)-C(17)-H(17B)	109.5
C(6)-C(7)-C(8)	119.29(11)	O(1)-C(17)-H(17C)	109.5
C(6)-C(7)-H(7)	120.4	H(17A)-C(17)-H(17C)	109.5
C(8)-C(7)-H(7)	120.4	H(17B)-C(17)-H(17C)	109.5
C(9)-C(8)-C(7)	122.08(11)	C(12)-C(18)-H(18A)	109.5
C(9)-C(8)-H(8)	119	C(12)-C(18)-H(18B)	109.5
C(7)-C(8)-H(8)	119	H(18A)-C(18)-H(18B)	109.5
C(8)-C(9)-C(4)	118.24(11)	C(12)-C(18)-H(18C)	109.5
C(8)-C(9)-C(10)	125.85(11)	H(18A)-C(18)-H(18C)	109.5
C(4)-C(9)-C(10)	115.79(10)	H(18B)-C(18)-H(18C)	109.5
N(1)-C(10)-C(9)	122.23(10)	N(1)-C(19)-C(20)	111.36(10)
N(1)-C(10)-C(1)	102.38(9)	N(1)-C(19)-H(19A)	109.4
C(9)-C(10)-C(1)	111.09(10)	C(20)-C(19)-H(19A)	109.4
N(1)-C(10)-H(10)	106.7	N(1)-C(19)-H(19B)	109.4
C(9)-C(10)-H(10)	106.7	C(20)-C(19)-H(19B)	109.4
C(1)-C(10)-H(10)	106.7	H(19A)-C(19)-H(19B)	108
O(2)-C(11)-N(1)	125.28(12)	C(21)-C(20)-C(25)	118.66(13)
O(2)-C(11)-C(12)	124.43(12)	C(21)-C(20)-C(19)	121.59(11)
N(1)-C(11)-C(12)	110.22(10)	C(25)-C(20)-C(19)	119.71(12)
C(13A)-C(12)-C(11)	121.15(19)	C(20)-C(21)-C(22)	120.74(13)
C(13A)-C(12)-C(18)	101.30(18)	C(20)-C(21)-H(21)	119.6
C(11)-C(12)-C(18)	105.80(10)	C(22)-C(21)-H(21)	119.6
C(13A)-C(12)-C(1)	114.8(2)	C(23)-C(22)-C(21)	119.97(13)
C(11)-C(12)-C(1)	100.95(9)	C(23)-C(22)-H(22)	120
C(18)-C(12)-C(1)	112.94(11)	C(21)-C(22)-H(22)	120
C(11)-C(12)-C(13)	103.42(18)	C(22)-C(23)-C(24)	119.78(14)
C(18)-C(12)-C(13)	117.47(19)	C(22)-C(23)-H(23)	120.1
C(1)-C(12)-C(13)	113.9(2)	C(24)-C(23)-H(23)	120.1
C(14)-C(13)-C(12)	109.0(3)	C(23)-C(24)-C(25)	120.39(13)

C(14)-C(13)-H(13A)	109.9	C(23)-C(24)-H(24)	119.8
C(12)-C(13)-H(13A)	109.9	C(25)-C(24)-H(24)	119.8
C(14)-C(13)-H(13B)	109.9	C(24)-C(25)-C(20)	120.45(13)
C(12)-C(13)-H(13B)	109.9	C(24)-C(25)-H(25)	119.8
H(13A)-C(13)-H(13B)	108.3	C(20)-C(25)-H(25)	119.8
C(15)-C(14)-C(13)	108.7(3)	C(11)-N(1)-C(19)	117.58(10)
C(15)-C(14)-H(14A)	109.9	C(11)-N(1)-C(10)	110.11(10)
C(13)-C(14)-H(14A)	109.9	C(19)-N(1)-C(10)	123.17(10)
C(15)-C(14)-H(14B)	109.9	C(6)-O(1)-C(17)	116.80(9)

Table 2.12: Anisotropic displacement parameters ($Å^2$x 10^3)for sarpong122. The anisotropic displacement factor exponent takes the form: -2$\sqrt{}$2[$h^2a^{*2}U^{11}$ + ... + 2 h k a* b* U^{12}]

	U11	U22	U33	U23	U13	U12
C(1)	19(1)	22(1)	17(1)	3(1)	0(1)	7(1)
C(2)	20(1)	25(1)	22(1)	6(1)	1(1)	11(1)
C(3)	22(1)	25(1)	24(1)	2(1)	1(1)	13(1)
C(4)	16(1)	17(1)	21(1)	4(1)	2(1)	5(1)
C(5)	18(1)	18(1)	24(1)	3(1)	4(1)	7(1)
C(6)	19(1)	18(1)	18(1)	2(1)	4(1)	5(1)
C(7)	20(1)	23(1)	19(1)	5(1)	1(1)	10(1)
C(8)	20(1)	21(1)	21(1)	3(1)	3(1)	10(1)
C(9)	17(1)	16(1)	19(1)	3(1)	2(1)	5(1)
C(10)	20(1)	18(1)	19(1)	4(1)	2(1)	9(1)
C(11)	34(1)	20(1)	18(1)	4(1)	0(1)	12(1)
C(12)	23(1)	26(1)	17(1)	4(1)	1(1)	8(1)
C(13)	28(1)	21(2)	20(2)	2(1)	-3(1)	6(2)
C(14)	27(1)	25(1)	26(1)	2(1)	-3(1)	6(1)
C(13A)	28(1)	21(2)	20(2)	2(1)	-3(1)	6(2)
C(14A)	27(1)	25(1)	26(1)	2(1)	-3(1)	6(1)
C(15)	22(1)	29(1)	28(1)	7(1)	2(1)	5(1)
C(16)	24(1)	23(1)	18(1)	3(1)	2(1)	7(1)
C(17)	29(1)	31(1)	18(1)	0(1)	0(1)	16(1)
C(18)	47(1)	39(1)	22(1)	13(1)	9(1)	29(1)
C(19)	30(1)	30(1)	19(1)	3(1)	2(1)	20(1)
C(20)	24(1)	32(1)	20(1)	2(1)	3(1)	20(1)
C(21)	26(1)	41(1)	21(1)	0(1)	3(1)	19(1)
C(22)	25(1)	36(1)	35(1)	-4(1)	2(1)	14(1)
C(23)	27(1)	37(1)	42(1)	12(1)	8(1)	16(1)
C(24)	33(1)	49(1)	27(1)	12(1)	5(1)	19(1)
C(25)	30(1)	37(1)	20(1)	2(1)	1(1)	15(1)
N(1)	26(1)	21(1)	17(1)	1(1)	1(1)	13(1)
O(1)	26(1)	30(1)	17(1)	-1(1)	0(1)	14(1)

Table 2.12: Anisotropic displacement parameters ($Å^2$x 10^3)for sarpong122. The anisotropic displacement factor exponent takes the form: -2$\sqrt{}$2[$h^2a^{*2}U^{11}$ + ... + 2 h k a* b* U^{12}]

	U11	U22	U33	U23	U13	U12
O(2)	63(1)	33(1)	22(1)	-5(1)	-8(1)	32(1)
O(3)	29(1)	32(1)	26(1)	12(1)	1(1)	8(1)

Table 2.13: Hydrogen coordinates (x 10^4) and isotropic displacement parameters ($Å^2$x 10^3) for sarpong122.

	x	y	z	U(eq)
H(2A)	962	7410	2876	26
H(2B)	2816	8477	2776	26
H(3A)	2510	9425	4573	28
H(3B)	1236	7855	4823	28
H(5)	3220	9385	6698	24
H(7)	6509	7783	7283	25
H(8)	6132	6734	5320	24
H(10)	4888	7808	3150	22
H(13A)	687	3916	492	30
H(13B)	930	3264	1622	30
H(14A)	-586	5257	1643	34
H(14B)	-1592	3488	1505	34
H(13C)	885	3972	473	30
H(13D)	258	5195	953	30
H(14C)	114	2810	2101	34
H(14D)	-1410	2969	1542	34
H(15A)	-962	3442	3333	33
H(15B)	-951	5055	3491	33
H(17A)	6003	8296	9135	38
H(17B)	6208	9845	9875	38
H(17C)	7296	9826	8824	38
H(18A)	3234	6172	189	47
H(18B)	4143	7490	1260	47
H(18C)	2333	7116	795	47
H(19A)	6333	4932	2548	29
H(19B)	6626	5781	3863	29
H(21)	8462	8380	4307	34
H(22)	10236	10568	3714	39
H(23)	10360	10708	1738	40
H(24)	8717	8658	357	42

Table 2.13: Hydrogen coordinates (x 10^4) and isotropic displacement parameters (Å^{2}x 10^3) for sarpong122.

	x	y	z	U(eq)
H(25)	6913	6489	941	35

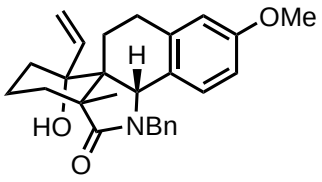

2.46b

A colorless prism 0.050 x 0.040 x 0.040 mm in size was mounted on a Cryoloop with Paratone oil. Data were collected in a nitrogen gas stream at 100(2) K using and scans. Crystal-to-detector distance was 60 mm and exposure time was 5 seconds per frame using a scan width of 2.0°. Data collection was 98.5% complete to 67.000°in θ. A total of 36493 reflections were collected covering the indices, -10<=h<=10, -14<=k<=14, -12<=l<=14. 3978 reflections were found to be symmetry independent, with an Rint of 0.0430. Indexing and unit cell refinement indicated a primitive, triclinic lattice. The space group was found to be P -1 (No. 2). The data were integrated using the Bruker SAINT software program and scaled using the SADABS software program. Solution by iterative methods (SHELXT-2014) produced a complete heavy-atom phasing model consistent with the proposed structure. All non-hydrogen atoms were refined anisotropically by full-matrix least-squares (SHELXL-2014). All hydrogen atoms were placed using a riding model. Their positions were constrained relative to their parent atom using the appropriate HFIX command in SHELXL-2014.

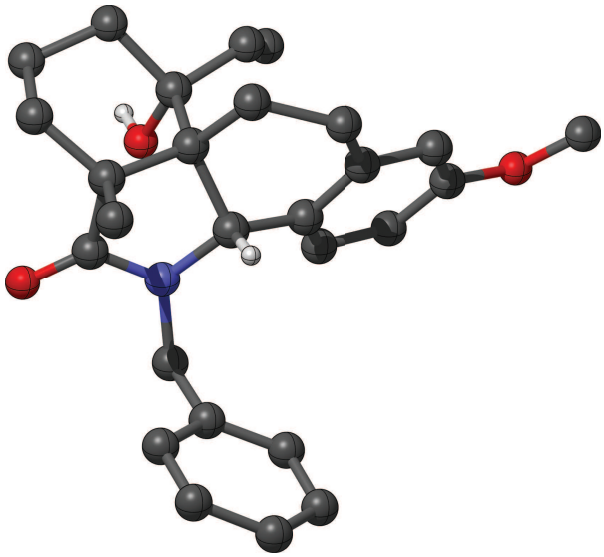

Table 2.14: Crystal data and structure refinement for **2.46b**.

X-ray ID	sarpong131	
Sample/notebook ID	kro6.008a	
Empirical formula	C27 H31 N O3	
Formula weight	417.53	
Temperature	100(2) K	
Wavelength	1.54178 Å	
Crystal system	Triclinic	
Space group	P -1	
Unit cell dimensions	a = 8.6339(5) Å	a= 67.177(2)°.
	b = 11.8023(7) Å	b= 79.596(3)°.
	c = 12.0475(7) Å	g = 78.562(3)°.
Volume	1101.73(11) Å3	
Z	2	
Density (calculated)	1.259 Mg/m^3	
Absorption coefficient	0.641 mm^{-1}	
F(000)	448	
Crystal size	0.050 x 0.040 x 0.040 mm^3	
Theta range for data collection	4.007 to 68.264°.	
Index ranges	-10<=h<=10, -14<=k<=14, -12<=l<=14	
Reflections collected	36493	
Independent reflections	3978 [R(int) = 0.0430]	
Completeness to theta = 67.000°	98.50%	
Absorption correction	Semi-empirical from equivalents	
Max. and min. transmission	0.929 and 0.858	
Refinement method	Full-matrix least-squares on F2	
Data / restraints / parameters	3978 / 0 / 283	
Goodness-of-fit on F2	1.037	
Final R indices [I>2sigma(I)]	R1 = 0.0420, wR2 = 0.1088	
R indices (all data)	R1 = 0.0449, wR2 = 0.1119	
Extinction coefficient	n/a	
Largest diff. peak and hole	0.480 and -0.254 $e.Å^{-3}$	

Table 2.15: Atomic coordinates (x 10^4) and equivalent isotropic displacement parameters (Å^{2}x 10^3) for sarpong131. U(eq) is defined as one third of the trace of the orthogonalized U^{ij} tensor.

	x	y	z	U(eq)
C(1)	5587(2)	2885(1)	7167(1)	24(1)
C(2)	6574(2)	2461(1)	6208(1)	27(1)
C(3)	8021(2)	1688(1)	6280(1)	31(1)
C(4)	8776(2)	1395(2)	5293(2)	37(1)
C(5)	8074(2)	1865(2)	4220(2)	37(1)
C(6)	6598(2)	2589(2)	4151(1)	35(1)
C(7)	5833(2)	2881(1)	5146(1)	31(1)
C(8)	4176(2)	3606(2)	5112(1)	39(1)
C(9)	3049(2)	3270(1)	6311(1)	31(1)
C(10)	3898(2)	2492(1)	7449(1)	24(1)
C(11)	3927(2)	1060(1)	7749(1)	26(1)
C(12)	2296(2)	672(2)	8426(1)	32(1)
C(13)	1956(2)	834(2)	9642(1)	33(1)
C(14)	1902(2)	2188(2)	9451(1)	32(1)
C(15)	3312(2)	2794(1)	8622(1)	26(1)
C(16)	4847(2)	2419(1)	9224(1)	23(1)
C(17)	8397(3)	2194(2)	2111(2)	51(1)
C(18)	4233(2)	651(1)	6666(1)	30(1)
C(19)	5327(2)	-297(2)	6591(2)	42(1)
C(20)	2903(2)	4203(1)	8374(1)	32(1)
C(21)	7633(2)	2730(1)	8554(1)	27(1)
C(22)	7869(2)	4086(1)	8002(1)	26(1)
C(23)	7025(2)	4925(2)	8529(1)	35(1)
C(24)	7259(2)	6165(2)	8046(2)	39(1)
C(25)	8363(2)	6575(2)	7037(2)	36(1)
C(26)	9195(2)	5754(2)	6503(1)	34(1)
C(27)	8928(2)	4522(1)	6974(1)	30(1)
N(1)	6103(1)	2530(1)	8359(1)	24(1)
O(1)	8923(2)	1537(1)	3281(1)	47(1)
O(2)	5118(1)	423(1)	8537(1)	26(1)
O(3)	4932(1)	2170(1)	10306(1)	27(1)

Table 2.16: Bond lengths [Å] for sarpong131.

C(1)-N(1)	1.4585(17)	C(14)-H(14A)	0.99
C(1)-C(2)	1.494(2)	C(14)-H(14B)	0.99
C(1)-C(10)	1.5572(18)	C(15)-C(16)	1.5313(19)
C(1)-H(1)	1	C(15)-C(20)	1.5493(19)

C(2)-C(3)	1.388(2)	C(16)-O(3)	1.2327(16)
C(2)-C(7)	1.403(2)	C(16)-N(1)	1.3493(18)
C(3)-C(4)	1.381(2)	C(17)-O(1)	1.427(2)
C(3)-H(3)	0.95	C(17)-H(17A)	0.98
C(4)-C(5)	1.393(2)	C(17)-H(17B)	0.98
C(4)-H(4)	0.95	C(17)-H(17C)	0.98
C(5)-O(1)	1.376(2)	C(18)-C(19)	1.334(2)
C(5)-C(6)	1.383(2)	C(18)-H(18)	0.95
C(6)-C(7)	1.392(2)	C(19)-H(19A)	0.95
C(6)-H(6)	0.95	C(19)-H(19B)	0.95
C(7)-C(8)	1.513(2)	C(20)-H(20A)	0.98
C(8)-C(9)	1.546(2)	C(20)-H(20B)	0.98
C(8)-H(8A)	0.99	C(20)-H(20C)	0.98
C(8)-H(8B)	0.99	C(21)-N(1)	1.4612(17)
C(9)-C(10)	1.5427(18)	C(21)-C(22)	1.5166(19)
C(9)-H(9A)	0.99	C(21)-H(21A)	0.99
C(9)-H(9B)	0.99	C(21)-H(21B)	0.99
C(10)-C(15)	1.5627(19)	C(22)-C(27)	1.385(2)
C(10)-C(11)	1.5807(19)	C(22)-C(23)	1.396(2)
C(11)-O(2)	1.4198(17)	C(23)-C(24)	1.390(2)
C(11)-C(18)	1.523(2)	C(23)-H(23)	0.95
C(11)-C(12)	1.552(2)	C(24)-C(25)	1.388(2)
C(12)-C(13)	1.519(2)	C(24)-H(24)	0.95
C(12)-H(12A)	0.99	C(25)-C(26)	1.382(2)
C(12)-H(12B)	0.99	C(25)-H(25)	0.95
C(13)-C(14)	1.517(2)	C(26)-C(27)	1.392(2)
C(13)-H(13A)	0.99	C(26)-H(26)	0.95
C(13)-H(13B)	0.99	C(27)-H(27)	0.95
C(14)-C(15)	1.531(2)	O(2)-H(2)	0.84

Table 2.17: Bond lengths [°] for sarpong131.

N(1)-C(1)-C(2)	121.80(12)	C(13)-C(14)-H(14A)	108.6
N(1)-C(1)-C(10)	104.06(10)	C(15)-C(14)-H(14A)	108.6
C(2)-C(1)-C(10)	111.11(11)	C(13)-C(14)-H(14B)	108.6
N(1)-C(1)-H(1)	106.3	C(15)-C(14)-H(14B)	108.6
C(2)-C(1)-H(1)	106.3	H(14A)-C(14)-H(14B)	107.6
C(10)-C(1)-H(1)	106.3	C(14)-C(15)-C(16)	113.82(12)
C(3)-C(2)-C(7)	119.29(14)	C(14)-C(15)-C(20)	106.66(12)
C(3)-C(2)-C(1)	128.33(13)	C(16)-C(15)-C(20)	103.42(11)
C(7)-C(2)-C(1)	112.29(13)	C(14)-C(15)-C(10)	117.44(12)
C(4)-C(3)-C(2)	120.53(15)	C(16)-C(15)-C(10)	101.21(11)
C(4)-C(3)-H(3)	119.7	C(20)-C(15)-C(10)	113.52(12)

C(2)-C(3)-H(3)	119.7	O(3)-C(16)-N(1)	124.94(13)
C(3)-C(4)-C(5)	119.91(16)	O(3)-C(16)-C(15)	125.80(13)
C(3)-C(4)-H(4)	120	N(1)-C(16)-C(15)	108.93(11)
C(5)-C(4)-H(4)	120	O(1)-C(17)-H(17A)	109.5
O(1)-C(5)-C(6)	123.92(16)	O(1)-C(17)-H(17B)	109.5
O(1)-C(5)-C(4)	115.80(16)	H(17A)-C(17)-H(17B)	109.5
C(6)-C(5)-C(4)	120.27(15)	O(1)-C(17)-H(17C)	109.5
C(5)-C(6)-C(7)	119.85(15)	H(17A)-C(17)-H(17C)	109.5
C(5)-C(6)-H(6)	120.1	H(17B)-C(17)-H(17C)	109.5
C(7)-C(6)-H(6)	120.1	C(19)-C(18)-C(11)	123.25(14)
C(6)-C(7)-C(2)	119.99(15)	C(19)-C(18)-H(18)	118.4
C(6)-C(7)-C(8)	120.48(14)	C(11)-C(18)-H(18)	118.4
C(2)-C(7)-C(8)	119.48(14)	C(18)-C(19)-H(19A)	120
C(7)-C(8)-C(9)	116.98(12)	C(18)-C(19)-H(19B)	120
C(7)-C(8)-H(8A)	108.1	H(19A)-C(19)-H(19B)	120
C(9)-C(8)-H(8A)	108.1	C(15)-C(20)-H(20A)	109.5
C(7)-C(8)-H(8B)	108.1	C(15)-C(20)-H(20B)	109.5
C(9)-C(8)-H(8B)	108.1	H(20A)-C(20)-H(20B)	109.5
H(8A)-C(8)-H(8B)	107.3	C(15)-C(20)-H(20C)	109.5
C(10)-C(9)-C(8)	114.12(12)	H(20A)-C(20)-H(20C)	109.5
C(10)-C(9)-H(9A)	108.7	H(20B)-C(20)-H(20C)	109.5
C(8)-C(9)-H(9A)	108.7	N(1)-C(21)-C(22)	112.70(11)
C(10)-C(9)-H(9B)	108.7	N(1)-C(21)-H(21A)	109.1
C(8)-C(9)-H(9B)	108.7	C(22)-C(21)-H(21A)	109.1
H(9A)-C(9)-H(9B)	107.6	N(1)-C(21)-H(21B)	109.1
C(9)-C(10)-C(1)	106.02(11)	C(22)-C(21)-H(21B)	109.1
C(9)-C(10)-C(15)	117.98(11)	H(21A)-C(21)-H(21B)	107.8
C(1)-C(10)-C(15)	99.10(10)	C(27)-C(22)-C(23)	118.38(14)
C(9)-C(10)-C(11)	110.22(11)	C(27)-C(22)-C(21)	121.19(13)
C(1)-C(10)-C(11)	113.34(11)	C(23)-C(22)-C(21)	120.43(13)
C(15)-C(10)-C(11)	109.78(11)	C(24)-C(23)-C(22)	120.89(15)
O(2)-C(11)-C(18)	109.89(12)	C(24)-C(23)-H(23)	119.6
O(2)-C(11)-C(12)	108.77(11)	C(22)-C(23)-H(23)	119.6
C(18)-C(11)-C(12)	106.08(11)	C(25)-C(24)-C(23)	119.86(15)
O(2)-C(11)-C(10)	106.43(10)	C(25)-C(24)-H(24)	120.1
C(18)-C(11)-C(10)	116.09(11)	C(23)-C(24)-H(24)	120.1
C(12)-C(11)-C(10)	109.43(12)	C(26)-C(25)-C(24)	119.71(14)
C(13)-C(12)-C(11)	111.88(12)	C(26)-C(25)-H(25)	120.1
C(13)-C(12)-H(12A)	109.2	C(24)-C(25)-H(25)	120.1
C(11)-C(12)-H(12A)	109.2	C(25)-C(26)-C(27)	120.12(14)
C(13)-C(12)-H(12B)	109.2	C(25)-C(26)-H(26)	119.9
C(11)-C(12)-H(12B)	109.2	C(27)-C(26)-H(26)	119.9
H(12A)-C(12)-H(12B)	107.9	C(22)-C(27)-C(26)	120.98(14)
C(14)-C(13)-C(12)	109.76(13)	C(22)-C(27)-H(27)	119.5
C(14)-C(13)-H(13A)	109.7	C(26)-C(27)-H(27)	119.5

C(12)-C(13)-H(13A)	109.7	C(16)-N(1)-C(1)	111.09(11)
C(14)-C(13)-H(13B)	109.7	C(16)-N(1)-C(21)	121.03(11)
C(12)-C(13)-H(13B)	109.7	C(1)-N(1)-C(21)	124.05(11)
H(13A)-C(13)-H(13B)	108.2	C(5)-O(1)-C(17)	116.86(15)
C(13)-C(14)-C(15)	114.70(12)	C(11)-O(2)-H(2)	109.5

Table 2.18: Anisotropic displacement parameters ($Å^2$x 10^3)for sarpong131. The anisotropic displacement factor exponent takes the form: -2$\sqrt{}$2[$h^2a^{*2}U^{11}$ + ... + 2 h k a* b* U^{12}]

	U^{11}	U^{22}	U^{33}	U^{23}	U^{13}	U^{12}
C(1)	27(1)	22(1)	22(1)	-5(1)	-5(1)	-6(1)
C(2)	29(1)	28(1)	24(1)	-8(1)	0(1)	-11(1)
C(3)	30(1)	33(1)	31(1)	-13(1)	-1(1)	-9(1)
C(4)	33(1)	39(1)	42(1)	-20(1)	6(1)	-10(1)
C(5)	45(1)	42(1)	31(1)	-20(1)	10(1)	-21(1)
C(6)	45(1)	39(1)	24(1)	-10(1)	1(1)	-18(1)
C(7)	36(1)	33(1)	24(1)	-8(1)	-2(1)	-12(1)
C(8)	42(1)	45(1)	25(1)	-6(1)	-11(1)	-3(1)
C(9)	31(1)	31(1)	30(1)	-11(1)	-11(1)	1(1)
C(10)	24(1)	26(1)	24(1)	-8(1)	-4(1)	-3(1)
C(11)	26(1)	27(1)	25(1)	-9(1)	-4(1)	-6(1)
C(12)	30(1)	37(1)	34(1)	-15(1)	-1(1)	-12(1)
C(13)	28(1)	41(1)	33(1)	-14(1)	3(1)	-14(1)
C(14)	24(1)	42(1)	32(1)	-18(1)	1(1)	-5(1)
C(15)	25(1)	27(1)	27(1)	-11(1)	-4(1)	-2(1)
C(16)	28(1)	18(1)	24(1)	-8(1)	-3(1)	-4(1)
C(17)	72(1)	59(1)	33(1)	-26(1)	12(1)	-26(1)
C(18)	36(1)	30(1)	26(1)	-10(1)	-3(1)	-10(1)
C(19)	56(1)	40(1)	32(1)	-17(1)	-7(1)	-4(1)
C(20)	33(1)	30(1)	34(1)	-14(1)	-8(1)	4(1)
C(21)	25(1)	30(1)	28(1)	-11(1)	-6(1)	-4(1)
C(22)	24(1)	31(1)	27(1)	-12(1)	-5(1)	-6(1)
C(23)	39(1)	39(1)	32(1)	-19(1)	4(1)	-13(1)
C(24)	47(1)	38(1)	42(1)	-23(1)	-1(1)	-9(1)
C(25)	39(1)	32(1)	40(1)	-11(1)	-8(1)	-12(1)
C(26)	26(1)	38(1)	33(1)	-6(1)	-2(1)	-9(1)
C(27)	23(1)	35(1)	31(1)	-13(1)	-2(1)	-2(1)
N(1)	25(1)	24(1)	22(1)	-8(1)	-3(1)	-5(1)
O(1)	53(1)	57(1)	38(1)	-29(1)	14(1)	-19(1)
O(2)	30(1)	22(1)	26(1)	-6(1)	-6(1)	-5(1)
O(3)	33(1)	26(1)	22(1)	-9(1)	-3(1)	-5(1)

Table 2.19: Hydrogen coordinates (x 10^4) and isotropic displacement parameters ($Å^2$x 10^3) for sarpong108.

	x	y	z	U(eq)
H(1)	5432	3813	6815	29
H(3)	8497	1358	7014	37
H(4)	9773	874	5346	44
H(6)	6107	2886	3426	42
H(8A)	3664	3496	4496	47
H(8B)	4277	4498	4833	47
H(9A)	2473	4048	6404	37
H(9B)	2249	2802	6258	37
H(12A)	1443	1182	7917	38
H(12B)	2288	-208	8556	38
H(13A)	924	555	10058	40
H(13B)	2797	319	10159	40
H(14A)	1858	2256	10250	38
H(14B)	909	2660	9103	38
H(17A)	7333	2014	2121	77
H(17B)	9137	1930	1509	77
H(17C)	8360	3088	1900	77
H(18)	3613	1092	6011	36
H(19A)	5961	-753	7234	50
H(19B)	5472	-515	5895	50
H(20A)	2744	4337	9143	48
H(20B)	1927	4534	7978	48
H(20C)	3779	4630	7845	48
H(21A)	8499	2244	8196	33
H(21B)	7704	2420	9436	33
H(23)	6281	4646	9227	41
H(24)	6665	6729	8405	47
H(25)	8545	7417	6716	43
H(26)	9951	6032	5813	41
H(27)	9480	3971	6585	36
H(2)	5062	-342	8818	40

Chapter 3

Synthesis of Arcutine

3.1 Introduction

Given the difficulties we had accessing many of the key substrates in our retrosynthesis as described in Chapter 2, it became apparent that a redesign of the route was necessary. With a more clear idea of what would be possible, we set out to develop a new retrosynthesis that addressed the deficiencies of our old approaches. We were also able to draw upon the new literature towards these molecules had been published since our initial approaches.

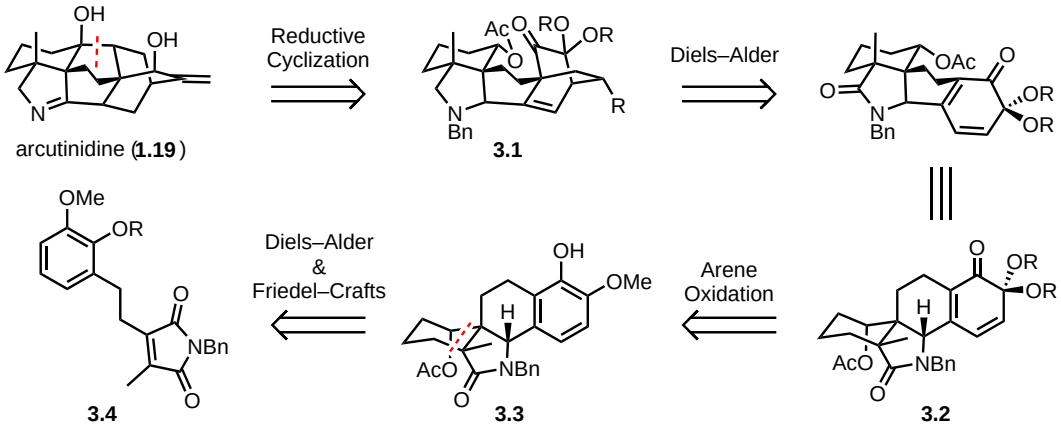

Figure 3.1: Retrosynthesis of arcutinidine (**1.19**) utilizing a reductive coupling to form the B ring and an oxidative dearomatization/Diels–Alder sequence to form the C & D rings.

3.2 Optimized Imide Synthesis

During our earlier efforts, we found an overlooked report[1] that greatly simplified the synthesis of our starting imide (**2.35**) as shown in Scheme 3.1. On the basis of this report, we developed a new approach to a series of more oxidized imide precursors (**3.4a**,**b**), and eventually identified one that could be used for our oxidative dearomatization. N-benzyl citraconimide (**3.5**) was synthesized from the commercial anhydride in high yields, and on more than 50 gram scale. Treating this imide

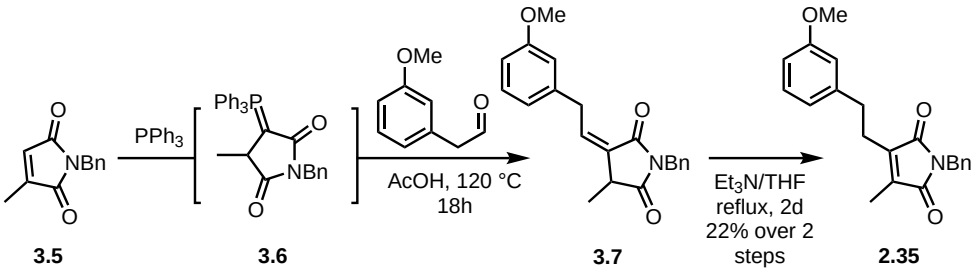

Scheme 3.1: Improved synthesis of imide **2.35**.

with PPh_3 in AcOH gave an ylide (**3.6**) that underwent Wittig reaction with a variety of aldehydes to give imides with an exocyclic olefin such as **3.7**. In the original report, these exocyclic products were refluxed for 2 days in a mixture of THF and Et_3N to give the desired maleimides, such as **2.35**. We found that using methyl enol ethers as masked aldehyde equivalents, gave higher overall yields. These enol ethers could be synthesized in one step from the corresponding benzaldehydes using a Wittig reaction, and purified by simple filtration to remove the bulk of the PPh_3O. We also found that 1,8-diazabicyclo[5.4.0]undec-7-ene (DBU) facilitated isomerization to the maleimides under milder conditions, and in only a few hours. This modular approach allowed us to synthesize a series of imides (**3.4a**,**b**) in only three steps with only a single chromatographic separation.

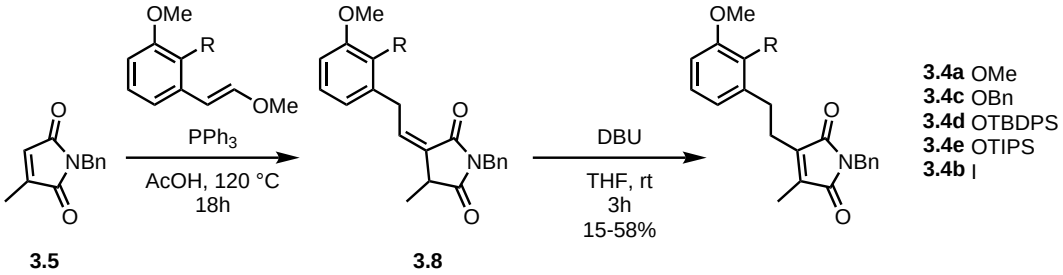

Scheme 3.2: Scalable, modular synthesis of a variety of maleimides with disubstituted aryl groups.

3.3 Oxopyrrolium Diels Alder

The most dramatic improvement to our route came from our efforts to improve the regioselectivity of the Diels–Alder step. Throughout all of our early Diels–Alder-based approaches, lack of regioselectivity in this key step led to mixtures of products that were often difficult to separate, and resulted in half of the material eventually being discarded. Our key insight came when we considered changing the order of operations in the synthesis of our tetracycle. Whether it was a Friedel–Crafts, as in our early approaches or an anionic cyclization in the later one, forging the C–C bond between the arene and heterocyclic portion of the molecule was proving difficult. To that end we discussed forming that bond before installation of the A ring (Figure 3.2). We realized that if done earlier in the sequence, the resulting hemiaminal could prove useful for facilitating the Diels–Alder that had been so inefficient in earlier approaches. Upon elimination of hydroxide, the resulting N-acyliminium (**3.9**) would be substantially activated toward a cycloaddition reaction.

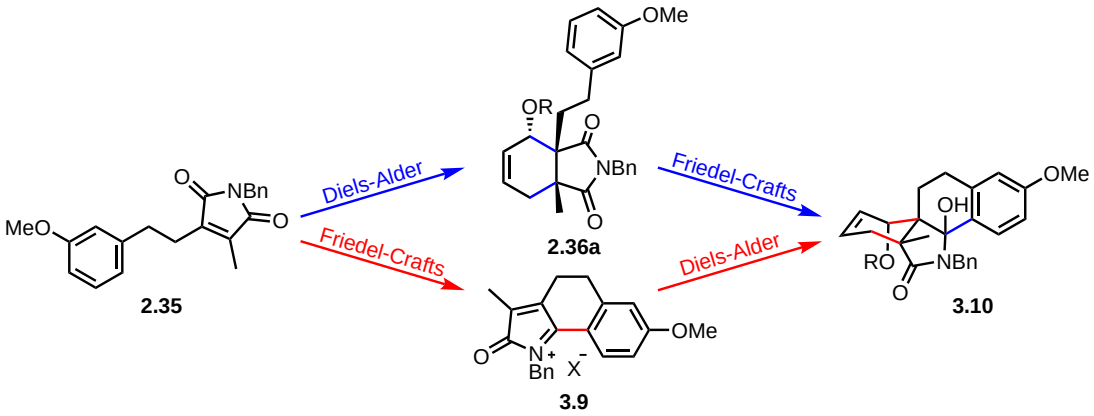

Figure 3.2: Two possible routes to our key tetracycle (**3.10**)

Preliminary DFT calculations showed that this N-acyliminium ion not only displayed the desired polarization of the LUMO, but also significantly lowered the LUMO energy (Figure 3.3). We hoped that this polarization would give us some regioselectivity in the Diels–Alder cycloaddition, and that the lower energy LUMO would facilitate the reaction at temperatures lower than 170 °C (as was required previously). In the acyclic precursor (**2.35**), the LUMO has a calculated energy of -2.3 eV whereas the cyclized iminium ion dienophile (**3.9**) had a LUMO energy of -4.0 eV; as a result, the HOMO/LUMO gap was decreased by a factor of 2. This type of analysis has shown to be a strong predictor of both reactivity and selectivity in Diels-Alder reactions.[2] With these computational results in hand, we were confident that this approach would solve our selectivity issues, assuming that we could synthesize the requisite tricycle (**3.9**).

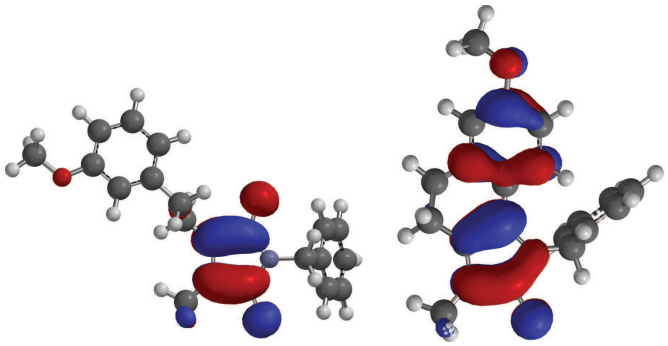

Figure 3.3: The LUMO's of **2.35** and **3.9** calculated using ETD2/6-31+G* and visualized in Spartan.

Using our series of more highly oxidized imide precursors (**3.4a**,**b**), we attempted the Friedel–Crafts alkylation to give us the tricyclic dienophile precursors. While there was little precedent for forming these types of heterocycles, one report[3] demonstrated the desired reactivity using phthalimides with N tethered aryl groups and trifluoromethanesulfonic acid (TfOH) to facilitate the reaction. We were pleased to find that the desired cyclization worked well as long as the starting materials could tolerate the strongly acidic conditions. Imides with benzyl and silyl protected guia-

cols gave poor yields, but the 3-methoxy and 2,3-dimethoxy substrates gave the tricyclic products (**3.9** and **3.11**) in high yields.

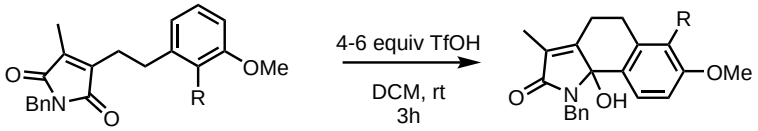

2.35

3.9 R = H 98%
3.11 R = OMe 86%

Scheme 3.3: Oxopyrrolium dienophile precursor synthesis.

With these dienophile precursors in hand, we set out to explore conditions for the Diels-Alder reaction. Initial attempts at performing this reaction under thermal conditions were unsuccessful, as these tricycles were prone to aromatization at high temperatures. Screening by a visiting scholar, Sohei Ueno, eventually hit upon several promising Lewis acid catalysts including $BF_3 \cdot Et_2O$ and $AlCl_3$ that allowed the reaction to proceed at lower temperatures. After some optimization, we found that 3 equivalents of $AlCl_3$ and 3 equivalents of diene in acetonitrile at 40 °C gave the desired tetracycle (**3.15**) as a single isomer and in good yields, validating our hypothesis. The switch to a Lewis acidic catalyst also required a more acid stable diene, namely 1-acetoxybutadiene, as the 1-silyloxybutadiene used in previous approaches was prone to decomposition under these conditions. With this new approach we were able to access decagram quantities of our key tetracycle much more efficiently than with previous routes. This synthesis was exploited for much of the later work from Chapter 2 utilizing the monomethoxy substrates. Since this chapter focuses on our current approach toward the arcutines we will only discuss the dimethoxy substrates.

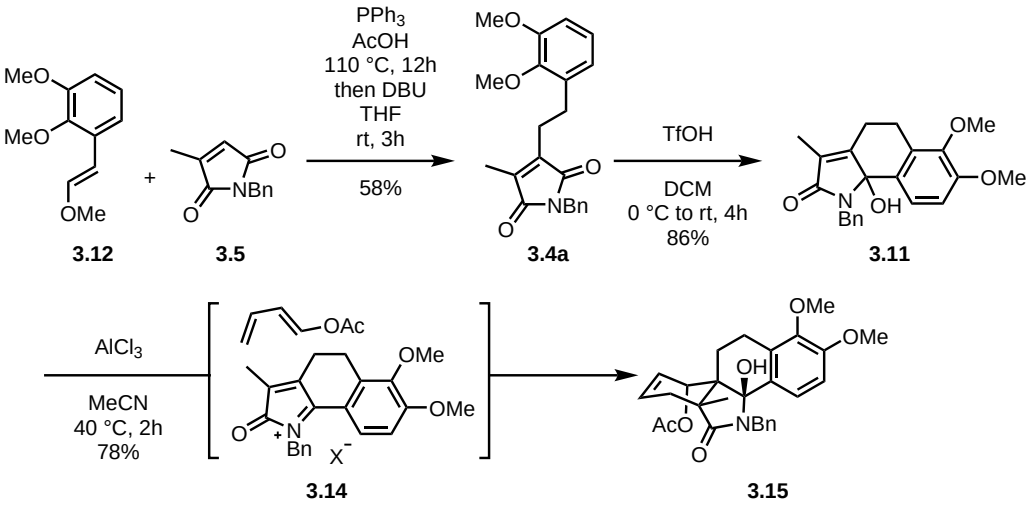

3.12 **3.5** **3.4a** **3.11**

3.14 **3.15**

Scheme 3.4: Synthesis of dimethoxy tetracycle **3.15**.

3.4 Tetracycle Functionalization

With Diels-Alder adduct **3.15** in hand, we were ready to explore the later steps toward the oxidative dearomatization. Fortunately, the Rh on Al_2O_3 catalyzed hydrogenation and ionic reduction conditions previously developed for the monomethoxy substrate (**2.42**) were applicable to the dimethoxy substrate (**3.15**). Using this approach, we were able to access large quantities of **3.17**, which served as the staging point for many of our approaches since it could be stored for months at –20 °C without any apparent degradation.

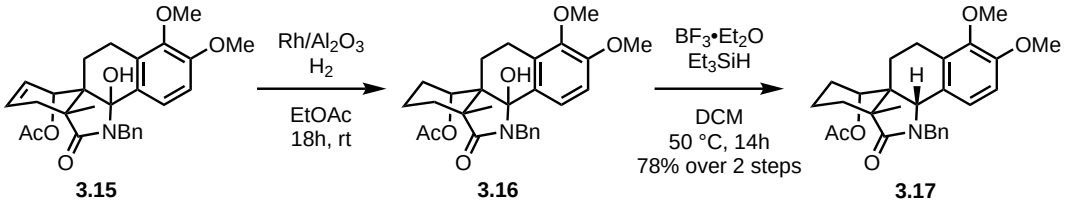

Scheme 3.5: Reduction of Diels–Alder adduct **3.15** to lactam **3.17**.

3.5 Oxidative Dearomatization & Diels-Alder Investigations

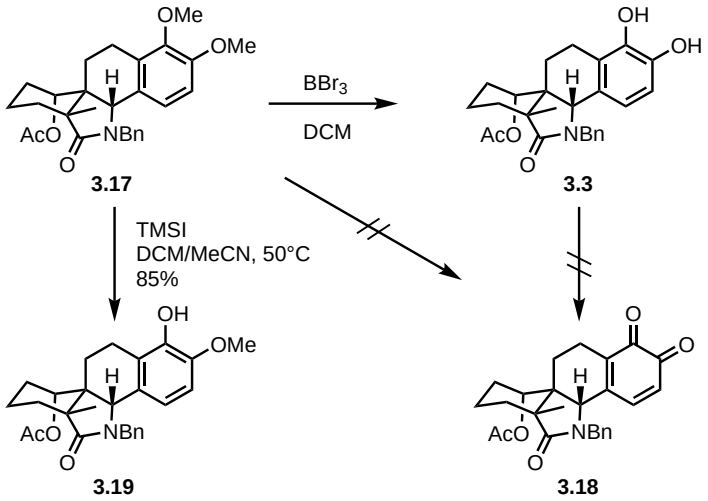

Scheme 3.6: Initial approaches to the oxidative dearomatization of **3.17**.

At this stage, we had several options for the oxidative dearomatization. Direct dearomatization of 1,2-dimethoxy arenes to orthoquinones is known with some cerium oxidants including CAN[4] and $Ce(SO_4)_2$ with $HClO_4$.[5] This was recently demonstrated by the Qin group in their synthesis of a variety of atisane-type diterpenoids. Under these conditions we only observed undesired oxidation elsewhere in the molecule. Unlike our monomethoxy substrate, demethylation of **3.17** with excess BBr_3 worked reliably to give catechol **3.18**. Attempts to perform a monodemethylation with 1 equivalent of BBr_3 gave a statistical mixture of demethylated products. Oxidation of

the catechol to the diketone (**3.19**) with DDQ, Ag_2O and $Ce(SO_4)_2$ gave complex mixtures or decomposition. Like the monomethoxy substrate, the dimethoxy compound was resistant to EtSNa mediated demethylation. Fortunately, upon treating **3.17** with 10 equivalents of TMSI, a selective monodemethylation occurred to give guiacol **3.3**. The selectivity was confirmed by comparison to a sample synthesized from the benzyl protected imide (**3.4c**).

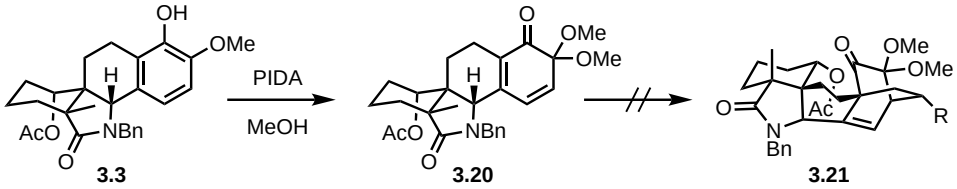

Scheme 3.7: Oxidative dearomatization of **3.3** with PIDA.

With this guiacol (**3.3**) in hand we were able to test the oxidative dearomatization conditions that had been so effective for Qin, Kobayashi, and others. Treatment with diacetoxyiodobenzene (PIDA) in methanol led to the expected masked orthobenzoquinone (MOB) (**3.20**). While the crude reaction was relatively clean, this MOB was unstable to silica gel. Therefore the intermolecular Diels–Alder cycloadditions were attempted on crude material. Benzyl propargyl ether, trimethylsilylacetylene, and ethyl vinyl ether were chosen as dienophiles since they would lead to products at roughly the correct level of oxidation. However, upon heating to 180 °C, no desired product was detected and only slow decomposition of the starting diene was observed. Since we had expected the intermolecular Diels–Alder cycloaddition would be challenging, we next explored options to install a pendant dienophile such as an allyl group in the oxidative dearomatization.

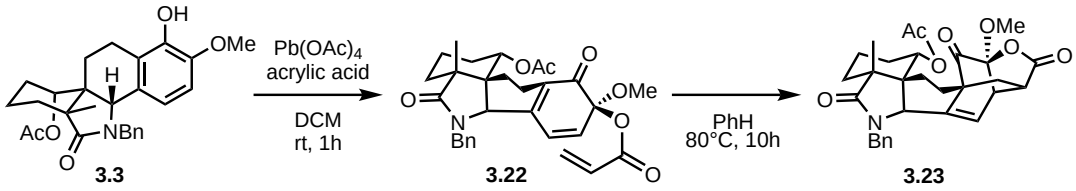

Scheme 3.8: Wessley oxidation of **3.3** and subsequent Diels–Alder to form the ACDEF ring system of arcutine.

Treating guiacol **3.3** with allyl alcohol[6] and PIDA gave complex mixtures. On the other hand, treating this guiacol with a solution of lead (IV) acrylate (generated from lead (IV) acetate and a large excess of acrylic acid) gave the Wessley[7] oxidation product (**3.22**) possessing a diene and an acrylate moiety ortho to the ketone. Isolating this compound by chromatography proved difficult as it was also unstable to SiO_2, but upon heating to reflux in benzene, a new product formed that was consistent with the desired Diels–Alder product. While we were relatively confident that the acrylate would react from the less hindered β face, we confirmed the connectivity and stereochemistry of this product using X-ray crystallography (Figure 3.4).

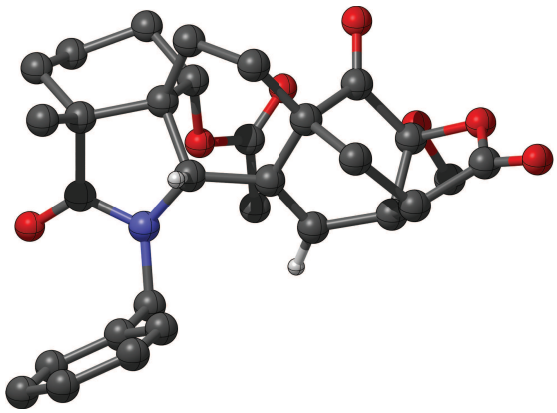

Figure 3.4: X-ray structure of **3.23**, visualized in CYLview.

3.6 Pentacyclic Amide Functionalization

With cycloadduct **3.23** in hand, we only needed to form the B ring in order to complete the arcutine skeleton. Given the precedent set by Qin, we wanted to form the B ring via a reductive cyclization utilizing SmI_2. To mimic their substrate, we would need to convert the acetate group in **3.23** to a ketone and install an alkene in the [2.2.2] bicycle as in **3.24**. Alternatively, a 1,6 diketone would be well poised for a pinacol coupling as in **3.25** (see Figure 3.5).

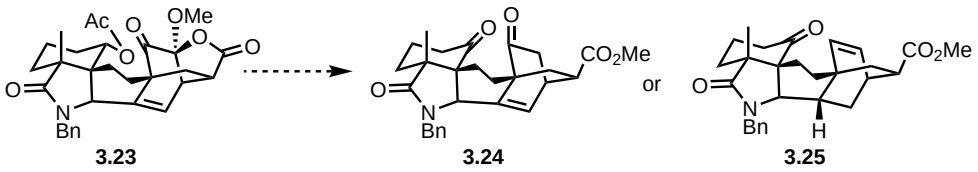

Figure 3.5: Possible precursors for B ring closure via a pinacol (**3.24**), or Qin's reductive cyclization (**3.25**).

Screening of various hydride and dissolving metal reduction conditions gave only decomposition. Treating **3.23** with an excess of SmI_2 gave reduction of the masked 1,2 diketone with concomitant formation of the carboxylic acid. This acid was not isolated but instead methylated with $TMSCHN_2$ to give the methyl ester (**3.26**). While this reduction was a useful step toward the targeted B ring precursors **3.24** and **3.25**, the reaction suffered from one major shortcoming. During the reduction a transient 1,4 cyclohexadiene (**3.27**, Scheme 3.9) forms, which can undergo a retro Diels–Alder through loss of acrylate to give **3.72**. Our initial attempts using SmI_2 in methanol gave nearly a 1:1 mixture of the desired reduction product and the guiacol. Fortunately, guiacol **3.3** could be recycled since it was our oxidative dearomatization precursor. Common additives such as hexamethylphosphoramide (HMPA) and 1,3-dimethyl-3,4,5,6-tetrahydro-2(1H)-pyrimidinone (DMPU) were examined, but these led to more of the retro Diels–Alder product. We then looked at different temperatures and found that, while the overall rate of this reaction was sensitive to temperature, little difference in product ratio was observed at temperatures between –78 °C and room temperature. The one factor that did improve the reaction slightly was the use of more acidic cosolvents such as trifluoroethanol (TFE) or hexafluoroisopropanol (HFIP). These improved the

ratio to roughly 70:30 in favor of the desired reduction product. We believe that these solvents facilitate the tautomerization between the initial enol tautomer (**3.73**) that can rapidly undergo a retro Diels–Alder and the relatively stable keto tautomer (**3.73**).

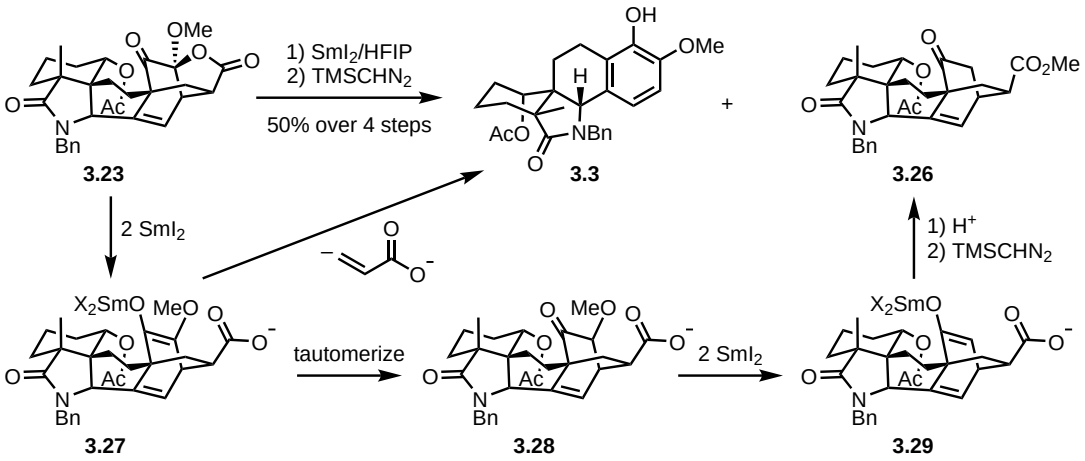

Scheme 3.9: Reduction of **3.23** to **3.26** as well as guiacol **3.3**.

In order to suppress the retro Diels–Alder cycloaddition, we tried to reduce the alkene in the [2.2.2] bicycle of **3.23**. Heterogeneous catalysts including Pd and $Pd(OH)_2$ on charcoal, Rh on charcoal, Rh on Al_2O_3, PtO_2, and Pt on Al_2O_3 at 50 atm were explored, as were additives such as AcOH. In the end, none of the desired alkene reduced product (**3.33**) was ever detected, and only starting material, retro Diels–Alder products, and reduction of the benzyl group to the methylenecyclohexyl group occurred. After examining a 3D model of this system, we realized that pyramidalization of the sp^2carbons would force the carbonyl in the [2.2.2] bicycle into a severe steric clash with the acetate, which could prevent the desired reduction.

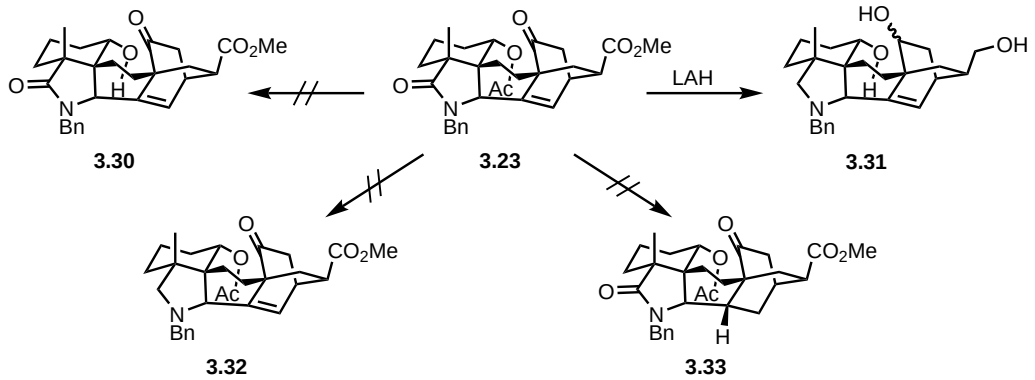

Scheme 3.10: Attempted transformations of Diels–Alder product **3.23**.

One way to mitigate this steric clash would be to convert the ketone group in the C ring to something smaller. Since the Qin group was able to form the B ring via a reductive cyclization onto an alkene at that position we attempted to install an alkene in the [2.2.2] bicycle. Treatment with $LiBH_4$ afforded the desired alcohol **3.34** as a single diastereomer. Attempts to sulfonylate this alcohol with triflic anhydride or mesyl chloride failed, presumably due to the highly sterically

encumbered environment. Treatment with Burgess reagent or Martin's sulfurane led to a new product, which appeared to be the result of a rearrangement arising from the formation of a secondary carbocation.[8] While the structure of this product was not fully elucidated, it was apparent that it lacked the desired alkene group by ^{1}H analysis. Installation of a vinyl triflate resulted in rapid retro Diels–Alder to give the triflated guiacol. Given that formation of alkene would be impossible due to the heavily favored retro Diels–Alder, we decided to pursue removal of the acetyl group.

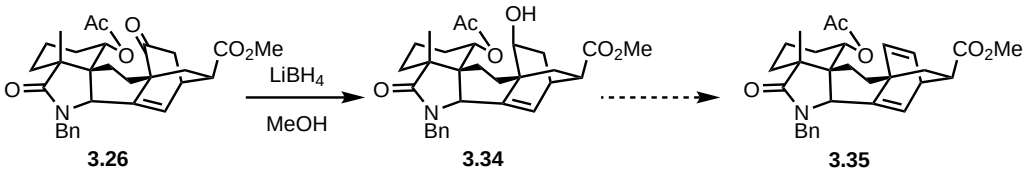

Scheme 3.11: Attempted formation of diene **3.74**.

Selective removal of the acetyl group to give **3.30** proved challenging and we were only successful at removing it by global reduction to the triol (**3.31**). Reoxidation to the diketoaldehyde proved somewhat feasible but the compound proved challenging to isolate. Because we sought to keep the methyl ester intact, a variety of methanolysis conditions were explored. Under basic conditions, only epimerization of the methyl ester was ever observed. The acetate was also completely resistant to acidic methanolysis conditions.

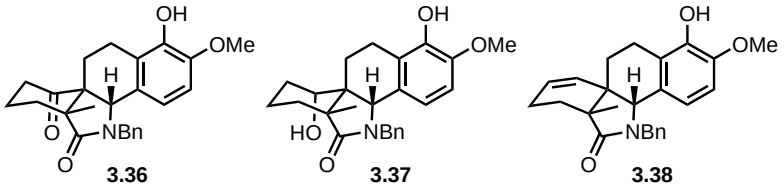

Scheme 3.12: Alternative oxidative dearomatization substrates.

With our attempts to remove this acetyl group faltering, we decided to remove it at an earlier stage in the synthesis. We synthesized a variety of oxidative dearomatization precursors bearing a ketone (**3.36**), alcohol (**3.37**), and alkene (**3.38**) instead of the acetate. In all cases, oxidative dearomatization gave complex mixtures, possibly due to poor diastereoselectivity in the acrylate addition due to lack of steric influence from the acetate. After workup, the crude oxidative dearomatization products were heated to reflux in benzene, but no Diels-Alder product formation was evident. At this stage, it appeared that the acetate was ideally suited for this approach since it was oxidatively stable and bulky enough to enforce a diastereoselective oxidative dearomatization.

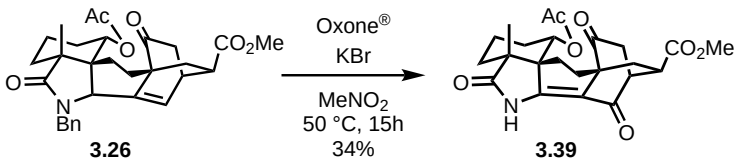

Scheme 3.13: Preparation of vinylogous imide **3.39** using Oxone®.

Our final effort to salvage this approach was to remove the benzyl group since we were unsure whether it could interfere with acetate removal or double bond hydrogenation. Given our exhaustive attempts to reduce the alkene group in the [2.2.2] bicycle, we knew that hydrogenolysis was unlikely to work since debenzylation was never detected in those attempts. Selective reduction of the amide to give **3.32**, which would render hydrogenolysis more feasible, gave none of the desired product. Therefore, we explored a variety of oxidative and acidic debenzylation conditions. Treatment with $AlCl_3$ or TfOH and various other acids at temperatures up to 150 °C returned only starting material or decomposition products. Oxidation to the benzoyl group also proved challenging but we did achieve some success with the combination of KBr and Oxone®.[9] Under anhydrous conditions, this combination gave a mixture of oxidized products, one of which also lacked the benzyl group. Addition of a small amount of water gave good conversion to the debenzylated product albeit with over oxidation to the vinylogous imide **3.39**. With imide **3.39** in hand we once again looked at a battery of reductive and methanolytic conditions to cleave the acetyl group with no success.

3.7 Synthesis of the Arcutine Core

Given that the only positive results at this point involved moving toward highly oxidized substrates like **3.39** rather than more reduced products closer to the natural products, we once again decided to revisit an earlier stage in the synthesis. Modification or removal of the acetyl group had already been explored with no success. Therefore, we decided to convert the N-benzyl lactam to something that could be more readily removed. This meant reducing the lactam to the amine, which would render hydrogenolysis feasible, or replacing the benzyl group entirely. We chose to explore the latter option first. Once again we revisited our key tetracyclic lactam (**3.17**) as a staging point for these attempts. Given our previous experience with Birch reductions on similar substrates, we knew that the dimethoxy arene would be resistant to reduction using dissolving metal conditions. Birch reduction with Na or Li on both the guiacol (**3.3**) and veratrol (**3.17**) tetracycles provided the debenzylated products (**3.40** and **3.42**), albeit with loss of the acetyl group as well. Upon treating the debenzylated veratol (**3.40**) with TMSI, we observed an unexpected rearrangement to the aminolactone (**3.41**) that we had originally targeted in one of our very first approaches. While Birch reduction of the guiacol afforded the expected product, it rearranged on silica to the same amino lactone (**3.41**).

Lithium aluminum hydride (LAH) reduction of **3.40** gave the expected secondary amine. Reprotection of the nitrogen with a Boc group proved facile, however reintroduction of a protecting group on the oxygen proved challenging. Rather than continue with that approach, we opted to explore the N-benzylated amine (**3.43**), which would give us the benefit of having orthogonal protecting groups on the nitrogen and oxygen. Global reduction of **3.17** with LAH provided the tertiary amine bearing a 2°hydroxyl in good yields. Reacylation under forcing conditions provided the desired amino acetate (**3.43**). Attempts to access this compound directly from the amide have been unsuccessful so far, as even amide selective reducing conditions gave primarily reduction of the ester.[10–12]

To our surprise, these tertiary amine substrates were relatively oxidatively stable, and surprisingly nonpolar, making them easy to purify. Using conditions similar to those developed for the amide substrates, we were able to successfully access the guiacol (**3.44**) and perform the oxidative

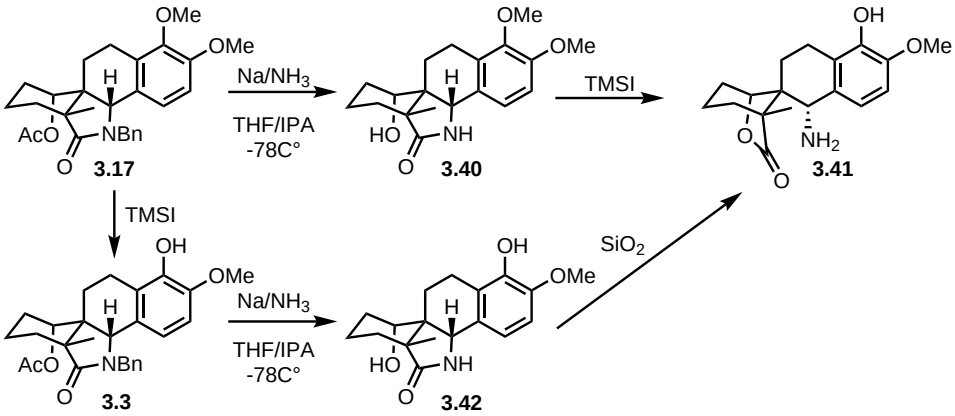

Scheme 3.14: Debenzylation of **3.17** led to unexpected spirolactonization.

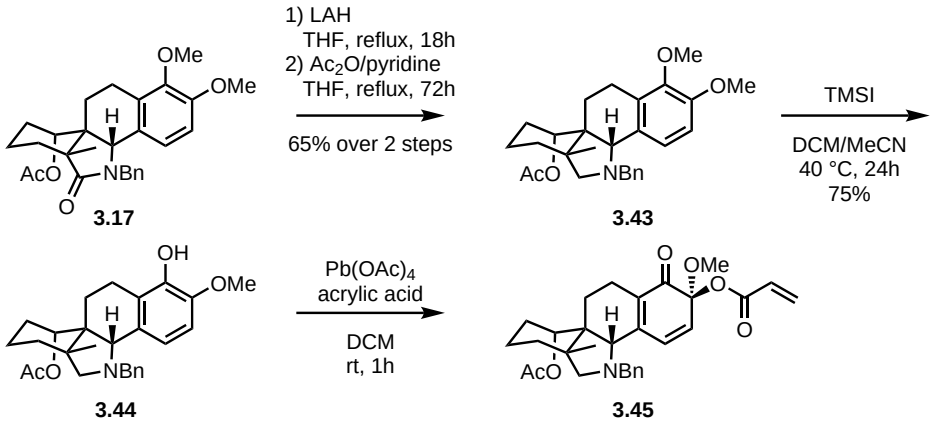

Scheme 3.15: Oxidative dearomatization and installation of an acrylate to give **3.45**.

dearomatization with lead (IV) acrylate to give **3.45**. Upon heating to reflux in benzene, we were only able to isolate a small amount of the desired Diels–Alder product (**3.47**). Upon examination, the bulk of the crude material appeared to be a diastereomeric mixture of isomerized starting material (**3.46**, Scheme 3.16). This was presumably due to the basic nitrogen facilitating a proton transfer. Fortunately, conducting the Diels-Alder at higher temperatures greatly improved the product ratios and heating the oxidative dearomatization products in toluene or xylenes at reflux gave mostly the desired product as roughly a 15:1 mixture of diastereomers.

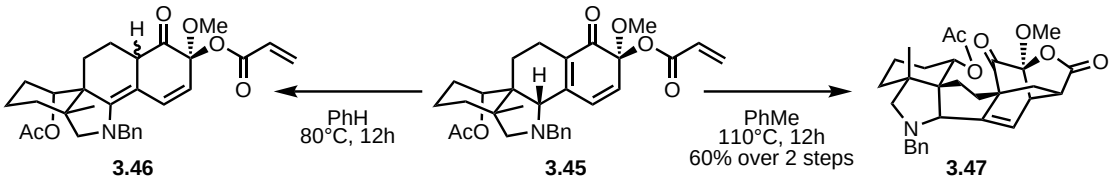

Scheme 3.16: Temperature dependence of the Diels–Alder reaction of **3.45**.

With this new Diels–Alder product in hand (**3.47**), we explored several of the conditions that had shown promise with the lactam-containing substrate (**3.23**). To our dismay, nearly all condi-

tions that we tried led to complex mixtures, including the SmI_2-mediated reduction conditions that had worked previously for α-keto reduction. Serendipitously, during an attempted reduction using $NaBH_4$ in methanol, we found that the colorless starting material turned bright yellow after several minutes of stirring, but before any other reagents were added. TLC confirmed full conversion to a new product that had the same mass as the starting material by LCMS. This new product decomposed slowly in solution, but we were able to isolate it and collect NMR data. This confirmed that methanolysis of the lactone in the [2.2.2] bicycle occurred to give diketone **3.48**. ^{13}C NMR showed characteristic 1,2-dicarbonyl resonances, and when **3.47** was stirred in CD_3OD, the diketone was isolated with the fully deuterated of the methyl ester. Since many of our initial studies had been done in methanol, we believed that the resulting complex mixtures were due to partial conversion of the starting material before other reactions could occur.

After allowing the starting material to fully isomerize to the diketone, we reexamined our initial reaction conditions. Methanolysis of the acetyl group proved difficult given how prone the diketone was to decomposition. Treatment of **3.48** with a wide array of borohydride reducing reagents led to complex mixtures of diastereomeric products. After isomerization to the diketone, reduction with SmI_2 proceeded smoothly (Scheme 3.17). When methanol was used as the sole cosolvent, the ketone containing product (**3.50**) was formed. When water was used, reduction to alcohol **3.49**, largely obtained as a single isomer, occurred.[13]

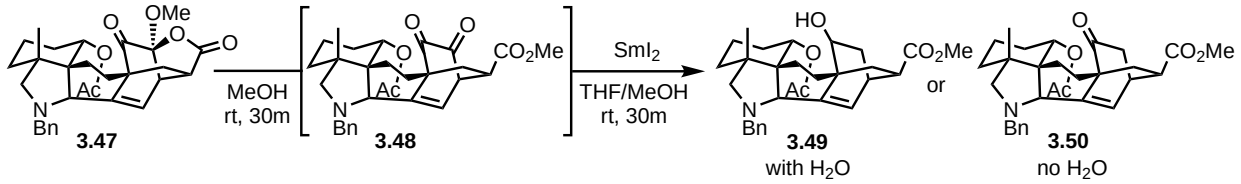

Scheme 3.17: Isomerization and reduction of Diels–Alder product **3.47**.

With ketone **3.50** and alcohol **3.75** in hand, we looked toward achieving the transformations necessary to form the final ring of the arcutine core. Once again, we found the acetate was resistant to basic methanolysis; acidic methanolytic conditions, however, showed some promise. While the ketone containing substrate (**3.50**) proved unreactive, removal of the acetyl group in **3.49** occurred with several acids at high temperatures. Eventually we found that Amberlyst®15 resin at 100 °C gave good conversion to diol **3.51**, which was isolated by simply filtering off the resin and concentrating. Treatment of the resulting diol with DMP gave the diketone (**3.52**) in modest yields. With this compound in hand we were ready to attempt a pinacol coupling to form the last C–C bond in the arcutine skeleton. Treating diketone **3.52** with SmI_2 gave two new products with the correct masses by LCMS in roughly a 10:1 ratio. 2D NMR studies of the major product seemed to confirm that it had the desired connectivity, but it was difficult to confirm which diasteromer was formed. Calculations showed that only two of the four possible diasteromers (epimeric at the A ring alcohol) were energetically feasible, with the undesired A ring stereochemistry being energetically favored by approximately 3 kcal/mol. While still attempting to determine the structure of this product, we explored a variety of other samarium based reductants. We found that the diastereomeric ratio could be tuned to favor the other diastereomer, in a roughly 2:1 ratio, using $SmBr_2$ conditions developed by Riesman during their synthesis of maoecrystal Z.[14] We were able to obtain an X-ray quality crystal of the major diastereomer from the SmI_2 mediated reaction, which confirmed

that it was the pinacol product with the desired stereochemistry. This may be due to chelation of both alkoxides by the samarium to give the syn product. This is somewhat supported by the observation that conditions with additives like LiBr or water tend to favor the anti diasteromer. These nucleophiles could disrupt any chelation and thereby give the thermodynamically favored diastereomer.

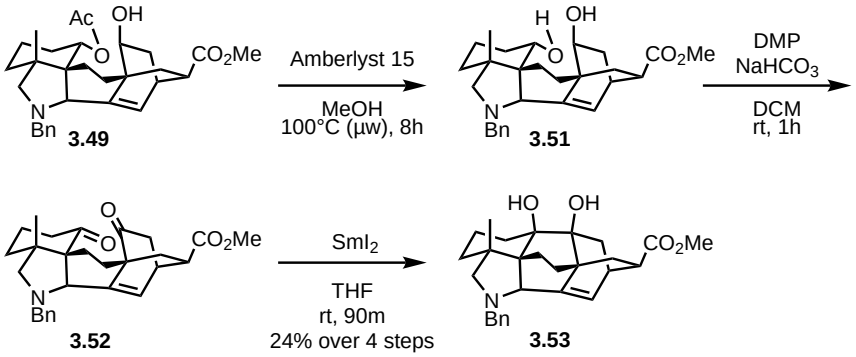

Scheme 3.18: Synthesis of the completed arcutine skeleton.

During the exploratory phase of this synthetic sequence (from **3.47** to **3.53**) we isolated every intermediate, leading to an overall yield of less than 5%. Eventually, we found that we could reproducibly access pinacol product **3.53** in a single series of operations starting from the Diels–Alder adduct (**3.47**). After isomerization to the diketone in methanol, the reaction mixture was diluted with THF and water and degassed before SmI_2 was added. Once the reduction was complete, it was worked up, and immediately subjected to methanolysis overnight. After filtration, the crude diol was oxidized to the diketone with DMP, and after workup and azeotropic drying, the crude diketone was treated with SmI_2 to give the desired pinacol product. Unlike many of the intermediates in this sequence, the pinacol product was stable enough to isolate without significant losses during purification. Yields suffered when more than 400 mg of the Diels–Alder product (**3.49**) was used. With this approach, we have accessed nearly a gram of the pinacol product (**3.53**) to date.

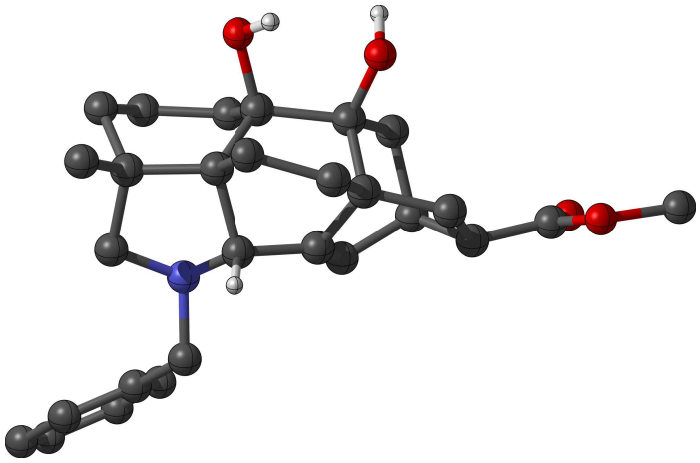

Figure 3.6: X-ray structure of pinacol product **3.53**. Visualized in CYLview.

3.8 Synthetic Studies Toward Arcutinidine

With the skeleton of arcutine in place, we needed several redox manipulations to complete the natural product. We expected the largest challenge to be the selective deoxygenation of the diol that resulted from the pincaol coupling. Based on the X-ray structure, there was relatively little differentiation between the two tertiary alcohol groups in **3.53**. Our initial attempts were directed at installing some sort of functionality, such as a thiocarbonate, that could be used in a radical deoxygenation. Unfortunately, all attempts to install a thiocarbonate with thiophosgene, thiocarbonyldiimidaziole, and phenyl chlorothionocarbonate failed to give any thiocarbonate products. In stark contrast, use of a variety of boron sources such as $BF_3 \cdot Et_2O$ and $NaBH_4$ resulted in rapid incorporation of the boron atom to give a borate (**3.56**), which was confirmed by HRMS and ^{11}B NMR. Interestingly, small amounts of this product were also detected in the crude pinacol reaction mixture. A report by Baran and coworkers demonstrated that polyols such as **3.53** can actually react with the boron in borosilicate glass.[15] Attempts to convert one of the tertiary alcohols to a chloride with $SOCl_2$ led to the formation of cyclic sulfite **3.57**.

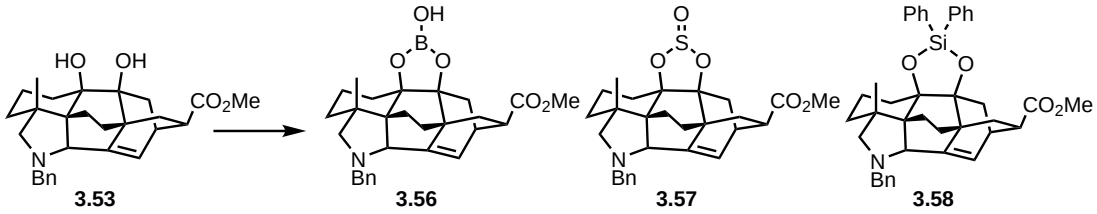

Scheme 3.19: Heterocycles accessible from pinacol product **3.53**.

The most interesting results were obtained using a procedure for the deoxygenation of tertiary alcohols.[16] Treatment of **3.53** with $InCl_3$ and a silane based reductant, Ph_2SiHCl, led to the formation of a new product with both hydroxyls removed, one reductively and the other by loss of water. Attempts to scale this reaction up were initially frustrated by the formation of a cyclic silane (**3.58**). After some investigation it became clear that on small scales, we were using a larger excess of $InCl_3$ than thought, and significantly more than the 5 mol% used in the original report. After further studies we found that with two equivalents of $InCl_3$ we were able to achieve consistently good yields of the deoxygenated product (**3.55**).

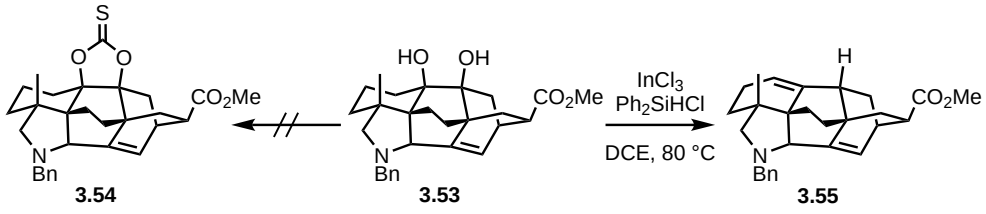

Scheme 3.20: Thiocarbonate **3.54** proved elusive, but deoxygenation to give **3.55** was successful.

Concurrently, we were also exploring other applications of the pinacol product. Hydrogenation with Pd on charcoal led to a very surprising result. After hydrogenolysis of the benzyl group occurred, a rapid isomerization took place to give an imine with a saturated [2.2.2] bicycle (**3.60**, Scheme 3.21). Extended reaction times and higher pressure failed to further reduce the resulting

imine. While this isomerization was initially surprising, DFT calculations showed that the isomerized product was favored by a staggering 30 kcal/mol, demonstrating just how much strain energy there is in this fused ring system. Unlike substrates without the B ring in place, the now highly strained trisubstituted alkene in the rightmost [2.2.2] bicycle was readily reduced with diimide to give the saturated framework (**3.61**).

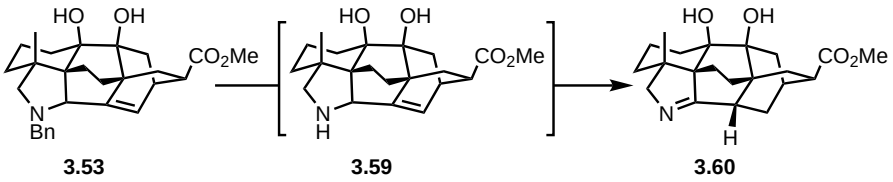

Scheme 3.21: Hydrogenolysis and unexpected isomerization of **3.53**.

Under our optimized conditions we were also able to deoxygenate the diimide reduction product (**3.61**) in good yields. Meanwhile, all attempts to deoxygenate imine **3.60** failed to deliver any of the desired product. Instead the cyclic silane product was formed in all attempts.

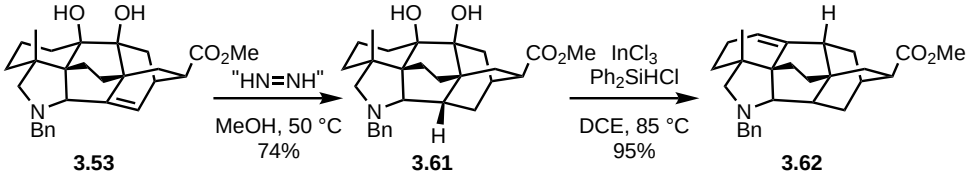

Scheme 3.22: Double deoxygenation of **3.53**.

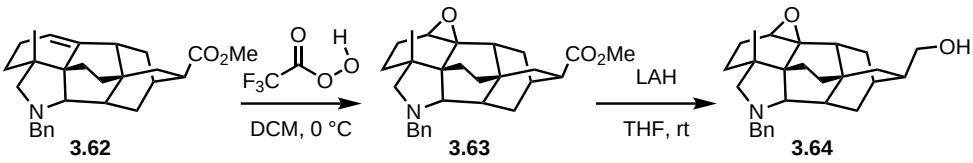

Scheme 3.23: Epoxidation and reduction of **3.62**. No reduction of the epoxide opening occurs, even at elevated temperatures.

With these deoxygenation products (**3.55** and **3.62**) in hand, we attempted to progress further toward arcutinidine (**1.19**). At this stage the remaining transformations needed were the reintroduction of a hydroxyl group in the A ring, debenzylation, formation of the imine, installation of the exomethylene, and an allylic oxidation. In order to reinstall the oxygen that was eliminated in the previous step we examined various alkene hydration conditions. Treating **3.55** and **3.62** with standard Mukaiyama hydration conditions led to complex mixtures, especially in the case where two alkene groups were present. Treating the pinacol deoxygenation product (**3.55**) with $Hg(OAc)_2$ or mCPBA led to rapid functionalization of the strained alkene in the [2.2.2] bicycle. Oxymercuration of monounsaturated **3.62** led to oxidation at the nitrogen[17] rather than the desired oxymercurated product. Treatment with mCPBA gave some epoxidized product, with poor conversion, and more forcing conditions led to decomposition. Upon switching to the much more reactive trifluoroperacetic acid (TFPAA), we were able to access the epoxide as a single diastereomer. Since we

were unsure whether the nitrogen was directing the epoxidation, the reaction was conducted under acidic conditions, which is known to suppress any directing effects of the nitrogen.[18] These conditions gave the same product as when the reaction was run under buffered conditions. X-ray crystallography confirmed that the epoxide (**3.63**) was formed with the desired stereochemistry.

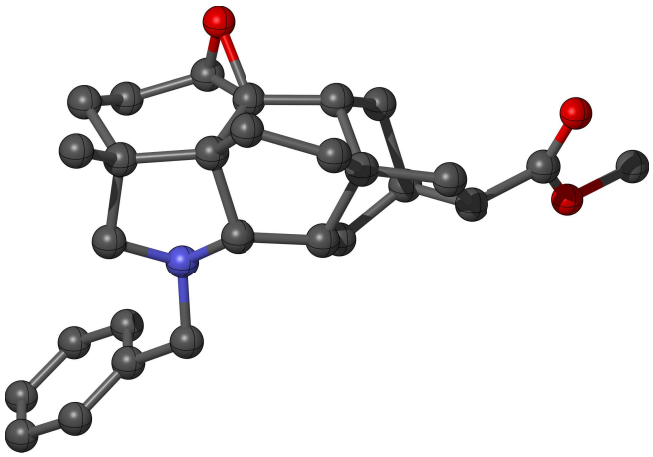

Figure 3.7: X-ray structure of **3.63** with the desired epoxide stereochemistry. Visualized in CYLview.

When epoxide **3.63** was treated with LAH, the ester was cleanly reduced, but no epoxide opening was observed, even at 150 °C. Under very forcing conditions, or when treated with LAH and a Lewis acid, a mixture of products was formed, with the predominant one bearing an alkene group where the epoxide once was. This could result from reductive ring opening and subsequent elimination of the tertiary alkoxide.

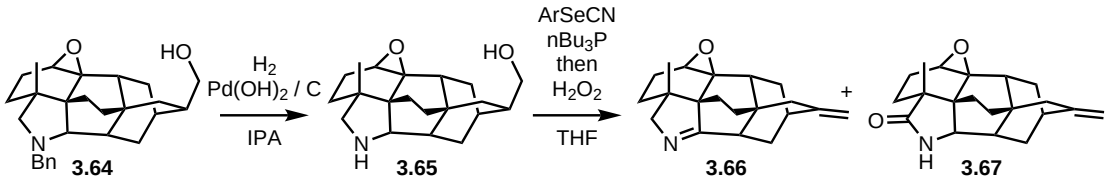

Scheme 3.24: Exomethylene installation and unexpected amine oxidation.

When primary hydroxyl bearing substrate **3.64** was subjected to hydrogenolysis conditions in methanol, the expected secondary amine was not isolated. Instead the N-methylated amine was formed, presumably via Pd mediated oxidation of methanol and condensation of the resulting formaldehyde with the unveiled 2°amine. Changing the solvent to isopropanol avoided this complication and gave the expected secondary amine (**3.65**). Treating this amine with Grieco elimination[19] conditions gave the expected elimination of the primary hydroxyl. Unexpected oxidation of the nitrogen also occurred, presumably via selenation of the amine and extrusion of a selenoxide upon treatment with H_2O_2. This elimination was relatively unselective as two products (**3.66** and **3.67**) were isolated. Imine **3.66** could arise directly from the selenoxide extrusion whereas the lactam **3.67** could arise from elimination and further oxidation.

To date, imine **3.66** represents our closest intermediate towards arcutinidine (**1.19**). Reductive ring opening of the epoxide and allylic oxidation would give arcutinidine, and from there all 3

alkaloid natural products should be achievable in one step. Efforts are currently underway to identify conditions to open epoxide **3.63** via elimination or reduction.

3.9 Experimental Contributors

Initial optimization of the oxopyrrolium Diels–Alder cycloaddition was conducted by Sohei Ueno (S.U.) under the supervision of Kyle Owens (K.O.). All other chemistry in Chapter 3 was developed by K.O.. Scale up and route optimization, as well as some exploratory chemistry that was not discussed was performed by Shelby McCowen (S.V.M.).

3.10 Experimental Details

Materials and Methods for the Experiments in Chapter 3 Unless stated otherwise, reactions were performed in flame or oven dried glassware sealed with rubber septa under a nitrogen atmosphere and were stirred with Teflon-coated magnetic stir bars. Liquid reagents and solvents were transferred by syringe using standard Schlenk techniques. Reaction temperatures above room temperature (rt), 23 °C, were controlled by a temperature modulated stir plate. Reaction temperatures below room temperature were performed in appropriate cold baths maintained with dry ice, liquid N_2, or a portable cryostat. THF, Et_2O, PhH, PhMe, MeCN, Et_3N and MeOH were dried by passage over a column of activated alumina; DCM was distilled over calcium hydride; other solvents were obtained in a sure-seal bottles; all other reagents and solvents were used as received from commercial sources unless stated otherwise. Thin layer chromatography was performed using precoated (0.25 mm) silica gel 60 F-254 plates, which were visualized by UV irradiation and CAM or anisaldehyde stain when necessary. Silica gel (particle size 40-63 μm) was used for flash chromatography, or the reaction products were isolated and purified using an automated YamazenâĎć flash system. $CDCl_3$ and C_6D_6 were obtained from commercial suppliers and were used as purchased. NMR experiments were performed on Bruker spectrometers operating at 300, 400, 500, 600 or 700 MHz for 1H nuclei, 75, 100, 126, 151, or 176 MHz for 13C experiments, and 376 MHz when 19F was observed. Chemical shifts (δ) are reported relative to TMS using the residual solvent signal as internal reference ($CDCl_3$: 7.26 ppm for 1H, 77.16 ppm for 13C; C_6D_6: 7.16 ppm for 1H, 128.06 ppm for 13C). NMR data are reported as follows: chemical shift (multiplicity, coupling constants J [Hz] where applicable, number of hydrogens). Abbreviations are as follows: s (singlet), d (doublet), t (triplet), q (quartet), sep (septet), m (multiplet), b (broad). High-resolution mass spectral data were obtained from the UCB Mass Spectral Facility using a Finnigan/Thermo LTQ/FT instrument for ESI, and a Waters Autospec Premiere instrument for EI. X-Ray data were collected on a Bruker APEX-II CCD diffractometer with Mo-Kα radiation (λ = 0.71073 Å) or a MicroStar-H X8 APEX-II diffractometer with Cu-Kα radiation (λ = 1.54178 Å) and analyzed by Dr. Antonio DiPasquale and Nick Settineri (University of California, Berkeley), structures were visualized with CYLview.

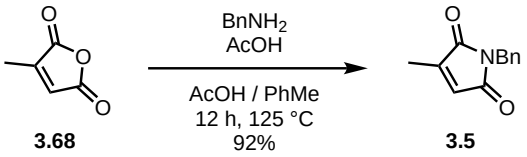

3.68 **3.5**

Benzylamine (30 mL, 275 mmol, 1.1 equiv) was added to a dry flask and cooled to 0 °C. Citraconic anhydride (22.5 mL, 250 mmol, 1 equiv) was added slowly followed by AcOH (250 mL, 1M) and PhMe (25 mL, 0.1M). The flask was fitted with a Dean-Stark trap and a condenser and heated to 125 °C overnight. After 12 hours the reaction mixture was moved to room temperature, concentrated under reduced pressure and azeotroped with PhMe. The crude mixture was diluted with EtOAc (300 mL), washed with 1N HCl, H_2O, then twice with sat. $NaHCO_3$ before being dried over Na_2SO_4, filtered, and concentrated to an orange oil. The crude product was purified by flash chromatography (5% EtOAc in Hx) to give N-benzylcitraconimide (**3.5**) (46.32 g, 92%) as a white solid.

Spectral data was consistent with the literature reports.[20]

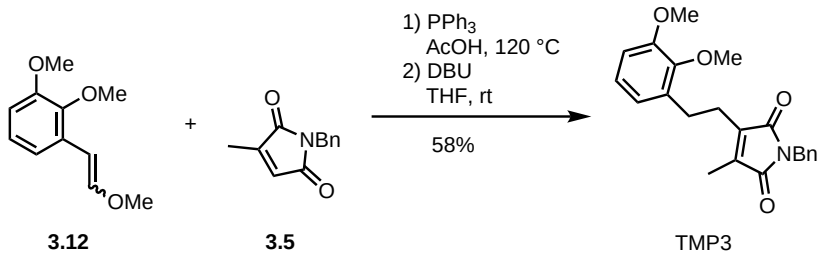

3.12 **3.5** TMP3

N-benzyl citraconimide (10.41 g, 51.72 mmol, 1 equiv) and PPh_3 (16.23 g, 62.06 mmol, 1.2 equiv) were added to a 1 L flask and dissolved in AcOH (260 mL, 0.2M). The mixture was stirred until homogeneous (about 15 minutes) under N_2 then for an additional 30 minutes. Methyl enol ether **3.12**[21] (11.05 g, 56.89 mmol, 1.1 equiv) was added and the flask was fitted with a reflux condenser, flushed with N_2 and heated to reflux. After 24 hours the flask was cooled and concentrated to remove the bulk of the acetic acid. The crude residue was azeotroped with PhMe (3x100 mL) to further remove any trace acetic acid and dried overnight under vacuum to give a thick orange paste. This paste was redissolved in THF (260 mL, 0.2M) and put under N_2 atmosphere. DBU (7.7 mL, 51.72 mmol, 1 equiv) was added to give a deep red solution. After 8 hours the mixture was quenched by the addition of 2N HCl (50 mL) and H_2O and concentrated under reduced pressure to remove most of the THF. The mixture was extracted with Et_2O (3x200 mL), washed with H_2O, brine, dried over $MgSO_4$, filtered and concentrated to give a yellow oil that was purified by flash chromatography (5%–10% EtOAc in Hx) to give imide **3.4a** (11.0 g, 58%) as a yellow oil. **^{1}H NMR:** (700 MHz, $CDCl_3$) δ 7.38–7.29 (m, 4H), 7.29–7.24 (m, 1H), 6.92 (t, J = 7.9 Hz, 1H), 6.78 (d, J = 8.6 Hz, 1H), 6.67 (d, J = 7.6 Hz, 1H), 4.65 (s, 2H), 3.83 (s, 3H), 3.77 (s, 3H), 2.84 (t, J = 7.4 Hz, 2H), 2.67 (t, J = 7.4 Hz, 2H), 1.66 (s, 3H); **^{13}C NMR:** (176 MHz, $CDCl_3$) δ 172.0, 171.8, 152.9, 147.5, 140.3, 138.2, 136.9, 134.3, 128.7, 128.4, 127.7, 124.1, 122.2, 111.2, 60.7, 55.9, 41.5, 28.9, 25.0, 8.4; **HRMS (ESI) m/z:** calculated for $[C_{22}H_{23}NO_4Na]^+$ 388.1519, found 388.1514.

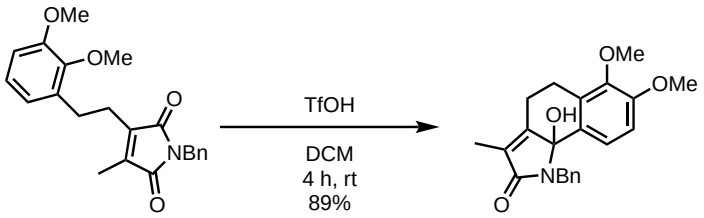

3.4a **3.11**

A solution of imide **3.4a** (10.93 g, 29.91 mmol, 1 equiv) in DCM (300 mL, 0.1M) was cooled to 0 °C. Triflic acid (15.9 mL, 179.46 mmol, 6 equiv) was added over 5 minutes and then the solution was removed from the ice bath and stirred at room temperature. Note: TfOH will rapidly destroy plastic syringes, use greased glass syringes when working with TfOH. After 4 hours the reaction was quenched by very careful addition of sat. $NaHCO_3$. A color change from red to yellow occurs near the end of the quench. Once the aqueous layer has a pH >8 it was extracted with DCM (3x200 mL), washed with sat. $NaHCO_3$, brine, dried over $MgSO_4$, filtered and concentrated to give an orange foam. The crude product was purified by flash chromatography (33%–50% EtOAc in Hx) to give tricycle **3.11** (9.73 g, 89%) as a pale orange foam. **^{1}H NMR:** (700 MHz, C_6D_6) δ 7.47 (d, J = 7.6 Hz, 2H), 7.20–7.14 (m, 2H), 7.07 (t, J = 7.8 Hz, 2H), 6.20 (d, J = 8.6 Hz, 1H), 5.12 (d, J = 16.3 Hz, 1H), 4.97 (d, J = 16.3 Hz, 1H), 3.60 (s, 2H), 3.14 (s, 3H), 3.12–3.04 (m, 2H), 2.89 (dt, J = 15.4, 6.7 Hz, 1H), 2.42 (dt, J = 14.6, 7.0 Hz, 1H), 2.27 (dt, J = 14.6, 6.6 Hz, 1H), 1.71 (s, 3H); **^{13}C NMR:** (176 MHz, $CDCl_3$) δ 173.9, 155.0, 153.0, 146.7, 140.2, 132.3, 130.8, 128.9, 128.5, 128.3, 127.2, 126.1, 122.7, 110.6, 88.9, 60.1, 55.3, 45.0, 37.0, 23.5, 21.3, 8.7; **R_f:** 0.33 in 1:1 Hx:EtOAc; **HRMS (ESI) m/z:** calculated for $[C_{22}H_{23}NO_4Na]^+$ 388.1519, found 388.1513.

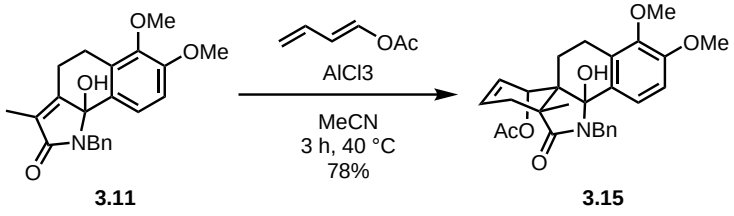

3.11 **3.15**

Tricycle **3.11** (3.65 g, 10 mmol, 1 equiv) and 1-acetoxybutadiene[22] (3.36 g, 30 mmol, 3 equiv) was added to a 200 mL flask and dissolved in MeCN (100 mL, 0.1M). The flask was cooled to 0 °C and $AlCl_3$ (4.0 g, 30 mmol, 3 equiv) was added (exotherm and color change from yellow to dark red). The flask was sealed, and heated to 40 °C for 3 hours, then cooled to room temperature, and the contents were poured into H_2O (150 mL) in a separatory funnel. The mixture was extracted with EtOAc (4x150 mL), washed with sat. $NaHCO_3$ twice, brine, dried over Na_2SO_4, filtered and concentrated to an orange foam. The crude product was purified by flash chromatography (20%–33% EtOAc in Hx) to give **3.15** (3.74 g, 78%) as a pale yellow foam.

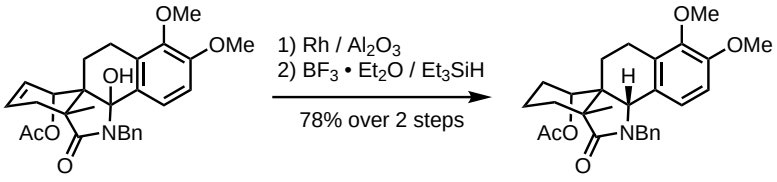

3.15 **3.17**

Diels–Alder adduct **3.15** (3.74 g, 7.83 mmol, 1 equiv) was dissolved in EtOAc (300 mL, 0.025M) and Rh on Al_2O_3 (5% rhodium, 935 mg, 25 %wt) was added. The flask was backfilled with H_2 5 times and then stirred vigorously overnight. After approximately 15 hours the reaction progress was checked by NMR and checked every few hours until >90% conversion was observed by NMR. Prolonged reaction times lead to overreduction to the N-methylenecyclohexyl product, which is difficult to separate chromatographically. Once complete, the reaction mixture was filtered through a pad of celite with EtOAc and concentrated to a white foam that was used without purification. **^{1}H NMR:** (600 MHz, $CDCl_3$) δ 7.41 (d, J = 8.6 Hz, 1H), 7.15–7.05 (m, 3H), 6.99 (dd, J = 7.7, 1.8 Hz, 2H), 6.82 (d, J = 8.6 Hz, 1H), 4.97 (dd, J = 11.5, 6.7 Hz, 1H), 4.28 (d, J = 15.2 Hz, 1H), 4.12 (d, J = 15.2 Hz, 1H), 3.86 (s, 3H), 3.51 (s, 3H), 2.65 (s, 1H), 2.59 (ddd, J = 16.2, 7.4, 4.3 Hz, 1H), 2.19 (ddd, J = 16.5, 9.6, 4.2 Hz, 2H), 1.97–1.84 (m, 3H), 1.84–1.78 (m, 2H), 1.53 (s, 3H), 1.43 (ddd, J = 14.0, 9.5, 4.4 Hz, 1H), 1.32 (s, 3H).

The crude hydrogenation product (3.61 g, 7.53 mmol, 1 equiv) was dissolved in DCM (75 mL, 0.1M) and transferred to a 250 mL Schlenck flask. Triethylsilane (12.0 mL, 75.3 mmol, 10 equiv) then $BF_3 \cdot Et_2O$ (9.3 mL, 75.3 mmol, 10 equiv) were added and the flask was sealed and heated to 50 °C overnight. After 14 hours the reaction mixture was cooled to 0 °C and carefully vented to release any built up pressure. The reaction mixture was poured into ca was quenched by careful slow addition of sat. $NaHCO_3$ until no more gas evolution was observed. The mixture was extracted with DCM (3x100 mL), dried over $MgSO_4$, filtered, and concentrated to a pale yellow foam. The crude product was purified by repeated Yamazen flash chromatograph to give lactam **3.17** (2.84 g, 78% over 2 steps) as a white solid. **^{1}H NMR:** (500 MHz, $CDCl_3$) δ 7.23–7.11 (m, 5H), 6.88 (d, J = 8.4 Hz, 1H), 6.61 (d, J = 8.3 Hz, 1H), 5.14 (d, J = 14.7 Hz, 1H), 4.47 (d, J = 14.6 Hz, 1H), 4.07 (s, 1H), 4.01–3.95 (m, 1H), 3.73 (s, 3H), 3.68 (s, 3H), 3.14 (ddd, J = 17.2, 9.5, 3.4 Hz, 1H), 2.35 (ddd, J = 16.9, 10.8, 5.6 Hz, 1H), 2.19 (d, J = 12.7 Hz, 1H), 1.86 (ddd, J = 14.2, 10.8, 3.5 Hz, 1H), 1.69 (s, 3H), 1.56–1.47 (m, 1H), 1.46–1.32 (m, 2H), 1.32–1.18 (m, 2H), 1.10 (td, J = 13.6, 4.5 Hz, 1H), 0.83 (s, 3H); **^{13}C NMR:** (126 MHz, $CDCl_3$) δ 181.8, 169.0, 151.1, 146.9, 136.5, 129.5, 128.9, 128.6, 128.5, 128.4, 127.7, 118.4, 109.4, 71.1, 60.6, 60.5, 55.8, 47.9, 45.2, 30.8, 25.9, 23.0, 21.6, 21.4, 19.2, 16.6; **HRMS (ESI) m/z:** calculated for $[C_{28}H_{34}NO_5]^+$ 464.2432, found 464.2427.

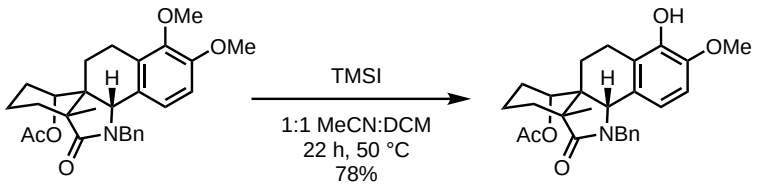

3.17 **3.3**

Lactam **3.17** (1000 mg, 2.16 mmol, 1 equiv) was dissolved in DCM (22 mL, 0.1M) and transferred to a dry 100 mL Schlenck flask by cannula. The residual material was dissolved in MeCN (22 mL, 0.1M) and transferred to the Schlenck flask. The flask was sealed and transferred to a glove box where trimethylsilyl iodide (3.06 mL, 10 equiv was added). The flask was sealed and remove from the glove box and transferred to 40 °C oil bath. After 22 hours the reaction mixture was carefully diluted with sat. NaH_3CO_3 and $Na_2S_2O_3$ solution. The mixture was extracted with DCM (3x 100 mL), washed with sat. $NaHCO_3$ and $Na_2S_2O_3$, dried over $MgSO_4$, filtered, and concentrated. The crude residue was dry loaded onto celite and flushed through a 2 cm plug of silica with 5% EtOAc in Hx to remove a non polar byproduct. The resulting solution was concentrated and purified by Yamazen flash chromatography to give guiacol **3.3** (759 mg, 78%) as a white solid. **^{1}H NMR:** (500 MHz, $CDCl_3$) δ 7.32–7.19 (m, 5H), 6.80 (d, J = 8.3 Hz, 1H), 6.66 (d, J = 8.3 Hz, 1H), 5.76 (s, 1H), 5.27 (d, J = 14.6 Hz, 1H), 4.55 (d, J = 14.5 Hz, 1H), 4.19–4.14 (m, 2H), 3.85 (s, 3H), 3.20 (ddd, J = 17.3, 9.6, 3.9 Hz, 1H), 2.44 (ddd, J = 16.8, 10.8, 5.2 Hz, 1H), 2.28 (dq, J = 13.5, 3.1, 2.6 Hz, 1H), 1.95 (ddd, J = 14.5, 10.9, 4.0 Hz, 1H), 1.81 (s, 3H), 1.65–1.59 (m, 1H), 1.57–1.44 (m, 2H), 1.43–1.31 (m, 2H), 1.21 (td, J = 13.6, 4.7 Hz, 1H), 0.92 (s, 3H).

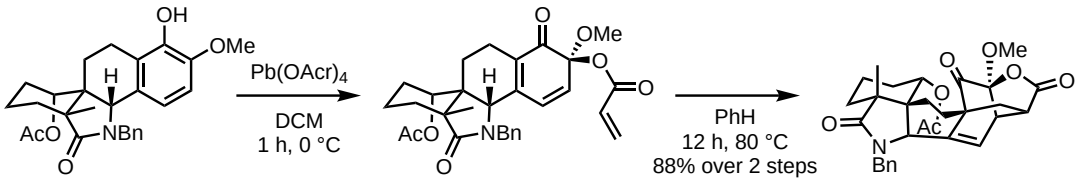

3.3 **3.22** **3.23**

$Pb(OAc)_4$ (895 mg, 2.02 mmol, 1.2 equiv) was dissolved in DCM (28 mL, 0.06M). Acrylic acid (7.4 mL, 108.1 mmol, 64 equiv) was added and the resulting solution of $Pb(OAcr)_4$ was stirred for 30 minutes. Meanwhile, a solution of guiacol **3.3** (759 mg, 1.69 mmol, 1 equiv) in DCM (57 mL, 0.03M) was prepared. Once the lead solution had stirred for 30 minutes it was cooled to 0 °C and the guiacol solution was added. After stirring 1 hour at 0 °C the reaction was quenched by the addition of ethylene glycol (200 μL), poured in to ice water, and extracted with DCM (3x100 mL). The organic layers were combined, washed with sat. $NaHCO_3$, dried over MgSO4, and concentrated to give masked orthobenzoquinone **3.22** as a yellow foam.

The crude masked orthobenzoquinone **3.22** was dissolved in PhH (85 mL, 0.02M) in a 200 mL flask. The solution was sparged with N_2 for 5 minutes and then the flask fitted with a condenser and refluxed overnight. After 12 hours the solution was concentrated under reduced pressure and purified by flash chromatography (0%–5% MeOH in DCM) to give Diels–Alder product **3.23** (775 mg) as a yellow foam. **^{1}H NMR:** (700 MHz, $CDCl_3$) δ 7.30–7.27 (m, 3H), 7.18–7.15 (m, 2H), 6.06 (dd, J = 6.8, 1.9 Hz, 1H), 5.30 (d, J = 14.5 Hz, 1H), 4.10 (d, J = 14.5 Hz, 1H), 4.07–4.06 (m, 1H), 3.87 (d, J = 2.5 Hz, 1H), 3.75 (s, 3H), 3.59 (dd, J = 6.7, 5.1 Hz, 1H), 2.77 (ddd, J = 10.5, 5.1, 1.2 Hz, 1H), 2.24 (dd, J = 14.6, 7.6 Hz, 1H), 2.22–2.19 (m, 1H), 1.94 (s, 4H), 1.93–1.91 (m, 1H), 1.87 (dd, J = 14.9, 8.7 Hz, 1H), 1.80 (d, J = 14.5 Hz, 1H), 1.55–1.52 (m, 1H), 1.44 (tt, J = 13.2, 3.6 Hz, 1H), 1.39–1.31 (m, 4H), 1.14 (td, J = 13.5, 4.6 Hz, 1H), 0.92 (s, 3H); **^{13}C NMR:** (176 MHz, $CDCl_3$) δ 199.7, 179.6, 174.2, 168.6, 142.3, 135.7, 128.7, 128.6, 128.2, 116.9, 99.6, 73.5, 57.1, 55.1, 53.4, 45.9, 45.4, 45.2, 44.9, 40.2, 37.1, 30.3, 25.2, 23.5, 22.3, 21.4, 20.7, 16.3.

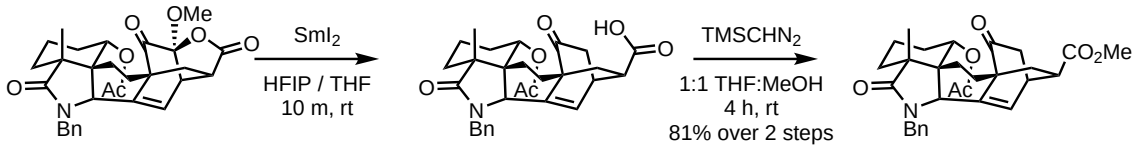

3.23 **3.69** **3.26**

Diels–Alder product **3.23** (486 mg, 0.935 mmol, 1 equiv) was dissolved in N_2 sparged HFIP (9.8 mL, 93.5 mmol, 100 equiv) under N_2 atmosphere. SmI_2 (0.09M in THF, 66 mL, 5.97 mmol, 4 equiv) was added and the solution was stirred at room temperature. After 1 hour the reaction was quenched by the slow addition of 2N HCl (5 mL). The reaction mixture was concentrated to remove most of the THF and then diluted with H_2O to dissolve Sm salts and extracted with Et_2O, washed with brine, dried over $MgSO_4$, filtered and concentrated to give a pale yellow foam (roughly 60:40 product:**3.3**). The crude extract was redissolved in Et_2O and extracted with sat. $NaHCO_3$ (3x50 mL). The combined bicarbonate extracts were acidified with conc. HCl (white solid precipitated) and extracted with Et_2O (3x50 mL). The organic extracts were concentrated to give the crude carboxylic acid **3.69** (366 mg) as a white foam. **^{1}H NMR:** (500 MHz, $CDCl_3$) δ 7.38–7.32 (m, 3H), 7.25 (dd, J = 7.2, 2.3 Hz, 2H), 6.40 (dd, J = 6.8, 2.3 Hz, 1H), 5.37 (d, J = 14.4 Hz, 1H), 4.31 (s, 1H), 4.13 (d, J = 14.3 Hz, 1H), 3.89 (d, J = 2.4 Hz, 1H), 3.41 (s, 1H), 2.80–2.71 (m, 1H), 2.38–2.22 (m, 4H), 2.12 (dd, J = 13.4, 5.3 Hz, 1H), 1.86 (dd, J = 14.7, 8.4 Hz, 1H), 1.61–1.07 (m, 13H), 0.95 (s, 3H).

The SmI_2 reduction product (366 mg, 0.74 mmol, 1 equiv) was dissolved in 1:1 THF:MeOH (15 mL, 0.05M) and $TMSCHN_2$ (2M in Et_2O, 740 μL, 1.47 mmol, 2 equiv) was added. After stirring 4 hours at room temperature the reaction was quenched with AcOH (200 μL), and the reaction mixture was concentrated and azeotroped with PhMe to give a white foam. The crude product was purified by Yamazen flash chromatography using (0%–3% MeOH in DCM). The resulting methyl ester **3.26** (354 mg) was a white foam containing 10% of an impurity that could be removed by preparative TLC (2 runs with 15% Et_2O in DCM). **^{1}H NMR:** (700 MHz, $CDCl_3$) δ 7.31–7.27 (m, 3H), 7.19 (dd, J = 7.5, 2.0 Hz, 2H), 6.33 (dd, J = 6.8, 2.3 Hz, 1H), 5.31 (d, J = 14.3 Hz, 1H), 4.25 (d, J = 2.5 Hz, 1H), 4.07 (d, J = 14.3 Hz, 1H), 3.83 (d, J = 2.4 Hz, 1H), 3.71 (s, 3H), 3.31 (dq, J = 5.6, 2.7 Hz, 1H), 2.65 (ddt, J = 11.1, 5.2, 2.3 Hz, 1H), 2.30–2.22 (m, 2H), 2.21–2.13 (m, 2H), 2.06 (dd, J = 13.5, 5.4 Hz, 1H), 1.94 (s, 3H), 1.79 (dd, J = 14.8, 8.4 Hz, 1H), 1.58–1.54 (m, 1H), 1.52–1.43 (m, 2H), 1.42–1.36 (m, 1H), 1.31 (dd, J = 13.6, 11.3 Hz, 2H), 1.24–1.20 (m, 1H), 1.13 (td, J = 13.6, 4.9 Hz, 1H), 0.89 (s, 3H); **^{13}C NMR:** (176 MHz, $CDCl_3$) δ 210.7, 179.7, 173.8, 169.4, 138.5, 135.9, 128.7, 128.6, 128.1, 125.6, 72.8, 56.9, 53.0, 52.4, 45.6, 45.2, 44.6, 42.4, 36.4, 35.2, 33.3, 30.0, 25.6, 23.6, 22.1, 21.7, 20.6, 16.5; **HRMS (ESI) m/z:** calculated for $[C_{30}H_{35}NO_6Na]^+$ 528.2357, found 528.2363.

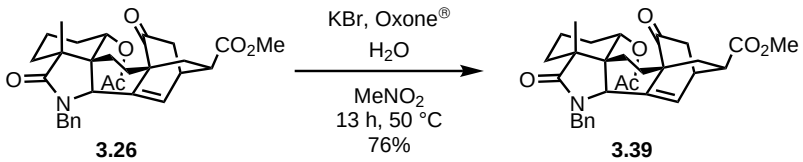

3.26 **3.39**

Pentacycle **3.26** (49 mg, 97 μmol, 1 equiv) was dissolved in $MeNO_2$ (4.85 mL, 0.02M) in a dry 20 mL vial. KBr (35 mg, 291 μmol, 3 equiv), H_2O (49 uL, 2.72 mmol, 30 equiv), and Oxone® (357 mg, 581 μmol, 6 equiv) were added and the vial sealed and heated to 50 °C under fluorescent (fume hood lights) bulbs. After 13 hours the mixture was cooled to room temperature, diluted with sat. $NaHCO_3$ and aqueous $Na_2S_2O_3$, extracted with EtOAC (3x10 mL), washed with sat. $NaHCO_3$, brine, dried over $MgSO_4$, filtered and concentrated. The crude residue was purified by flash chromatography (25%–66% EtOAc in Hx) to give vinylogous imide **3.39** (31 mg, 76%) as a white foam. **^{1}H NMR:** (700 MHz, $CDCl_3$) δ 9.73 (s, 1H), 5.32 (dd, J = 3.8, 2.4 Hz, 1H), 3.73 (s, 3H), 3.08 (q, J = 2.7 Hz, 1H), 3.00 (ddt, J = 10.4, 6.1, 1.8 Hz, 1H), 2.82 (td, J = 15.0, 4.6 Hz, 1H), 2.71 (dd, J = 19.4, 2.8 Hz, 1H), 2.49 (ddd, J = 19.4, 3.0, 1.8 Hz, 1H), 2.26–2.14 (m, 3H), 1.89 (s, 3H), 1.84 (td, J = 14.3, 4.5 Hz, 1H), 1.78–1.70 (m, 2H), 1.64 (dddd, J = 16.7, 12.8, 8.4, 3.8 Hz, 1H), 1.57–1.44 (m, 3H), 1.28 (ddd, J = 14.4, 12.9, 4.9 Hz, 1H), 1.08 (s, 3H).

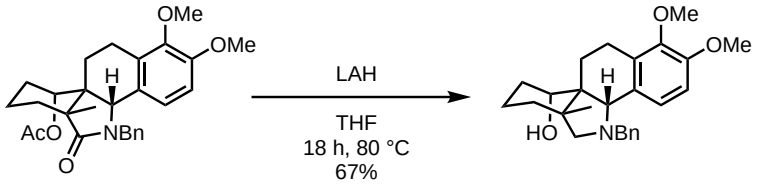

3.17 **3.70**

Lactam **3.17** (5.42 g, 11.69 mmol, 1 equiv) was dissolved in THF (230 mL, 0.05M) and LAH (2M in THF, 29.2 mL, 58.45 mmol, 5 equiv) was added and the mixture was refluxed overnight. After 18 hours the mixture was cooled to 0 °C and quenched by the careful sequential addition of 1 mL H_2O, 1 mL 15% NaOH, and 3 mL of H_2O. The mixture was diluted with Et_2O and $MgSO_4$ was added until and stirred until a fine and flocculent. The mixture was filtered through a pad of celite with Et_2O and concentrated to give a white foam. The crude material was purified by flash chromatography (20%–25% EtOAch In Hx) to give amino alcohol **3.70** (3.20 g, 67%) as a white solid. **^{1}H NMR:** (700 MHz, $CDCl_3$) δ 7.43 (d, J = 7.2 Hz, 2H), 7.38 (t, J = 7.7 Hz, 2H), 7.29 (t, J = 7.5 Hz, 1H), 7.13 (d, J = 8.3 Hz, 1H), 6.82 (d, J = 8.3 Hz, 1H), 6.08 (bs, 1H), 4.54 (d, J = 14.3 Hz, 1H), 4.17 (s, 1H), 3.85 (s, 3H), 3.80 (s, 3H), 3.62 (d, J = 10.6 Hz, 1H), 3.58 (d, J = 14.4 Hz, 1H), 3.21 (ddd, J = 16.5, 8.7, 3.4 Hz, 1H), 3.06 (dd, J = 4.0, 2.0 Hz, 1H), 2.52 (ddd, J = 16.9, 10.0, 7.3 Hz, 1H), 2.33 (d, J = 10.5 Hz, 1H), 1.98 (ddd, J = 13.7, 10.1, 3.4 Hz, 1H), 1.88–1.79 (m, 1H), 1.56–1.46 (m, 2H), 1.37–1.30 (m, 2H), 1.27–1.14 (m, 2H), 1.12 (s, 3H); **^{13}C NMR:** (700 MHz, $CDCl_3$) δ 151.2, 146.3, 138.9, 130.9, 130.5, 128.7, 128.0, 127.3, 118.2, 109.9, 70.1, 69.0, 65.9, 61.4, 60.7, 55.8, 49.6, 40.1, 33.3, 29.3, 28.4, 23.7, 20.7, 15.6.

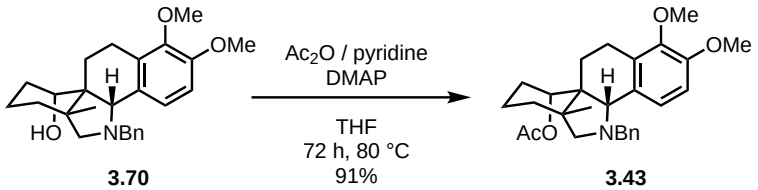

3.70 **3.43**

Amino alcohol **3.76** (3.20 g, 7.85 mmol, 1 equiv) was dissolved in THF (80 mL, 0.1M). DMAP (192 mg, 1.57 mmol, 0.2 equiv), pyridine (3.17 mL, 39.25 mmol, 5 equiv) and Ac_2O (3.71 mL, 39.25 mmol, 5 equiv) were added. The flask was fitted with a reflux condenser and refluxed for three days, or until NMR of an aliquot showed full conversion. Once complete the flask was cooled to room temperature, quenched with sat. $NaHCO_3$ until no more gas evolution occurred, then concentrated in vacuo to remove most of the THF. The mixture was extracted with DCM (3x100 mL), dried over $MgSO_4$, filtered and concentrated to an orange foam. The crude product was purified by flash chromatography (20%–33% EtAOc in Hx) to give amino acetate **3.43** (3.22 g, 91%) as a white foam. **^{1}H NMR:** (700 MHz, $CDCl_3$) δ 7.54 (d, J = 7.6 Hz, 2H), 7.37 (t, J = 7.6 Hz, 2H), 7.28 (t, J = 7.6 Hz, 1H), 6.95 (d, J = 1.2 Hz, 1H), 6.69 (d, J = 8.3 Hz, 1H), 4.39 (s, 1H), 4.27 (d, J = 14.8 Hz, 1H), 4.15 (s, 1H), 3.81 (d, J = 2.2 Hz, 6H), 3.77–3.70 (m, 2H), 3.16 (ddd, J = 17.9, 9.7, 5.8 Hz, 1H), 2.73 (ddd, J = 17.9, 10.6, 3.5 Hz, 1H), 2.27 (s, 1H), 2.06–1.99 (m, 1H), 1.96 (s, 3H), 1.71–1.43 (m, 6H), 1.34–1.28 (m, 1H), 1.23 (td, J = 13.5, 4.5 Hz, 1H), 1.13 (s, 3H); **^{13}C NMR:** (176 MHz, $CDCl_3$) δ 169.6, 150.9, 147.0, 141.6, 132.2, 129.2, 128.4, 127.9, 126.7, 118.0, 109.8, 71.2, 70.0, 65.0, 62.2, 60.3, 56.0, 48.4, 41.6, 33.0, 28.2, 27.0, 24.9, 21.7, 20.6, 16.2; **HRMS (ESI) m/z:** calculated for $[C_{28}H_{36}NO_4]^+$ 450.2639, found 450.2635.

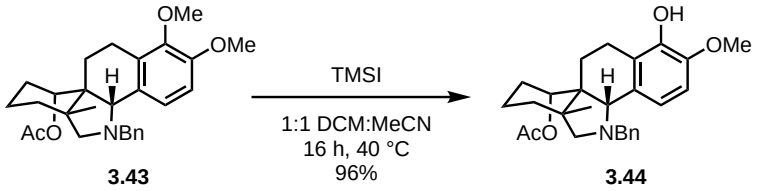

Amino veratrol **3.43** (3.22 g, 7.16 mmol, 1 equiv) was dissolved in DCM (65 mL, 0.11M) and cannulated into a dry 250 mL Schlenck flask. The residual starting material was dissolved in MeCN (65 mL, 0.11M) and cannulated to the Schlenck flask. The flask was sealed and transferred to a glove box where TMSI (10.2 mL, 71.62 mmol, 10 equiv) was added. The flask was removed from the glove box and heated to 40 °C overnight. After 16 hours the reaction mixture was cooled to room temperature, diluted with Et_2O and poured into a solution of $Na_2S_2O_3$. Sat. $NaHCO_3$ was carefully added until no more gas evolved when shaken. The resulting emulsion was extracted with Et_2O (3x200 mL) and DCM (2x200 mL) the combine organics were washed with a solution of $NaHCO_3$ and $Na_2S_2O_3$ three times until the aqueous layer was clear then the organic layer was washed with brine, dried over $MgSO_4$, filtered and concentrated. The crude product was purified by flash chromatography (25%–33% EtOAc in Hx) to give the guaicol **3.44** (2.99 g, 96%) as a white solid. **^{1}H NMR:** (500 MHz, C_6D_6) δ 7.62 (d, J = 7.6 Hz, 2H), 7.35 (t, J = 7.7 Hz, 2H), 7.21 (t, J = 7.4 Hz, 1H), 6.84 (d, J = 8.1 Hz, 1H), 6.37 (d, J = 8.1 Hz, 1H), 5.79 (s, 1H), 4.68 (s, 1H), 4.27 (d, J = 14.9 Hz, 1H), 3.98 (s, 1H), 3.73 (d, J = 10.5 Hz, 1H), 3.61 (d, J = 14.9 Hz, 1H), 3.30 (ddd, J = 18.1, 9.7, 6.5 Hz, 1H), 3.22 (s, 3H), 2.72 (ddd, J = 18.2, 10.4, 2.9 Hz, 1H), 2.13 (d, J = 10.4 Hz, 1H), 1.91 (s, 3H), 1.72–1.58 (m, 2H), 1.52 (qt, J = 13.7, 3.7 Hz, 1H), 1.34–1.22 (m, 2H), 1.15 (tdd, J = 13.8, 3.9, 2.3 Hz, 1H), 1.05 (d, J = 13.3 Hz, 1H), 0.91 (td, J = 13.8, 4.8 Hz, 1H), 0.82 (s, 3H); **^{13}C NMR:** (126 MHz, C_6D_6) δ 168.4, 145.0, 143.8, 142.2, 132.8, 128.6, 128.2, 126.9, 121.3, 113.6, 108.0, 71.5, 69.5, 65.4, 62.6, 55.6, 48.5, 41.5, 33.0, 27.9, 27.2, 25.0, 21.5, 20.7, 16.5; **HRMS (ESI) m/z:** calculated for $[C_{27}H_{34}NO_4]^+$ 436.2482, found 436.2478.

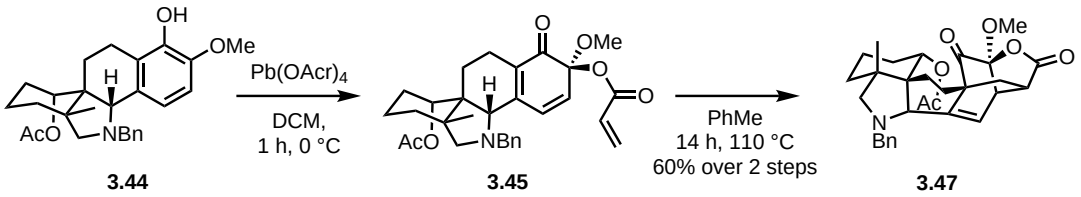

3.44 **3.45** **3.47**

A dry recovery flask was charged with $Pb(OAc)_4$ (3.77 g, 8.51 mmol, 1.1 equiv) and DCM (60 mL). Acrylic acid (32.8 mL, 464 mmol, 60 equiv) was added and the solution was stirred for 30 minutes. Meanwhile, guiacol **3.44** (3.37 g, 7.74 mmol, 1 equiv) was dissolved in DCM (180 mL, 0.04M) and cooled to 0 °C under N_2. After stirring for 20 minutes the lead solution was cannulated into the guiacol solution. After stirring for an additional hour the reaction was quenched by the addition of ethylene glycol (1 mL) and transferred to an Erlenmeyer flask in an ice bath. Ice cold 2N KOH(200 mL) was added followed by aqueous K_2CO_3 until potassium polyacrylate precipitated and the aqueous layer was basic. This emulsion was extracted with DCM (3x200 mL), washed with sat. $NaHCO_3$ twice, brine, dried over Na_2SO_4, filtered and concentrated to an orange foam (4.18 g, 106% mass balance) that was azeotroped with PhMe and used without purification.

The crude Wessley oxidation product **3.45** was dissolved in PhMe (240 mL, 0.04M) and sparged with N_2 5 minutes before the flask was fitted with a condenser and heated to 120 °C overnight. After 14 hours the reaction mixture was concentrated and purified by flash chromatography (0%–6% Et_2O in DCM) to give the desired Diels–Alder product **3.47** (2.33 g, 60% over 2 steps) as a pale orange solid. **^{1}H NMR:** (500 MHz, $CDCl_3$) δ 7.41 (d, J = 7.6 Hz, 2H), 7.37–7.30 (m, 2H), 7.24 (t, J = 7.3 Hz, 1H), 5.85 (dd, J = 6.5, 2.5 Hz, 1H), 4.16–4.13 (m, 1H), 4.03 (d, J = 14.1 Hz, 1H), 3.94 (d, J = 2.6 Hz, 1H), 3.76 (s, 3H), 3.63–3.44 (m, 4H), 2.74 (ddd, J = 10.5, 5.1, 1.2 Hz, 1H), 2.40–2.31 (m, 1H), 2.17 (d, J = 10.5 Hz, 1H), 2.08 (s, 3H), 2.03 (d, J = 13.8 Hz, 1H), 1.97–1.88 (m, 1H), 1.80 (d, J = 13.8 Hz, 1H), 1.70 (dd, J = 13.6, 10.5 Hz, 1H), 1.54–1.38 (m, 5H), 1.29–1.23 (m, 1H), 1.16 (td, J = 13.7, 4.7 Hz, 1H), 1.06 (d, J = 0.9 Hz, 3H); **^{13}C NMR:** (176 MHz, $CDCl_3$) δ 200.2, 175.0, 169.3, 145.4, 140.7, 128.4, 126.9, 126.9, 114.7, 100.3, 73.2, 68.4, 64.1, 61.3, 54.9, 53.1, 48.3, 45.3, 41.2, 40.6, 37.6, 32.6, 28.0, 25.9, 24.0, 23.5, 21.7, 15.9. **HRMS (ESI) m/z:** calculated for $[C_{30}H_{36}NO_6]^+$ 506.2537, found 506.2531.

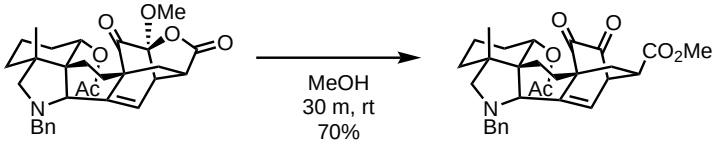

3.47 **3.48**

Diels–Alder product **3.47** (20 mg, 40 μmol, 1 equiv) was dissolved in MeOH (2 mL, 0.02M) under N_2. After several minutes the colorless solution turned bright yellow, and after 30 minutes the reaction mixture was concentrated and purified by flash chromatography (20%–33% EtOAc in Hx) to give diketone **3.48** (14 mg, 70%) as a yellow solid. **^{1}H NMR:** (700 MHz, C_6D_6) δ 7.39 (d, J = 7.6 Hz, 2H), 7.27 (t, J = 7.5 Hz, 2H), 7.18 (t, J = 7.2 Hz, 1H), 5.66 (dd, J = 6.8, 2.4 Hz, 1H), 4.47 (s, 1H), 3.82 (d, J = 14.0 Hz, 1H), 3.61 (d, J = 2.5 Hz, 1H), 3.48 (d, J = 10.5 Hz, 1H), 3.44 (dd,

J = 6.7, 2.9 Hz, 1H), 3.35 (d, J = 14.1 Hz, 1H), 3.23 (s, 3H), 2.48 (ddd, J = 11.7, 5.1, 2.9 Hz, 1H), 2.26 (dd, J = 14.4, 7.6 Hz, 1H), 2.15 (dd, J = 13.6, 5.0 Hz, 1H), 1.95 (d, J = 10.5 Hz, 1H), 1.80 (s, 3H), 1.48 (dd, J = 14.8, 8.7 Hz, 1H), 1.42–1.29 (m, 3H), 1.27–1.22 (m, 1H), 1.20–1.09 (m, 3H), 0.95–0.91 (m, 1H), 0.77 (td, J = 13.7, 4.8 Hz, 1H), 0.72 (s, 3H); **^{13}C NMR:** (176 MHz, C_6D_6) δ 189.9, 185.7, 172.9, 168.3, 145.1, 141.0, 128.6, 128.4, 128.3, 127.2, 117.7, 71.7, 68.8, 64.2, 61.7, 53.3, 52.1, 51.1, 49.3, 42.0, 40.9, 33.9, 32.4, 27.8, 26.6, 23.8, 23.7, 21.4, 16.2.

3.47 **3.50**

Diels–Alder product **3.47** (10 mg, 20 μmol, 1 equiv) was dissolved in MeOH (1 mL, 0.02M) and stirred for 30 minutes until full conversion to diketone **3.48** was observed by TLC. The crude diketone solution was concentrated and the residue was redissolved in 5:1 THF:MeOH (1.2 mL, 0.017M). SmI_2 (0.07M in THF, 2.3 mL, 160 μmol, 8 equiv) was added. The resulting dark blue solution was stirred for 20 minutes after which it faded to a pale gray/yellow. The reaction was quenched with sat. $NaHCO_3$, extracted with DCM (4x10 mL), dried over $MgSO_4$, filtered and concentrated. The resulting yellow residue was purified by preparative TLC (1/4 plate, 50% EtOAc in Hx) to give ketone **3.50**. **^{1}H NMR:** (700 MHz, C_6D_6) δ 7.44 (d, J = 7.5 Hz, 2H), 7.29 (t, J = 7.7 Hz, 2H), 7.19 (t, J = 7.7 Hz, 1H), 5.89 (dd, J = 6.6, 2.5 Hz, 1H), 4.64 (d, J = 2.2 Hz, 1H), 3.92 (d, J = 14.1 Hz, 1H), 3.65 (d, J = 2.5 Hz, 1H), 3.51 (d, J = 10.4 Hz, 1H), 3.35 (d, J = 14.1 Hz, 1H), 3.26 (s, 3H), 2.94 (dq, J = 5.6, 2.7 Hz, 1H), 2.58 (dt, J = 18.5, 2.5 Hz, 1H), 2.46–2.36 (m, 2H), 2.34–2.26 (m, 2H), 1.99 (d, J = 10.4 Hz, 1H), 1.89 (s, 3H), 1.60–1.37 (m, 3H), 1.29–1.12 (m, 4H), 0.95 (d, J = 13.8 Hz, 1H), 0.83–0.78 (m, 1H), 0.76 (s, 4H); **^{13}C NMR:** (176 MHz, C_6D_6) δ 210.0, 174.0, 169.0, 141.5, 128.5, 128.4, 128.4, 127.0, 123.4, 72.4, 68.3, 64.3, 61.6, 52.8, 51.5, 48.3, 42.8, 40.8, 36.9, 35.6, 34.1, 32.5, 28.0, 26.5, 24.2, 23.9, 21.7, 16.3.

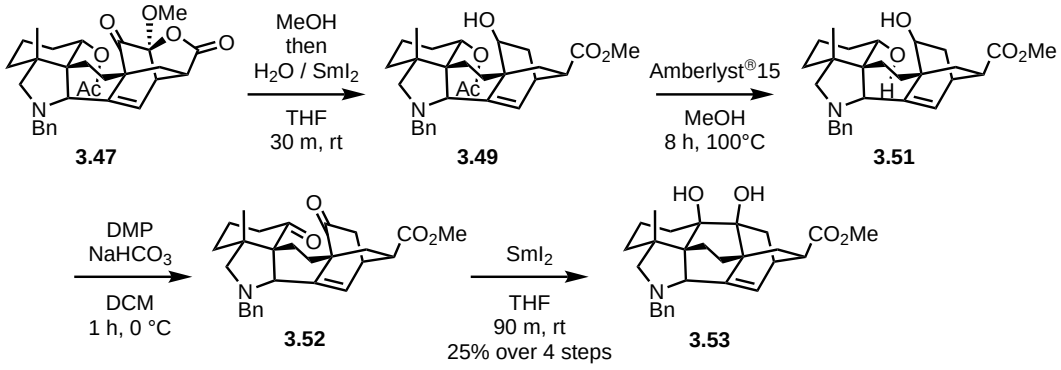

3.47 **3.49** **3.51** **3.52** **3.53**

Diels–Alder product **3.47** (300 mg, 593 μmol, 1 equiv) was dissolved in MeOH (6 mL, 0.1M) and stirred 30 minutes until full conversion to diketone **3.48** was observed by TLC. THF (30 mL,

0.02M) and H_2O (6 mL, 0.1M) were added and the solution was sparged with N_2 for 20 minutes then SmI_2 (0.099M in THF, 48 mL, 4.75 mmol, 8 equiv) was added and the solution was stirred. Additional SmI_2 (2 equiv) was added whenever the reaction mixture turned from deep purple to grey/yellow until the dark purple color had persisted for at least 30 minutes (12 equiv of SmI_2 total, variable from batch to batch). Upon completion, the reaction was quenched by the addition of sat. $NaHCO_3$ and aqueous $Na_2S_2O_3$. The mixture was extracted with Et_2O (3x100 mL), filtered through a 2 cm silica plug with additional Et_2O and concentrated to give alcohol **3.50** as a pale yellow foam (284 mg). **^{1}H NMR:** (700 MHz, C_6D_6) δ 7.45 (d, J = 7.5 Hz, 2H), 7.29 (t, J = 7.7 Hz, 2H), 7.19 (t, J = 7.5 Hz, 1H), 5.92 (dd, J = 6.7, 2.7 Hz, 1H), 5.85 (dd, J = 4.0, 2.2 Hz, 1H), 4.02 (d, J = 14.2 Hz, 1H), 3.95 (s, 1H), 3.63 (d, J = 2.8 Hz, 1H), 3.57–3.51 (m, 2H), 3.33 (d, J = 14.1 Hz, 1H), 3.32 (s, 3H), 2.74 (dq, J = 6.0, 2.9 Hz, 1H), 2.47 (ddd, J = 13.8, 9.0, 3.1 Hz, 1H), 2.24 (ddd, J = 14.6, 8.0, 4.6 Hz, 1H), 2.21 (dq, J = 11.2, 2.3, 1.8 Hz, 1H), 2.02 (dd, J = 13.2, 4.6 Hz, 1H), 2.01 (d, J = 10.8 Hz, 1H), 1.91 (s, 3H), 1.62 (ddd, J = 13.7, 8.9, 4.6 Hz, 1H), 1.59–1.48 (m, 2H), 1.44 (dt, J = 14.5, 8.4 Hz, 2H), 1.37 (ddt, J = 13.7, 4.7, 2.4 Hz, 1H), 1.32 (ddd, J = 14.0, 4.0, 2.2 Hz, 1H), 1.25–1.18 (m, 1H), 1.09 (dd, J = 12.9, 11.1 Hz, 1H), 1.06–1.01 (m, 1H), 0.92 (dd, J = 13.7, 5.0 Hz, 1H), 0.80 (d, J = 0.9 Hz, 3H).

A dry 20 mL microwave vial was charged with Amberlyst®15 resin (140 mg, 50% wt.) and evacuated. Crude **3.50** (284 mg) was dissolved in MeOH (14.3 mL, 0.04M) and transferred to the microwave vial. The solution was sparged with N_2 for 5 minutes then subjected to microwave heating at 100 °C for 8 hours. Upon cooling the solution was filtered through a celite plug, which was washed with MeOH containing 5% Et_3N. The resulting solution was concentrated and flushed through a 2 cm silica pad with large amounts of Et_2O and concentrated. This was repeated until the mass was constant after concentrating to give crude diol **3.51** (171 mg) as a yellow foam. **^{1}H NMR:** (600 MHz, $CDCl_3$) δ 7.36–7.21 (m, 5H), 6.73 (bs, 1H), 6.27 (dd, J = 6.7, 2.5 Hz, 1H), 4.37 (dd, J = 3.9, 2.0 Hz, 1H), 4.34 (d, J = 13.9 Hz, 1H), 3.84 (dd, J = 9.6, 4.1 Hz, 2H), 3.68 (s, 3H), 3.45 (d, J = 10.5 Hz, 1H), 3.35 (d, J = 13.9 Hz, 1H), 2.91 (dq, J = 6.0, 2.9 Hz, 1H), 2.40 (ddt, J = 11.0, 4.6, 2.4 Hz, 1H), 2.20 (ddd, J = 13.7, 8.9, 3.2 Hz, 1H), 2.17 (d, J = 10.5 Hz, 1H), 1.99–1.91 (m, 2H), 1.88 (dd, J = 13.1, 4.5 Hz, 1H), 1.81 (dt, J = 13.0, 3.7 Hz, 1H), 1.79–1.74 (m, 1H), 1.64–1.53 (m, 3H), 1.43 (s, 1H), 1.42–1.38 (m, 1H), 1.36–1.29 (m, 1H), 1.27–1.24 (m, 1H), 1.17–1.09 (m, 1H), 0.97 (s, 3H).

A dry flask was charged with the crude diol **3.51** (171 mg, 380 μmol, 1 equiv) and DCM (38 mL, 0.01M). $NaHCO_3$ (255 mg, 3.03 mmol, 8 equiv) and DMP (640 mg, 1.51 mmol, 4 equiv) were added and the reaction was stirred at room temperature under N_2. Reaction progress was monitored by LCMS. After 1 hour the reaction was quenched by aqueous $Na_2S_2O_3$ and stirred for 10 minutes. The mixture was extracted with DCM (3x100 mL), washed with sat. $NaHCO_3$, brine, dried over $MgSO_4$, filtered through a celite plug, and concentrated. The crude residue was azeotroped with PhMe to give the crude diketone **3.52** (166 mg) as a yellow/brown solid. **^{1}H NMR:** (500 MHz, $CDCl_3$) δ 7.37–7.28 (m, 4H), 7.26–7.21 (m, 1H), 6.24 (dd, J = 6.8, 2.6 Hz, 1H), 4.30 (d, J = 14.0 Hz, 1H), 3.70 (s, 3H), 3.63 (d, J = 2.6 Hz, 1H), 3.41 (d, J = 14.0 Hz, 1H), 3.29 (dq, J = 5.5, 2.7 Hz, 1H), 3.22 (d, J = 11.0 Hz, 1H), 2.77 (ddt, J = 11.4, 5.0, 2.3 Hz, 1H), 2.43–2.09 (m, 7H), 1.93 (ddd, J = 14.9, 7.6, 1.7 Hz, 1H), 1.79–1.68 (m, 3H), 1.64 (dd, J = 13.6, 11.4 Hz, 1H), 1.53–1.39 (m, 4H), 1.03 (s, 3H).

Crude diketone **3.52** (166 mg, 0.37 mmol, 1 equiv) was dissolved in THF (18 mL, 0.02M) and sparged with N_2 for 10 minutes. SmI_2 (0.099M in THF, 15 mL, 1.48 mmol, 4 equiv) was added and the resulting deep blue solution was stirred until the blue color had persisted for at least

90 minutes. In some cases additional SmI_2 was needed to maintain the appropriate color for the duration of the reaction. After the reaction was complete it was quenched with sat. $NaHCO_3$ and aqueous $Na_2S_2O_3$, extracted with Et_2O (3x50 mL), washed sequentially with $NaHCO_3$ and aqueous $Na_2S_2O_3$, H_2O, and brine. The organic layer was dried over $MgSO_4$, filtered and concentrated to give a crude brown residue that was purified by Yamazen flash chromatography (25%–45% EtOAc in Hx) to give the pinacol product **3.53** (93 mg, 25% over 4 steps) as a white solid. **^{1}H NMR:** (500 MHz, $CDCl_3$) δ 7.40 (d, J = 7.3 Hz, 2H), 7.33 (t, J = 7.5 Hz, 2H), 7.29–7.22 (m, 1H), 6.24 (ddd, J = 6.4, 2.2, 0.8 Hz, 1H), 4.25 (d, J = 13.4 Hz, 1H), 3.71 (s, 3H), 3.21 (d, J = 2.1 Hz, 1H), 3.09 (s, 1H), 2.93 (d, J = 9.4 Hz, 1H), 2.88 (td, J = 4.1, 1.9 Hz, 1H), 2.83 (d, J = 13.5 Hz, 1H), 2.67 (s, 1H), 2.60 (ddt, J = 11.4, 7.7, 1.8 Hz, 1H), 2.31 (ddd, J = 14.1, 4.8, 1.8 Hz, 1H), 2.23 (td, J = 12.6, 12.0, 3.4 Hz, 1H), 2.18 (dd, J = 14.0, 7.7 Hz, 1H), 2.03 (td, J = 13.2, 12.8, 5.4 Hz, 1H), 1.98–1.90 (m, 2H), 1.89–1.77 (m, 2H), 1.68–1.64 (m, 1H), 1.58 (s, 1H), 1.57–1.47 (m, 2H), 1.45–1.36 (m, 2H), 1.09 (ddd, J = 12.8, 6.1, 1.3 Hz, 1H), 0.92 (s, 3H); **^{13}C NMR:** (176 MHz, $CDCl_3$) δ 175.7, 146.9, 140.0, 128.4, 128.2, 127.0, 126.8, 81.8, 77.9, 74.6, 71.2, 60.5, 56.3, 52.0, 43.7, 42.9, 40.6, 36.3, 35.1, 34.9, 33.4, 27.0, 25.7, 23.1, 22.0, 16.8; **R_f:** 0.33 in 2:1 Hx:EtOAc; **HRMS (ESI) m/z:** calculated for $[C_{28}H_{36}NO_4]^+$ 450.2639, found 450.2635.

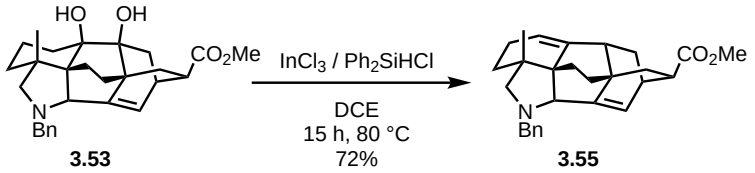

3.53 **3.55**

Pinacol product **3.53** (10.0 mg, 22 μmol, 1 equiv) in a 4 mL vial was transferred to a glovebox and DCE (1.11 mL, 0.02M), $InCl_3$ (9.8 mg, 46 μmol, 2 equiv) and Ph_2SiHCl (13 μL, 67 μmol, 3 equiv) were added. The vial was sealed and transferred to a 80 °C heating block. After stirring for 15 hours the vial was cooled to room temperature, and the reaction quenched with sat. $NaHCO_3$, extracted with DCM (3x2 mL), dried over $MgSO_4$, filtered, and concentrated. The resulting crude residue was purified by pipette column to give the deoxygenation product **3.55** (6.7 mg, 72%) as a colorless residue. **^{1}H NMR:** (700 MHz, $CDCl_3$) δ7.38 (d, J = 7.6 Hz, 2H), 7.31 (t, J = 7.6 Hz, 2H), 7.23 (t, J = 7.3 Hz, 1H), 6.20 (dd, J = 6.3, 1.5 Hz, 1H), 5.28 (dt, J = 4.9, 2.4 Hz, 1H), 4.05 (d, J = 13.7 Hz, 1H), 3.70 (s, 3H), 3.62 (d, J = 1.9 Hz, 1H), 3.43 (d, J = 13.7 Hz, 1H), 3.06 (d, J = 10.1 Hz, 1H), 2.95 (ddt, J = 6.5, 3.3, 1.4 Hz, 1H), 2.50 (ddt, J = 11.2, 7.5, 1.9 Hz, 1H), 2.38 (d, J = 6.5 Hz, 1H), 2.13 (d, J = 10.2 Hz, 1H), 2.08–1.90 (m, 3H), 1.88–1.78 (m, 1H), 1.73 (dd, J = 13.7, 7.4 Hz, 1H), 1.58–1.48 (m, 2H), 1.47–1.35 (m, 2H), 1.31–1.18 (m, 3H), 0.96 (s, 3H); **^{13}C NMR:** (176 MHz, $CDCl_3$) δ 176.0, 151.5, 147.5, 140.4, 134.5, 128.6, 128.3, 126.8, 125.4, 121.7, 73.4, 65.8, 60.7, 56.1, 51.9, 48.6, 42.1, 40.0, 39.4, 36.1, 35.1, 32.1, 28.6, 28.4, 27.1, 26.6, 21.7.

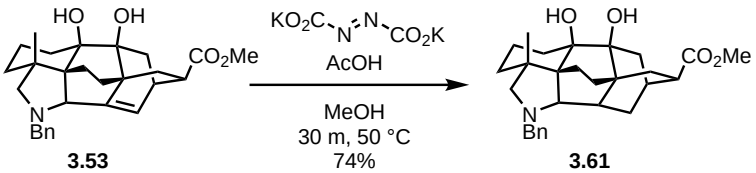

3.53 **3.61**

Pinacol product **3.53** (90 mg, 200 μmol, 1 equiv) was suspended in MeOH (4 mL, 0.05M) in a 20 mL vial. Potassium azodicarboxylate (5 equiv, 1.0 mmol, 194 mg) and AcOH (114 μL, 2.0 mmol, 10 equiv) were added and the vial was sealed and heated to 50 °C. After 15 minutes the reaction mixture was concentrated and the crude residue was purified by flash chromatography (20% EtOAc in Hx) to give the saturated hexacycle **3.61** (66 mg, 74%) as a white solid. **^{1}H NMR:** (700 MHz, $CDCl_3$) δ 7.41–7.29 (m, 4H), 7.24 (t, J = 7.1 Hz, 1H), 4.01 (d, J = 13.5 Hz, 1H), 3.70 (s, 3H), 3.64 (s, 1H), 3.46 (s, 1H), 3.07 (d, J = 10.1 Hz, 1H), 2.81 (d, J = 10.8 Hz, 1H), 2.76 (d, J = 13.5 Hz, 1H), 2.59 (dd, J = 11.1, 6.1 Hz, 1H), 2.54 (ddd, J = 12.7, 10.0, 6.8 Hz, 1H), 2.35 (dd, J = 15.2, 2.1 Hz, 1H), 2.13 (ddt, J = 8.3, 5.9, 3.1 Hz, 2H), 2.09 (dd, J = 14.2, 6.0 Hz, 1H), 2.03 (qd, J = 11.6, 11.0, 5.2 Hz, 2H), 1.88–1.82 (m, 2H), 1.75 (d, J = 10.1 Hz, 1H), 1.74–1.55 (m, 4H), 1.44 (dt, J = 15.2, 2.8 Hz, 1H), 1.28 (td, J = 12.2, 3.8 Hz, 2H), 1.24 (dd, J = 14.2, 11.2 Hz, 1H), 1.14 (ddd, J = 13.4, 12.0, 4.9 Hz, 1H), 1.08 (dd, J = 13.3, 7.9 Hz, 1H), 0.88 (s, 3H); **^{13}C NMR:** (176 MHz, $CDCl_3$) δ 177.8, 140.0, 128.4, 128.0, 126.9, 75.3, 73.0, 70.4, 68.9, 61.7, 52.2, 49.9, 42.0, 40.7, 35.8, 35.4, 35.1, 31.3, 30.6, 30.4, 29.5, 28.0, 26.7, 26.1, 22.9, 17.1; **R_f:** 0.27 in 2:1 Hx:EtOAc; **HRMS (ESI) m/z:** calculated for $[C_{28}H_{38}NO_4]^+$ 452.2795, found 452.2791.

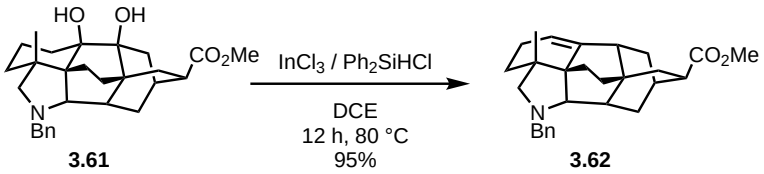

3.61 **3.62**

Saturated hexacycle **3.61** (66 mg, 147 μmol, 1 equiv) in a dry 20 mL vial was transferred to a glovebox. DCE (7.3 mL, 0.02M), $InCl_3$ (64 mg, 293 μmol, 2 equiv) and Ph_2SiHCl (86 μL, 440 μmol, 3 equiv) were added and the vial was sealed and heated to 80 °C. After 12 hours the vial was cooled to room temperature and the reaction was quenched with sat. $NaHCO_3$, extracted with DCM (3x15 mL), dried over $MgSO_4$, filtered, and concentrated. The crude residue was purified by flash chromatography (5%–10% EtOAc in Hx) to give the deoxygenated product **3.62** (61 mg, >95%) as a white solid. **^{1}H NMR:** (700 MHz, $CDCl_3$) δ 7.33 (d, J = 7.2 Hz, 2H), 7.29 (t, J = 7.6 Hz, 2H), 7.22 (t, J = 7.2 Hz, 1H), 5.60 (d, J = 5.9 Hz, 1H), 3.88 (d, J = 13.4 Hz, 1H), 3.68 (s, 3H), 3.07 (dd, J = 14.8, 11.7 Hz, 2H), 2.90 (d, J = 9.2 Hz, 1H), 2.54 (dd, J = 10.3, 8.5 Hz, 1H), 2.26 (ddd, J = 13.2, 7.1, 2.0 Hz, 1H), 2.07–2.01 (m, 3H), 1.99–1.94 (m, 1H), 1.94–1.86 (m, 2H), 1.80 (dddd, J = 11.3, 9.2, 7.0, 2.2 Hz, 1H), 1.78–1.69 (m, 2H), 1.63 (dd, J = 13.3, 4.6 Hz, 1H), 1.55–1.46 (m, 2H), 1.42 (dddd, J = 13.4, 11.2, 4.2, 2.7 Hz, 1H), 1.38–1.28 (m, 3H), 1.20 (td, J = 12.3, 5.3 Hz, 1H), 0.92 (s, 3H).

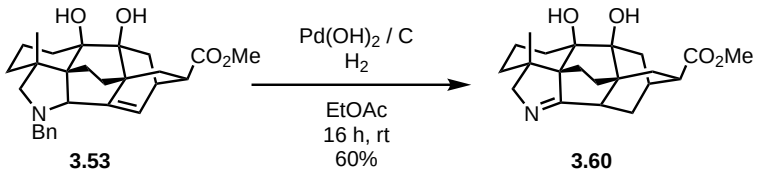

3.53 **3.60**

Pinacol product **3.53** (5 mg, 11 μmol, 1 equiv) was dissolved in EtOAc (560 μL, 0.02M) and $Pd(OH)_2$ C (2.5 mg, 50 %wt.) was added. The solution was sparged with H_2 for 30 seconds and then stirred under a balloon of H_2 overnight. After 16 hours the mixture was filtered and purified by preparative TLC to give imine **3.60** (2.4 mg, 60%) as a white solid. **^{1}H NMR:** (700 MHz, $CDCl_3$) δ 5.05 (s, 1H), 3.90 (s, 1H), 3.86 (dd, J = 15.6, 3.7 Hz, 1H), 3.72 (q, J = 1.2 Hz, 3H), 3.49 (dd, J = 15.5, 2.8 Hz, 1H), 2.73 (d, J = 11.6 Hz, 1H), 2.41 (d, J = 10.7 Hz, 1H), 2.24 (dd, J = 13.2, 4.7 Hz, 1H), 2.17–1.96 (m, 4H), 1.93–1.82 (m, 2H), 1.83–1.54 (m, 4H), 1.50–1.24 (m, 6H), 1.13 (t, J = 11.9 Hz, 1H), 0.85 (s, 2H); **^{13}C NMR:** (176 MHz, $CDCl_3$) δ 179.6, 75.9, 73.4, 72.9, 60.2, 52.7, 41.7, 41.6, 38.8, 35.0, 32.1, 30.8, 27.7, 27.6, 26.5, 26.4, 25.1, 19.8, 16.5.

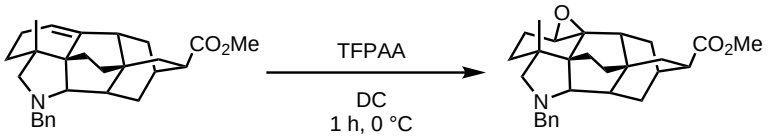

3.62 **3.63**

A 0.1M solution of trifluoroperacetic acid (TFPAA) was prepared by dissolving TFAA (138 μL, 0.98 mmol, 1.2 equiv) in DCM (8.2 mL, 0.1M) and adding H_2O_2 (50% in H_2O, 47 μL, 0.82 mmol, 1 equiv) and stirring at room temperature for 1 hour. Deoxygenation product **3.62** (34 mg, 82 μL, 1 equiv) was dissolved in DCM (4.1 mL, 0.02M) and cooled to 0 °C. The TFPAA solution (3.28 mL, 328 μmol, 4 equiv) was added dropwise and stirred for 30 minutes. LCMS showed 50% conversion so another 4 equivalents of TFPAA was added. After and additional 30 minutes the reaction appeared complete by LCMS. The reaction was quenched with sat. $NaHCO_3$, extracted with DCM (3x10 mL), dried over $MgSO_4$, filtered, and concentrated. The crude residue was purified by flash chromatography (5%–20% EtOAc in Hx) to give epoxide **3.63** (16 mg, 45%) as a white solid. **^{1}H NMR:** (700 MHz, $CDCl_3$) δ 7.33 (d, J = 7.2 Hz, 2H), 7.29 (t, J = 7.6 Hz, 2H), 7.22 (t, J = 7.2 Hz, 1H), 5.60 (d, J = 5.9 Hz, 1H), 3.88 (d, J = 13.4 Hz, 1H), 3.68 (s, 3H), 3.07 (dd, J = 14.8, 11.7 Hz, 2H), 2.90 (d, J = 9.2 Hz, 1H), 2.54 (dd, J = 10.3, 8.5 Hz, 1H), 2.26 (ddd, J = 13.2, 7.1, 2.0 Hz, 1H), 2.07–2.01 (m, 3H), 1.99–1.94 (m, 1H), 1.94–1.86 (m, 2H), 1.80 (dddd, J = 11.3, 9.2, 7.0, 2.2 Hz, 1H), 1.78–1.69 (m, 2H), 1.63 (dd, J = 13.3, 4.6 Hz, 1H), 1.55–1.46 (m, 2H), 1.42 (dddd, J = 13.4, 11.2, 4.2, 2.7 Hz, 1H), 1.38–1.28 (m, 3H), 1.20 (td, J = 12.3, 5.3 Hz, 1H), 0.92 (s, 3H).

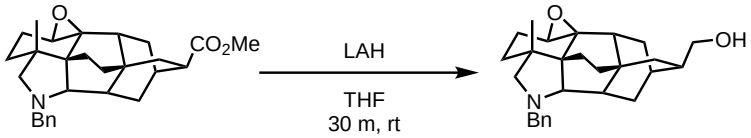

3.63 **3.64**

Epoxide **3.63** (22 mg, 50 μmol, 1 equiv) was dissolved in THF (2.5 mL, 0.02M) and LAH (2M in THF, 50 μL, 100 μmol, 2 equiv) wad added and the reaction was stirred at room temperature. After 30 minutes the reaction was quenched by the sequential addition of 4 μL H_2, 4 μL15% NaOH, and 12 μL H_2O. The reaction was then diluted with EtOAc and dried with $MgSO_4$. The

mixture was filtered through a pad of celite and concentrated. The crude residue was purified by flash chromatography (33%–50% EtOAc in Hx) to give the amino alcohol **3.64** (9.6 mg, 47%) as a white solid. **^{1}H NMR:** (500 MHz, $CDCl_3$) δ 7.38–7.28 (m, 4H), 7.26 (s, 2H), 4.04 (d, J = 13.1 Hz, 1H), 3.64 (d, J = 3.8 Hz, 1H), 3.56–3.46 (m, 2H), 2.72 (d, J = 9.5 Hz, 1H), 2.64 (d, J = 13.0 Hz, 1H), 2.58 (d, J = 9.4 Hz, 1H), 2.20 (ddd, J = 13.0, 7.3, 2.0 Hz, 1H), 2.02–1.92 (m, 2H), 1.91–1.71 (m, 5H), 1.68–1.41 (m, 9H), 0.94 (dt, J = 12.5, 3.2 Hz, 1H), 0.84 (s, 3H), 0.82 (dd, J = 13.3, 8.5 Hz, 1H).

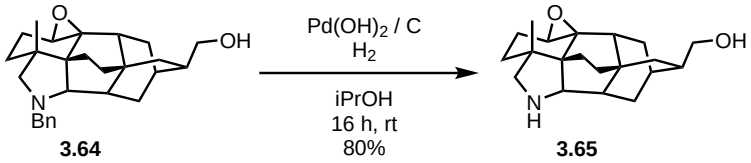

3.64 **3.65**

Alcohol **3.64** (5 mg, 12 μmol, 1 equiv) was dissolved in dry iPrOH (600 μL, 0.02M) and $Pd(OH)_2$\C (2.5 mg, 50 %wt.) and AcOH (1M in iPrOH, 12 μL, 12 μmol, 1 equiv) was added. The solution was sparged with H_2 for 1 minuted and then stirred under a balloon of H_2 overnight. After 16 hours the crude reaction mixture was filtered through a silica plug with 20% MeOH in DCM with 1% Et_3N. The filtrate was concentrated and azeotroped with PhMe then purified by preparative TLC (25% MeOH, 5% Et_3N in DCM) to give the secondary amine **3.65** (3.1 mg, 80%) as a white solid; **^{1}H NMR:** (700 MHz, $CDCl_3$) δ 3.46 (dt, J = 34.6, 9.4 Hz, 2H), 3.32 (s, 1H), 3.21 (d, J = 10.9 Hz, 1H), 3.07 (d, J = 10.9 Hz, 1H), 2.59 (d, J = 11.0 Hz, 1H), 2.03 (t, J = 11.5 Hz, 1H), 1.99–1.79 (m, 6H), 1.74 (s, 1H), 1.57 (dt, J = 25.4, 12.5 Hz, 3H), 1.50–1.41 (m, 5H), 1.40–1.31 (m, 2H), 1.07 (d, J = 13.5 Hz, 1H), 0.84 (s, 3H), 0.80 (dd, J = 14.5, 2.7 Hz, 1H).

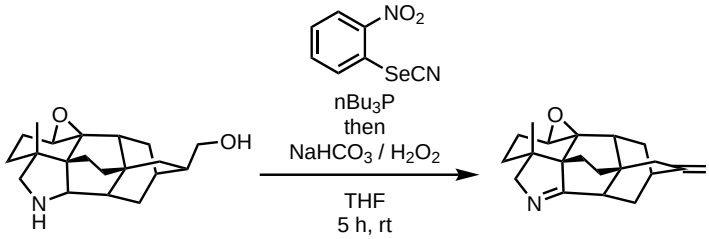

3.65 **3.66**

Amino alcohol **3.65** (1.5 mg, 5 μmol, 1 equiv) and o-nitrophenyl selenocyanate (3.3 mg, 15 μmol, 3 equiv) were dissolved in THF (250 μL, 0.02M) in a dry 4 mL vial. The vial was sealed and transferred to a glovebox where nBu_3P (3.7 μL, 15 μmol, 3 equiv) was added. The resulting deep red solution was stirred at room temperature for 90 minutes after which the red had faded to yellow. $NaHCO_3$ (13 mg, 154 μmol, 31 equiv) and H_2O_2 (35%, 16 μL, 186 μmol, 37 equiv) were added and the reaction was stirred an additional 3 hours, after which LCMS showed no starting material or intermediate selenide. Two products with m/z of 296 and 314 were observed alongside various phosphine related masses. Crude NMR showed two new products with exo-methylene groups in a 3:2 ratio. The lower molecular weight product was isolated by preparative TLC with

(1:2 Hx:EtOAc with 1% Et_3N. The higher molecular weight product could not be separated from the phosphine related products. **^{1}H NMR:** (600 MHz, $CDCl_3$) δ 4.76 (s, 1H), 4.63 (s, 1H), 3.78 (d, J = 15.5 Hz, 1H), 3.52 (d, J = 15.4 Hz, 1H), 3.14 (s, 1H), 2.51–2.23 (m, 4H), 2.14 (d, J = 16.8 Hz, 1H), 1.99 (dd, J = 36.3, 13.1 Hz, 3H), 1.91–1.57 (m, 6H), 1.43 (s, 1H), 1.24–1.13 (m, 2H), 0.87 (s, 3H) (major product, m/z 296).

3.11 References

1. (a) Hedaya, E.; Theodoropulos, S. *Tetrahedron* **1968**, *24*, 2241–2254; (b) Argade, N. P.; Easwar, S. *Synthesis* **2006**, *2006*, 831–838.
2. Houk, K. N. *J. Am. Chem. Soc.* **1973**, *95*, 4092–4094.
3. Selvakumar, J.; Ramanathan, C. R. *Org. Biomol. Chem.* **2011**, *9*, 7643–7646.
4. Jacob, P.; Callery, P. S.; Shulgin, A. T.; Castagnoli, N. *J. Org. Chem.* **1976**, *41*, 3627–3629.
5. Song, L.; Zhu, G.; Liu, Y.; Liu, B.; Qin, S. *J. Am. Chem. Soc.* **2015**, *137*, 13706–13714.
6. Yang, Q.; Njardarson, J. T.; Draghici, C.; Li, F. *Angew. Chem. Int. Ed.* **2013**, *52*, 8648–8651.
7. Morton, J. G.; Draghici, C.; Kwon, L. D.; Njardarson, J. T. *Org. Lett.* **2009**, *11*, 4492–4495.
8. Paquette, A. L.; Jendralla, H.; Cottrell, C. E. *J. Am. Chem. Soc.* **1986**, *108*, 3739–3744.
9. Moriyama, K.; Nakamura, Y.; Togo, H. *Org. Lett.* **2014**, *16*, 3812–3815.
10. (a) Mercado-Marin, E. V.; Sarpong, R. *Chem. Sci.* **2015**, *6*, 5048–5052; (b) Mukai, K.; de Sant'Ana, D. P.; Hirooka, Y.; Mercado-Marin, E. V.; Stephens, D. E.; Kou, K. G. M.; Richter, S. C.; Kelley, N.; Sarpong, R. *Nat. Chem.* **2018**, *10*, 38–44.
11. (a) Das, S.; Addis, D.; Zhou, S.; Junge, K.; Beller, M. *J. Am. Chem. Soc.* **2010**, *132*, 1770–1771; (b) Das, S.; Addis, D.; Junge, K.; Beller, M. *Chem. Eur. J.* **2011**, *17*, 12186–12192; (c) Das, S.; Join, B.; Junge, K.; Beller, M. *ChemComm* **2012**, *48*, 2683–2685; (d) Pisiewicz, S.; Junge, K.; Beller, M. *Eur. J. Inorg. Chem.* **2014**, *2014*, 2345–2349; (e) Das, S.; Li, Y.; Bornschein, C.; Pisiewicz, S.; Kiersch, K.; Michalik, D.; Gallou, F.; Junge, K.; Beller, M. *Angew. Chem. Int. Ed.* **2015**, *54*, 12389–12393.
12. Hanada, S.; Tsutsumi, E.; Motoyama, Y.; Nagashima, H. *J. Am. Chem. Soc.* **2009**, *131*, 15032–15040.
13. Szostak, M.; Spain, M.; Parmar, D.; Procter, D. J. *ChemComm* **2012**, *48*, 330–346.
14. Cha, J. Y.; Yeoman, J. T.; Reisman, S. E. *J. Am. Chem. Soc.* **2011**, *133*, 14964–14967.
15. Renata, H.; Zhou, Q.; Dunstl, G.; Felding, J.; Merchant, R. R.; Yeh, C. H.; Baran, P. S. *J. Am. Chem. Soc.* **2015**, *137*, 1330–1340.
16. Yasuda, M.; Onishi, Y.; Ueba, M.; Miyai, T.; Baba, A. *J. Org. Chem.* **2001**, *66*, 7741–7744.
17. Leonard, N. J.; Hay, A. S.; Fulmer, R. W.; Gash, V. W. *J. Am. Chem. Soc.* **1955**, *77*, 439–444.
18. Quick, J.; Khandelwal, Y.; Meltzer, P. C.; Weinberg, J. S. *J. Org. Chem.* **1983**, *48*, 5199–5203.
19. Grieco, P. A.; Nishizawa, M. *J. Org. Chem.* **1977**, *42*, 1717–1720.
20. Mukherjee, S.; Corey, E. J. *Org. Lett.* **2010**, *12*, 632–635.
21. Beierlein, J. M.; Frey, K. M.; Bolstad, D. B.; Pelphrey, P. M.; Joska, T. M.; Smith, A. E.; Priestley, N. D.; Wright, D. L.; Anderson, A. C. *J Med Chem* **2008**, *51*, 7532–7540.
22. Pietruszka, J.; Böse, D.; Frey, W. *Synthesis* **2014**, *46*, 2524–2532.

3.A NMR Spectral Data for Chapter 3

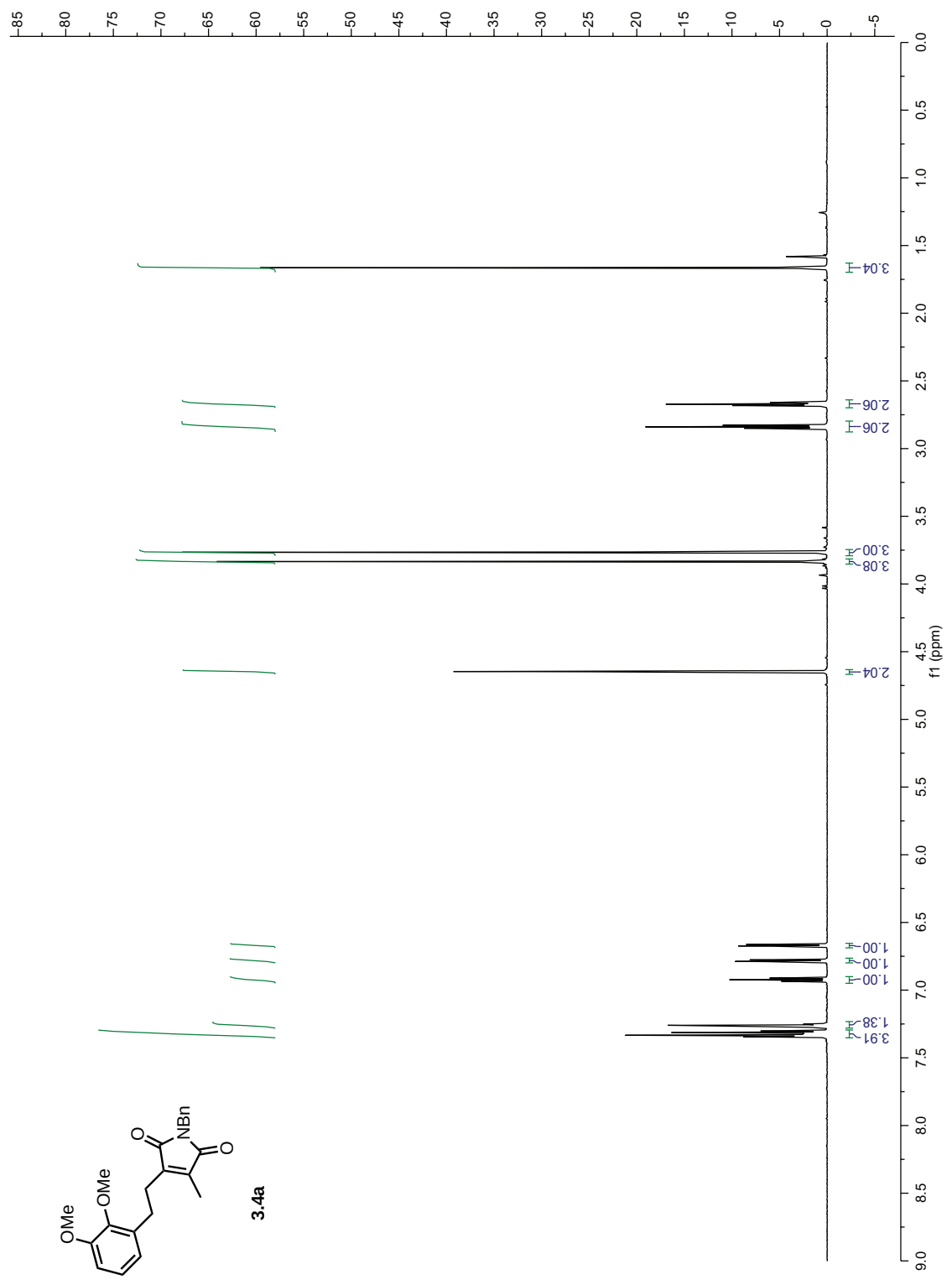

Figure 3.A.1: ^{1}H NMR of **3.4a**

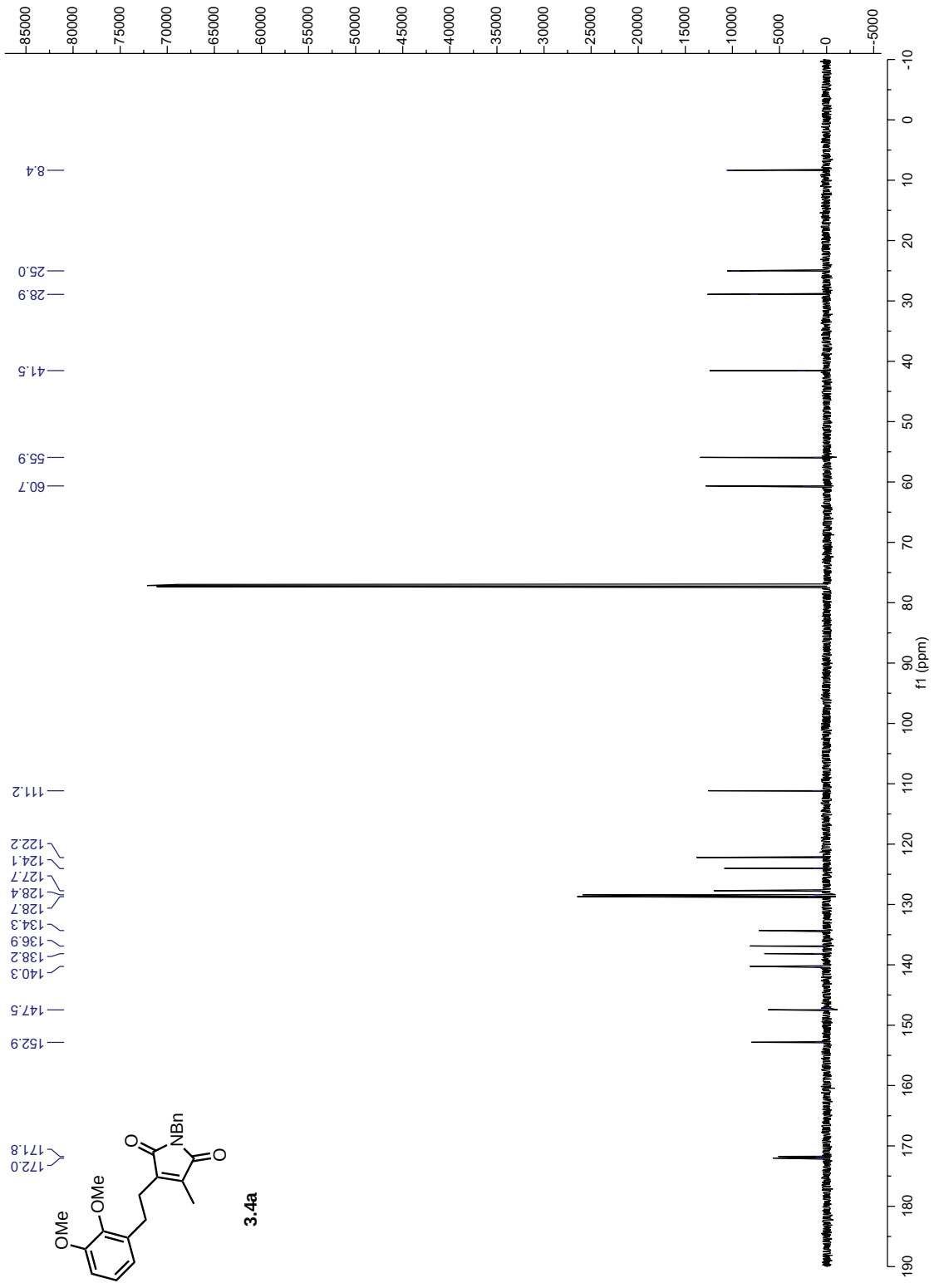

Figure 3.A.2: ^{13}C NMR of **3.4a**

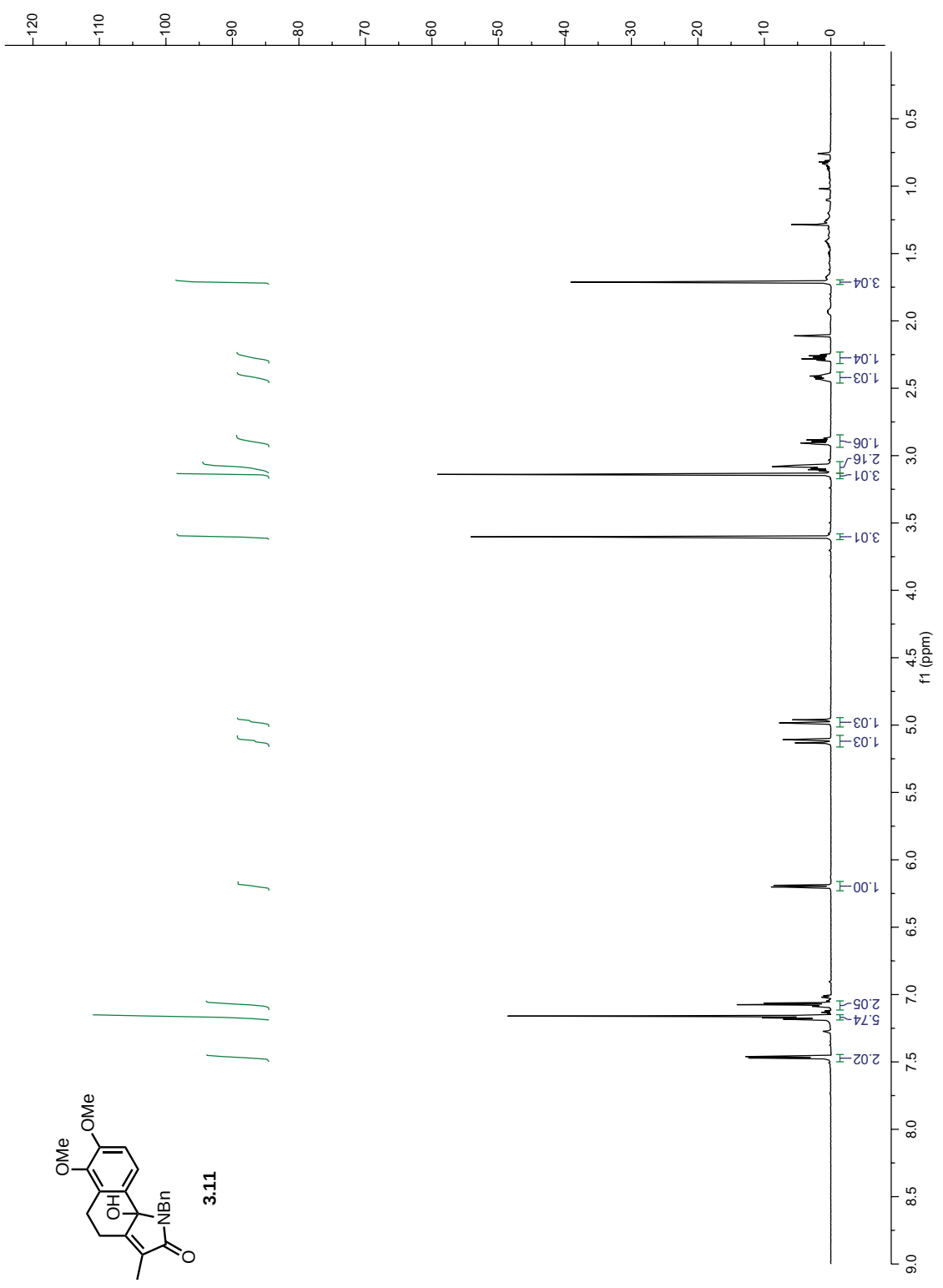

Figure 3.A.3: ^{1}H NMR of **3.11**

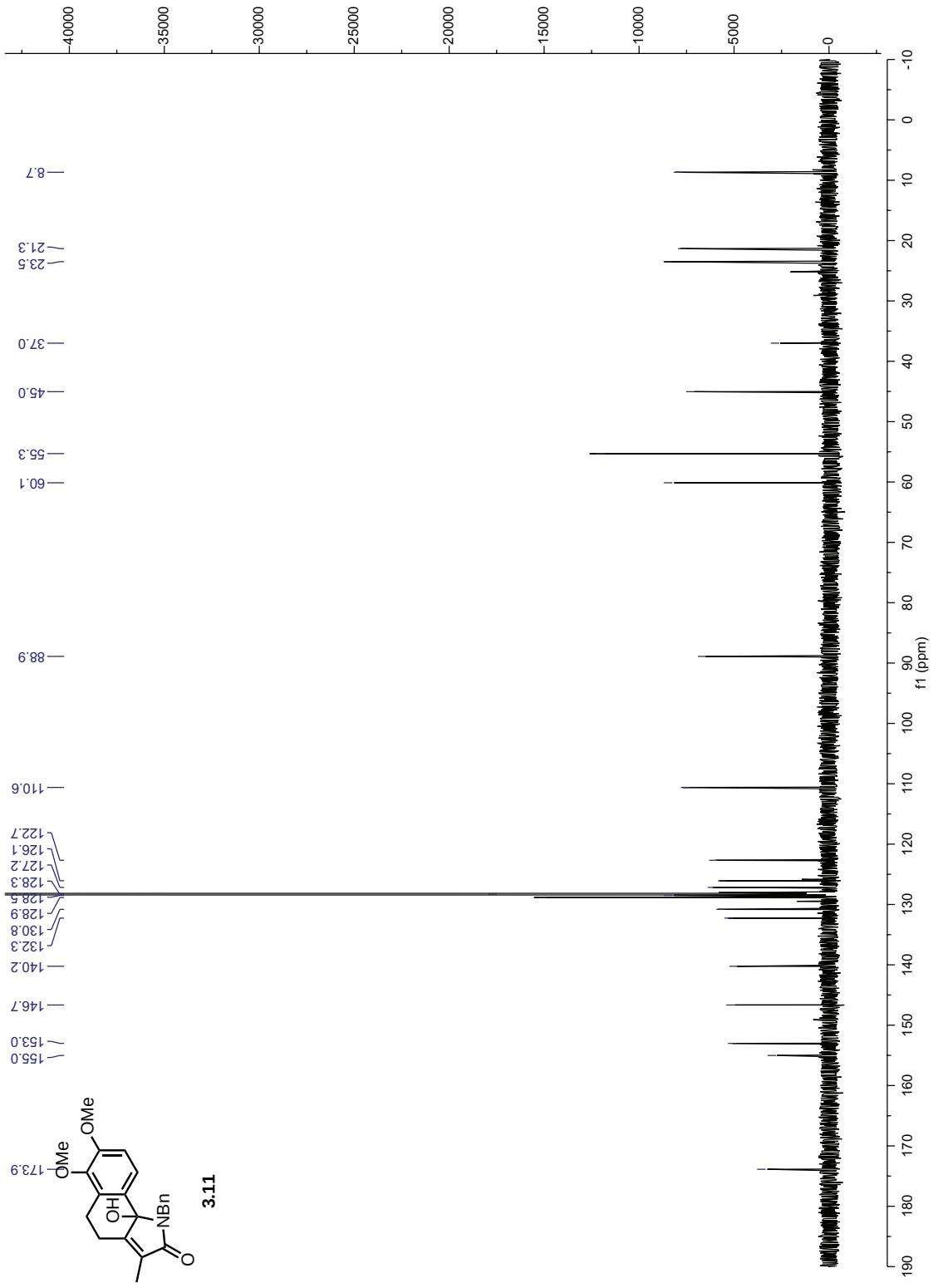

Figure 3.A.4: ^{13}C NMR of **3.11**

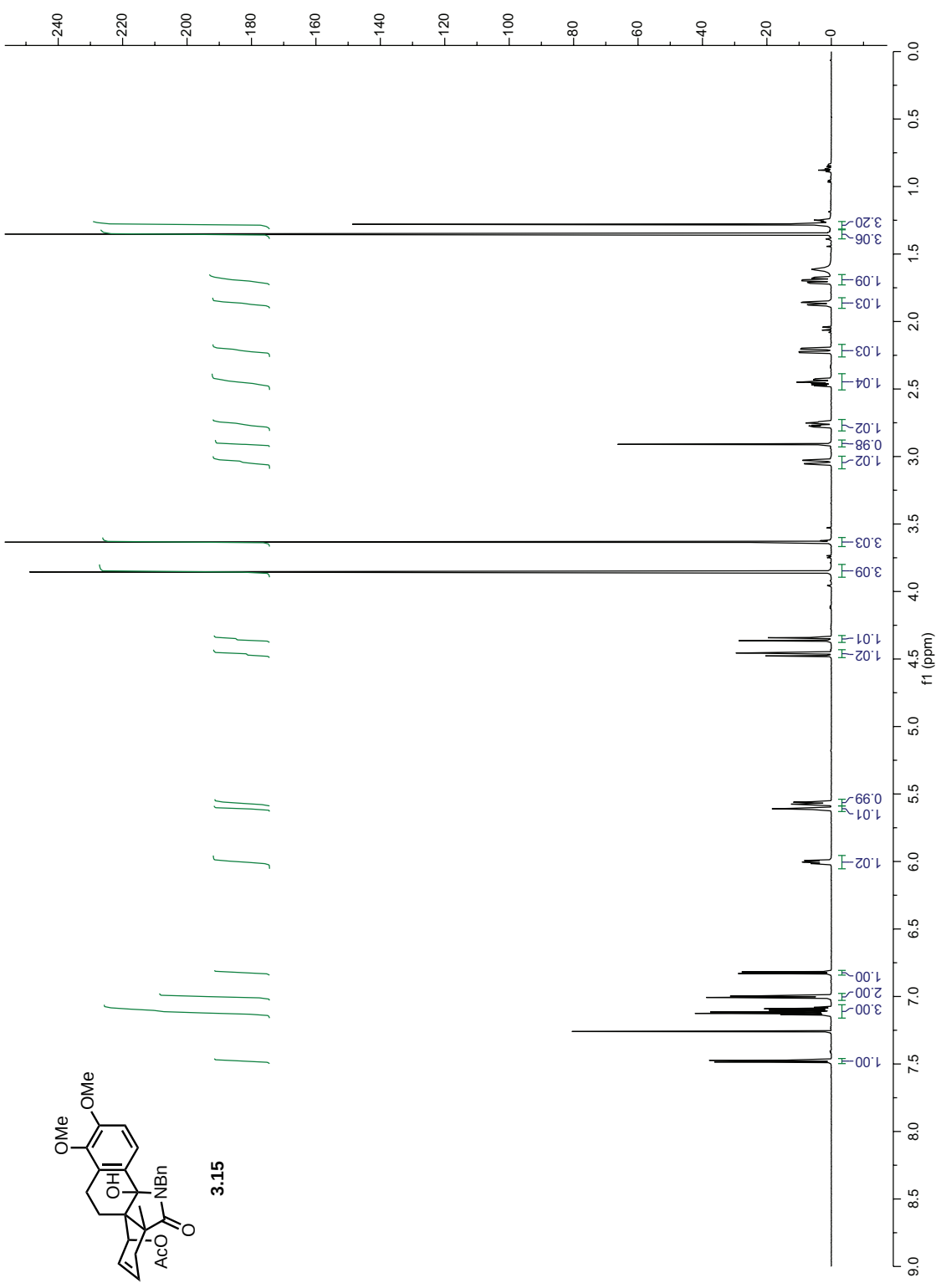

Figure 3.A.5: ^{1}H NMR of **3.15**

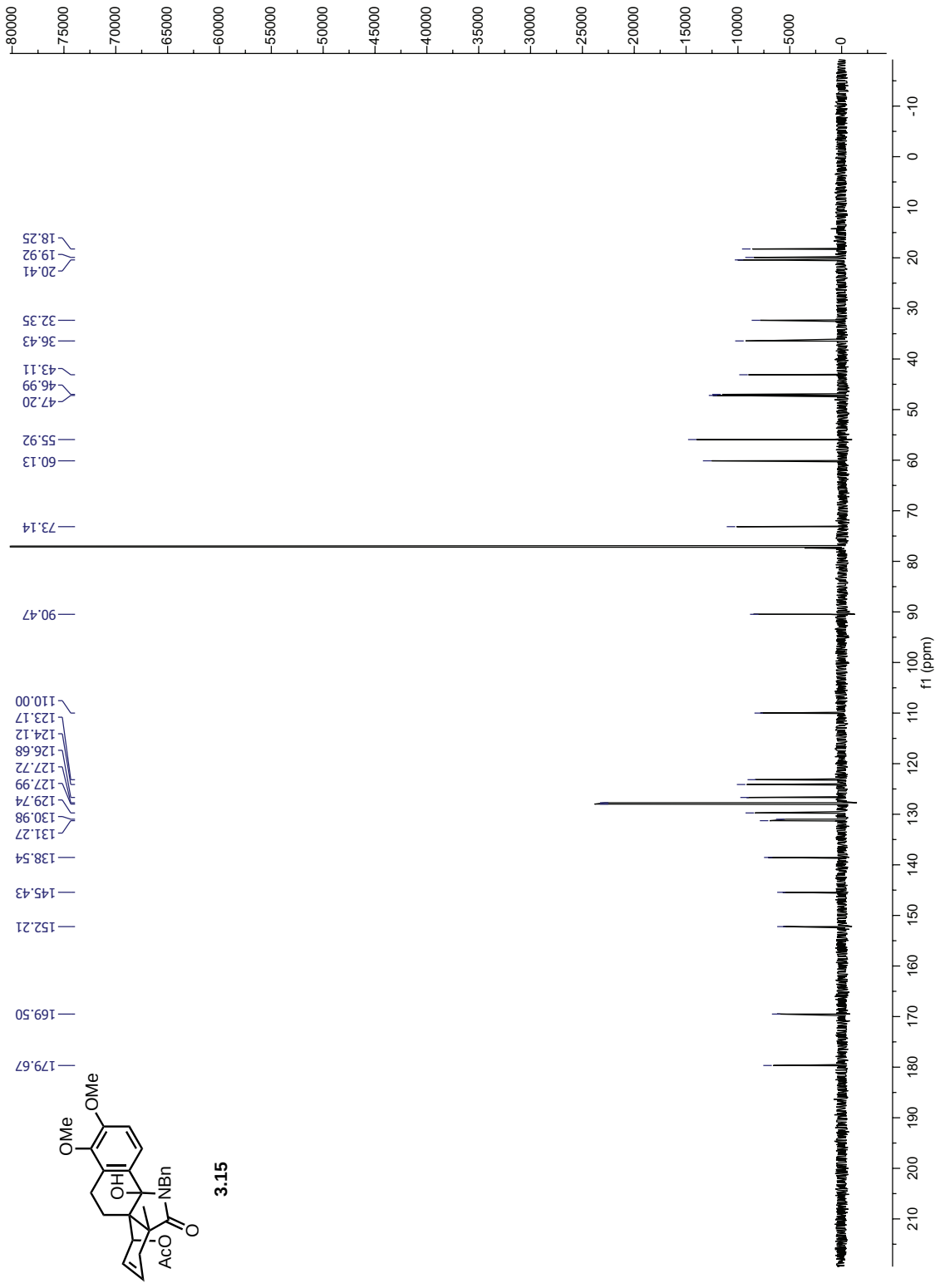

Figure 3.A.6: ^{13}C NMR of **3.15**

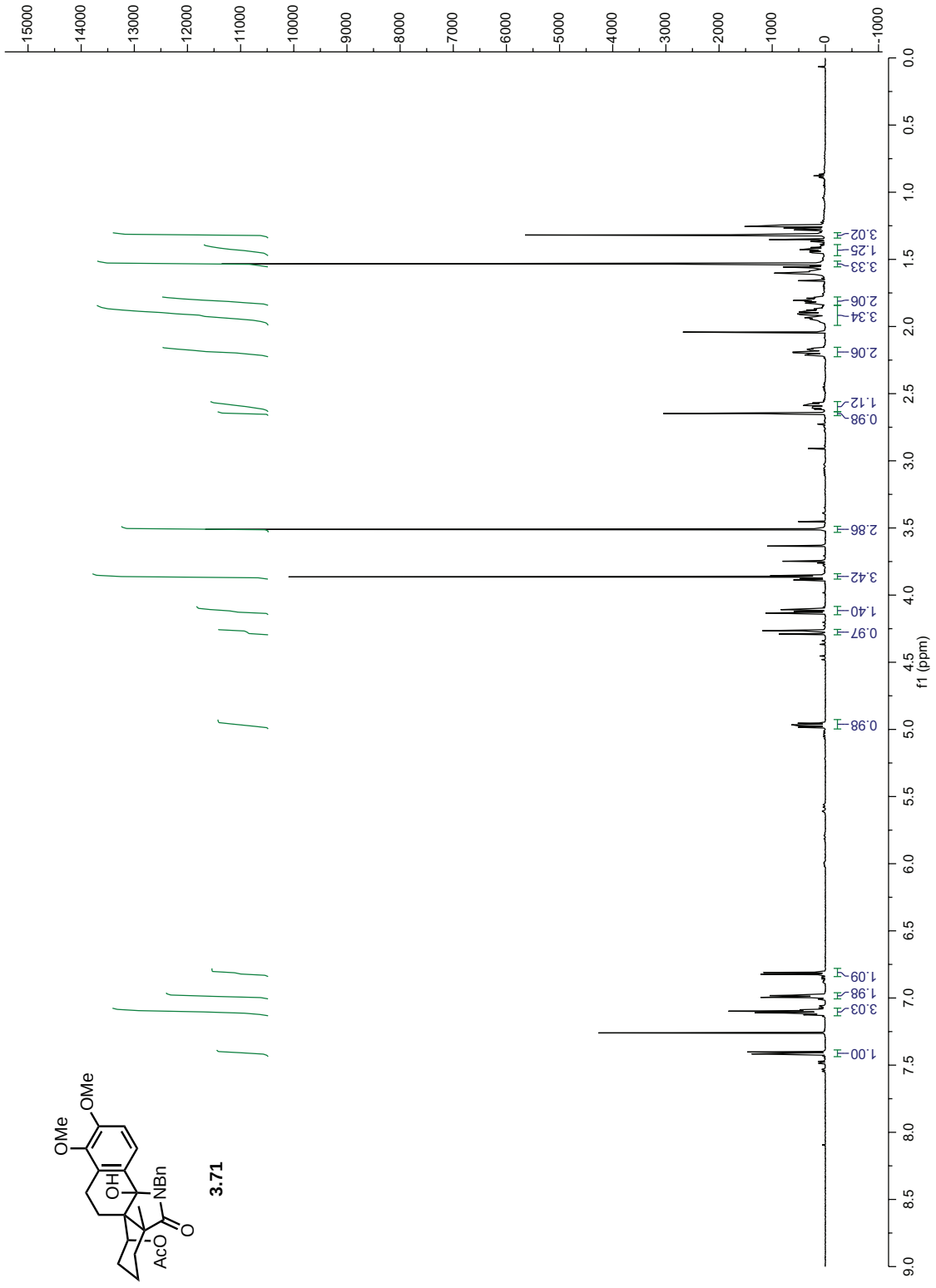

Figure 3.A.7: ^{1}H NMR of **3.71**

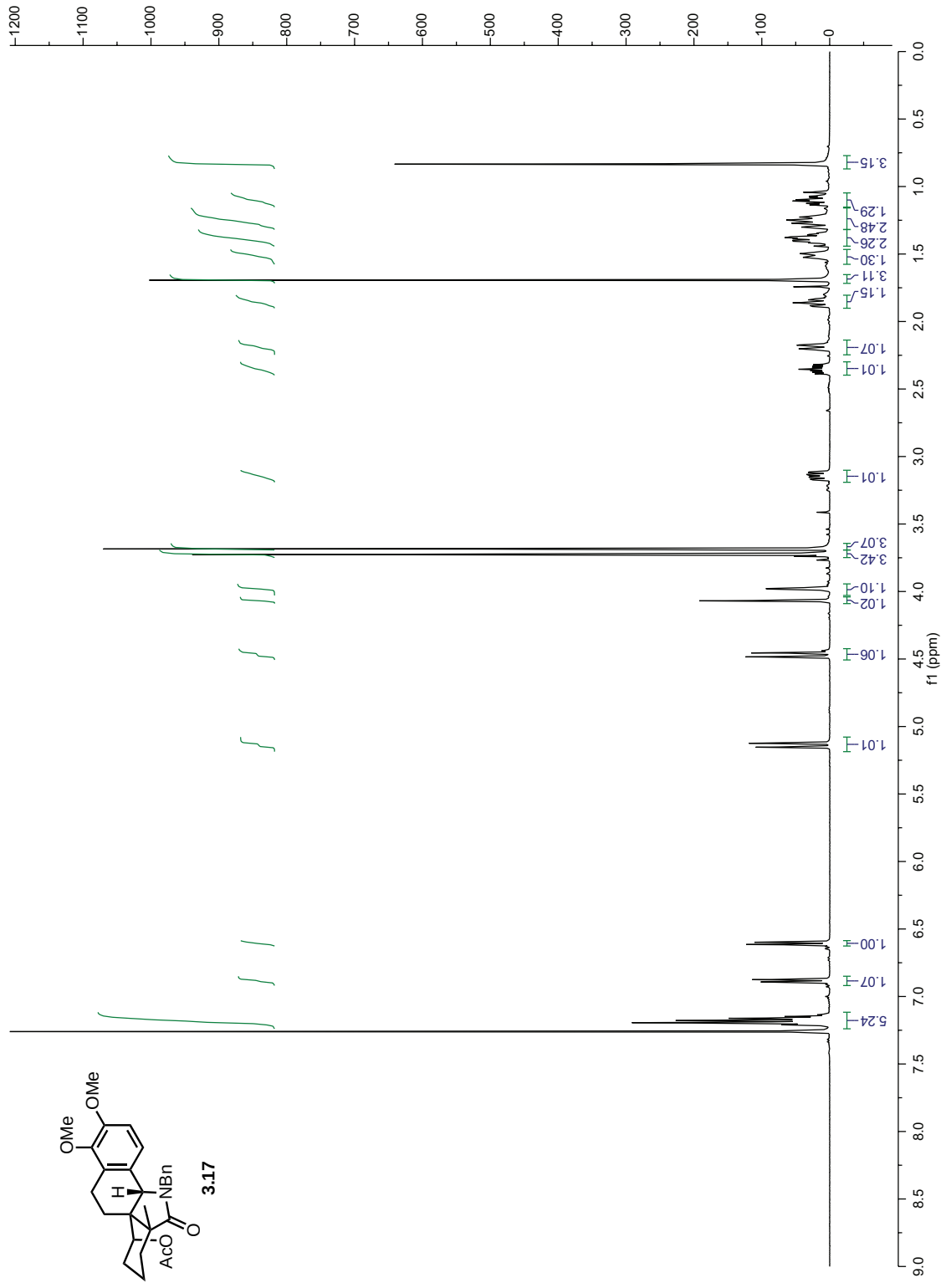

Figure 3.A.8: ^{1}H NMR of **3.17**

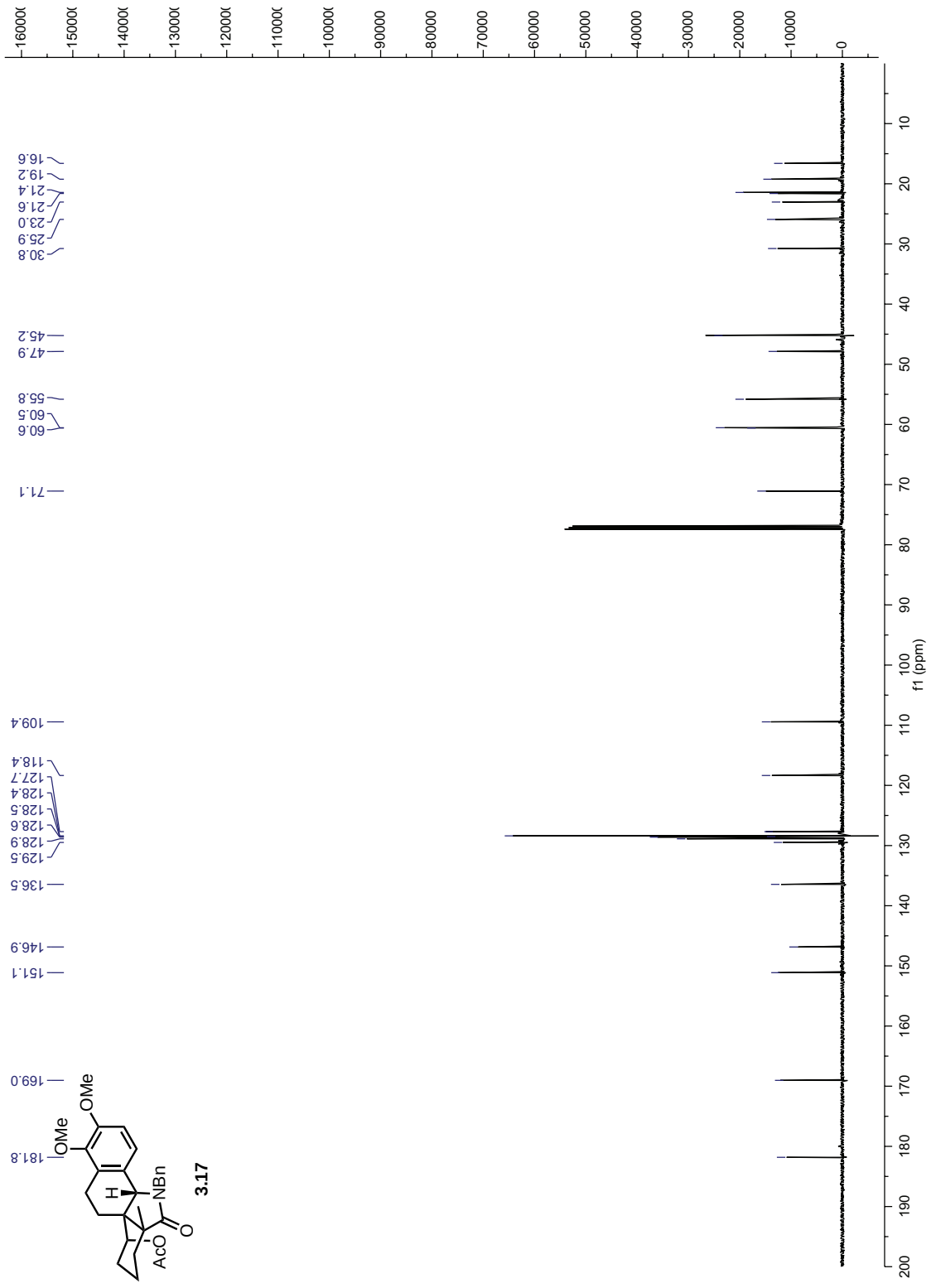

Figure 3.A.9: ^{13}C NMR of **3.17**

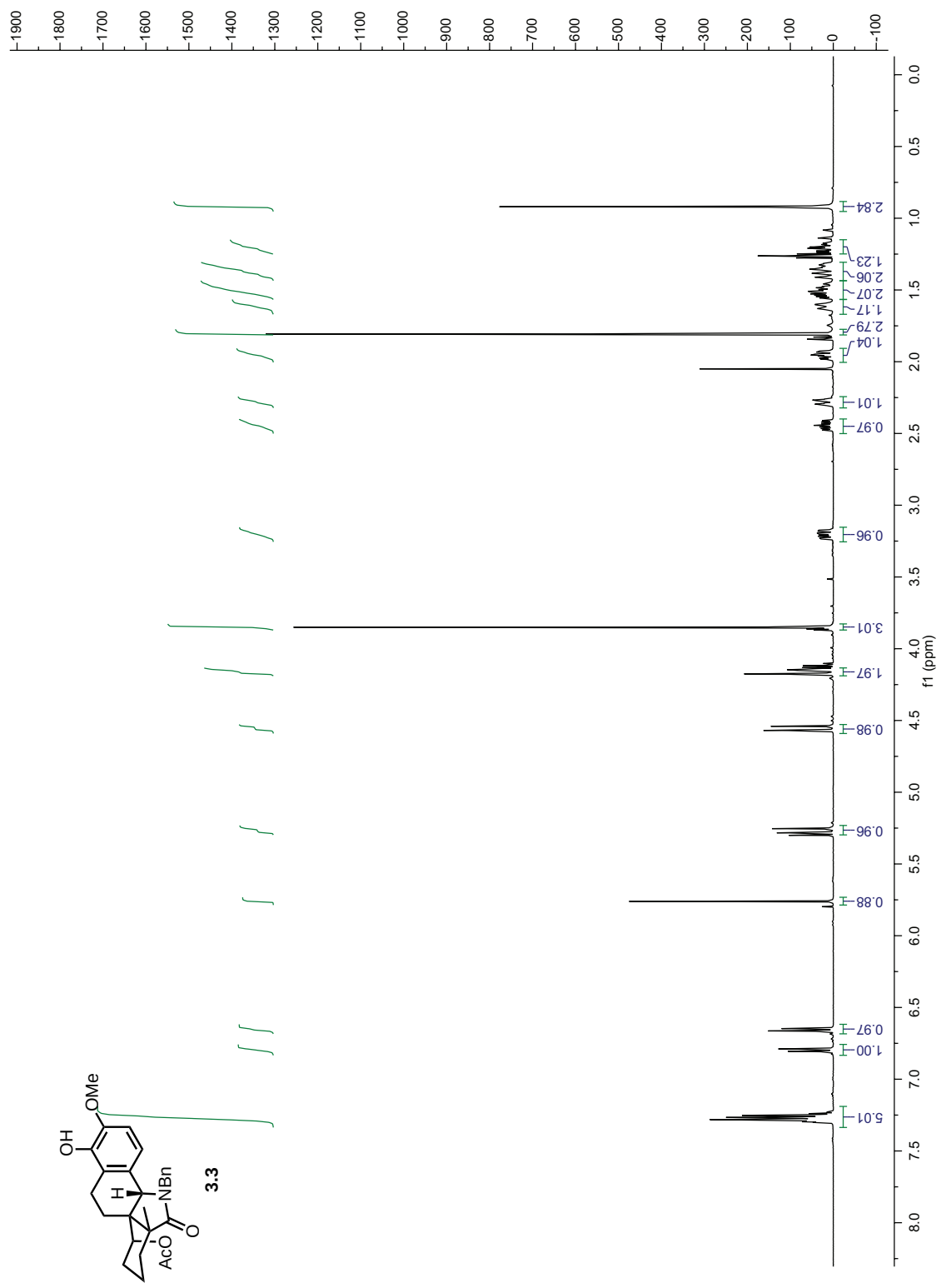

Figure 3.A.10: ^{1}H NMR of **3.3**

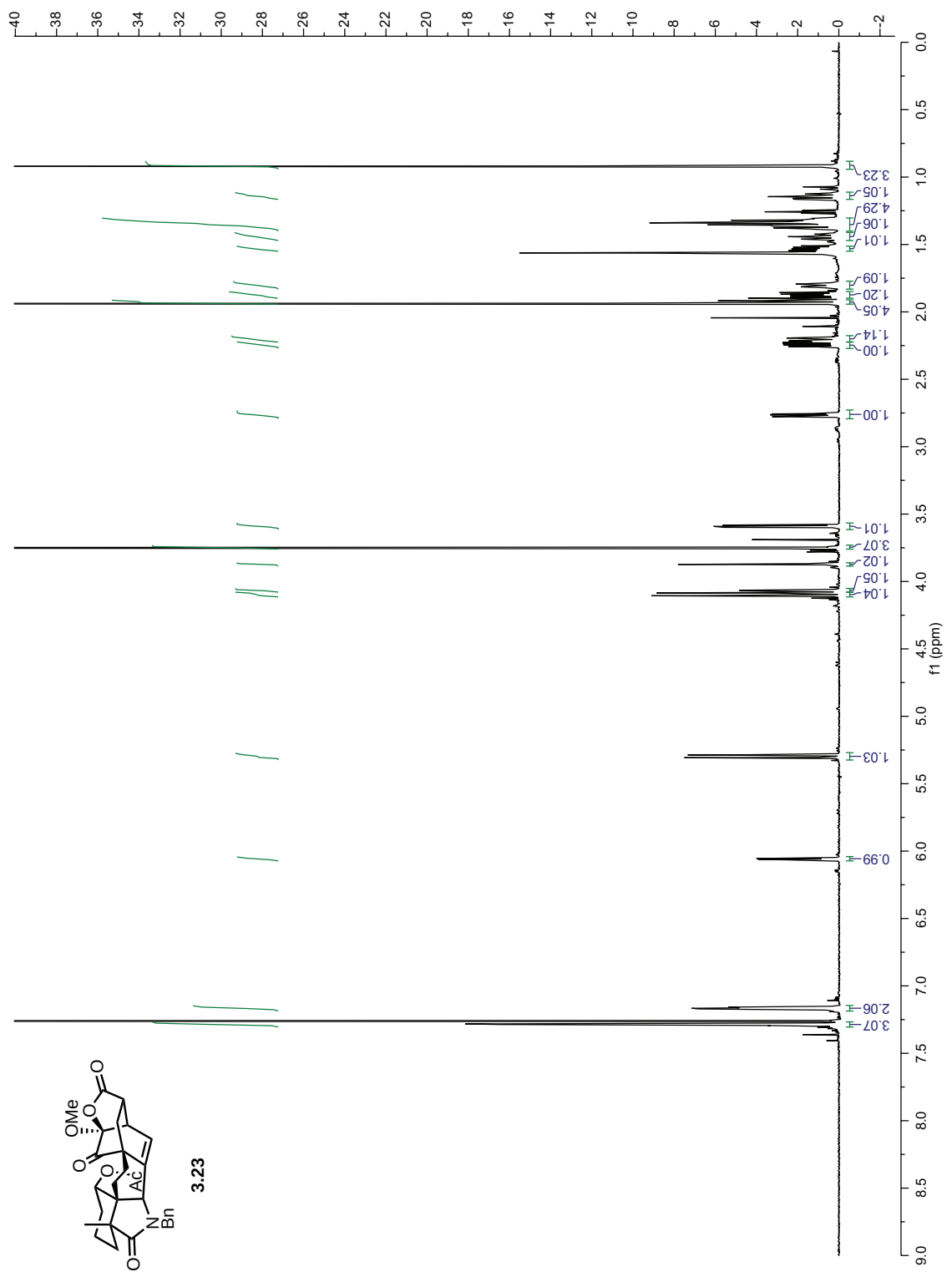

Figure 3.A.11: ^{1}H NMR of **3.23**

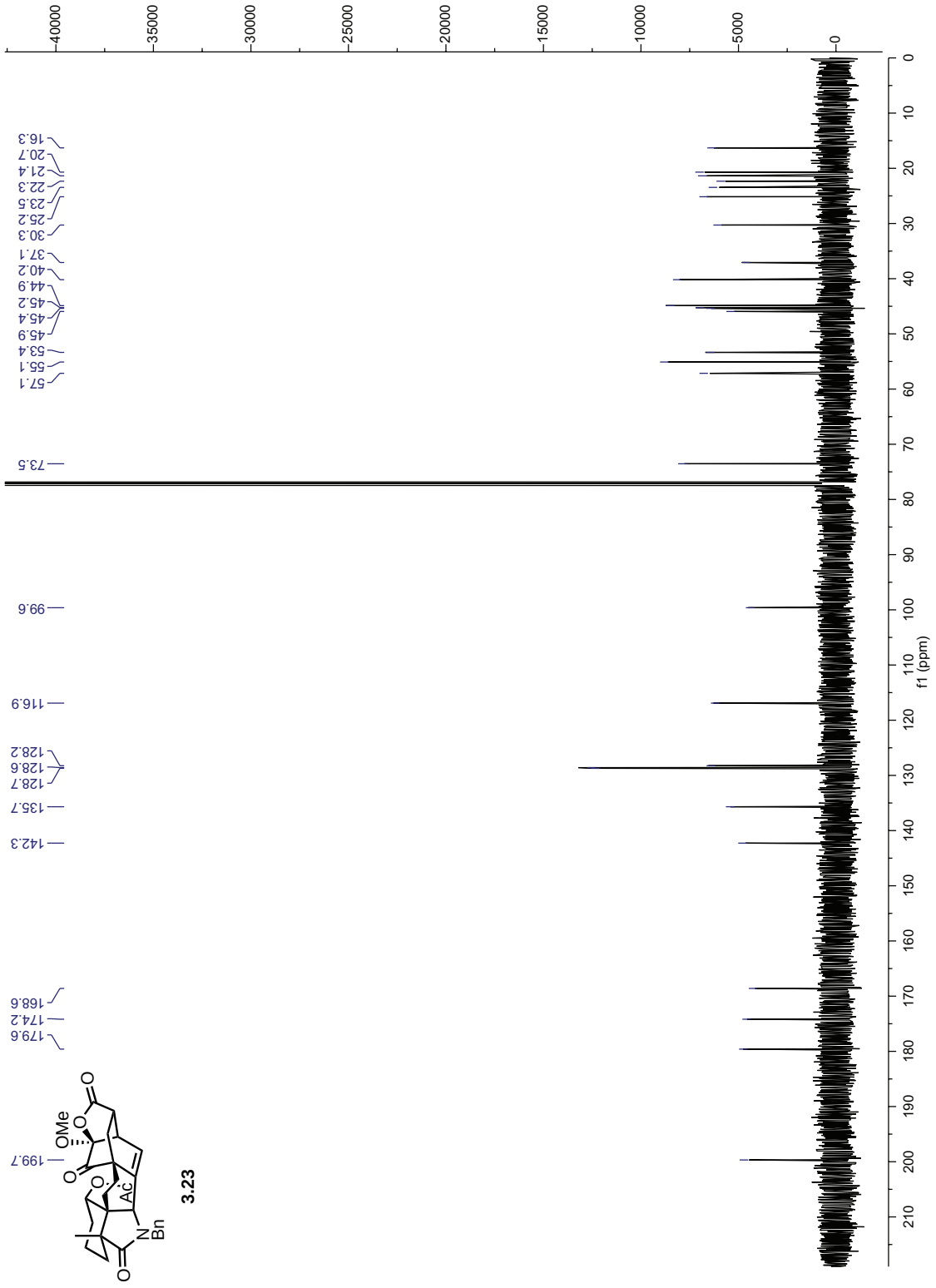

Figure 3.A.12: ^{13}C NMR of **3.23**

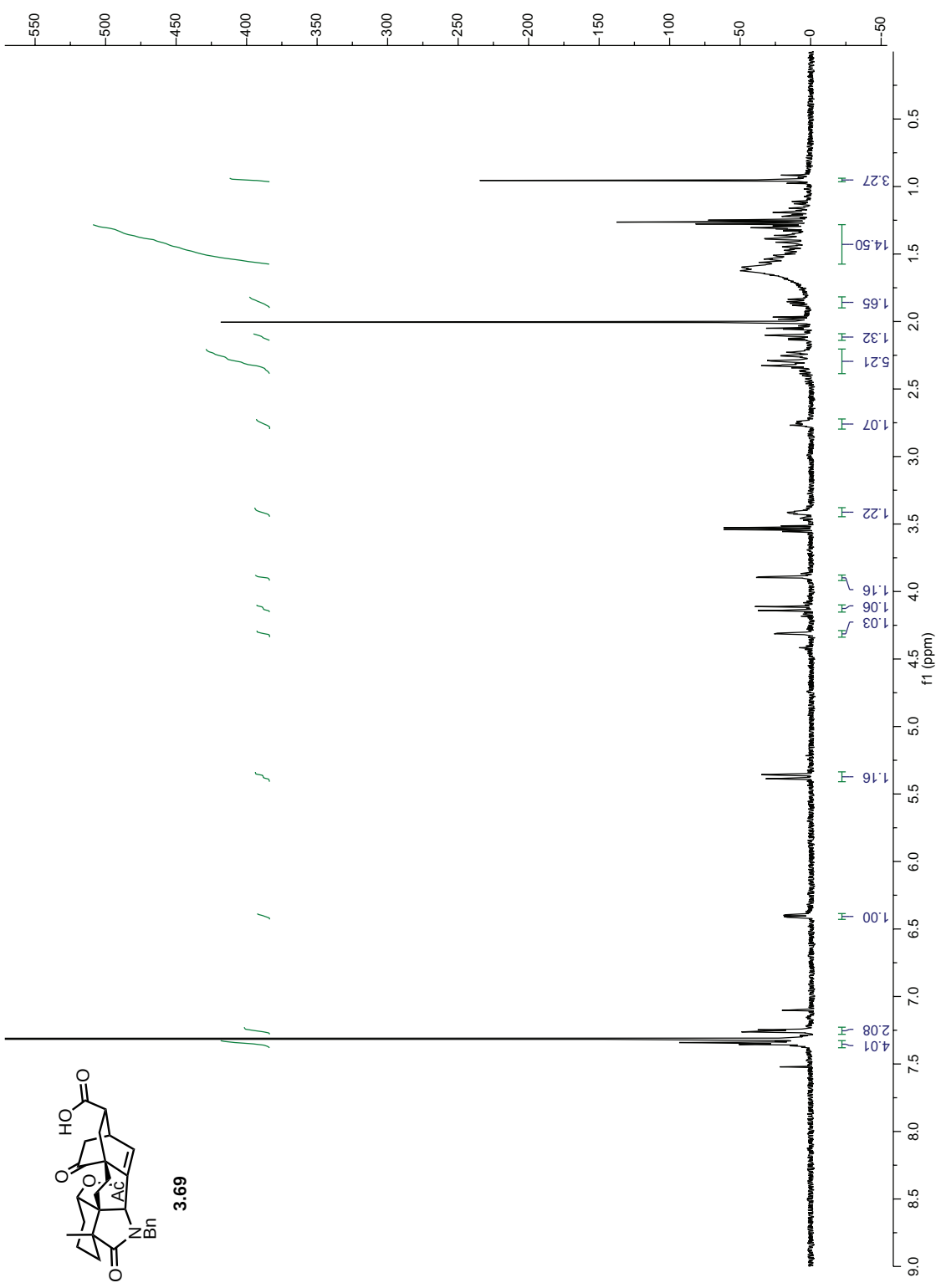

Figure 3.A.13: ^{1}H NMR of **3.69**

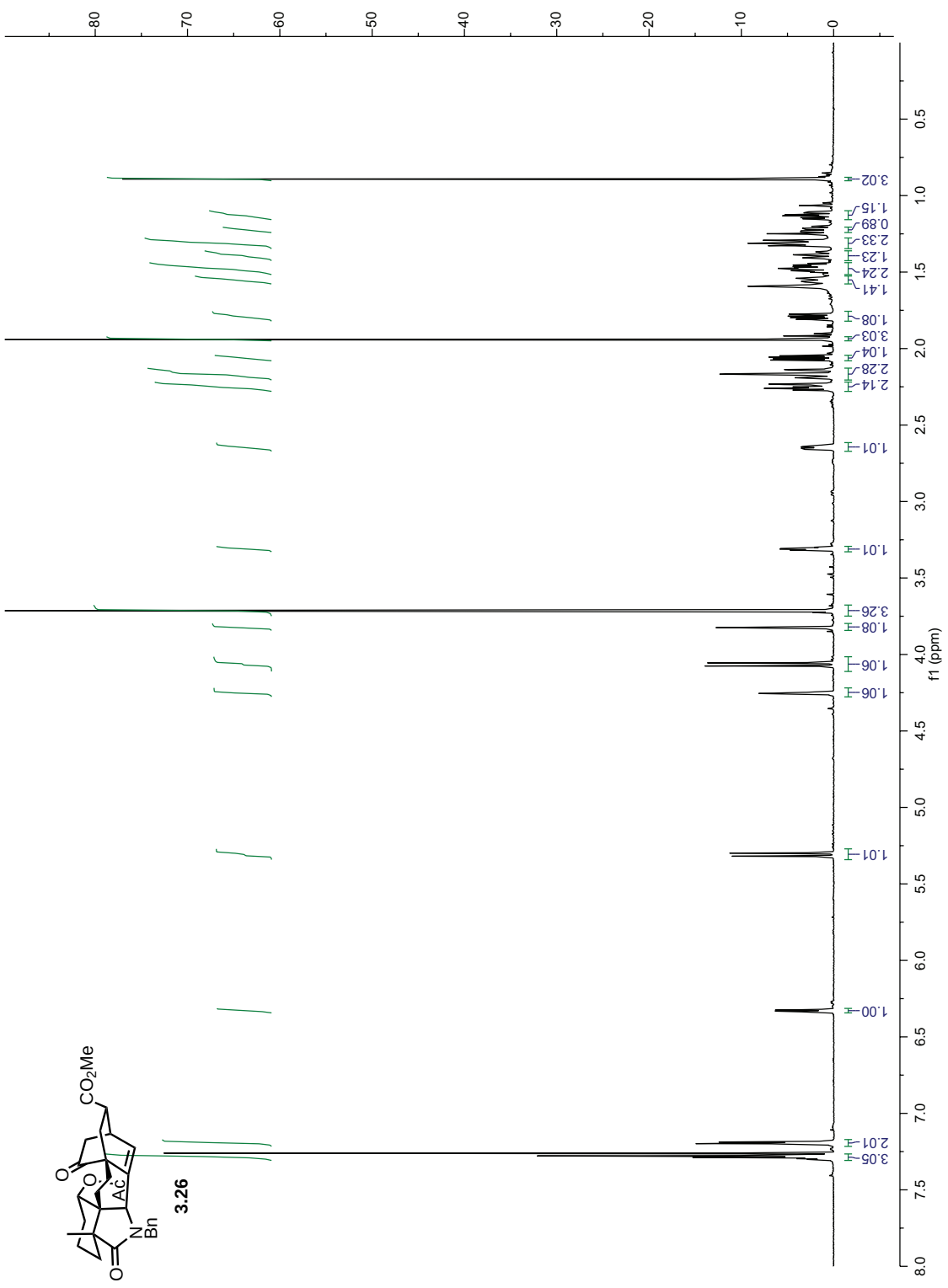

Figure 3.A.14: ^{1}H NMR of **3.26**

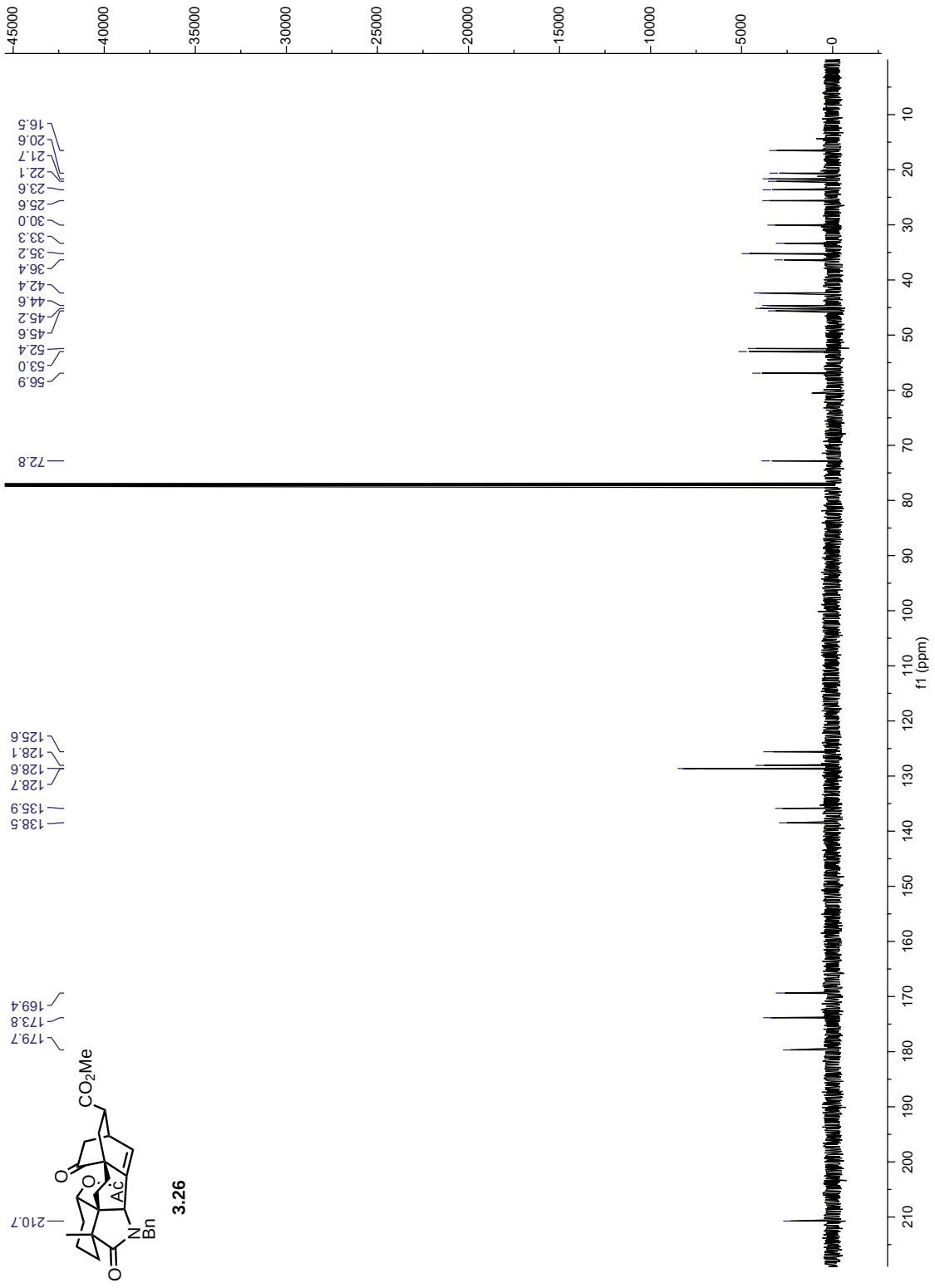

Figure 3.A.15: ^{13}C NMR of **3.26**

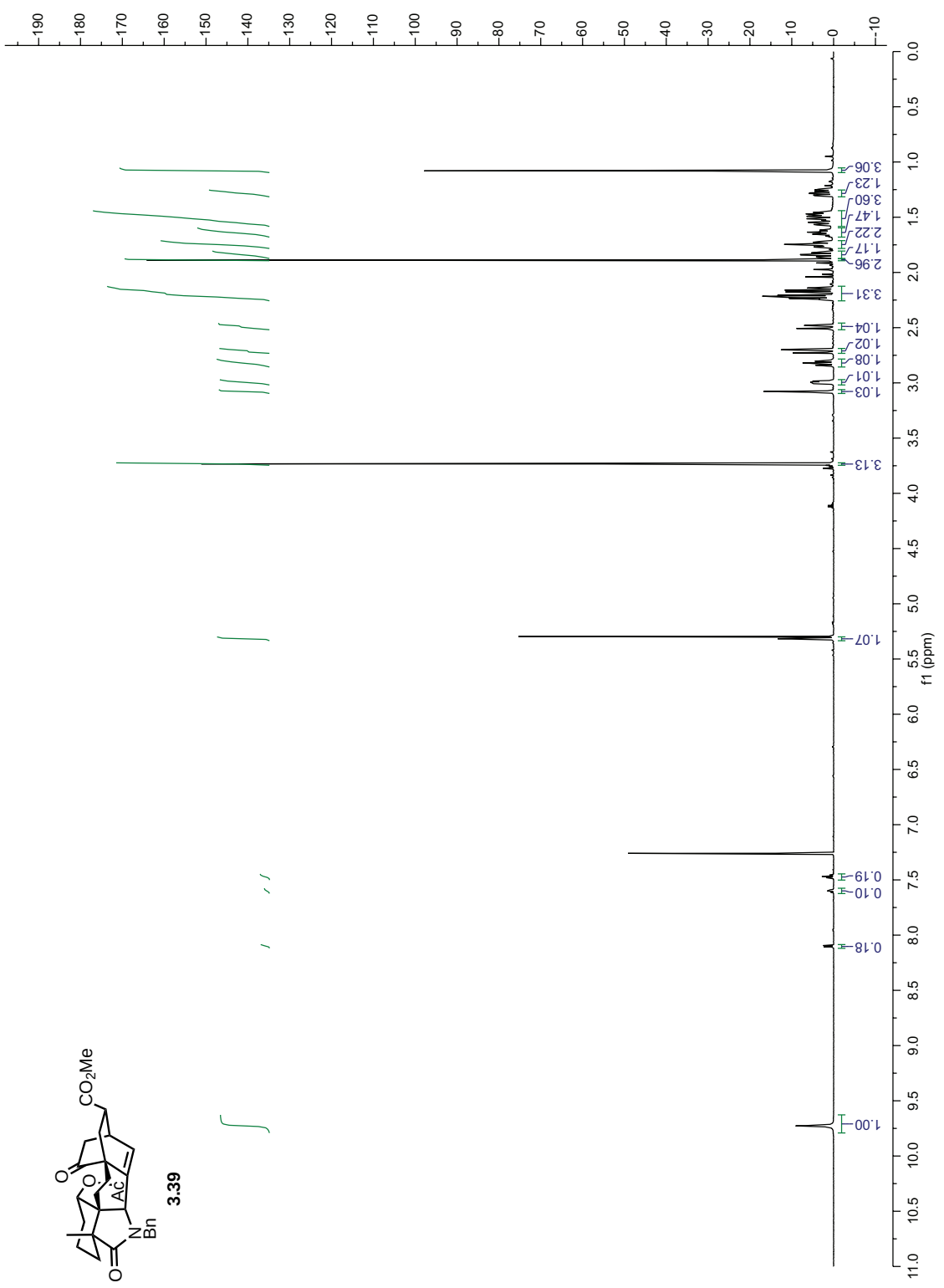

Figure 3.A.16: ^{1}H NMR of **3.39**

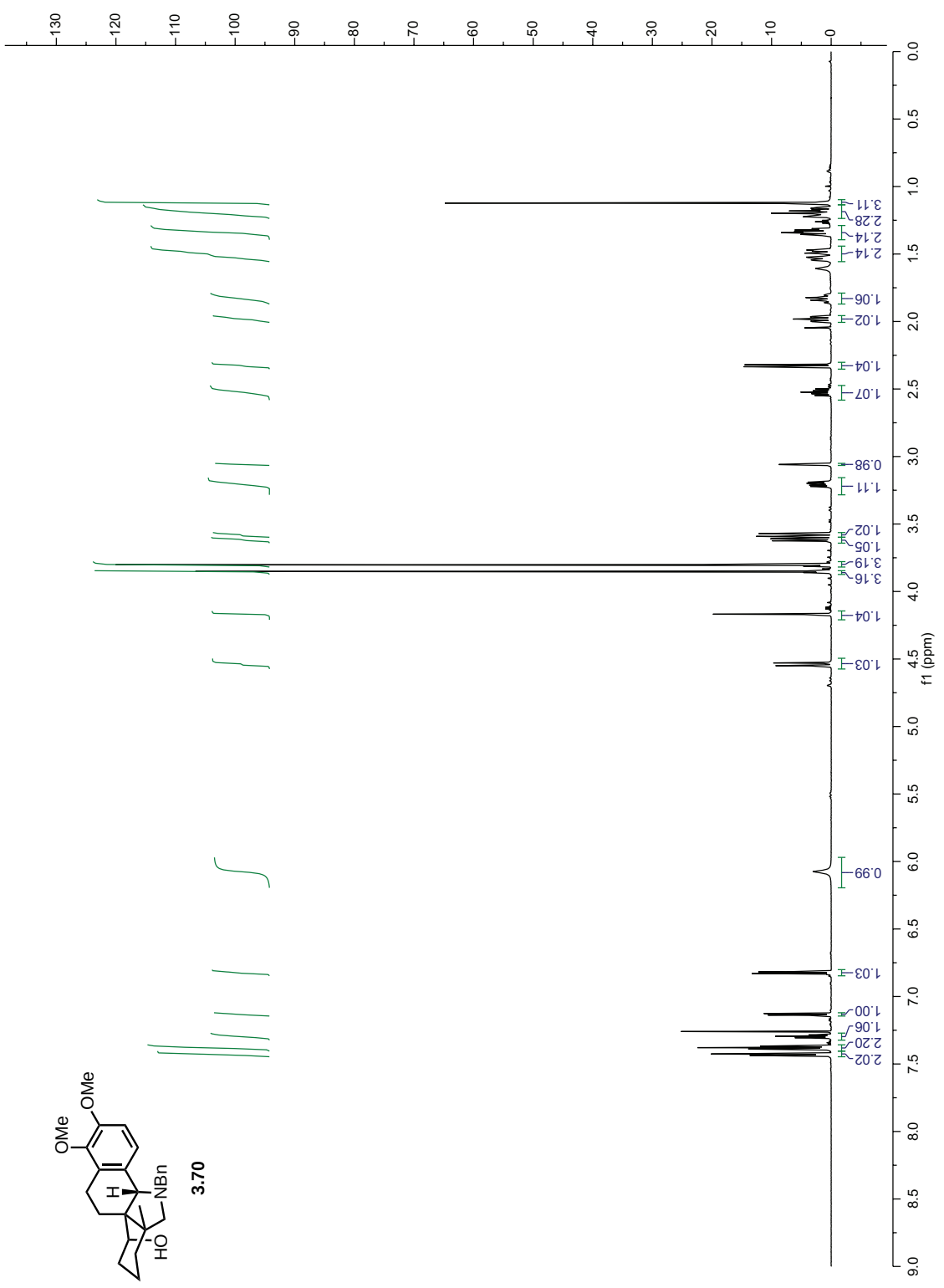

Figure 3.A.17: ^{1}H NMR of **3.70**

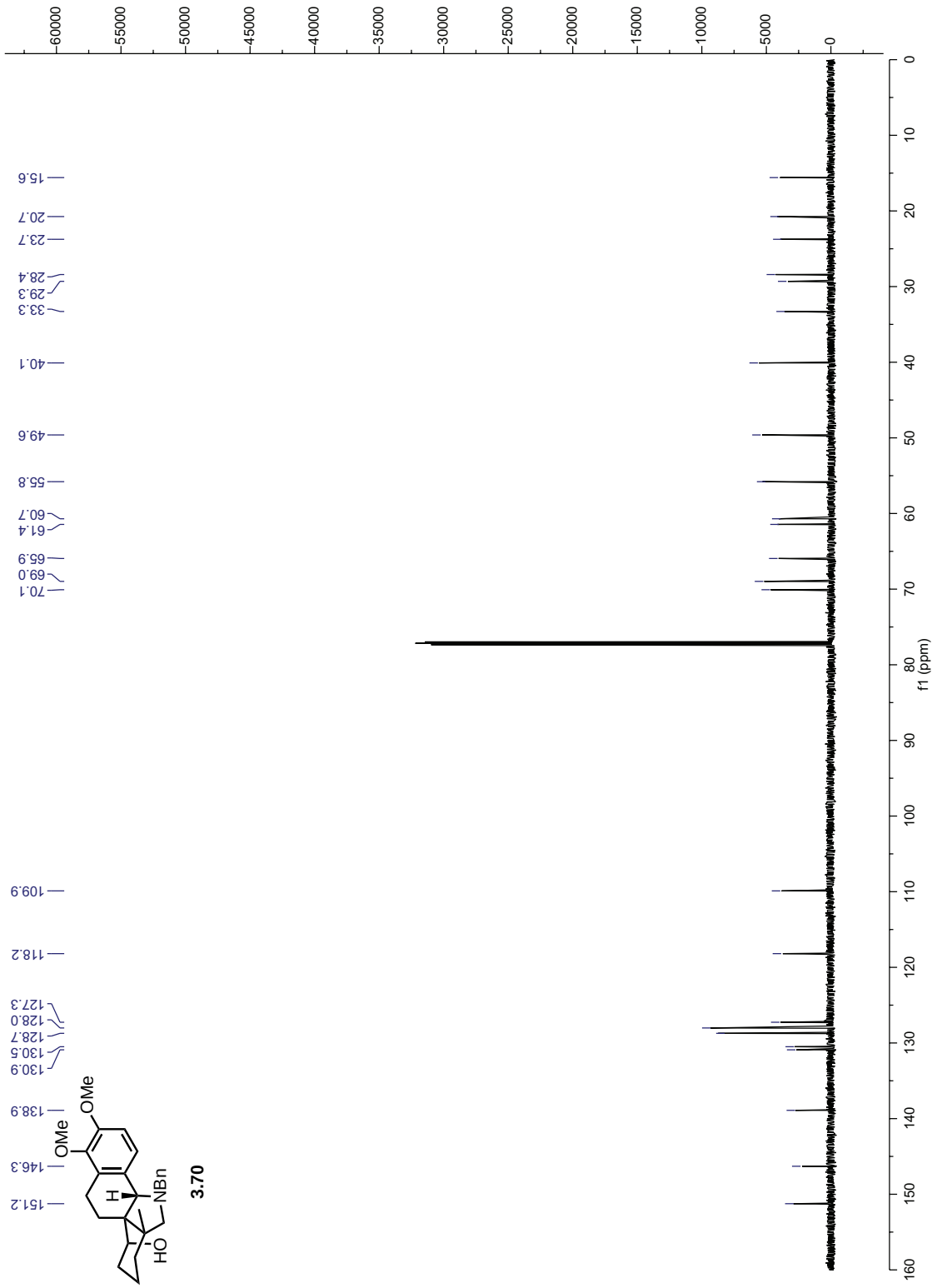

Figure 3.A.18: ^{13}C NMR of **3.70**

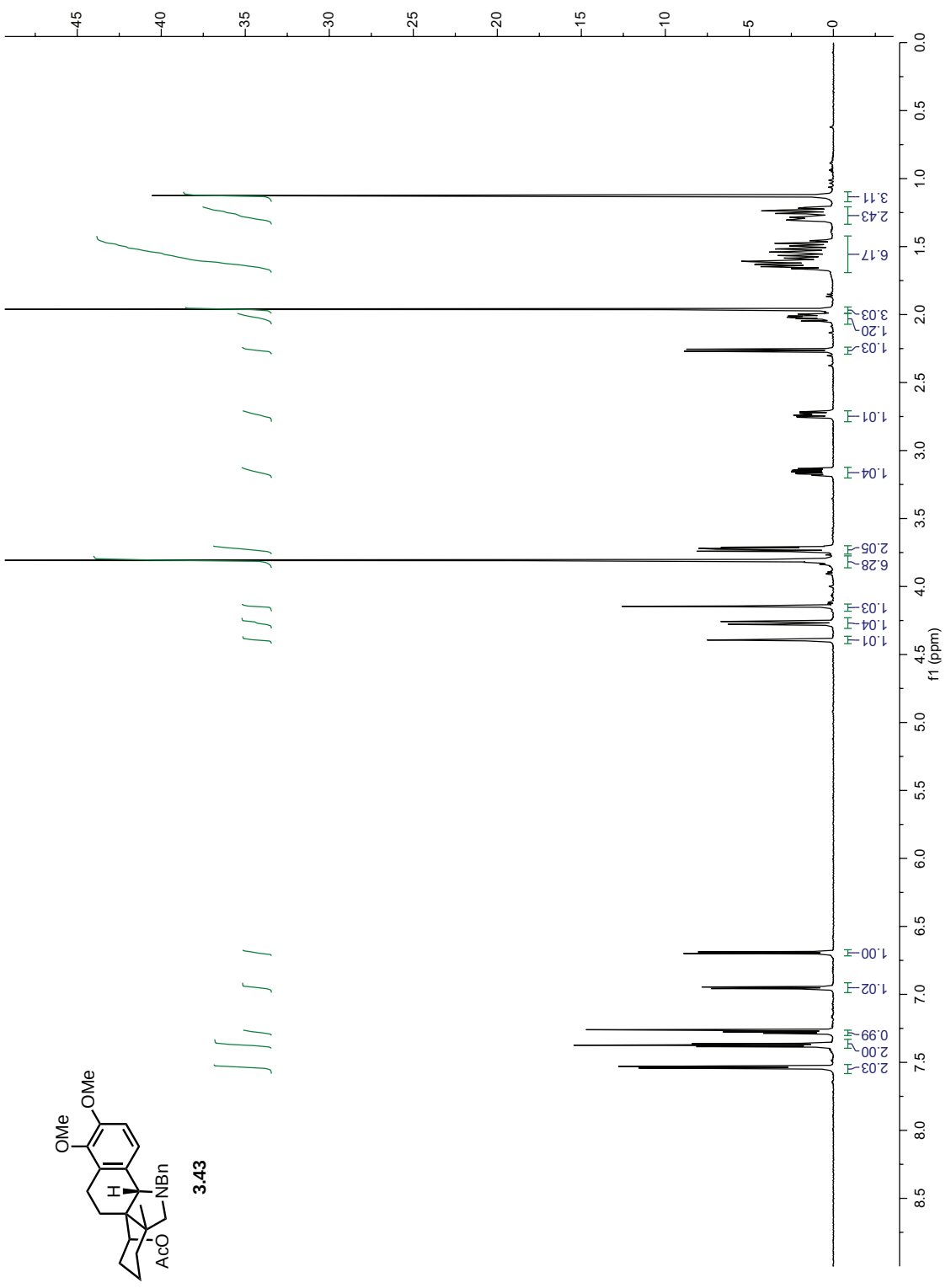

Figure 3.A.19: ^{1}H NMR of **3.43**

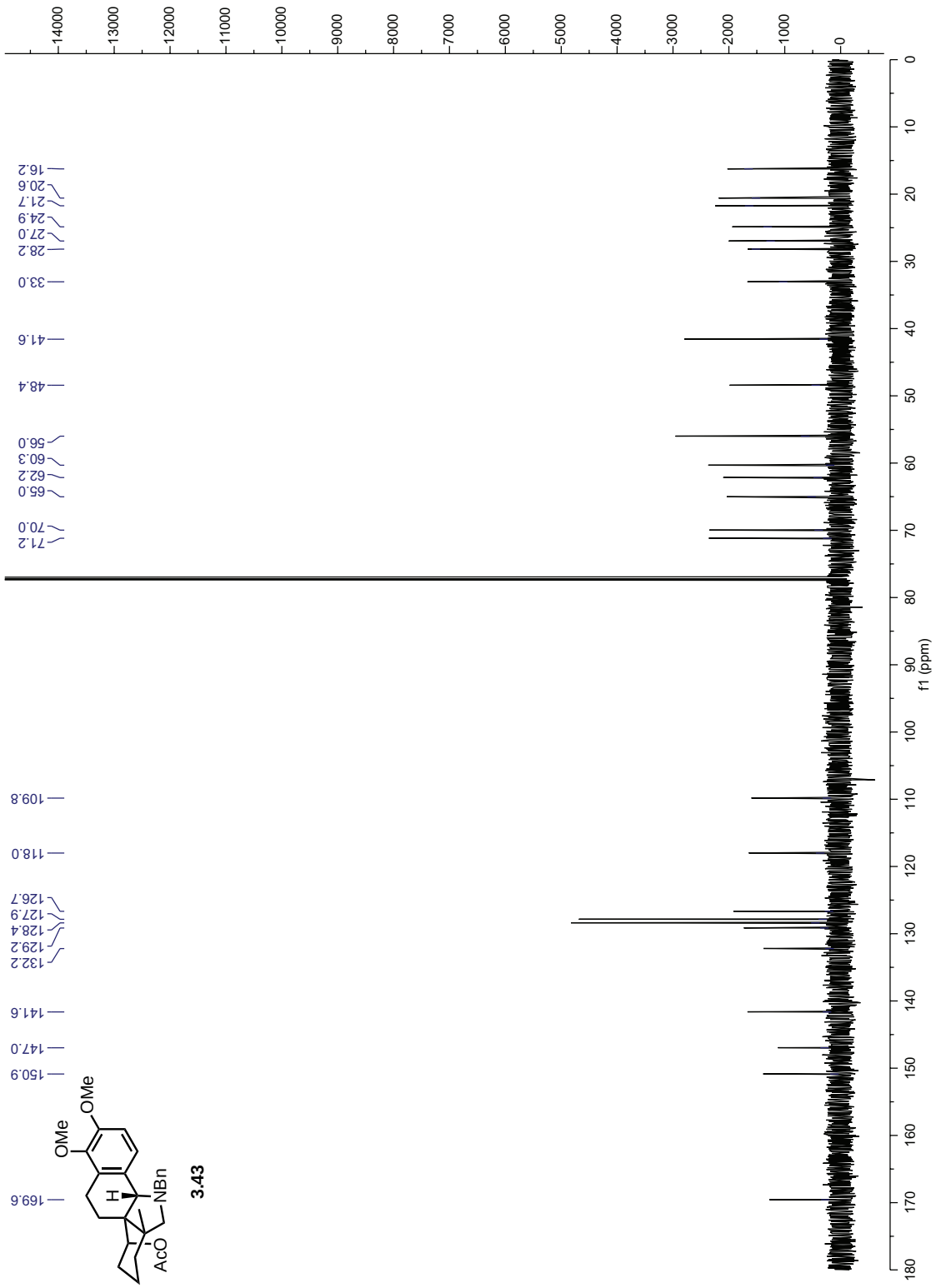

Figure 3.A.20: ^{13}C NMR of **3.43**

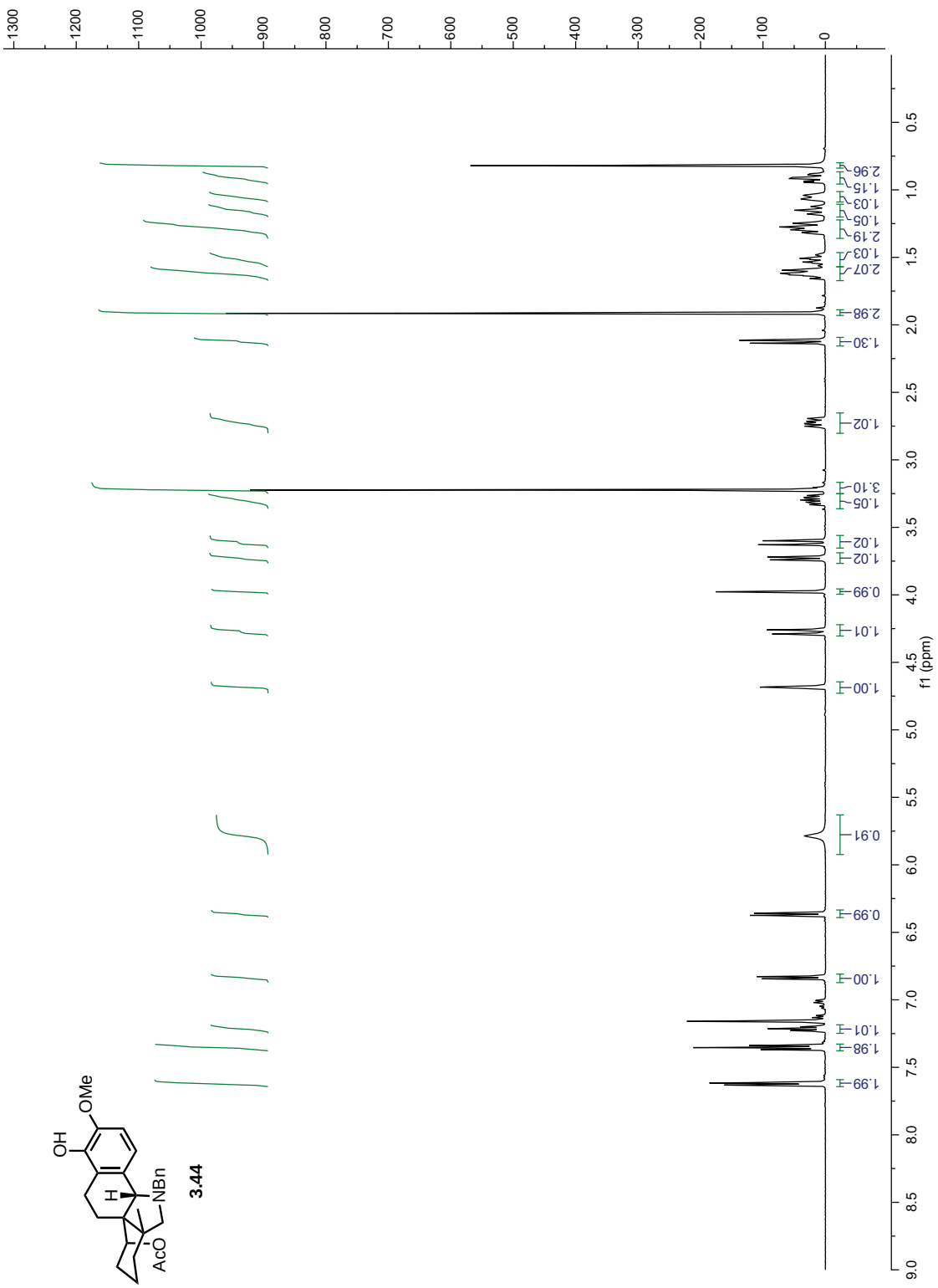

Figure 3.A.21: ^{1}H NMR of **3.44**

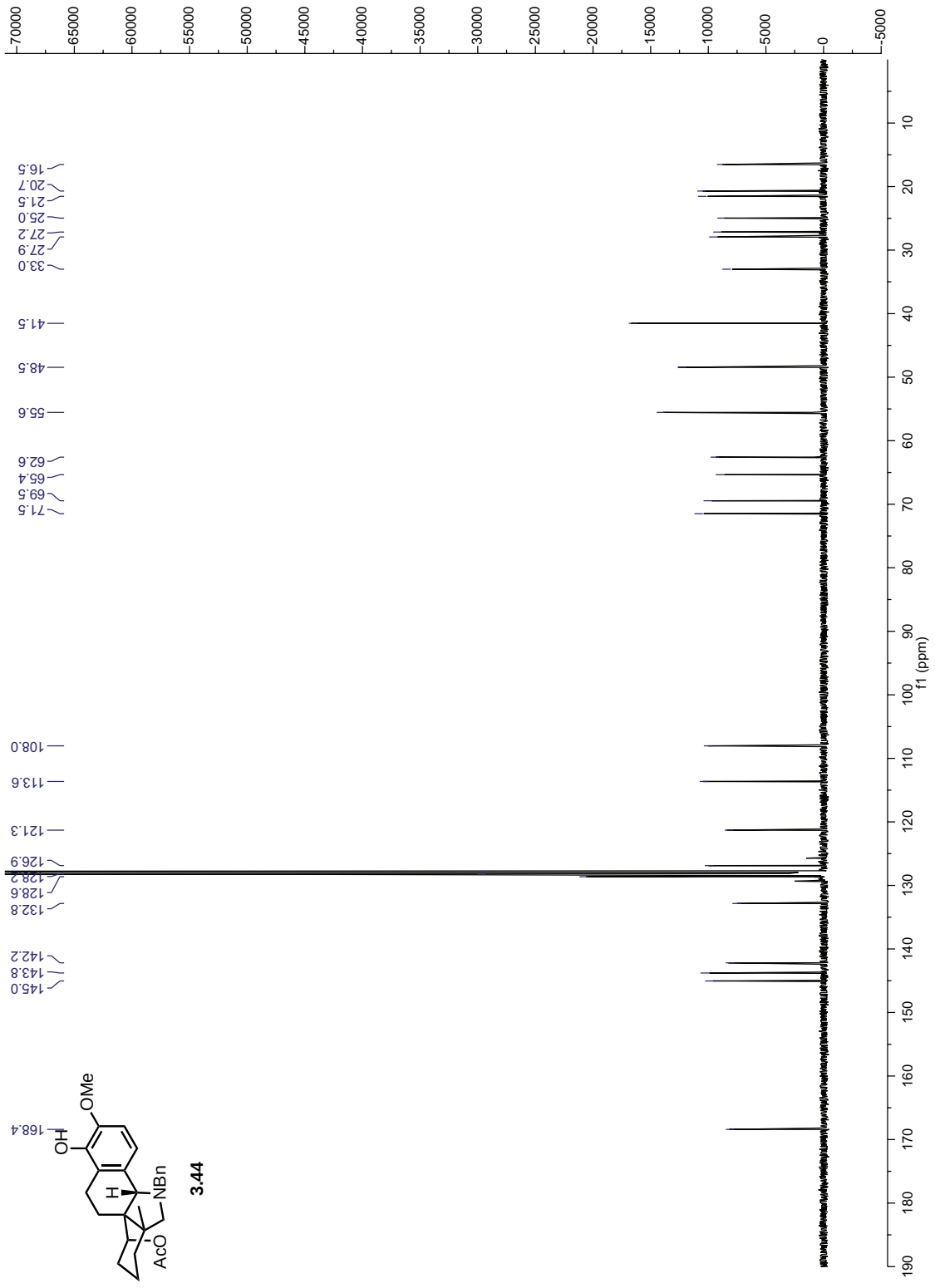

Figure 3.A.22: ^{13}C NMR of **3.44**

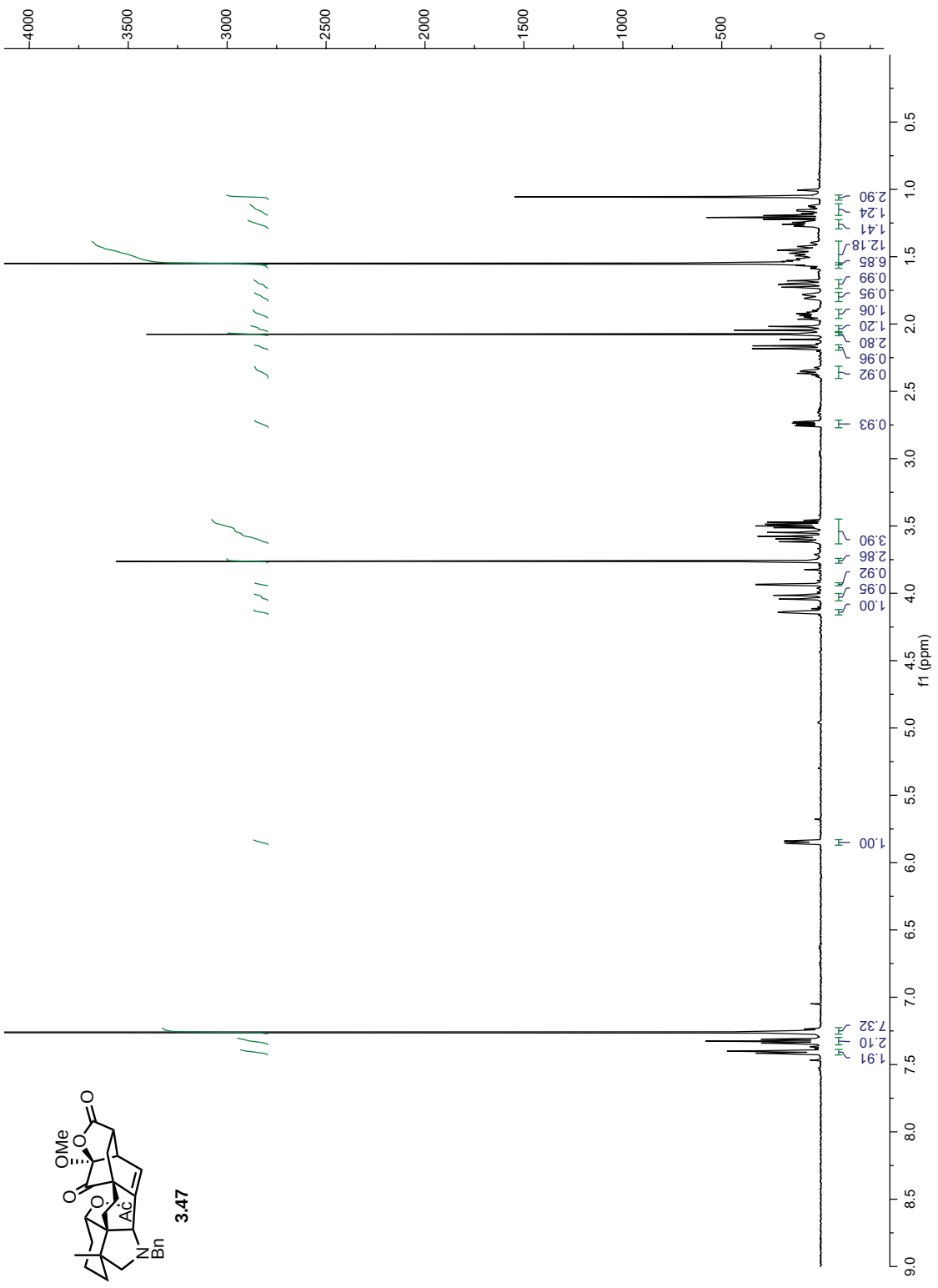

Figure 3.A.23: ^{1}H NMR of **3.47**

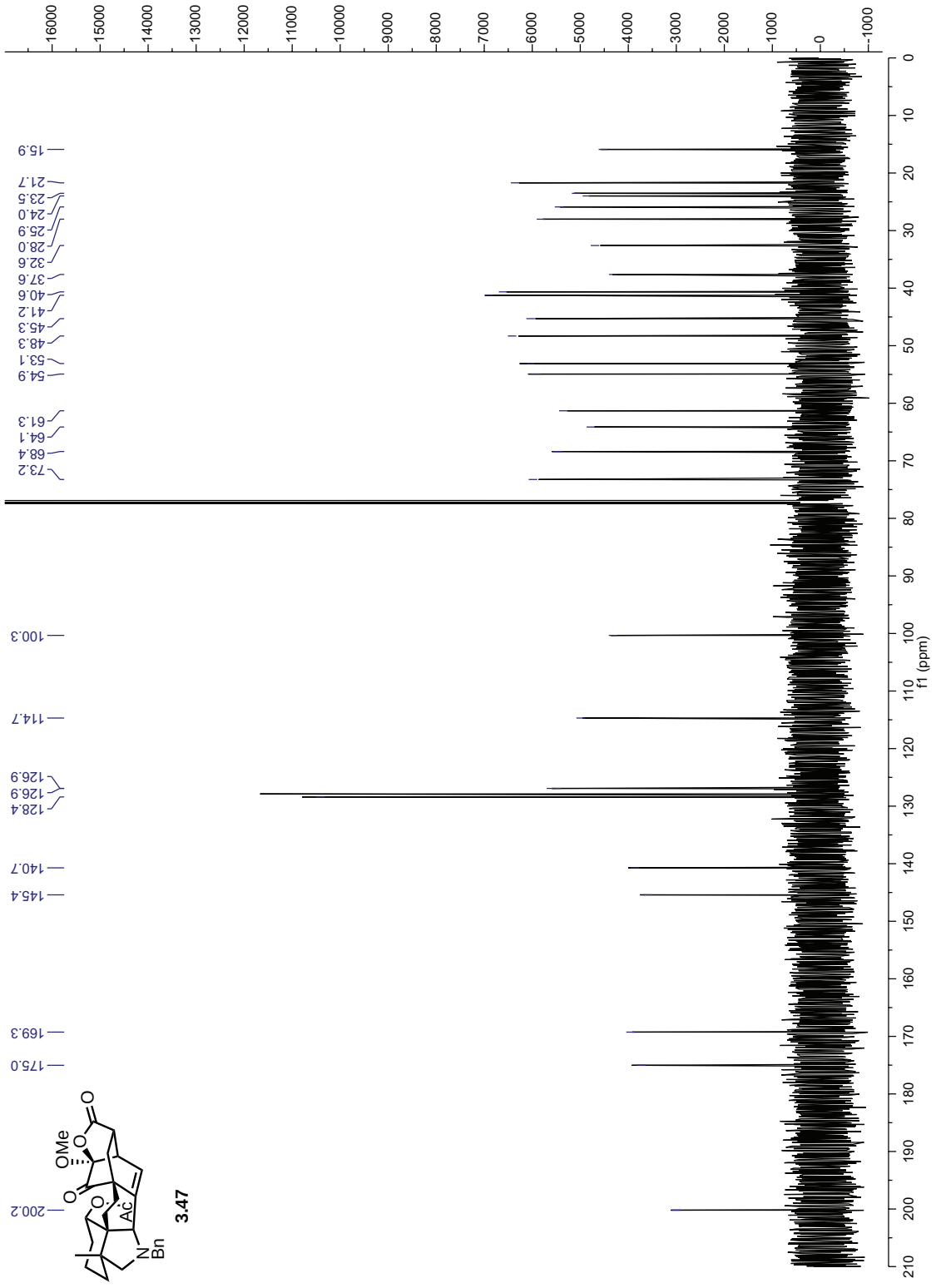

Figure 3.A.24: ^{13}C NMR of **3.47**

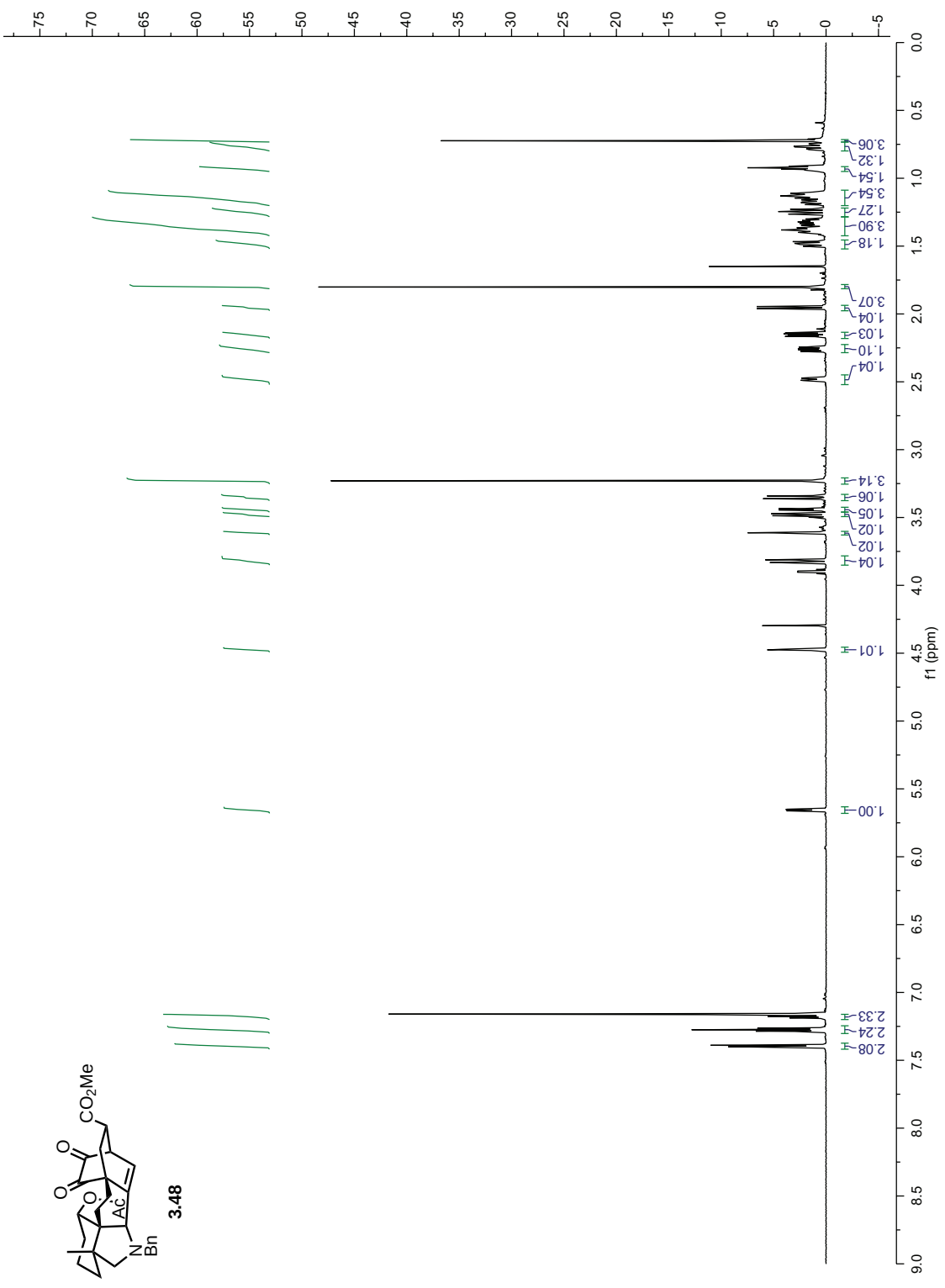

Figure 3.A.25: ^{1}H NMR of **3.48**

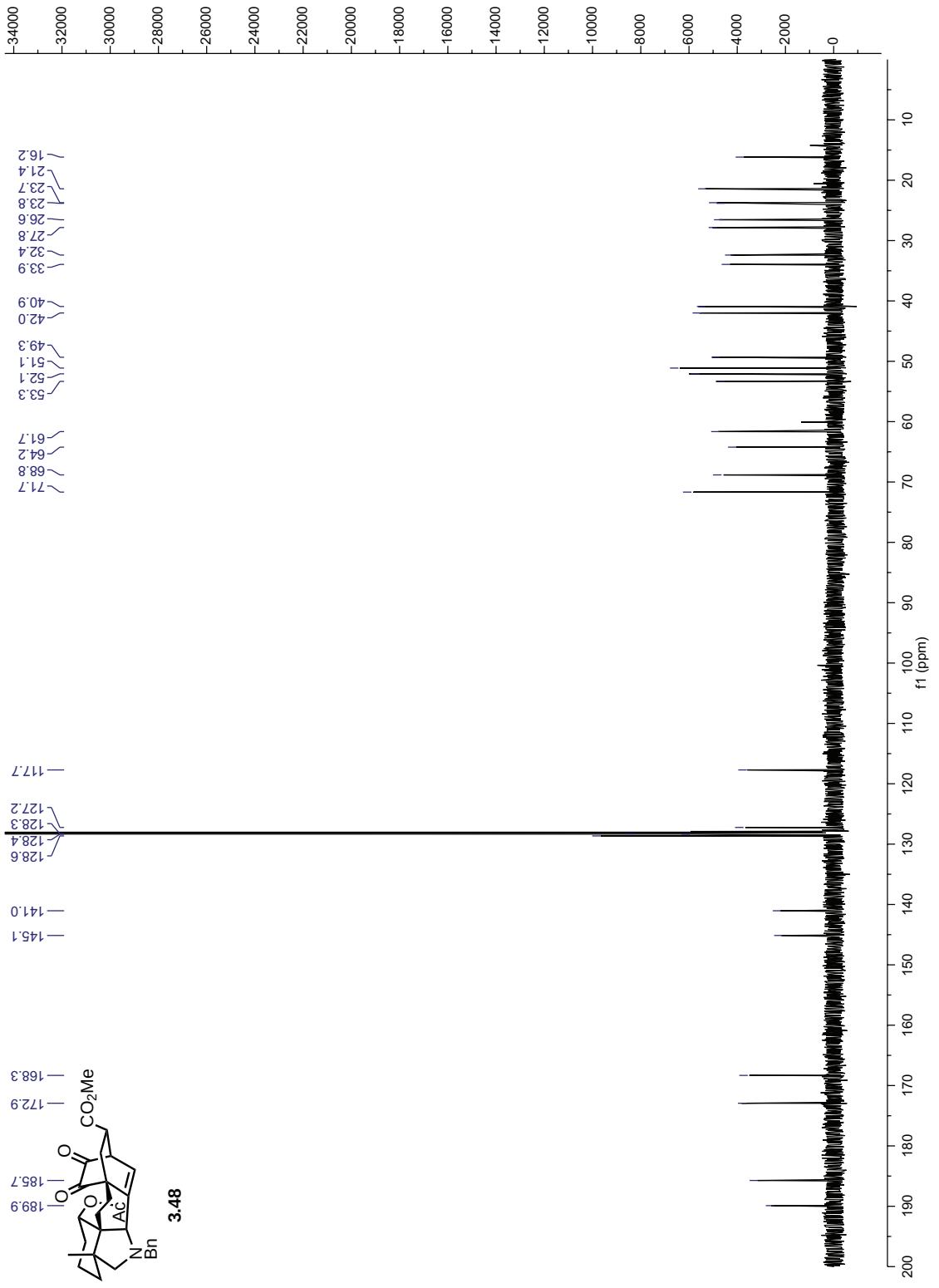

Figure 3.A.26: ^{13}C NMR of **3.48**

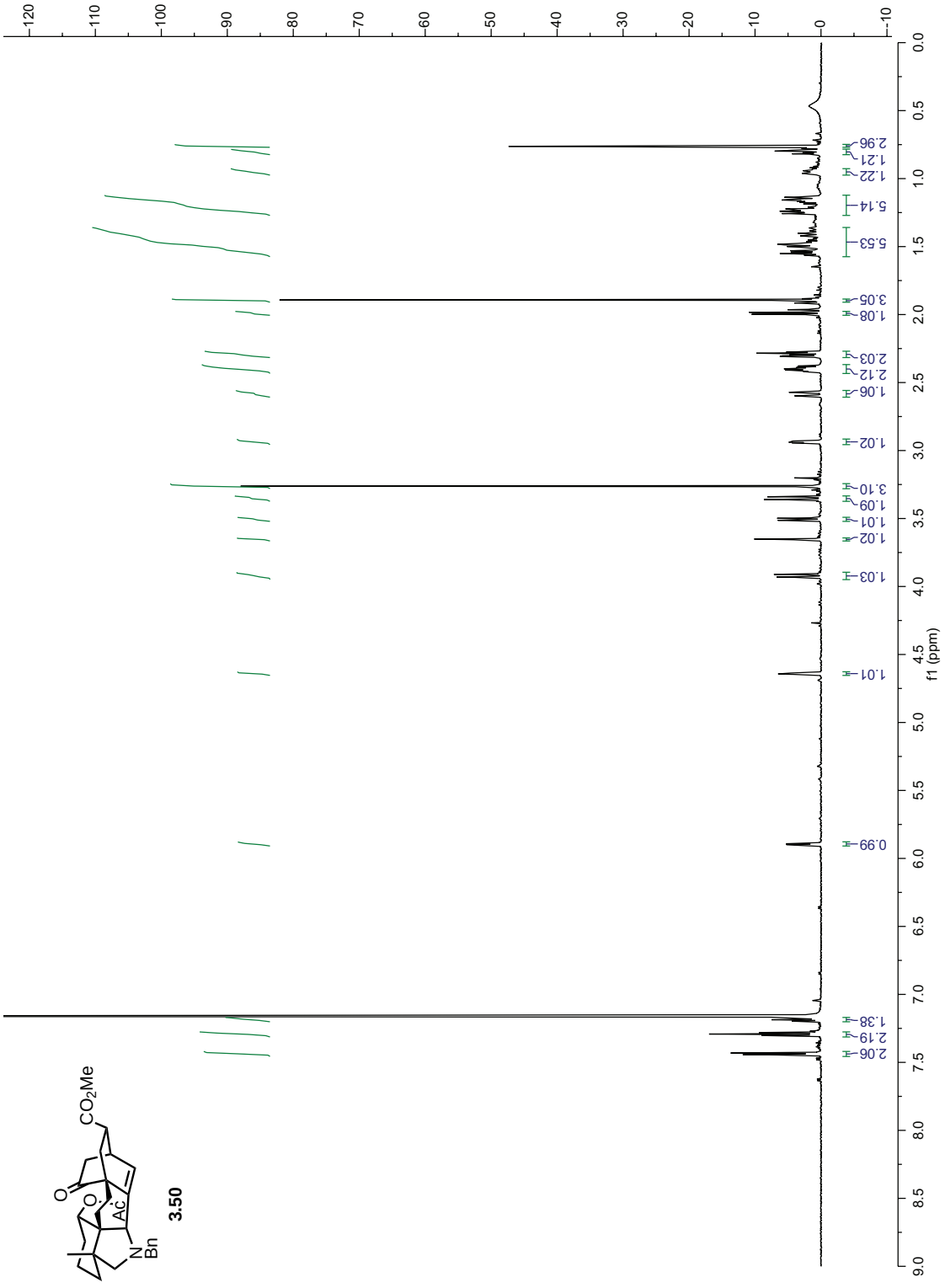

Figure 3.A.27: ^{1}H NMR of **3.50**

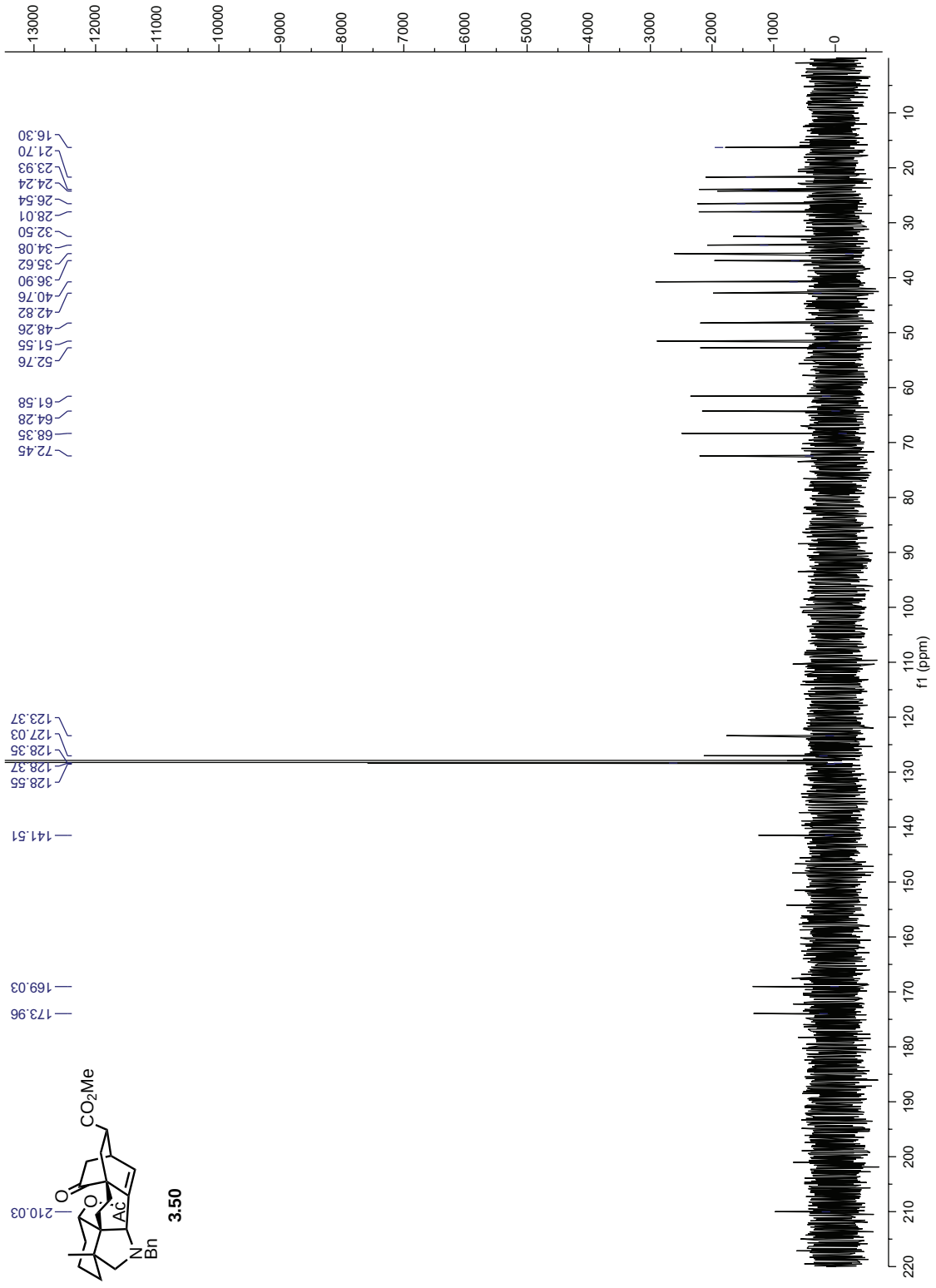

Figure 3.A.28: ^{13}C NMR of **3.50**

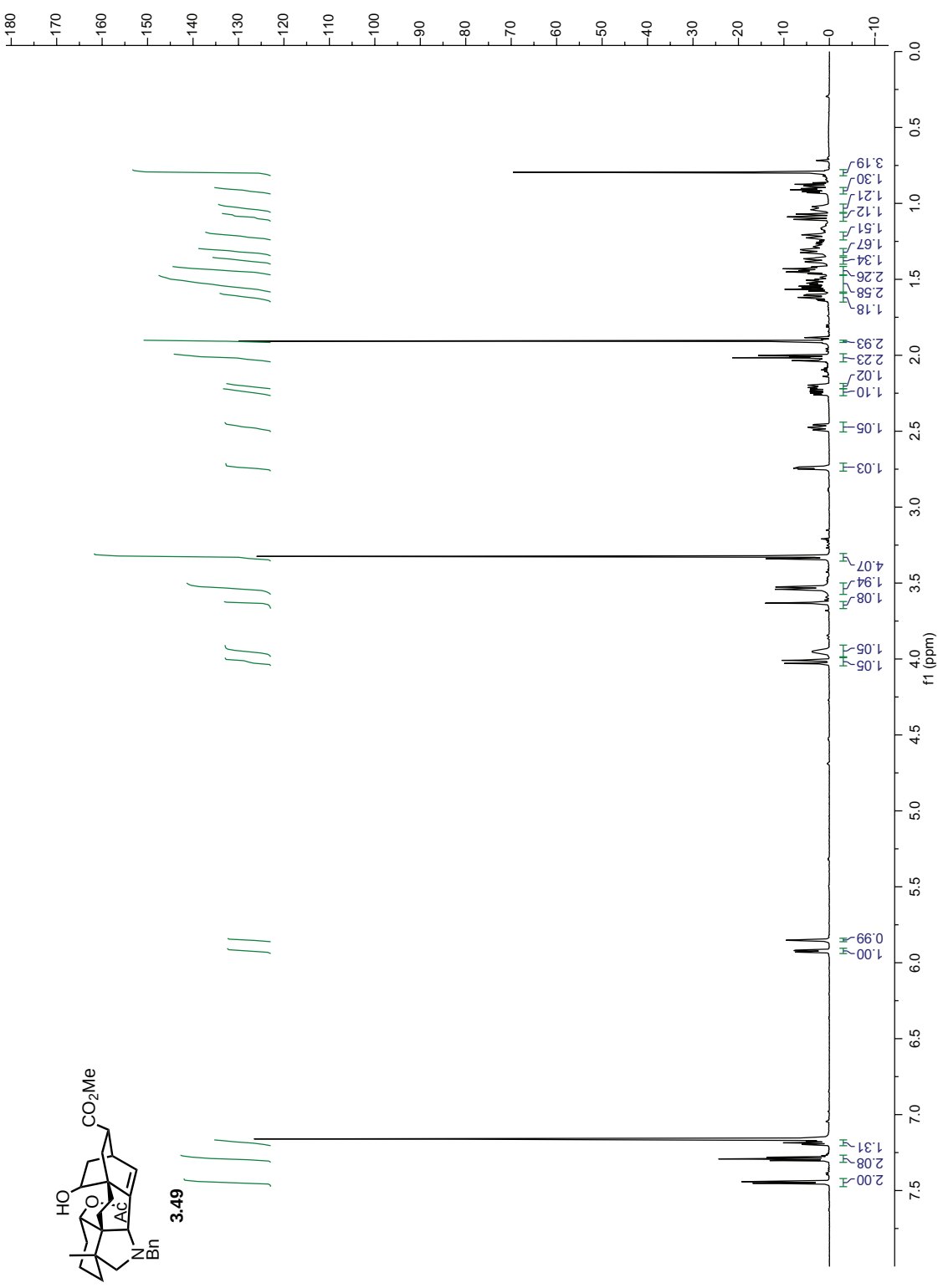

Figure 3.A.29: ^{1}H NMR of **3.49**

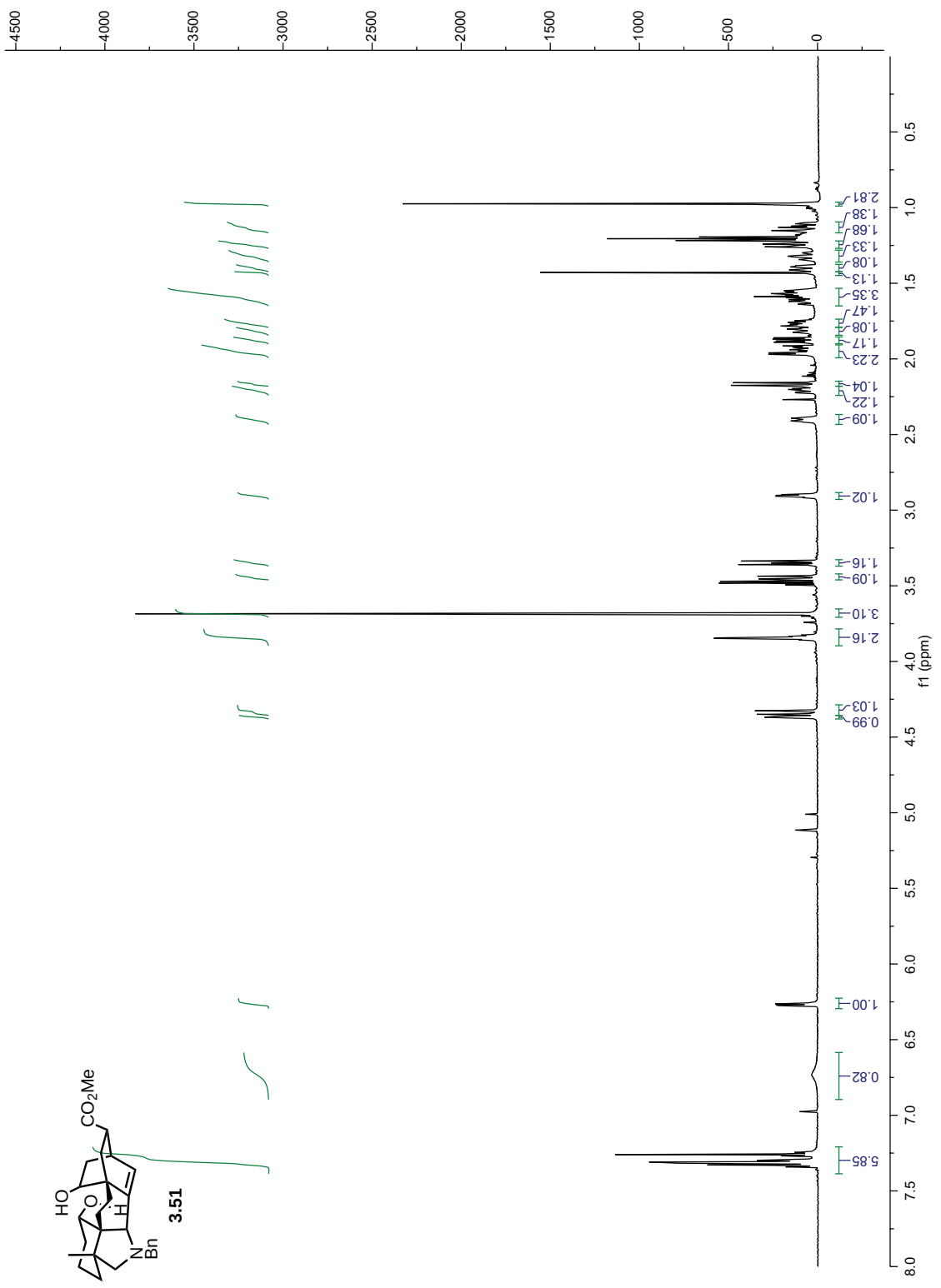

Figure 3.A.30: ^{1}H NMR of **3.51**

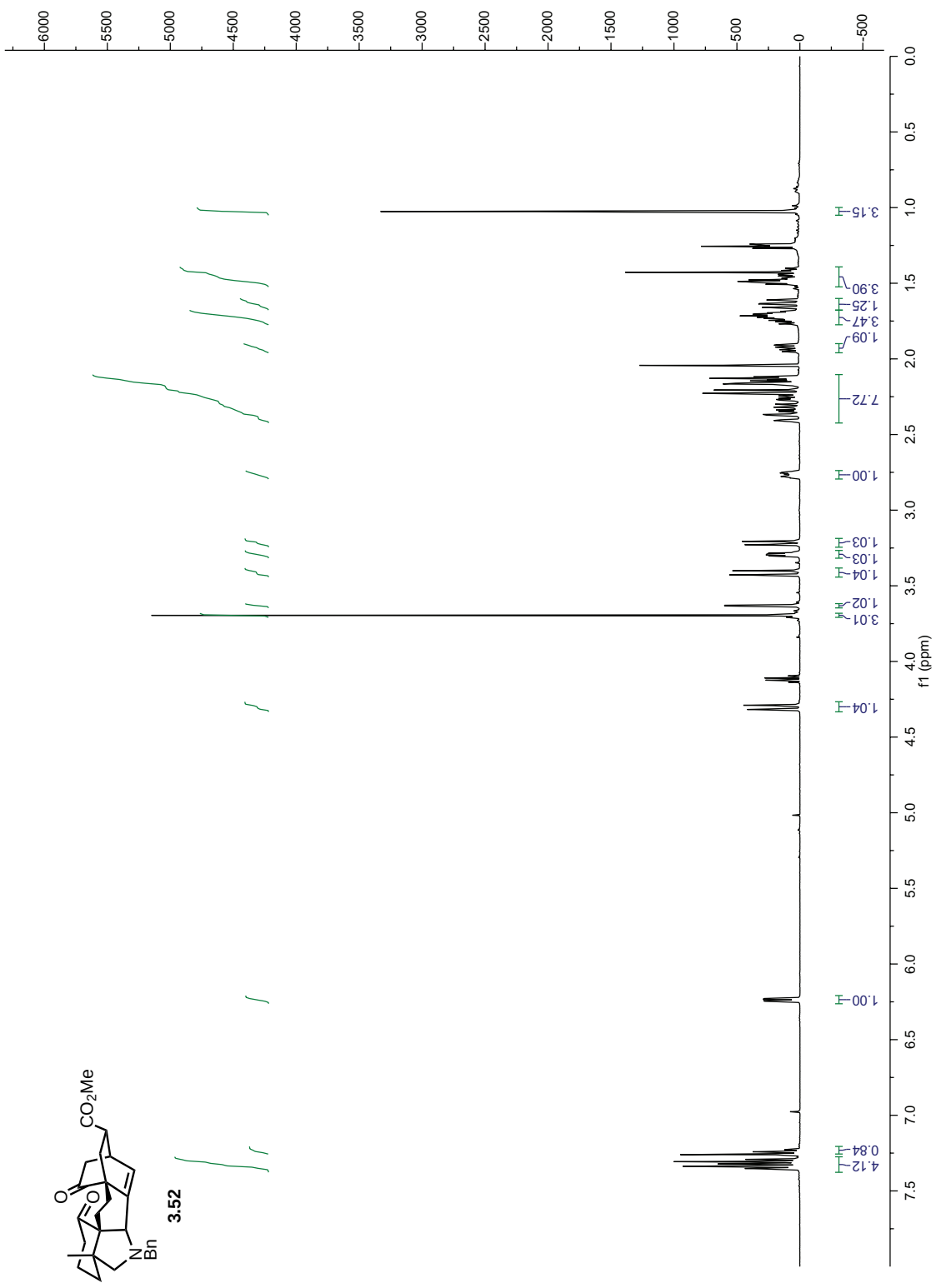

Figure 3.A.31: ^{1}H NMR of **3.52**

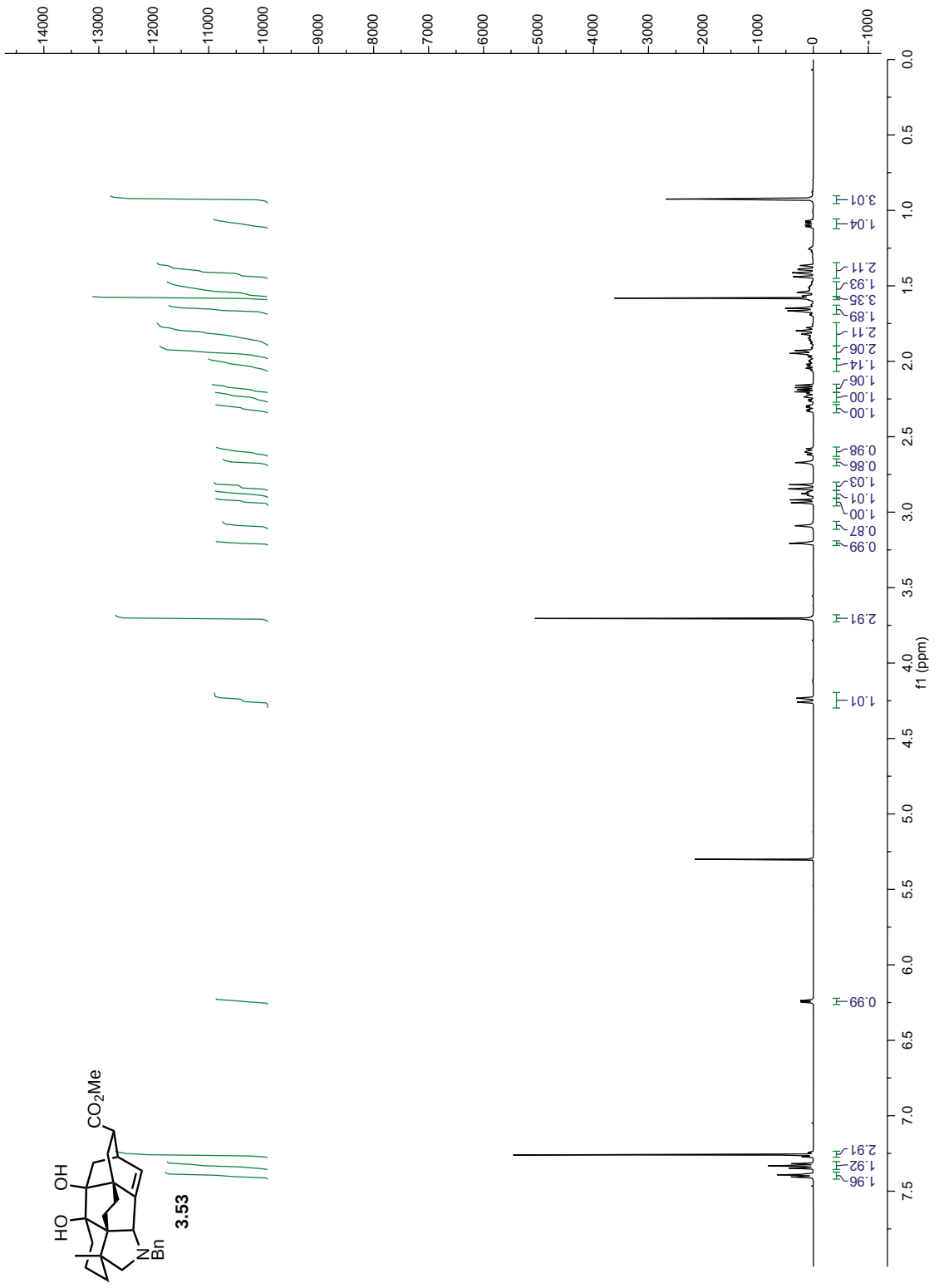

Figure 3.A.32: ^{1}H NMR of **3.53**

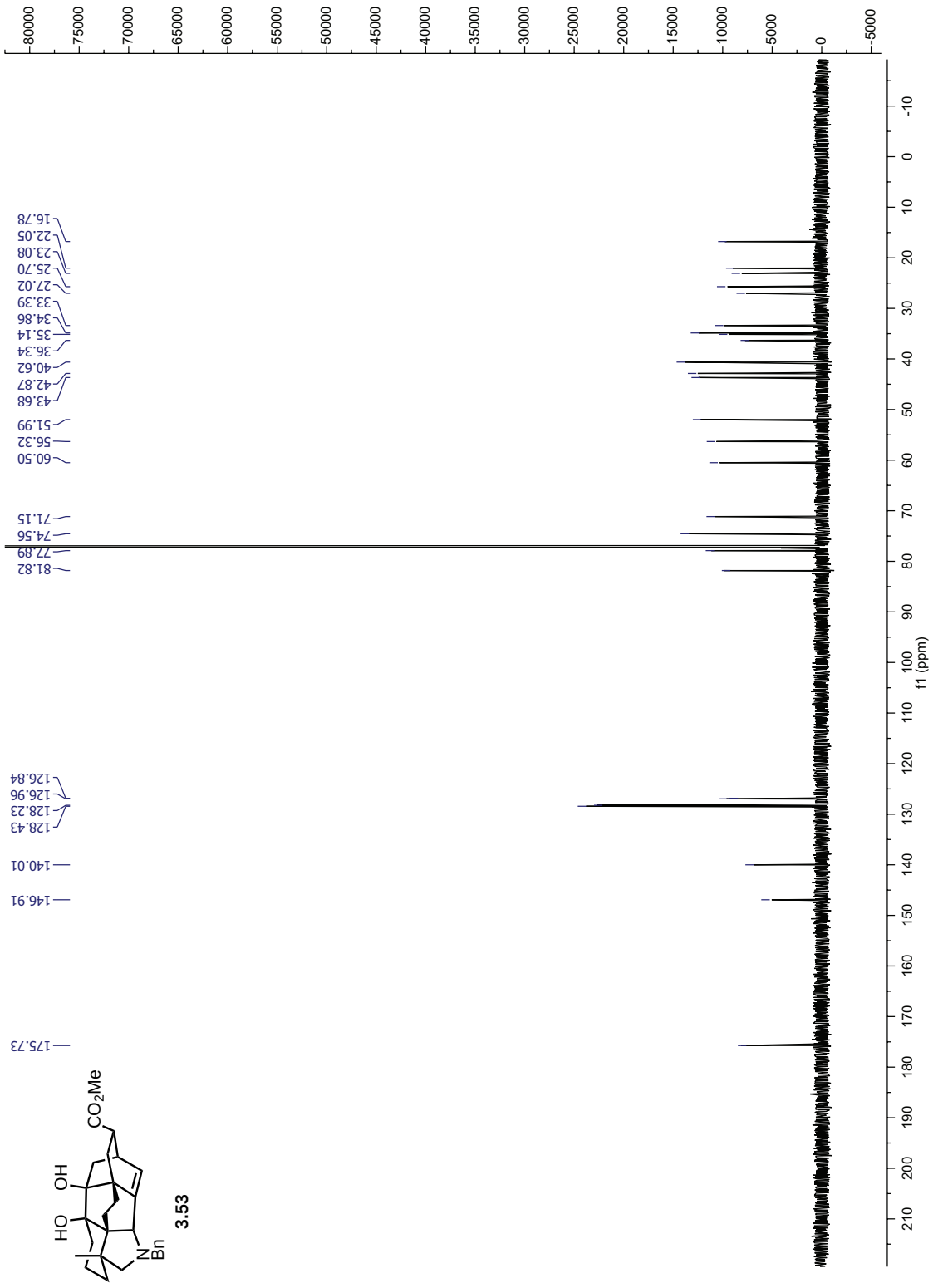

Figure 3.A.33: ^{13}C NMR of **3.53**

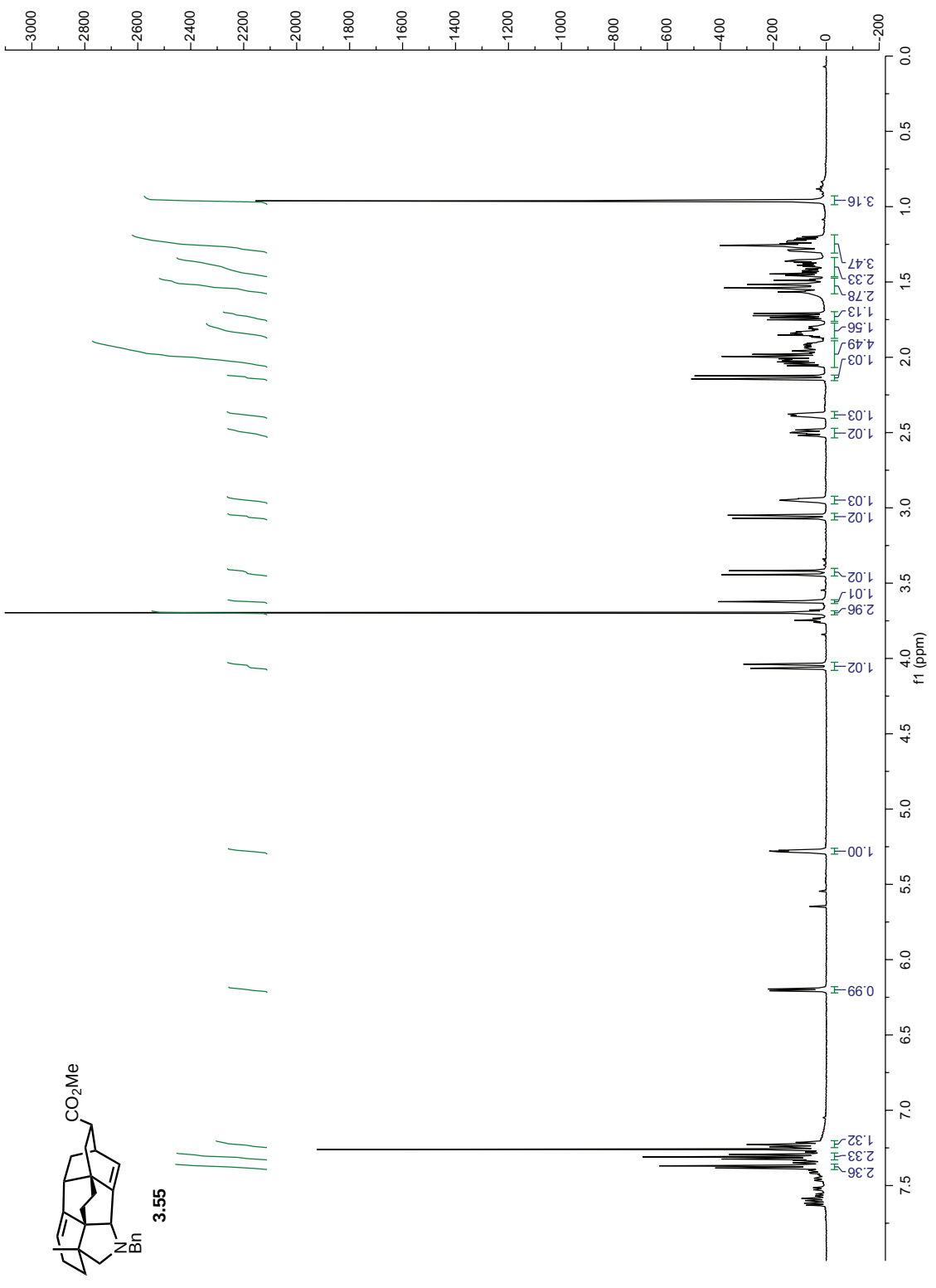

Figure 3.A.34: ^{1}H NMR of **3.55**

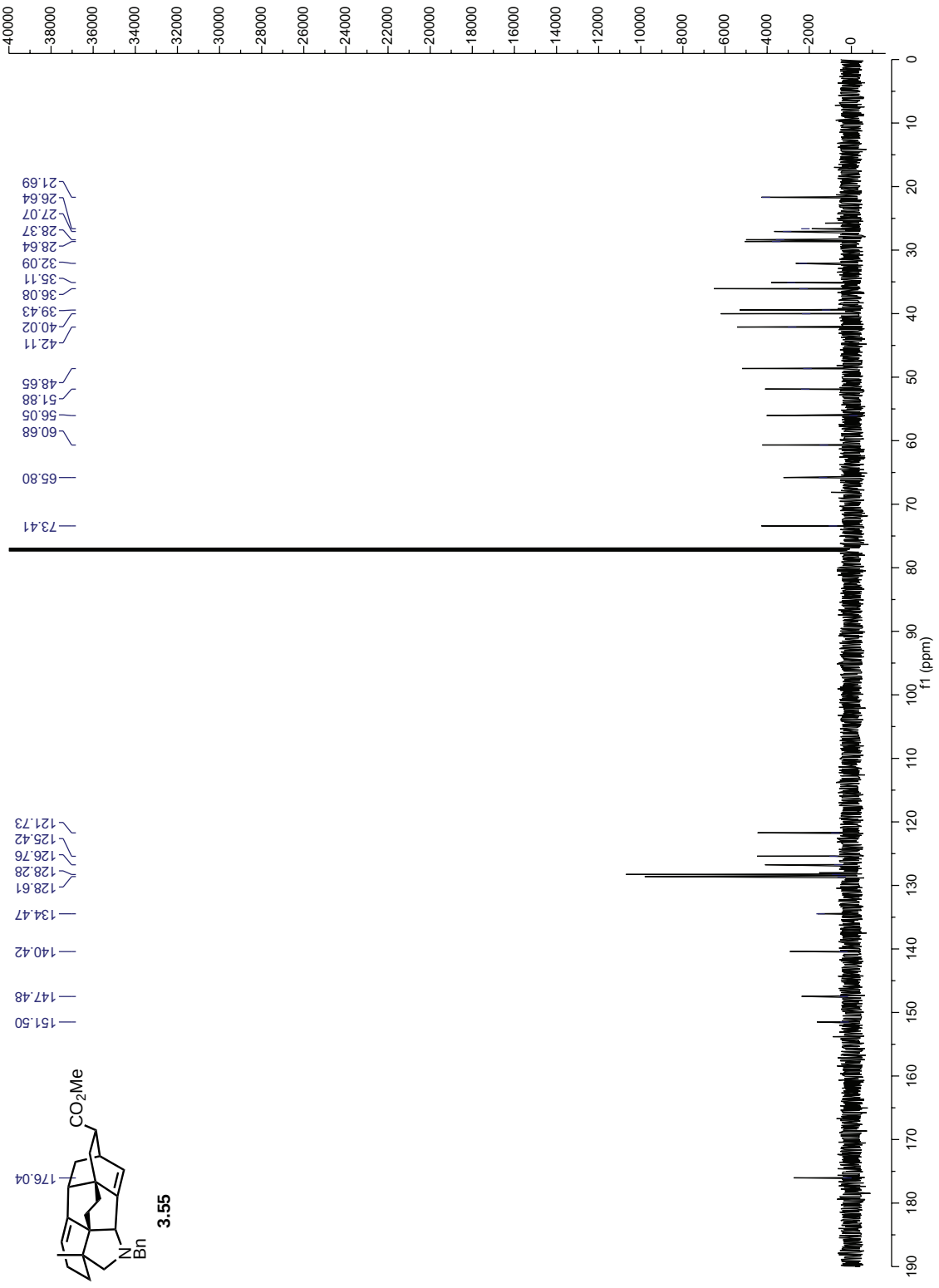

Figure 3.A.35: ^{13}C NMR of **3.55**

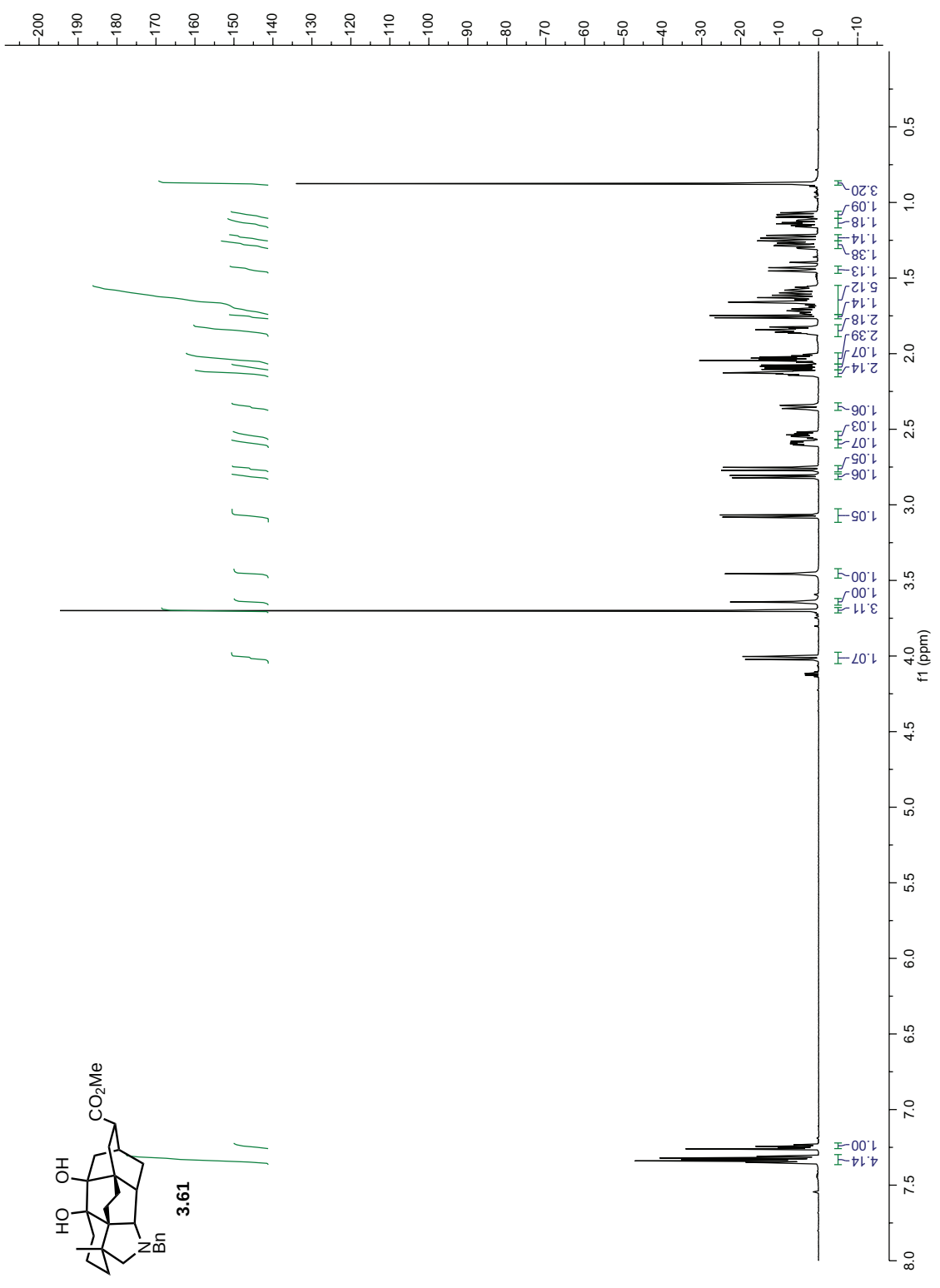

Figure 3.A.36: ^{1}H NMR of **3.61**

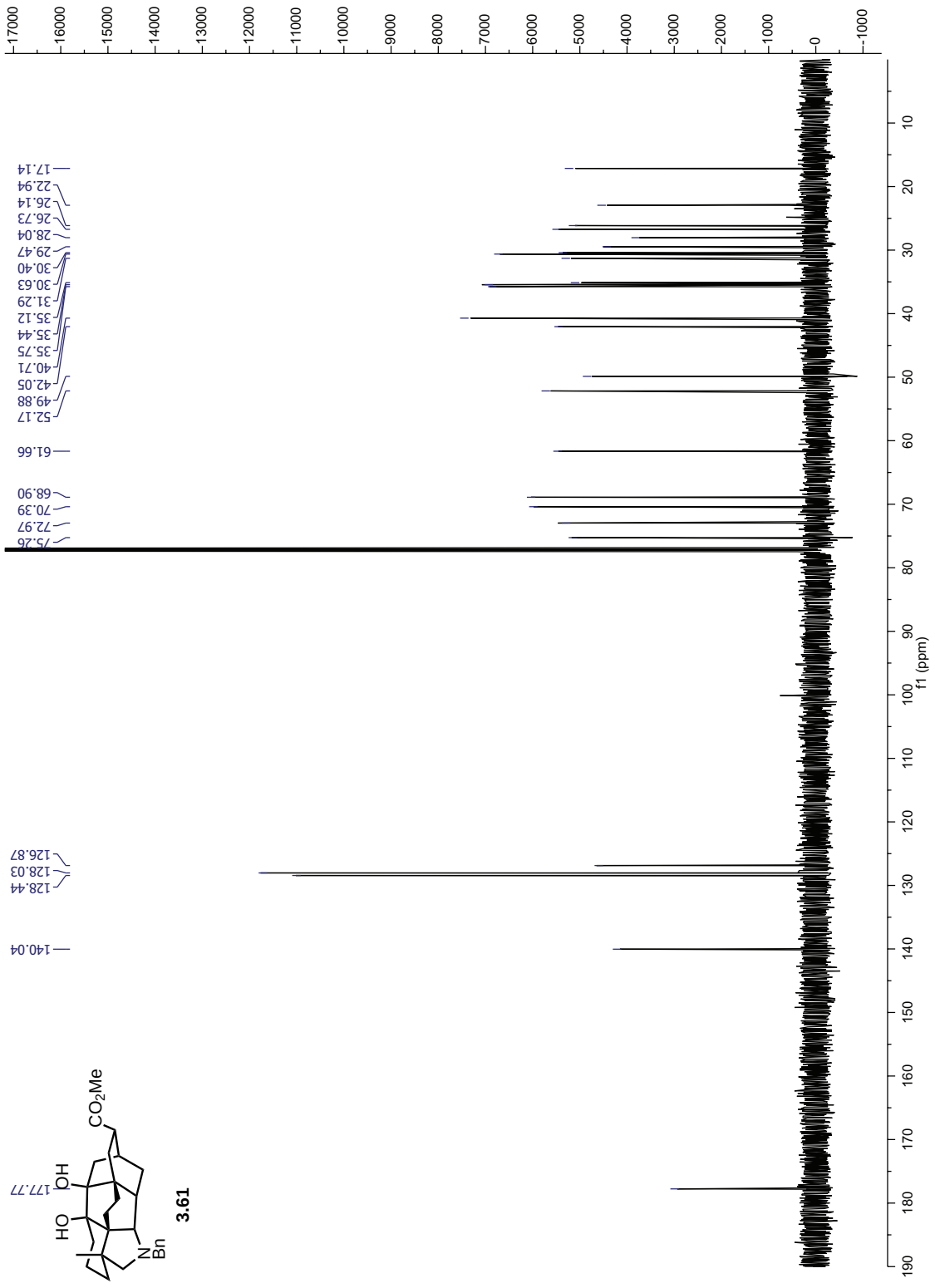

Figure 3.A.37: ^{13}C NMR of **3.61**

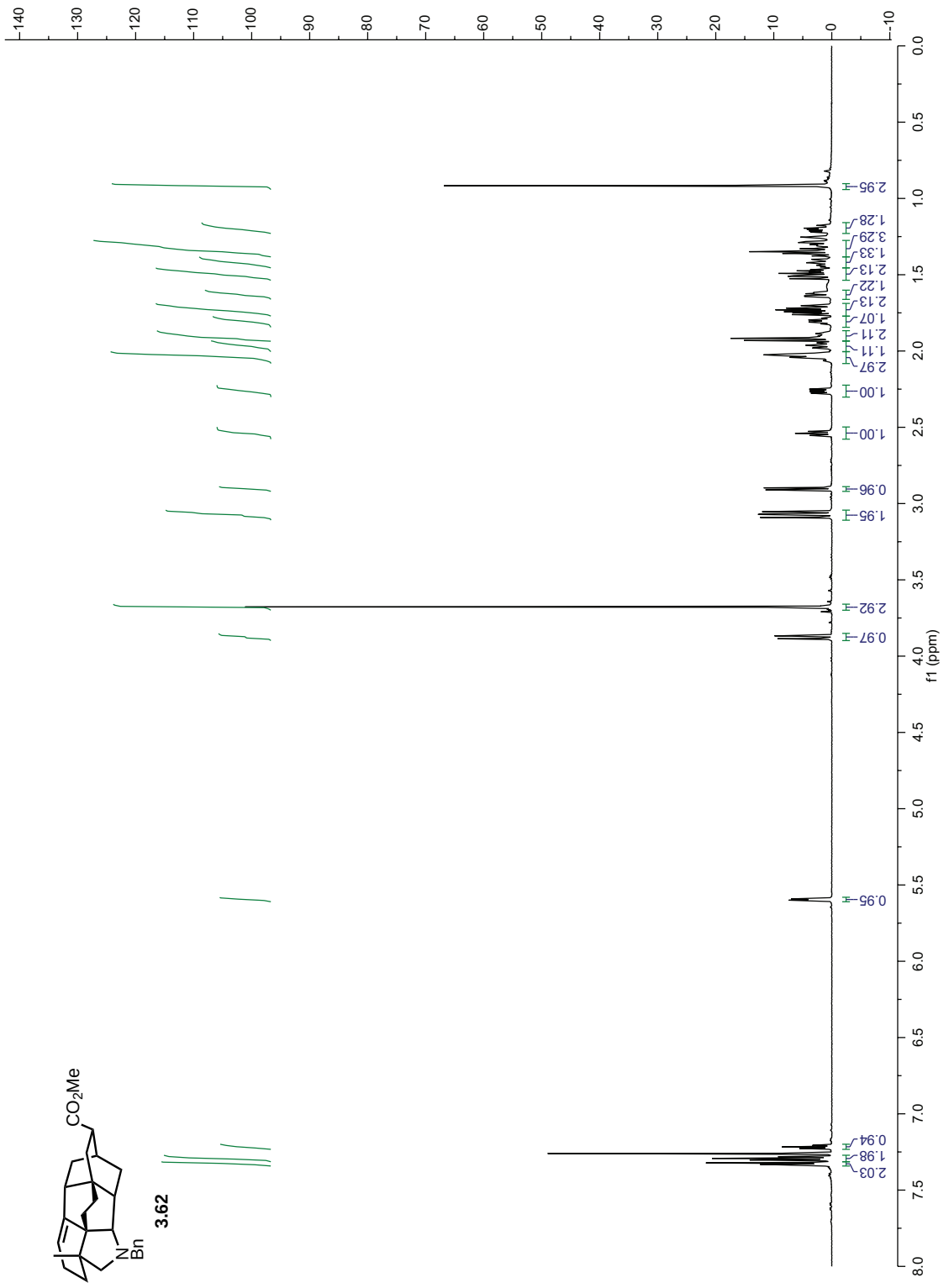

Figure 3.A.38: ^{1}H NMR of **3.62**

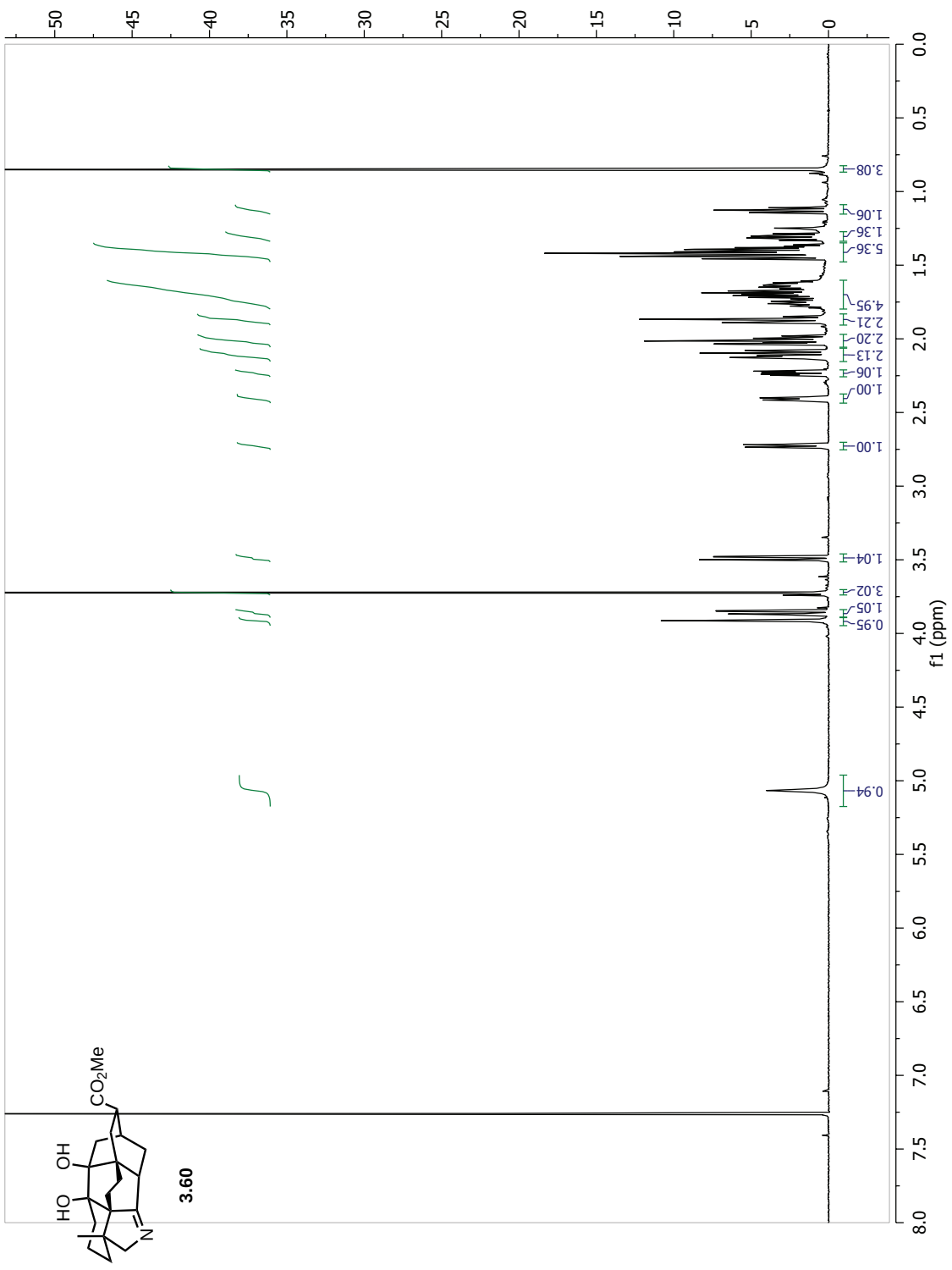

Figure 3.A.39: ^{1}H NMR of **3.60**

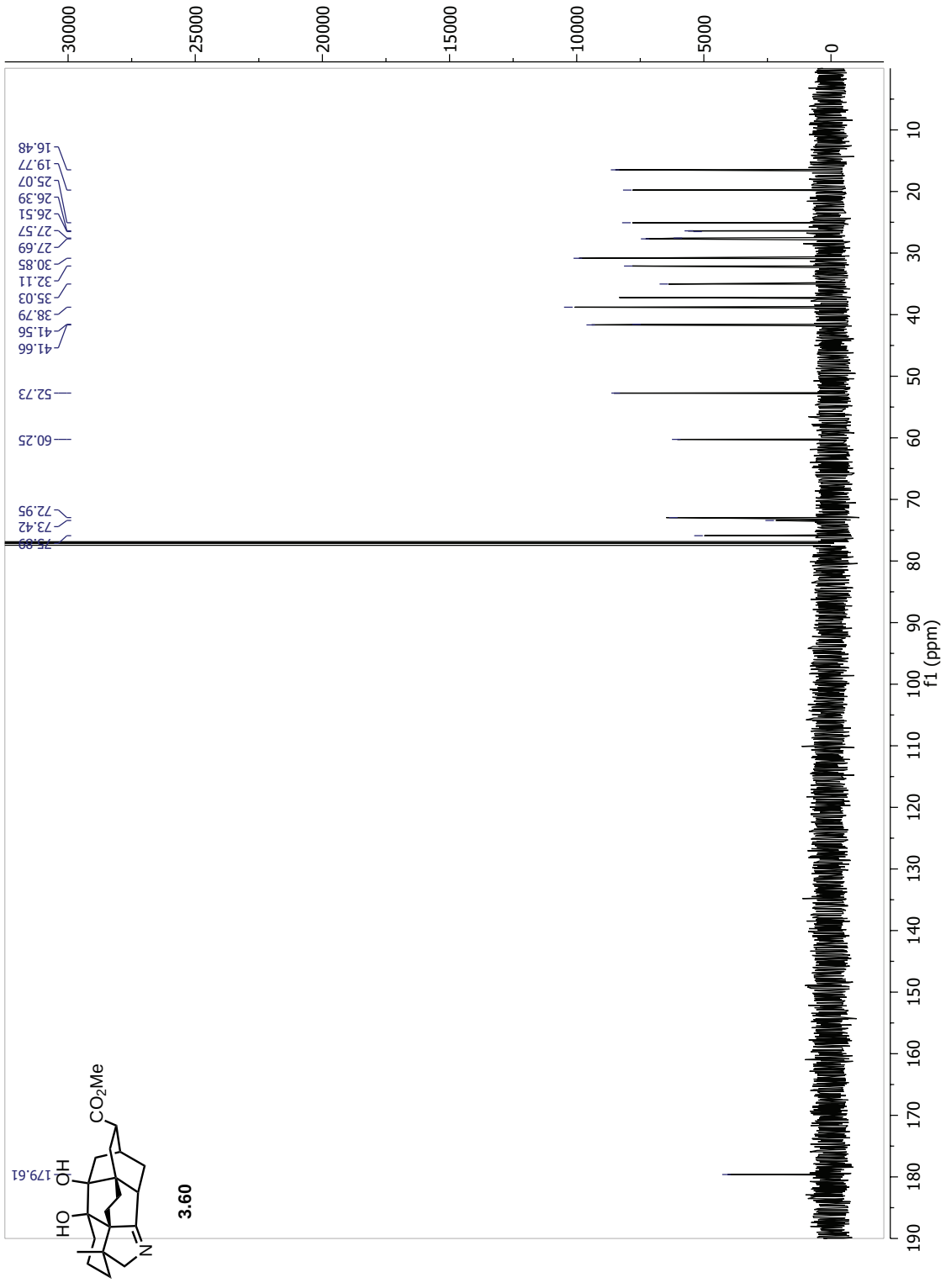

Figure 3.A.40: ^{13}C NMR of **3.60**

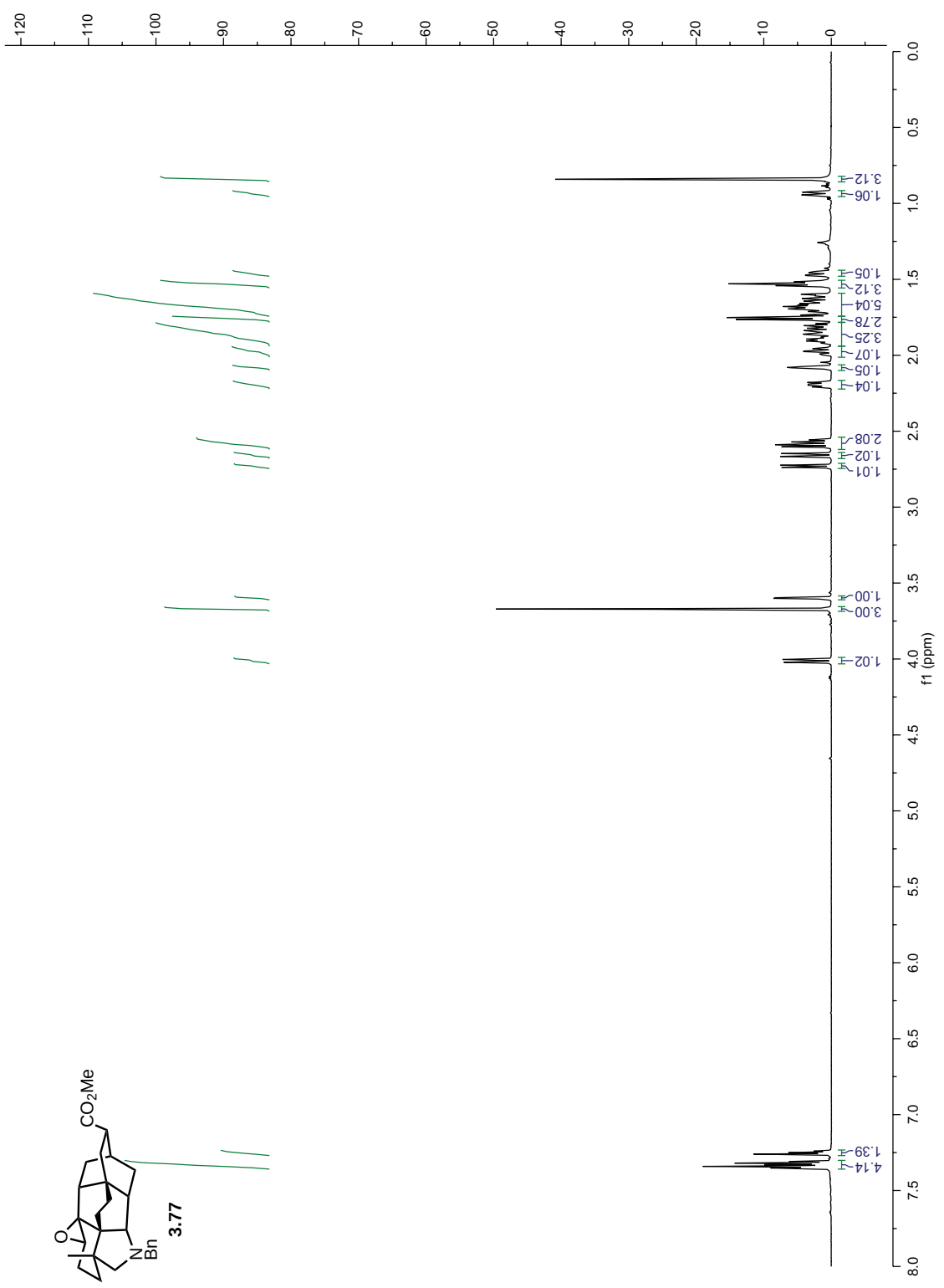

Figure 3.A.41: ^{1}H NMR of **3.77**

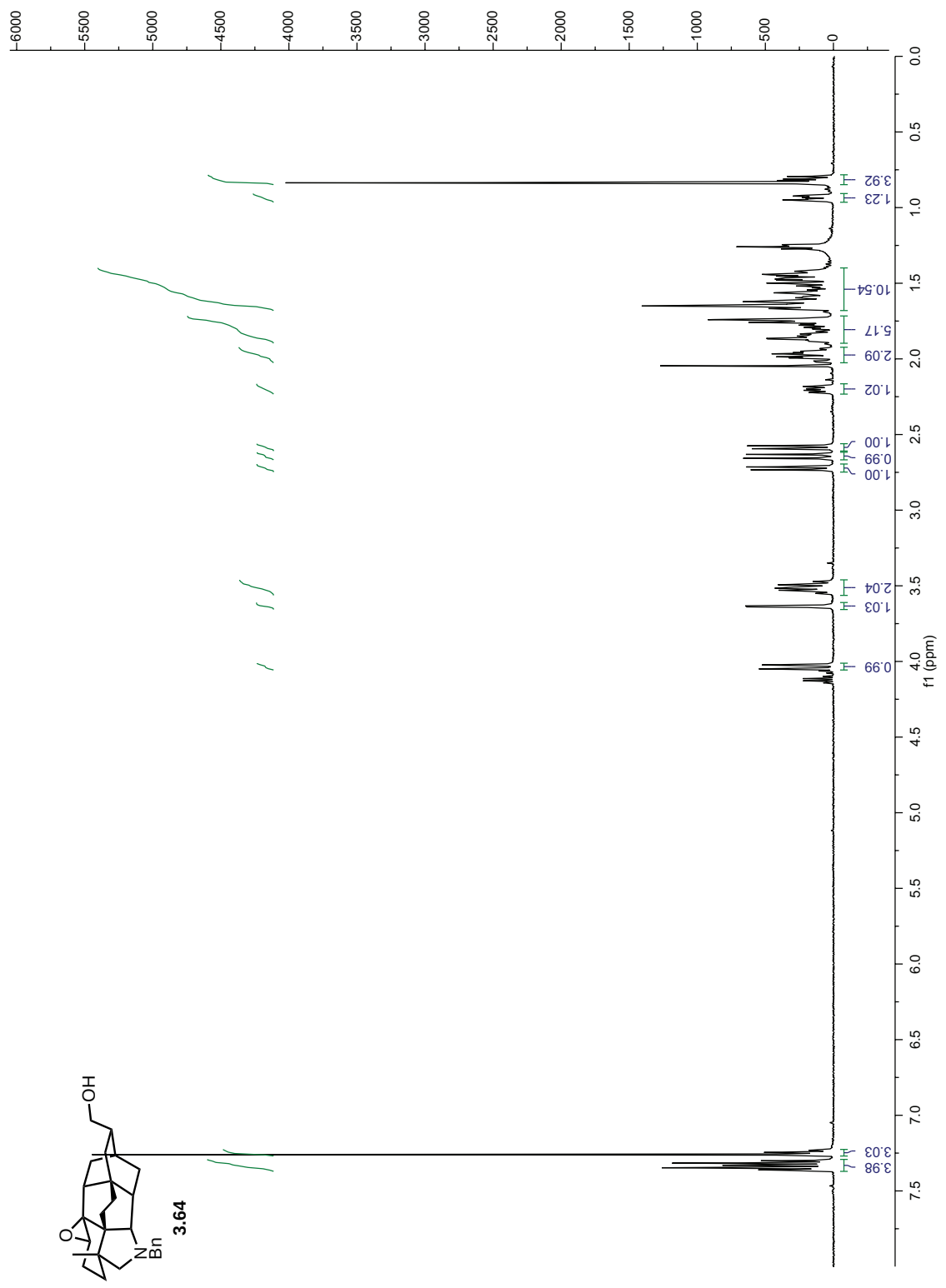

Figure 3.A.42: ^{1}H NMR of **3.64**

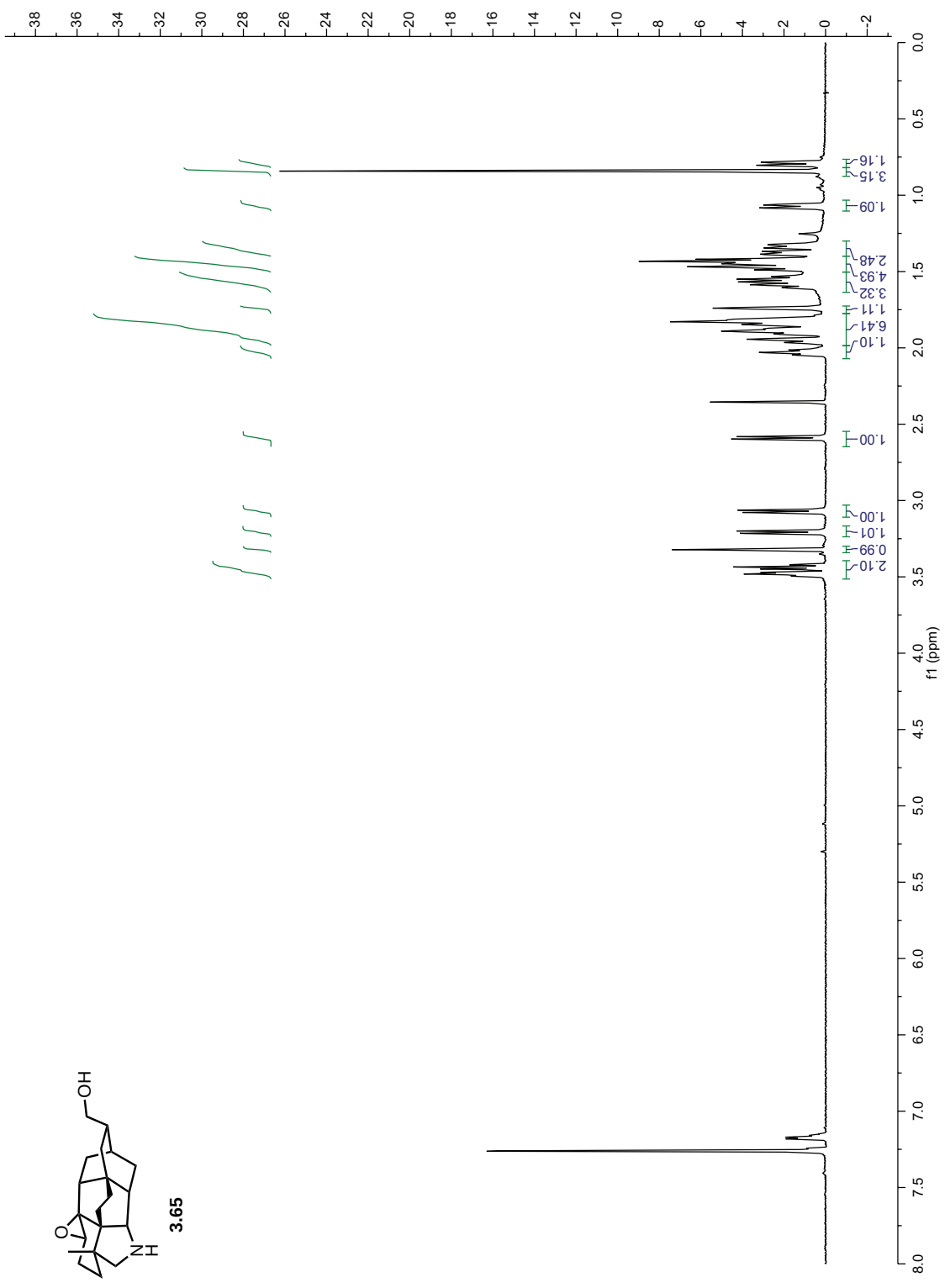

Figure 3.A.43: ^{1}H NMR of **3.65**

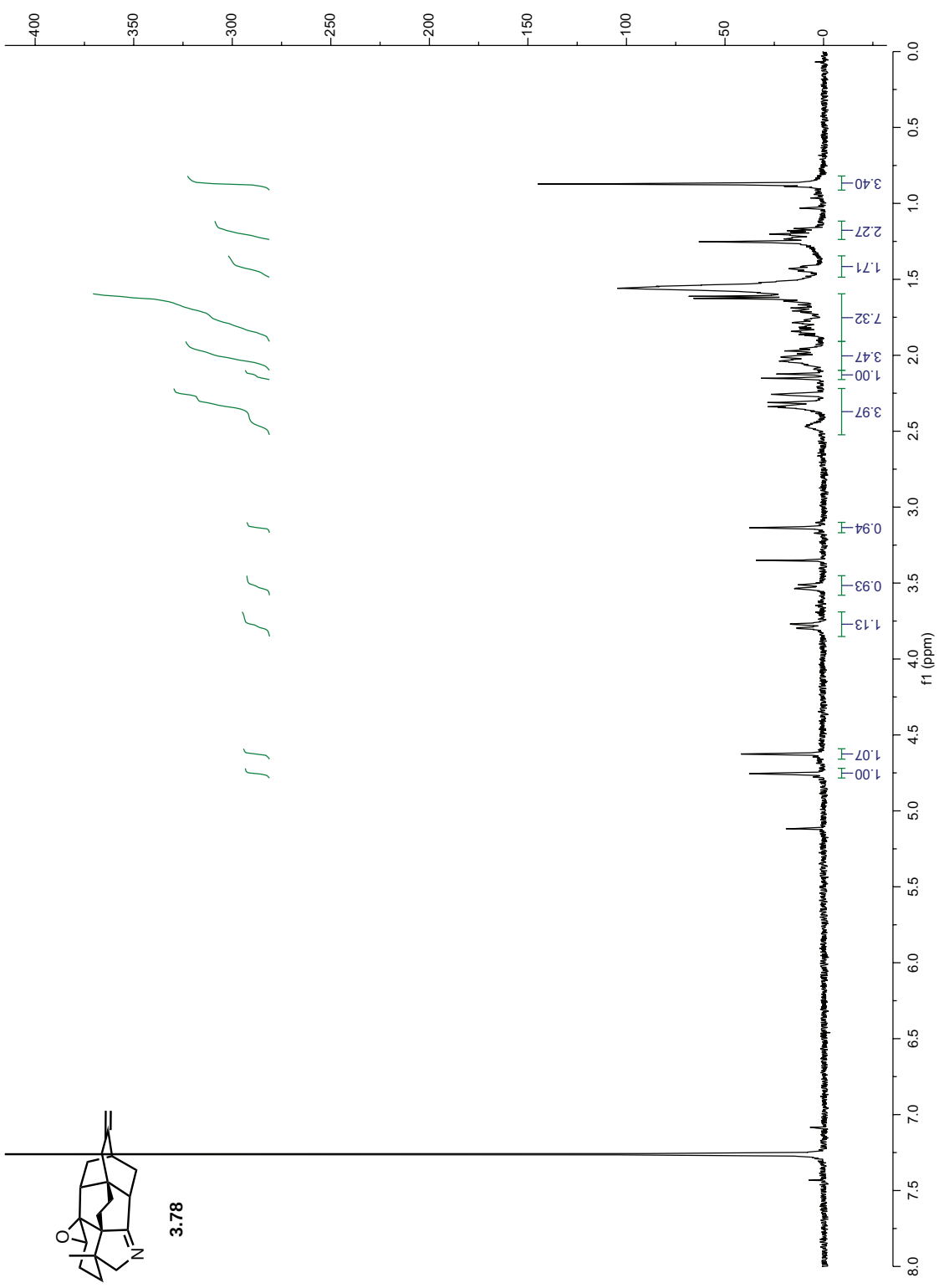

Figure 3.A.44: ^{1}H NMR of **3.78**

3.B X-ray Crystallography Data for Chapter 3

X-ray crystallography data for 3.23

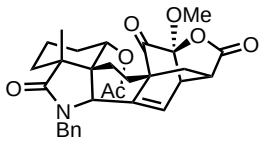

3.23

A colorless rod 0.080 x 0.040 x 0.040 mm in size was mounted on a Cryoloop with Paratone oil. Data were collected in a nitrogen gas stream at 100(2) K using and scans. Crystal-to-detector distance was 60 mm and exposure time was 1 seconds per frame using a scan width of 2.0°. Data collection was 98.4% complete to 67.000°in θ. A total of 40188 reflections were collected covering the indices, $-9 \leq h \leq 12$, $-16 \leq k \leq 18$, $-21 \leq l \leq 22$. 10098 reflections were found to be symmetry independent, with an R^{int} of 0.0336. Indexing and unit cell refinement indicated a primitive, triclinic lattice. The space group was found to be P -1 (No. 2). The data were integrated using the Bruker SAINT software program and scaled using the SADABS software program. Solution by iterative methods (SHELXT-2014) produced a complete heavy-atom phasing model consistent with the proposed structure. All non-hydrogen atoms were refined anisotropically by full-matrix least-squares (SHELXL-2016). All hydrogen atoms were placed using a riding model. Their positions were constrained relative to their parent atom using the appropriate HFIX command in SHELXL-2016.

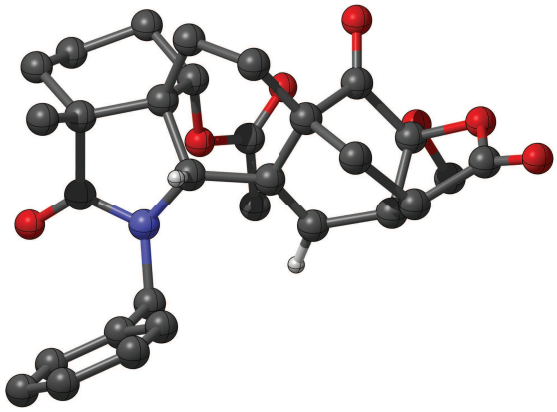

Table 3.1: Crystal data and structure refinement for **3.23**.

X-ray ID	sarpong137	
Sample/notebook ID	kro7-072C	
Empirical formula	C30 H33 N O7	
Formula weight	519.57	
Temperature	100(2) K	
Wavelength	1.54178 Å	
Crystal system	Triclinic	
Space group	P -1	
Unit cell dimensions	a = 10.4084(4) Å	α = 80.465(2)°.
	b = 15.0798(7) Å	β = 85.870(2)°.
	c = 18.4956(9) Å	γ = 78.653(2)°.
Volume	2804.6(2) $Å^3$	
Z	4	
Density (calculated)	1.231 Mg/m^3	
Absorption coefficient	0.716 mm^{-1}	
F(000)	1104	
Crystal size	0.080 x 0.040 x 0.040 mm^3	
Theta range for data collection	2.424 to 68.450°.	
Index ranges	$-9\leq h\leq 12$, $-16\leq k\leq 18$, $-21\leq l\leq 22$	
Reflections collected	40188	
Independent reflections	10098 [R(int) = 0.0336]	
Completeness to theta = 67.000°	98.4 %	
Absorption correction	Semi-empirical from equivalents	
Max. and min. transmission	0.929 and 0.744	
Refinement method	Full-matrix least-squares on F^2	
Data / restraints / parameters	10098 / 0 / 691	
Goodness-of-fit on F2	1.021	
Final R indices [I>2sigma(I)]	R1 = 0.0416, wR2 = 0.1042	
R indices (all data)	R1 = 0.0464, wR2 = 0.1082	
Extinction coefficient	n/a	
Largest diff. peak and hole	0.420 and -0.204 $e.Å^{-3}$	

Table 3.2: Atomic coordinates (x 10^4) and equivalent isotropic displacement parameters (Å^{2}x 10^3) for sarpong137. U(eq) is defined as one third of the trace of the orthogonalized U^{ij} tensor.

	x	y	z	U(eq)
C(1)	5037(2)	7609(1)	4857(1)	26(1)
C(2)	3812(1)	8246(1)	4535(1)	26(1)
C(3)	2565(2)	8152(1)	5004(1)	32(1)
C(4)	2108(2)	7262(1)	4986(1)	31(1)
C(5)	1962(1)	7145(1)	4196(1)	28(1)
C(6)	3262(1)	7116(1)	3753(1)	23(1)
C(7)	3859(1)	7988(1)	3751(1)	23(1)
C(8)	3182(1)	8716(1)	3133(1)	25(1)
C(9)	4043(1)	8827(1)	2416(1)	26(1)
C(10)	5017(1)	7977(1)	2243(1)	25(1)
C(11)	4380(1)	7291(1)	1939(1)	25(1)
C(12)	5408(1)	6467(1)	1729(1)	27(1)
C(13)	6418(2)	7191(1)	730(1)	37(1)
C(14)	6961(2)	7381(1)	1418(1)	32(1)
C(15)	6749(1)	6536(1)	1976(1)	27(1)
C(16)	6625(1)	6685(1)	2762(1)	25(1)
C(17)	5742(1)	7408(1)	2907(1)	22(1)
C(18)	5362(1)	7822(1)	3589(1)	23(1)
C(19)	6100(2)	8246(1)	1665(1)	32(1)
C(20)	4089(2)	9217(1)	4539(1)	31(1)
C(21)	4080(2)	5515(1)	3800(1)	26(1)
C(22)	5221(2)	4765(1)	4015(1)	34(1)
C(23)	5843(2)	4845(1)	1872(1)	39(1)
C(24)	7295(1)	7090(1)	4426(1)	27(1)
C(25)	7965(1)	7904(1)	4363(1)	25(1)

Table 3.3: Bond lengths [Å] for sarpong137.

C(1)-O(2)	1.2211(19)	C(31)-O(9)	1.2251(19)
C(1)-N(1)	1.369(2)	C(31)-N(2)	1.360(2)
C(1)-C(2)	1.530(2)	C(31)-C(32)	1.537(2)
C(2)-C(3)	1.525(2)	C(32)-C(33)	1.521(2)
C(2)-C(20)	1.549(2)	C(32)-C(50)	1.549(2)
C(2)-C(7)	1.556(2)	C(32)-C(37)	1.551(2)
C(3)-C(4)	1.517(2)	C(33)-C(34)	1.511(2)
C(3)-H(3A)	0.99	C(33)-H(33A)	0.99
C(3)-H(3B)	0.99	C(33)-H(33B)	0.99
C(4)-C(5)	1.523(2)	C(34)-C(35)	1.527(2)

C(4)-H(4A)	0.99	C(34)-H(34A)	0.99
C(4)-H(4B)	0.99	C(34)-H(34B)	0.99
C(5)-C(6)	1.527(2)	C(35)-C(36)	1.524(2)
C(5)-H(5A)	0.99	C(35)-H(35A)	0.99
C(5)-H(5B)	0.99	C(35)-H(35B)	0.99
C(6)-O(3)	1.4586(17)	C(36)-O(10)	1.4629(17)
C(6)-C(7)	1.5609(19)	C(36)-C(37)	1.560(2)
C(6)-H(6)	1	C(36)-H(36)	1
C(7)-C(8)	1.551(2)	C(37)-C(48)	1.5456(19)
C(7)-C(18)	1.5510(19)	C(37)-C(38)	1.553(2)
C(8)-C(9)	1.550(2)	C(38)-C(39)	1.544(2)
C(8)-H(8A)	0.99	C(38)-H(38A)	0.99
C(8)-H(8B)	0.99	C(38)-H(38B)	0.99
C(9)-C(10)	1.534(2)	C(39)-C(40)	1.529(2)
C(9)-H(9A)	0.99	C(39)-H(39A)	0.99
C(9)-H(9B)	0.99	C(39)-H(39B)	0.99
C(10)-C(11)	1.531(2)	C(40)-C(41)	1.524(2)
C(10)-C(17)	1.531(2)	C(40)-C(47)	1.5351(19)
C(10)-C(19)	1.563(2)	C(40)-C(49)	1.567(2)
C(11)-O(5)	1.2044(18)	C(41)-O(12)	1.2056(17)
C(11)-C(12)	1.554(2)	C(41)-C(42)	1.547(2)
C(12)-O(6)	1.3661(19)	C(42)-O(13)	1.3644(18)
C(12)-O(1)	1.4702(19)	C(42)-O(8)	1.4730(18)
C(12)-C(15)	1.527(2)	C(42)-C(45)	1.5296(19)
C(13)-O(7)	1.200(2)	C(43)-O(14)	1.195(2)
C(13)-O(1)	1.359(2)	C(43)-O(8)	1.367(2)
C(13)-C(14)	1.519(2)	C(43)-C(44)	1.516(2)
C(14)-C(15)	1.543(2)	C(44)-C(45)	1.550(2)
C(14)-C(19)	1.547(2)	C(44)-C(49)	1.550(2)
C(14)-H(14)	1	C(44)-H(44)	1
C(15)-C(16)	1.501(2)	C(45)-C(46)	1.495(2)
C(15)-H(15)	1	C(45)-H(45)	1
C(16)-C(17)	1.331(2)	C(46)-C(47)	1.329(2)
C(16)-H(16)	0.95	C(46)-H(46)	0.95
C(17)-C(18)	1.492(2)	C(47)-C(48)	1.488(2)
C(18)-N(1)	1.4554(19)	C(48)-N(2)	1.4594(18)
C(18)-H(18)	1	C(48)-H(48)	1
C(19)-H(19A)	0.99	C(49)-H(49A)	0.99
C(19)-H(19B)	0.99	C(49)-H(49B)	0.99
C(20)-H(20A)	0.98	C(50)-H(50A)	0.98
C(20)-H(20B)	0.98	C(50)-H(50B)	0.98
C(20)-H(20C)	0.98	C(50)-H(50C)	0.98
C(21)-O(4)	1.2063(19)	C(51)-O(11)	1.2061(19)
C(21)-O(3)	1.3495(18)	C(51)-O(10)	1.3450(18)
C(21)-C(22)	1.496(2)	C(51)-C(52)	1.502(2)

C(22)-H(22A)	0.98	C(52)-H(52A)	0.98
C(22)-H(22B)	0.98	C(52)-H(52B)	0.98
C(22)-H(22C)	0.98	C(52)-H(52C)	0.98
C(23)-O(6)	1.4401(19)	C(53)-O(13)	1.4330(19)
C(23)-H(23A)	0.98	C(53)-H(53A)	0.98
C(23)-H(23B)	0.98	C(53)-H(53B)	0.98
C(23)-H(23C)	0.98	C(53)-H(53C)	0.98
C(24)-N(1)	1.4644(18)	C(54)-N(2)	1.4671(19)
C(24)-C(25)	1.511(2)	C(54)-C(55)	1.511(2)
C(24)-H(24A)	0.99	C(54)-H(54A)	0.99
C(24)-H(24B)	0.99	C(54)-H(54B)	0.99
C(25)-C(26)	1.389(2)	C(55)-C(56)	1.386(2)
C(25)-C(30)	1.392(2)	C(55)-C(60)	1.396(3)
C(26)-C(27)	1.385(2)	C(56)-C(57)	1.395(3)
C(26)-H(26)	0.95	C(56)-H(56)	0.95
C(27)-C(28)	1.388(2)	C(57)-C(58)	1.369(4)
C(27)-H(27)	0.95	C(57)-H(57)	0.95
C(28)-C(29)	1.377(2)	C(58)-C(59)	1.374(4)
C(28)-H(28)	0.95	C(58)-H(58)	0.95
C(29)-C(30)	1.390(2)	C(59)-C(60)	1.388(3)
C(29)-H(29)	0.95	C(59)-H(59)	0.95
C(30)-H(30)	0.95	C(60)-H(60)	0.95

Table 3.4: Bond angles [°] for sarpong137.

O(2)-C(1)-N(1)	124.90(14)	C(33)-C(32)-C(37)	116.22(13)
O(2)-C(1)-C(2)	126.26(14)	C(31)-C(32)-C(37)	101.56(12)
N(1)-C(1)-C(2)	108.66(13)	C(50)-C(32)-C(37)	113.21(13)
C(3)-C(2)-C(1)	113.26(13)	C(34)-C(33)-C(32)	113.87(13)
C(3)-C(2)-C(20)	107.95(13)	C(34)-C(33)-H(33A)	108.8
C(1)-C(2)-C(20)	103.74(12)	C(32)-C(33)-H(33A)	108.8
C(3)-C(2)-C(7)	116.30(12)	C(34)-C(33)-H(33B)	108.8
C(1)-C(2)-C(7)	101.50(12)	C(32)-C(33)-H(33B)	108.8
C(20)-C(2)-C(7)	113.36(13)	H(33A)-C(33)-H(33B)	107.7
C(4)-C(3)-C(2)	113.32(13)	C(33)-C(34)-C(35)	110.42(13)
C(4)-C(3)-H(3A)	108.9	C(33)-C(34)-H(34A)	109.6
C(2)-C(3)-H(3A)	108.9	C(35)-C(34)-H(34A)	109.6
C(4)-C(3)-H(3B)	108.9	C(33)-C(34)-H(34B)	109.6
C(2)-C(3)-H(3B)	108.9	C(35)-C(34)-H(34B)	109.6
H(3A)-C(3)-H(3B)	107.7	H(34A)-C(34)-H(34B)	108.1
C(3)-C(4)-C(5)	110.01(13)	C(36)-C(35)-C(34)	110.93(12)
C(3)-C(4)-H(4A)	109.7	C(36)-C(35)-H(35A)	109.5
C(5)-C(4)-H(4A)	109.7	C(34)-C(35)-H(35A)	109.5

C(3)-C(4)-H(4B)	109.7	C(36)-C(35)-H(35B)	109.5
C(5)-C(4)-H(4B)	109.7	C(34)-C(35)-H(35B)	109.5
H(4A)-C(4)-H(4B)	108.2	H(35A)-C(35)-H(35B)	108
C(4)-C(5)-C(6)	111.57(12)	O(10)-C(36)-C(35)	108.45(11)
C(4)-C(5)-H(5A)	109.3	O(10)-C(36)-C(37)	110.77(11)
C(6)-C(5)-H(5A)	109.3	C(35)-C(36)-C(37)	112.48(12)
C(4)-C(5)-H(5B)	109.3	O(10)-C(36)-H(36)	108.3
C(6)-C(5)-H(5B)	109.3	C(35)-C(36)-H(36)	108.3
H(5A)-C(5)-H(5B)	108	C(37)-C(36)-H(36)	108.3
O(3)-C(6)-C(5)	109.52(12)	C(48)-C(37)-C(32)	99.31(11)
O(3)-C(6)-C(7)	110.40(11)	C(48)-C(37)-C(38)	108.97(12)
C(5)-C(6)-C(7)	112.57(12)	C(32)-C(37)-C(38)	118.00(12)
O(3)-C(6)-H(6)	108.1	C(48)-C(37)-C(36)	113.31(11)
C(5)-C(6)-H(6)	108.1	C(32)-C(37)-C(36)	111.94(12)
C(7)-C(6)-H(6)	108.1	C(38)-C(37)-C(36)	105.50(11)
C(8)-C(7)-C(18)	109.00(12)	C(39)-C(38)-C(37)	113.20(12)
C(8)-C(7)-C(2)	118.24(12)	C(39)-C(38)-H(38A)	108.9
C(18)-C(7)-C(2)	99.61(11)	C(37)-C(38)-H(38A)	108.9
C(8)-C(7)-C(6)	105.79(11)	C(39)-C(38)-H(38B)	108.9
C(18)-C(7)-C(6)	112.78(11)	C(37)-C(38)-H(38B)	108.9
C(2)-C(7)-C(6)	111.54(12)	H(38A)-C(38)-H(38B)	107.8
C(9)-C(8)-C(7)	113.54(12)	C(40)-C(39)-C(38)	116.50(12)
C(9)-C(8)-H(8A)	108.9	C(40)-C(39)-H(39A)	108.2
C(7)-C(8)-H(8A)	108.9	C(38)-C(39)-H(39A)	108.2
C(9)-C(8)-H(8B)	108.9	C(40)-C(39)-H(39B)	108.2
C(7)-C(8)-H(8B)	108.9	C(38)-C(39)-H(39B)	108.2
H(8A)-C(8)-H(8B)	107.7	H(39A)-C(39)-H(39B)	107.3
C(10)-C(9)-C(8)	117.01(12)	C(41)-C(40)-C(39)	113.51(12)
C(10)-C(9)-H(9A)	108	C(41)-C(40)-C(47)	104.41(11)
C(8)-C(9)-H(9A)	108	C(39)-C(40)-C(47)	113.82(12)
C(10)-C(9)-H(9B)	108	C(41)-C(40)-C(49)	106.91(12)
C(8)-C(9)-H(9B)	108	C(39)-C(40)-C(49)	111.71(12)
H(9A)-C(9)-H(9B)	107.3	C(47)-C(40)-C(49)	105.83(11)
C(11)-C(10)-C(17)	103.98(12)	O(12)-C(41)-C(40)	125.23(13)
C(11)-C(10)-C(9)	113.74(12)	O(12)-C(41)-C(42)	122.35(13)
C(17)-C(10)-C(9)	114.32(12)	C(40)-C(41)-C(42)	112.40(11)
C(11)-C(10)-C(19)	106.93(12)	O(13)-C(42)-O(8)	109.66(12)
C(17)-C(10)-C(19)	106.14(12)	O(13)-C(42)-C(45)	119.33(12)
C(9)-C(10)-C(19)	111.07(12)	O(8)-C(42)-C(45)	104.23(11)
O(5)-C(11)-C(10)	125.11(13)	O(13)-C(42)-C(41)	108.81(12)
O(5)-C(11)-C(12)	122.75(14)	O(8)-C(42)-C(41)	105.15(11)
C(10)-C(11)-C(12)	112.12(12)	C(45)-C(42)-C(41)	108.72(12)
O(6)-C(12)-O(1)	109.90(12)	O(14)-C(43)-O(8)	121.44(16)
O(6)-C(12)-C(15)	118.82(13)	O(14)-C(43)-C(44)	129.59(17)
O(1)-C(12)-C(15)	104.60(12)	O(8)-C(43)-C(44)	108.93(13)

O(6)-C(12)-C(11)	109.05(12)	C(43)-C(44)-C(45)	101.08(12)
O(1)-C(12)-C(11)	104.74(12)	C(43)-C(44)-C(49)	110.34(12)
C(15)-C(12)-C(11)	108.79(12)	C(45)-C(44)-C(49)	109.00(12)
O(7)-C(13)-O(1)	121.50(17)	C(43)-C(44)-H(44)	112
O(7)-C(13)-C(14)	129.08(18)	C(45)-C(44)-H(44)	112
O(1)-C(13)-C(14)	109.40(14)	C(49)-C(44)-H(44)	112
C(13)-C(14)-C(15)	101.59(13)	C(46)-C(45)-C(42)	109.80(12)
C(13)-C(14)-C(19)	109.28(14)	C(46)-C(45)-C(44)	114.18(12)
C(15)-C(14)-C(19)	108.90(13)	C(42)-C(45)-C(44)	97.42(11)
C(13)-C(14)-H(14)	112.2	C(46)-C(45)-H(45)	111.6
C(15)-C(14)-H(14)	112.2	C(42)-C(45)-H(45)	111.6
C(19)-C(14)-H(14)	112.2	C(44)-C(45)-H(45)	111.6
C(16)-C(15)-C(12)	109.12(12)	C(47)-C(46)-C(45)	115.22(13)
C(16)-C(15)-C(14)	114.59(13)	C(47)-C(46)-H(46)	122.4
C(12)-C(15)-C(14)	97.43(13)	C(45)-C(46)-H(46)	122.4
C(16)-C(15)-H(15)	111.6	C(46)-C(47)-C(48)	132.84(13)
C(12)-C(15)-H(15)	111.6	C(46)-C(47)-C(40)	115.39(13)
C(14)-C(15)-H(15)	111.6	C(48)-C(47)-C(40)	111.63(12)
C(17)-C(16)-C(15)	115.50(14)	N(2)-C(48)-C(47)	121.34(12)
C(17)-C(16)-H(16)	122.3	N(2)-C(48)-C(37)	103.67(11)
C(15)-C(16)-H(16)	122.3	C(47)-C(48)-C(37)	111.38(11)
C(16)-C(17)-C(18)	132.73(14)	N(2)-C(48)-H(48)	106.5
C(16)-C(17)-C(10)	115.12(13)	C(47)-C(48)-H(48)	106.5
C(18)-C(17)-C(10)	112.03(12)	C(37)-C(48)-H(48)	106.5
N(1)-C(18)-C(17)	121.36(12)	C(44)-C(49)-C(40)	110.17(12)
N(1)-C(18)-C(7)	103.39(11)	C(44)-C(49)-H(49A)	109.6
C(17)-C(18)-C(7)	112.21(12)	C(40)-C(49)-H(49A)	109.6
N(1)-C(18)-H(18)	106.3	C(44)-C(49)-H(49B)	109.6
C(17)-C(18)-H(18)	106.3	C(40)-C(49)-H(49B)	109.6
C(7)-C(18)-H(18)	106.3	H(49A)-C(49)-H(49B)	108.1
C(14)-C(19)-C(10)	110.46(13)	C(32)-C(50)-H(50A)	109.5
C(14)-C(19)-H(19A)	109.6	C(32)-C(50)-H(50B)	109.5
C(10)-C(19)-H(19A)	109.6	H(50A)-C(50)-H(50B)	109.5
C(14)-C(19)-H(19B)	109.6	C(32)-C(50)-H(50C)	109.5
C(10)-C(19)-H(19B)	109.6	H(50A)-C(50)-H(50C)	109.5
H(19A)-C(19)-H(19B)	108.1	H(50B)-C(50)-H(50C)	109.5
C(2)-C(20)-H(20A)	109.5	O(11)-C(51)-O(10)	124.34(14)
C(2)-C(20)-H(20B)	109.5	O(11)-C(51)-C(52)	125.00(14)
H(20A)-C(20)-H(20B)	109.5	O(10)-C(51)-C(52)	110.66(13)
C(2)-C(20)-H(20C)	109.5	C(51)-C(52)-H(52A)	109.5
H(20A)-C(20)-H(20C)	109.5	C(51)-C(52)-H(52B)	109.5
H(20B)-C(20)-H(20C)	109.5	H(52A)-C(52)-H(52B)	109.5
O(4)-C(21)-O(3)	123.48(14)	C(51)-C(52)-H(52C)	109.5
O(4)-C(21)-C(22)	125.05(14)	H(52A)-C(52)-H(52C)	109.5
O(3)-C(21)-C(22)	111.47(13)	H(52B)-C(52)-H(52C)	109.5

C(21)-C(22)-H(22A)	109.5	O(13)-C(53)-H(53A)	109.5
C(21)-C(22)-H(22B)	109.5	O(13)-C(53)-H(53B)	109.5
H(22A)-C(22)-H(22B)	109.5	H(53A)-C(53)-H(53B)	109.5
C(21)-C(22)-H(22C)	109.5	O(13)-C(53)-H(53C)	109.5
H(22A)-C(22)-H(22C)	109.5	H(53A)-C(53)-H(53C)	109.5
H(22B)-C(22)-H(22C)	109.5	H(53B)-C(53)-H(53C)	109.5
O(6)-C(23)-H(23A)	109.5	N(2)-C(54)-C(55)	111.85(12)
O(6)-C(23)-H(23B)	109.5	N(2)-C(54)-H(54A)	109.2
H(23A)-C(23)-H(23B)	109.5	C(55)-C(54)-H(54A)	109.2
O(6)-C(23)-H(23C)	109.5	N(2)-C(54)-H(54B)	109.2
H(23A)-C(23)-H(23C)	109.5	C(55)-C(54)-H(54B)	109.2
H(23B)-C(23)-H(23C)	109.5	H(54A)-C(54)-H(54B)	107.9
N(1)-C(24)-C(25)	111.53(12)	C(56)-C(55)-C(60)	118.71(17)
N(1)-C(24)-H(24A)	109.3	C(56)-C(55)-C(54)	120.75(17)
C(25)-C(24)-H(24A)	109.3	C(60)-C(55)-C(54)	120.51(15)
N(1)-C(24)-H(24B)	109.3	C(55)-C(56)-C(57)	120.3(2)
C(25)-C(24)-H(24B)	109.3	C(55)-C(56)-H(56)	119.8
H(24A)-C(24)-H(24B)	108	C(57)-C(56)-H(56)	119.8
C(26)-C(25)-C(30)	118.92(14)	C(58)-C(57)-C(56)	119.8(2)
C(26)-C(25)-C(24)	120.67(14)	C(58)-C(57)-H(57)	120.1
C(30)-C(25)-C(24)	120.34(14)	C(56)-C(57)-H(57)	120.1
C(27)-C(26)-C(25)	120.75(15)	C(57)-C(58)-C(59)	120.9(2)
C(27)-C(26)-H(26)	119.6	C(57)-C(58)-H(58)	119.5
C(25)-C(26)-H(26)	119.6	C(59)-C(58)-H(58)	119.5
C(26)-C(27)-C(28)	119.81(16)	C(58)-C(59)-C(60)	119.5(2)
C(26)-C(27)-H(27)	120.1	C(58)-C(59)-H(59)	120.3
C(28)-C(27)-H(27)	120.1	C(60)-C(59)-H(59)	120.3
C(29)-C(28)-C(27)	120.02(15)	C(59)-C(60)-C(55)	120.7(2)
C(29)-C(28)-H(28)	120	C(59)-C(60)-H(60)	119.7
C(27)-C(28)-H(28)	120	C(55)-C(60)-H(60)	119.7
C(28)-C(29)-C(30)	120.17(15)	C(1)-N(1)-C(18)	110.65(12)
C(28)-C(29)-H(29)	119.9	C(1)-N(1)-C(24)	119.40(13)
C(30)-C(29)-H(29)	119.9	C(18)-N(1)-C(24)	124.38(12)
C(29)-C(30)-C(25)	120.32(15)	C(31)-N(2)-C(48)	110.39(12)
C(29)-C(30)-H(30)	119.8	C(31)-N(2)-C(54)	120.04(12)
C(25)-C(30)-H(30)	119.8	C(48)-N(2)-C(54)	124.60(12)
O(9)-C(31)-N(2)	125.38(14)	C(13)-O(1)-C(12)	107.53(12)
O(9)-C(31)-C(32)	125.82(14)	C(21)-O(3)-C(6)	116.30(11)
N(2)-C(31)-C(32)	108.57(12)	C(12)-O(6)-C(23)	115.42(12)
C(33)-C(32)-C(31)	112.87(13)	C(43)-O(8)-C(42)	107.99(11)
C(33)-C(32)-C(50)	108.12(13)	C(51)-O(10)-C(36)	116.10(11)
C(31)-C(32)-C(50)	104.16(12)	C(42)-O(13)-C(53)	116.07(12)

Table 3.5: Anisotropic displacement parameters ($Å^2$x 10^3)for sarpong137. The anisotropic displacement factor exponent takes the form: -2$\sqrt{}$2[$h^2a^{*2}U^{11}$ + ... + 2 h k a* b* U^{12}]

	U^{11}	U^{22}	U^{33}	U^{23}	U^{13}	U^{12}
C(1)	27(1)	22(1)	34(1)	-9(1)	-2(1)	-12(1)
C(2)	25(1)	25(1)	29(1)	-9(1)	1(1)	-7(1)
C(3)	27(1)	38(1)	32(1)	-11(1)	4(1)	-8(1)
C(4)	24(1)	36(1)	36(1)	-8(1)	4(1)	-9(1)
C(5)	20(1)	28(1)	37(1)	-6(1)	-2(1)	-7(1)
C(6)	19(1)	21(1)	30(1)	-5(1)	-5(1)	-3(1)
C(7)	18(1)	21(1)	29(1)	-7(1)	1(1)	-4(1)
C(8)	22(1)	21(1)	32(1)	-6(1)	0(1)	-1(1)
C(9)	24(1)	21(1)	32(1)	-5(1)	1(1)	-2(1)
C(10)	21(1)	22(1)	30(1)	-6(1)	1(1)	-3(1)
C(11)	22(1)	26(1)	26(1)	-5(1)	0(1)	-2(1)
C(12)	23(1)	30(1)	31(1)	-12(1)	-2(1)	-3(1)
C(13)	30(1)	39(1)	37(1)	-11(1)	8(1)	6(1)
C(14)	23(1)	34(1)	40(1)	-11(1)	7(1)	-4(1)
C(15)	19(1)	26(1)	38(1)	-13(1)	1(1)	-2(1)
C(16)	16(1)	24(1)	36(1)	-9(1)	-2(1)	-5(1)
C(17)	16(1)	21(1)	32(1)	-6(1)	-1(1)	-7(1)
C(18)	19(1)	20(1)	32(1)	-7(1)	-2(1)	-5(1)
C(19)	29(1)	28(1)	37(1)	-6(1)	7(1)	-6(1)
C(20)	32(1)	25(1)	38(1)	-12(1)	1(1)	-5(1)
C(21)	31(1)	24(1)	26(1)	-5(1)	0(1)	-9(1)
C(22)	41(1)	24(1)	36(1)	-7(1)	-4(1)	-4(1)
C(23)	28(1)	26(1)	64(1)	-20(1)	-3(1)	1(1)
C(24)	22(1)	22(1)	37(1)	-7(1)	-8(1)	-3(1)
C(25)	16(1)	22(1)	36(1)	-8(1)	-4(1)	-1(1)
C(26)	26(1)	34(1)	35(1)	-11(1)	-2(1)	-8(1)
C(27)	35(1)	40(1)	38(1)	-3(1)	-1(1)	-17(1)
C(28)	32(1)	29(1)	49(1)	-6(1)	-8(1)	-14(1)
C(29)	26(1)	29(1)	42(1)	-13(1)	-6(1)	-6(1)
C(30)	22(1)	28(1)	36(1)	-8(1)	-4(1)	-5(1)
C(31)	25(1)	23(1)	28(1)	-7(1)	1(1)	0(1)
C(32)	27(1)	22(1)	30(1)	-6(1)	-2(1)	-3(1)
C(33)	35(1)	26(1)	38(1)	-4(1)	-3(1)	-11(1)
C(34)	31(1)	32(1)	36(1)	-5(1)	3(1)	-14(1)
C(35)	22(1)	33(1)	32(1)	-8(1)	1(1)	-8(1)
C(36)	20(1)	25(1)	24(1)	-6(1)	-2(1)	-3(1)
C(37)	21(1)	23(1)	25(1)	-7(1)	-1(1)	-4(1)
C(38)	24(1)	26(1)	26(1)	-7(1)	-4(1)	-5(1)
C(39)	23(1)	28(1)	22(1)	-8(1)	-1(1)	-4(1)

Table 3.5: Anisotropic displacement parameters ($Å^2 x\ 10^3$)for sarpong137. The anisotropic displacement factor exponent takes the form: $-2\sqrt{2}[\ h^2 a^{*2} U^{11} + ... + 2\ h\ k\ a^*\ b^*\ U^{12}]$

	U^{11}	U^{22}	U^{33}	U^{23}	U^{13}	U^{12}
C(40)	19(1)	25(1)	21(1)	-5(1)	-1(1)	-4(1)
C(41)	22(1)	24(1)	18(1)	-1(1)	-1(1)	-5(1)
C(42)	23(1)	21(1)	27(1)	-3(1)	-5(1)	-4(1)
C(43)	37(1)	35(1)	31(1)	-1(1)	-9(1)	-18(1)
C(44)	22(1)	33(1)	27(1)	-2(1)	-1(1)	-11(1)
C(45)	20(1)	25(1)	26(1)	-5(1)	-2(1)	-6(1)
C(46)	16(1)	26(1)	23(1)	-5(1)	-2(1)	-3(1)
C(47)	15(1)	26(1)	21(1)	-5(1)	1(1)	-2(1)
C(48)	19(1)	24(1)	22(1)	-7(1)	-1(1)	-1(1)
C(49)	22(1)	34(1)	22(1)	-5(1)	0(1)	-6(1)
C(50)	40(1)	26(1)	37(1)	-11(1)	-2(1)	-2(1)
C(51)	26(1)	22(1)	27(1)	-6(1)	5(1)	-4(1)
C(52)	37(1)	32(1)	34(1)	-14(1)	0(1)	-7(1)
C(53)	32(1)	50(1)	51(1)	-32(1)	0(1)	-8(1)
C(54)	25(1)	27(1)	32(1)	-6(1)	-9(1)	-1(1)
C(55)	21(1)	29(1)	51(1)	-13(1)	-9(1)	-5(1)
C(56)	28(1)	33(1)	74(1)	-10(1)	-14(1)	-2(1)
C(57)	29(1)	50(1)	118(2)	-43(1)	-10(1)	4(1)
C(58)	31(1)	94(2)	107(2)	-59(2)	11(1)	-5(1)
C(59)	43(1)	96(2)	67(2)	-31(1)	16(1)	-29(1)
C(60)	34(1)	51(1)	47(1)	-11(1)	3(1)	-17(1)
N(1)	21(1)	23(1)	31(1)	-5(1)	-5(1)	-6(1)
N(2)	21(1)	24(1)	24(1)	-4(1)	-3(1)	0(1)
O(1)	28(1)	43(1)	35(1)	-16(1)	0(1)	0(1)
O(2)	36(1)	33(1)	31(1)	-5(1)	-5(1)	-13(1)
O(3)	22(1)	20(1)	30(1)	-6(1)	-4(1)	-5(1)
O(4)	39(1)	30(1)	38(1)	-8(1)	-10(1)	-12(1)
O(5)	21(1)	30(1)	36(1)	-9(1)	-3(1)	-1(1)
O(6)	21(1)	25(1)	48(1)	-16(1)	-3(1)	-2(1)
O(7)	45(1)	55(1)	38(1)	-9(1)	11(1)	6(1)
O(8)	30(1)	27(1)	38(1)	1(1)	-9(1)	-7(1)
O(9)	38(1)	27(1)	32(1)	0(1)	-5(1)	-2(1)
O(10)	21(1)	22(1)	24(1)	-7(1)	-1(1)	-2(1)
O(11)	29(1)	30(1)	35(1)	-8(1)	2(1)	4(1)
O(12)	19(1)	29(1)	27(1)	-6(1)	-3(1)	-5(1)
O(13)	22(1)	30(1)	35(1)	-15(1)	-2(1)	-4(1)
O(14)	49(1)	45(1)	38(1)	9(1)	-10(1)	-24(1)

Table 3.6: Hydrogen coordinates (x 10^4) and isotropic displacement parameters ($Å^2$x 10^3) for sarpong137.

	x	y	z	U(eq)
H(3A)	2724	8193	5517	38
H(3B)	1859	8670	4829	38
H(4A)	1255	7265	5261	38
H(4B)	2752	6742	5225	38
H(5A)	1303	7660	3963	34
H(5B)	1640	6570	4191	34
H(6)	3097	7078	3234	28
H(8A)	2357	8542	3022	30
H(8B)	2950	9313	3311	30
H(9A)	3452	9043	2001	31
H(9B)	4544	9315	2439	31
H(14)	7907	7432	1348	39
H(15)	7424	5983	1903	33
H(16)	7141	6290	3131	30
H(18)	5612	8439	3493	27
H(19A)	5682	8650	1234	38
H(19B)	6656	8588	1881	38
H(20A)	3386	9675	4296	47
H(20B)	4929	9275	4277	47
H(20C)	4129	9316	5047	47
H(22A)	4951	4171	4055	51
H(22B)	5525	4832	4489	51
H(22C)	5934	4800	3641	51
H(23A)	6210	4887	1367	58
H(23B)	5382	4327	1978	58
H(23C)	6554	4752	2212	58
H(24A)	7713	6692	4066	32
H(24B)	7410	6729	4923	32
H(26)	8204	8106	3251	36
H(27)	9165	9395	3151	44
H(28)	9507	9968	4208	42
H(29)	8872	9260	5355	37
H(30)	7899	7971	5457	33
H(33A)	-703	1114	2252	39
H(33B)	165	640	2940	39
H(34A)	-667	1848	3576	38
H(34B)	-1882	1504	3300	38
H(35A)	-2084	2720	2289	34
H(35B)	-2228	3123	3046	34

Table 3.6: Hydrogen coordinates (x 10^4) and isotropic displacement parameters (Å^{2}x 10^3) for sarpong137.

	x	y	z	U(eq)
H(36)	-821	3866	2190	27
H(38A)	132	2413	970	30
H(38B)	-909	3242	1229	30
H(39A)	1517	3318	447	29
H(39B)	147	3997	300	29
H(44)	3553	5646	856	32
H(45)	2437	5954	1992	28
H(46)	2723	4404	2572	26
H(48)	2464	2704	1552	26
H(49A)	3070	4376	504	31
H(49B)	1919	5079	66	31
H(50A)	1996	470	1992	51
H(50B)	2434	1359	1522	51
H(50C)	1098	1072	1355	51
H(52A)	1166	4446	3837	50
H(52B)	541	3685	4378	50
H(52C)	-159	4739	4305	50
H(53A)	1014	6244	2880	63
H(53B)	-438	6813	2984	63
H(53C)	527	7176	2339	63
H(54A)	3878	2189	3407	34
H(54B)	3916	3114	2845	34
H(56)	5308	809	3185	54
H(57)	6947	17	2466	76
H(58)	7475	688	1293	89
H(59)	6428	2155	823	78
H(60)	4808	2959	1537	51

X-ray crystallography data for 3.53

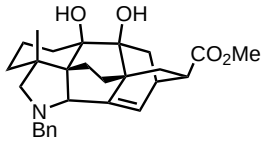

3.53

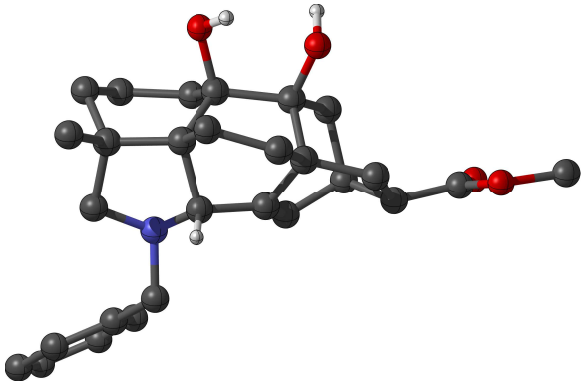

Table 3.7: Crystal data and structure refinement for **3.53**.

Identification code	KO001	
Empirical formula	C28 H35 N O4	
Formula weight	449.57	
Temperature	100(2) K	
Wavelength	0.71073 Å	
Crystal system	Monoclinic	
Space group	P 21/n	
Unit cell dimensions	a = 12.7300(9) Å	a= 90°.
	b = 8.7313(6) Å	b= 94.110(4)°.
	c = 20.2583(14) Å	g = 90°.
Volume	2245.9(3) $Å^3$	
Z	4	
Density (calculated)	1.330 Mg/m^3	
Absorption coefficient	0.088 mm^{-1}	
F(000)	968	
Crystal size	0.260 x 0.180 x 0.100 mm^3	
Theta range for data collection	1.832 to 28.354°.	
Index ranges	$-16 \leq h \leq 16$, $-11 \leq k \leq 11$, $-26 \leq l \leq 27$	
Reflections collected	121138	
Independent reflections	5589 [R(int) = 0.0405]	
Completeness to theta = 28.000°	100.00%	
Absorption correction	Semi-empirical from equivalents	
Max. and min. transmission	0.746 and 0.710	
Refinement method	Full-matrix least-squares on F2	
Data / restraints / parameters	5589 / 0 / 308	
Goodness-of-fit on F2	1.046	
Final R indices [I>2sigma(I)]	R1 = 0.0462, wR2 = 0.1205	
R indices (all data)	R1 = 0.0523, wR2 = 0.1255	
Extinction coefficient	n/a	
Largest diff. peak and hole	0.434 and -0.211 $e.Å^{-3}$	

Table 3.8: Atomic coordinates (x 10^4) and equivalent isotropic displacement parameters (Å^{2}x 10^3) for ko001. U(eq) is defined as one third of the trace of the orthogonalized U^{ij} tensor.

	x	y	z	U(eq)
C(1)	8311(1)	2828(2)	3629(1)	24(1)
C(2)	8194(1)	4342(1)	3996(1)	16(1)
C(3)	8246(1)	4010(2)	4739(1)	20(1)
C(4)	8104(1)	5437(2)	5159(1)	22(1)
C(5)	7145(1)	6425(1)	4919(1)	16(1)
C(6)	6475(1)	5744(1)	4338(1)	14(1)
C(7)	5513(1)	6857(1)	4057(1)	14(1)
C(8)	5395(1)	8437(1)	4404(1)	17(1)
C(9)	5860(1)	9749(1)	3989(1)	17(1)
C(10)	5160(1)	9988(2)	3342(1)	18(1)
C(11)	4226(1)	11018(2)	3430(1)	22(1)
C(12)	2553(1)	11807(2)	2967(1)	41(1)
C(13)	4908(1)	8403(2)	3036(1)	17(1)
C(14)	5706(1)	7212(1)	3324(1)	14(1)
C(15)	6815(1)	7868(1)	3429(1)	14(1)
C(16)	6897(1)	9152(1)	3785(1)	16(1)
C(17)	7628(1)	6658(1)	3400(1)	13(1)
C(18)	7165(1)	5252(1)	3754(1)	13(1)
C(19)	6409(1)	4491(1)	3225(1)	17(1)
C(20)	5652(1)	5733(1)	2917(1)	16(1)
C(21)	9104(1)	5423(1)	3827(1)	18(1)
C(22)	9288(1)	7969(2)	3357(1)	16(1)
C(23)	10317(1)	8446(2)	3717(1)	16(1)
C(24)	10337(1)	9634(2)	4173(1)	20(1)
C(25)	11279(1)	10123(2)	4498(1)	23(1)
C(26)	12216(1)	9405(2)	4369(1)	24(1)
C(27)	12207(1)	8206(2)	3922(1)	23(1)
C(28)	11262(1)	7731(2)	3592(1)	20(1)
N(1)	8651(1)	6963(1)	3748(1)	15(1)
O(1)	6017(1)	4368(1)	4595(1)	19(1)
O(2)	4542(1)	6026(1)	4062(1)	19(1)
O(3)	4195(1)	11994(1)	3850(1)	34(1)
O(4)	3450(1)	10788(1)	2953(1)	29(1)

Table 3.9: Bond lengths [Å] for ko001.

C(1)-C(2)	1.5292(18)	C(13)-C(14)	1.5391(16)
C(1)-H(1A)	0.98	C(13)-H(13A)	0.99

C(1)-H(1B)	0.98	C(13)-H(13B)	0.99
C(1)-H(1C)	0.98	C(14)-C(15)	1.5240(16)
C(2)-C(3)	1.5311(17)	C(14)-C(20)	1.5305(17)
C(2)-C(21)	1.5511(17)	C(15)-C(16)	1.3333(17)
C(2)-C(18)	1.5803(16)	C(15)-C(17)	1.4832(16)
C(3)-C(4)	1.5260(19)	C(16)-H(16)	0.95
C(3)-H(3A)	0.99	C(17)-N(1)	1.4599(14)
C(3)-H(3B)	0.99	C(17)-C(18)	1.5581(16)
C(4)-C(5)	1.5448(17)	C(17)-H(17)	1
C(4)-H(4A)	0.99	C(18)-C(19)	1.5386(16)
C(4)-H(4B)	0.99	C(19)-C(20)	1.5515(17)
C(5)-C(6)	1.5240(16)	C(19)-H(19A)	0.99
C(5)-H(5A)	0.99	C(19)-H(19B)	0.99
C(5)-H(5B)	0.99	C(20)-H(20A)	0.99
C(6)-O(1)	1.4490(14)	C(20)-H(20B)	0.99
C(6)-C(18)	1.5827(17)	C(21)-N(1)	1.4681(16)
C(6)-C(7)	1.6341(17)	C(21)-H(21A)	0.99
C(7)-O(2)	1.4336(14)	C(21)-H(21B)	0.99
C(7)-C(14)	1.5552(16)	C(22)-N(1)	1.4662(15)
C(7)-C(8)	1.5594(17)	C(22)-C(23)	1.5100(16)
C(8)-C(9)	1.5622(18)	C(22)-H(22A)	0.99
C(8)-H(8A)	0.99	C(22)-H(22B)	0.99
C(8)-H(8B)	0.99	C(23)-C(24)	1.3893(19)
C(9)-C(16)	1.5044(17)	C(23)-C(28)	1.3941(18)
C(9)-C(10)	1.5452(17)	C(24)-C(25)	1.3926(18)
C(9)-H(9)	1	C(24)-H(24)	0.95
C(10)-C(11)	1.5119(17)	C(25)-C(26)	1.388(2)
C(10)-C(13)	1.5410(18)	C(25)-H(25)	0.95
C(10)-H(10)	1	C(26)-C(27)	1.384(2)
C(11)-O(3)	1.2062(18)	C(26)-H(26)	0.95
C(11)-O(4)	1.3459(18)	C(27)-C(28)	1.3966(18)
C(12)-O(4)	1.4496(17)	C(27)-H(27)	0.95
C(12)-H(12A)	0.98	C(28)-H(28)	0.95
C(12)-H(12B)	0.98	O(1)-H(1)	0.89(2)
C(12)-H(12C)	0.98	O(2)-H(2)	0.89(3)

Table 3.10: Bond angles [°] for ko001.

C(2)-C(1)-H(1A)	109.5	H(13A)-C(13)-H(13B)	108.2
C(2)-C(1)-H(1B)	109.5	C(15)-C(14)-C(20)	113.46(10)
H(1A)-C(1)-H(1B)	109.5	C(15)-C(14)-C(13)	112.27(10)
C(2)-C(1)-H(1C)	109.5	C(20)-C(14)-C(13)	111.33(9)
H(1A)-C(1)-H(1C)	109.5	C(15)-C(14)-C(7)	98.60(9)

H(1B)-C(1)-H(1C)	109.5	C(20)-C(14)-C(7)	110.00(10)
C(1)-C(2)-C(3)	108.45(10)	C(13)-C(14)-C(7)	110.51(10)
C(1)-C(2)-C(21)	108.58(10)	C(16)-C(15)-C(17)	126.31(11)
C(3)-C(2)-C(21)	110.58(10)	C(16)-C(15)-C(14)	115.32(11)
C(1)-C(2)-C(18)	113.05(10)	C(17)-C(15)-C(14)	111.66(10)
C(3)-C(2)-C(18)	112.12(10)	C(15)-C(16)-C(9)	113.81(11)
C(21)-C(2)-C(18)	103.97(9)	C(15)-C(16)-H(16)	123.1
C(4)-C(3)-C(2)	113.32(10)	C(9)-C(16)-H(16)	123.1
C(4)-C(3)-H(3A)	108.9	N(1)-C(17)-C(15)	116.85(10)
C(2)-C(3)-H(3A)	108.9	N(1)-C(17)-C(18)	106.01(9)
C(4)-C(3)-H(3B)	108.9	C(15)-C(17)-C(18)	104.76(9)
C(2)-C(3)-H(3B)	108.9	N(1)-C(17)-H(17)	109.6
H(3A)-C(3)-H(3B)	107.7	C(15)-C(17)-H(17)	109.6
C(3)-C(4)-C(5)	113.75(10)	C(18)-C(17)-H(17)	109.6
C(3)-C(4)-H(4A)	108.8	C(19)-C(18)-C(17)	105.00(9)
C(5)-C(4)-H(4A)	108.8	C(19)-C(18)-C(2)	117.53(10)
C(3)-C(4)-H(4B)	108.8	C(17)-C(18)-C(2)	101.88(9)
C(5)-C(4)-H(4B)	108.8	C(19)-C(18)-C(6)	106.57(9)
H(4A)-C(4)-H(4B)	107.7	C(17)-C(18)-C(6)	112.22(9)
C(6)-C(5)-C(4)	114.28(10)	C(2)-C(18)-C(6)	113.37(9)
C(6)-C(5)-H(5A)	108.7	C(18)-C(19)-C(20)	108.52(10)
C(4)-C(5)-H(5A)	108.7	C(18)-C(19)-H(19A)	110
C(6)-C(5)-H(5B)	108.7	C(20)-C(19)-H(19A)	110
C(4)-C(5)-H(5B)	108.7	C(18)-C(19)-H(19B)	110
H(5A)-C(5)-H(5B)	107.6	C(20)-C(19)-H(19B)	110
O(1)-C(6)-C(5)	105.27(9)	H(19A)-C(19)-H(19B)	108.4
O(1)-C(6)-C(18)	107.63(9)	C(14)-C(20)-C(19)	111.76(10)
C(5)-C(6)-C(18)	111.96(10)	C(14)-C(20)-H(20A)	109.3
O(1)-C(6)-C(7)	107.87(9)	C(19)-C(20)-H(20A)	109.3
C(5)-C(6)-C(7)	113.65(10)	C(14)-C(20)-H(20B)	109.3
C(18)-C(6)-C(7)	110.10(9)	C(19)-C(20)-H(20B)	109.3
O(2)-C(7)-C(14)	107.59(9)	H(20A)-C(20)-H(20B)	107.9
O(2)-C(7)-C(8)	109.50(10)	N(1)-C(21)-C(2)	106.70(9)
C(14)-C(7)-C(8)	106.31(10)	N(1)-C(21)-H(21A)	110.4
O(2)-C(7)-C(6)	108.82(9)	C(2)-C(21)-H(21A)	110.4
C(14)-C(7)-C(6)	106.54(9)	N(1)-C(21)-H(21B)	110.4
C(8)-C(7)-C(6)	117.61(9)	C(2)-C(21)-H(21B)	110.4
C(7)-C(8)-C(9)	110.75(10)	H(21A)-C(21)-H(21B)	108.6
C(7)-C(8)-H(8A)	109.5	N(1)-C(22)-C(23)	113.50(10)
C(9)-C(8)-H(8A)	109.5	N(1)-C(22)-H(22A)	108.9
C(7)-C(8)-H(8B)	109.5	C(23)-C(22)-H(22A)	108.9
C(9)-C(8)-H(8B)	109.5	N(1)-C(22)-H(22B)	108.9
H(8A)-C(8)-H(8B)	108.1	C(23)-C(22)-H(22B)	108.9
C(16)-C(9)-C(10)	106.12(10)	H(22A)-C(22)-H(22B)	107.7
C(16)-C(9)-C(8)	105.54(10)	C(24)-C(23)-C(28)	118.63(12)

C(10)-C(9)-C(8)	109.71(10)	C(24)-C(23)-C(22)	120.07(11)
C(16)-C(9)-H(9)	111.7	C(28)-C(23)-C(22)	121.29(12)
C(10)-C(9)-H(9)	111.7	C(23)-C(24)-C(25)	121.18(12)
C(8)-C(9)-H(9)	111.7	C(23)-C(24)-H(24)	119.4
C(11)-C(10)-C(13)	115.98(11)	C(25)-C(24)-H(24)	119.4
C(11)-C(10)-C(9)	113.08(11)	C(26)-C(25)-C(24)	119.69(13)
C(13)-C(10)-C(9)	108.09(10)	C(26)-C(25)-H(25)	120.2
C(11)-C(10)-H(10)	106.3	C(24)-C(25)-H(25)	120.2
C(13)-C(10)-H(10)	106.3	C(27)-C(26)-C(25)	119.85(12)
C(9)-C(10)-H(10)	106.3	C(27)-C(26)-H(26)	120.1
O(3)-C(11)-O(4)	123.53(12)	C(25)-C(26)-H(26)	120.1
O(3)-C(11)-C(10)	124.61(13)	C(26)-C(27)-C(28)	120.24(12)
O(4)-C(11)-C(10)	111.72(12)	C(26)-C(27)-H(27)	119.9
O(4)-C(12)-H(12A)	109.5	C(28)-C(27)-H(27)	119.9
O(4)-C(12)-H(12B)	109.5	C(23)-C(28)-C(27)	120.40(13)
H(12A)-C(12)-H(12B)	109.5	C(23)-C(28)-H(28)	119.8
O(4)-C(12)-H(12C)	109.5	C(27)-C(28)-H(28)	119.8
H(12A)-C(12)-H(12C)	109.5	C(17)-N(1)-C(22)	110.93(9)
H(12B)-C(12)-H(12C)	109.5	C(17)-N(1)-C(21)	102.41(9)
C(14)-C(13)-C(10)	109.99(10)	C(22)-N(1)-C(21)	112.26(10)
C(14)-C(13)-H(13A)	109.7	C(6)-O(1)-H(1)	106.1(15)
C(10)-C(13)-H(13A)	109.7	C(7)-O(2)-H(2)	110.5(16)
C(14)-C(13)-H(13B)	109.7	C(11)-O(4)-C(12)	115.68(13)
C(10)-C(13)-H(13B)	109.7		

Table 3.11: Anisotropic displacement parameters ($Å^2$x 10^3)for ko001. The anisotropic displacement factor exponent takes the form: $-2\sqrt{2}[\ h^2a^{*2}U^{11} + ... + 2\ h\ k\ a^*\ b^*\ U^{12}]$

	U^{11}	U^{22}	U^{33}	U^{23}	U^{13}	U^{12}
C(1)	28(1)	16(1)	29(1)	-1(1)	2(1)	5(1)
C(2)	17(1)	13(1)	18(1)	2(1)	1(1)	2(1)
C(3)	22(1)	19(1)	19(1)	6(1)	0(1)	5(1)
C(4)	23(1)	25(1)	17(1)	1(1)	-4(1)	5(1)
C(5)	17(1)	17(1)	14(1)	0(1)	-1(1)	0(1)
C(6)	15(1)	14(1)	14(1)	1(1)	2(1)	-2(1)
C(7)	12(1)	17(1)	14(1)	0(1)	1(1)	-1(1)
C(8)	16(1)	19(1)	16(1)	-1(1)	0(1)	3(1)
C(9)	18(1)	15(1)	18(1)	-1(1)	-1(1)	3(1)
C(10)	17(1)	18(1)	18(1)	2(1)	2(1)	4(1)
C(11)	21(1)	25(1)	21(1)	8(1)	5(1)	7(1)
C(12)	28(1)	55(1)	40(1)	18(1)	7(1)	24(1)
C(13)	14(1)	20(1)	16(1)	1(1)	-1(1)	3(1)
C(14)	12(1)	15(1)	14(1)	0(1)	-1(1)	-1(1)

Table 3.11: Anisotropic displacement parameters ($Å^2$x 10^3)for ko001. The anisotropic displacement factor exponent takes the form: -2$\sqrt{}$2[$h^2a^{*2}U^{11}$ + ... + 2 h k a* b* U^{12}]

	U^{11}	U^{22}	U^{33}	U^{23}	U^{13}	U^{12}
C(15)	12(1)	15(1)	15(1)	3(1)	0(1)	0(1)
C(16)	15(1)	15(1)	19(1)	2(1)	-1(1)	-1(1)
C(17)	12(1)	13(1)	14(1)	1(1)	0(1)	-1(1)
C(18)	14(1)	12(1)	14(1)	1(1)	1(1)	-1(1)
C(19)	19(1)	14(1)	17(1)	-2(1)	0(1)	-2(1)
C(20)	16(1)	17(1)	15(1)	-2(1)	-2(1)	-2(1)
C(21)	16(1)	17(1)	22(1)	3(1)	1(1)	3(1)
C(22)	14(1)	20(1)	15(1)	4(1)	-1(1)	-2(1)
C(23)	14(1)	19(1)	16(1)	6(1)	0(1)	-3(1)
C(24)	17(1)	19(1)	25(1)	2(1)	0(1)	0(1)
C(25)	24(1)	21(1)	24(1)	1(1)	-2(1)	-5(1)
C(26)	17(1)	30(1)	26(1)	7(1)	-3(1)	-8(1)
C(27)	14(1)	32(1)	23(1)	7(1)	2(1)	0(1)
C(28)	17(1)	24(1)	19(1)	2(1)	3(1)	0(1)
N(1)	11(1)	15(1)	17(1)	4(1)	-1(1)	-1(1)
O(1)	19(1)	18(1)	20(1)	5(1)	0(1)	-5(1)
O(2)	14(1)	23(1)	20(1)	0(1)	3(1)	-4(1)
O(3)	38(1)	35(1)	29(1)	-2(1)	6(1)	19(1)
O(4)	21(1)	37(1)	28(1)	8(1)	0(1)	12(1)

Table 3.12: Hydrogen coordinates (x 10^4) and isotropic displacement parameters ($Å^2$x 10^3) for ko001.

	x	y	z	U(eq)
H(1A)	8978	2340	3783	36
H(1B)	8307	3025	3152	36
H(1C)	7724	2148	3716	36
H(3A)	7691	3259	4829	24
H(3B)	8936	3539	4874	24
H(4A)	8749	6071	5157	26
H(4B)	8024	5118	5622	26
H(5A)	6696	6575	5293	19
H(5B)	7400	7445	4789	19
H(8A)	5767	8409	4850	20
H(8B)	4640	8642	4456	20
H(9)	5949	10718	4250	21
H(10)	5607	10529	3030	21
H(12A)	2242	11713	3394	61

Table 3.12: Hydrogen coordinates (x 10^4) and isotropic displacement parameters ($Å^2$x 10^3) for ko001.

	x	y	z	U(eq)
H(12B)	2026	11531	2610	61
H(12C)	2783	12865	2905	61
H(13A)	4187	8092	3133	20
H(13B)	4937	8456	2550	20
H(16)	7550	9645	3899	20
H(17)	7726	6395	2928	16
H(19A)	6001	3674	3429	20
H(19B)	6813	4024	2877	20
H(20A)	5838	5958	2461	20
H(20B)	4921	5335	2892	20
H(21A)	9671	5413	4188	22
H(21B)	9404	5091	3413	22
H(22A)	8875	8899	3233	20
H(22B)	9439	7434	2944	20
H(24)	9697	10121	4266	24
H(25)	11281	10945	4805	28
H(26)	12861	9736	4588	29
H(27)	12846	7705	3838	28
H(28)	11263	6916	3281	24
H(1)	5436(19)	4180(30)	4337(12)	55(7)
H(2)	4350(20)	5930(30)	4474(13)	63(7)

X-ray crystallography data for 3.77

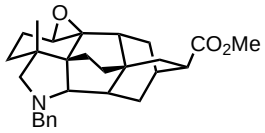

3.77

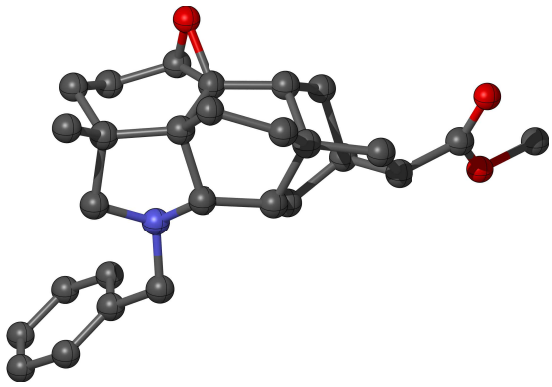

Table 3.13: Crystal data and structure refinement for **3.77**.

Identification code	KRO_11_051_finished
Empirical formula	C28H35NO3
Formula weight	433.57
Temperature/K	100(2)
Crystal system	orthorhombic
Space group	Pbca
a/Å	15.00270(10)
b/Å	13.12140(10)
c/Å	22.87130(10)
α/°	90
β/°	90
γ/°	90
Volume/Å^3	4502.36(5)
Z	8
ρcalcg/cm^3	1.279
Îij/mm 1	0.644
F(000)	1872.0
Crystal size/mm^3	0.33 ÃŮ 0.1 ÃŮ 0.06
Radiation	CuKα (λ = 1.54184)
2θ range for data collection/°	9.726 to 158.352
Index ranges	-19 ≤ h ≤ 19, -16 ≤ k ≤ 13, -28 ≤ l ≤ 29
Reflections collected	48143
Independent reflections	4848 [Rint = 0.0394, Rsigma = 0.0182]
Data/restraints/parameters	4848/0/291
Goodness-of-fit on F2	1.031
Final R indexes [I>=2σ (I)]	R1 = 0.0380, wR2 = 0.0966
Final R indexes [all data]	R1 = 0.0401, wR2 = 0.0983
Largest diff. peak/hole / e Å^3	0.26/-0.17

Table 3.14: Atomic coordinates (x 10^4) and equivalent isotropic displacement parameters (Å^{2}x 10^3) for KRO_11_051_finished. U(eq) is defined as one third of the trace of the orthogonalized U^{ij} tensor.

	x	y	z	U(eq)
O1	2614.4(5)	6778.7(6)	4784.1(3)	24.91(18)
O3	5766.4(6)	5344.8(6)	7037.2(3)	29.8(2)
O2	4472.8(6)	6044.0(7)	7317.4(4)	33.3(2)
N1	5155.6(6)	7916.2(7)	4294.9(4)	18.41(19)
C16	4784.6(7)	8313.3(8)	4838.1(4)	18.4(2)
C8	4628.0(7)	8451.6(8)	3853.7(5)	21.5(2)
C6	6447.9(7)	7677.9(8)	3658.9(5)	21.2(2)
C7	6110.1(7)	8102.9(8)	4230.4(5)	21.7(2)
C12	3510.2(7)	6488.3(8)	3887.2(5)	21.9(2)
C13	3389.2(7)	6294.1(8)	4529.9(5)	20.9(2)
C14	3503.0(7)	7124.8(8)	4953.1(4)	18.8(2)
C21	3684.8(7)	6953.9(8)	5608.8(4)	20.2(2)
C27	5096.2(8)	6020.3(8)	6987.5(5)	23.4(2)
C20	3305.6(8)	8935.0(8)	5180.8(5)	23.5(2)
C17	5104.9(7)	7837.9(8)	5416.4(4)	19.5(2)
C18	4287.0(7)	7828.4(8)	5827.9(4)	19.6(2)
C9	3652.5(7)	8402.5(8)	4071.8(5)	20.7(2)
C22	4113.0(8)	5928.8(8)	5784.0(5)	24.5(2)
C19	3761.9(8)	8824.8(8)	5786.7(5)	24.0(2)
C23	5110.8(8)	6094.0(8)	5883.8(5)	23.4(2)
C15	3764.9(7)	8198.0(8)	4749.4(4)	19.0(2)
C26	5240.5(8)	6699.8(8)	6461.3(5)	22.2(2)
C25	4599.3(8)	7616.9(8)	6453.5(5)	22.9(2)
C24	5481.5(8)	6735.7(8)	5377.9(5)	23.5(2)
C11	3170.2(7)	7548.2(9)	3737.1(5)	23.3(2)
C5	6333.7(8)	6649.5(9)	3528.5(5)	27.0(2)
C1	6867.8(8)	8297.2(9)	3252.2(5)	27.9(2)
C10	3174.2(9)	9402.6(9)	3926.6(5)	29.4(3)
C4	6621.7(8)	6250.5(10)	2999.1(6)	31.8(3)
C3	7027.0(9)	6885.2(10)	2591.2(6)	33.6(3)
C28	5679.7(10)	4612.1(10)	7505.3(5)	33.7(3)
C2	7155.2(9)	7905.9(10)	2720.2(6)	35.5(3)

Table 3.15: Bond lengths [Å] for KRO_11_051_finished.

O1	C13	1.4470(13)	C21	C22	1.5435(15)
O1	C14	1.4605(12)	C27	C26	1.5134(15)

O3	C27	1.3452(14)	C20	C19	1.5523(15)
O3	C28	1.4449(14)	C20	C15	1.5439(14)
O2	C27	1.2022(14)	C17	C18	1.5465(14)
N1	C16	1.4577(13)	C17	C24	1.5552(15)
N1	C8	1.4623(13)	C18	C19	1.5293(14)
N1	C7	1.4602(13)	C18	C25	1.5309(14)
C16	C17	1.5392(14)	C9	C15	1.5819(14)
C16	C15	1.5506(14)	C9	C11	1.5382(15)
C8	C9	1.5475(15)	C9	C10	1.5320(15)
C6	C7	1.5087(15)	C22	C23	1.5298(17)
C6	C5	1.3926(16)	C23	C26	1.5537(15)
C6	C1	1.3866(15)	C23	C24	1.5353(15)
C12	C13	1.5028(14)	C26	C25	1.5408(15)
C12	C11	1.5205(15)	C5	C4	1.3882(17)
C13	C14	1.4677(14)	C1	C2	1.3891(17)
C14	C21	1.5405(14)	C4	C3	1.3905(18)
C14	C15	1.5345(14)	C3	C2	1.3848(19)
C21	C18	1.5440(14)			

Table 3.16: Bond angles [°] for KRO_11_051_finished.

C13	O1	C14	60.64(6)	C19	C18	C21	108.30(9)
C27	O3	C28	115.71(9)	C19	C18	C17	111.36(9)
C16	N1	C8	102.11(8)	C19	C18	C25	111.73(8)
C16	N1	C7	113.61(8)	C25	C18	C21	110.35(9)
C7	N1	C8	112.37(8)	C25	C18	C17	109.11(9)
N1	C16	C17	117.93(8)	C8	C9	C15	102.82(8)
N1	C16	C15	103.31(8)	C11	C9	C8	108.35(9)
C17	C16	C15	112.38(8)	C11	C9	C15	114.46(9)
N1	C8	C9	105.64(8)	C10	C9	C8	109.72(9)
C5	C6	C7	120.16(10)	C10	C9	C15	114.05(9)
C1	C6	C7	121.15(10)	C10	C9	C11	107.22(9)
C1	C6	C5	118.69(10)	C23	C22	C21	108.82(9)
N1	C7	C6	110.79(9)	C18	C19	C20	111.21(8)
C13	C12	C11	109.60(9)	C22	C23	C26	108.78(9)
O1	C13	C12	114.55(9)	C22	C23	C24	108.64(9)
O1	C13	C14	60.14(6)	C24	C23	C26	108.34(9)
C14	C13	C12	120.34(9)	C16	C15	C9	102.52(8)
O1	C14	C13	59.23(6)	C14	C15	C16	107.61(8)
O1	C14	C21	111.97(8)	C14	C15	C20	105.46(8)
O1	C14	C15	116.02(8)	C14	C15	C9	115.20(8)
C13	C14	C21	123.68(9)	C20	C15	C16	107.20(8)
C13	C14	C15	120.73(9)	C20	C15	C9	118.17(9)

C15	C14	C21	112.57(8)	C27	C26	C23	110.89(9)
C14	C21	C18	108.14(8)	C27	C26	C25	112.34(9)
C14	C21	C22	116.95(8)	C25	C26	C23	108.15(9)
C22	C21	C18	108.65(9)	C18	C25	C26	110.09(8)
O3	C27	C26	110.40(9)	C23	C24	C17	109.62(9)
O2	C27	O3	123.06(10)	C12	C11	C9	113.35(9)
O2	C27	C26	126.53(10)	C4	C5	C6	120.93(11)
C15	C20	C19	108.37(9)	C6	C1	C2	120.80(11)
C16	C17	C18	106.17(8)	C5	C4	C3	119.70(12)
C16	C17	C24	116.21(8)	C2	C3	C4	119.80(12)
C18	C17	C24	108.38(8)	C3	C2	C1	120.07(11)
C21	C18	C17	105.83(8)				

Table 3.17: Anisotropic displacement parameters ($Å^2$x 10^3)for KRO_11_051_finished . The anisotropic displacement factor exponent takes the form: -2$\sqrt{}$2[$h^2a^{*2}U^{11}$ + ... + 2 h k a* b* U^{12}]

	U^{11}	U^{22}	U^{33}	U^{23}	U^{13}	U^{12}
O1	18.4(4)	30.7(4)	25.6(4)	-6.1(3)	2.5(3)	-3.5(3)
O3	38.4(5)	29.7(4)	21.2(4)	7.1(3)	2.8(3)	8.5(4)
O2	35.8(5)	39.9(5)	24.4(4)	7.9(3)	6.7(4)	4.0(4)
N1	19.2(4)	21.0(4)	15.0(4)	2.0(3)	-0.6(3)	-0.9(3)
C16	22.2(5)	15.5(4)	17.5(5)	0.2(4)	-0.9(4)	-1.0(4)
C8	24.1(5)	22.1(5)	18.4(5)	3.3(4)	-3.0(4)	-1.1(4)
C6	17.1(5)	26.0(5)	20.6(5)	3.7(4)	-0.9(4)	-0.7(4)
C7	20.7(5)	24.9(5)	19.6(5)	2.4(4)	-1.2(4)	-4.7(4)
C12	23.6(5)	22.5(5)	19.5(5)	-3.6(4)	-0.9(4)	-3.2(4)
C13	21.3(5)	20.3(5)	21.1(5)	-2.5(4)	1.6(4)	-1.9(4)
C14	17.7(5)	19.5(5)	19.1(5)	-1.9(4)	1.5(4)	-0.2(4)
C21	22.9(5)	20.3(5)	17.5(5)	-1.7(4)	3.6(4)	-1.4(4)
C27	29.2(6)	23.8(5)	17.1(5)	-0.8(4)	-1.5(4)	0.5(4)
C20	26.6(5)	20.7(5)	23.2(5)	-3.3(4)	-1.1(4)	5.9(4)
C17	21.7(5)	19.9(5)	17.0(5)	-0.2(4)	-0.6(4)	-0.6(4)
C18	23.5(5)	17.9(5)	17.3(5)	-2.3(4)	0.9(4)	0.9(4)
C9	23.1(5)	19.0(5)	20.0(5)	0.7(4)	-3.4(4)	1.9(4)
C22	37.3(6)	18.0(5)	18.1(5)	-0.2(4)	0.8(4)	-2.5(4)
C19	30.9(6)	19.7(5)	21.3(5)	-4.9(4)	-0.3(4)	4.1(4)
C23	33.8(6)	20.4(5)	16.1(5)	0.9(4)	2.4(4)	6.8(4)
C15	21.2(5)	17.2(5)	18.6(5)	-1.7(4)	-1.2(4)	1.8(4)
C26	26.9(5)	23.2(5)	16.6(5)	1.2(4)	0.7(4)	1.7(4)
C25	30.0(5)	21.5(5)	17.2(5)	-2.8(4)	1.2(4)	1.8(4)
C24	27.6(6)	25.4(5)	17.6(5)	2.7(4)	2.9(4)	7.5(4)
C11	22.7(5)	26.5(5)	20.7(5)	-1.2(4)	-4.2(4)	-0.4(4)

Table 3.17: Anisotropic displacement parameters ($Å^2$x 10^3)for KRO_11_051_finished . The anisotropic displacement factor exponent takes the form: -2$\sqrt{}$2[$h^2a^{*2}U^{11}$ + ... + 2 h k a* b* U^{12}]

	U^{11}	U^{22}	U^{33}	U^{23}	U^{13}	U^{12}
C5	27.9(6)	26.1(6)	27.1(6)	3.1(4)	5.4(5)	-3.7(4)
C1	29.3(6)	25.7(5)	28.6(6)	5.0(5)	5.2(5)	-1.8(4)
C10	35.9(6)	24.1(5)	28.2(6)	1.4(4)	-6.2(5)	7.9(5)
C4	30.8(6)	30.0(6)	34.5(6)	-4.3(5)	5.8(5)	-2.6(5)
C3	33.4(6)	40.5(7)	27.0(6)	-1.9(5)	9.3(5)	2.0(5)
C28	47.5(7)	31.4(6)	22.2(5)	8.9(5)	-1.1(5)	5.6(5)
C2	40.7(7)	36.3(7)	29.7(6)	7.4(5)	14.4(5)	-0.3(5)

Table 3.18: Hydrogen coordinates (x 10^4) and isotropic displacement parameters ($Å^2$x 10^3) for KRO_11_051_finished.

	x	y	z	U(eq)
H16	4920.99	9058.83	4853.71	22
H8A	4686.31	8114.75	3468.32	26
H8B	4826.8	9168.15	3816.8	26
H7A	6434.4	7779.84	4558.66	26
H7B	6225.7	8845.3	4244.76	26
H12A	3177.3	5971.95	3659.31	26
H12B	4149.14	6433.07	3783.85	26
H13	3531.42	5591.46	4671.17	25
H21	3102.07	7008.84	5818.67	24
H20A	2663.93	8767.86	5212.74	28
H20B	3361.66	9645.08	5039.12	28
H17	5571.9	8289.82	5589.86	23
H22A	3831.96	5668.31	6145.97	29
H22B	4020.59	5420.28	5469.98	29
H19A	4170.27	9407.09	5850.16	29
H19B	3302.76	8840.62	6097.41	29
H23	5427.29	5424.31	5905.68	28
H26	5865.85	6962.82	6472.82	27
H25A	4077.63	7471.37	6705.03	28
H25B	4905.95	8225.98	6611.01	28
H24A	5309.71	6424.9	4999.91	28
H24B	6140.44	6753.69	5399.09	28
H11A	2525.08	7583.14	3825.97	28
H11B	3244.5	7663.79	3312.15	28
H5	6054.68	6214.87	3805.75	32

Table 3.18: Hydrogen coordinates (x 10^4) and isotropic displacement parameters ($Å^2$x 10^3) for KRO_11_051_finished.

	x	y	z	U(eq)
H1	6959.99	8997.55	3338.29	33
H10A	3482.81	9970.45	4117.66	44
H10B	2557.7	9369.71	4067.01	44
H10C	3176.14	9507.36	3502.39	44
H4	6542.25	5547.02	2915.79	38
H3	7215.5	6619.38	2225.13	40
H28A	5178.98	4154.71	7422.57	51
H28B	5571.23	4971.04	7874.29	51
H28C	6230.13	4213.66	7536.68	51
H2	7439.9	8338.9	2444.7	43

Chapter 4

Synthesis of Natural Product Like Molecules Using C–C Activation

4.1 Introduction

In addition to the diterpenoid alkaloids, our group is interested in a wide range of non-alkaloidal diterpenoid natural products. This broad class of natural products possesses more structural diversity than can easily be quantified as well as a correspondingly large assortment of biological activities. One common approach to the syntheses of diterpenoids is to utilize the large number of commercially available and inexpensive monoterpenoid natural products as building blocks. These cheap, abundant, and renewable chemical feedstocks are an ideal starting point for any synthesis that can utilize their stereochemical and structural diversity.[1] This group of molecules, referred to as the "chiral pool" has long dictated which enantiopure targets are easily within reach, and which require difficult to employ enantioselective methods or chiral resolutions.[2] By converting chiral pool molecules to new scaffolds via deep-seated structural changes, chemists can access chiral building blocks with novel structural motifs that enable the syntheses of new targets.

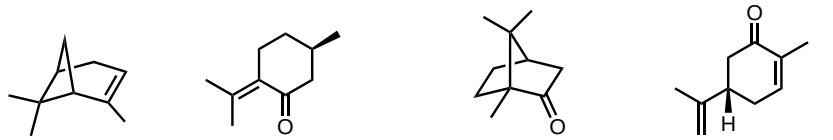

(+)-pinene (**4.1**) (+)-pulegone (**4.2**) (+)-camphor (**4.3**) (+)-carvone (**4.4**)

Figure 4.1: Common terpenoid natural products used as chiral pool building blocks.

In addition to natural product synthesis, there has been a recent surge in interest in the synthesis of natural product like compounds. In this context, we consider "natural product like" to mean compounds that occupy chemical space that is closely related to known natural products, but are not simple derivatives (i.e., esterification, saponification, etc.).[3,4] One approach to these molecules is to transform commercially available complex natural products to novel natural product like scaffolds via ring expansion or contraction.[5] Alternatively, rearrangements and fragmentations can also lead to new scaffolds that still possess the stereochemical and structural complexity generally associated with natural products.[6]

Our approach relies on transforming simple natural products into complex terpenoid building blocks with unusual scaffolds. While many applications of chiral pool molecules rely on well established chemistry that incorporates their skeletons directly into their targets, methods that utilize rearrangements of these scaffolds enable the synthesis of new scaffolds and expand the synthetic toolbox. Our interest in this field began in 2015 when we found that unnaturally hydroxylated pinene derivatives such as **4.7** could undergo a Rh catalyzed C–C bond activation (Scheme 4.1) to furnish novel chiral building blocks.[7] These unusual pinene derivatives could in turn be synthesized from the cheap and abundant chiral pool molecule carvone (**4.4**), which is conveniently available in both enantiomers.[8] Using this method, we were able to transform carvone to a wide variety of interesting enantiopure scaffolds. Mechanistically, this reaction proceeds through a Rh mediated C–C bond cleavage that occurs with selectivity orthogonal to more traditional methods such as Lewis acids.

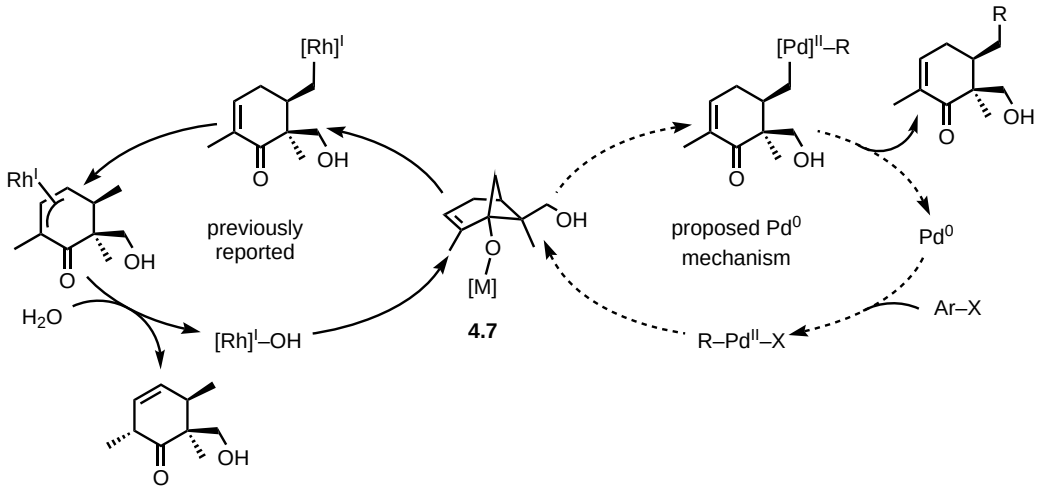

Scheme 4.1: Mechanisms of Rh and Pd mediated cyclobutanol opening reactions.

Methods that activate unreactive bonds such as C–H and C–C bonds, have become a powerful tool for organic chemists. C–H bond activation in particular has garnered a significant amount of interest over the past decade and has become a mainstay in many fields of chemistry. C–C activation, however has received comparatively less attention.[9] This is largely due to the increased challenge compared to C–H bond activation. While C–C bonds are generally weaker than C–H bonds, considerations regarding orbital overlap and the relative weakness of carbon metal bonds mean that this process is substantially more difficult. One way to overcome this challenge is to couple C–C bond activation with a strain releasing process in order to render the desired reaction more favorable. To that end, a large body of work toward C–C activation employing cyclopropanols[10] and cyclobutanols[11,12] has been reported.

In our initial report, we used these pinene-type cyclobutanols to access transient organorhodium species. While this C–C activation was a useful tool for accessing new scaffolds, we wanted to further develop this strategy to allow us to form new C–C bonds. We sought to develop a Pd–based system (Scheme 4.1) that achieved C–C bond activation as well as sp^3–sp^2 cross-couplings from the resulting alkylpalladium species. That work forms the basis of this chapter.[13]

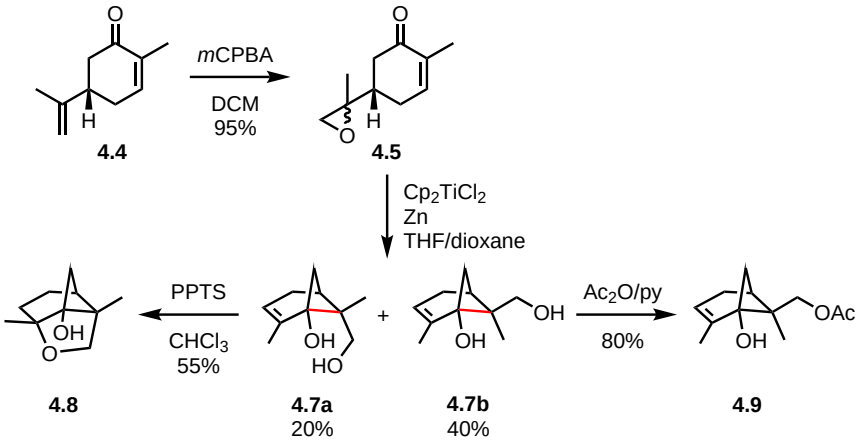

Scheme 4.2: Bermejo's synthesis of hydroxylated pinene scaffolds.

4.2 Taxagifine: An Unusual Taxoid Natural Product

Our motivation for developing this methodology was the realization that with the proper cross-coupling partner, this approach could provide rapid access to a variety of natural product scaffolds. In particular, tricyclic cyclobutanol **4.8** mapped directly onto several taxoid natural products such as taxagifine (**4.10**), which possesses an additional tetrahydrofuran ring system that is not found in most taxoids. The taxoids paclitaxel (**4.11**) and docetaxel (**4.12**) have become some of the most important chemotherapy drugs on the market today, and are the front line treatment for a variety of common cancers. Given their broad applications to a variety of diseases, concerns over drug resistance have driven chemists to search for other biologically active taxoid natural products. Taxagifine is particularly interesting as it lacks several of the characteristic structural features of paclitaxel that are thought to confer its bioactivity. Despite these differences, taxagifine possess comparable potency in Ca^{2+} induced microtubule depolymerization assays.[14] A scalable synthesis of taxagfine and related compounds would facilitate additional studies of their mechanism of action.

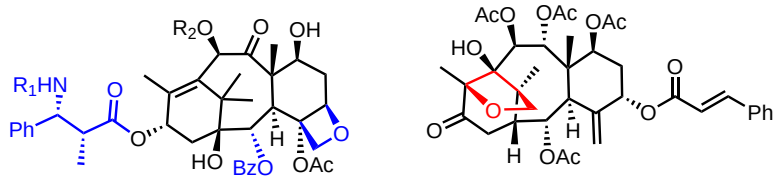

Figure 4.1: The two most commonly prescribed taxoids, as well as taxagifine. Functionalities absent in taxagifine are shown in blue, the unusual tetrahydrofuran ring in taxagifine is shown in red.

Our retrosynthesis of taxagifine identified two key disconnections that took the natural product back to two fragments of similar complexity. Diketone **4.24** would be converted to **4.13** by an aldol reaction to form the eight-membered ring in the taxoid skeleton. This was an ambitious disconnec-

tion as there was little precedent for forming 8-membered rings of this type via an aldol reaction because eight membered rings are generally difficult to form as a result of the high transannular strain and the inherent reversibility of the aldol reaction.[15] Our second disconnection cut the aldol precursor into two similarly sized fragments. In the forward direction this would occur via a Pd-catalyzed C–C bond activation of a strained cyclobutanol (**4.8**), followed by cross-coupling with an appropriately functionalized partner. While the synthesis of taxagifine would require a complex coupling partner, we opted to use a simple acetophenone substrate (2'-bromoacetophenone) to determine the feasibility of this approach. This would allow us to synthesize the [6.8.6] tricyclic core of the taxoids while using a commercially available coupling partner.

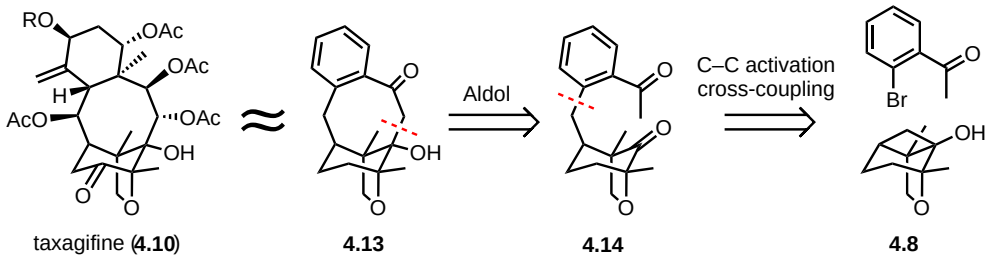

Figure 4.2: Retrosynthesis of the taxagifine skeleton.

4.3 Palladium Mediated C–C Bond Activation / Cross-Coupling

While our ultimate goal was to synthesize a variety of natural product and natural product like molecules, we wanted to develop a general method that demonstrated the utility of these interesting chiral building blocks. This cross-coupling was explored with a variety of aryl and heteroaryl cross-coupling partners as well as two cyclobutanols, a tricycle (**4.8**) arising from the minor diastereomer of the Ti (III)-mediated cyclization and an acetoxy-protected cyclobutanol (**4.9**) from the major diastereomer. Tricycle **4.8** was chosen since it possesses the same THF ring found in taxagifine.

Building on the previous work on cyclobutanols by Uemura[11] we found a metal complex and solvent system that was generally applicable to a variety of cross-coupling partners. Simple electron-rich and electron-deficient aryl bromides such as **4.16a**–**c** gave the desired cross-coupling products (**4.15a**–**c**) in high yields with 5% $Pd(OAc)_2$ and 5% (*R*)-BINAP loadings. Bulky ortho-substituted cross-coupling partners such as **4.16l** also gave high yields, but required slightly elevated catalyst loadings. Heteroaryl cross-coupling partners (**4.16d**–**h**) also worked in moderate to good yields. In these cases, it was beneficial to decrease reaction temperatures and extend the reaction times. Unfortunately, when we attempted this cross-coupling with 2'-bromoacetophenone (**4.16m**), we were unable to isolate any of the desired product. We were concerned that the methyl ketone might be forming an unreactive palladacycle (Figure 4.1) so we examined a variety of other substrates that could be transformed into the desired acetophenone.[16] The protected and free benzylic alcohols also failed to give any desired product, as did the aldehyde and ketal substrates. Palladium complexes with bulky monodentate ligands are known to exhibit substantially increased reactivity.[17] With this in mind, we explored other ligands with our original substrate (**4.16m**) and found that the we could perform the desired cross-coupling as long as a large excess of the ligand

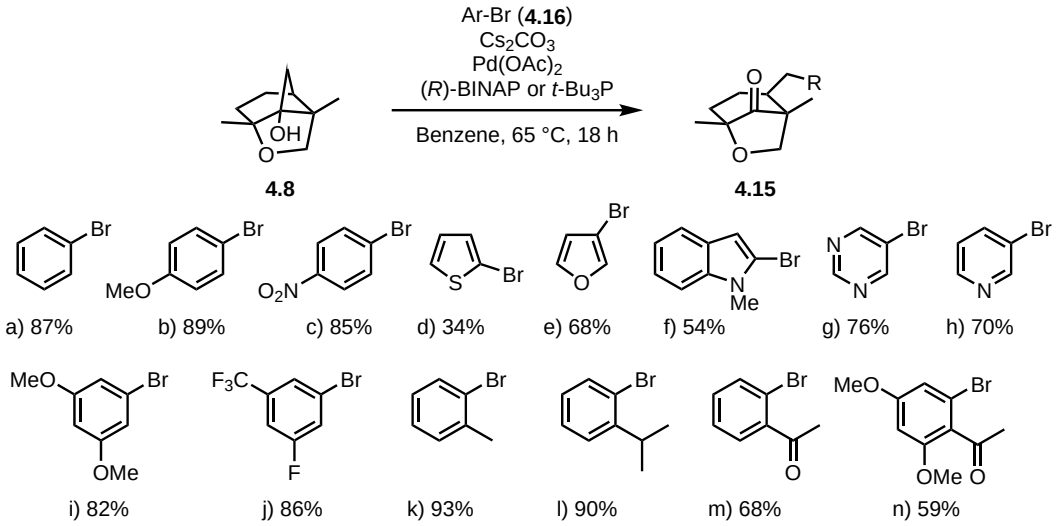

Scheme 4.3: Substrate scope of the cross-coupling with tricycle **4.8**.

P(*t*-Bu)$_3$ was used. With these conditions, we were able to access the desired taxoid core precursor (**4.15m**) in 68% yield.

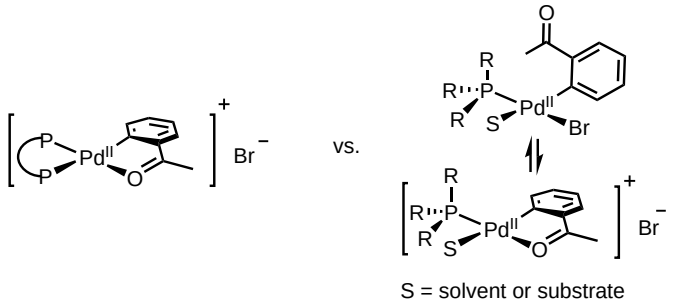

Figure 4.1: Formation of a deactivated palladacycle by chelation with a carbonyl.

Next, we explored cross-couplings with our acetoxy-protected cyclobutanol (**4.9**). Under our optimized conditions, a variety of aryl and indole electrophiles underwent cross-coupling in good yields. Other heteroaromatic electrophiles were not well tolerated with this substrate. Based on our results with **4.8**, these cross-couplings should be possible with individualized optimization. We also explored a single non-aromatic cross-coupling partner (**4.18g**), which gave the corresponding prenylated cross-coupling product (**4.17g**) in 49% yield.

We have examined the role of (*R*)-BINAP in our system. In our previous studies under Rh catalysis, we found a strong matched-mismatched effect with (R)- and (*S*)-BINAP. Under our palladium conditions, however, we observed only minor matched-mismatched effects (Scheme 4.4). (*S*)-BINAP giving slightly lower yields when **4.9** was used, and a somewhat improved yield when the unprotected cyclobutanol (**4.7b**) was used.

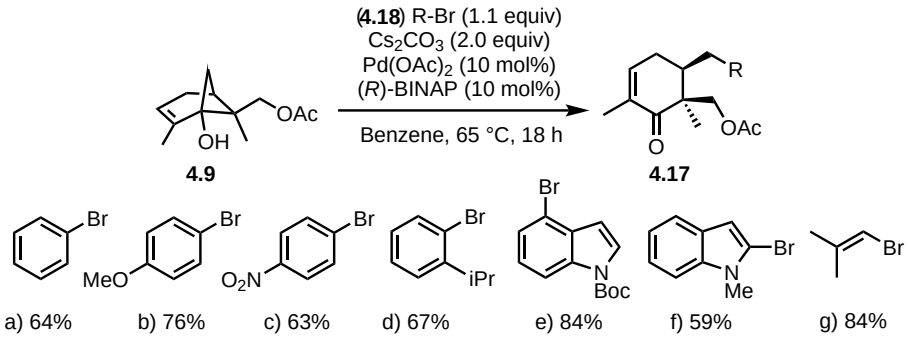

Figure 4.2: Substrate scope of the cross-coupling with **4.9**.

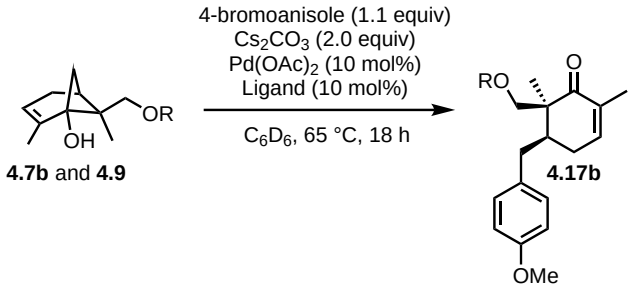

Entry	R	Ligand	Yield (%)
1	H	(*R*)-BINAP	46
2	H	(*S*)-BINAP	72
3	Ac	(*R*)-BINAP	76
4	Ac	(*S*)-BINAP	70

Scheme 4.4: Ligand matched-mismatched effects with **4.7b** and **4.9**.

4.4 Synthesis of Natural Product Like Scaffolds

With these cross-coupled products in hand, we next turned our attention toward using them to access more complex molecules. In addition to the taxoid scaffold, we were interested in using the inherent functionality of these products to form novel polycyclic scaffolds. The two indole containing cross-coupling products (**4.17e** and **4.17f**) were especially interesting since they possessed a nucleophilic indole unit as well as an electrophilic enone. When heated in the presence of $Yb(OTf)_3$, **4.17f** cyclized to form **4.21** containing a [3.3.1] bicycle. In the case of Boc protected indole **4.17e**, thermolysis of the carbamate followed by addition of Amberlyst®15 and $Yb(OTf)_3$ provided tetracycle **4.19**, which features a [4.3.1] bicycle. The structure and stereochemistry of these molecules was confirmed by X-ray crystallography. The tetracycle derived from **4.17e** possessed a framework reminiscent of the welwitindolinones (**4.22**) with slightly different connectivity in the bicyclic portion that would be difficult to access via semisynthesis.

Finally, we explored conditions to form the taxoid core with the tetrahydrofuran ring found in taxagifine (**4.10**). After examining a variety of bases, we found that lithium bis(trimethylsilyl)amide (LHMDS) facilitated the desired aldol reaction in good yields. The counter ion of our base proved very important as potassium bases gave only starting material. Subsequent work by our group has

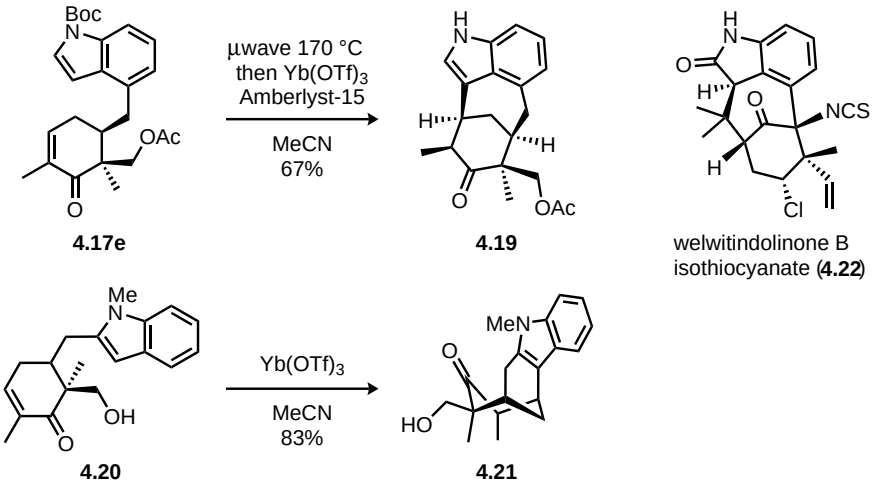

Scheme 4.5: Cyclization of indole containing cross coupled products to form bicyclic systems.

shown that the thermodynamics of this reaction can vary greatly due to relatively minor changes and that using potassium bases, the reaction equilibrium favors the starting materials. We were able to confirm the structure of our desired product **4.13**. This methodology provided us with the first synthesis of the taxagifine core in only 4 steps from carvone.

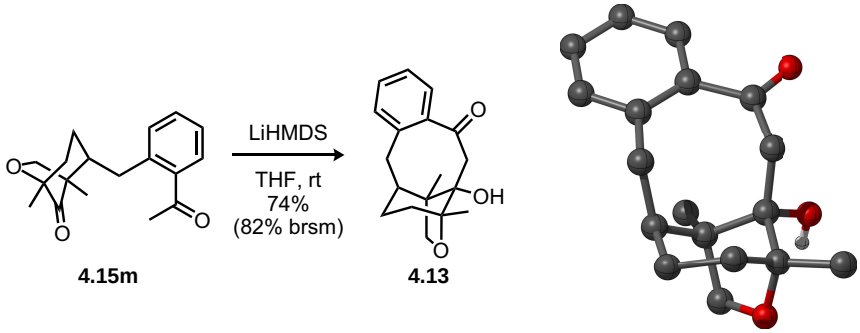

Scheme 4.6: Synthesis of the taxoid core using an aldol reaction. X-ray crystallography confirmed the structure of the product. Visualized in CYLview.

4.5 Experimental Contributors

Synthesis of cyclobutanols **4.7a** and **4.7b** was conducted by Dr. Manuel Weber (M.W.) and Dr. Ahmad Masarwa (A.M.) A method for obtaining pure **4.7b** was developed by Kyle Owens (K.O.). All cross couplings and subsequent transformations and characterization related to **4.7a** were conducted by M.W. and all cross couplings and subsequent transformations and characterization related to **4.25a** were conducted by K.O.. Non-commercial aryl bromide coupling partners were synthesized by K.O..

4.6 Experimental Details

Materials and Methods for the Experiments in Chapter 4 Unless stated otherwise, reactions were performed in flame or oven dried glassware sealed with rubber septa under a nitrogen atmosphere and were stirred with Teflon-coated magnetic stir bars. Liquid reagents and solvents were transferred by syringe using standard Schlenk techniques. Reaction temperatures above room temperature (RT), 23 °C, were controlled by a temperature modulated stir plate. Tetrahydrofuran (THF) and diethyl ether Et_2O were dried by passage over a column of activated alumina; dichloromethane was distilled over calcium hydride; dimethylformamide (DMF) was obtained in a sure-seal bottle; benzene was de-oxygenated by stirring under N_2, continuously exchanging the atmosphere; non-commercially available aryl bromides were synthesized as according to literature protocols; all other reagents and solvents were used as received from commercial sources unless stated otherwise. Thin layer chromatography was performed using pre-coated (0.25 mm) silica gel 60 F-254 plates, which were visualized by UV irradiation and anisaldehyde or $KMnO_4$ stain when necessary. Silica gel (particle size 40-63 μm) was used for flash chromatography, or the reaction products were isolated and purified using an automated Yamazen flash system. $CDCl_3$ and C_6D_6 were obtained from commercial suppliers and were used as purchased. NMR experiments were performed on Bruker spectrometers operating at 300, 400, 500 or 600 MHz for 1H nuclei, 75, 100, 125, or 150 MHz for 13C experiments, and 376 MHz when 19F was observed. Chemical shifts (δ) are reported relative to TMS using the residual solvent signal as internal reference ($CDCl_3$: 7.26 ppm for 1H, 77.16 ppm for 13C; C_6D_6: 7.16 ppm for 1H, 128.06 ppm for 13C). NMR data are reported as follows: chemical shift (multiplicity, coupling constants J [Hz] where applicable, number of hydrogens). Abbreviations are as follows: s (singlet), d (doublet), t (triplet), q (quartet), sep (septet), m (multiplet), b (broad). Melting points were recorded on a Mel-Temp II by Laboratory Devices Inc., USA and are uncorrected. Optical rotations were recorded on a Perkin Elmer Polarimeter 241 at the Na D-line (1.0 dm path length), c = 10 mg mL-1. IR spectra were recorded on a Bruker Alpha Platinum ATR spectrometer and are reported in frequency of absorption [cm-1]. High-resolution mass spectral data were obtained from the UCB Mass Spectral Facility using a Finnigan/Thermo LTQ/FT instrument for ESI, and a Waters Autospec Premiere instrument for EI. X-Ray data were collected on a Bruker APEX-II CCD diffractometer with Mo-Kα radiation (λ = 0.71073 Å) or a MicroStar-H X8 APEX-II diffractometer with Cu-Kα radiation (λ = 1.54178 Å) and analyzed by Dr. Antonio DiPasquale and Dr. Lena J. Daumann (University of California, Berkeley), structures were visualized with CYLview.

General Procedure for the Palladium-Catalyzed Ring-Opening/Cross-Coupling reaction of cyclobutanol 4.8 (GP1) Cyclobutanol **4.8**, $Pd(OAc)_2$, Cs_2CO_3, aryl bromide **4.16**, and a magnetic stir bar were added to a dry 4 ml vial. The vial was brought into a N_2 atmosphere glovebox. The ligand and benzene (2.1 mL, 0.1M) were added. The vial was sealed with a Teflon cap and the resulting mixture was stirred at room temperature for 5-10 min then the vial was placed into a pre-heated metal block and was stirred with heating for the indicated time. After cooling to room temperature, the mixture was filtered through celite using ethyl acetate and concentrated. The crude product was purified by Yamazen flash chromatography.

Conditions A: 4.8 (1.0 equiv, 208 μmol, 35.0 mg), $Pd(OAc)_2$ (0.05 equiv, 10.4 μmol, 2.3 mg), Cs_2CO_3 (2.0 equiv, 416 μmol, 135.6 mg), **4.16** (1.25 equiv, 260 μmol), (R)-BINAP (0.05 equiv, 10

μmol, 6.5 mg), 80 °C, 4 h.
Conditions B: 4.8 (1.0 equiv, 208 μmol, 35.0 mg), $Pd(OAc)_2$ (0.10 equiv, 20.8 μmol, 4.7 mg), Cs_2CO_3 (2.0 equiv, 416 μmol, 135.6 mg), **4.16** (2.0 equiv, 416 μmol), (R)-BINAP (0.1 equiv, 21 μmol, 13.0 mg) , 80 °C, 22 h.
Conditions C: 4.8 (1.0 equiv, 208 μmol, 35.0 mg), $Pd(OAc)_2$ (0.05 equiv, 10.4 μmol, 2.3 mg), Cs_2CO_3 (2.0 equiv, 416 μmol, 135.6 mg), **4.16** (1.25 equiv, 260 μmol), (R)-BINAP (0.05 equiv, 10 μmol, 6.5 mg) , 65 °C, 22 h.
Conditions D: 4.8 (1.0 equiv, 208 μmol, 35.0 mg), $Pd(OAc)_2$ (0.15 equiv, 31.2 μmol, 7.0 mg), Cs_2CO_3 (2.0 equiv, 416 μmol, 135.6 mg), **4.16** (1.0 equiv, 208 μmol), (R)-BINAP (0.15 equiv, 31 μmol, 19.4 mg) , 65 °C, 43 h.
Conditions E: 4.8 (1.0 equiv, 208 μmol, 35.0 mg), $Pd(OAc)_2$ (0.15 equiv, 31.2 μmol, 7.0 mg), Cs_2CO_3 (2.0 equiv, 416 μmol, 135.6 mg), **4.16** (2.0 equiv, 416 μmol), $P(tBu)_3$ (1.5 equiv, 312 μmol, 63.1 mg) , 65 °C, 22 h.

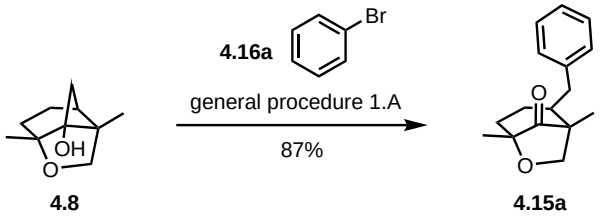

4.8 **4.15a**

Cyclobutanol **4.8** was treated according to general procedure 1.A using **4.18a** (40.8 mg, 27 μL) to give **4.17a** (44.0 mg, 180 μmol, 87%) as a colorless solid. **^{1}H NMR:** (400 MHz, $CDCl_3$) δ 7.31–7.25 (m, 2 H), 7.22–7.17 (m, 1 H), 7.10–7.05 (m, 2 H), 4.28 (d, J = 8.5, 1 H), 3.89 (d, J = 8.3, 1 H), 2.86 (dd, J = 13.7, 2.6, 1 H), 2.25–2.17 (m, 1 H), 2.07 (dd, J = 13.7, 12.3, 1 H), 2.02–1.84 (m, 3 H), 1.38–1.31 (m, 1 H), 1.26 (s, 3 H), 1.19 (s, 3 H); **^{13}C NMR:** (100 MHz, $CDCl_3$) δ 214.7, 140.6, 129.1, 128.6, 126.3, 80.0, 75.1, 52.7, 50.5, 39.3, 34.1, 20.8, 18.5, 14.1; **m.p.** 54–56 °C; **[α]D^{23}:** –24.8° (c = 0.307, CH_2Cl_2); **IR (ATR, neat) ν_{max}:** 2933, 2875, 1751, 1492, 1453, 1381, 1146, 1115, 1019, 988, 954, 923, 874, 850, 755, 740, 701, 613, 544, 498; **HRMS (EI) m/z:** calculated for $[C_{16}H_{20}O_2]^+$ 244.1463, found 244.1466.

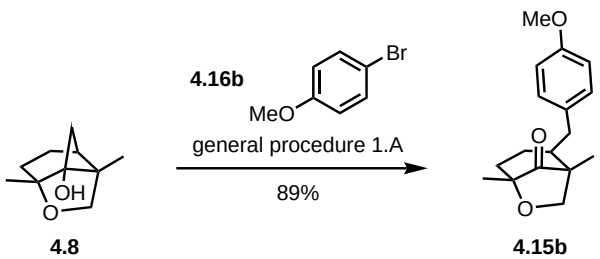

4.8 **4.15b**

Cyclobutanol **4.8** was treated according to general procedure 1.A using **4.18b** (46.8 mg, 33 μL) to give **4.17b** (51.0 mg, 186 μmol, 89%) as a colorless oil. **^{1}H NMR:** (400 MHz, $CDCl_3$)

δ 7.01–6.95 (m, 2 H), 6.84–6.79 (m, 2 H), 4.27 (d, J = 8.5, 1 H), 3.88 (d, J = 8.2, 1 H), 3.78 (s, 3 H), 2.79 (dd, J = 13.3, 2.6, 1 H), 2.19–2.11 (m, 1 H), 2.00 (dd, J = 14.0, 12.2, 1 H), 1.99–183 (m, 3 H), 1.38–1.30 (m, 1 H), 1.24 (s, 3 H), 1.18 (s, 3 H); **^{13}C NMR:** (100 MHz, $CDCl_3$) δ 214.8, 158.1, 132.6, 130.0, 114.0, 80.0, 75.2, 55.4, 52.9, 50.5, 39.3, 33.2, 20.8, 18.5, 14.1 **[α]D^{23}:** –39.9° (c = 0.193 , CH_2Cl_2); **IR (ATR, neat) ν_{max}:** 2929, 2873, 2755, 1611, 1510, 1444, 1297, 1244, 1175, 1148, 1033, 1019, 993, 853, 833, 822, 796, 742, 540, 522; **HRMS (EI) m/z:** calculated for $[C_{17}H_{22}O_3]^+$ 274.1569, found 274.1571.

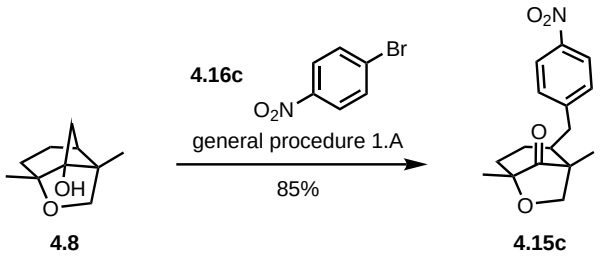

4.8 **4.15c**

Cyclobutanol **4.8** was treated according to general procedure 1.A using **4.18c** (52.5 mg) to give **4.17c** (51.1 mg, 177 μmol, 85%) as a pale yellow solid. **^{1}H NMR:** (300 MHz, $CDCl_3$) δ 8.17–8.10 (m, 2 H), 7.26–7.20 (m, 2 H), 4.28 (d, J = 8.5, 1 H), 3.84 (d, J = 8.5, 1 H), 2.99–2.86 (m, 1 H), 2.30–2.15 (m, 2 H), 2.08–1.95 (m, 1 H), 1.94–1.78 (m, 2 H), 1.26–1.17 (m, 1 H), 1.24 (s, 3 H), 1.18 (s, 3 H); **^{13}C NMR:** (300 MHz, $CDCl_3$) δ 214.4, 148.5, 146.7, 129.9, 123.9, 79.9, 75.0, 52.2, 50.4, 39.2, 34.3, 21.0, 18.4, 14.1; **m.p.** 126–128 °C; **[α]D^{23}:** –47.3° (c = 0.427, CH_2Cl_2); **IR (ATR, neat) ν_{max}:** 2934, 2886, 2873, 1756, 1593, 1512, 1492, 1446, 1377, 1339, 1314, 1256, 1207, 1170, 1146, 1106, 1092, 1034, 1016, 994, 951, 924, 882, 863, 854, 826, 807, 750, 739, 699, 651, 630, 596, 548, 528; **HRMS (EI) m/z:** calculated for $[C_{16}H_{19}NO_4]^+$ 289.1314, found 289.1316.

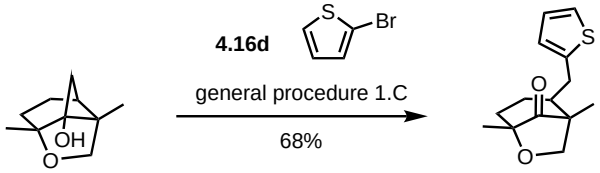

4.8 **4.15d**

Cyclobutanol **4.8** was treated according to general procedure 1.C using **4.18d** (42.4 mg, 25 μL) to give **4.17d** (35.3 mg, 142 μmol, 68%) as a colorless oil. **^{1}H NMR:** (400 MHz, $CDCl_3$) δ 7.20–7.15 (m, 1 H), 6.98–6.92 (m, 1 H), 6.79–6.74 (m, 1 H), 4.33 (d, J = 8.1, 1 H), 3.92 (d, J = 8.3, 1 H), 3.07–2.99 (m, 1 H), 2.42 (dd, J = 15.0, 12.1, 1 H), 2.33–2.23 (m, 1 H), 2.14–2.01 (m, 1 H), 1.98–1.80 (m, 1 H), 1.56–1.46 (m, 1 H), 1.34–1.17 (m, 1 H), 1.28 (s, 3 H), 1.21 (s, 3 H); **^{13}C NMR:** (100 MHz, $CDCl_3$) δ 214.6, 143.2, 127.0, 125.5, 123.8, 80.0, 75.1, 53.1, 50.4, 39.3, 28.6, 21.3, 18.5, 13.9; **[α]D^{23}:** –27.1° (c = 0.447, CH_2Cl_2); **IR (ATR, neat) ν_{max}:** 2977, 2928, 2872, 1754, 1443, 1377, 1295, 1257, 1220, 1196, 1162, 1131, 1118, 1102, 1078, 1045, 1019, 994, 924, 878, 852, 840, 804, 756, 745, 691, 627, 587, 546, 508; **HRMS (EI) m/z:** calculated for $[C_{14}H_{18}O_2S]^+$ 250.1028, found 250.1027.

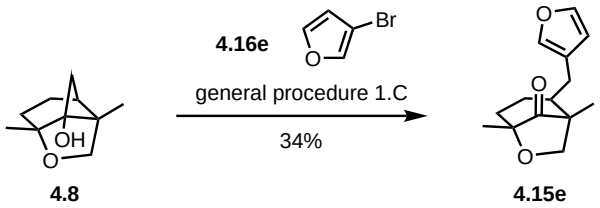

4.8 **4.15e**

Cyclobutanol **4.8** was treated according to general procedure 1.C using **4.18e** (38.2 mg, 23 μL) to give **4.17e** (16.4 mg, 70 μmol, 34%) as a colorless solid. **^{1}H NMR:** (400 MHz, $CDCl_3$) δ 7.35 (t, J = 1.5, 1 H), 7.17 (s, 1 H), 6.18 (d, J = 0.9, 1 H), 4.28 (d, J = 8.2, 1 H), 3.87 (d, J = 8.2, 1 H), 2.60–2.54 (m, 1 H), 2.16–2.08 (m, 1 H), 2.08–1.93 (m, 2 H), 1.90–1.73 (m, 2 H), 1.48–1.40 (m, 1 H), 1.23 (s, 3 H), 1.14 (s, 3 H); **^{13}C NMR:** (100 MHz, $CDCl_3$) δ 214.7, 143.3, 139.7, 123.2, 110.4, 80.0, 75.2, 51.3, 50.4, 39.3, 23.4, 21.3, 18.5, 14.0; **[α]D^{23}:** 6.5° (c =0.413, CH_2Cl_2); **IR (ATR, neat) ν_{max}:** 2976, 2930, 2875, 1754, 1501, 1447, 1378, 1218, 1175, 1160, 1144, 1117, 1065, 1041, 1020, 993, 924, 872, 847, 826, 810, 776, 755, 726, 622; **HRMS (EI) m/z:** calculated for $[C_{14}H_{18}O_3]^+$ 234.1256, found 234.1259

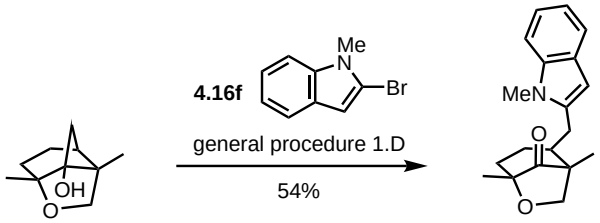

4.8 **4.15f**

Cyclobutanol **4.8** was treated according to general procedure 1.D using **4.18f** (43.7 mg) to give **4.17f** (33.5 mg, 113 μmol, 54%) as a pale yellow solid. **^{1}H NMR:** (400 MHz, $CDCl_3$) δ 7.53 (dt, J = 7.8, 0.9, 1 H), 7.27 (dt, J = 8.3, 0.9, 1 H), 7.18 (td, J = 6.9, 1.1, 1 H), 7.09 (td, J = 7.8, 1.0, 1 H), 6.21 (b, 1 H), 4.34 (d, J = 8.3, 1 H), 3.92 (d, J = 8.4, 1 H), 3.64 (s, 3 H), 2.97–2.84 (m, 1 H), 2.42–2.27 (m, 2 H), 2.15–2.02 (m, 1 H), 1.98–1.83 (m, 2 H), 1.64–1.55 (m, 1 H), 1.28 (s, 3 H), 1.23 (s, 3 H); **^{13}C NMR:** (100 MHz, $CDCl_3$) δ 214.7, 138.7, 137.5, 127.8, 121.0, 119.9, 119.6, 109.0, 100.5, 80.1, 75.1, 50.4, 50.1, 39.6, 29.8, 25.5, 21.6, 18.5, 14.0; **m.p.** 92–94 °C; **[α]D^{23}:** –50.9° (c = 0.513, CH_2Cl_2); **IR (ATR, neat) ν_{max}:** 2980, 2931, 2885, 2846, 1747, 1543, 1467, 1448, 1396, 1376, 1360, 1334, 1313, 1216, 1154, 1138, 1116, 1095, 1023, 992, 922, 904, 882, 855, 840, 826, 816, 783, 774, 750, 704, 683, 629, 565; **HRMS (ESI) m/z:** calculated for $[C_{19}H_{24}NO_2]^+$ 298.1802, found 298.1800.

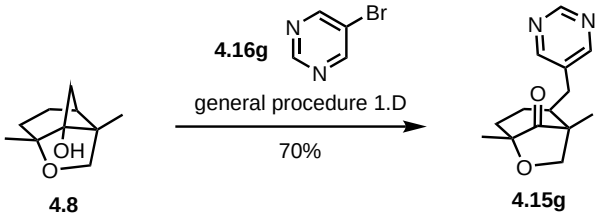

Cyclobutanol **4.8** was treated according to general procedure 1.D using **4.18g** (33.1 mg) to give **4.17g** (36.1 mg, 147 μmol, 70%) as a colorless solid. **^{1}H NMR:** (400 MHz, $CDCl_3$) δ 9.06 (s, 1 H), 8.47 (s, 2 H), 4.27 (d, J = 8.4, 1 H), 3.84 (d, J = 8.6, 1 H), 2.82 (dd, J = 13.6, 1.5, 1 H), 2.23–2.14 (m, 1 H), 2.10–1.97 (m, 1 H), 2.07 (dd, J = 14.0, 12.1, 1 H), 1.96–1.75 (m, 2 H), 1.26–1.16 (m, 1 H), 1.24 (s, 3 H), 1.18 (s, 3 H); **^{13}C NMR:** (100 MHz, $CDCl_3$) δ 214.2, 157.2, 133.7, 79.9, 74.9, 51.8, 50.3, 39.1, 29.0, 20.9, 18.4, 14.1; **m.p.** 101–103 °C; **[α]D^{23}:** –23.1° (c = 0.333, CH_2Cl_2); **IR (ATR, neat) ν_{max}:** 2978, 2959, 2932, 2881, 1754, 1558, 1452, 1434, 1406, 1378, 1341, 1288, 1237, 1218, 1202, 1173, 1147, 1105, 1041, 1020, 991, 954, 925, 910, 876, 851, 829, 808, 752, 731, 631, 592; **HRMS (ESI) m/z:** calculated for $[C_{14}H_{19}N_2O_2]^+$ 247.1441, found 247.1441.

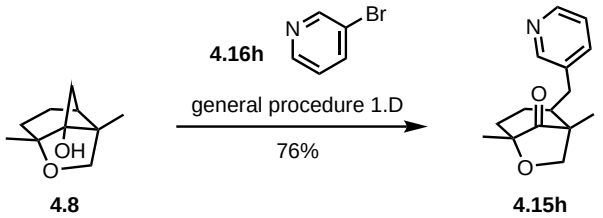

Cyclobutanol **4.8** was treated according to general procedure 1.D using **4.18h** (32.9 mg, 20 μL) to give **4.17h** (38.7 mg, 158 μmol, 76%) as a colorless solid. **^{1}H NMR:** (400 MHz, $CDCl_3$) δ 8.44 (dd, J = 4.7, 1.5, 1 H), 8.33 (d, J = 2.1, 1 H), 7.38 (dt, J = 7.8, 1.9, 1 H), 7.20 (ddd, J = 7.8, 4.8, 0.7, 1 H), 4.26 (d, J = 8.4, 1 H), 3.88 (d, J = 8.3, 1 H), 2.82 (dd, J = 14.0, 2.3, 1 H), 2.21–2.14 (m, 1 H), 2.07 (dd, J = 13.9, 12.4, 1 H), 2.03–1.92 (m, 1 H), 1.92–1.78 (m, 2 H), 1.29–1.25 (m, 1 H), 1.23 (s, 3 H), 1.18 (s, 3 H); **^{13}C NMR:** (100 MHz, $CDCl_3$) δ 214.4, 150.4, 147.9, 136.4, 135.9, 123.5, 80.0, 75.0, 52.3, 50.4, 39.2, 31.4, 20.8, 18.4, 14.1; **m.p.** 71–73 °C; **[α]D^{23}:** –22.2° (c = 0.36, CH_2Cl_2); **IR (ATR, neat) ν_{max}:** 2984, 2932, 2874, 1754, 1575, 1476, 1452, 1423, 1377, 1298, 1219, 1196, 1172, 1148, 1115, 1096, 1041, 1021, 994, 925, 878, 852, 830, 810, 785, 751, 714, 633, 613, 584, 548, 509; **HRMS (ESI) m/z:** calculated for $[C_{15}H_{20}NO_2]^+$ 246.1489, found 246.1486.

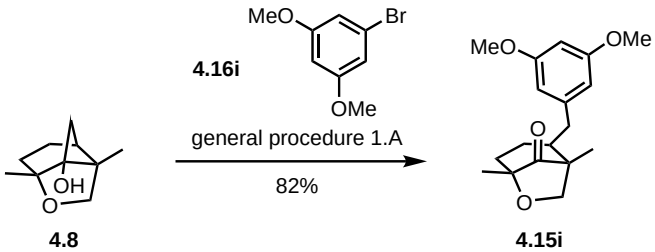

Cyclobutanol **4.8** was treated according to general procedure 1.A using **4.18i** (56.5 mg) to give **4.17i** (51.7 mg, 170 μmol, 82%) as a colorless solid. **^{1}H NMR:** (400 MHz, $CDCl_3$) δ 6.29 (t, J = 2.4 1 H), 6.21 (d, J = 2.3, 2 H), 4.27 (d, J = 8.3, 1 H), 3.87 (d, J = 8.2, 1 H), 3.75 (s, 6 H), 2.78 (dd, J = 13.7, 3.1, 1 H), 2.25–2.15 (m, 1 H), 1.98 (dd, J = 13.8, 12.4, 1 H), 2.01–1.90 (m, 1 H), 1.89–1.80 (m, 2 H), 1.41–1.32 (m, 1 H), 1.23 (s, 3 H), 1.16 (s, 3 H); **^{13}C NMR:** (100 MHz, $CDCl_3$) δ 214.7, 160.9, 142.9, 107.2, 97.8, 80.0, 75.1, 55.3, 52.4, 50.4, 39.4, 34.4, 21.0, 18.5, 14.0; **m.p.** 88–90 °C; **[α]D^{23}:** –21.4° (c = 0.467, CH_2Cl_2); **IR (ATR, neat) ν_{max}:** 3002, 2929, 2881, 2838, 1750, 1611, 1586, 1501, 1457, 1430, 1378, 1315, 1202, 1158, 1108, 1063, 1019, 990, 958, 944, 935, 917, 848, 809, 753, 706, 687, 639, 622, 593; **HRMS (EI) m/z:** calculated for $[C_{18}H_{24}O_4]^+$ 304.1675, found 304.1678.

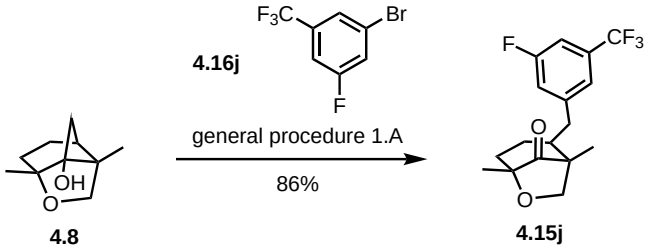

Cyclobutanol **4.8** was treated according to general procedure 1.A using **4.18j** (63.2 mg, 42 μL) to give **4.17j** (59.4 mg, 180 μmol, 86%) as a colorless solid. **^{1}H NMR:** (400 MHz, $CDCl_3$) δ 7.15 (d, 8.3, 1 H), 7.11 (m, 1 H), 6.97 (d, J = 9.2, 1 H), 4.28 (d, J = 8.4, 1 H), 3.89 (d, J = 8.4, 1 H), 2.88 (d, J = 13.3, 1 H), 2.26–2.18 (m, 1 H), 2.15 (dd, J = 13.3, 12.3, 1 H), 2.08–1.95 (m, 1 H), 1.94 (m, 2 H), 1.28–1.20 (m, 1 H), 1.24 (s, 3 H), 1.17 (s, 3 H); **^{13}C NMR:** (100 MHz, $CDCl_3$) δ 214.3, 163.5, 161.8, 144.5 (d, 7.3), 132.7 (qd, 33.1, 8.6), 123.3 (qd, 272.5, 3.1), 121.5 (m), 119.5 (d, 119.4), 80.0, 75.0, 52.2, 50.4, 39.3, 34.1, 21.0, 18.4, 14.0; **m.p.** 117–119°C; **[α]D^{23}:** –19.6° (c = 0.46, CH_2Cl_2); **IR (ATR, neat) ν_{max}:** 2979, 2932, 2890, 2850, 1755, 1598, 1455, 1358, 13333, 1283, 1265, 1230, 1164, 1121, 1087, 1043, 1020, 996, 983, 955, 926, 983, 955, 926, 912, 895, 882, 875, 864, 848, 827, 806, 754, 720, 656, 639, 626, 587, 563; **HRMS (EI) m/z:** calculated for $[C_{17}H_{18}F_4O_2]^+$]+ 330.1243, found 330.1249.

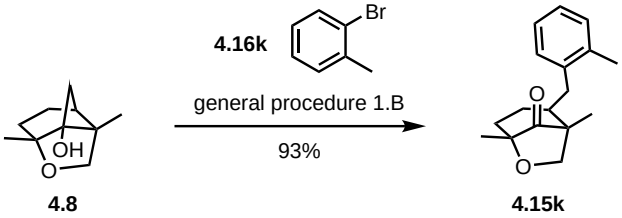

Cyclobutanol **4.8** was treated according to general procedure 1.B using **4.18k** (71.2 mg, 50 μL) to give **4.17k** (49.0 mg, 193 μmol, 93%) as a colorless solid. **^{1}H NMR:** (400 MHz, $CDCl_3$) δ 7.16–7.08 (m, 3 H), 7.01–6.95 (m, 1 H), 4.29 (d, 8.4, 1 H), 3.89 (d, J = 8.4, 1 H), 2.84 (dd, J = 13.7, 2.0, 1 H), 2.27 (s, 3 H), 2.24–2.17 (m, 1 H), 2.13 (dd, J = 13.6, 12.3, 1 H), 2.03–1.88 (m, 3

H), 1.42–1.33 (m, 1 H), 1.26 (s, 3 H), 1.22 (s, 3 H); **^{13}C NMR:** (100 MHz, $CDCl_3$) δ 214.7, 138.6, 136.2, 130.6, 130.2, 126.5, 126.0, 80.0, 75.2, 51.0, 50.6, 39.7, 31.3, 20.8, 19.7, 18.5, 13.9; **m.p.** 80–82°C; **[α]D^{23}:** –15.6° (c = 0.82, CH_2Cl_2); **IR (ATR, neat) ν_{max}:** 2976, 2963, 2946, 2927, 2872, 1756, 1714, 1488, 1453, 1378, 1297, 1220, 1175, 1151, 1120, 1095, 1055, 1038, 1019, 1000, 954, 941, 923, 883, 868, 858, 825, 752, 738, 618, 592; **HRMS (EI) m/z:** calculated for $[C_{17}H_{22}O_2]^+$ 258.1620, found 258.1625.

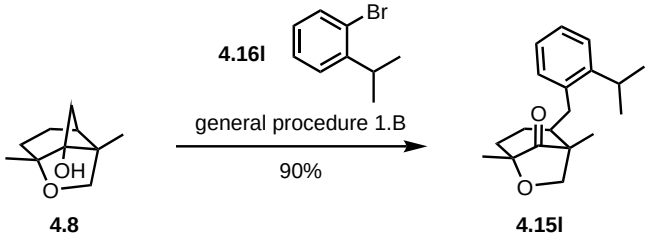

4.8 **4.15l**

Cyclobutanol **4.8** was treated according to general procedure 1.B using **4.18l** (82.8 mg, 64 μL) to give **4.17l** (53.3 mg, 186 μmol, 90%) as a colorless solid. **^{1}H NMR:** (400 MHz, $CDCl_3$) δ 7.27 (dd, J = 7.8, 1.3, 1 H), 7.20 (td, J = 7.4, 1.2, 1 H), 7.08 (td, J = 7.5, 1.5, 1 H), 6.97 (dd, J = 7.5, 1.1, 1 H), 4.29 (d, J = 8.3, 1 H), 3.90 (d, J = 8.4, 1 H), 3.02 (sep, 6.9, 1 H), 2.95–2.82 (m, 1 H), 2.21–2.07 (m, 2 H), 2.02–1.87 (m, 3 H), 1.41–1.34 (m, 1 H), 1.27 (s, 3 H), 1.23 (s, 3 H), 1.22 (d, J = 4.1, 3 H), 1.21 (d, J = 4.1, 3 H); **^{13}C NMR:** (100 MHz, $CDCl_3$) δ 214.7, 147.1, 136.9, 130.6, 126.9, 125.6, 80.1, 75.3, 52.3, 50.7, 39.7, 30.6, 28.8, 24.2, 20.6, 18.5, 13.9; **m.p.** 118–120 °C; **[α]D^{23}:** –15.3° (c = 0.347, CH_2Cl_2); **IR (ATR, neat) ν_{max}:** 2968, 2957, 2929, 2889, 2873, 1747, 1490, 1449, 1380, 1361, 1221, 1163, 1147, 1113, 1079, 1020, 989, 951, 926, 867, 849, 826, 763, 750, 719, 615, 593, 555; **HRMS (EI) m/z:** calculated for $[C_{19}H_{26}O_2]^+$ 286.1933, found 286.1933.

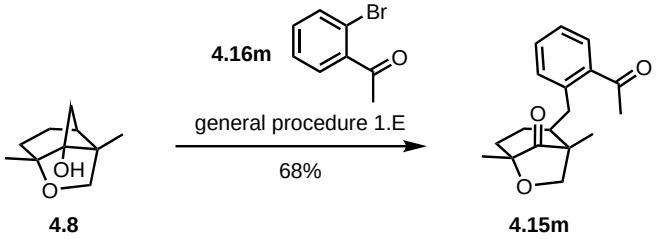

4.8 **4.15m**

Cyclobutanol **4.8** was treated according to general procedure 1.A using **4.18m** (82.8 mg, 56 μL) to give **4.17m** (40.5 mg, 141 μmol, 68%) as an off white solid.

^{1}H NMR: (400 MHz, $CDCl_3$) δ 7.70 (d, J = 7.8, 1 H), 7.38 (tt, J = 8.6, 0.9, 1 H), 7.29 (tt, J = 7.5, 0.9, 1 H), 7.08 (d, J = 7.7, 1 H), 4.25 (d, J = 8.3, 1 H), 3.86 (d, J = 8.3, 1 H), 2.56 (s, 3 H), 2.32–2.24 (m, 1 H), 2.22 (dd, J = 12.5, 12.0, 1 H), 2.00–1.82 (m, 3 H), 1.27–1.18 (m, 2 H), 1.24 (s, 6 H); **^{13}C NMR:** (100 MHz, $CDCl_3$) δ 215.0, 201.6, 140.8, 137.6, 132.9, 131.6, 130.2, 126.5, 80.0, 75.4, 51.5, 50.8, 39.8, 32.3, 29.9, 20.7, 18.5, 13.6; **m.p.** 118–120 °C; **[α]D^{23}:** –45.5° (c = 0.62 , CH_2Cl_2); **IR (ATR, neat) ν_{max}:** 2976, 2930, 2873, 1755, 1682, 1598, 1570, 1485, 1444, 1377, 1354, 1296, 1250, 1223, 1193, 1175, 1154, 1129, 1098, 1071, 1046, 1019, 993, 950, 921,

883, 871, 851, 825, 806, 760, 732, 639, 615, 599, 584, 550, 509; **HRMS (ESI) m/z:** calculated for $[C_{18}H_{22}O_3Na]^+$ 309.1461, found 309.1461.

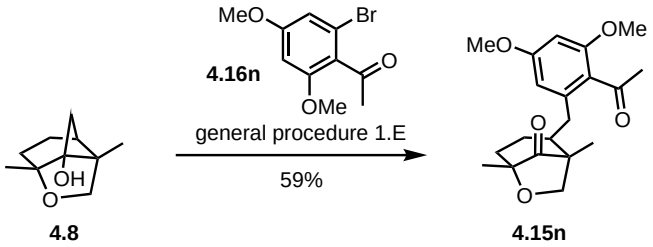

Cyclobutanol **4.8** was treated according to general procedure 1.A using **4.18n** (107.8 mg) to give **4.17n** (42.4 mg, 122 μmol, 59%) as a yellow oil.

^{1}H NMR: (500 MHz, $CDCl_3$) δ 6.31 (d, J = 1.9, 1 H), 6.15 (d, J = 1.8, 1 H), 4.24 (d, J = 8.4, 1 H), 3.83 (d, J = 8.2, 1 H), 3.79 (s, 3 H), 3.78 (s, 3 H), 2.80 (dd, J = 13.7, 2.8, 1 H), 2.42 (s, 3 H), 2.26–2.13 (m, 1 H), 2.06–1.78 (m, 4 H), 1.42–1.31 (m, 1 H), 1.21 (s, 3 H), 1.12 (s, 3 H); **^{13}C NMR:** (125 MHz, $CDCl_3$) δ 214.8, 204.6, 161.1, 158.6, 140.2, 124.5, 107.9, 96.2, 80.0, 75.2, 55.7, 55.5, 52.2, 50.5, 39.6, 32.8, 31.5, 20.6, 18.5, 13.7; **[α]D^{23}:** –24.5° (c = 0.366, CH_2Cl_2); **IR (ATR, neat) ν_{max}:** 2932, 2874, 2841, 1754, 1684, 1599, 1577, 1454, 1419, 1378, 1349, 1317, 1291, 1258, 1222, 1202, 1155, 1113, 1086, 1043, 1019, 994, 956, 917, 880, 846, 731, 644, 592, 568, 542, 511; **HRMS (ESI) m/z:** calculated for $[C_{20}H_{26}O_5Na]^+$ 369.1672, found 369.1673.

General Procedure for the Palladium-Catalyzed Ring-Opening/Cross-Coupling reaction of cyclobutanol 4.9 (GP2) Cyclobutanol **4.9** (1.0 equiv, 197 μmol, 41.4 mg), $Pd(OAc)_2$ (0.1 equiv, 19.7 μmol, 4.4 mg), Cs_2CO_3 (2.0 equiv, 394 μmol, 128.0 mg), aryl bromide **4.18** (1.1 equiv, 216 μmol), and a magnetic stir bar were added into a 4 ml vial. The vial was brought intoa a N_2 atmosphere glove box and (R)-BINAP (0.1 equiv, 19.7 μmol, 12.3 mg) followed by benzene (2.0 mL, 0.1M) were added. The vial was sealed with a Teflon cap and the resulting mixture was stirred at room temperature for 5-10 min. After this time, the vial was placed into a pre-heated (65 °C) metal block and stirred for 18 hours. After cooling to room temperature, the mixture was filtered through celite using ethyl acetate and concentrated. The crude product was purified by Yamazen flash chromatography.

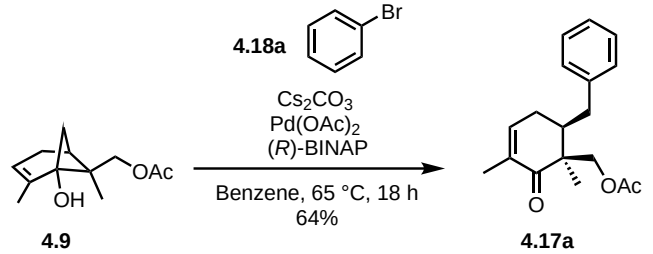

Cyclobutanol **4.9** was treated according to general procedure 2 using **4.18a** (21.0 mg) to give **4.17a** (36.1 mg, 126 μmol, 64%) as a colorless oil. **^{1}H NMR:** (600 MHz, $CDCl_3$) δ 7.29 (t, J = 7.6, 2 H), 7.21 (t, J = 7.3, 1 H), 7.10 (d, J = 7.4, 2 H), 6.52 (s, 1 H), 4.35 (d, J = 11.4, 1 H), 4.27 (d, J = 11.4, 1 H), 2.97 (dd, J = 13.2, 2.7, 1 H), 2.37 (t, J = 12.4, 1 H), 2.21 (d, J = 21.2, 2 H), 2.12 (d, J = 17.1, 1 H), 2.07 (s, 3 H), 1.78 (s, 3 H), 1.34 (s, 3 H); **^{13}C NMR:** (151 MHz, $CDCl_3$) δ 201.5, 170.9, 142.0, 140.3, 134.3, 129.1, 128.6, 126.4, 66.4, 48.5, 44.0, 35.8, 27.6, 21.0, 19.7, 16.4; **[α]D^{23}:** 4.3° (c = 0.938, CH_2Cl_2); **IR (ATR, neat) ν_{max}:** 3025, 2975, 2923, 1738, 1664, 1602, 1494, 1452, 1433, 1364, 1230, 1077, 1029, 999, 950, 913, 865, 834, 767, 740, 702, 632, 603, 505, 454; **HRMS (ESI) m/z:** calculated for $[C_{18}H_{22}O_3Na]^+$ 309.1461, found 309.1461.

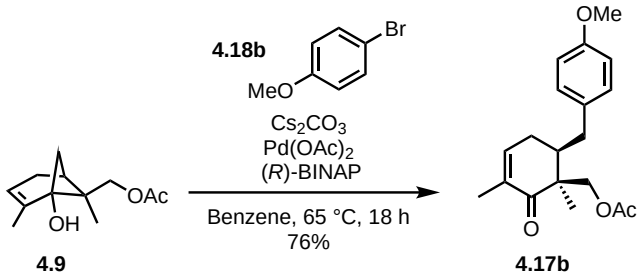

4.9 **4.17b**

Cyclobutanol **4.9** was treated according to general procedure 2 using **4.18b** (37.8 mg) to give **4.17b** (47.2 mg, 149 μmol, 76%) as a colorless oil. **^{1}H NMR:** (600 MHz, $CDCl_3$) δ 7.01 (d, J = 8.5, 2 H), 6.88–6.78 (m, 2 H), 6.53 (s, 1 H), 4.34 (d, J = 11.4, 1 H), 4.26 (d, J = 11.4, 1 H), 3.79 (s, 3 H), 2.91 (dd, J = 13.3, 2.7, 1 H), 2.31 (dd, J = 13.4, 11.5, 1 H), 2.25–2.15 (m, 2 H), 2.14–2.09 (m, 1 H), 2.07 (s, 3 H), 1.77 (d, J = 1.7, 3 H), 1.32 (s, 3 H); **^{13}C NMR:** (151 MHz, $CDCl_3$) δ 201.6, 171.0, 158.2, 142.1, 134.2, 132.2, 130.0, 114.0, 66.4, 55.4, 48.5, 44.1, 34.8, 27.6, 21.1, 19.7, 16.5; **[α]D^{23}:** 5.8° (c = 1.075, CH_2Cl_2); **IR (ATR, neat) ν_{max}:** 2923, 2835, 1739, 1664, 1610, 1583, 1511, 1457, 1364, 1299, 1235, 1177, 1106, 1086, 1032, 998, 950, 903, 867, 841, 809, 758, 600, 523; **HRMS (ESI) m/z:** calculated for $[C_{19}H_{24}O_4Na]^+$ 339.1576, found 339.1576.

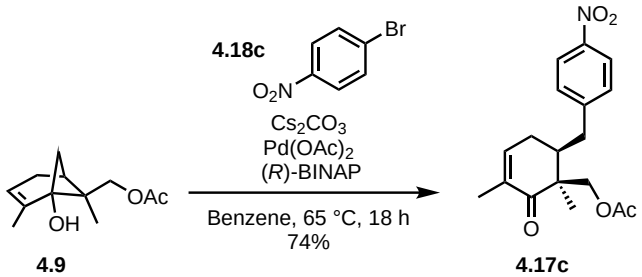

4.9 **4.17c**

Cyclobutanol **4.9** was treated according to general procedure 2 using **4.18c** (41.4 mg) to give **4.17c** (48.1 mg, 145 μmol, 74%) as a yellow solid. **^{1}H NMR:** (600 MHz, $CDCl_3$) δ = 8.15 (d, J = 8.6, 2 H), 7.27 (d, J = 8.5, 2 H), 6.51 (s, 1 H), 4.34 (d, J = 11.5, 1 H), 4.28 (d, J = 11.5, 1 H), 3.06 (dd, J = 13.3, 3.1, 1 H), 2.52 (dd, J = 13.2, 11.9, 1 H), 2.31–2.26 (m, 1 H), 2.21 (d, J = 21.2, 1 H), 2.12–2.04 (m, 1 H), 2.08 (s, 3 H), 1.78 (d, J = 1.4, 3 H), 1.34 (s, 3 H); **^{13}C NMR:** (151

MHz, $CDCl_3$) δ 200.9, 170.8, 148.2, 146.9, 141.1, 134.6, 129.9, 123.9, 66.2, 48.5, 43.7, 35.7, 27.4, 21.0, 19.9, 16.4; **m.p.** 85–88 °C; **[α]D^{23}:** 5.8° (c = 1.203, CH_2Cl_2); **IR (ATR, neat) ν_{max}:** 2977, 2923, 1739, 1665, 1599, 1517, 1451, 1434, 1365, 1344, 1233, 1109, 1033, 999, 952, 906, 856, 831, 806, 744, 707, 630, 602, 583; **HRMS (ESI) m/z:** calculated for $[C_{18}H_{22}NO_5]^+$ 332.1492, found 332.1488.

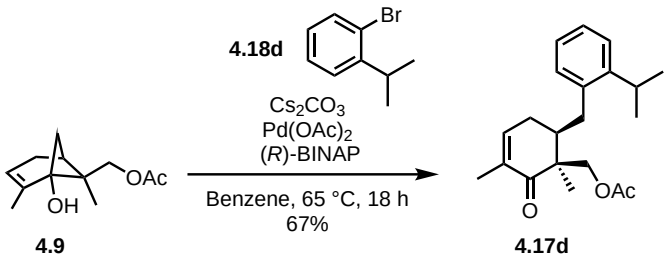

Cyclobutanol **4.9** was treated according to general procedure 2 using **4.18d** (44.2, 34 μL) to give **4.17d** (43.1 mg, 132 μmol, 67%) as a colorless oil. **^{1}H NMR:** (600 MHz, $CDCl_3$) δ 7.27 (d, J = 7.8, 1 H), 7.20 (t, J = 7.4, 1 H), 7.09 (t, J = 7.2, 1 H), 6.98 (d, J = 7.4, 1 H), 6.53 (s, 1 H), 4.41 (d, J = 11.4, 1 H), 4.31 (d, J = 11.4, 1 H), 3.08 (sep, J = 7.3, 6.8, 1 H), 2.99 (dd, J = 13.2, 1.5, 1 H), 2.43 (t, J = 12.4, 1 H), 2.22 (d, J = 14.4, 2 H), 2.16–2.10 (m, 1 H), 2.09 (s, 3 H), 1.79 (s, 3 H), 1.35 (s, 3 H), 1.25–1.16 (m, 6H); **^{13}C NMR:** (151 MHz, $CDCl_3$) δ 201.8, 171.0, 147.1, 142.0, 136.4, 134.1, 126.9, 125.7, 125.6, 100.1, 66.4, 48.6, 42.9, 32.0, 28.6, 26.9, 24.2, 21.0, 19.9, 16.4; **[α]D^{23}:** 9.8° (c = 1.042, CH_2Cl_2); **IR (ATR, neat) ν_{max}:** 2961, 2925, 2871, 1740, 1664, 1488, 1451, 1381, 1362, 1230, 1081, 1031, 998, 949, 905, 833, 760, 737, 701, 602, 501; **HRMS (ESI) m/z:** calculated for $[C_{21}H_{28}O_3Na]^+$ 331.1931, found 331.1931.

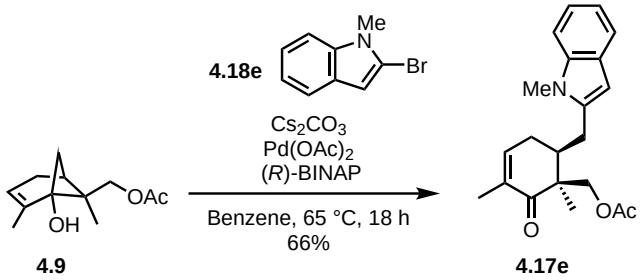

Cyclobutanol **4.9** (82 mg, 390 μmol) was treated according to general procedure 2 scale using **4.18e** (82.0 mg) to give **4.17e** (134.0 mg, 320 μmol, 81%) as a white solid. **^{1}H NMR:** (500 MHz, $CDCl_3$) δ 8.03 (d, J = 8.2, 1 H), 7.60 (s, 1 H), 7.24 (t, J = 7.8, 1 H), 6.95 (d, J = 7.3, 1 H), 6.53 (d, J = 3.9, 1 H), 6.49 (s, 1 H), 4.46 (d, J = 11.5, 1 H), 4.33 (d, J = 11.4, 1 H), 3.19 (dd, J = 13.2, 3.4, 1 H), 2.64 (t, J = 12.6, 1 H), 2.42–2.33 (m, 1 H), 2.13 (s, 3 H), 2.19–2.03 (m, 2 H), 1.79 (s, 3 H), 1.67 (s, 9 H), 1.39 (s, 3 H); **^{13}C NMR:** (126 MHz, $CDCl_3$) δ 201.7, 171.0, 149.8, 142.1, 135.3, 134.1, 132.5, 130.0, 125.8, 124.4, 123.4, 113.5, 105.2, 83.9, 66.5, 48.6, 43.0, 32.7, 28.3, 27.4, 21.1, 19.9, 16.4; **m.p.** 123–126 °C; **[α]D^{23}:** 16.5° (c = 0.803, CH_2Cl_2); **IR (ATR, neat) ν_{max}:** 2977, 2930,

1732, 1665, 1599, 1533, 1481, 1454, 1428, 1383, 1369, 1344, 1324, 1297, 1282, 1232, 1154, 1122, 1028, 999, 983, 950, 909, 851, 825, 796, 760, 731, 646, 603, 460; **HRMS (ESI) m/z:** calculated for $[C_{25}H_{28}NO_5Na]^+$ 448.2904, found 448.2903.

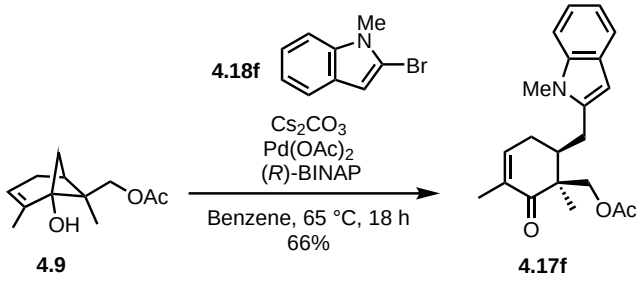

Cyclobutanol **4.9** was treated according to general procedure 2 using **4.18f** (41.4 mg) to give **4.17f** (44 mg, 130 μmol, 66%) as a yellow solid. **^{1}H NMR:** (500 MHz, $CDCl_3$) δ 7.54 (d, J = 7.8, 1 H), 7.28 (d, J = 8.2, 1 H), 7.19 (t, J = 7.6, 1 H), 7.10 (t, J = 7.4, 1 H), 6.56 (s, 1 H), 6.25 (s, 1 H), 4.44 (d, J = 11.6, 1 H), 4.33 (d, J = 11.6, 1 H), 3.66 (s, 3 H), 3.03 (dd, J = 14.7, 2.6, 1 H), 2.67 (dd, J = 14.6, 11.8, 1 H), 2.46–2.32 (m, 2 H), 2.28 (d, J = 19.0, 1 H), 2.09 (s, 3 H), 1.81 (s, 3 H), 1.38 (s, 3 H); **^{13}C NMR:** (126 MHz, $CDCl_3$) δ 201.4, 170.9, 142.0, 138.3, 137.6, 134.2, 127.8, 121.1, 119.9, 119.7, 109.0, 101.0, 66.3, 48.4, 41.2, 29.7, 27.5, 26.7, 21.1, 20.1, 16.4; **m.p.** 75–77 °C; **[α]D^{23}:** –16.6° (c = 0.67, CH_2Cl_2); **IR (ATR, neat) ν_{max}:** 2972, 2927, 1741, 1665, 1544, 1467, 1433, 1382, 1364, 1339, 1315, 1234, 1087, 1032, 999, 905, 777, 749, 448; **HRMS (ESI) m/z:** calculated for $[C_{21}H_{26}NO_3]^+$ 340.1907, found 340.1908.

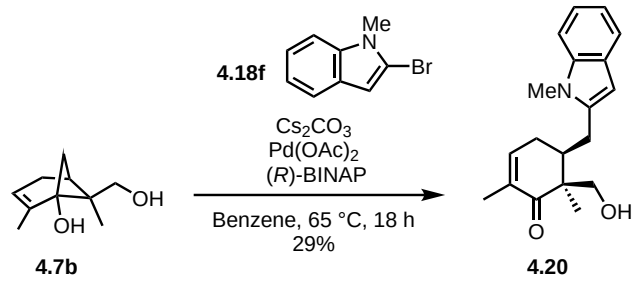

Cyclobutanol **4.7b** (300 mg, 1.78 mmol) was treated according to a modified general procedure 2 using a larger excess of **4.18f** (562 mg, 2.67 mmol, 1.5 equiv) to give **4.26** (155 mg, 0.516 mmol, 29%) as a pale yellow oil. **^{1}H NMR:** (400 MHz, $CDCl_3$) δ 7.57 (d, 7.9, 1 H), 7.30 (d, 8.2, 1 H), 7.21 (t, 7.1, 1 H), 7.13 (t, 7.4, 1 H), 6.61 (t, 4.3, 1 H), 6.27 (s, 1 H), 4.04 (dd, 11.1, 2.9, 1 H), 3.77 (dd, 10.9, 6.1, 1 H), 3.67 (s, 3 H), 3.11 (dd, 14.7, 2.5, 1 H), 2.73–2.59 (m, 2 H), 2.54–2.41 (m, 1 H), 2.39–2.27 (m, 1 H), 1.87 (s, 3 H), 1.39 (s, 3 H); **^{13}C NMR:** (100 MHz, $CDCl_3$) δ 204.6, 142.7, 138.8, 137.5, 134.1, 127.7, 120.9, 119.5, 109.0, 100.7, 66.1, 49.6, 41.9, 29.7, 27.2, 26.3, 20.1, 16.1; **[α]D^{23}:** –56.0° (c = 0.945, CH_2Cl_2); **IR (ATR, neat) ν_{max}:** 3458, 2924, 2886, 1656, 1541, 1466, 1433, 1400, 1362, 1338, 1314, 1233, 1202, 1181, 1046, 1024, 995, 906, 778, 748, 734; **HRMS (ESI) m/z:** calculated for $[C_{19}H_{24}NO_2]^+$ 298.1802, found 298.1801.

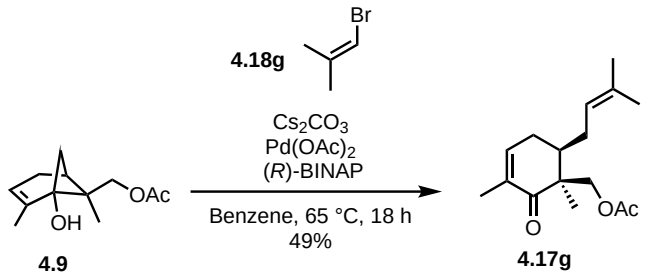

Cyclobutanol **4.9** was treated according to general procedure 2 using **4.18g** (33.0, 25 μL) to give **4.17g** (25.8 mg, 97 μmol, 49%) as a light yellow oil. **^{1}H NMR:** (500 MHz, $CDCl_3$) δ 6.57 (s, 1 H), 5.06–5.01 (m, 1 H), 4.28 (d, J = 11.3, 1 H), 4.16 (d, J = 11.3, 1 H), 2.47–2.40 (m, 1 H), 2.22–2.12 (m, 2 H), 2.02 (s, 3 H), 1.99–1.87 (m, 2 H), 1.76 (d, J = 1.5, 3 H), 1.69 (s, 3 H), 1.56 (s, 3 H), 1.24 (s, 3 H); **^{13}C NMR:** (151 MHz, $CDCl_3$) δ 202.0, 171.0, 142.2, 134.1, 133.7, 122.5, 66.5, 48.4, 42.5, 28.1, 27.9, 25.9, 21.0, 19.6, 18.0, 16.4; **[α]D^{23}:** –26.4° (c = 0.933, CH_2Cl_2); **IR (ATR, neat) ν_{max}:** 2969, 2920, 1740, 1665, 1555, 1537, 1451, 1433, 1363, 1231, 1104, 1031, 987, 907, 849, 830; **HRMS (ESI) m/z:** calculated for $[C_{16}H_{24}O_3Na]^+$ 287.1618, found 287.1612.

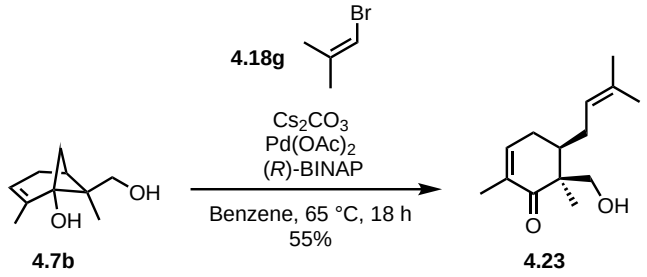

Cyclobutanol **4.7b** was treated according to a modified general procedure 2 using **4.18g** (33 mg, 25 μL) and S-BINAP (0.1 equiv) to give **4.23** (24.1 mg, 111 μmol, 55%) as a colorless oil. **^{1}H NMR:** (600 MHz, $CDCl_3$) δ 6.57 (t, 3.5, 1 H), 5.02 (t, 5.3, 1 H), 3.99 (dd, 11.1, 3.8, 1 H), 3.42 (dd, 11.3, 8.7), 2.57–2.38 (m, 2 H), 2.31–2.07 (m, 2 H), 1.97–1.80 (m, 2 H), 1.77 (s, 3 H), 1.68 (s, 3 H), 1.54 (s, 3 H), 1.27 (s, 3 H); **^{13}C NMR:** (151 MHz, $CDCl_3$) δ 205.9, 142.9, 134.0, 133.7, 122.9, 66.5, 49.5, 43.3, 27.7, 27.5, 25.9, 19.7, 18.0, 16.1; **[α]D^{23}:** –56.0° (c = .503, CH_2Cl_2); **IR (ATR, neat) ν_{max}:** 3465, 2968, 2922, 2882, 1659, 1450, 1435, 1376, 1255, 1202, 1172, 1090, 1050, 1023, 994, 941, 853, 824; **HRMS (ESI) m/z:** calculated for $[C_{14}H_{23}O_2]^+$ 223.1693, found 223.1689.

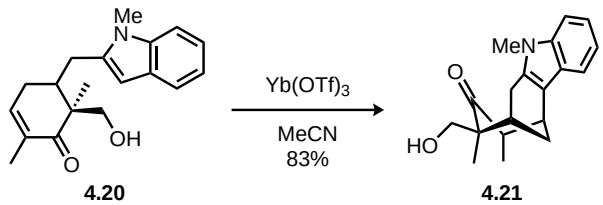

To a vial containing cross-coupling product **4.20** (51 mg, 172 μL, 1 equiv) in MeCN (0.57 mL, 0.3M) was added $Yb(OTf)_3$ (5.3 mg, 8,5 μmol, 0.05 equiv) and the reaction mixture was stirred under N_2. After 5 hours the mixture was concentrated to dryness and purified by Yamazen flash chromatography to give **4.21** (42.4 mg, 143 μmol, 83%, 2.6:1 dr, major shown) as an off white solid. **^{1}H NMR:** (400 MHz, $CDCl_3$) δ 7.45 (d, J = 7.9, 1 H_{minor}), 7.41 (d, J = 7.7, 1 H_{major}), 7.25 (d, J = 9.2, 1 H_{major}), 7.22 (d, J = 8.3, 1 H_{minor}), 7.17 (td, J = 7.1, 1.0, 1 H_{major}), 7.13 (td, J = 8.2, 1.0, 1 H_{minor}), 7.10–7.03 (m, 1 H_{minor} and 1 H_{major}), 3.85–3.77 (m, 1 H_{minor}), 3.69–3.58 (m, 1 H_{minor} and 2 H_{major}), 3.58 (s, 3 H_{major}), 3.57 (s, 3 H_{minor}), 3.49–3.44 (m, 1 H_{minor}), 3.31–3.08 (m, 2 H_{minor} and 2 H_{major}), 2.86–2.71 (m, 2 H_{minor} and 3 H_{major}), 2.70–2.60 (m, 1 H_{minor}), 2.57–2.49 (m, 1 H_{minor} and 1 H_{major}), 2.48–2.42 (m, 1 H_{major}), 2.09–2.01 (m, 1 H_{minor}), 2.01–1.93 (m, 1 H_{major}), 1.44 (d, 7.7, 3 H_{major}), 1.38 (s, 3 H_{minor}), 1.34 (s, 3 H_{major}), 1.14 (d, 6.7, 3 H_{minor}); **^{13}C NMR:** (100 MHz, $CDCl_3$, major diastereomer) δ 221.8, 137.5, 133.2, 125.6, 121.0, 119.0, 117.3, 113.0, 109.0, 68.6, 51.5, 51.1, 40.1, 33.7, 29.1, 25.2, 25.1, 24.3, 18.7; **^{13}C NMR:** (100 MHz, $CDCl_3$, minor diastereomer) δ 219.2, 137.2, 133.4, 127.6, 120.7, 119.0, 118.8, 110.1, 108.8, 68.1, 51.6, 47.7, 41.7, 36.9, 31.5, 29.2, 25.4, 23.7, 14.1; **m.p.** 145–150 °C; **[α]D^{23}:** 17.5° (c = 0.993, CH_2Cl_2); **IR (ATR, neat) ν_{max}:** 3518, 2922, 2872, 2851, 1674, 1612, 1558, 1467, 1416, 1371, 1330, 1252, 1192, 1170, 1144, 1131, 1101, 1062, 1032, 1013, 993, 967, 932, 919, 874, 842, 816, 740, 621, 559; **HRMS (ESI) m/z:** calculated for $[C_{19}H_{23}NO_2]^+$ 297.1729, found 297.1735.

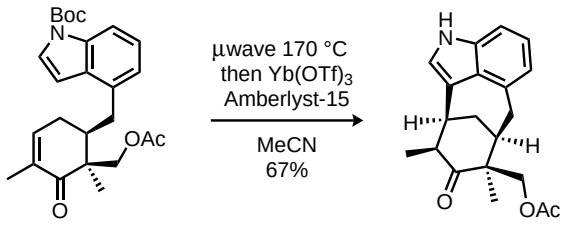

4.17e **4.19**

A microwave vial containing **4.17e** (22.5 mg, 53 μmol, 1 equiv) in MeCN (0.68 mL, 0.078M) was subjected to microwave heating at 170 °C for 50 minutes. Once cooled the vial was transferred to a glovebox with a N_2 atmosphere and $Yb(OTf)_3$ (2 mg, 3 μmol, 0.06 equiv) and Amberlyst® (2 mg) were added. The reaction was stirred for 4 hours at room temperature then diluted with H_2O, extracted with Et_2O (5x10 mL), washed with brine, dried over $MgSO_4$, filtered, and concentrated. The crude residue was purified by Yamazen flash chromatography to give **4.19** (11.6 mg, 36 μmol, 67%) as a white solid. **^{1}H NMR:** (600 MHz, $CDCl_3$) δ 8.04 (s, 1 H), 7.13 (d, J = 8.1, 1 H), 7.03 (t, J = 7.7, 1 H), 6.91 (d, J = 2.4, 1 H), 6.83 (d, J = 7.1, 1 H), 4.28 (dd, J = 17.6, 11.9, 2 H), 3.63 (s, 1 H), 3.31 (dd, J = 17.1, 3.6, 1 H), 3.19 (p, J = 6.7, 6.3, 6.0, 5.3, 1 H), 3.07 (dd, J = 17.1, 3.8, 1 H), 2.95 (dddd, J = 13.5, 6.6, 4.5, 1.8, 1 H), 2.75 (q, J = 4.9, 1 H), 2.25 (d, J = 14.1, 1 H), 2.12 (s, 3 H), 1.46 (s, 3 H), 0.79 (d, J = 6.5, 3 H); **^{13}C NMR:** (151 MHz, $CDCl_3$) δ 213.5, 171.2, 136.6, 132.2, 125.8, 122.6, 122.5, 120.1, 114.4, 109.0, 67.4, 50.0, 44.9, 44.6, 44.1, 40.1, 34.0, 24.5, 21.3, 13.3; **m.p.** 200 °C (decomposed); **[α]D^{23}:** 97.0° (c = .773, CH_2Cl_2); **IR (ATR, neat) ν_{max}:** 3366, 2970, 2927, 2882, 1735, 1697, 1613, 1449, 1427, 1370, 1303, 1235, 1168, 1142, 1107, 1086, 1043, 1006, 986, 914, 799, 781, 747, 610, 653; **HRMS (ESI) m/z:** calculated for $[C_{20}H_{23}NO_3Na]^+$ 348.1570, found 348.1560.

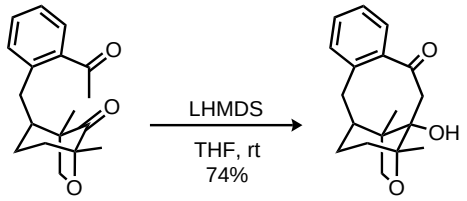

4.15m **4.13**

To a flask containing **4.17m** (30 mg, 105 μmol, 1 equiv) in THF (2.1 mL, 0.05M) was added LHMDS (1M in THF, 525 μL, 525 μmol, 5 equiv). After 10 minutes, 20 mL of H_2O was added and the resulting mixture was extracted with DCM (5x10 mL), washed with brine, dried over $MgSO_4$, filtered, and concentrated. The crude residue was purified by Yamazen flash chromatography to give **4.13** (22.3 mg, 78 μmol, 74%) as a white solid. **^{1}H NMR:** (400 MHz, $CDCl_3$) δ = 8.15 (dd, J = 7.9, 1.5, 1 H), 7.48 (td, J = 7.4, 1.6, 1 H), 7.36 (td, J = 8.1, 1.2, 1 H), 7.26 (d, J = 7.0, 1 H), 4.00 (d, J = 12.9, 1 H), 3.81 (d, J = 7.9, 1 H), 3.59 (d, J = 8.2, 1 H), 3.50 (dd, J = 15.4, 10.8, 1 H), 3.05 (dd, J = 15.4, 7.8, 1 H), 2.76 (d, J = 12.9, 1 H), 2.56, s, 1 H), 2.25–2.02 (m, 3 H), 1.83–1.72 (m, 1 H), 1.43–1.34 (m, 1 H), 1.30 (s, 3 H), 0.39 (s, 3 H); **^{13}C NMR:** (100 MHz, $CDCl_3$) δ 199.50, 141.43, 138.09, 134.02, 132.76, 129.96, 127.49, 87.90, 79.43, 79.24, 48.77, 47.46, 43.48, 43.02, 33.89, 26.24, 19.09, 16.67; **m.p.** 158–156 °C; **[α]D^{23}:** –44.5° (c = 0.196, CH_2Cl_2); **IR (ATR, neat) ν_{max}:** 3475, 2964, 2930, 2877, 1662, 1594, 1483, 1458, 1446, 1377, 1343, 1307, 1285, 1246, 1191, 1174, 1145, 1130, 1120, 1109, 1081, 1055, 1028, 914, 864, 814, 783, 755, 731, 626, 485, 472, 459, 444, 428; **HRMS (ESI) m/z:** calculated for $[C_{18}H_{22}O_3]^+$ 286.1569, found 286.1568.

4.7 References

1. (a) Blaser, H. U. *Chem. Rev.* **1992**, *92*, 935–952; (b) Liu, W. In *Handbook Of Chiral Chemicals*; Ager, D. J., Ed.; CRC Press: Baton Rouge, 1999.
2. Brill, Z. G.; Condakes, M. L.; Ting, C. P.; Maimone, T. J. *Chem. Rev.* **2017**, *117*, 11753–11795.
3. Wetzel, S.; Bon, R. S.; Kumar, K.; Waldmann, H. *Angew. Chem. Int. Ed.* **2011**, *50*, 10800–10826.
4. Koch, M. A.; Schuffenhauer, A.; Scheck, M.; Wetzel, S.; Casaulta, M.; Odermatt, A.; Ertl, P.; Waldmann, H. *Proc. Natl. Acad. Sci. U.S.A.* **2005**, *102*, 17272–17277.
5. (a) Huigens, r., R. W.; Morrison, K. C.; Hicklin, R. W.; Flood, J., T. A.; Richter, M. F.; Hergenrother, P. J. *Nat. Chem.* **2013**, *5*, 195–202; (b) Rafferty, R. J.; Hicklin, R. W.; Maloof, K. A.; Hergenrother, P. J. *Angew. Chem. Int. Ed.* **2014**, *53*, 220–224.
6. Morrison, K. C.; Hergenrother, P. J. *Nat. Prod. Rep.* **2014**, *31*, 6–14.
7. Masarwa, A.; Weber, M.; Sarpong, R. *J. Am. Chem. Soc.* **2015**, *137*, 6327–6334.
8. Bermejo, F. A.; Fernández Mateos, A.; Marcos Escribano, A.; Martín Lago, R.; Mateos Burón, L.; Rodríguez López, M.; Rubio González, R. *Tetrahedron* **2006**, *62*, 8933–8942.
9. (a) Souillart, L.; Cramer, N. *Chem. Rev.* **2015**, *115*, 9410–9464; (b) Chen, F.; Wang, T.; Jiao, N. *Chem. Rev.* **2014**, *114*, 8613–8661.
10. Orellana, A.; Rosa, D.; Nikolaev, A.; Nithiy, N. *Synlett* **2015**, *26*, 441–448.
11. (a) Nishimura, T.; Uemura, S. *J. Am. Chem. Soc.* **1999**, *121*, 11010–11011; (b) Matsumura, S.; Maeda, Y.; Nishimura, T.; Uemura, S. *J. Am. Chem. Soc.* **2003**, *125*, 8862–8869.

12. Muzart, J. *Tetrahedron* **2005**, *61*, 9423–9463.
13. Weber, M.; Owens, K.; Masarwa, A.; Sarpong, R. *Org. Lett.* **2015**, *17*, 5432–5435.
14. Shigemori, H.; Kobayashi, J. *J. Nat. Prod.* **2004**, *67*, 245–256.
15. Petasis, N. A.; Patane, M. A. *Tetrahedron* **1992**, *48*, 5757–5821.
16. Vicente, J.; Abad, J.-A.; Martínez-Viviente, E.; Ramírez de Arellano, M. C.; Jones, P. G. *Organometallics* **2000**, *19*, 752–760.
17. Stambuli, J. P.; Buhl, M.; Hartwig, J. F. *J. Am. Chem. Soc.* **2002**, *124*, 9346–9347.

4.A NMR Spectral Data for Chapter 4

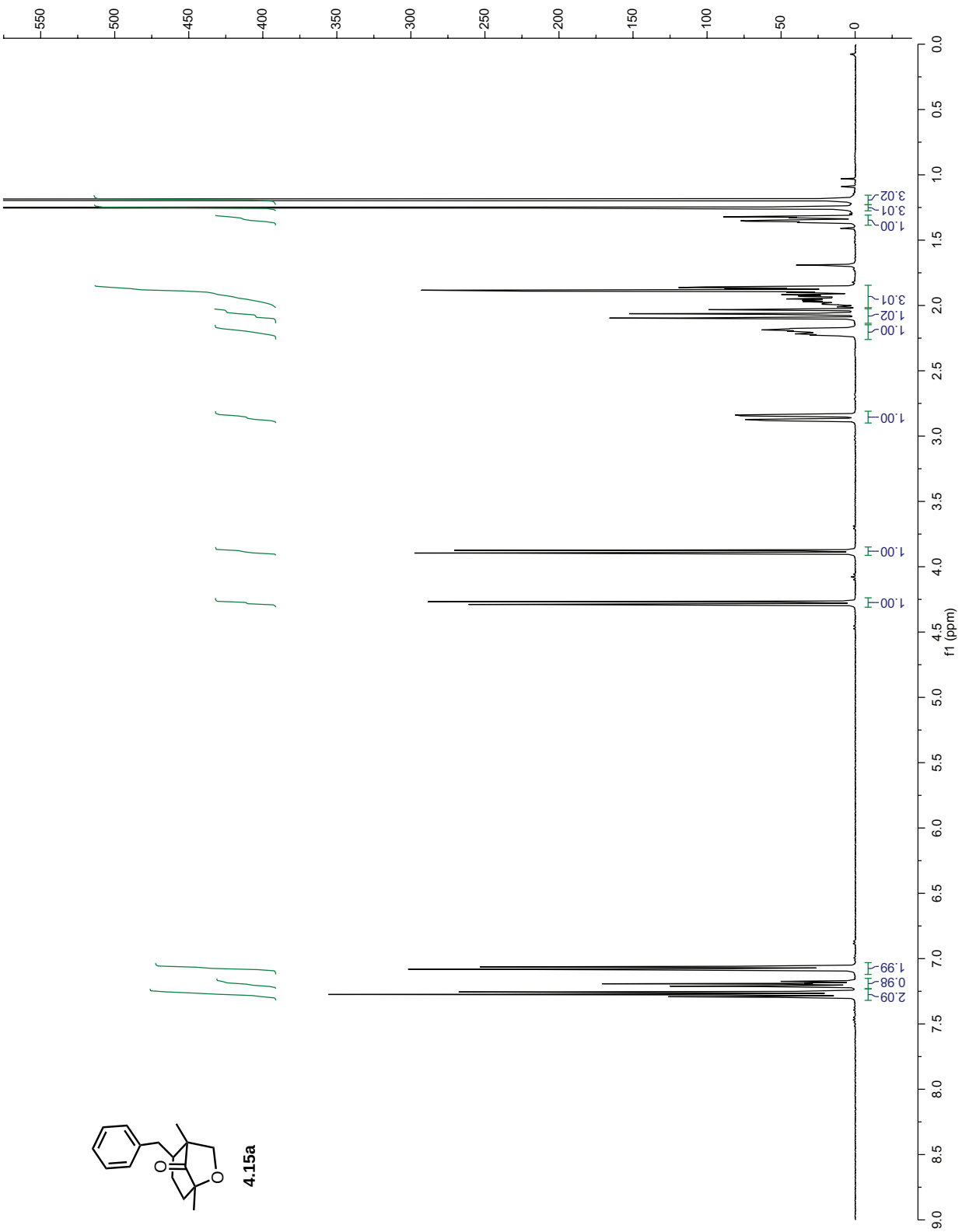

Figure 4.A.1: ^{1}H NMR of **4.15a**

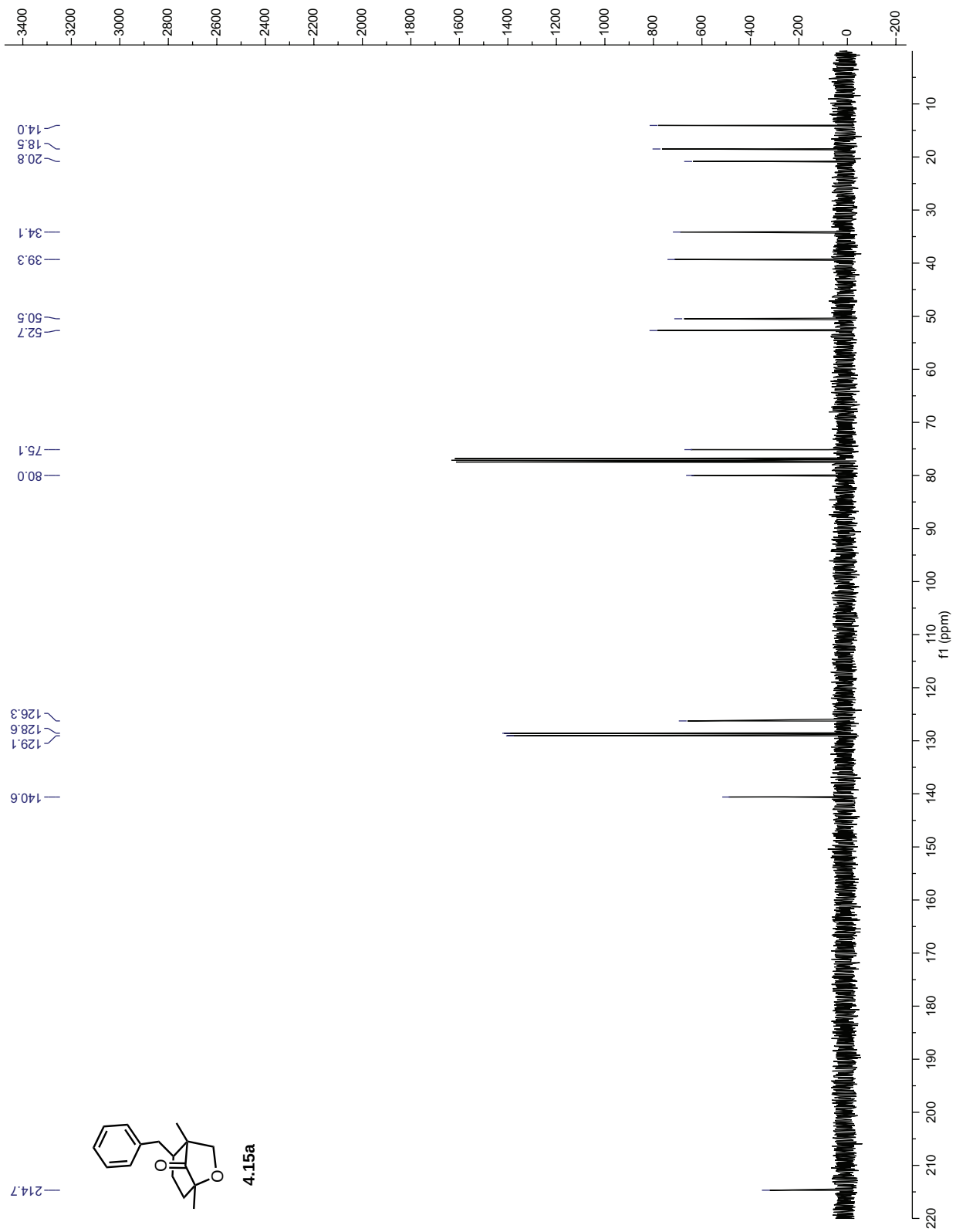

Figure 4.A.2: ^{13}C NMR of **4.15a**

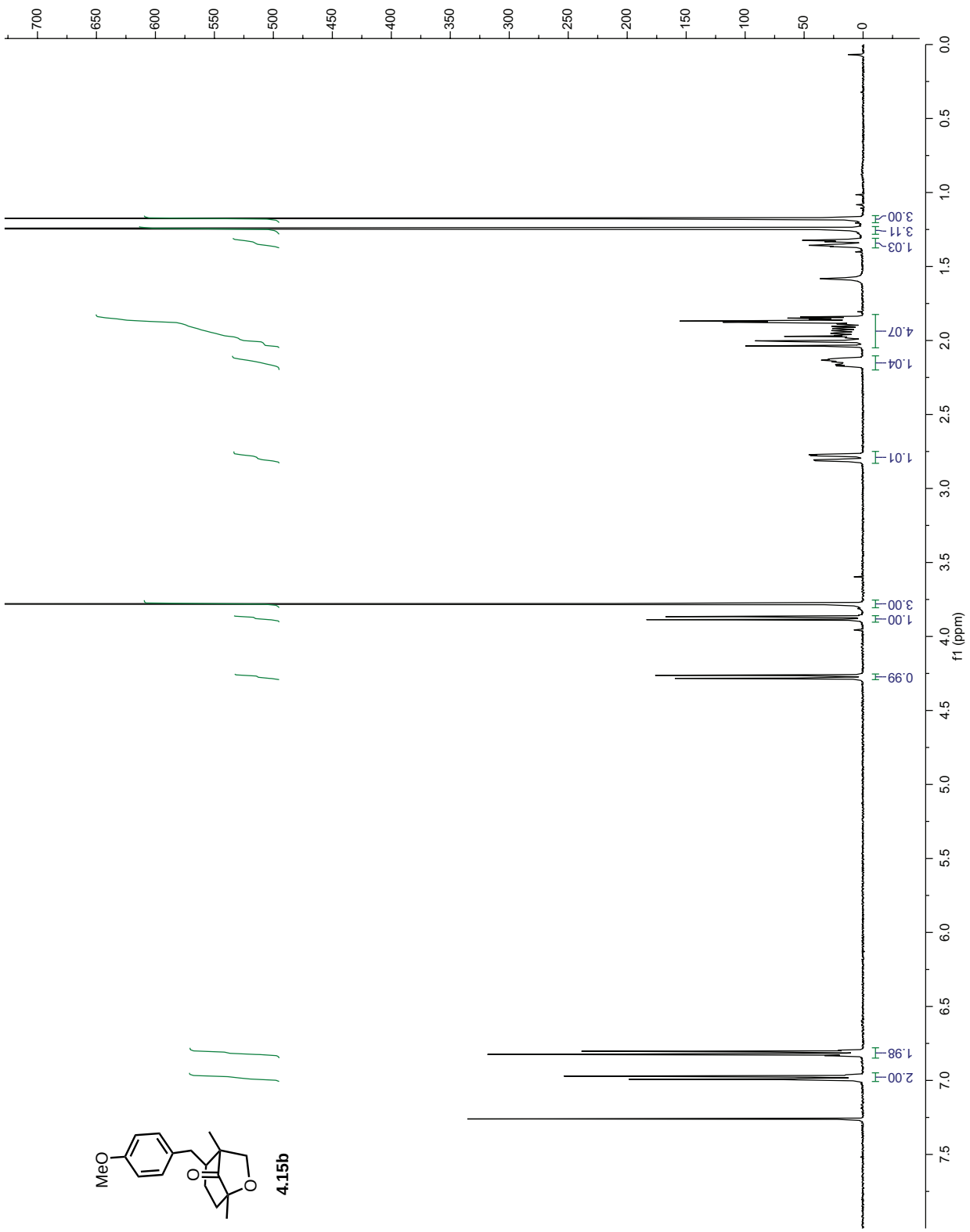

Figure 4.A.3: ^{1}H NMR of **4.15b**

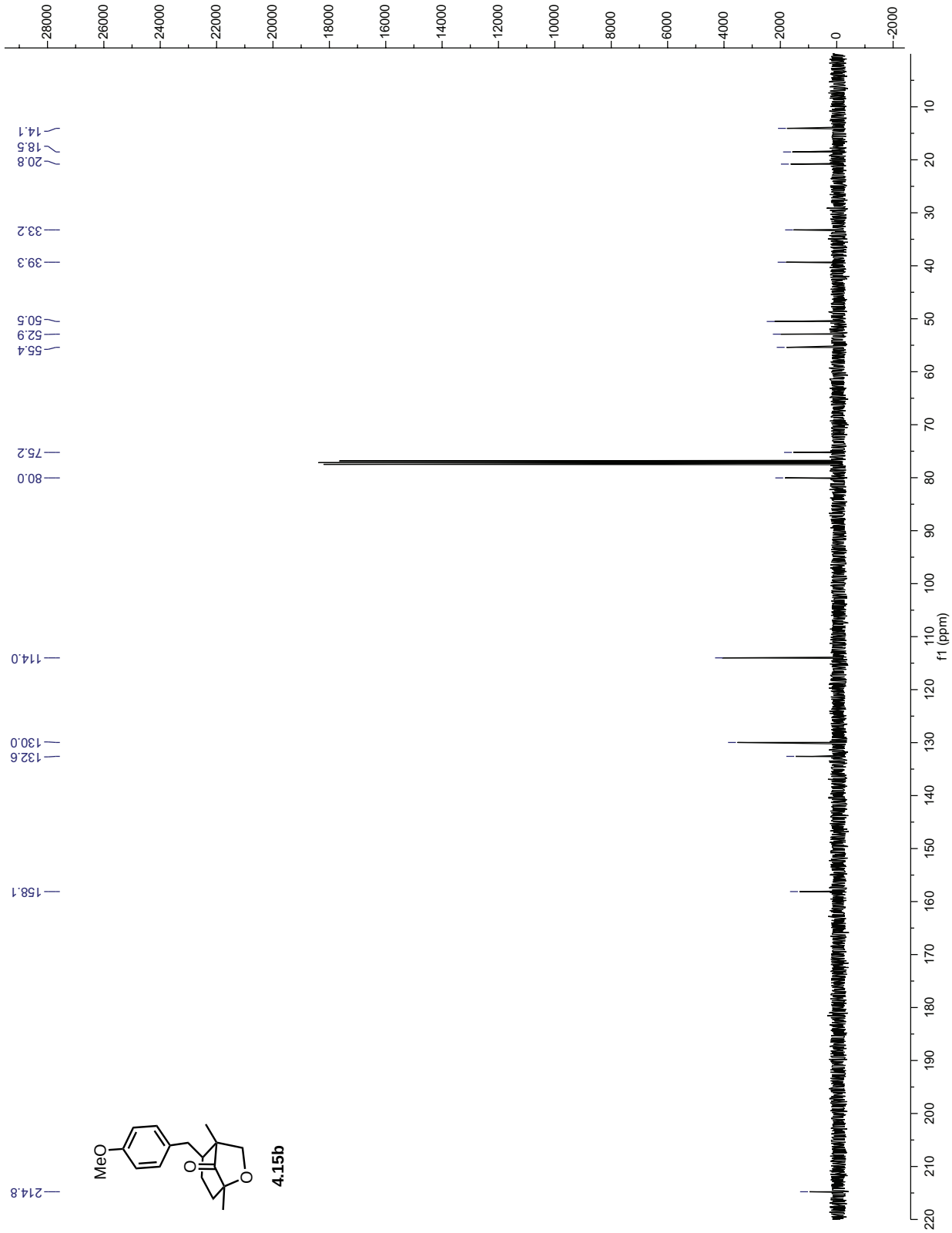

Figure 4.A.4: ^{13}C NMR of **4.15b**

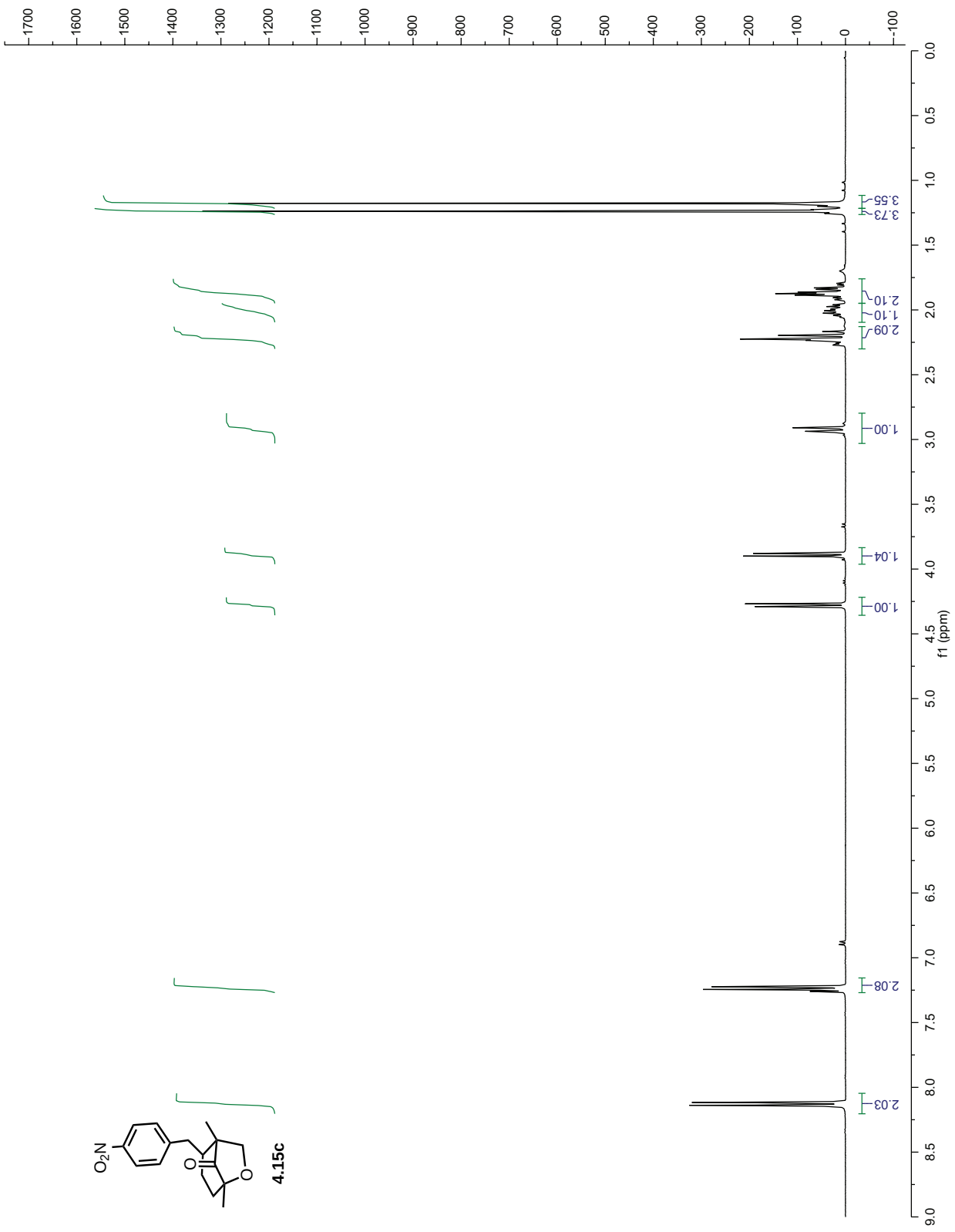

Figure 4.A.5: ^{1}H NMR of **4.15c**

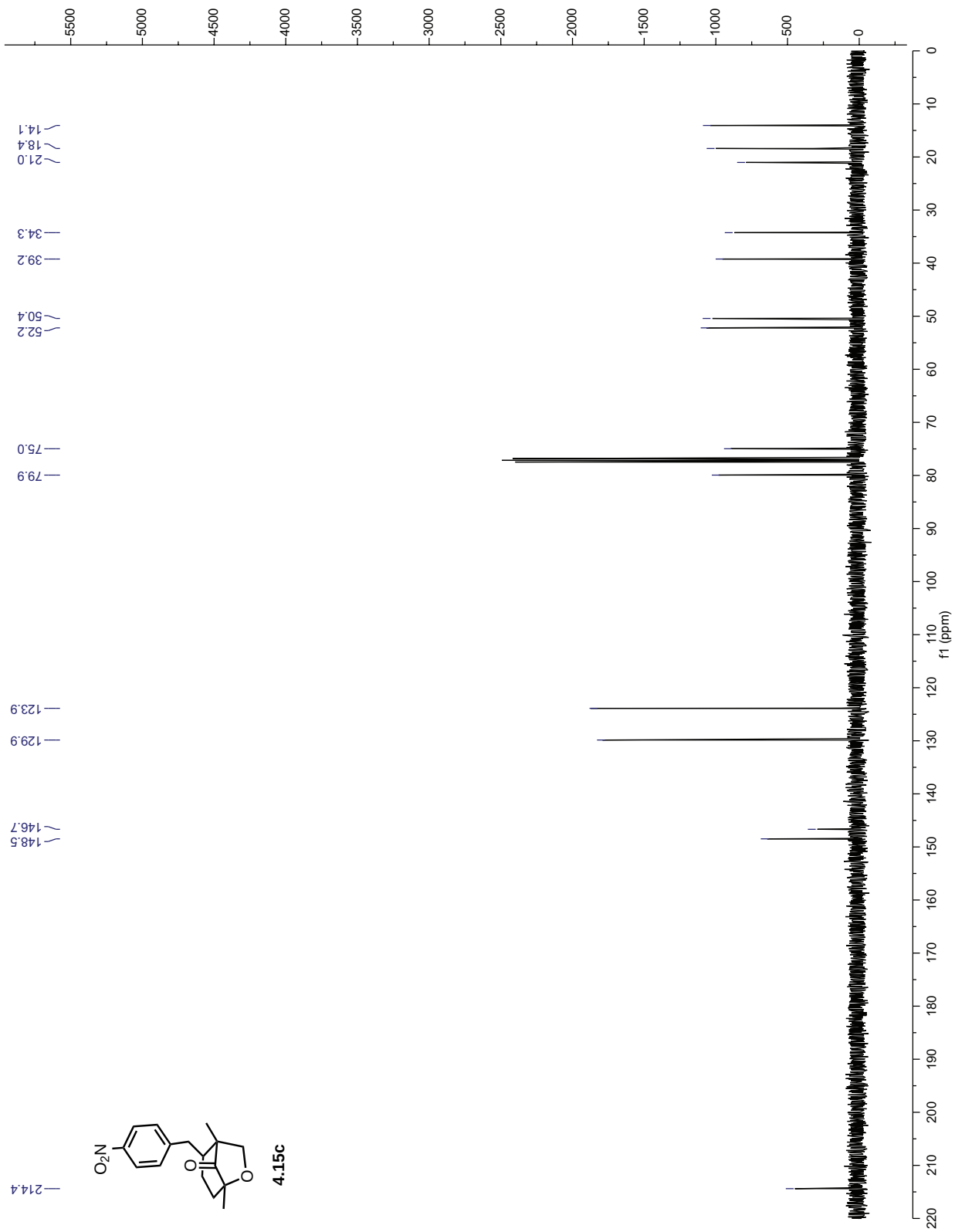

Figure 4.A.6: ^{13}C NMR of **4.15o**

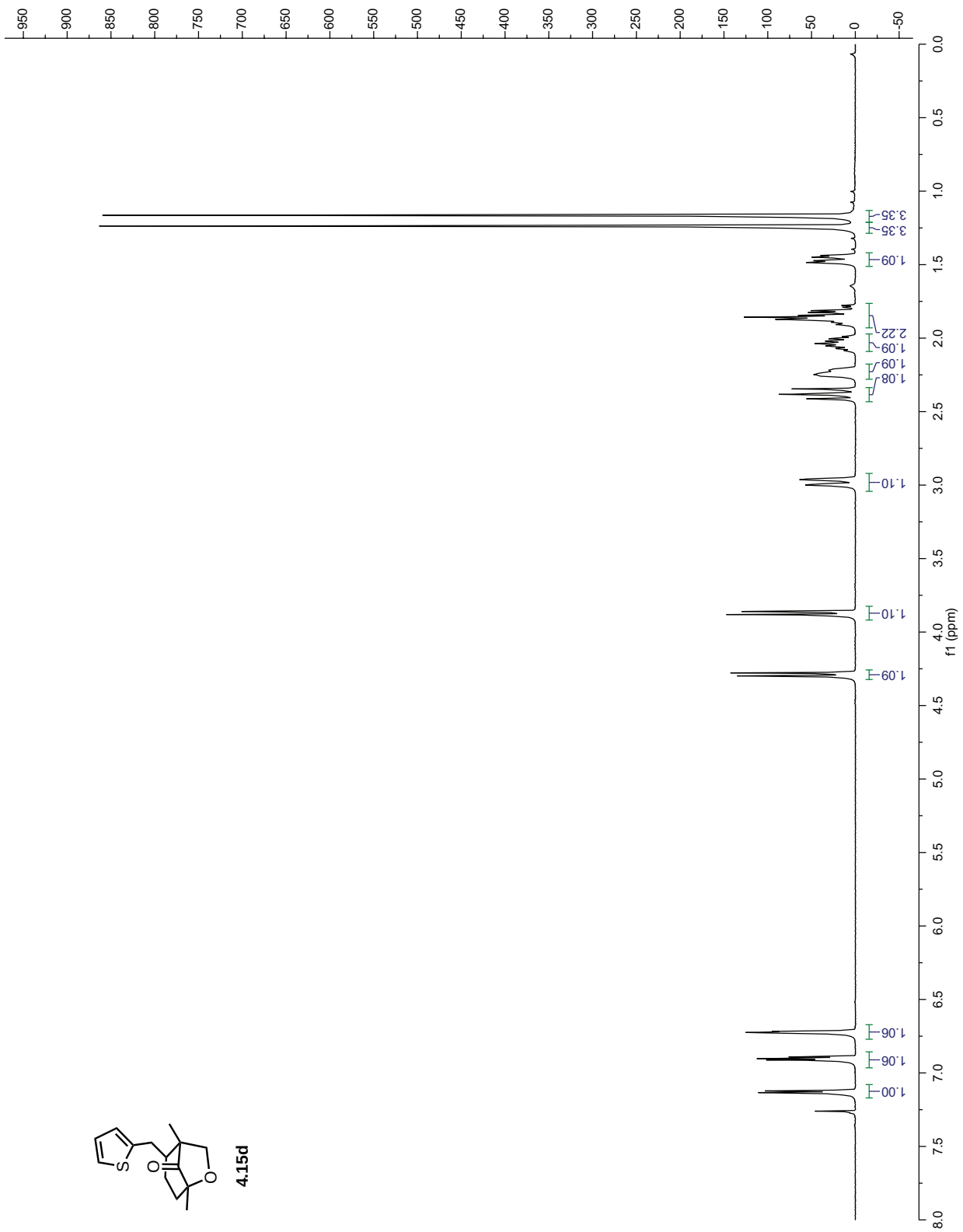

Figure 4.A.7: ^{1}H NMR of **4.15d**

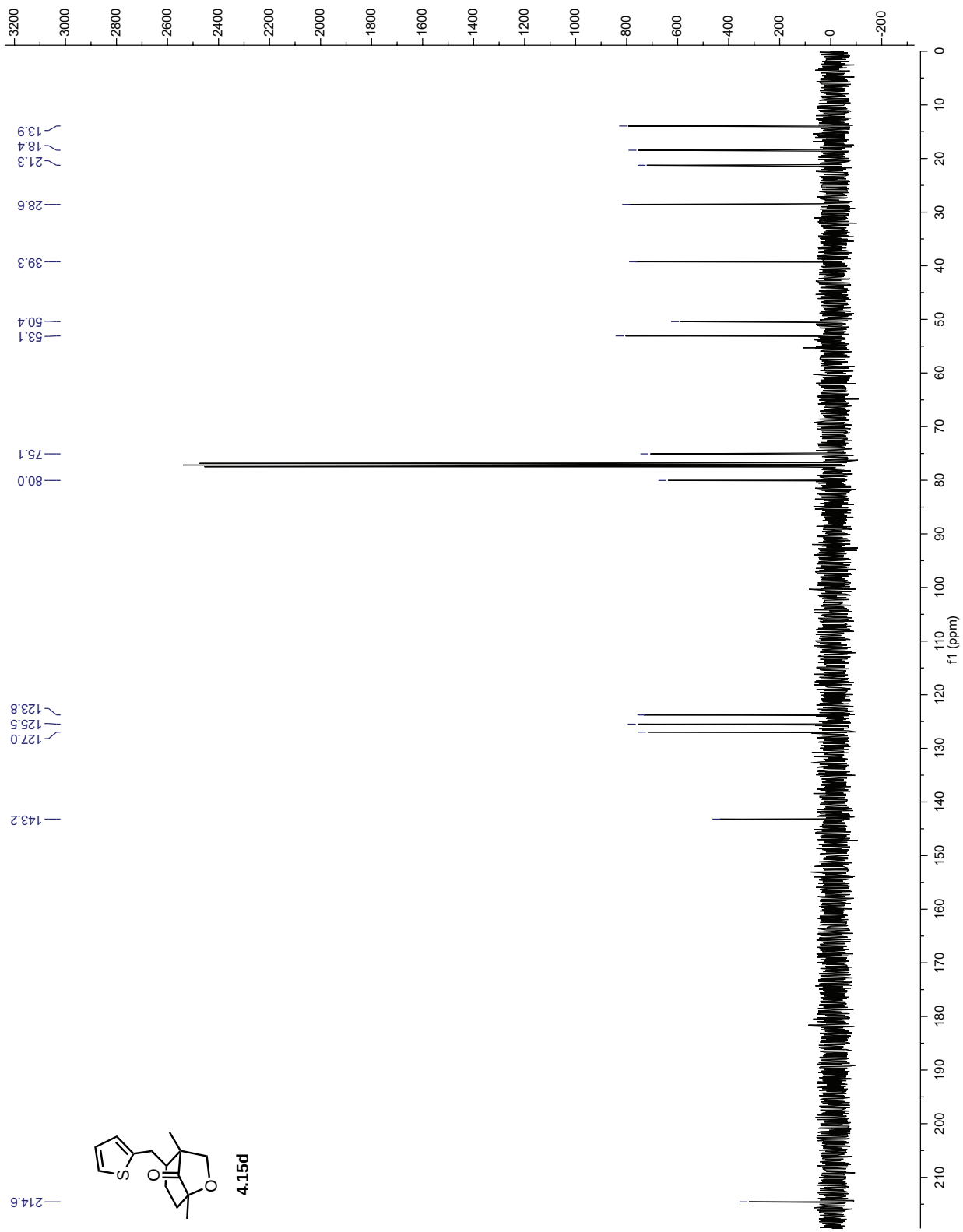

Figure 4.A.8: ^{13}C NMR of **4.15d**

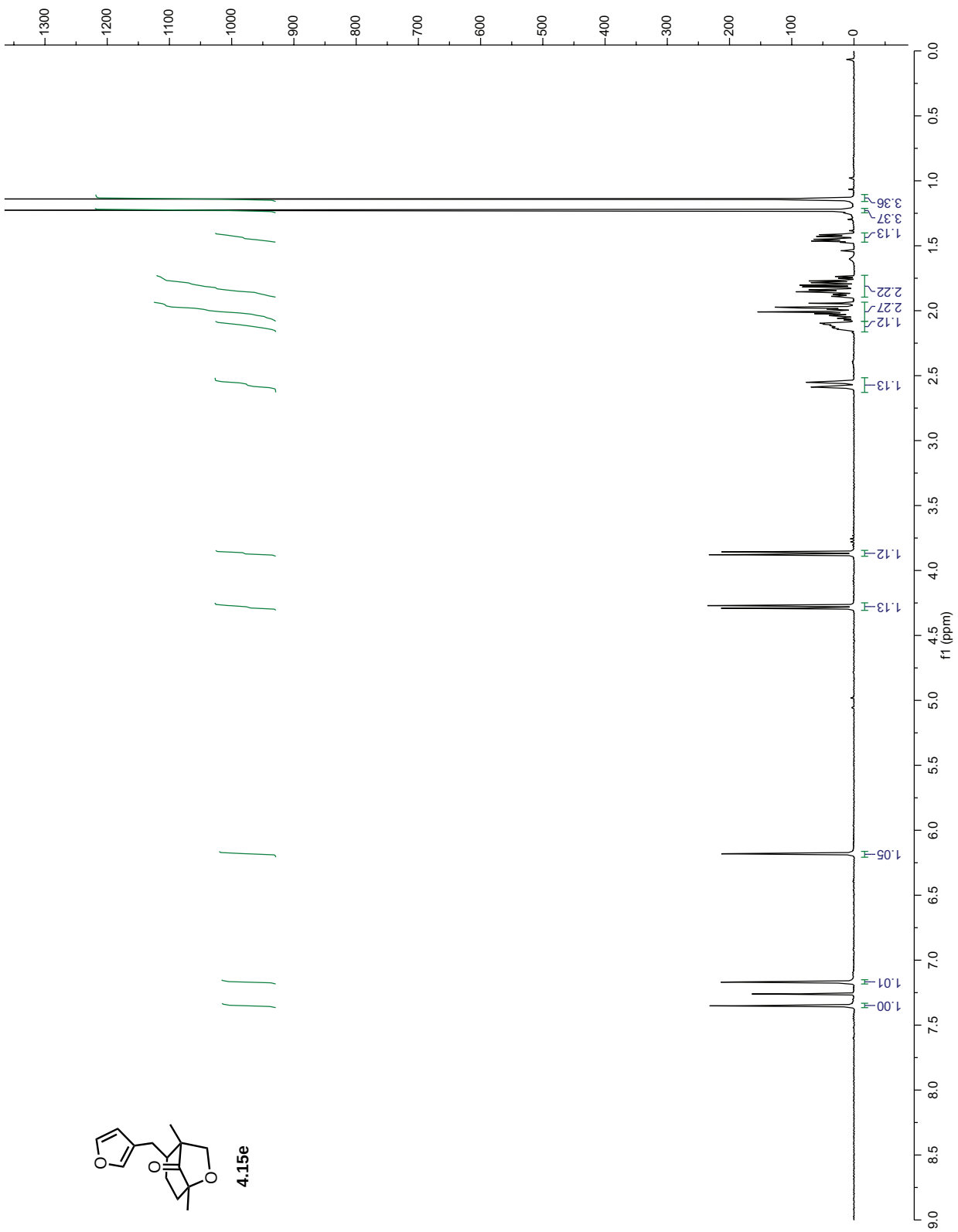

Figure 4.A.9: ^{1}H NMR of **4.15e**

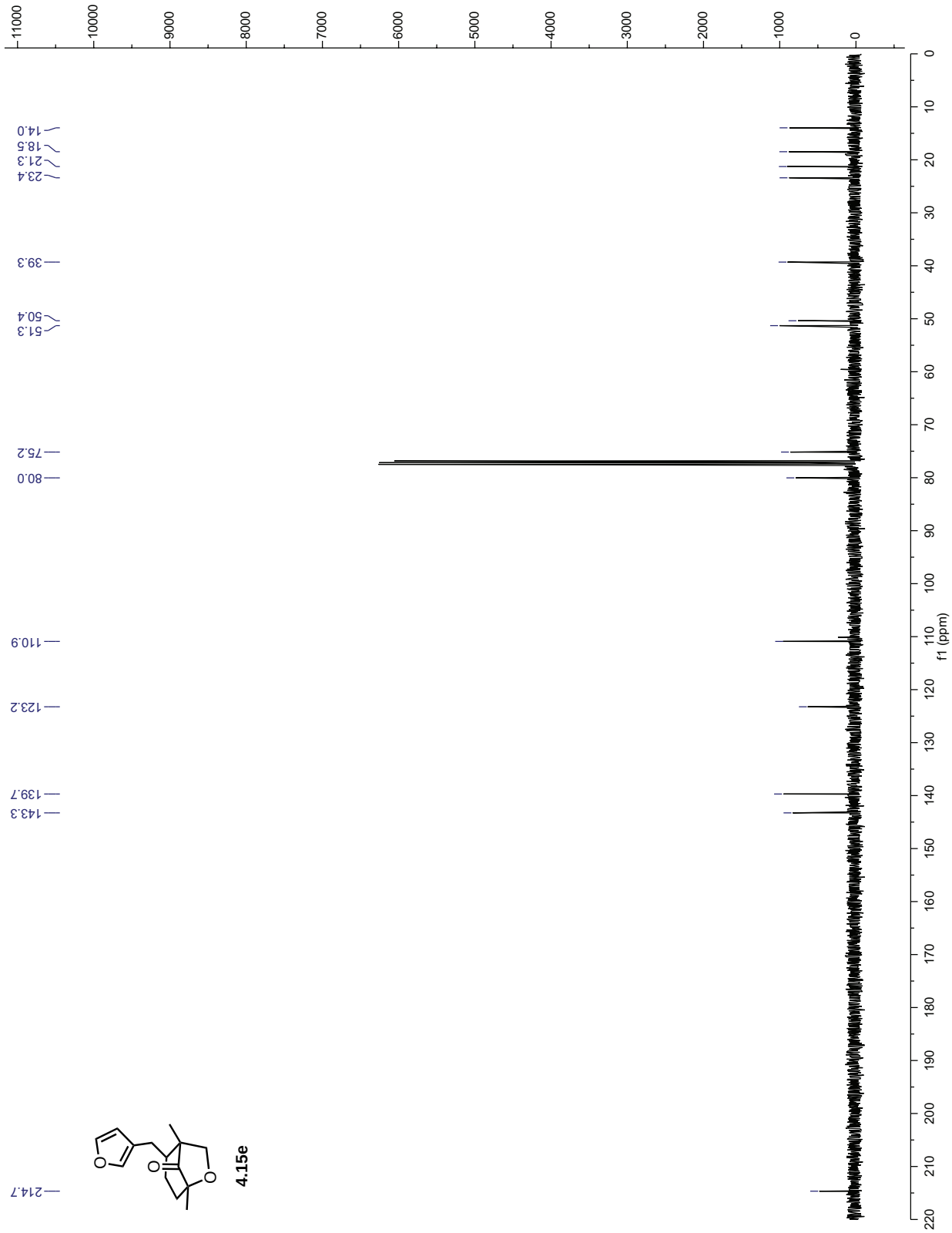

Figure 4.A.10: ^{13}C NMR of **4.15e**

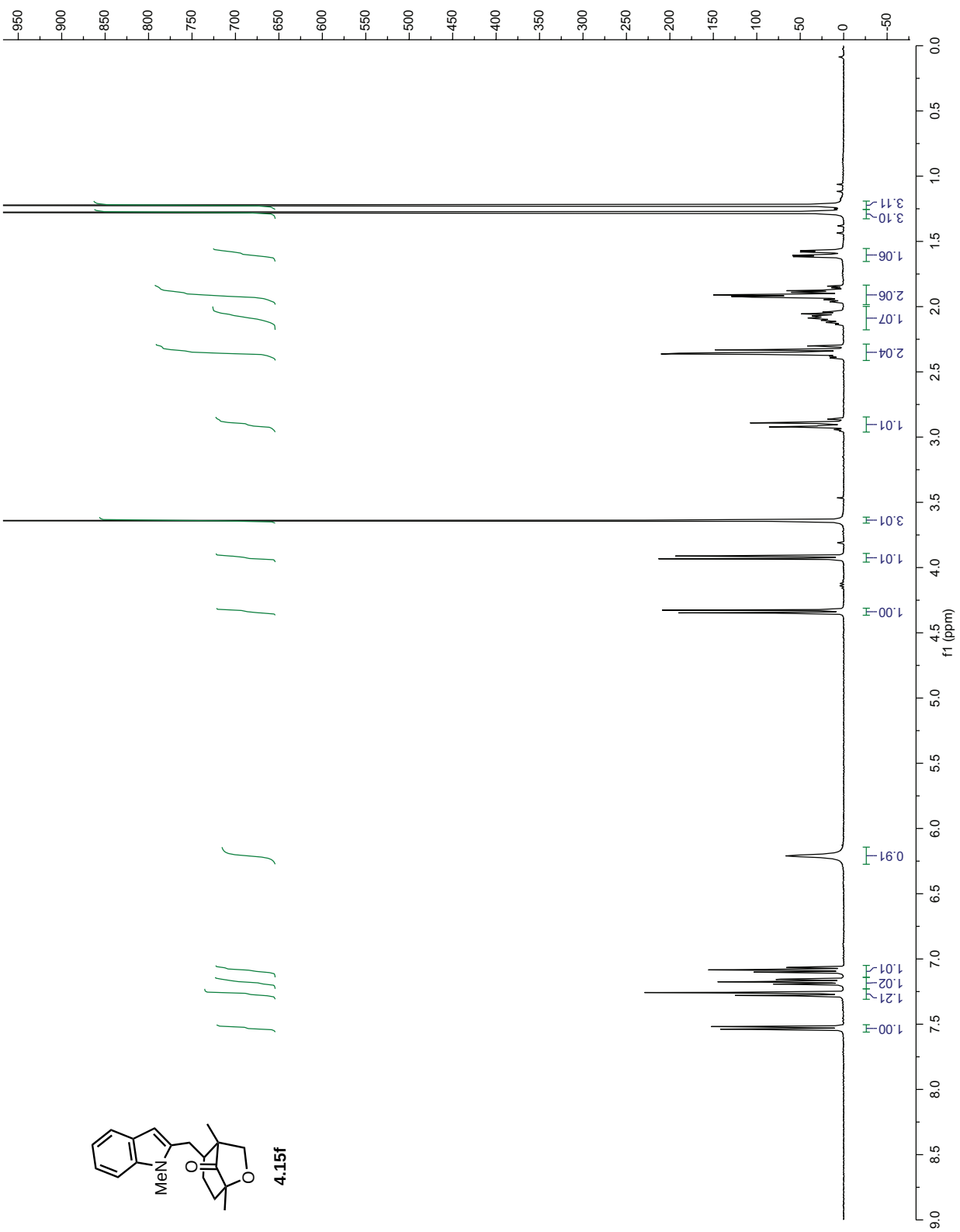

Figure 4.A.11: ^{1}H NMR of **4.15f**

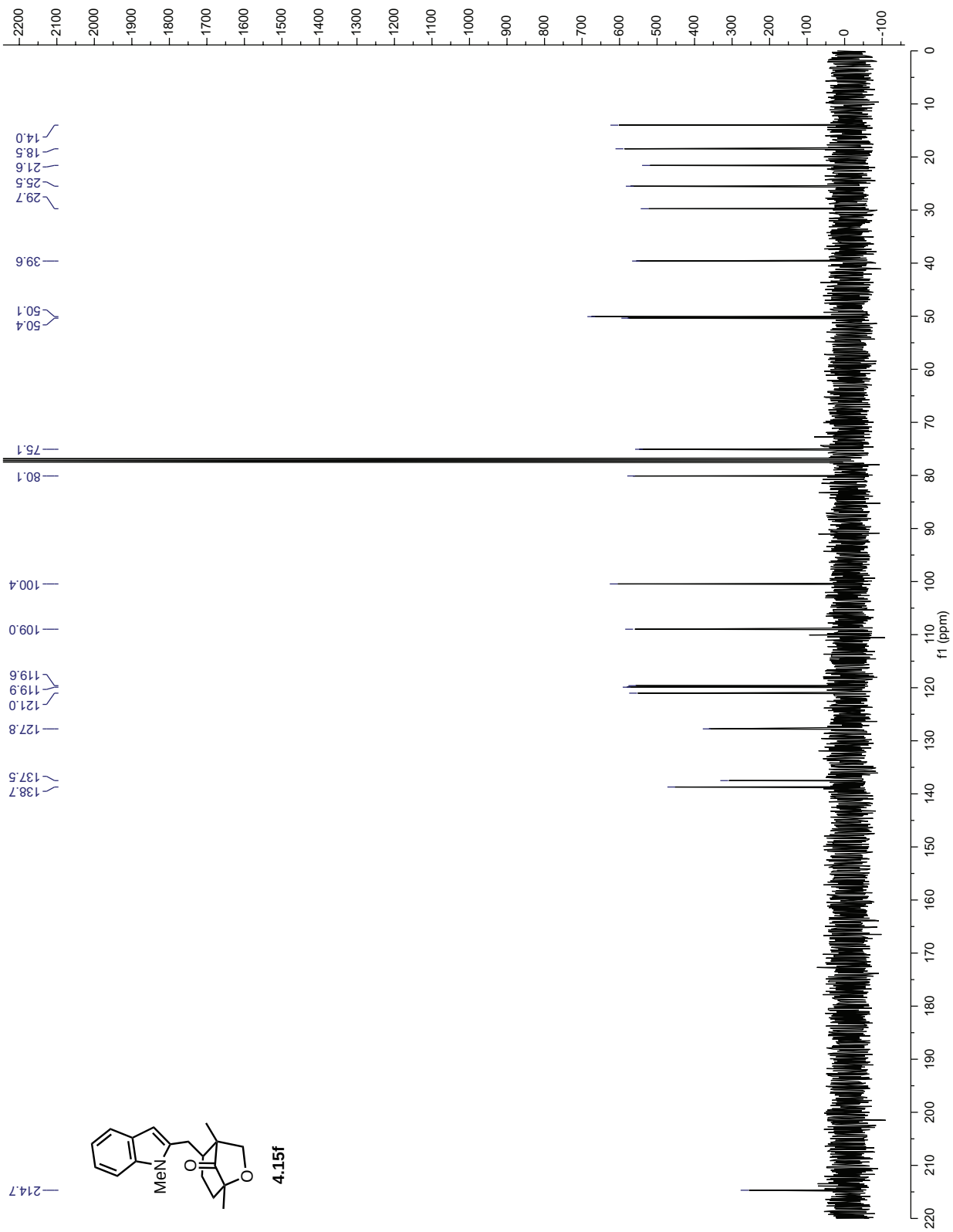

Figure 4.A.12: ^{13}C NMR of **4.15f**

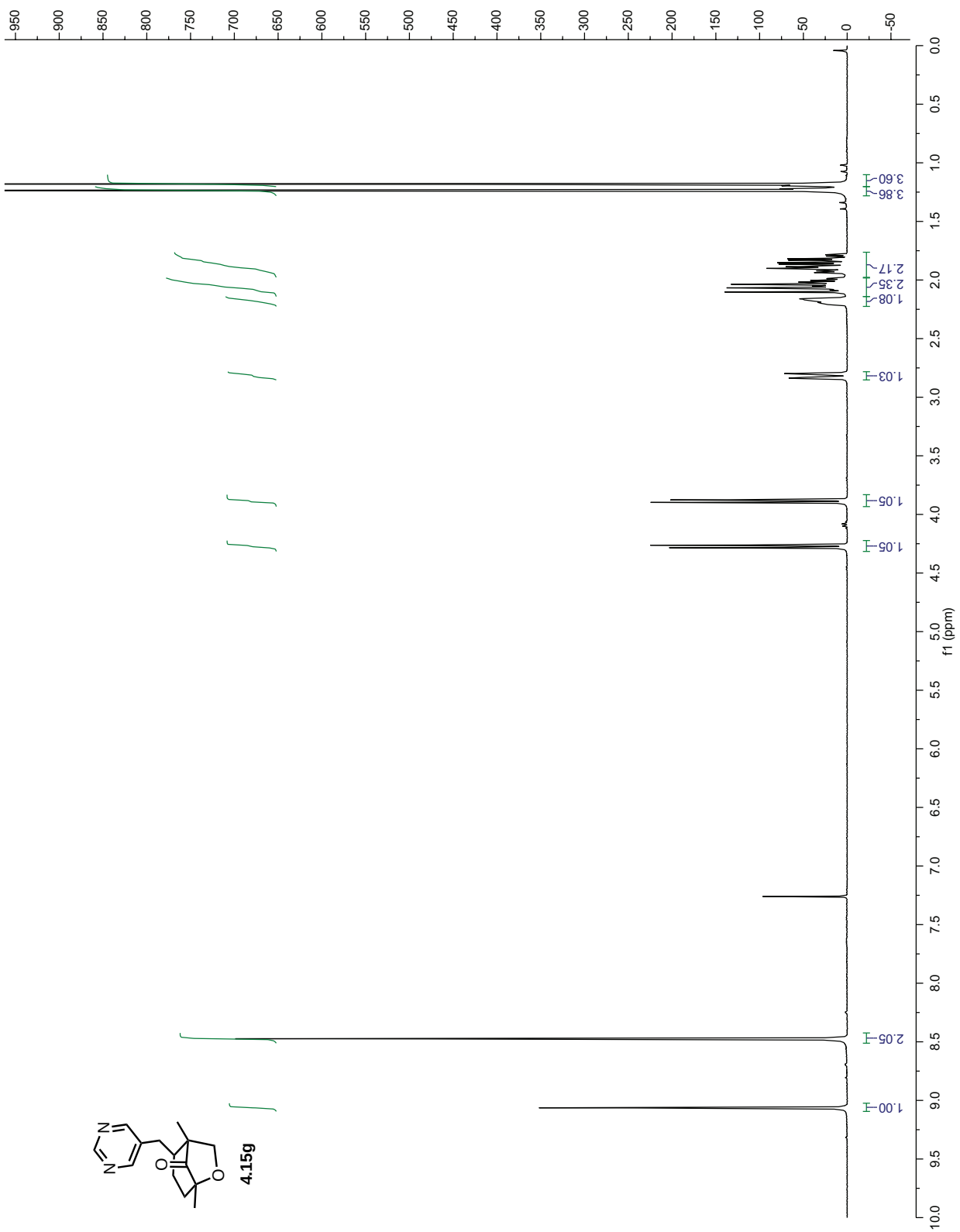

Figure 4.A.13: ^{1}H NMR of **4.15g**

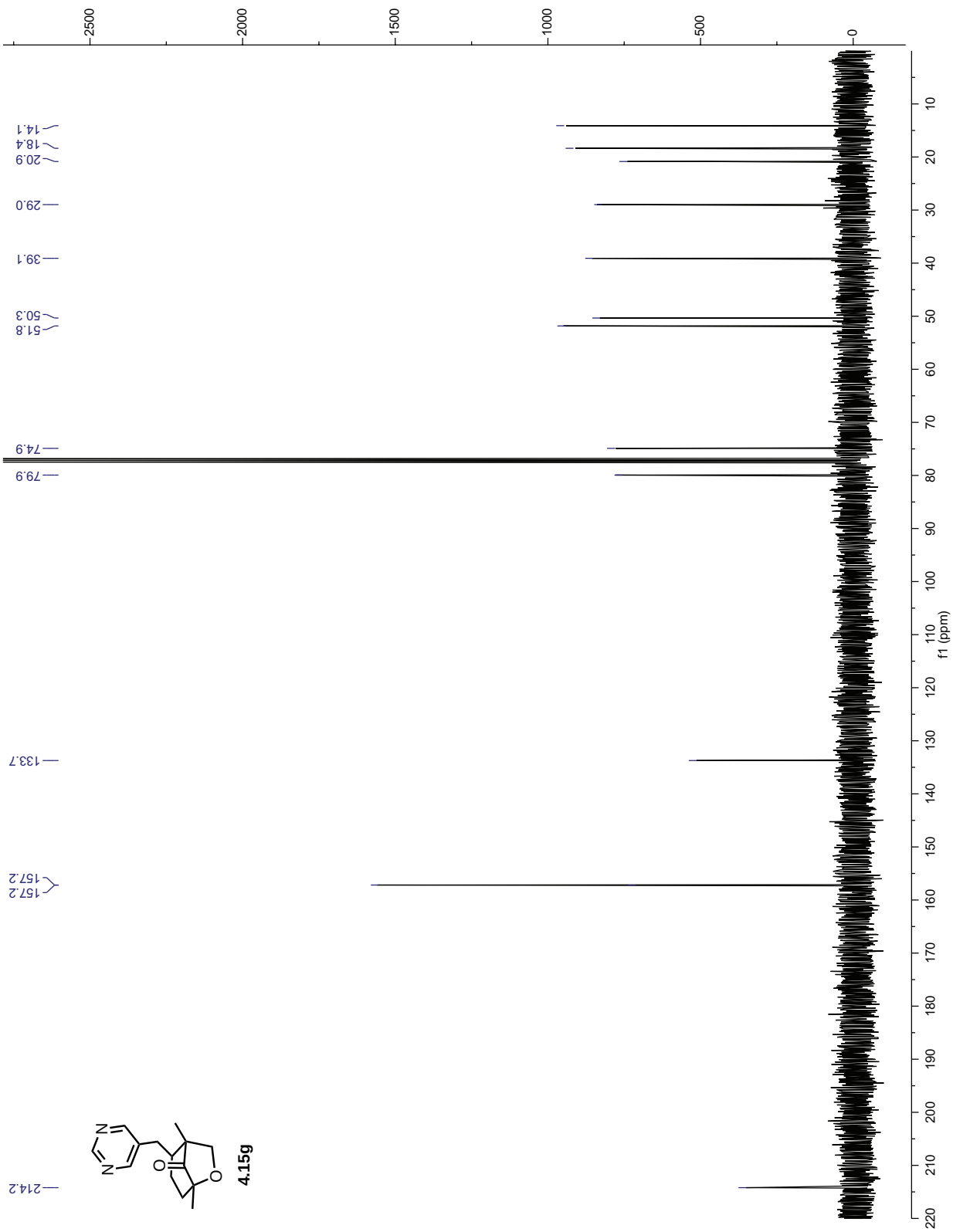

Figure 4.A.14: ^{13}C NMR of **4.15g**

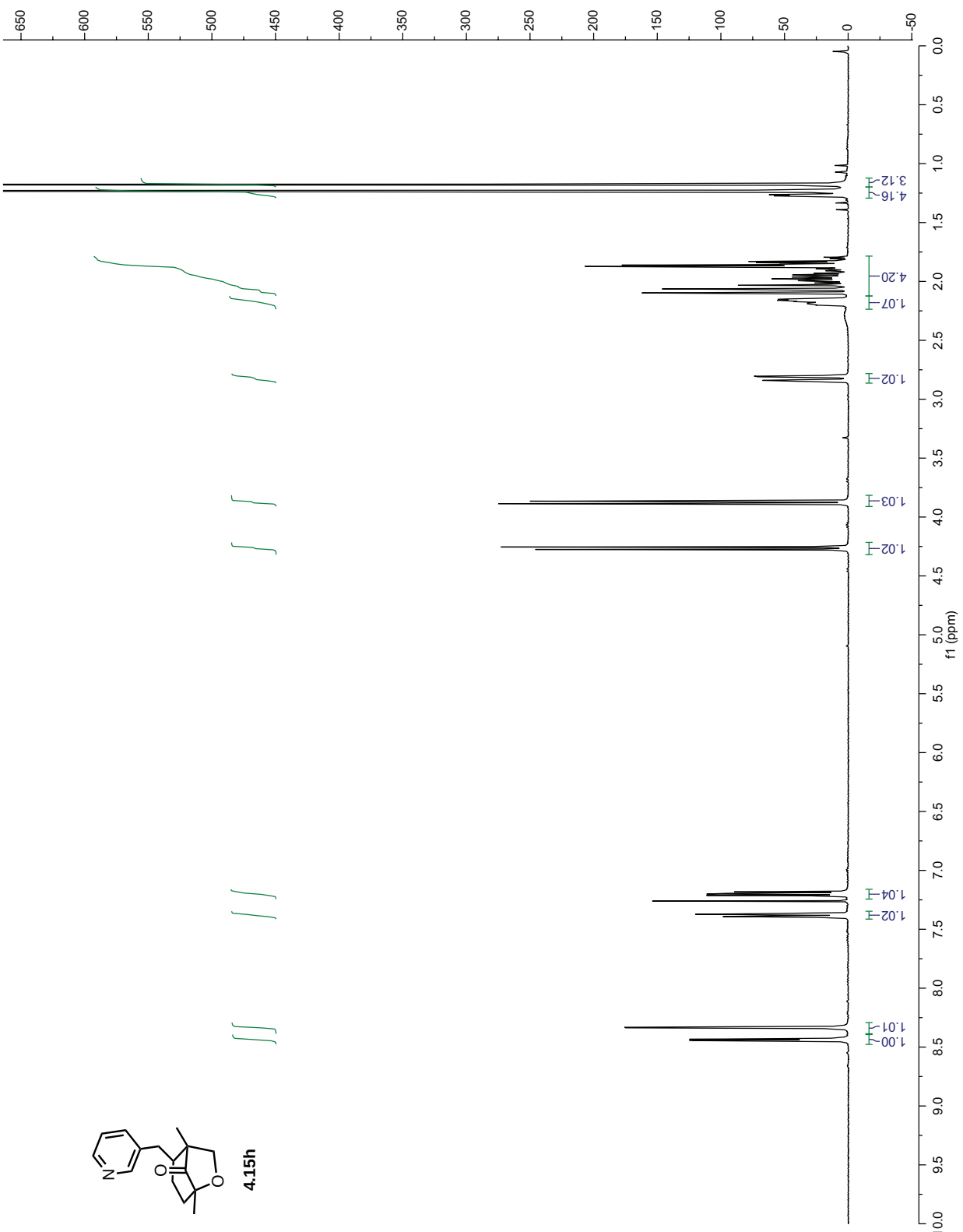

Figure 4.A.15: ^{1}H NMR of **4.15h**

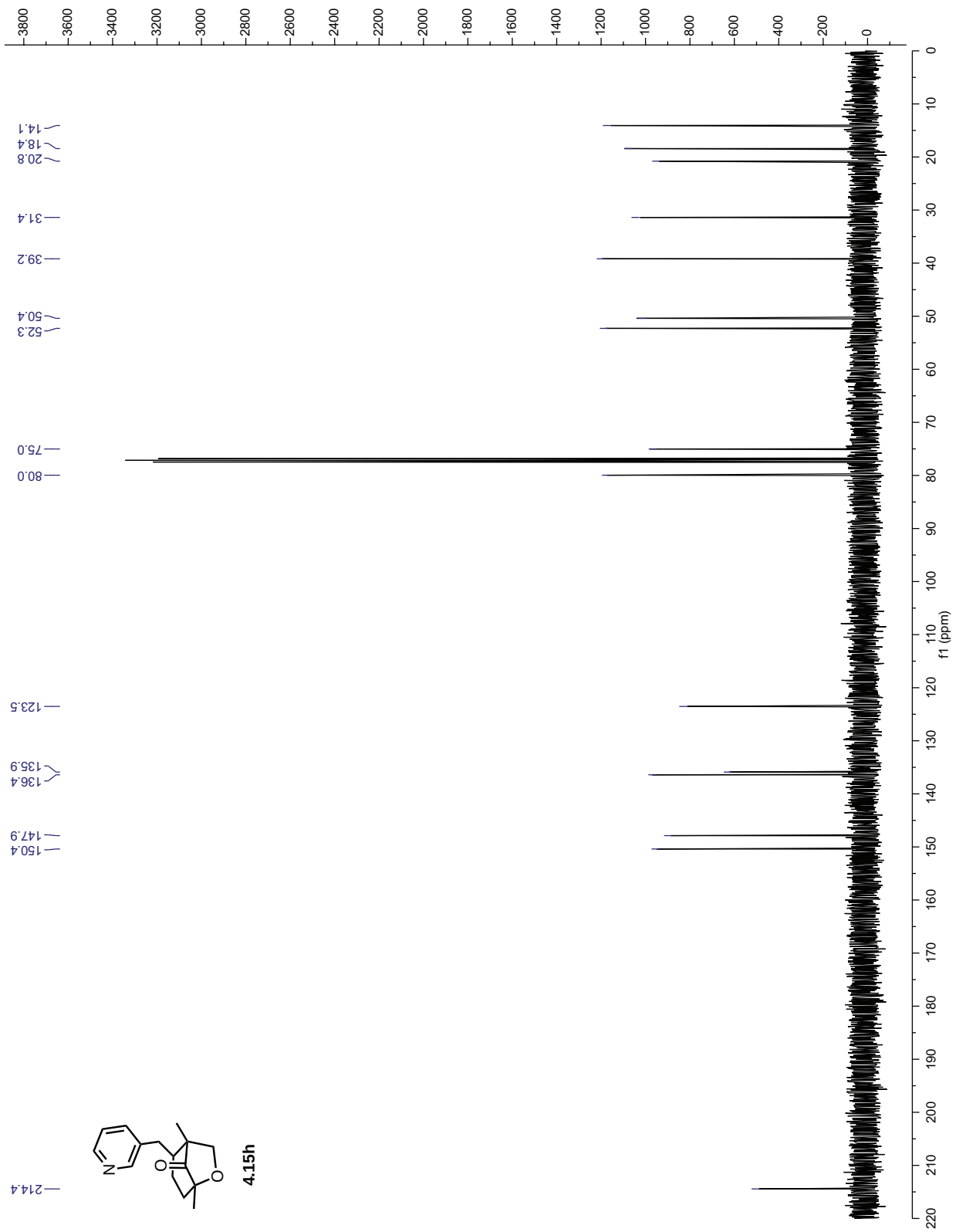

Figure 4.A.16: ^{13}C NMR of **4.15h**

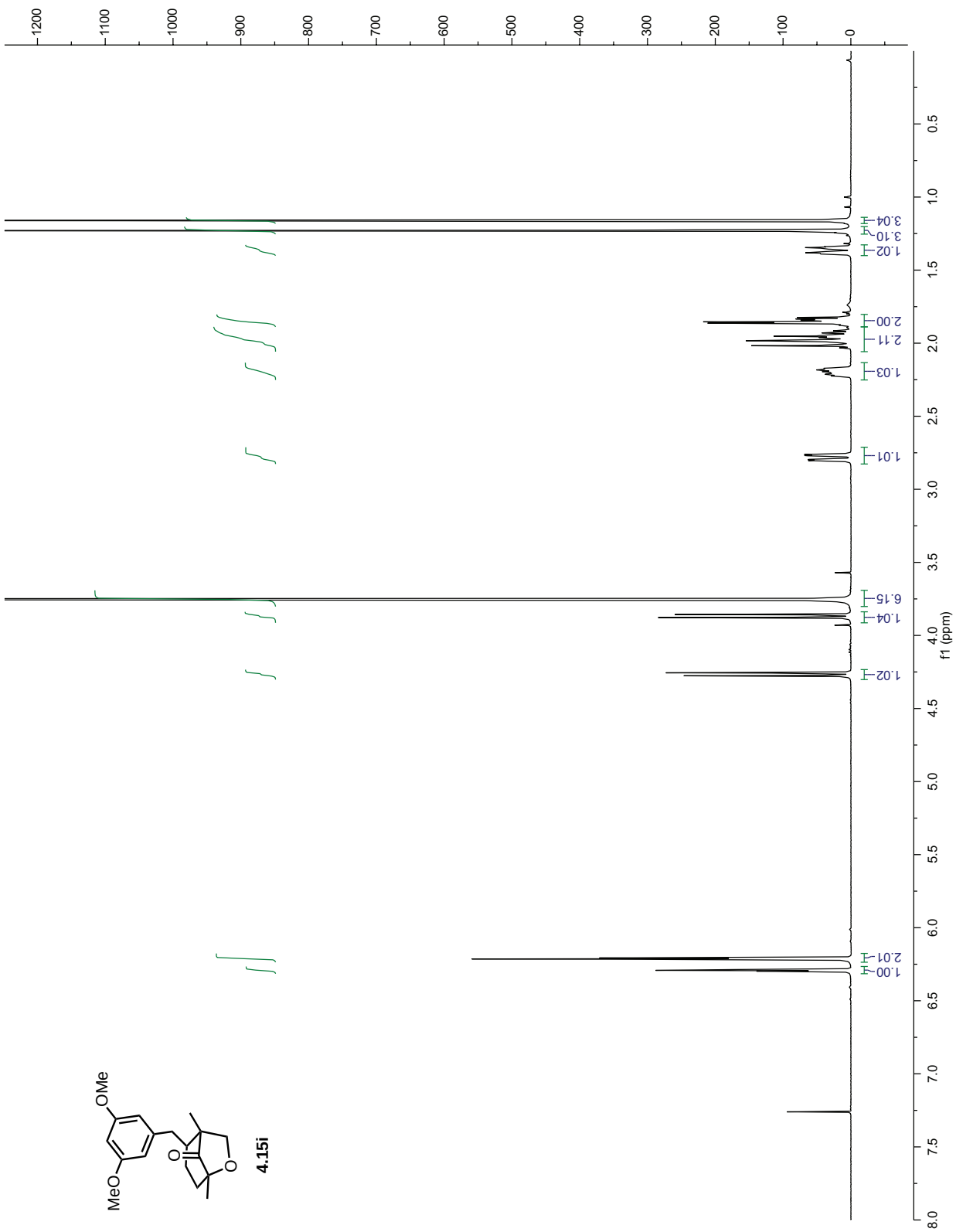

Figure 4.A.17: ^{1}H NMR of **4.15i**

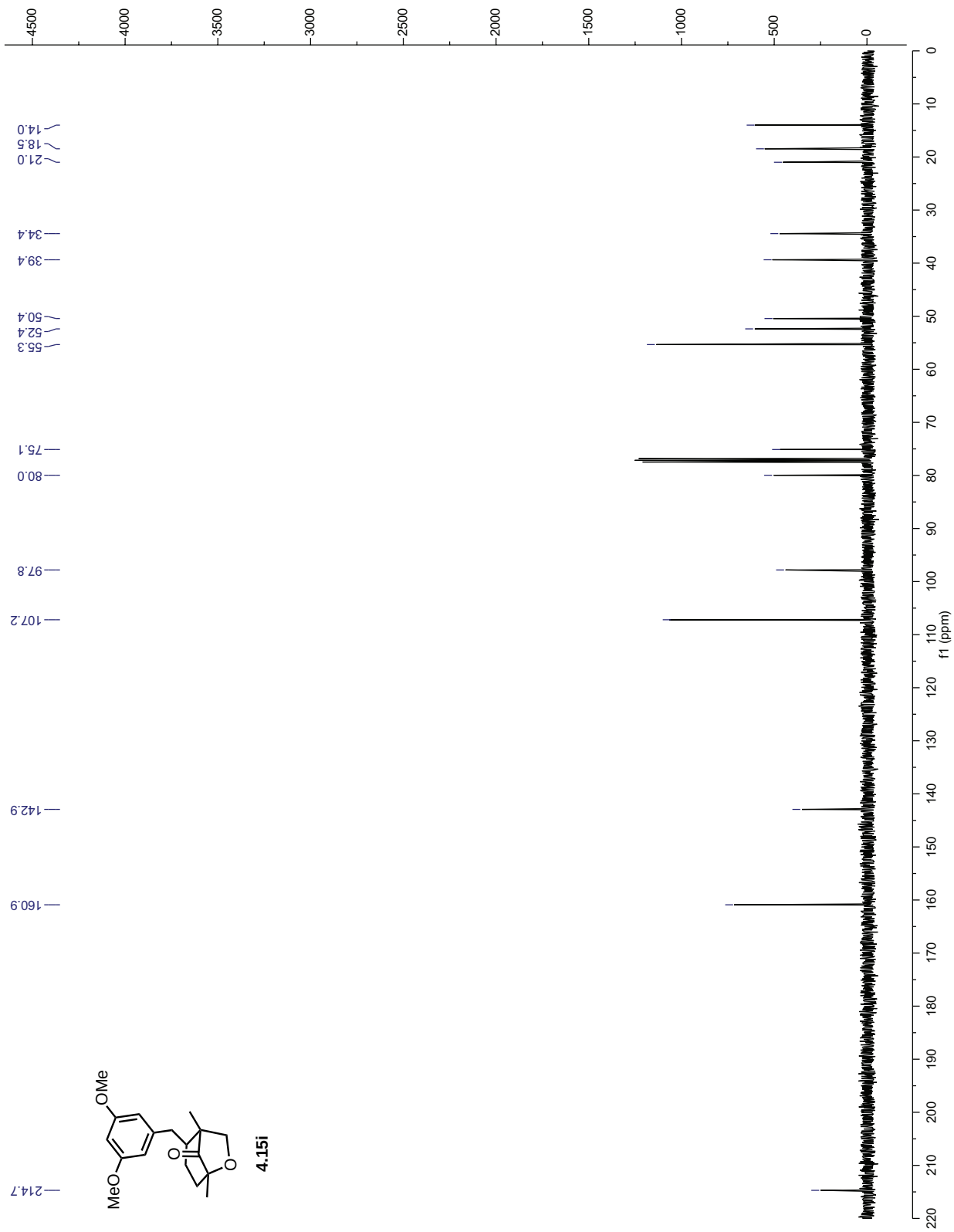

Figure 4.A.18: ^{13}C NMR of **4.15i**

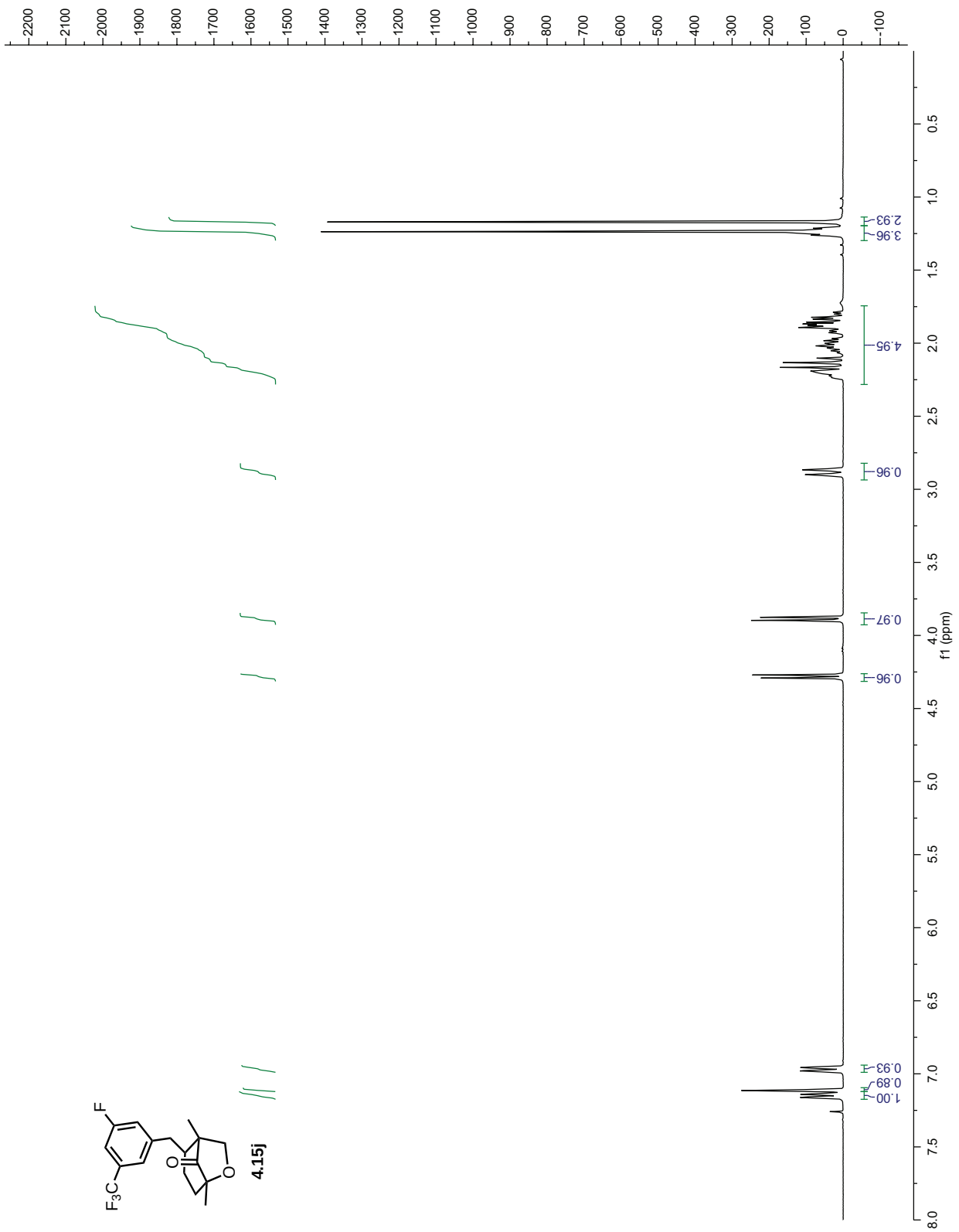

Figure 4.A.19: ^{1}H NMR of **4.15j**

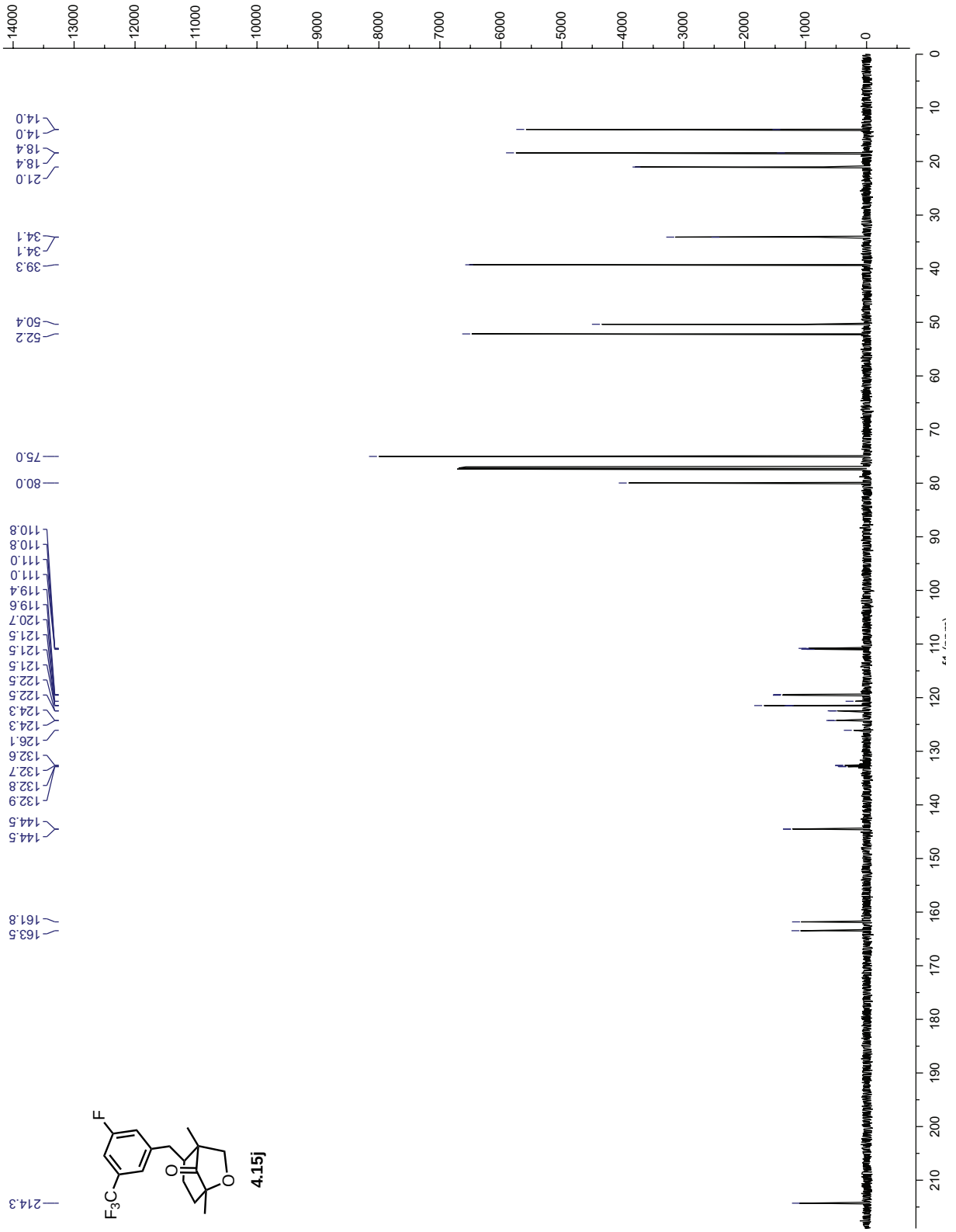

Figure 4.A.20: ^{13}C NMR of **4.15j**

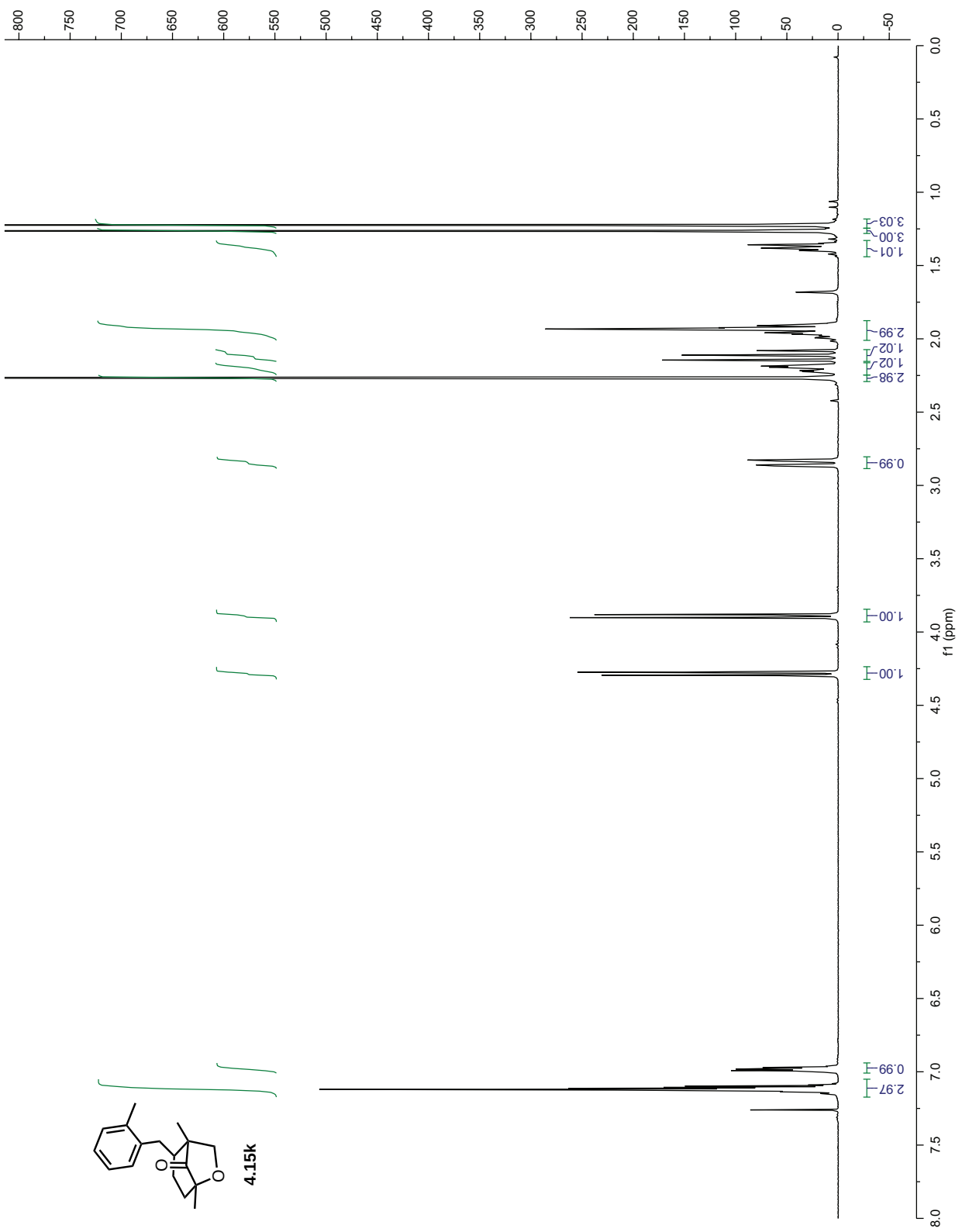

Figure 4.A.21: ^{1}H NMR of **4.15k**

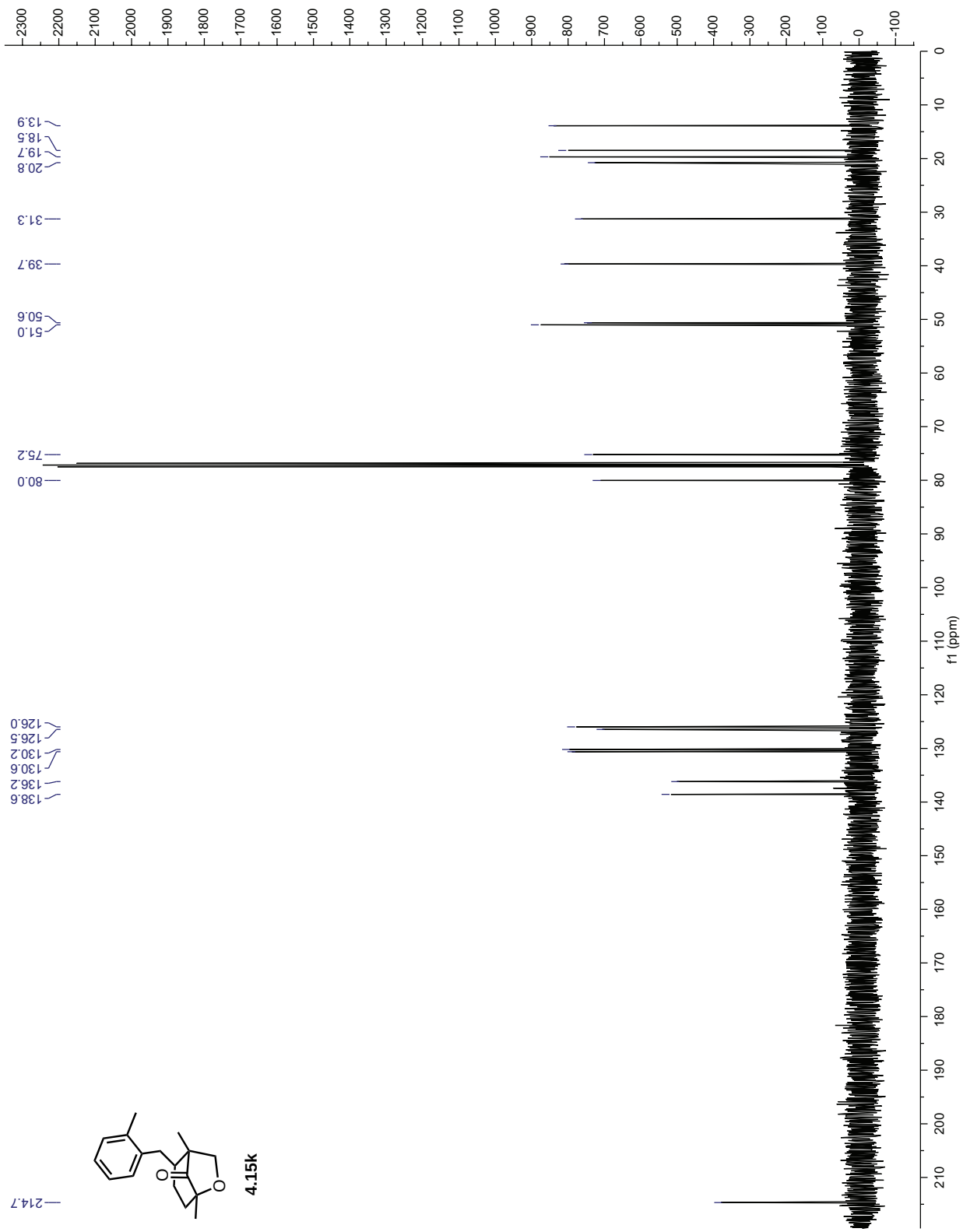

Figure 4.A.22: ^{13}C NMR of **4.15k**

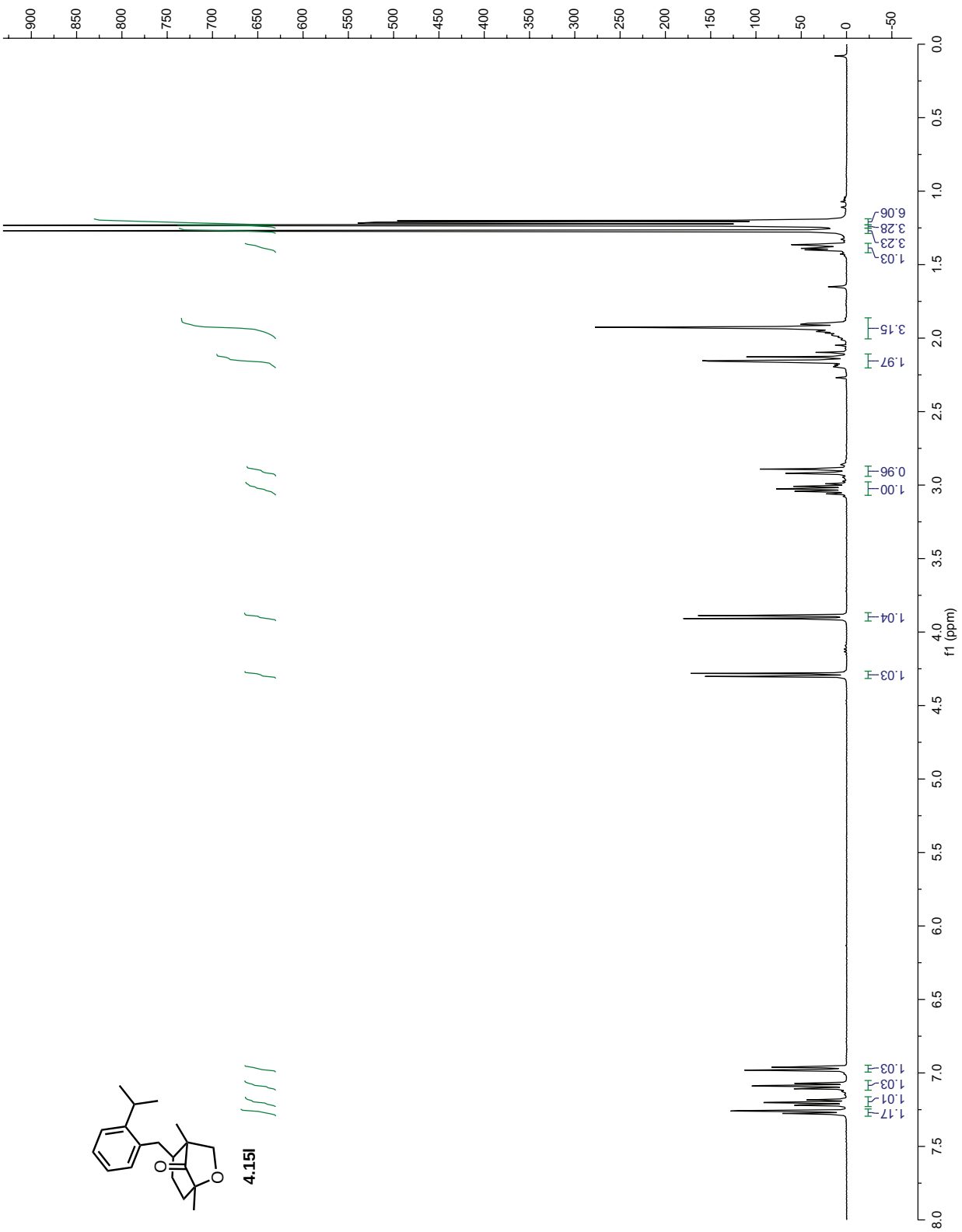

Figure 4.A.23: ^{1}H NMR of **4.15l**

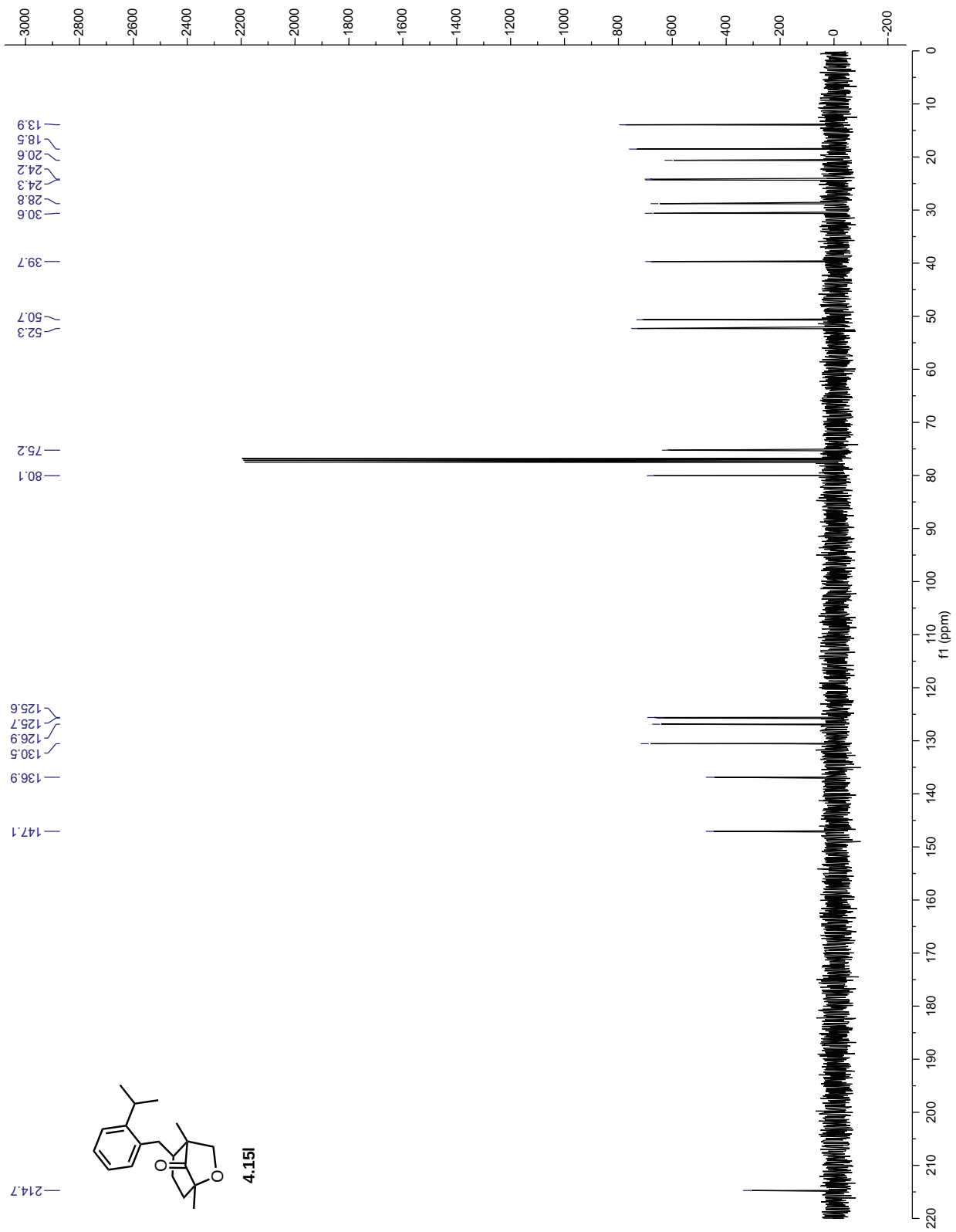

Figure 4.A.24: ^{13}C NMR of **4.15l**

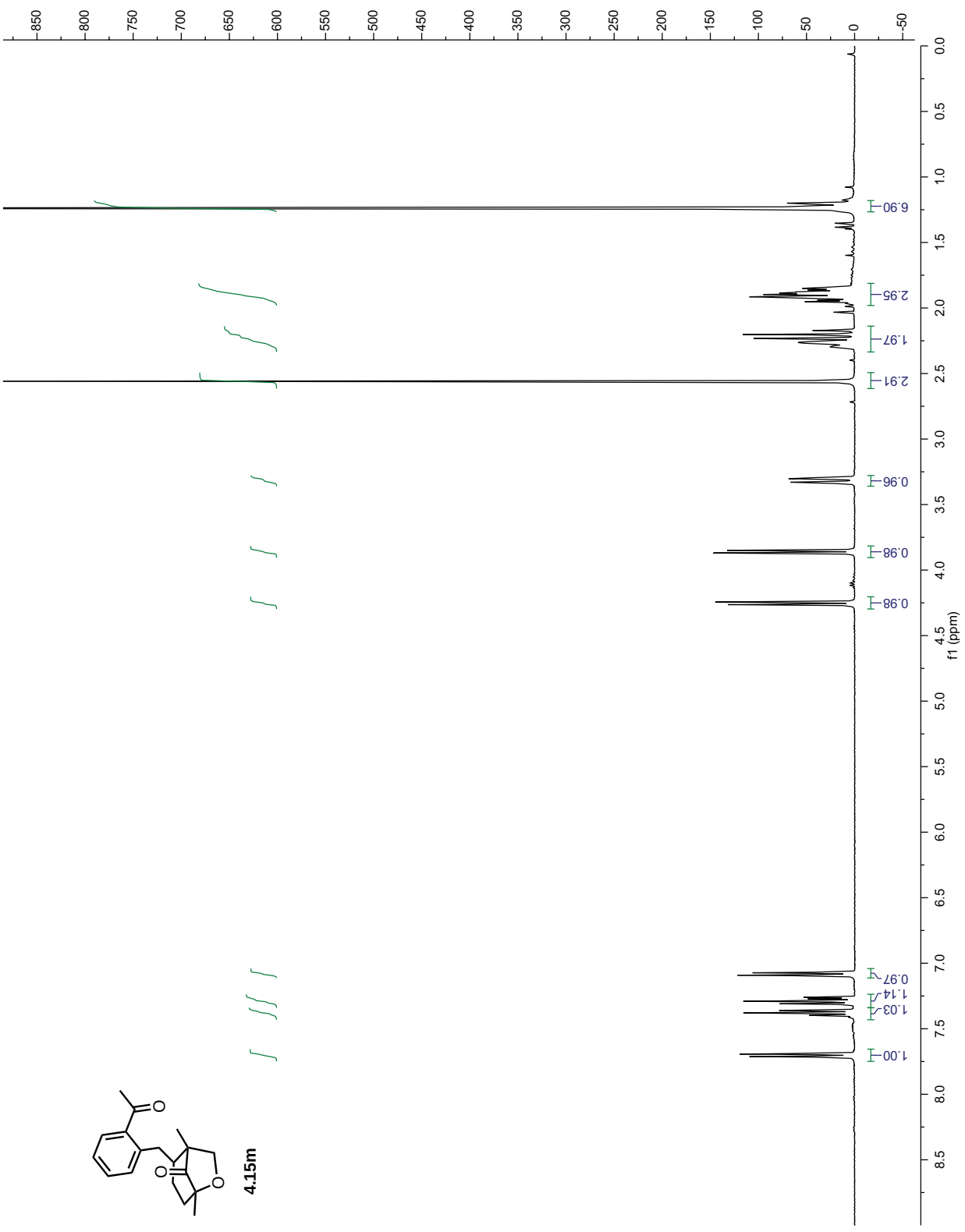

Figure 4.A.25: ^{1}H NMR of **4.15m**

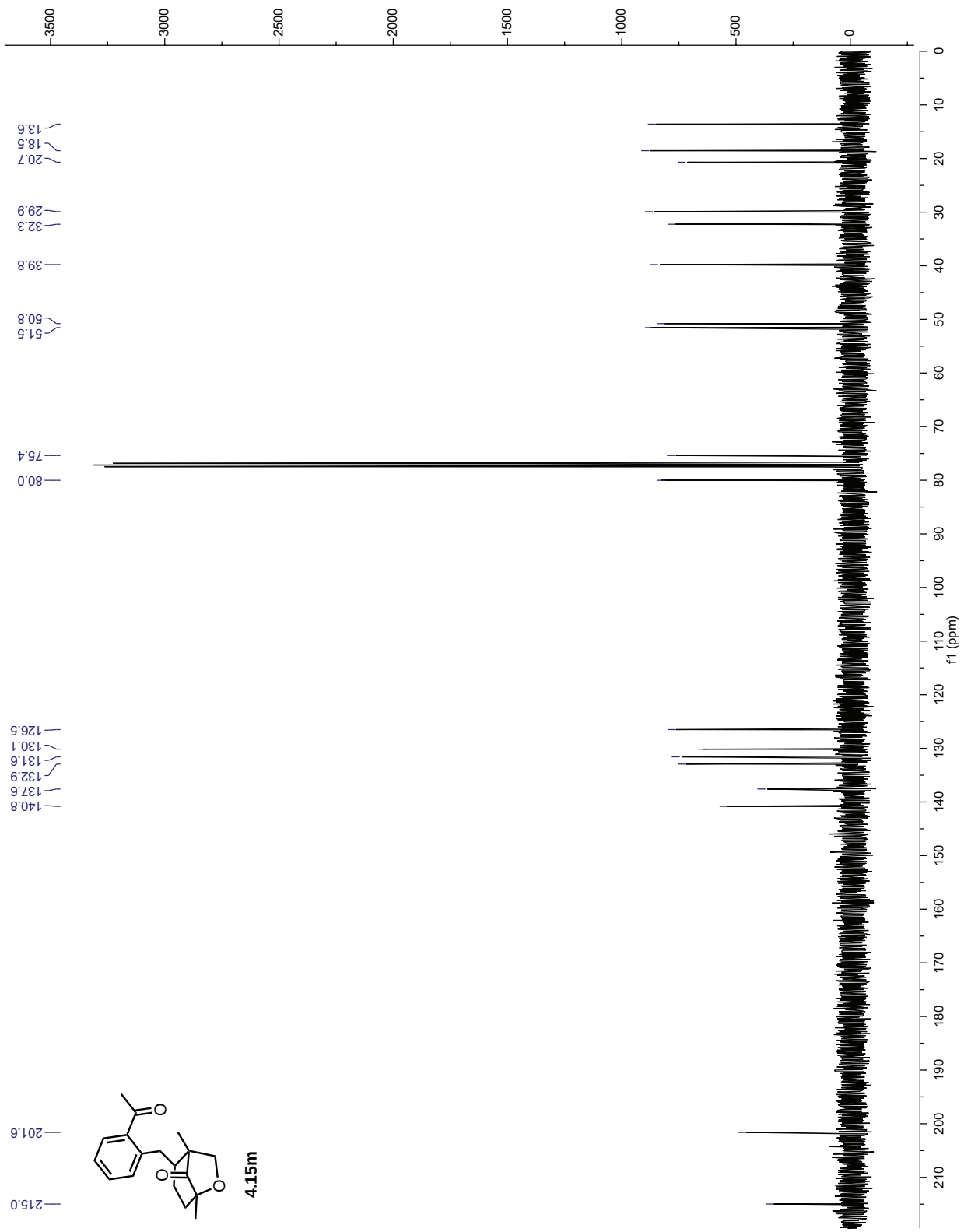

Figure 4.A.26: ^{13}C NMR of **4.15m**

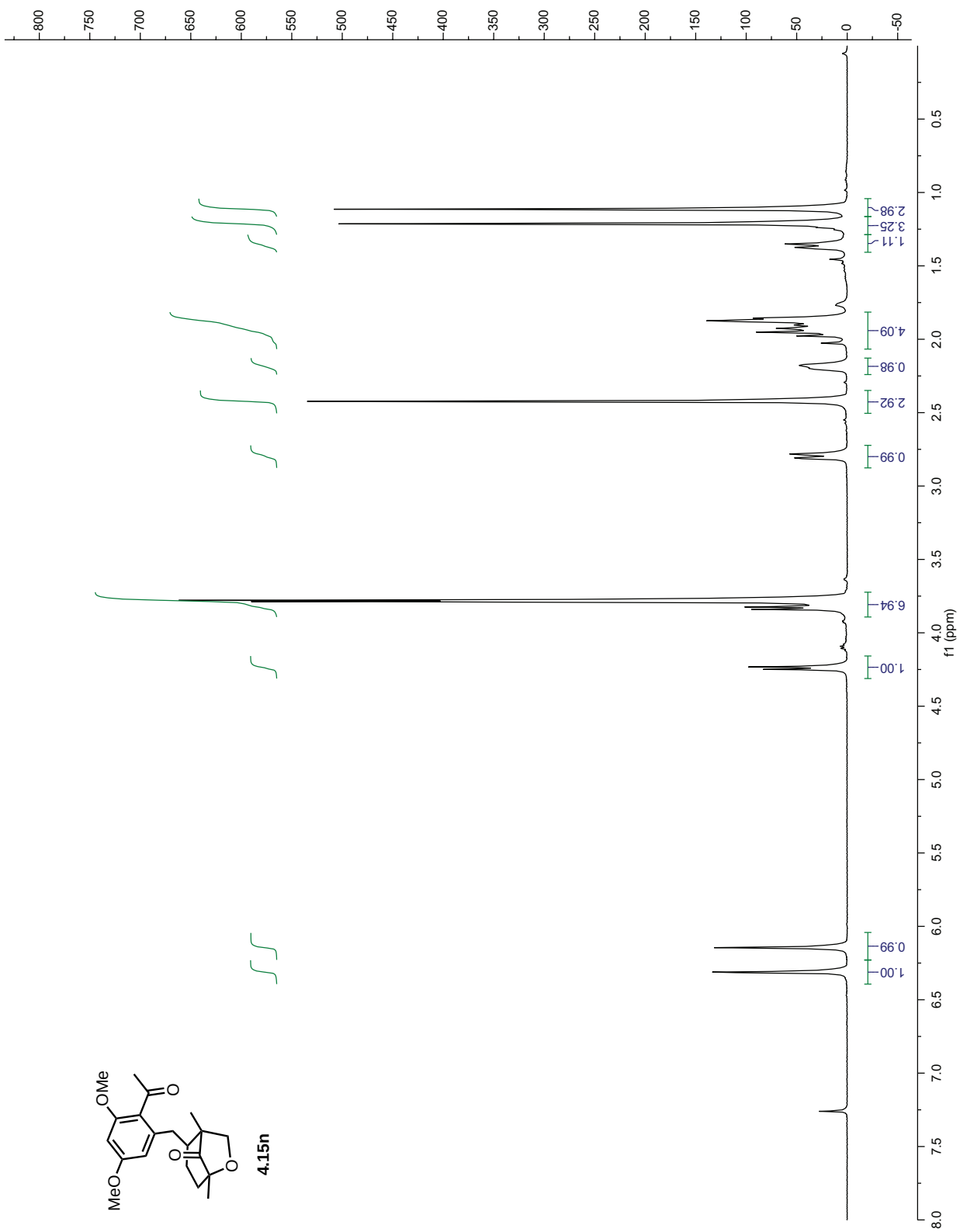

Figure 4.A.27: ^{1}H NMR of **4.15n**

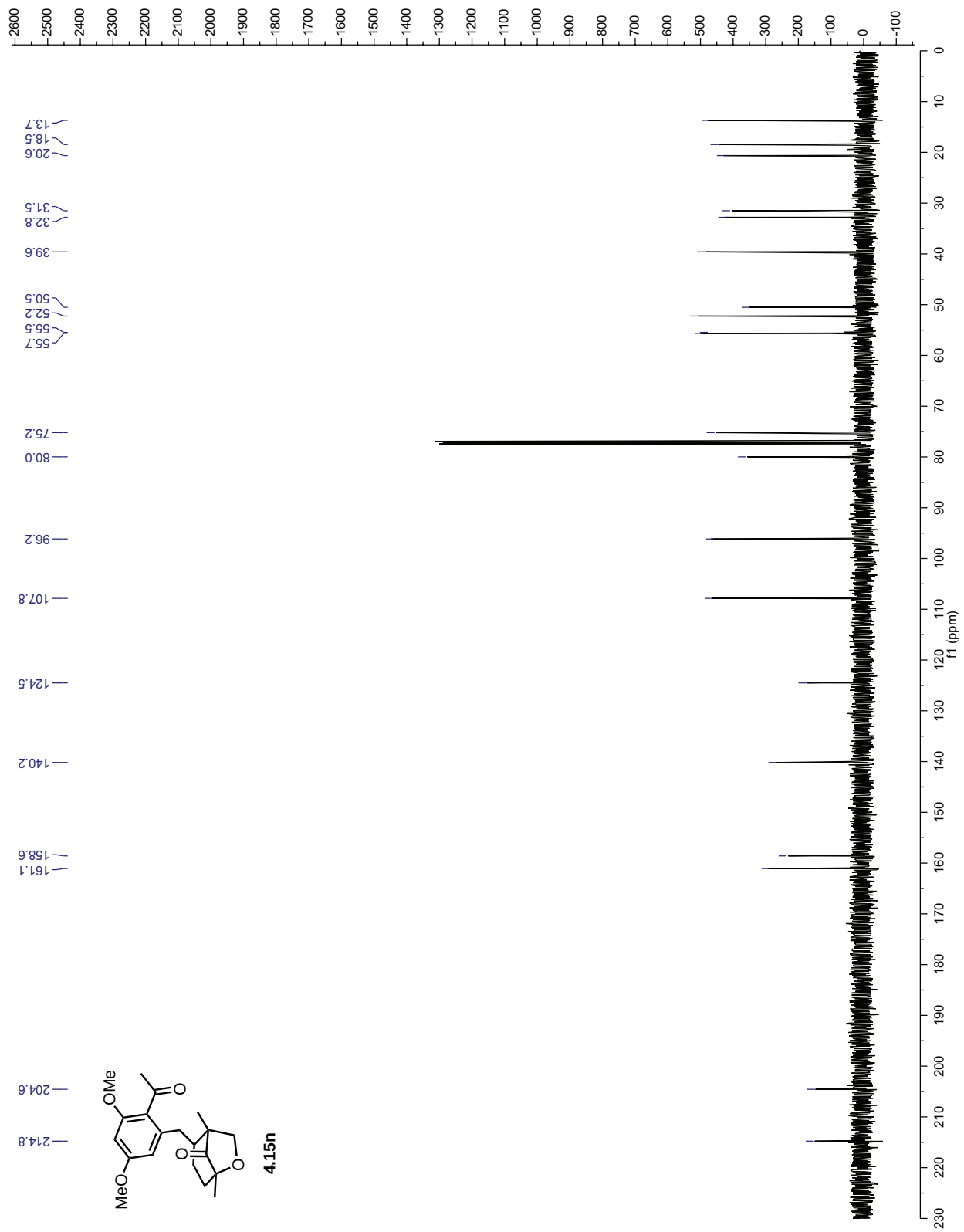

Figure 4.A.28: ^{13}C NMR of **4.15n**

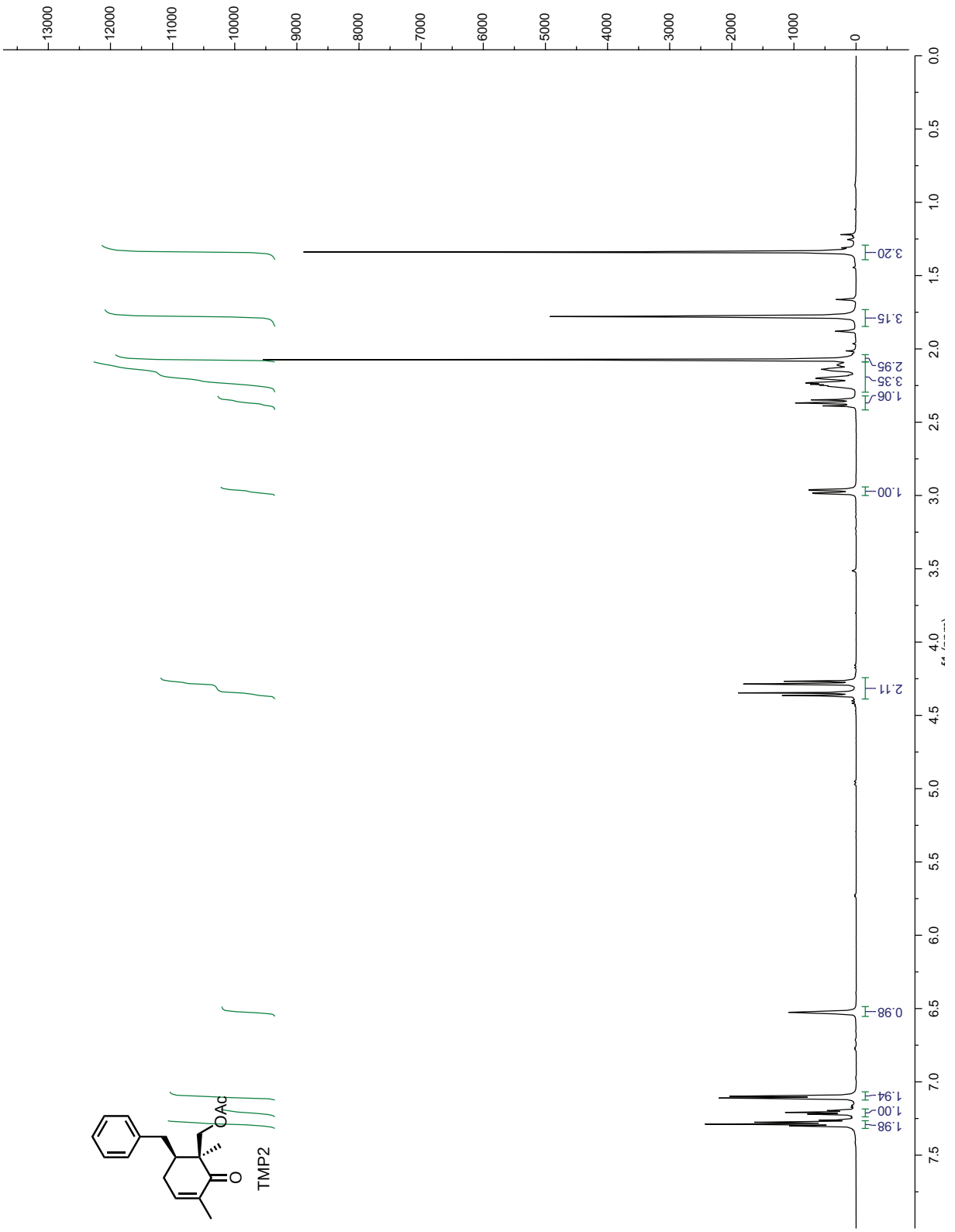

Figure 4.A.29: ^{1}H NMR of **4.17a**

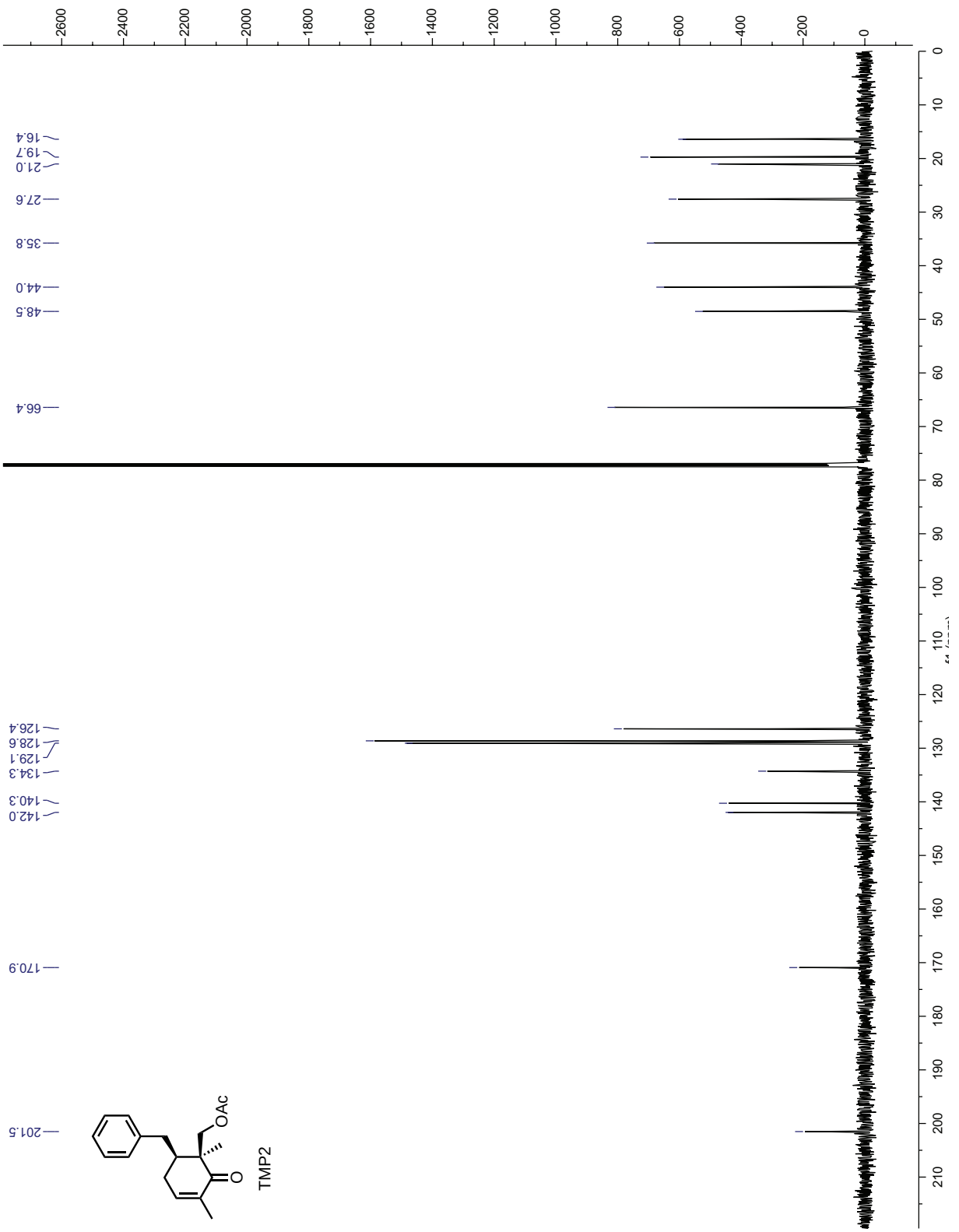

Figure 4.A.30: ^{13}C NMR of **4.17a**

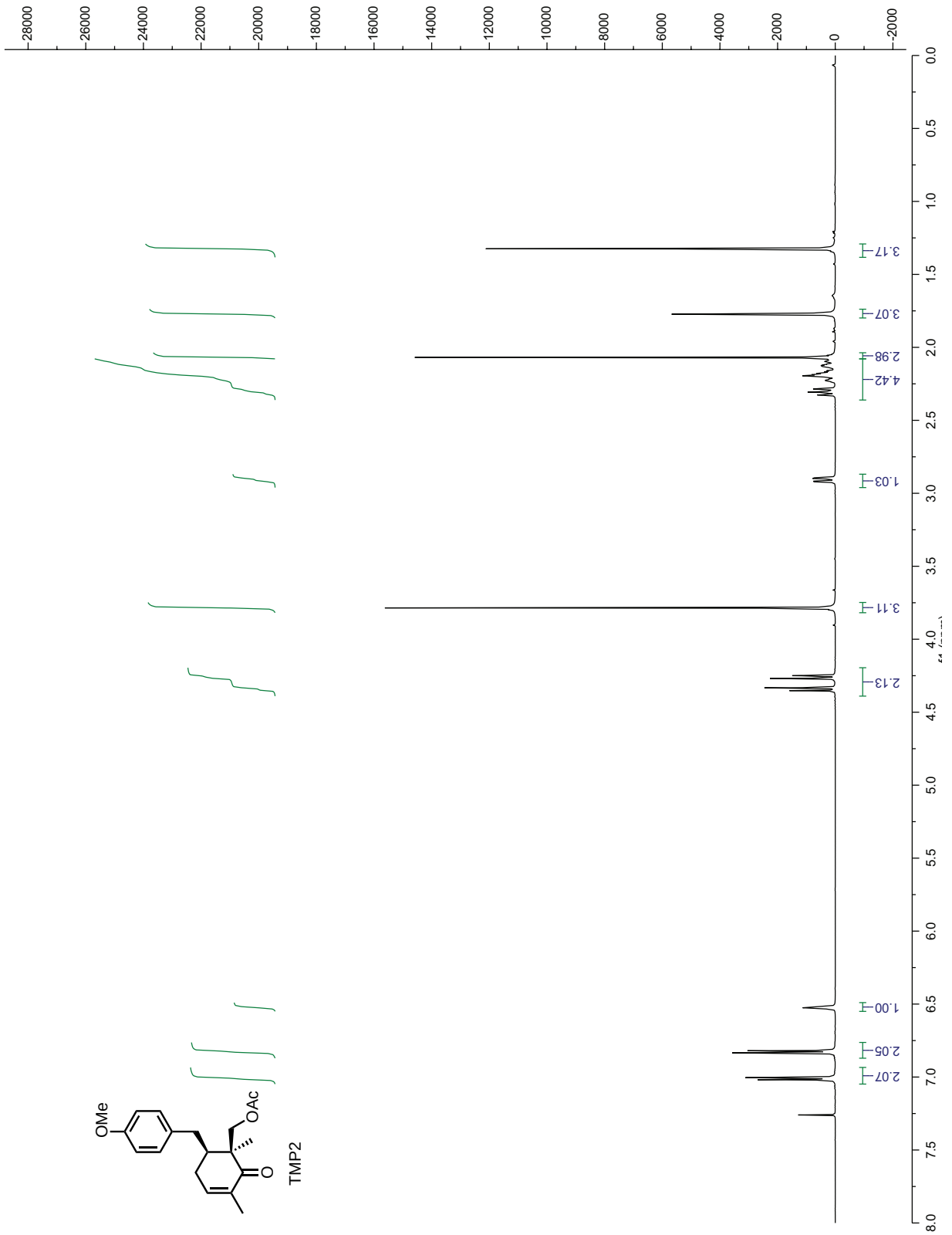

Figure 4.A.31: ^{1}H NMR of **4.17b**

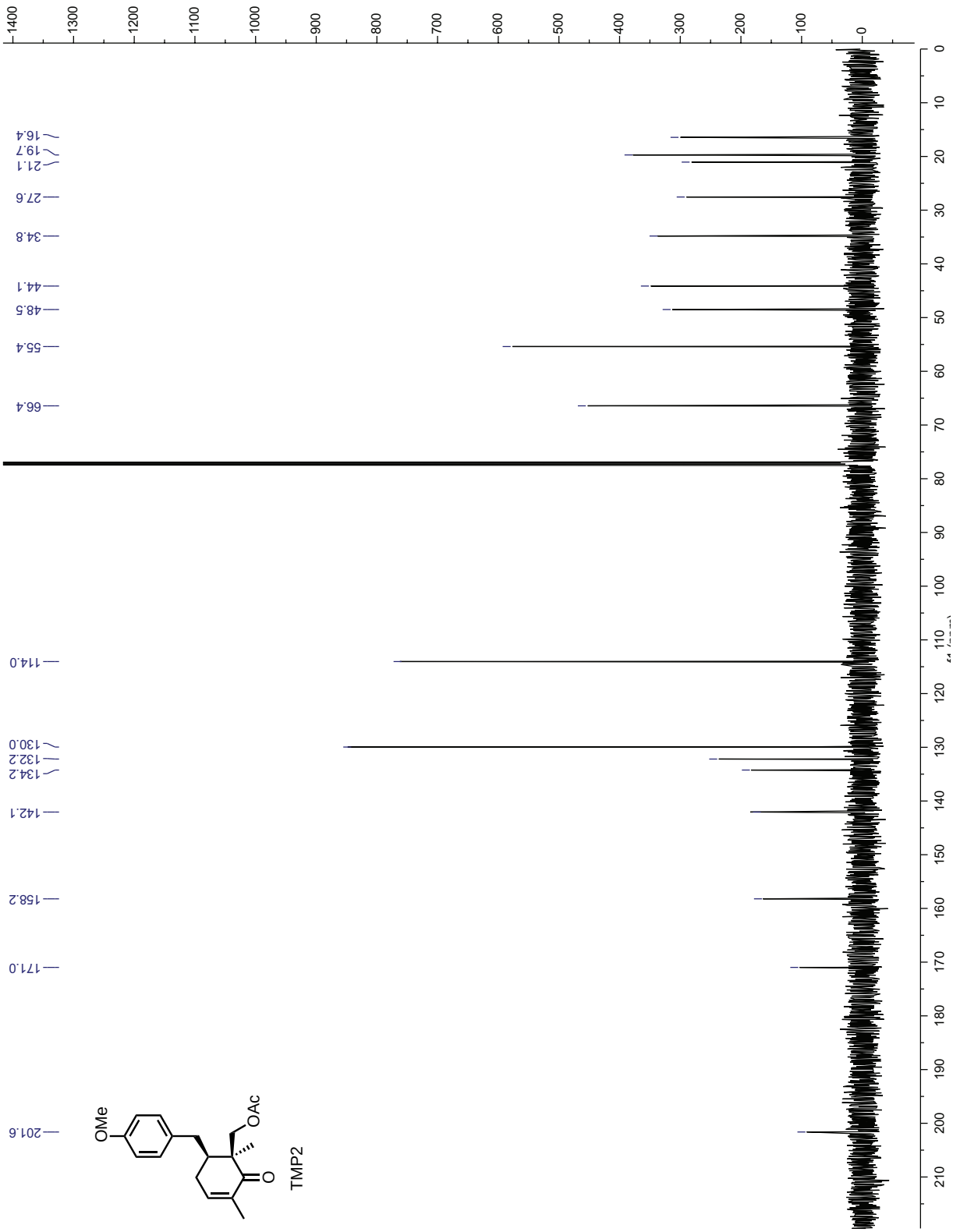

Figure 4.A.32: ^{13}C NMR of **4.17b**

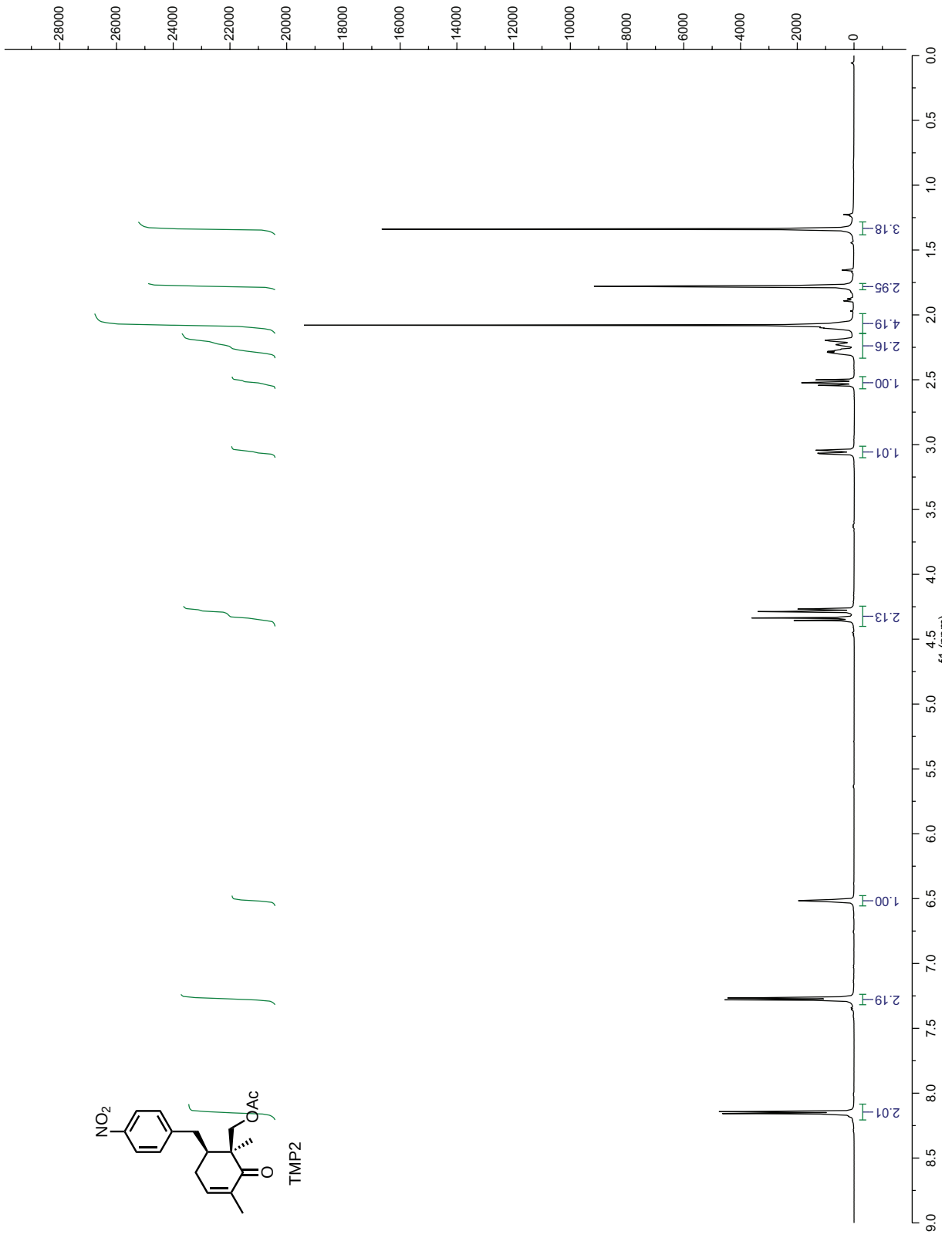

Figure 4.A.33: ^{1}H NMR of **4.17c**

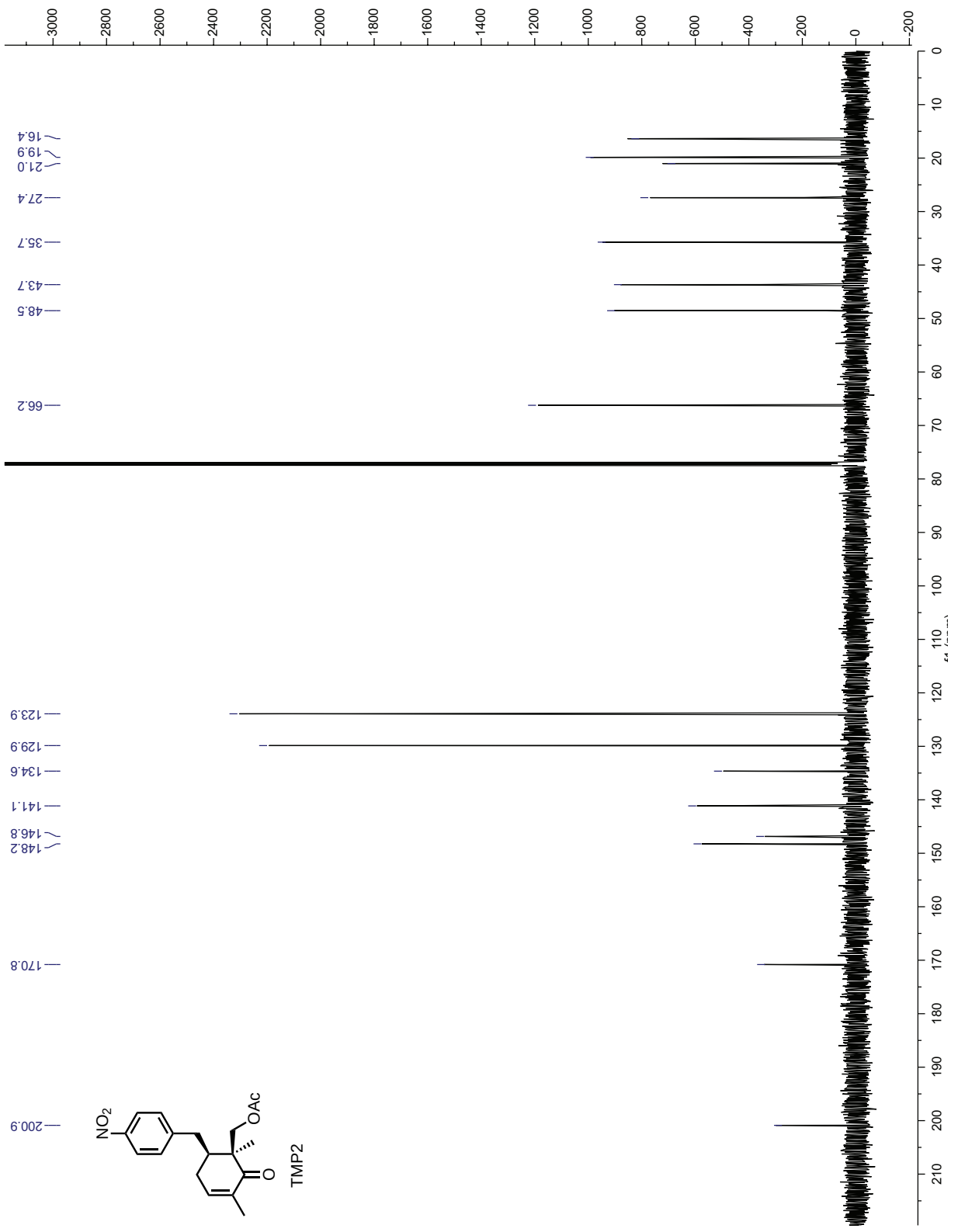

Figure 4.A.34: ^{13}C NMR of **4.17c**

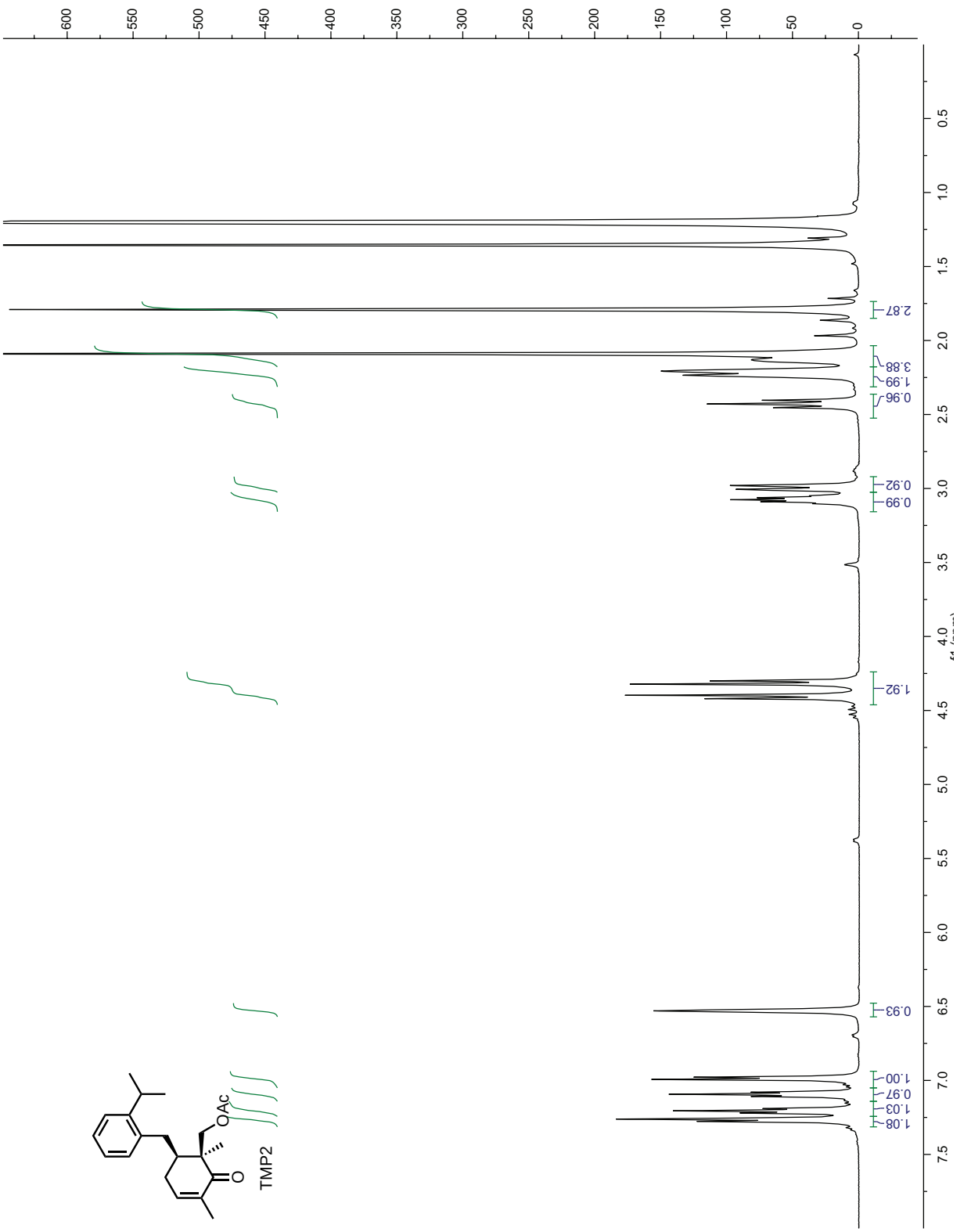

Figure 4.A.35: ^{1}H NMR of **4.17d**

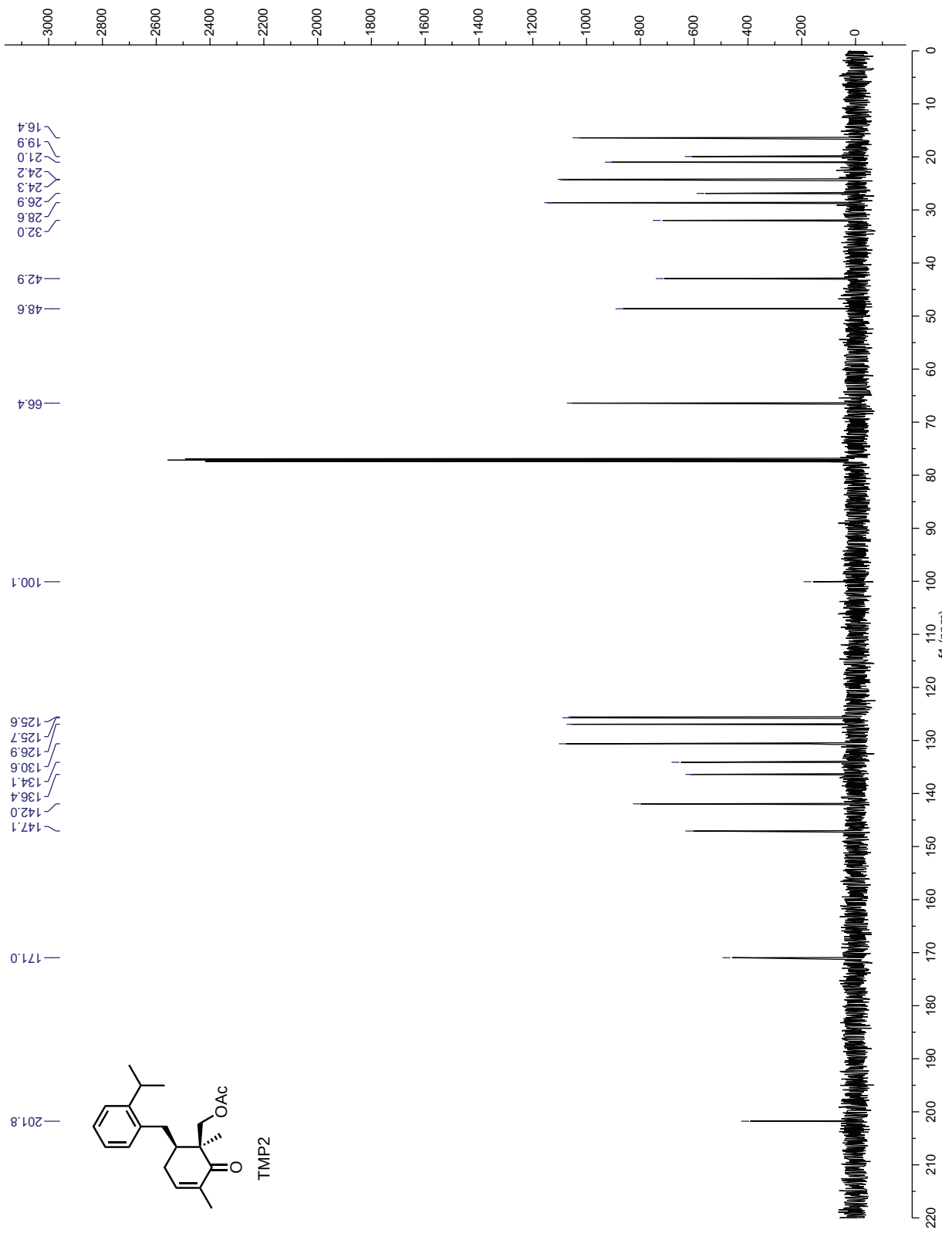

Figure 4.A.36: ^{13}C NMR of **4.17d**

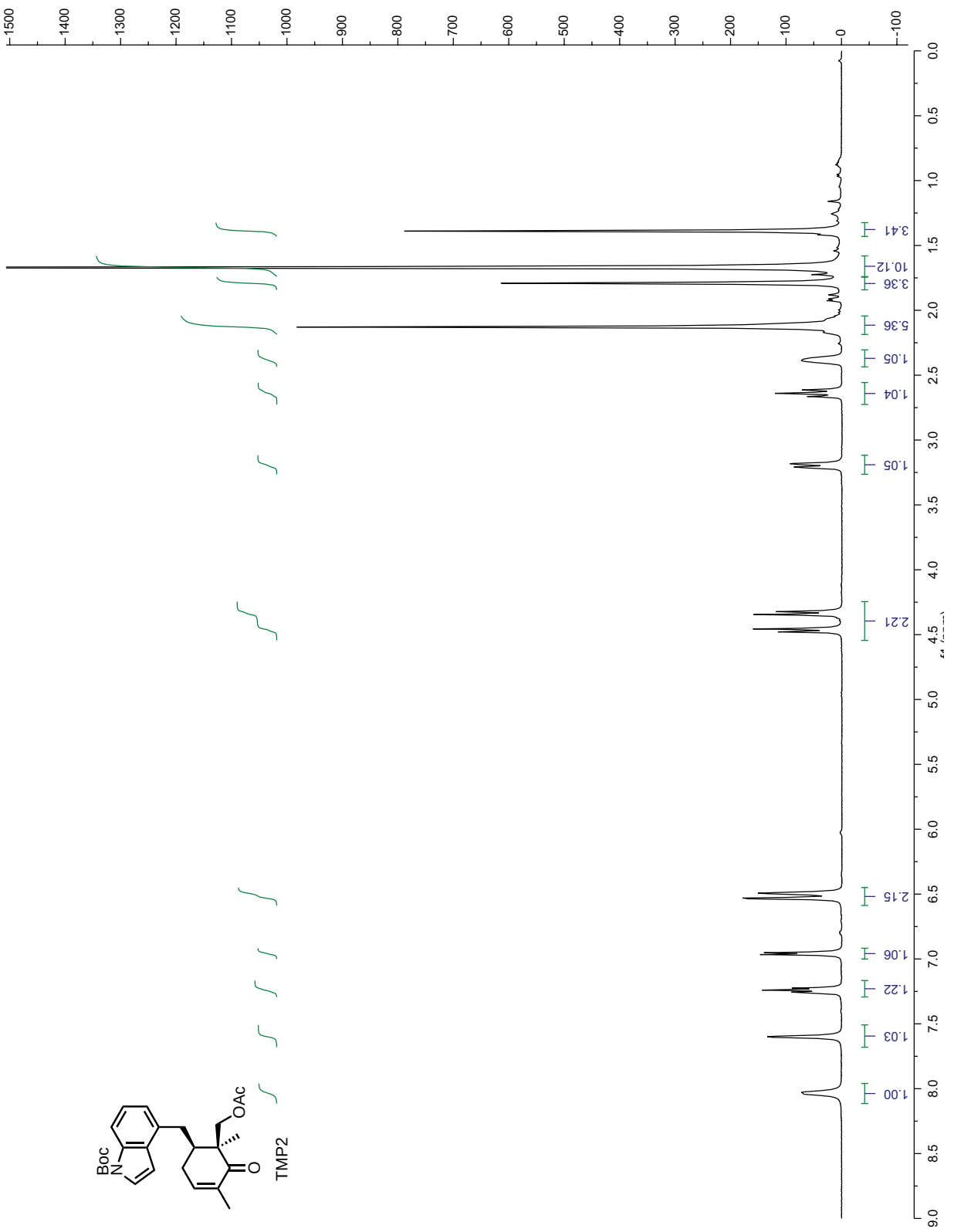

Figure 4.A.37: ^{1}H NMR of **4.17e**

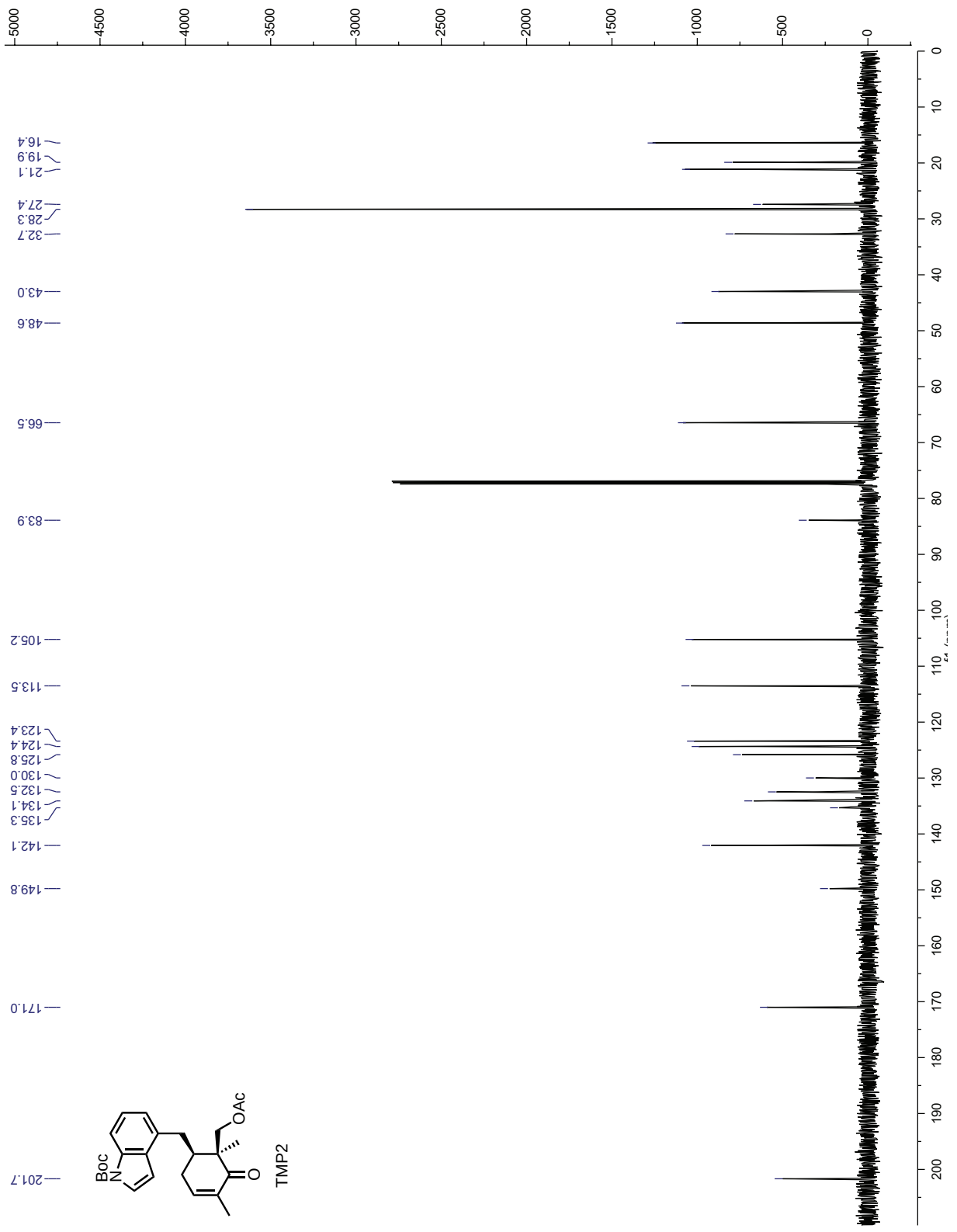

Figure 4.A.38: ^{13}C NMR of **4.17e**

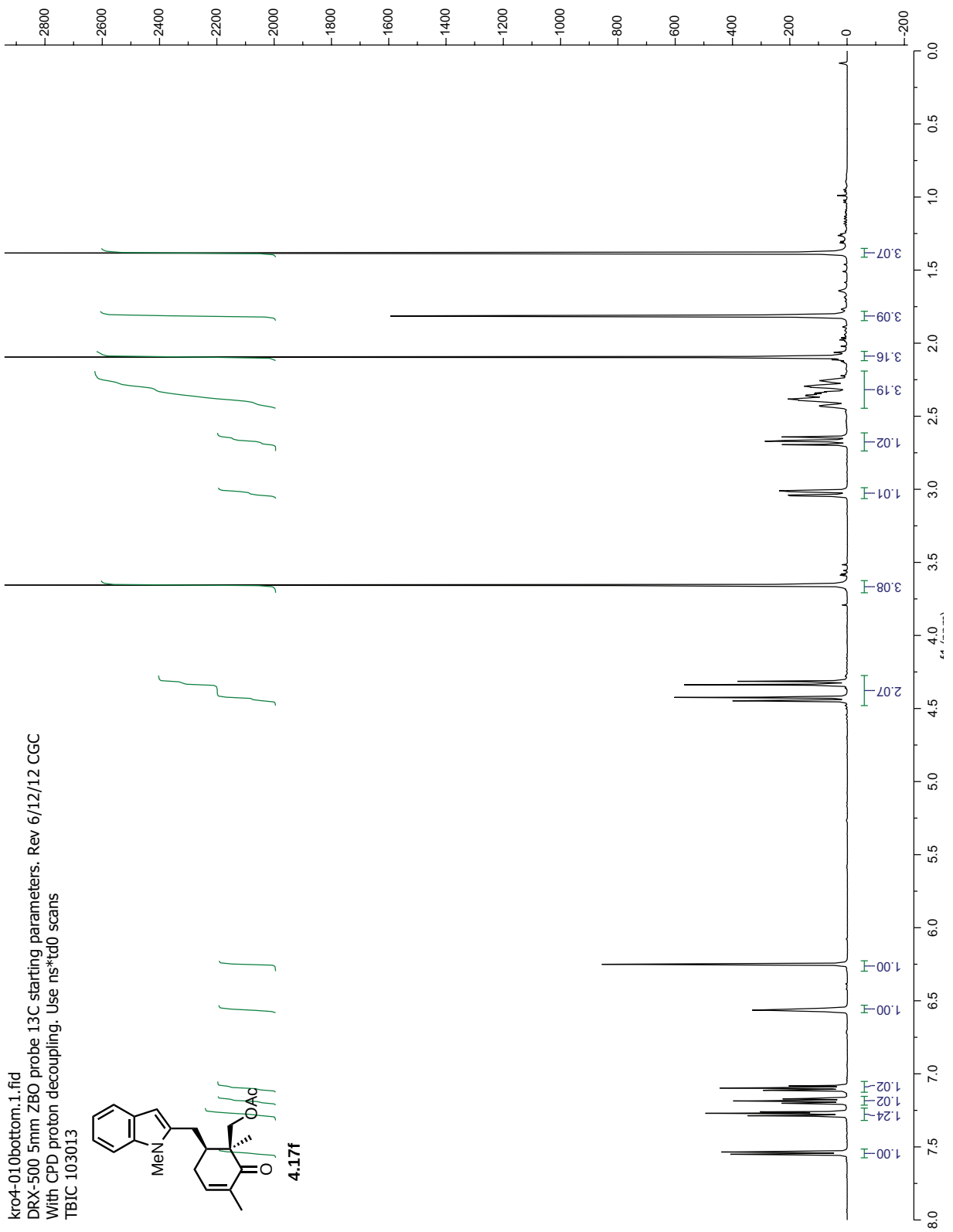

Figure 4.A.39: ^{1}H NMR of **4.17f**

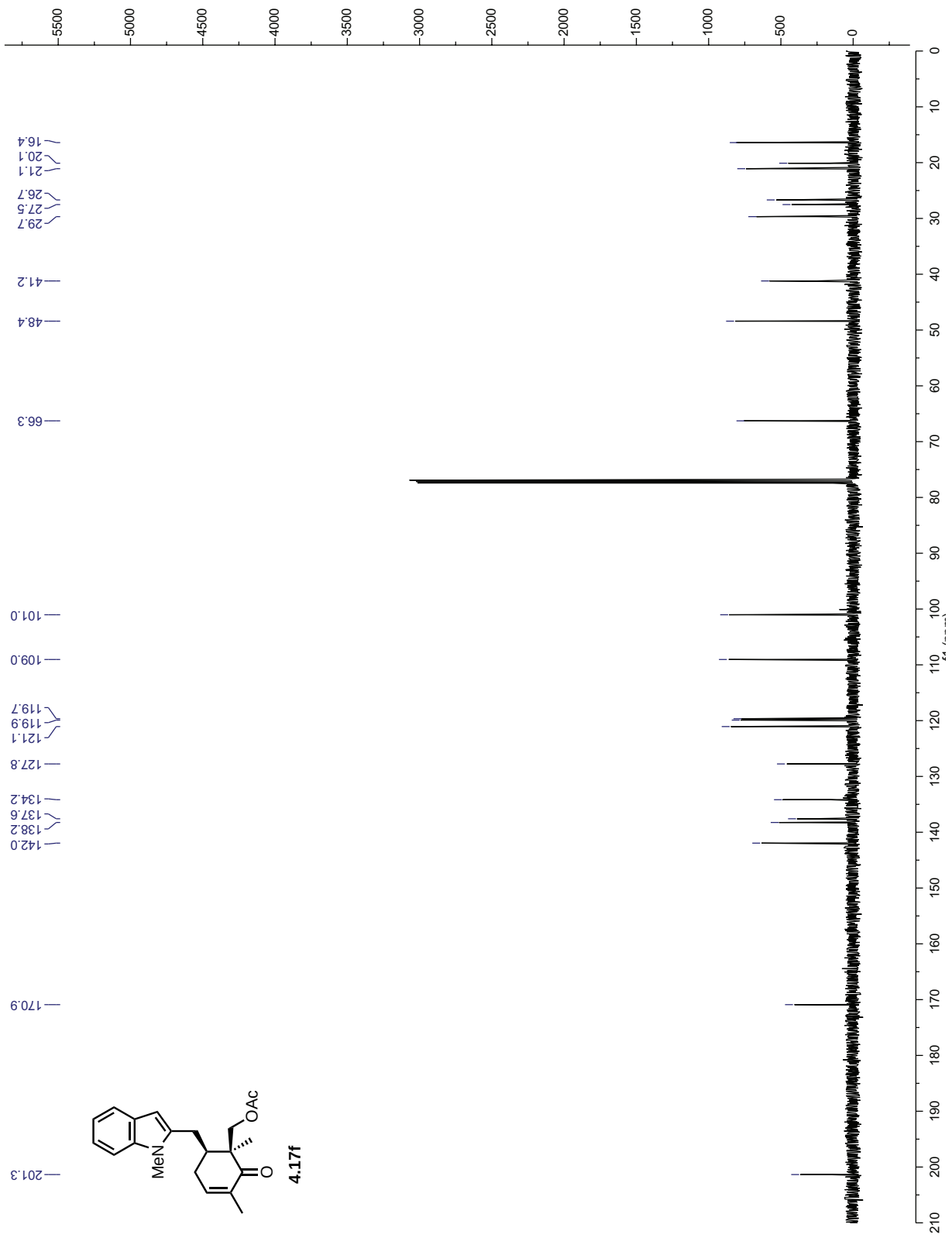

Figure 4.A.40: ^{13}C NMR of **4.17f**

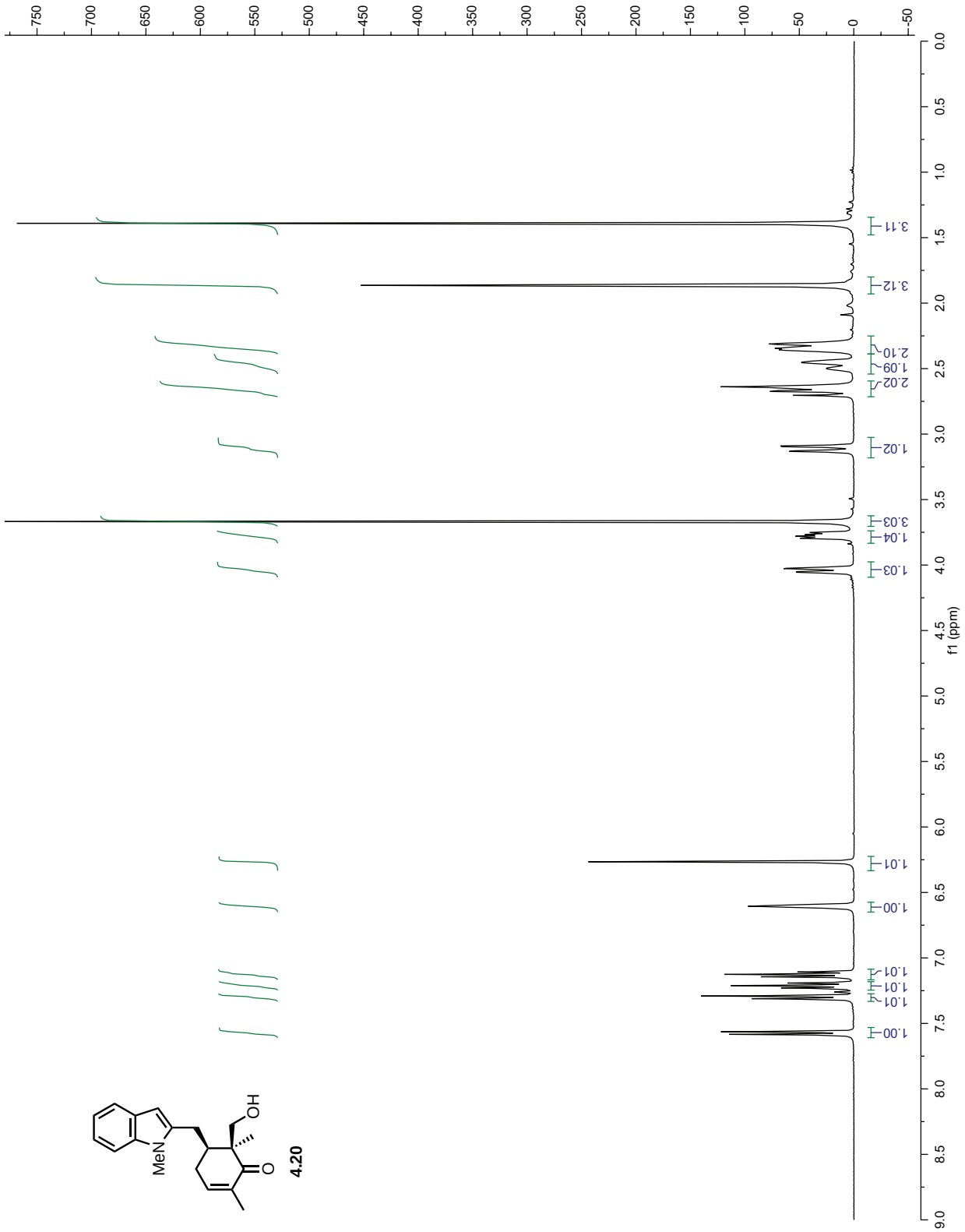

Figure 4.A.41: ^{1}H NMR of **4.20**

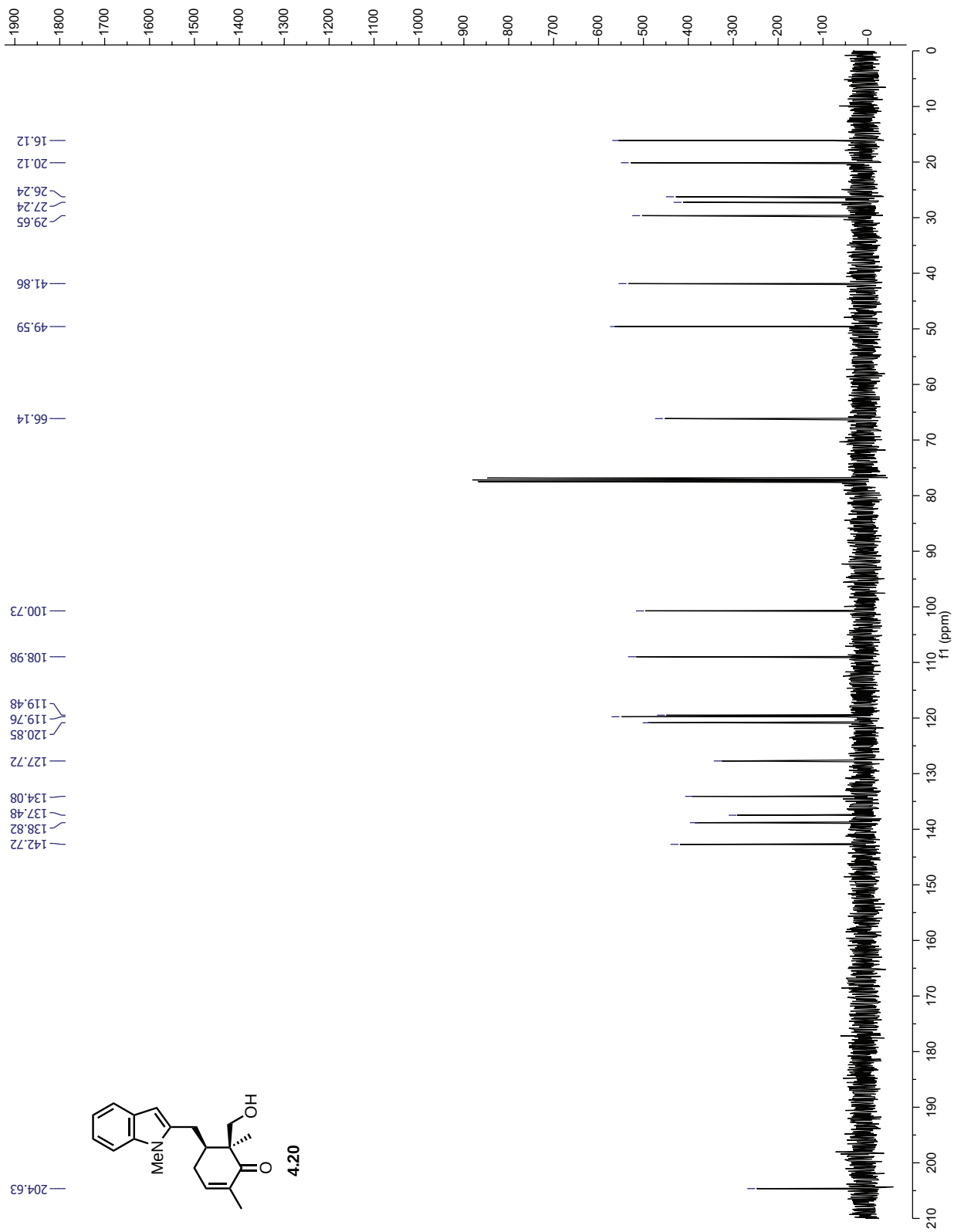

Figure 4.A.42: ^{13}C NMR of **4.20**

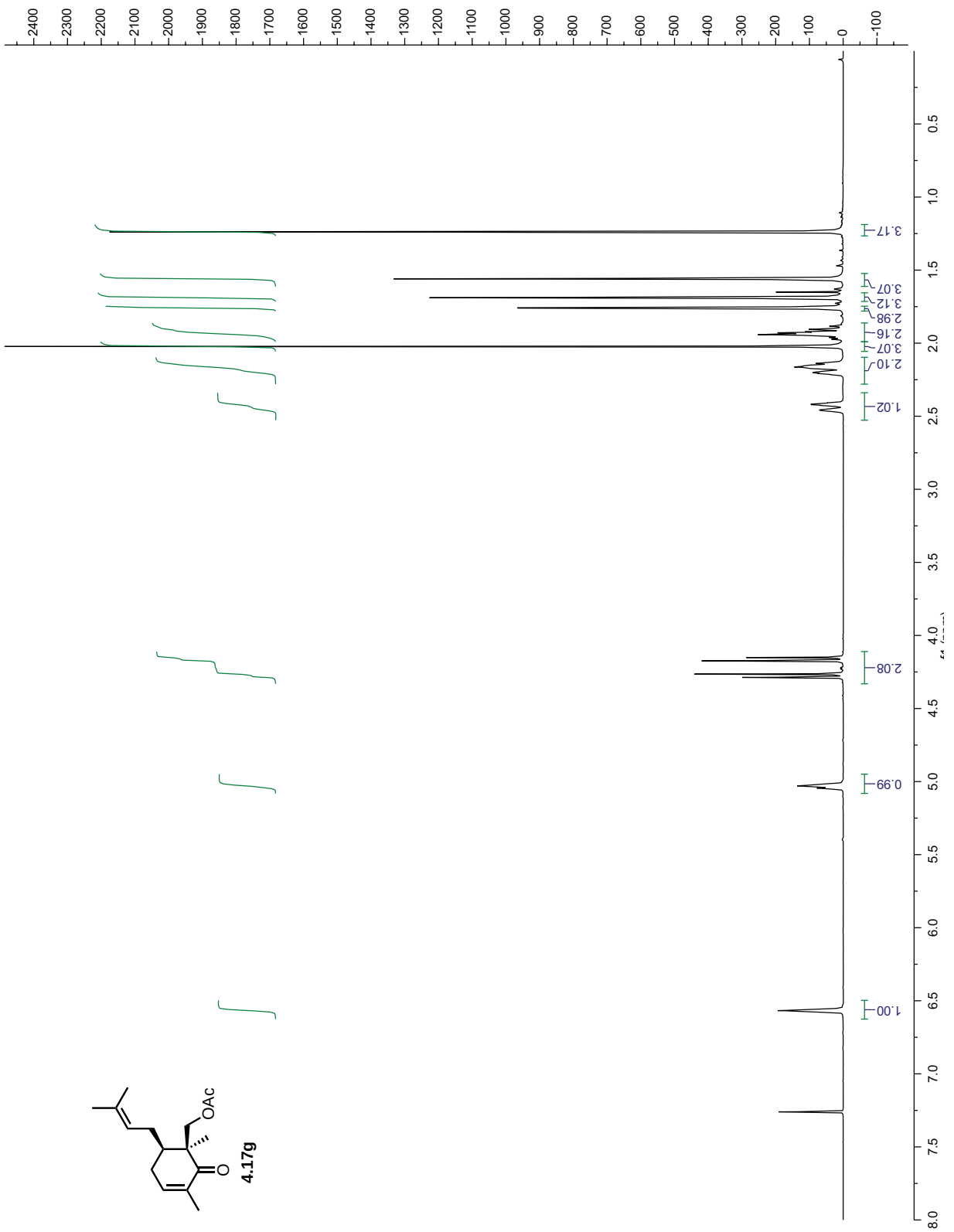

Figure 4.A.43: ^{1}H NMR of **4.17g**

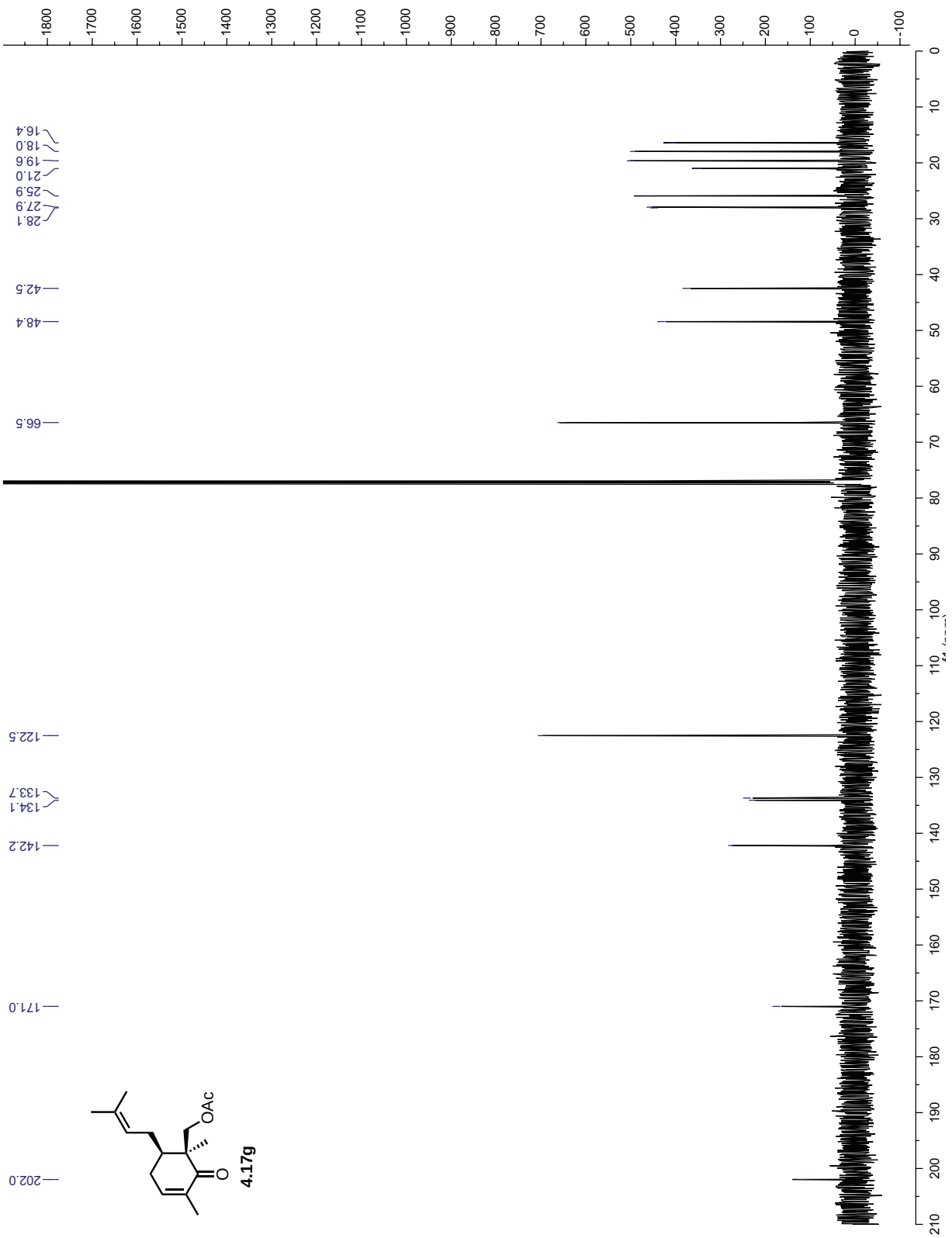

Figure 4.A.44: ^{13}C NMR of **4.17g**

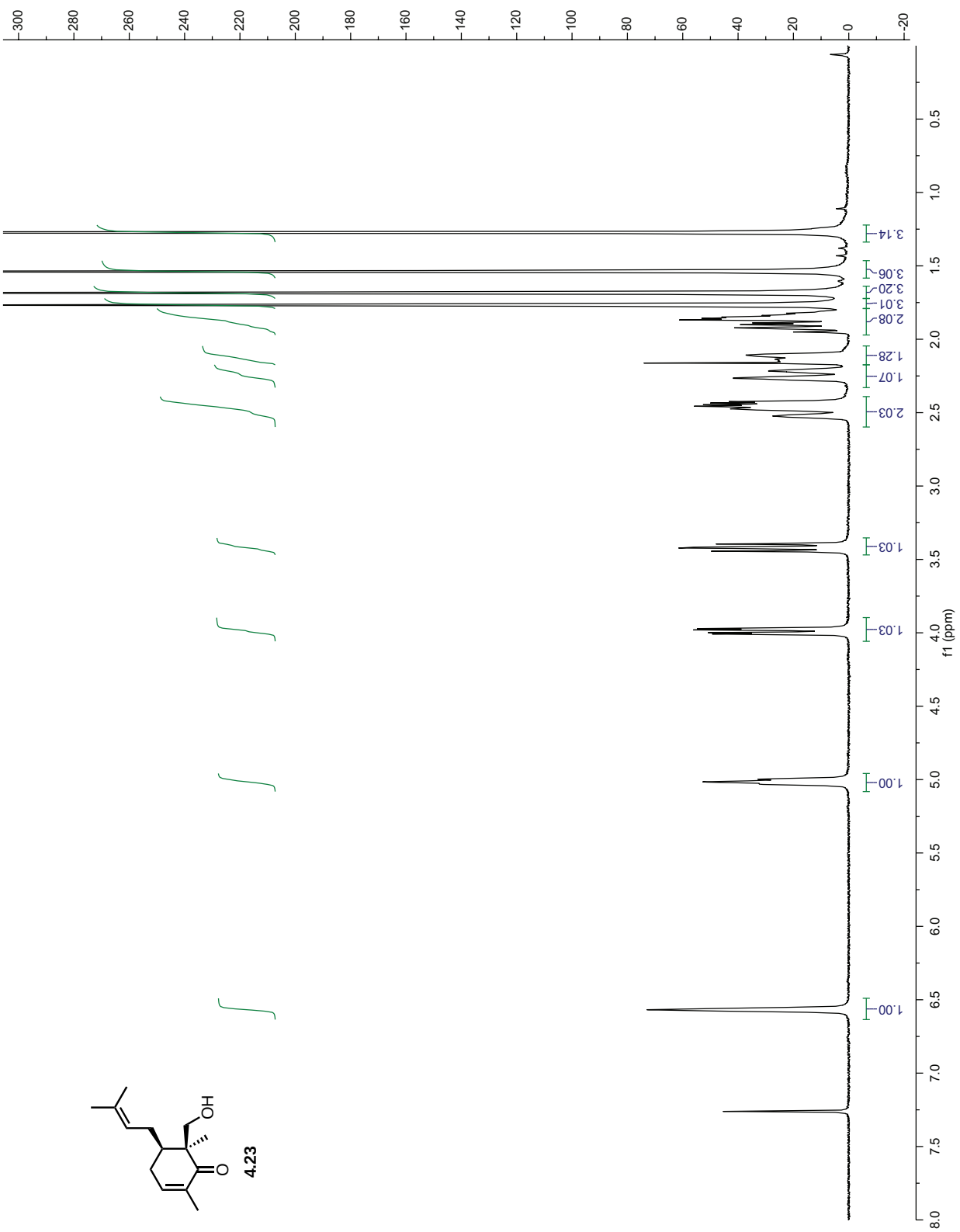

Figure 4.A.45: ^{1}H NMR of **4.23**

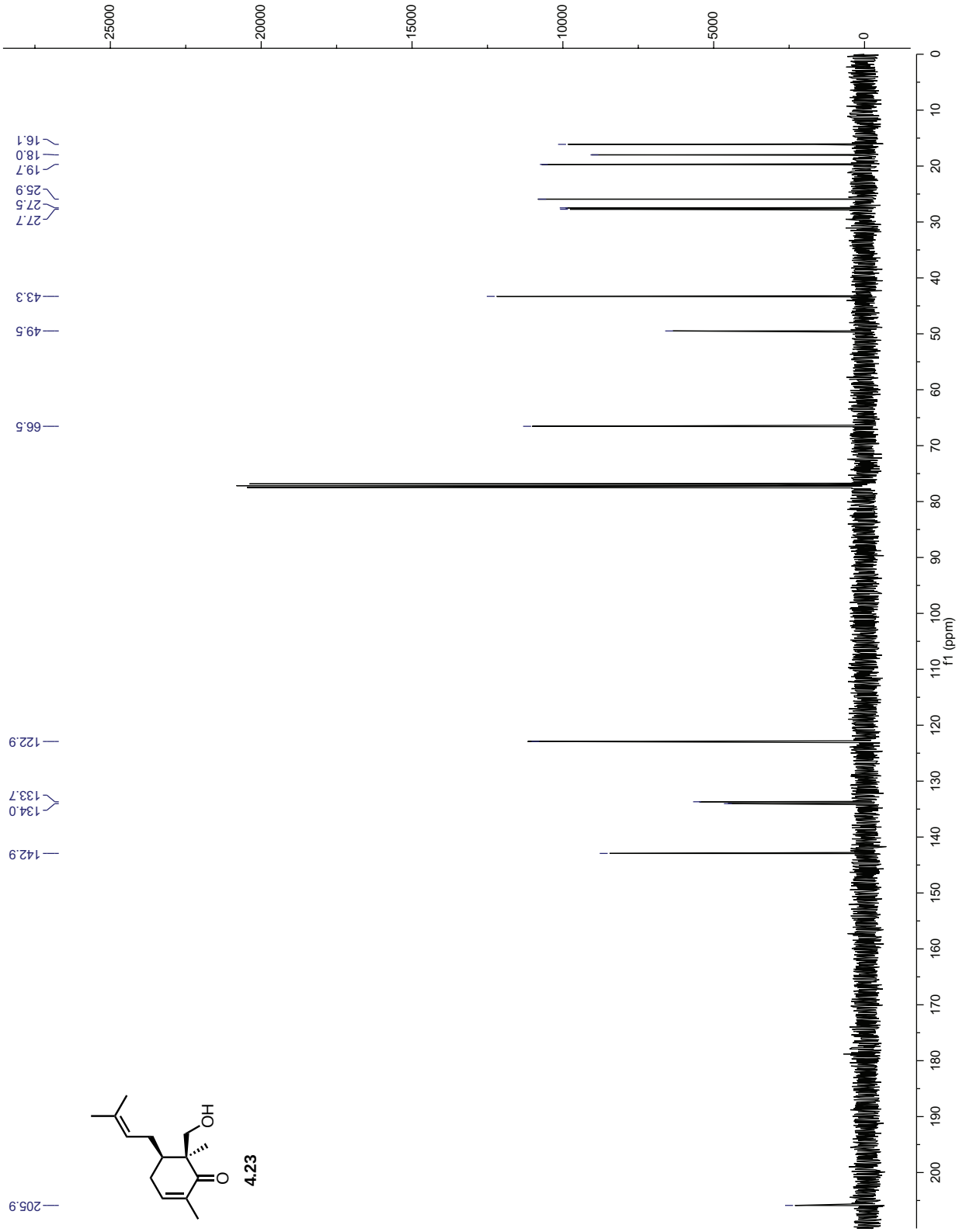

Figure 4.A.46: ^{13}C NMR of **4.23**

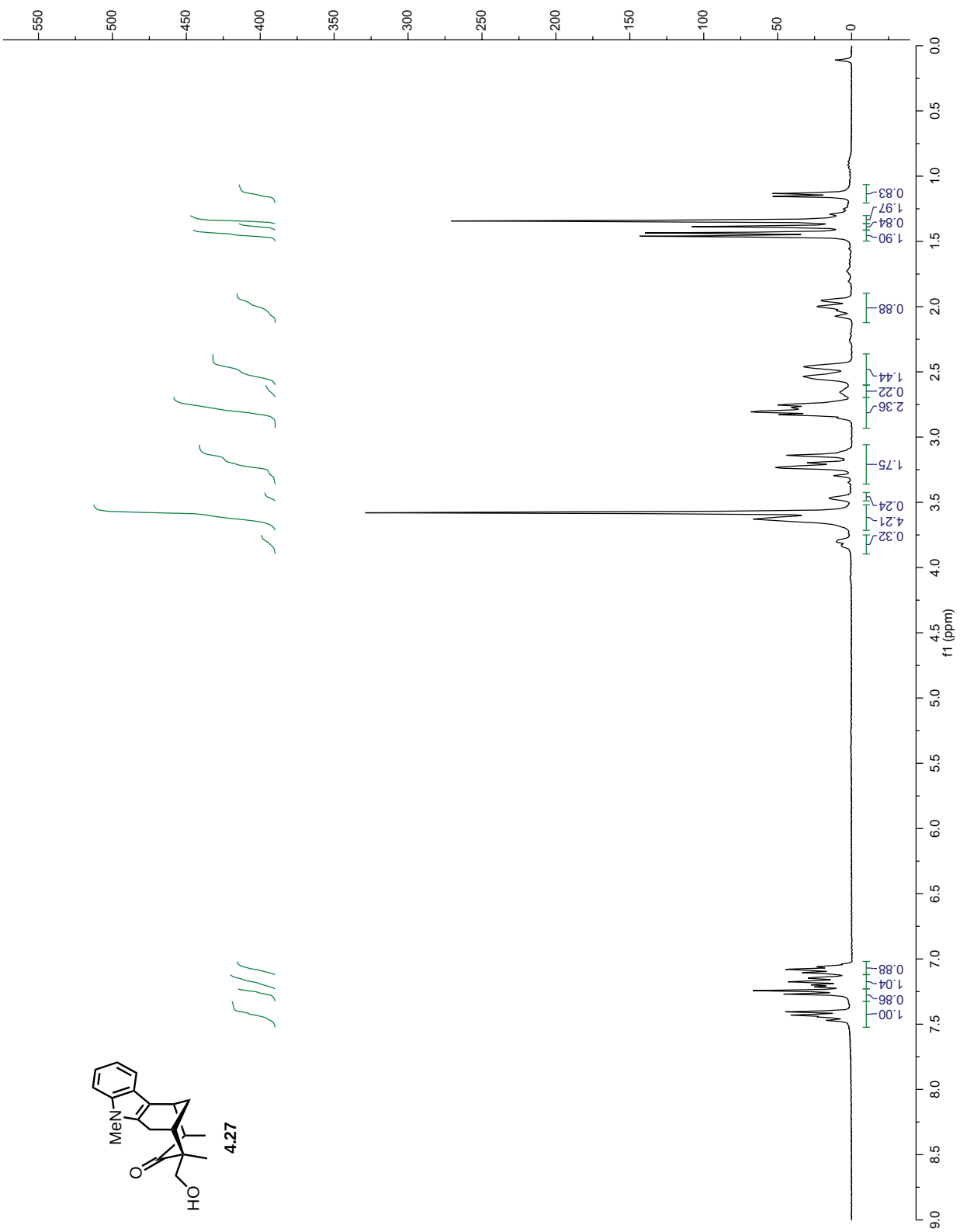

Figure 4.A.47: ^{1}H NMR of **4.27**

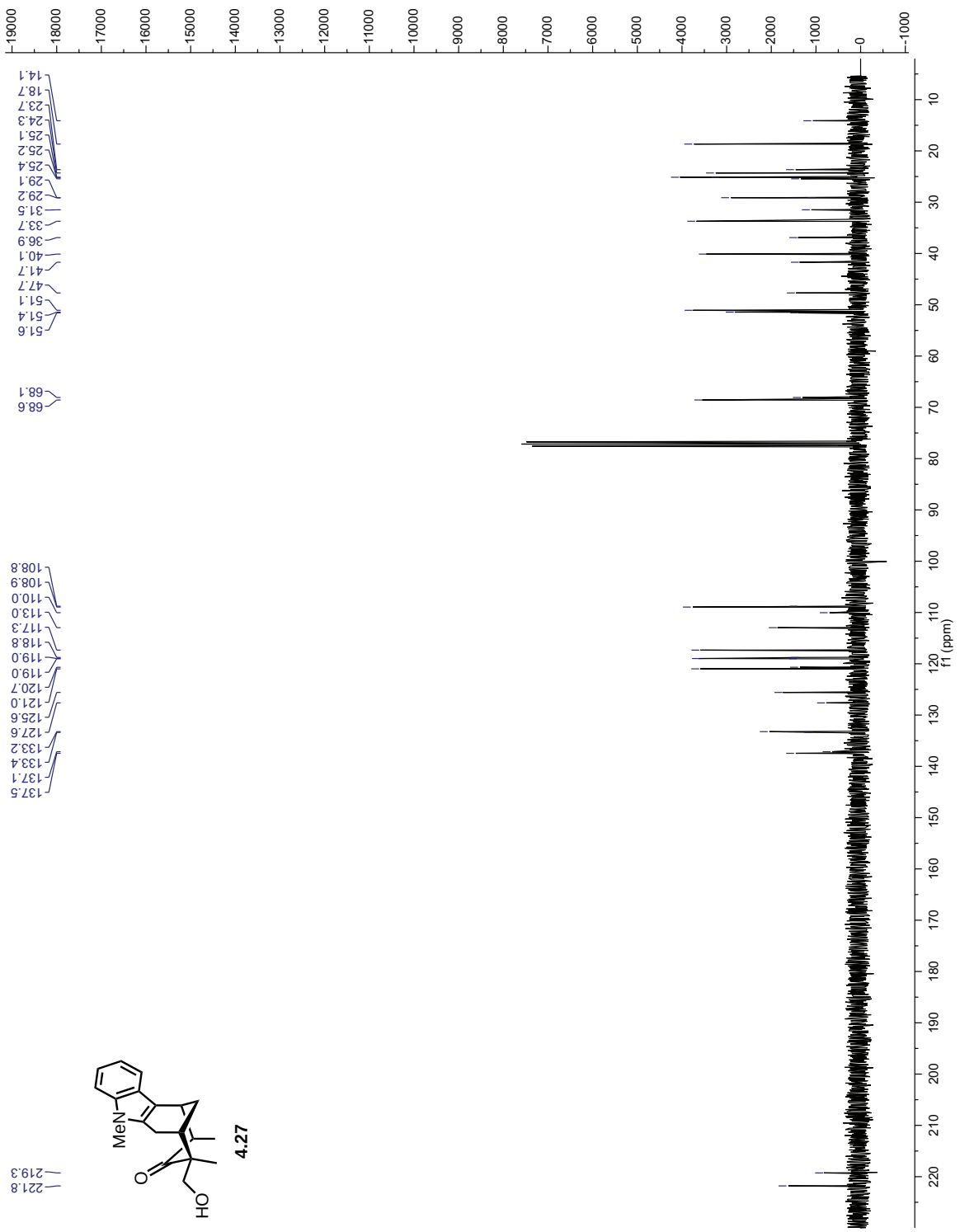

Figure 4.A.48: ^{13}C NMR of **4.27**

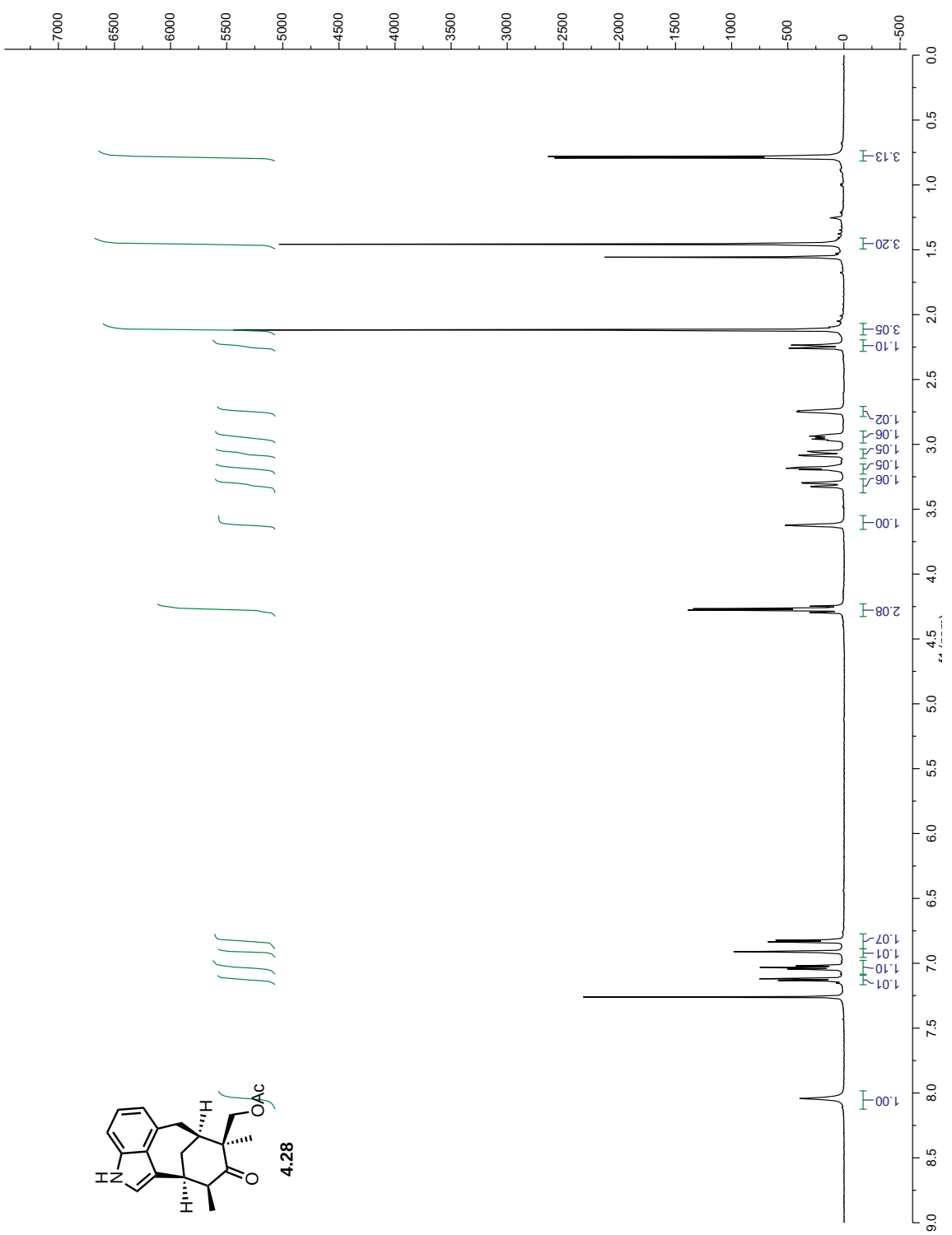

Figure 4.A.49: ^{1}H NMR of **4.28**

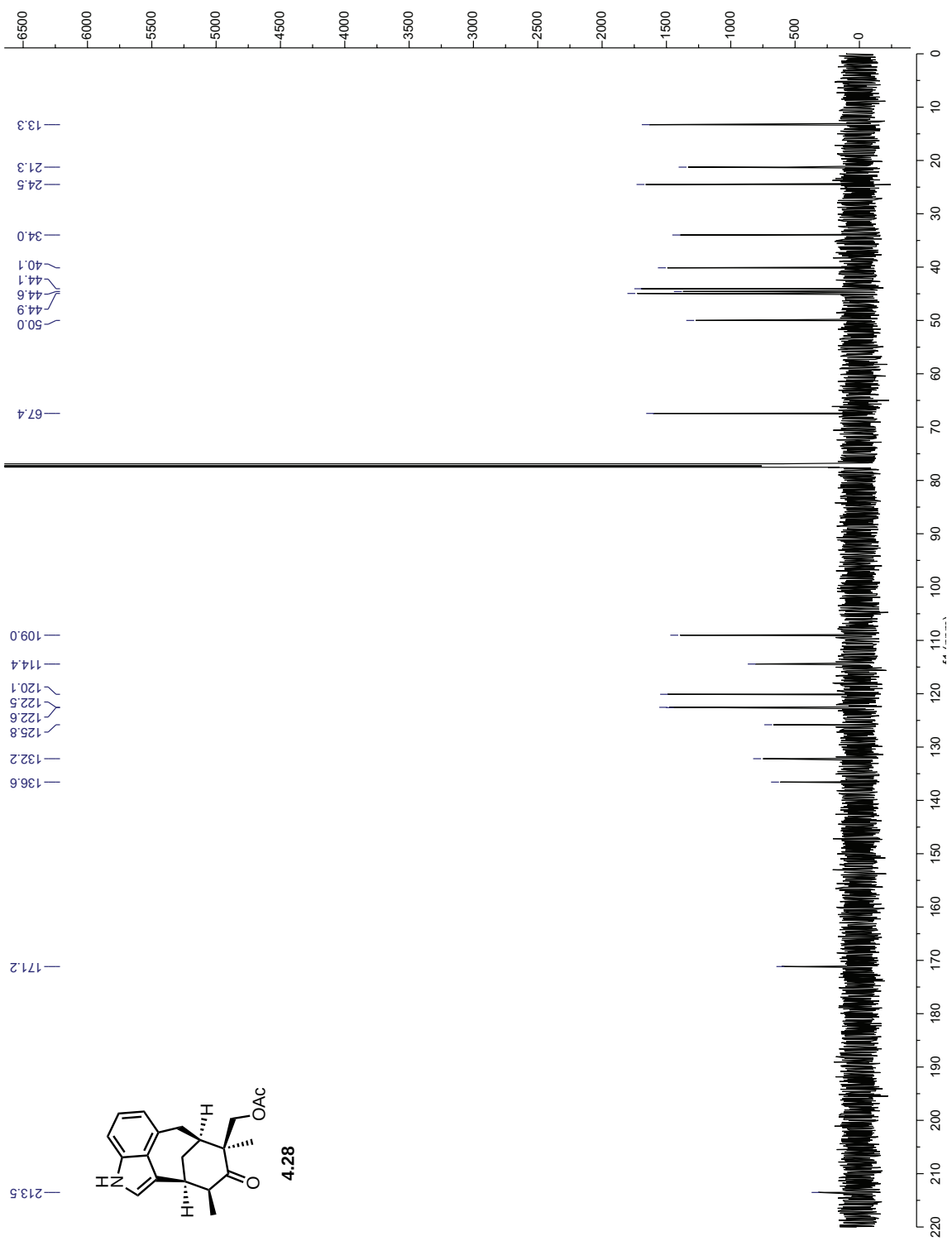

Figure 4.A.50: ^{13}C NMR of **4.28**

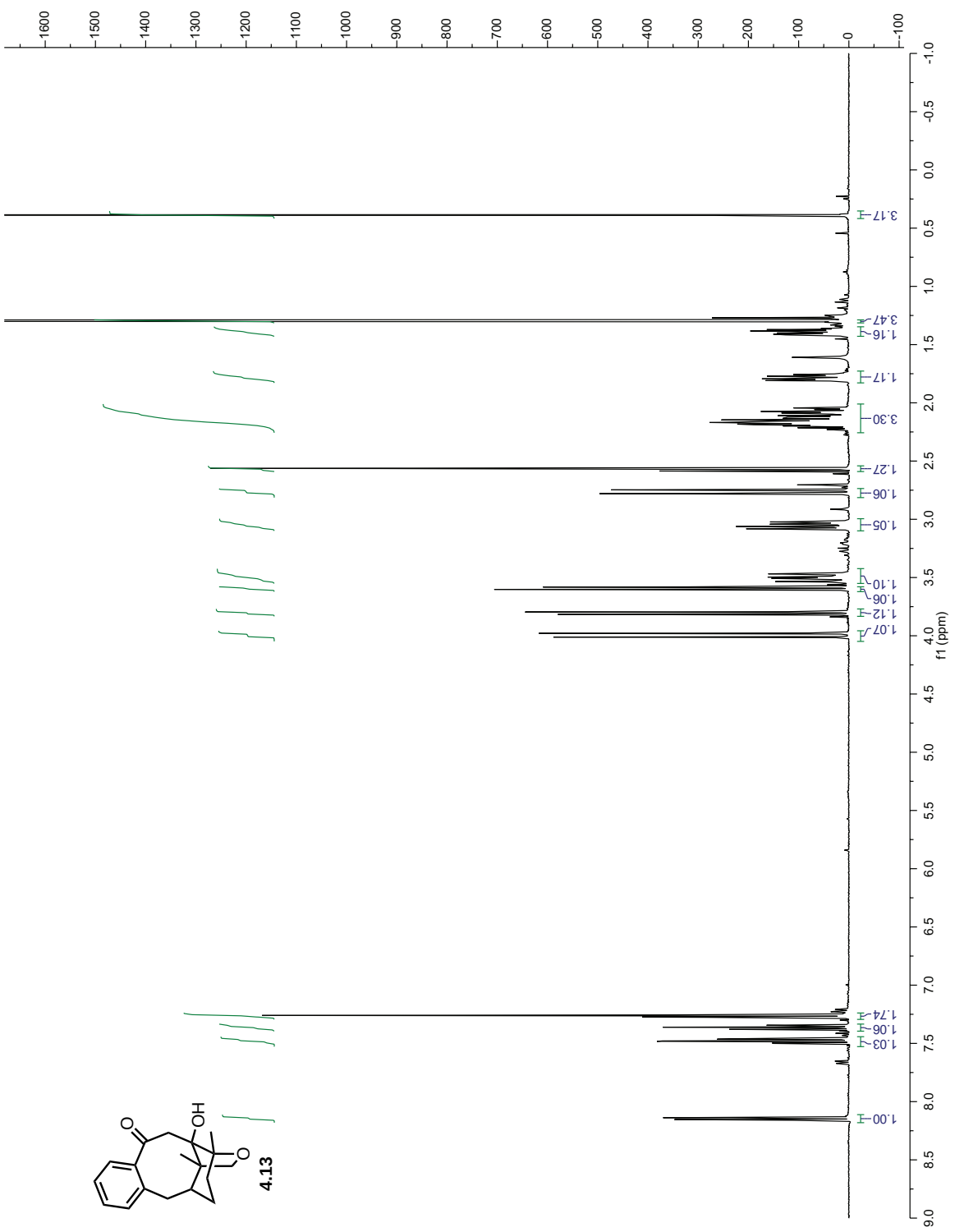

Figure 4.A.51: ^{1}H NMR of **4.13**

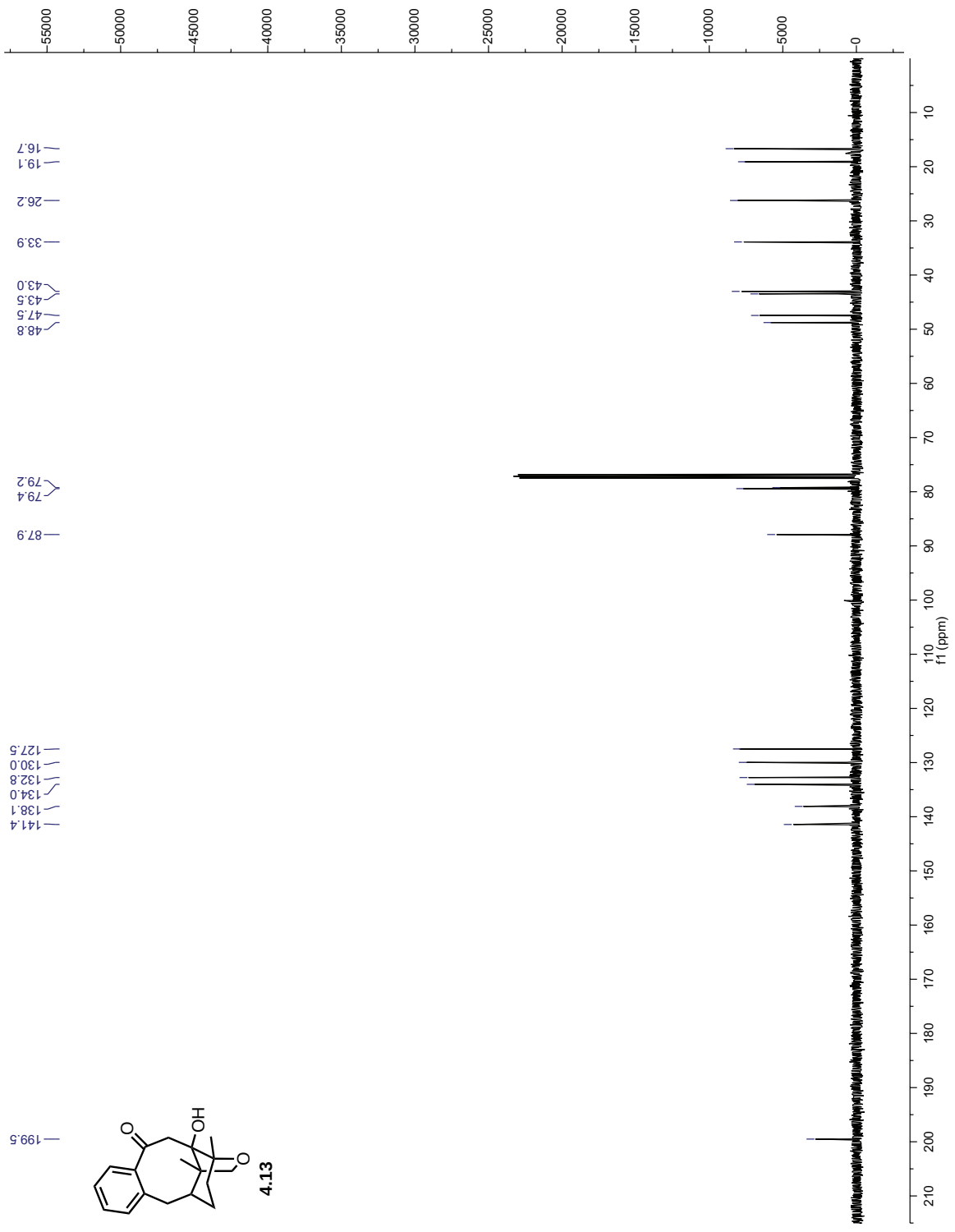

Figure 4.A.52: ^{13}C NMR of **4.13**

4.B X-ray Crystallography Data for Chapter 4

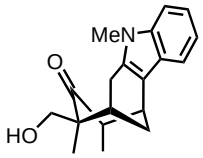

4.21

A colorless plate 0.050 x 0.040 x 0.020 mm in size was mounted on a Cryoloop with Paratone oil. Data were collected in a nitrogen gas stream at 100(2) K using phi and omega scans. Crystal-to-detector distance was 60 mm and exposure time was 20 seconds per frame using a scan width of 2.0°. Data collection was 99.3% complete to 67.000°in θ. A total of 9983 reflections were collected covering the indices, -8≤h≤9, -10≤k≤10, -14≤l≤14. 2771 reflections were found to be symmetry independent, with an Rint of 0.0769. Indexing and unit cell refinement indicated a primitive, monoclinic lattice. The space group was found to be P 21 (No. 4). The data were integrated using the Bruker SAINT software program and scaled using the SADABS software program. Solution by iterative methods (SHELXT) produced a complete heavy-atom phasing model consistent with the proposed structure. All non-hydrogen atoms were refined anisotropically by full-matrix least-squares (SHELXL-2014). All hydrogen atoms were placed using a riding model. Their positions were constrained relative to their parent atom using the appropriate HFIX command in SHELXL-2014. Absolute stereochemistry was unambiguously determined to be R at C1 and S at C3, C4, and C14, respectively.

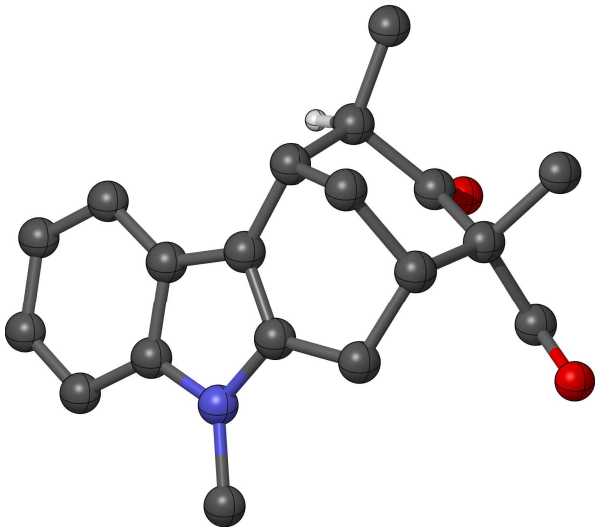

Table 4.1: Crystal data and structure refinement for **4.21**.

X-ray ID	sarpong114	
Sample/notebook ID	MW5-085	
Empirical formula	C19 H23 N O2	
Formula weight	297.38	
Temperature	100(2) K	
Wavelength	1.54178 Å	
Crystal system	Monoclinic	
Space group	P 21	
Unit cell dimensions	a = 7.5354(6) Å	a= 90°.
	b = 8.5029(8) Å	b= 90.259(6)°.
	c = 11.9989(11) Å	g = 90°.
Volume	768.79(12) Å3	
Z	2	
Density (calculated)	1.285 Mg/m3	
Absorption coefficient	0.651 mm-1	
F(000)	320	
Crystal size	0.050 x 0.040 x 0.020 mm3	
Theta range for data collection	3.684 to 68.816°.	
Index ranges	$-8 \leq h \leq 9$, $-10 \leq k \leq 10$, $-14 \leq l \leq 14$	
Reflections collected	9983	
Independent reflections	2771 [R(int) = 0.0769]	
Completeness to theta = 67.000°	99.30%	
Absorption correction	Semi-empirical from equivalents	
Max. and min. transmission	0.929 and 0.776	
Refinement method	Full-matrix least-squares on F^2	
Data / restraints / parameters	2771 / 1 / 203	
Goodness-of-fit on F2	1.064	
Final R indices [I>2sigma(I)]	R1 = 0.0585, wR2 = 0.1491	
R indices (all data)	R1 = 0.0691, wR2 = 0.1567	
Absolute structure parameter	-0.1(3)	
Extinction coefficient	n/a	
Largest diff. peak and hole	0.345 and -0.183 e.$Å^{-3}$	

Table 4.2: Atomic coordinates (x 10^4) and equivalent isotropic displacement parameters (Å^{2}x 10^3) for sarpong114. U(eq) is defined as one third of the trace of the orthogonalized U^{ij} tensor.

	x	y	z	U(eq)
C(1)	7314(7)	2684(5)	2390(4)	36(1)
C(2)	8379(6)	3811(5)	1676(4)	32(1)
C(3)	7423(6)	5123(5)	1009(4)	32(1)
C(4)	5782(6)	5803(5)	1618(4)	33(1)
C(5)	6198(7)	7061(5)	2506(4)	34(1)
C(6)	6696(5)	6271(5)	3580(4)	29(1)
C(7)	7720(6)	5942(6)	5321(4)	36(1)
C(8)	8396(7)	6152(8)	6393(5)	46(1)
C(9)	8617(7)	4844(9)	7042(5)	53(2)
C(10)	8185(7)	3334(8)	6648(4)	53(2)
C(11)	7476(7)	3121(7)	5588(5)	42(1)
C(12)	7216(6)	4450(6)	4900(4)	33(1)
C(13)	6557(6)	4699(5)	3803(4)	30(1)
C(14)	5789(6)	3554(5)	2970(4)	33(1)
C(15)	6836(7)	4346(7)	-103(4)	43(1)
C(16)	8799(6)	6395(6)	725(4)	38(1)
C(17)	4673(6)	4470(6)	2140(4)	37(1)
C(18)	7629(7)	8730(6)	4616(5)	42(1)
C(19)	6690(8)	1287(6)	1699(5)	44(1)
N(1)	7405(5)	7042(5)	4505(4)	34(1)
O(1)	9960(5)	3624(4)	1583(3)	38(1)
O(2)	7895(5)	7685(5)	213(3)	51(1)

Table 4.3: Bond lengths [Å] for sarpong114.

C(1)-C(2)	1.517(6)	C(10)-C(11)	1.389(8)
C(1)-C(19)	1.521(6)	C(10)-H(10)	0.95
C(1)-C(14)	1.536(6)	C(11)-C(12)	1.412(7)
C(1)-H(1)	1	C(11)-H(11)	0.95
C(2)-O(1)	1.207(6)	C(12)-C(13)	1.421(7)
C(2)-C(3)	1.549(6)	C(13)-C(14)	1.509(6)
C(3)-C(16)	1.537(7)	C(14)-C(17)	1.516(7)
C(3)-C(4)	1.551(6)	C(14)-H(14)	1
C(3)-C(15)	1.551(7)	C(15)-H(15A)	0.98
C(4)-C(5)	1.541(7)	C(15)-H(15B)	0.98
C(4)-C(17)	1.543(6)	C(15)-H(15C)	0.98
C(4)-H(4)	1	C(16)-O(2)	1.429(6)
C(5)-C(6)	1.500(7)	C(16)-H(16A)	0.99

C(5)-H(5A)	0.99	C(16)-H(16B)	0.99
C(5)-H(5B)	0.99	C(17)-H(17A)	0.99
C(6)-C(13)	1.367(6)	C(17)-H(17B)	0.99
C(6)-N(1)	1.393(6)	C(18)-N(1)	1.452(6)
C(7)-N(1)	1.374(7)	C(18)-H(18A)	0.98
C(7)-C(8)	1.392(7)	C(18)-H(18B)	0.98
C(7)-C(12)	1.417(7)	C(18)-H(18C)	0.98
C(8)-C(9)	1.368(10)	C(19)-H(19A)	0.98
C(8)-H(8)	0.95	C(19)-H(19B)	0.98
C(9)-C(10)	1.406(10)	C(19)-H(19C)	0.98
C(9)-H(9)	0.95	O(2)-H(2)	0.84

Table 4.4: Bond angles [°] for sarpong114.

C(2)-C(1)-C(19)	110.4(4)	C(11)-C(12)-C(13)	135.0(5)
C(2)-C(1)-C(14)	110.5(4)	C(7)-C(12)-C(13)	106.8(4)
C(19)-C(1)-C(14)	113.1(4)	C(6)-C(13)-C(12)	107.4(4)
C(2)-C(1)-H(1)	107.5	C(6)-C(13)-C(14)	122.1(4)
C(19)-C(1)-H(1)	107.5	C(12)-C(13)-C(14)	130.5(4)
C(14)-C(1)-H(1)	107.5	C(13)-C(14)-C(17)	108.3(4)
O(1)-C(2)-C(1)	119.6(4)	C(13)-C(14)-C(1)	109.0(4)
O(1)-C(2)-C(3)	120.2(4)	C(17)-C(14)-C(1)	111.4(4)
C(1)-C(2)-C(3)	120.1(4)	C(13)-C(14)-H(14)	109.4
C(16)-C(3)-C(2)	108.0(4)	C(17)-C(14)-H(14)	109.4
C(16)-C(3)-C(4)	112.4(4)	C(1)-C(14)-H(14)	109.4
C(2)-C(3)-C(4)	113.3(4)	C(3)-C(15)-H(15A)	109.5
C(16)-C(3)-C(15)	107.4(4)	C(3)-C(15)-H(15B)	109.5
C(2)-C(3)-C(15)	105.5(4)	H(15A)-C(15)-H(15B)	109.5
C(4)-C(3)-C(15)	109.9(4)	C(3)-C(15)-H(15C)	109.5
C(5)-C(4)-C(17)	109.8(4)	H(15A)-C(15)-H(15C)	109.5
C(5)-C(4)-C(3)	115.2(4)	H(15B)-C(15)-H(15C)	109.5
C(17)-C(4)-C(3)	110.6(4)	O(2)-C(16)-C(3)	108.3(4)
C(5)-C(4)-H(4)	107	O(2)-C(16)-H(16A)	110
C(17)-C(4)-H(4)	107	C(3)-C(16)-H(16A)	110
C(3)-C(4)-H(4)	107	O(2)-C(16)-H(16B)	110
C(6)-C(5)-C(4)	109.4(4)	C(3)-C(16)-H(16B)	110
C(6)-C(5)-H(5A)	109.8	H(16A)-C(16)-H(16B)	108.4
C(4)-C(5)-H(5A)	109.8	C(14)-C(17)-C(4)	110.1(4)
C(6)-C(5)-H(5B)	109.8	C(14)-C(17)-H(17A)	109.6
C(4)-C(5)-H(5B)	109.8	C(4)-C(17)-H(17A)	109.6
H(5A)-C(5)-H(5B)	108.2	C(14)-C(17)-H(17B)	109.6
C(13)-C(6)-N(1)	109.5(4)	C(4)-C(17)-H(17B)	109.6
C(13)-C(6)-C(5)	125.9(4)	H(17A)-C(17)-H(17B)	108.2

N(1)-C(6)-C(5)	124.6(4)	N(1)-C(18)-H(18A)	109.5
N(1)-C(7)-C(8)	129.2(5)	N(1)-C(18)-H(18B)	109.5
N(1)-C(7)-C(12)	108.1(4)	H(18A)-C(18)-H(18B)	109.5
C(8)-C(7)-C(12)	122.7(5)	N(1)-C(18)-H(18C)	109.5
C(9)-C(8)-C(7)	117.7(6)	H(18A)-C(18)-H(18C)	109.5
C(9)-C(8)-H(8)	121.1	H(18B)-C(18)-H(18C)	109.5
C(7)-C(8)-H(8)	121.1	C(1)-C(19)-H(19A)	109.5
C(8)-C(9)-C(10)	121.5(5)	C(1)-C(19)-H(19B)	109.5
C(8)-C(9)-H(9)	119.2	H(19A)-C(19)-H(19B)	109.5
C(10)-C(9)-H(9)	119.2	C(1)-C(19)-H(19C)	109.5
C(11)-C(10)-C(9)	121.0(6)	H(19A)-C(19)-H(19C)	109.5
C(11)-C(10)-H(10)	119.5	H(19B)-C(19)-H(19C)	109.5
C(9)-C(10)-H(10)	119.5	C(7)-N(1)-C(6)	108.2(4)
C(10)-C(11)-C(12)	118.9(5)	C(7)-N(1)-C(18)	126.0(5)
C(10)-C(11)-H(11)	120.6	C(6)-N(1)-C(18)	125.6(5)
C(12)-C(11)-H(11)	120.6	C(16)-O(2)-H(2)	109.5
C(11)-C(12)-C(7)	118.2(5)		

Table 4.5: Anisotropic displacement parameters ($Å^2 x\ 10^3$)for sarpong114. The anisotropic displacement factor exponent takes the form: $-2\sqrt{2}[\ h^2 a^{*2} U^{11} + ... + 2\ h\ k\ a^*\ b^*\ U^{12}]$

	U^{11}	U^{22}	U^{33}	U^{23}	U^{13}	U^{12}
C(1)	43(3)	24(2)	41(2)	-2(2)	0(2)	2(2)
C(2)	36(2)	30(2)	31(2)	-9(2)	4(2)	2(2)
C(3)	33(2)	32(2)	32(2)	0(2)	4(2)	3(2)
C(4)	27(2)	34(2)	36(2)	3(2)	3(2)	4(2)
C(5)	34(2)	26(2)	42(3)	3(2)	9(2)	5(2)
C(6)	28(2)	25(2)	34(2)	-2(2)	7(2)	-2(2)
C(7)	27(2)	45(3)	37(2)	-4(2)	8(2)	3(2)
C(8)	31(2)	68(4)	39(3)	-11(3)	4(2)	2(2)
C(9)	32(2)	93(5)	33(3)	-5(3)	5(2)	-9(3)
C(10)	35(3)	84(5)	40(3)	22(3)	4(2)	-3(3)
C(11)	35(3)	43(3)	49(3)	11(2)	9(2)	-5(2)
C(12)	27(2)	32(2)	39(2)	1(2)	10(2)	-3(2)
C(13)	26(2)	24(2)	40(2)	-3(2)	6(2)	-2(2)
C(14)	34(2)	22(2)	42(2)	-3(2)	8(2)	-8(2)
C(15)	42(3)	52(3)	36(3)	0(2)	0(2)	2(2)
C(16)	35(2)	38(2)	40(2)	7(2)	11(2)	7(2)
C(17)	32(2)	37(2)	41(3)	-7(2)	5(2)	-6(2)
C(18)	38(2)	28(2)	60(3)	-15(2)	12(2)	-5(2)
C(19)	54(3)	28(2)	50(3)	-5(2)	-2(2)	1(2)
N(1)	32(2)	27(2)	44(2)	-7(2)	6(2)	-3(2)
O(1)	38(2)	41(2)	35(2)	0(1)	4(1)	8(2)

Table 4.5: Anisotropic displacement parameters ($Å^2$x 10^3)for sarpong114. The anisotropic displacement factor exponent takes the form: -2$\sqrt{}$2[$h^2a^{*2}U^{11}$ + ... + 2 h k a* b* U^{12}]

	U^{11}	U^{22}	U^{33}	U^{23}	U^{13}	U^{12}
O(2)	50(2)	48(2)	54(2)	22(2)	22(2)	14(2)

Table 4.6: Hydrogen coordinates (x 10^4) and isotropic displacement parameters ($Å^2$x 10^3) for sarpong114.

	x	y	z	U(eq)
H(1)	8125	2272	2984	43
H(4)	5020	6317	1039	39
H(5A)	7188	7735	2251	41
H(5B)	5144	7737	2621	41
H(8)	8694	7168	6664	55
H(9)	9072	4958	7778	63
H(10)	8382	2446	7113	63
H(11)	7171	2100	5330	51
H(14)	5022	2777	3366	39
H(15A)	5767	3715	22	65
H(15B)	7790	3668	-378	65
H(15C)	6580	5165	-655	65
H(16A)	9410	6751	1412	45
H(16B)	9699	5964	210	45
H(17A)	3628	4922	2521	44
H(17B)	4242	3755	1547	44
H(18A)	6582	9181	4978	63
H(18B)	7772	9200	3876	63
H(18C)	8685	8950	5070	63
H(19A)	5890	1655	1107	66
H(19B)	6060	543	2179	66
H(19C)	7718	765	1365	66
H(2)	8472	7993	-343	76

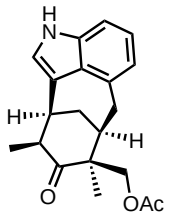

4.19

A colorless rod 0.050 x 0.030 x 0.030 mm in size was mounted on a Cryoloop with Paratone oil. Data were collected in a nitrogen gas stream at 100(2) K using phi and omega scans. Crystal-to-detector distance was 60 mm and exposure time was 10 seconds per frame using a scan width of 2.0°. Data collection was 100.0% complete to 67.000°in θ. A total of 46264 reflections were collected covering the indices, $-8 \leq h \leq 8$, $-14 \leq k \leq 14$, $-22 \leq l \leq 22$. 3061 reflections were found to be symmetry independent, with an Rint of 0.0412. Indexing and unit cell refinement indicated a primitive, orthorhombic lattice. The space group was found to be P 21 21 21 (No. 19). The data were integrated using the Bruker SAINT software program and scaled using the SADABS software program. Solution by iterative methods (SIR-2014) produced a complete heavy-atom phasing model consistent with the proposed structure. All non-hydrogen atoms were refined anisotropically by full-matrix least-squares (SHELXL-2014). All hydrogen atoms were placed using a riding model. Their positions were constrained relative to their parent atom using the appropriate HFIX command in SHELXL-2014. Absolute stereochemistry was unambiguously determined to be S at C1, C2, C11, and C12, respectively.

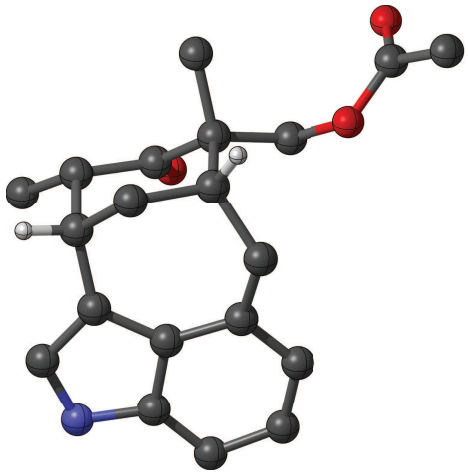

Table 4.7: Crystal data and structure refinement for **4.29**.

X-ray ID	sarpong115	
Sample/notebook ID	kro4-035	
Empirical formula	C20 H23 N O3	
Formula weight	325.39	
Temperature	100(2) K	
Wavelength	1.54178 Å	
Crystal system	Orthorhombic	
Space group	P 21 21 21	
Unit cell dimensions	a = 7.2672(2) Å	a= 90°.
	b = 12.3762(4) ÃĚ	b= 90°.
	c = 18.5597(5) ÃĚ	g = 90°.
Volume	1669.27(8) Å3	
Z	4	
Density (calculated)	1.295 Mg/m3	
Absorption coefficient	0.694 mm-1	
F(000)	696	
Crystal size	0.050 x 0.030 x 0.030 mm3	
Theta range for data collection	4.294 to 68.338Âř.	
Index ranges	-8≤h≤8, -14≤k≤14, -22≤l≤22	
Reflections collected	46264	
Independent reflections	3061 [R(int) = 0.0412]	
Completeness to theta = 67.000Âř	100.00%	
Absorption correction	Semi-empirical from equivalents	
Max. and min. transmission	0.929 and 0.859	
Refinement method	Full-matrix least-squares on F2	
Data / restraints / parameters	3061 / 0 / 220	
Goodness-of-fit on F2	1.089	
Final R indices [I>2sigma(I)]	R1 = 0.0291, wR2 = 0.0748	
R indices (all data)	R1 = 0.0296, wR2 = 0.0753	
Absolute structure parameter	0.08(5)	
Extinction coefficient	n/a	
Largest diff. peak and hole	0.248 and -0.189 e.Å-3	

Table 4.8: Atomic coordinates (x 10^4) and equivalent isotropic displacement parameters (Å^{2}x 10^3) for sarpong115. U(eq) is defined as one third of the trace of the orthogonalized U^{ij} tensor.

	x	y	z	U(eq)
C(1)	3790(3)	-748(2)	7532(1)	24(1)
C(2)	3286(2)	-1750(2)	8004(1)	23(1)
C(3)	4635(3)	-1908(1)	8609(1)	23(1)
C(4)	6204(3)	-2512(2)	8577(1)	27(1)
C(5)	6417(3)	-1623(1)	9626(1)	24(1)
C(6)	6982(3)	-1196(2)	10283(1)	29(1)
C(7)	5779(3)	-475(2)	10608(1)	29(1)
C(8)	4046(3)	-252(2)	10315(1)	26(1)
C(9)	3453(3)	-701(2)	9668(1)	23(1)
C(10)	1449(3)	-647(1)	9461(1)	23(1)
C(11)	845(2)	-597(1)	8667(1)	21(1)
C(12)	1507(3)	433(1)	8255(1)	22(1)
C(13)	3453(3)	280(2)	7955(1)	22(1)
C(14)	5717(3)	-792(2)	7210(1)	31(1)
C(15)	1279(3)	-1638(1)	8249(1)	23(1)
C(16)	4716(3)	-1349(1)	9290(1)	23(1)
C(17)	198(3)	643(2)	7615(1)	28(1)
C(18)	1520(3)	1431(1)	8739(1)	25(1)
C(19)	-1294(3)	2392(2)	8974(1)	26(1)
C(20)	-3104(3)	2289(2)	9354(1)	36(1)
N(1)	7275(2)	-2349(1)	9177(1)	27(1)
O(1)	4622(2)	976(1)	8029(1)	29(1)
O(2)	-255(2)	1513(1)	9098(1)	27(1)
O(3)	-821(2)	3139(1)	8609(1)	36(1)

Table 4.9: Bond lengths [Å] for sarpong115.

C(1)-C(13)	1.515(3)	C(11)-C(15)	1.537(2)
C(1)-C(14)	1.523(3)	C(11)-C(12)	1.561(2)
C(1)-C(2)	1.562(2)	C(11)-H(11)	1
C(1)-H(1)	1	C(12)-C(18)	1.528(2)
C(2)-C(3)	1.505(3)	C(12)-C(13)	1.531(3)
C(2)-C(15)	1.534(2)	C(12)-C(17)	1.544(2)
C(2)-H(2)	1	C(13)-O(1)	1.217(2)
C(3)-C(4)	1.365(3)	C(14)-H(14A)	0.98
C(3)-C(16)	1.441(3)	C(14)-H(14B)	0.98
C(4)-N(1)	1.372(3)	C(14)-H(14C)	0.98
C(4)-H(4)	0.95	C(15)-H(15A)	0.99

C(5)-N(1)	1.375(3)	C(15)-H(15B)	0.99
C(5)-C(6)	1.392(3)	C(17)-H(17A)	0.98
C(5)-C(16)	1.425(3)	C(17)-H(17B)	0.98
C(6)-C(7)	1.386(3)	C(17)-H(17C)	0.98
C(6)-H(6)	0.95	C(18)-O(2)	1.455(2)
C(7)-C(8)	1.399(3)	C(18)-H(18A)	0.99
C(7)-H(7)	0.95	C(18)-H(18B)	0.99
C(8)-C(9)	1.392(3)	C(19)-O(3)	1.197(3)
C(8)-H(8)	0.95	C(19)-O(2)	1.343(2)
C(9)-C(16)	1.406(3)	C(19)-C(20)	1.498(3)
C(9)-C(10)	1.507(3)	C(20)-H(20A)	0.98
C(10)-C(11)	1.539(2)	C(20)-H(20B)	0.98
C(10)-H(10A)	0.99	C(20)-H(20C)	0.98
C(10)-H(10B)	0.99	N(1)-H(1A)	0.88

Table 4.10: Bond angles [°] for sarpong115.

C(13)-C(1)-C(14)	112.48(16)	C(13)-C(12)-C(17)	108.08(14)
C(13)-C(1)-C(2)	109.78(14)	C(18)-C(12)-C(11)	111.90(14)
C(14)-C(1)-C(2)	114.02(16)	C(13)-C(12)-C(11)	111.22(14)
C(13)-C(1)-H(1)	106.7	C(17)-C(12)-C(11)	108.94(14)
C(14)-C(1)-H(1)	106.7	O(1)-C(13)-C(1)	122.61(17)
C(2)-C(1)-H(1)	106.7	O(1)-C(13)-C(12)	121.12(17)
C(3)-C(2)-C(15)	114.14(15)	C(1)-C(13)-C(12)	116.19(15)
C(3)-C(2)-C(1)	111.63(15)	C(1)-C(14)-H(14A)	109.5
C(15)-C(2)-C(1)	108.55(15)	C(1)-C(14)-H(14B)	109.5
C(3)-C(2)-H(2)	107.4	H(14A)-C(14)-H(14B)	109.5
C(15)-C(2)-H(2)	107.4	C(1)-C(14)-H(14C)	109.5
C(1)-C(2)-H(2)	107.4	H(14A)-C(14)-H(14C)	109.5
C(4)-C(3)-C(16)	105.46(17)	H(14B)-C(14)-H(14C)	109.5
C(4)-C(3)-C(2)	125.66(17)	C(2)-C(15)-C(11)	114.87(15)
C(16)-C(3)-C(2)	128.29(16)	C(2)-C(15)-H(15A)	108.5
C(3)-C(4)-N(1)	110.98(17)	C(11)-C(15)-H(15A)	108.5
C(3)-C(4)-H(4)	124.5	C(2)-C(15)-H(15B)	108.5
N(1)-C(4)-H(4)	124.5	C(11)-C(15)-H(15B)	108.5
N(1)-C(5)-C(6)	130.22(18)	H(15A)-C(15)-H(15B)	107.5
N(1)-C(5)-C(16)	106.47(17)	C(9)-C(16)-C(5)	118.94(17)
C(6)-C(5)-C(16)	123.31(18)	C(9)-C(16)-C(3)	133.12(18)
C(7)-C(6)-C(5)	116.04(18)	C(5)-C(16)-C(3)	107.76(16)
C(7)-C(6)-H(6)	122	C(12)-C(17)-H(17A)	109.5
C(5)-C(6)-H(6)	122	C(12)-C(17)-H(17B)	109.5
C(6)-C(7)-C(8)	121.72(18)	H(17A)-C(17)-H(17B)	109.5
C(6)-C(7)-H(7)	119.1	C(12)-C(17)-H(17C)	109.5

C(8)-C(7)-H(7)	119.1	H(17A)-C(17)-H(17C)	109.5
C(9)-C(8)-C(7)	122.38(18)	H(17B)-C(17)-H(17C)	109.5
C(9)-C(8)-H(8)	118.8	O(2)-C(18)-C(12)	108.67(14)
C(7)-C(8)-H(8)	118.8	O(2)-C(18)-H(18A)	110
C(8)-C(9)-C(16)	117.07(17)	C(12)-C(18)-H(18A)	110
C(8)-C(9)-C(10)	120.10(17)	O(2)-C(18)-H(18B)	110
C(16)-C(9)-C(10)	121.95(17)	C(12)-C(18)-H(18B)	110
C(9)-C(10)-C(11)	121.40(15)	H(18A)-C(18)-H(18B)	108.3
C(9)-C(10)-H(10A)	107	O(3)-C(19)-O(2)	124.09(18)
C(11)-C(10)-H(10A)	107	O(3)-C(19)-C(20)	125.73(18)
C(9)-C(10)-H(10B)	107	O(2)-C(19)-C(20)	110.18(17)
C(11)-C(10)-H(10B)	107	C(19)-C(20)-H(20A)	109.5
H(10A)-C(10)-H(10B)	106.7	C(19)-C(20)-H(20B)	109.5
C(15)-C(11)-C(10)	112.95(14)	H(20A)-C(20)-H(20B)	109.5
C(15)-C(11)-C(12)	111.97(14)	C(19)-C(20)-H(20C)	109.5
C(10)-C(11)-C(12)	114.48(14)	H(20A)-C(20)-H(20C)	109.5
C(15)-C(11)-H(11)	105.5	H(20B)-C(20)-H(20C)	109.5
C(10)-C(11)-H(11)	105.5	C(4)-N(1)-C(5)	109.26(16)
C(12)-C(11)-H(11)	105.5	C(4)-N(1)-H(1A)	125.4
C(18)-C(12)-C(13)	107.92(15)	C(5)-N(1)-H(1A)	125.4
C(18)-C(12)-C(17)	108.68(15)	C(19)-O(2)-C(18)	118.48(15

Table 4.11: Anisotropic displacement parameters ($Å^2$x 10^3)for sarpong115. The anisotropic displacement factor exponent takes the form: -2$\sqrt{}$2[$h^2a^{*2}U^{11}$ + ... + 2 h k a* b* U^{12}]

	U^{11}	U^{22}	U^{33}	U^{23}	U^{13}	U^{12}
C(1)	23(1)	28(1)	21(1)	0(1)	4(1)	-5(1)
C(2)	24(1)	22(1)	24(1)	-4(1)	4(1)	-3(1)
C(3)	26(1)	21(1)	24(1)	2(1)	5(1)	-5(1)
C(4)	27(1)	26(1)	29(1)	2(1)	7(1)	-1(1)
C(5)	20(1)	23(1)	28(1)	8(1)	6(1)	1(1)
C(6)	24(1)	34(1)	29(1)	9(1)	2(1)	-4(1)
C(7)	33(1)	31(1)	24(1)	1(1)	3(1)	-7(1)
C(8)	30(1)	24(1)	24(1)	1(1)	5(1)	-4(1)
C(9)	24(1)	20(1)	23(1)	4(1)	3(1)	-1(1)
C(10)	23(1)	20(1)	24(1)	2(1)	0(1)	1(1)
C(11)	17(1)	21(1)	24(1)	1(1)	1(1)	-2(1)
C(12)	21(1)	21(1)	24(1)	3(1)	-1(1)	-2(1)
C(13)	22(1)	25(1)	20(1)	6(1)	-1(1)	-3(1)
C(14)	29(1)	35(1)	29(1)	0(1)	9(1)	-4(1)
C(15)	23(1)	21(1)	25(1)	0(1)	2(1)	-5(1)
C(16)	25(1)	20(1)	25(1)	5(1)	3(1)	-3(1)
C(17)	25(1)	30(1)	30(1)	6(1)	-4(1)	-3(1)

Table 4.11: Anisotropic displacement parameters ($Å^2$x 10^3)for sarpong115. The anisotropic displacement factor exponent takes the form: -2$\sqrt{}$2[$h^2a^{*2}U^{11}$ + ... + 2 h k a* b* U^{12}]

	U^{11}	U^{22}	U^{33}	U^{23}	U^{13}	U^{12}
C(18)	21(1)	21(1)	33(1)	1(1)	3(1)	0(1)
C(19)	30(1)	24(1)	23(1)	-7(1)	-8(1)	5(1)
C(20)	30(1)	37(1)	40(1)	-13(1)	-3(1)	6(1)
N(1)	20(1)	29(1)	33(1)	6(1)	5(1)	6(1)
O(1)	25(1)	28(1)	32(1)	2(1)	2(1)	-7(1)
O(2)	22(1)	22(1)	37(1)	3(1)	4(1)	3(1)
O(3)	47(1)	28(1)	34(1)	3(1)	1(1)	11(1)

Table 4.12: Hydrogen coordinates (x 10^4) and isotropic displacement parameters ($Å^2$x 10^3) for sarpong115.

	x	y	z	U(eq)
H(1)	2910	-741	7118	29
H(2)	3360	-2403	7687	28
H(4)	6514	-2983	8192	32
H(6)	8124	-1387	10497	34
H(7)	6141	-124	11040	35
H(8)	3246	222	10567	31
H(10A)	924	-5	9703	27
H(10B)	843	-1287	9676	27
H(11)	-528	-546	8678	25
H(14A)	5905	-166	6895	47
H(14B)	5856	-1458	6929	47
H(14C)	6630	-781	7599	47
H(15A)	969	-2265	8558	28
H(15B)	475	-1670	7819	28
H(17A)	666	1248	7328	42
H(17B)	-1031	819	7797	42
H(17C)	129	-6	7313	42
H(18A)	2513	1368	9102	30
H(18B)	1747	2087	8447	30
H(20A)	-3616	3010	9440	53
H(20B)	-2923	1920	9816	53
H(20C)	-3957	1871	9055	53
H(1A)	8343	-2659	9260	33

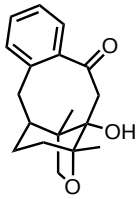

4.13

A colorless block 0.050 x 0.050 x 0.010 mm in size was mounted on a Cryoloop with Paratone oil. Data were collected in a nitrogen gas stream at 100(2) K using phi and omega scans. Crystal-to-detector distance was 60 mm and exposure time was 20 seconds per frame using a scan width of 0.3°. Data collection was 99.7% complete to 25.000°in θ. A total of 7289 reflections were collected covering the indices, $-7 \leq h \leq 9$, $-6 \leq k \leq 10$, $-26 \leq l \leq 21$. 2548 reflections were found to be symmetry independent, with an Rint of 0.0403. Indexing and unit cell refinement indicated a primitive, orthorhombic lattice. The space group was found to be P 21 21 21 (No. 19). The data were integrated using the Bruker SAINT software program and scaled using the SADABS software program. Solution by iterative methods (SHELXT) produced a complete heavy-atom phasing model consistent with the proposed structure. All non-hydrogen atoms were refined anisotropically by full-matrix least-squares (SHELXL-2014). All hydrogen atoms were placed using a riding model. Their positions were constrained relative to their parent atom using the appropriate HFIX command in SHELXL-2014.

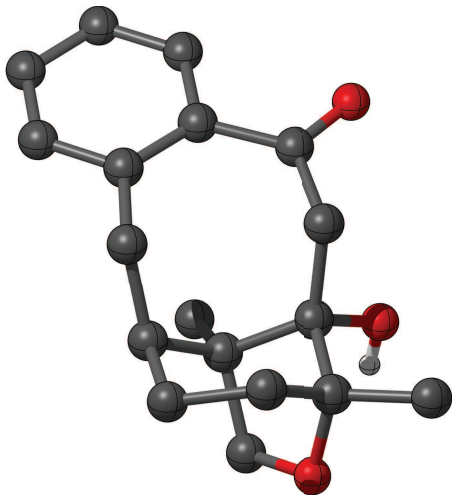

Table 4.13: Crystal data and structure refinement for **4.13**.

X-ray ID	sarpong118	
Sample/notebook ID	MW5128	
Empirical formula	C18 H22 O3	
Formula weight	286.35	
Temperature	100(2) K	
Wavelength	0.71073 Å	
Crystal system	Orthorhombic	
Space group	P 21 21 21	
Unit cell dimensions	a = 7.5988(4) Å	a= 90°.
	b = 8.4424(4) Å	b= 90°.
	c = 21.9530(10) Å	g = 90°.
Volume	1408.33(12) Å3	
Z	4	
Density (calculated)	1.351 Mg/m3	
Absorption coefficient	0.090 mm-1	
F(000)	616	
Crystal size	0.050 x 0.050 x 0.010 mm3	
Theta range for data collection	1.855 to 25.347°.	
Index ranges	-7≤h≤9, -6≤k≤10, -26≤l≤21	
Reflections collected	7289	
Independent reflections	2548 [R(int) = 0.0403]	
Completeness to theta = 25.000°	99.70%	
Absorption correction	Semi-empirical from equivalents	
Max. and min. transmission	0.745 and 0.686	
Refinement method	Full-matrix least-squares on F2	
Data / restraints / parameters	2548 / 0 / 193	
Goodness-of-fit on F2	1.045	
Final R indices [I>2sigma(I)]	R1 = 0.0314, wR2 = 0.0817	
R indices (all data)	R1 = 0.0320, wR2 = 0.0823	
Absolute structure parameter	-0.2(5)	
Extinction coefficient	n/a	
Largest diff. peak and hole	0.225 and -0.171 e.ÃĚ-3	

Table 4.14: Atomic coordinates (x 10^4) and equivalent isotropic displacement parameters (Å^{2}x 10^3) for sarpong118. U(eq) is defined as one third of the trace of the orthogonalized U^{ij} tensor.

	x	y	z	U(eq)
C(1)	2328(3)	6930(2)	4076(1)	13(1)
C(2)	4255(2)	6390(2)	3943(1)	12(1)
C(3)	4600(3)	6206(2)	3256(1)	13(1)
C(4)	6307(3)	5440(2)	3065(1)	13(1)
C(5)	6611(3)	3671(2)	3098(1)	13(1)
C(6)	8284(3)	3163(2)	2911(1)	15(1)
C(7)	8799(3)	1594(2)	2948(1)	17(1)
C(8)	7627(3)	486(2)	3180(1)	18(1)
C(9)	5960(3)	967(2)	3357(1)	16(1)
C(10)	5399(3)	2544(2)	3317(1)	14(1)
C(11)	3518(3)	2878(2)	3506(1)	15(1)
C(12)	3143(3)	3585(2)	4146(1)	14(1)
C(13)	1201(3)	4119(2)	4157(1)	16(1)
C(14)	960(3)	5738(2)	3850(1)	15(1)
C(15)	1938(3)	8601(2)	3860(1)	17(1)
C(16)	4344(2)	4944(2)	4379(1)	13(1)
C(17)	6178(3)	4359(2)	4565(1)	15(1)
C(18)	3493(3)	5712(2)	4946(1)	16(1)
O(1)	2277(2)	6910(2)	4739(1)	16(1)
O(2)	5480(2)	7595(2)	4119(1)	15(1)
O(3)	7474(2)	6283(2)	2862(1)	21(1)

Table 4.15: Bond lengths [Å] for sarpong118.

C(1)-O(1)	1.457(2)	C(11)-C(12)	1.554(3)
C(1)-C(15)	1.517(3)	C(11)-H(11A)	0.99
C(1)-C(14)	1.530(3)	C(11)-H(11B)	0.99
C(1)-C(2)	1.561(3)	C(12)-C(13)	1.543(3)
C(2)-O(2)	1.432(2)	C(12)-C(16)	1.552(3)
C(2)-C(3)	1.538(3)	C(12)-H(12)	1
C(2)-C(16)	1.552(3)	C(13)-C(14)	1.535(3)
C(3)-C(4)	1.509(3)	C(13)-H(13A)	0.99
C(3)-H(3A)	0.99	C(13)-H(13B)	0.99
C(3)-H(3B)	0.99	C(14)-H(14A)	0.99
C(4)-O(3)	1.222(2)	C(14)-H(14B)	0.99
C(4)-C(5)	1.513(3)	C(15)-H(15A)	0.98
C(5)-C(6)	1.403(3)	C(15)-H(15B)	0.98
C(5)-C(10)	1.408(3)	C(15)-H(15C)	0.98

C(6)-C(7)	1.384(3)	C(16)-C(17)	1.535(3)
C(6)-H(6)	0.95	C(16)-C(18)	1.546(3)
C(7)-C(8)	1.388(3)	C(17)-H(17A)	0.98
C(7)-H(7)	0.95	C(17)-H(17B)	0.98
C(8)-C(9)	1.385(3)	C(17)-H(17C)	0.98
C(8)-H(8)	0.95	C(18)-O(1)	1.444(2)
C(9)-C(10)	1.401(3)	C(18)-H(18A)	0.99
C(9)-H(9)	0.95	C(18)-H(18B)	0.99
C(10)-C(11)	1.514(3)	O(2)-H(2)	0.84

Table 4.16: Bond angles [°] for sarpong118.

O(1)-C(1)-C(15)	108.51(16)	C(13)-C(12)-C(16)	110.00(15)
O(1)-C(1)-C(14)	107.33(15)	C(13)-C(12)-C(11)	107.52(16)
C(15)-C(1)-C(14)	112.19(17)	C(16)-C(12)-C(11)	118.26(15)
O(1)-C(1)-C(2)	102.03(15)	C(13)-C(12)-H(12)	106.8
C(15)-C(1)-C(2)	113.37(16)	C(16)-C(12)-H(12)	106.8
C(14)-C(1)-C(2)	112.64(15)	C(11)-C(12)-H(12)	106.8
O(2)-C(2)-C(3)	103.03(15)	C(14)-C(13)-C(12)	111.56(16)
O(2)-C(2)-C(16)	111.35(15)	C(14)-C(13)-H(13A)	109.3
C(3)-C(2)-C(16)	121.14(16)	C(12)-C(13)-H(13A)	109.3
O(2)-C(2)-C(1)	110.60(15)	C(14)-C(13)-H(13B)	109.3
C(3)-C(2)-C(1)	111.88(15)	C(12)-C(13)-H(13B)	109.3
C(16)-C(2)-C(1)	98.93(15)	H(13A)-C(13)-H(13B)	108
C(4)-C(3)-C(2)	117.59(16)	C(1)-C(14)-C(13)	111.29(16)
C(4)-C(3)-H(3A)	107.9	C(1)-C(14)-H(14A)	109.4
C(2)-C(3)-H(3A)	107.9	C(13)-C(14)-H(14A)	109.4
C(4)-C(3)-H(3B)	107.9	C(1)-C(14)-H(14B)	109.4
C(2)-C(3)-H(3B)	107.9	C(13)-C(14)-H(14B)	109.4
H(3A)-C(3)-H(3B)	107.2	H(14A)-C(14)-H(14B)	108
O(3)-C(4)-C(3)	118.46(17)	C(1)-C(15)-H(15A)	109.5
O(3)-C(4)-C(5)	118.81(18)	C(1)-C(15)-H(15B)	109.5
C(3)-C(4)-C(5)	122.71(17)	H(15A)-C(15)-H(15B)	109.5
C(6)-C(5)-C(10)	119.08(17)	C(1)-C(15)-H(15C)	109.5
C(6)-C(5)-C(4)	115.19(18)	H(15A)-C(15)-H(15C)	109.5
C(10)-C(5)-C(4)	125.69(18)	H(15B)-C(15)-H(15C)	109.5
C(7)-C(6)-C(5)	122.13(19)	C(17)-C(16)-C(18)	107.44(16)
C(7)-C(6)-H(6)	118.9	C(17)-C(16)-C(12)	112.57(15)
C(5)-C(6)-H(6)	118.9	C(18)-C(16)-C(12)	109.19(15)
C(6)-C(7)-C(8)	118.98(19)	C(17)-C(16)-C(2)	117.21(16)
C(6)-C(7)-H(7)	120.5	C(18)-C(16)-C(2)	98.56(15)
C(8)-C(7)-H(7)	120.5	C(12)-C(16)-C(2)	110.68(15)
C(9)-C(8)-C(7)	119.51(19)	C(16)-C(17)-H(17A)	109.5

C(9)-C(8)-H(8)	120.2	C(16)-C(17)-H(17B)	109.5
C(7)-C(8)-H(8)	120.2	H(17A)-C(17)-H(17B)	109.5
C(8)-C(9)-C(10)	122.61(19)	C(16)-C(17)-H(17C)	109.5
C(8)-C(9)-H(9)	118.7	H(17A)-C(17)-H(17C)	109.5
C(10)-C(9)-H(9)	118.7	H(17B)-C(17)-H(17C)	109.5
C(9)-C(10)-C(5)	117.65(18)	O(1)-C(18)-C(16)	107.92(15)
C(9)-C(10)-C(11)	116.54(18)	O(1)-C(18)-H(18A)	110.1
C(5)-C(10)-C(11)	125.81(17)	C(16)-C(18)-H(18A)	110.1
C(10)-C(11)-C(12)	119.47(16)	O(1)-C(18)-H(18B)	110.1
C(10)-C(11)-H(11A)	107.5	C(16)-C(18)-H(18B)	110.1
C(12)-C(11)-H(11A)	107.5	H(18A)-C(18)-H(18B)	108.4
C(10)-C(11)-H(11B)	107.5	C(18)-O(1)-C(1)	107.81(14)
C(12)-C(11)-H(11B)	107.5	C(2)-O(2)-H(2)	109.5
H(11A)-C(11)-H(11B)	107		

Table 4.17: Anisotropic displacement parameters ($Å^2$x 10^3)for sarpong118. The anisotropic displacement factor exponent takes the form: -2$\sqrt{}$2[$h^2a^{*2}U^{11}$ + ... + 2 h k a* b* U^{12}]

	U^{11}	U^{22}	U^{33}	U^{23}	U^{13}	U^{12}
C(1)	14(1)	16(1)	10(1)	1(1)	1(1)	2(1)
C(2)	12(1)	12(1)	12(1)	0(1)	-1(1)	0(1)
C(3)	14(1)	12(1)	12(1)	1(1)	0(1)	0(1)
C(4)	15(1)	16(1)	9(1)	-1(1)	-2(1)	-2(1)
C(5)	15(1)	15(1)	10(1)	-3(1)	-1(1)	1(1)
C(6)	15(1)	18(1)	12(1)	-3(1)	-1(1)	-2(1)
C(7)	13(1)	20(1)	17(1)	-5(1)	-1(1)	3(1)
C(8)	21(1)	14(1)	18(1)	-2(1)	-4(1)	3(1)
C(9)	19(1)	15(1)	16(1)	-1(1)	0(1)	-3(1)
C(10)	15(1)	17(1)	11(1)	-2(1)	-2(1)	-1(1)
C(11)	15(1)	14(1)	17(1)	0(1)	2(1)	-3(1)
C(12)	14(1)	13(1)	14(1)	2(1)	2(1)	-1(1)
C(13)	14(1)	18(1)	15(1)	0(1)	1(1)	-3(1)
C(14)	11(1)	22(1)	14(1)	0(1)	1(1)	1(1)
C(15)	19(1)	17(1)	16(1)	3(1)	4(1)	7(1)
C(16)	14(1)	14(1)	10(1)	1(1)	-1(1)	-1(1)
C(17)	16(1)	16(1)	14(1)	2(1)	-3(1)	1(1)
C(18)	18(1)	17(1)	12(1)	1(1)	-1(1)	0(1)
O(1)	18(1)	17(1)	12(1)	0(1)	2(1)	3(1)
O(2)	18(1)	15(1)	13(1)	-1(1)	-1(1)	-4(1)
O(3)	17(1)	18(1)	29(1)	4(1)	6(1)	-2(1)

Table 4.18: Hydrogen coordinates (x 10^4) and isotropic displacement parameters ($Å^2$x 10^3) for sarpong118.

	x	y	z	U(eq)
H(3A)	3623	5579	3081	15
H(3B)	4550	7272	3069	15
H(6)	9089	3921	2754	18
H(7)	9938	1279	2816	20
H(8)	7965	-593	3217	21
H(9)	5167	196	3512	20
H(11A)	2858	1870	3474	18
H(11B)	3009	3610	3201	18
H(12)	3253	2697	4445	16
H(13A)	471	3322	3943	19
H(13B)	790	4181	4584	19
H(14A)	1070	5616	3403	18
H(14B)	-235	6144	3939	18
H(15A)	703	8856	3943	26
H(15B)	2158	8676	3421	26
H(15C)	2699	9350	4076	26
H(17A)	6928	5269	4663	23
H(17B)	6702	3760	4228	23
H(17C)	6077	3673	4924	23
H(18A)	2863	4900	5187	19
H(18B)	4411	6195	5207	19
H(2)	5590	7595	4499	23